REGULATION OF FRUIT RIPENING AND SENESCENCE

EDITED BY: Carlos R. Figueroa, Noam Alkan, Ana Margarida Fortes, Cai-Zhong Jiang and Carolina Andrea Torres

PUBLISHED IN: Frontiers in Plant Science

frontiers Research Topics

ISSN 1664-8714
ISBN 978-2-88971-389-9
DOI 10.3389/978-2-88971-389-9

About Frontiers

Frontiers is more than just an open-access publisher of scholarly articles: it is a pioneering approach to the world of academia, radically improving the way scholarly research is managed. The grand vision of Frontiers is a world where all people have an equal opportunity to seek, share and generate knowledge. Frontiers provides immediate and permanent online open access to all its publications, but this alone is not enough to realize our grand goals.

Frontiers Journal Series

The Frontiers Journal Series is a multi-tier and interdisciplinary set of open-access, online journals, promising a paradigm shift from the current review, selection and dissemination processes in academic publishing. All Frontiers journals are driven by researchers for researchers; therefore, they constitute a service to the scholarly community. At the same time, the Frontiers Journal Series operates on a revolutionary invention, the tiered publishing system, initially addressing specific communities of scholars, and gradually climbing up to broader public understanding, thus serving the interests of the lay society, too.

Dedication to Quality

Each Frontiers article is a landmark of the highest quality, thanks to genuinely collaborative interactions between authors and review editors, who include some of the world's best academicians. Research must be certified by peers before entering a stream of knowledge that may eventually reach the public - and shape society; therefore, Frontiers only applies the most rigorous and unbiased reviews.
Frontiers revolutionizes research publishing by freely delivering the most outstanding research, evaluated with no bias from both the academic and social point of view. By applying the most advanced information technologies, Frontiers is catapulting scholarly publishing into a new generation.

What are Frontiers Research Topics?

Frontiers Research Topics are very popular trademarks of the Frontiers Journals Series: they are collections of at least ten articles, all centered on a particular subject. With their unique mix of varied contributions from Original Research to Review Articles, Frontiers Research Topics unify the most influential researchers, the latest key findings and historical advances in a hot research area! Find out more on how to host your own Frontiers Research Topic or contribute to one as an author by contacting the Frontiers Editorial Office: frontiersin.org/about/contact

REGULATION OF FRUIT RIPENING AND SENESCENCE

Topic Editors:
Carlos R. Figueroa, University of Talca, Chile
Noam Alkan, Agricultural Research Organization (ARO), Israel
Ana Margarida Fortes, University of Lisbon, Portugal
Cai-Zhong Jiang, Crops Pathology and Genetics Research Unit, USDA-ARS, United States
Carolina Andrea Torres, Washington State University, United States

Citation: Figueroa, C. R., Alkan, N., Fortes, A. M., Jiang, C.-Z., Torres, C. A., eds. (2021). Regulation of Fruit Ripening and Senescence. Lausanne: Frontiers Media SA. doi: 10.3389/978-2-88971-389-9

Table of Contents

frontiers in Plant Science

EDITORIAL
published: 26 July 2021
doi: 10.3389/fpls.2021.711458

Editorial: Regulation of Fruit Ripening and Senescence

Carlos R. Figueroa[1], Cai-Zhong Jiang[2,3], Carolina A. Torres[4], Ana M. Fortes[5] and Noam Alkan[6]*

[1] Institute of Biological Sciences, Campus Talca, Universidad de Talca, Talca, Chile, [2] Crops Pathology and Genetics Research Unit, USDA-ARS, Davis, CA, United States, [3] Department of Plant Sciences, University of California, Davis, Davis, CA, United States, [4] Horticulture Department, Tree Fruit Research and Extension Center, Washington State University, Wenatchee, WA, United States, [5] Faculty of Sciences, BioISI - Biosystems and Integrative Sciences Institute, University of Lisbon, Lisbon, Portugal, [6] Department of Postharvest Science, Agricultural Research Organization (ARO), Rishon LeZion, Israel

Keywords: fruit ripening and senescence, hormonal regulation, cell wall-modifying enzymes, transcription factors, molecule signaling, exogenous molecule application, microbial interaction, postharvest fruit quality

Editorial on the Research Topic

Regulation of Fruit Ripening and Senescence

Fruit ripening and senescence comprise complex and highly coordinated molecular and biochemical processes involving ripening-associated genes, transcription factors, enzymes, repressors, signaling molecules, and metabolic pathways in both climacteric and non-climacteric fruits (Cherian et al., 2014; Fuentes et al., 2019), which account for fruit quality on one hand and post-harvest losses on the other. Therefore, studying the molecular mechanisms of fruit ripening and senescence have profound commercial implications. As the fruit ripens or enters senescence, it becomes susceptible to fungal pathogens (Alkan and Fortes, 2015), while fruit-pathogen interactions could accelerate ripening and senescence, resulting in fruit deterioration. Hence, common strategies to slow down senescence and preserve fruit quality include both pre- and post-harvest management practices and technological tools.

This Research Topic aimed to study and characterize the endogenous molecular and biochemical regulators (i.e., hormones, molecules, and genetic components) and their mechanisms of action to regulate ripening, senescence, and disease resistance in fruit. This collection includes 10 original research articles reporting new information on hormonal control of fruit ripening (Upadhyay et al.; Khaksar and Sirikantaramas; Fresno and Munné-Bosch), the effect of exogenous application of signal molecules in post-harvest fruit quality (Yu et al.; Yao et al.; García-Pastor et al.), genetics studies of the fruit cell wall and texture modification-related enzymes (Wen et al.; Nakano et al.), antioxidant-related proteomic changes during ripening (Song et al.), and the effect of mutations of key transcription factors on fruit quality traits (Adaskaveg et al.) (**Figure 1**). These studies included various fruit species such as tomato, peach, sweet cherry, strawberry, pomegranate, and durian. Moreover, two important reviews on the role of alternative oxidase (Hewitt and Dhingra) and sugar signaling (Durán-Soria et al.) during ripening were included in this Research Topic (**Figure 1**).

Upadhyay et al. investigated the regulation of two small heat shock proteins (sHSP) by ethylene and the inhibitor of ethylene receptor 1-methylcyclopropene (1-MCP) during tomato fruit ripening (SlHSP17.7A and SlHSP17.7B). This study showed that a transgenic tomato line silenced in one of the ACC synthase genes (*SlACS2*), whose fruit produced 50% less ethylene, had higher expression of both *sHSP* genes at the transition stages [breaker (BR) and BR+3 days] compared to control fruit. Moreover, the expression of *SlHSP 17.7A* and *SlHSP 17.7B* were significantly down and upregulated, respectively, in the tomato ripening mutants *rin*/*rin*, *nor*/*nor*, and *Nr*/*Nr* compared to the wild-type. Authors concluded that ethylene, directly or in combination with the transcription

OPEN ACCESS

Edited and reviewed by:
Claudio Bonghi, University of Padua, Italy

****Correspondence:***
Carlos R. Figueroa
cfigueroa@utalca.cl

Specialty section:
This article was submitted to Crop and Product Physiology, a section of the journal Frontiers in Plant Science

Received: *18 May 2021*
Accepted: *02 June 2021*
Published: *26 July 2021*

Citation:
Figueroa CR, Jiang C-Z, Torres CA, Fortes AM and Alkan N (2021) Editorial: Regulation of Fruit Ripening and Senescence. Front. Plant Sci. 12:711458. doi: 10.3389/fpls.2021.711458

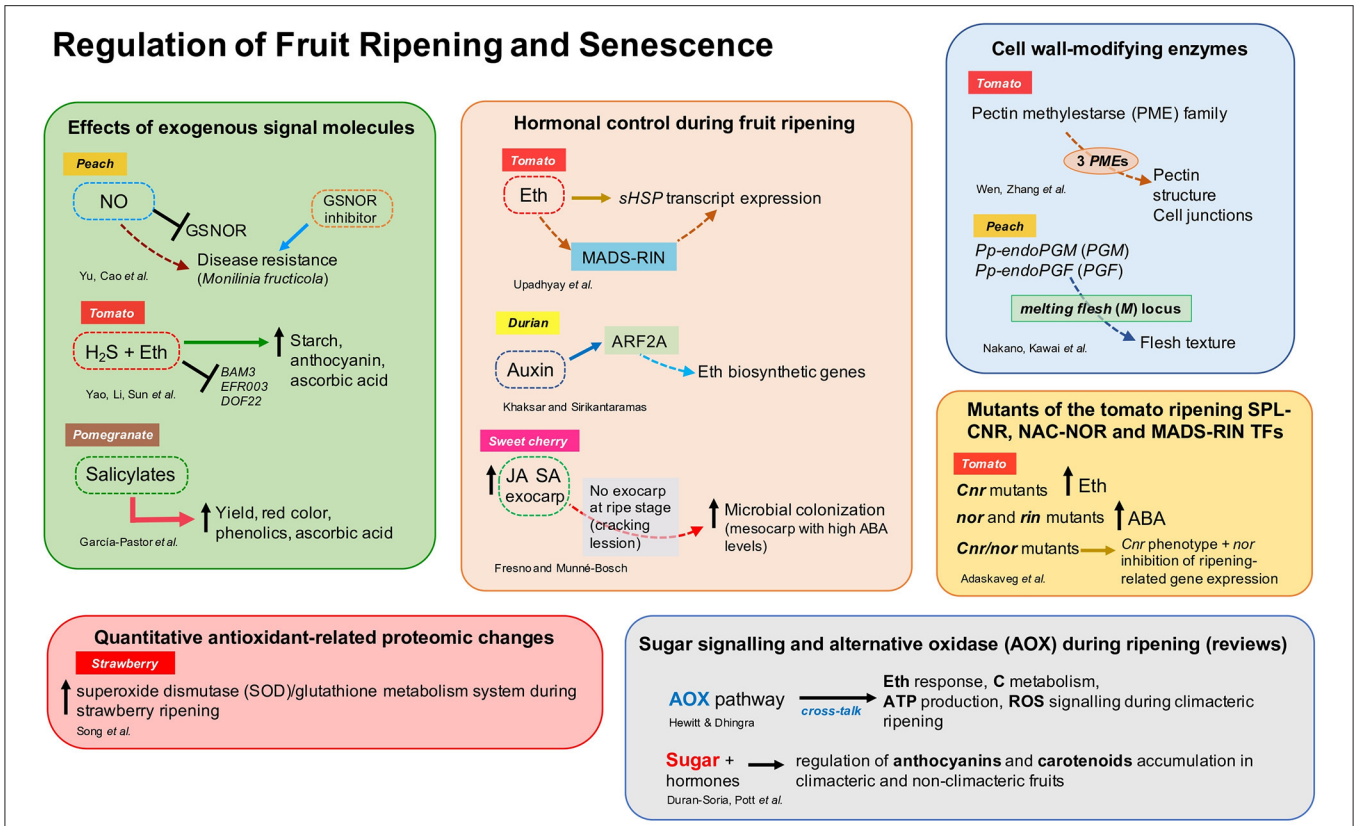

FIGURE 1 | Overview of the different aspects addressed by authors in the Research Topic "Regulation of Fruit Ripening and Senescence." ABA, abscisic acid; ARF, auxin response factor; Eth, ethylene; GSNOR, S-nitrosoglutathione reductase; H_2S, hydrogen sulfide; JA, jasmonic acid; NO, nitric oxide; SA, salicylic acid; sHSP, small heat-shock proteins; for other abbreviations, see the respective references.

factor *SlMADS-RIN,* regulates the *sHSP* transcript expression. Khaksar and Sirikantaramas showed that the auxin response factor (ARF), *DzARF2A*, transactivates ethylene biosynthetic genes. Also, *DzARF2A* expression was higher in fast-ripening durian cultivars and increased in response to auxin treatment. Therefore, DzARF2A was suggested to play an important role in auxin-ethylene crosstalk to regulate the fruit ripening process in durian. Fresno and Munné-Bosch analyzed three hormones (ABA, JA, and SA) that play a role in fruit development and fruit-microbe interactions on sweet cherry exocarp and mesocarp. The fruit's exocarp had significantly higher concentrations of JA and SA than the mesocarp, while ABA content was similar in both tissues. Authors also reported that endophytic microbial colonization was poor but increased with fruit development, while epiphytic fungi, such as *Alternaria* spp., increased in the mesocarp when the exocarp was cracked. Thus, the absence of concentrated levels of JA and SA and high ABA levels could probably stimulate microbial colonization of mesocarp tissues.

Yu et al. investigated the role of nitric oxide (NO)-induced resistance to *Monilinia fructicola* in peach. Exogenous NO enhanced disease resistance via inhibition of S-nitrosoglutathione reductase (GSNOR) expression and enzyme activity. Also, NO and GSNOR inhibitor (N6022) enhanced the expression of systemic-acquired resistance (SAR)-related genes contributing to disease resistance. In tomato, Yao et al. demonstrated that the addition of hydrogen sulfide (H_2S) to ethylene treatment maintained high chlorophyll, anthocyanin, and starch content during storage, attenuating the gene expression of the *beta*-amylase (*BAM3*) and ethylene-responsive transcription factors. H_2S affected pigments' metabolism and the transformation of macromolecular to small molecular metabolites. Altogether, H_2S delayed the ripening and senescence of tomato fruits during storage. García-Pastor et al. found that foliar spray application of salicylates (SA, ASA, or MeSA) produced a higher concentration of phenolics, anthocyanin, and ascorbic acid at harvest and during storage of pomegranate. Remarkably, salicylate treatments increased crop yield, and red color in pomegranate arils.

Cell wall-degrading enzymes play a key role in fruit ripening (Forlani et al., 2019). Wen et al. performed a genome-wide analysis of pectin methylesterase (PME) in tomato and identified 57 non-redundant PME genes. By analyzing gene expression, three new PME genes were suggested to play a role in fruit ripening, where PE1 and PE2 isoforms could be related to pectin structure at cell junctions and fruit softening. Nakano et al. studied post-harvest characteristics of two ultra-late maturing

peach cultivars and found that the cultivar "Daijumitsuto" (DJ) did not soften at all during 3 weeks of storage in response to endogenous and exogenous ethylene, compared to the normal melting flesh (MF) peach cultivar "Tobihaku" (TH). DNA-seq analysis demonstrated that the tandem endo-polygalacturonase (*endoPG*) genes *Pp-endoPGM* (*PGM*) and *Pp-endoPGF* (*PGF*) were deleted in the DJ cultivar, confirming that the *endoPG* genes at *melting flesh* (*M*) locus are responsible for controlling flesh texture in the ultra-late maturing cultivars. Furthermore, genomic analysis of the TH cultivar revealed that an unidentified *M* haplotype (M^0) is the common haplotype in MF peach accessions.

Song et al. analyzed the changes in the redox and antioxidant system in white, pink, and red stages of strawberry fruit development through proteomics analyses using LC-MS and multiple reaction monitoring (MRM) systems. Authors reported novel significant quantitative proteomic changes in antioxidant enzymes (46 proteins and isoforms) during ripening, suggesting that strawberry fruit ripening activates the antioxidant enzymes of a superoxide dismutase (SOD)/glutathione metabolism system.

Tomato ripening mutants SPL-CNR, NAC-NOR, and MADS-RIN were comprehensively characterized at physiological, molecular, and genetical levels during fruit development and ripening by Adaskaveg et al. Through gene expression analysis and direct measurement of hormones, authors found that *Cnr*, *nor*, and *rin* have alterations in the metabolism and signaling of plant hormones. Remarkably, *Cnr* mutants produce more than basal levels of ethylene, while *nor* and *rin* accumulate high concentrations of ABA. The homozygous *Cnr/nor* double mutant has a *Cnr* phenotype but displayed inhibition of ripening-related gene expression just like *nor* fruit. The fruit trait data generated in this study could be applied to improve the quality and inhibit ripening of tomato hybrids or at least identify tradeoffs between fruit traits.

Finally, two review articles are also included in this Research Topic. Hewitt and Dhingra reviewed the role of the alternative oxidase (AOX) respiratory pathway in mediating cross-talk between ethylene response, carbon metabolism, ATP production, and ROS signaling during climacteric ripening and provided perspectives in post-harvest ripening regulation by AOX. Durán-Soria et al. addressed the role of sugar and its associated molecular network with hormones in the regulation of the accumulation of health-promoting pigments such as anthocyanins and carotenoids both in climacteric and non-climacteric fruit.

Altogether, this Research Topic gathered new information and reviewed the scientific literature on the regulation of fruit ripening at the genetic, transcriptional, proteomic, hormonal, and metabolic levels and their impact on fruit quality. These data provided new insights that could be converted to future applications to improve fruit quality and reduce post-harvest fruit loss (Shipman et al., 2021).

AUTHOR CONTRIBUTIONS

CF wrote the first draft of the manuscript and performed the visualization. All authors contributed to conception of the Research Topic, manuscript revision, editing, and approved the submitted version.

FUNDING

CF was supported by the National Research and Development Agency (ANID, Chile) grant FONDECYT/Regular 1210941. C-ZJ's work was supported by United States Department of Agriculture (USDA) CRIS project 2032-21000-025-00D. CT was supported by the USDA National Institute of Food and Agriculture Hatch project 1014919, titled Crop Improvement and Sustainable Production Systems (WSU reference 00011). AF's research was supported by the FCT-funded project GrapInfectomics(PTDC/ASP-HOR/28485/2017).

REFERENCES

Alkan, N., and Fortes, A. M. (2015). Insights into molecular and metabolic events associated with fruit response to post-harvest fungal pathogens. *Front. Plant Sci.* 6:889. doi: 10.3389/fpls.2015.00889

Cherian, S., Figueroa, C. R., and Nair, H. (2014). 'Movers and shakers' in the regulation of fruit ripening: a cross-dissection of climacteric versus non-climacteric fruit. *J. Exp. Bot.* 65, 4705–4722. doi: 10.1093/jxb/eru280

Forlani, S., Masiero, S., and Mizzotti, C. (2019). Fruit ripening: the role of hormones, cell wall modifications, and their relationship with pathogens. *J. Exp. Bot.* 70, 2993–3006. doi: 10.1093/jxb/erz112

Fuentes, L., Figueroa, C. R., and Valdenegro, M. (2019). Recent advances in hormonal regulation and cross-talk during non-climacteric fruit development and ripening. *Horticulturae* 5:45. doi: 10.3390/horticulturae5020045

Shipman, E. N., Yu, J., Zhou, J., Albornoz, K., and Beckles, D. M. (2021). Can gene editing reduce postharvest waste and loss of fruit, vegetables, and ornamentals?. *Hortic. Res.* 8:1. doi: 10.1038/s41438-020-00428-4

Conflict of Interest: The authors declare that the research was conducted in the absence of any commercial or financial relationships that could be construed as a potential conflict of interest.

frontiers in Plant Science

ORIGINAL RESEARCH
published: 03 March 2020
doi: 10.3389/fpls.2020.00238

Characterization of the Tomato (*Solanum lycopersicum*) Pectin Methylesterases: Evolution, Activity of Isoforms and Expression During Fruit Ripening

Bo Wen†, Feng Zhang†, Xiaozhen Wu and Huan Li*

School of Horticulture, Anhui Agricultural University, Hefei, China

Pectin methylesterase (PME, EC 3.1.1.11) is a hydrolytic enzyme of pectin that plays multiple roles in different plant development processes and responses to biotic stress. To characterize the molecular evolution and functional divergence of the PME gene family, a genome-wide analysis of the PME gene family in the tomato was performed. In total, 57 non-redundant PME genes were identified, and these PME genes were divided into five groups based on their phylogeneny; their classification was supported by similar gene structures and domain distributions. The PME genes were found to be unevenly distributed among 12 chromosomes of the tomato. In addition, 11 segmental duplication and 11 tandem duplication events occurred in these PME genes, implying that both contributed to the expansion of the tomato PME gene family. Non-synonymous/synonymous mutation ratio analysis revealed that positive selection played a key role in the functional divergence of PME genes. Interspecific collinear analysis indicated a large divergence in the PME gene family after the divergence of monocot and dicot plants in ancient times. Gene expression pattern analysis suggested that PMEs plays roles in the different parts of the tomato plant, including the fruit. Three newly identified candidate genes (Solyc03g083360, Solyc07g071600, and Solyc12g098340) may have functions during fruit ripening. Immunoassays suggested that the tomato isoform PE1 and PE2 may change pectin structure at cell junctions, which could be associated with fruit softening. In addition, our analysis indicate that two undescribed PE isoforms might be active in leaves and fruits. This study increases our understanding of the PME gene family in the tomato and may facilitate further functional analyses to elucidate PME function, especially during fruit ripening.

Keywords: tomato, pectin methylesterase genes, cell wall, fruit softening, ethylene, functional divergence

OPEN ACCESS

Edited by:
Ana Margarida Fortes, University of Lisbon, Portugal

Reviewed by:
Vincenzo Lionetti, Sapienza University of Rome, Italy
Catherine Rayon, University of Picardie Jules Verne, France

****Correspondence:***
Bo Wen
hgm7901@163.com

†These authors have contributed equally to this work

Specialty section:
This article was submitted to Crop and Product Physiology, a section of the journal Frontiers in Plant Science

Received: *28 November 2019*
Accepted: *17 February 2020*
Published: *03 March 2020*

Citation:
Wen B, Zhang F, Wu X and Li H (2020) Characterization of the Tomato (Solanum lycopersicum) Pectin Methylesterases: Evolution, Activity of Isoforms and Expression During Fruit Ripening. Front. Plant Sci. 11:238. doi: 10.3389/fpls.2020.00238

INTRODUCTION

Pectin is one of the most abundant macromolecules within the plant cell wall in both the middle lamella and primary wall. Pectin is a highly complex group of polysaccharides that can be divided into four types of pectic polysaccharides: homogalacturonan (HGA), rhamnogalacturonan I (RG-I), rhamnogalacturonan II (RG II), and xylogalacturonan (XGA). HGAs are a major pectic form and homopolymer of (1–4) α-D-GalA, and they are synthesized in the Golgi apparatus and deposited

in the cell wall in a highly methylesterified form. During cell growth and development, some of these methyl groups can be removed by enzymes in the cell wall, such as pectin methylesterase (PME). PME (EC 3.1.1.11, CE8 of CAZy), also called pectinesterase, is widely present in plants and some microorganisms that possess a cell wall degradation function. PMEs can catalyze the de-esterification of methylesterified galacturonic acid residues of pectin, generating carboxyl groups and releasing free methanol in the cell wall. After de-esterification, the blocks of de-esterified HGA can be cross-linked by calcium to form a structure called "egg box," which may stiffen the cell wall (Micheli, 2001). Otherwise, the de-esterified HGA could be cleaved by other cell wall enzymes, such as polygalacturonase (PG), which could result in cell wall loosening (Seymour et al., 1987).

According to the presence or absence of the PME inhibitor (PMEI) domain, PMEs can be classified into either Type I (with both PME and PMEI domains) or Type II (with the PME domain only) (Jolie et al., 2010). In plants, PME exists as multigene families, and different PME genes exhibit different expression specificities (Jeong et al., 2018). Genomic sequencing programs have revealed that there are 66 PME genes in *Arabidopsis thaliana* (Louvet et al., 2006), 89 in *Populus* (Geisler-Lee et al., 2006; Pelloux et al., 2007), 43 in *Oryza sativa* (Jeong et al., 2015), and 105 in *Linum usitatissimum* (Pinzon-Latorre and Deyholos, 2013). Research has revealed that PME plays multiple roles in plants, including methanol accumulation (Jolie et al., 2010), abscission (Sexton and Roberts, 1982), plant defense (Bethke et al., 2014), pollen tube growth (Bosch and Hepler, 2005), cotton fiber elongation (Qin and Zhu, 2011), cell release from the root cap (Stephenson and Hawes, 1994), plant pathogenesis (Raiola et al., 2011; Lionetti et al., 2012; Giancaspro et al., 2018), increasing ascorbic acid content (Rigano et al., 2018), plant systemic infection by the tobacco mosaic virus (Dorokhov et al., 1999; Chen and Citovsky, 2003), heat and salt tolerance (Wu et al., 2017; Yan et al., 2018), microspore development (Yue et al., 2018), and maintenance of tomato fruit tissue integrity and texture during postharvest shelf life (Tieman and Handa, 1994; Phan et al., 2007; Wen et al., 2013).

In the tomato, three PME isoforms have been isolated, which are named PE1, PE2, and PE3 (Simons and Tucker, 1999). PE2 is a fruit-specific isoform and represents a dominant isoform accumulated during fruit ripening (Tieman et al., 1992; Hall et al., 1993). Tieman et al. (1992) generated a PE2 antisense line, in which fruit tomato integrity was lost during ripening. The *Pmeu1* gene has also been successfully downregulated by antisense technology, and the aforementioned transgenic plant showed the loss of the PE1 isoform, and fruit softened faster (Phan et al., 2007). In a previous study, we generated a double antisense line. In double antisense fruit, only 10% of normal PE activity was remained and ripening associated pectin de-esterification was almost completely blocked. However, PE1/PE2 line only mimicked the phenotype of Pmeu1 as, and further change in fruit firmness was not observed. Comparing to PE1 isoform, PE2 was found to play a major role in pectin de-esterification and act on during fruit ripening (Wen et al., 2013).

In this study, a genome-wide analysis of the PME gene family of the tomato was conducted using genomic sequencing tools including the phylogenetic tree as well as motif composition, gene structure and domains, chromosome distribution, and gene duplication events. Furthermore, expression patterns of PME genes in different vegetative tissues and during fruit ripening was investigated. Using a PE1/PE2 double antisense line, the isoforms in different tomato tissues and esterification pattern changes during fruit ripening were characterized. Our results provide valuable information on PME gene evolution and function that will support future research of this gene family in plants, predominantly their role in fruit ripening.

MATERIALS AND METHODS

Identification of PME Family Members in the Tomato Genome

The tomato protein sequence was downloaded from the phytozome (JGI[1]). To identify tomato PME candidates, hidden Markov model (HMM) analysis was used for the search. We downloaded an HMM profile of PMEs (Pfam01095) from the Pfam protein family database[2]. After removing all redundant sequences and short sequences, the output putative PME protein sequences were submitted to the Conserved Domain Database (CDD)[3], Pfam[4] (Pelloux et al., 2007), and Simple Modular Architecture Research Tool (SMART)[5] (Letunic et al., 2004) to confirm the conserved PME domains. The predicted protein sequences lacking the PME domain were excluded. Finally, a reliable list of PME family genes was obtained.

Multiple Alignment and Phylogenetic Analysis

The conserved domain sequences of PMEs derived from *A. thaliana* and tomato were used for phylogenetic analysis. Multiple sequence alignment was performed using ClustalX1.81 software with default parameters. Based on alignment, phylogenetic trees were constructed with the neighbor-joining (NJ) method using ClustalX1.81. Bootstrap analysis was performed using 1000 replicates. A phylogenetic tree including all tomato and Arabidopsis PME protein sequences was constructed from the ClustalW-aligned PME proteins using MEGA6.0 software (Tamura et al., 2013) with default parameters. Tomato PME genes were classified into different groups according to the topology of the phylogenetic tree and the classifications of PMEs in *A. thaliana*.

[1]https://phytozome.jgi.doe.gov/pz/portal.html

[2]http://pfam.xfam.org/

[3]https://www.ncbi.nlm.nih.gov/Structure/bwrpsb/bwrpsb.cgi

[4]http://pfam.xfam.org/search

[5]http://smart.embl-heidelberg.de/

Sequence Analysis, Gene Structure Analysis, and Identification of Conserved Motifs

Physical parameters of the predicted PME proteins, including the amino acid (aa) length, molecular weight (MW), and isoelectric point (pI), for each gene product was calculated using the online ExPASY tool[6] (Gasteiger et al., 2003). Exon and intron structures of individual PME genes were analyzed using Gene Structure Display Server 2.0 (GSDS[7]) through alignment of cDNAs with their corresponding genomic DNA sequences (Guo et al., 2007). The presence of signal peptide and transmembrane domains was predicted using SignalP 4.0 and TMHMM v.2.0, respectively. We used the online MEME tool (version 4.12.0[8]) to analyze the conserved motif structures of the proteins encoded by tomato PME genes (Bailey et al., 2009) with the following parameters: any number of repetitions, maximum of 10 misfits, and an optimum motif width of 6–50 aa residues. The exon–intron structures of tomato PME genes were identified using the GSDS[9] (Hu et al., 2015).

Chromosomal Localization and Gene Duplication

The chromosomal positions of tomato PME genes were acquired from the tomato (*Solanum lycopersicum*) using the JGI genome browser. MapChart software (version 2.32) (Voorrips, 2002) was used for the mapping of tomato PME genes' chromosomal positions and relative distances. Tomato PME gene duplication was confirmed based on two criteria: (a) the length of the shorter aligned sequence covered >70% of the longer sequence and (b) the similarity of the two aligned sequences was >70% (Gu et al., 2002; Yang et al., 2008). Two genes separated by five or fewer genes in a 100-kb chromosome fragment were considered as tandem duplicated genes (Wang L. et al., 2010). MCScanX software was used for collinearity, gene doubling, and tandem duplication analyses, and Circos was used for mapping.

Calculation of Non-synonymous to Synonymous Substitutions

Duplicated PME gene pairs in the tomato genome were aligned using ClustalW. Next, the non-synonymous substitution rate (Ka) and synonymous substitution rate (Ks) values were calculated using KaKs_Calculator 2.0 software (Wang D. et al., 2010). The calculated Ka/Ks ratios were then analyzed to explore the selection pressure on each duplicated gene pair. Generally, a Ka/Ks ratio greater than, equal to, or less than 1 indicates positive (diversifying) selection, neutral evolution, or negative (purifying) selection, respectively.

Plant Material and Ethylene Treatment

All tomato plants, *Lycopersicon esculentum* Mill cv. Ailsa Craig (S.A. Bowes, Glasshouse Crops Research Institute) wild-type along with the PE1, PE2, and double PE1as/2as antisense lines, were grown under glasshouse conditions with a cycle of 16 h light at 22°C and 8 h dark at 14°C. The plants reached maturity within 3–4 months. The fruit were tagged at anthesis (defined as the time of petal drop and fruit set) and harvested at different stages. The stages were defined as follows: immature green (IMG, 25 days after anthesis), mature green (MG, 40 days after anthesis), Breaker (B, fruit picked at first color change from green to yellow), and red ripe (B + X, fruit picked at X days after breaker). For the ethylene response experiment, 0.1% ethephon was applied to the stalk of the MG fruit. Leaves and fruit tissues were collected and frozen at −80°C until required.

RNA Extraction and Real-Time Quantitative PCR Analysis

To examine tomato PME gene expression, tomato leaf, and fruit samples were collected from the greenhouse. Total RNA was extracted from the collected samples using Trizol Reagent (Invitrogen). Then, DNase-treated RNA was reverse transcribed using reverse transcriptase (Takara No. 6110A). Primers (**Supplementary Table S1**) were designed for real-time quantitative PCR (q-PCR) using Primer Premier 5 software. PME genes were used as an internal reference, and the primers for these gene were synthesized by Sangon Biotech, Co., Ltd. (Shanghai, China). q-PCR was performed using a CFX96 instrument to examine the gene expression in cDNA samples from cross-pollinated varieties at different developmental stages. Each reaction was performed in triplicate. The relative expression levels of tomato PME genes were calculated using the $2^{-\Delta\Delta CT}$ method (Livak and Schmittgen, 2001). The reaction mixtures (Takara, No. RR820A) contained the following in a total volume of 20 μL: 10 μL SYBR Premix Ex Taq II (2×), 2 μL template cDNA, 1 μL forward and reverse primers, and 6 μL water. PCR amplification was conducted under the following conditions: 95°C for 1.5 min, followed by 40 cycles of 95°C for 1.5 min, 95°C for 15 s, and 60°C for 30 s. This experiment was carried out in four biological replicates for each measurement.

Extraction of Protein From Tomato Fruit

The tomato pericarp was homogenized in dH_2O, 1:2 (w/v). The homogenate was then transferred to a 50-mL Falcon tube and spun for 20 min at approximately 3000 rpm. A further spin was sometimes necessary when the supernatant was not clear of fruit debris. The supernatant was discarded, and care was taken not to lose any debris. The pellet was then resuspended in 20 mL extraction buffer (1 M NaCl, 0.05 M NaAc), adjusted to pH 6.0, and left at 4°C, with stirring for 3 h. A further spin at 3000 rpm for 20 min was performed after the extraction, and the supernatant was adjusted to 80% saturation with ammonium sulfate (0.57 g/mL). It was ensured that ammonium sulfate was completely dissolved before the samples were placed at 4°C overnight. The precipitate (white) was spun down at 15,000 rpm for 20 min and resuspended in 5 mL dialysis buffer (0.15 M NaCl, 0.05 M NaAc, pH 6.0). A dialysis membrane (Medicell International, London, United Kingdom) was prepared by boiling the tubes in dH_2O for 5 min. The samples were then

[6]http://web.expasy.org/compute_pi/

[7]http://gsds.cbi.pku.edu.cn/

[8]http://alternate.meme-suite.org/tools/meme

[9]http://gsds.cbi.pku.edu.cn/

loaded into the tubing and immersed in additional dialysis buffer and left overnight. After this overnight dialysis, the samples were ready to load into a column.

Extraction of Protein From Tomato Leaf and Stem by Preparation of Acetone-Insoluble Solids

Tomato leaf and stem was homogenized in four volumes of acetone at −20°C, filtered through Miracloth (Calicoes, CA, United States), and washed with 10 volumes of 80% acetone at 4°C. An additional wash with 10 volumes of 100% acetone at 4°C was performed before drying the acetone-insoluble solids (AIS) in a vacuum overnight. The dried AIS were then resuspended in 20 mL extraction buffer (1 M NaCl, 0.05 M NaAc), rehomogenized (AIS were rather clumpy at this stage), adjusted to pH 6.0, and left at 4°C for 3 h, with stirring. An additional spin at 3000 rpm for 20 min was performed after the extraction, and the supernatant was adjusted to 80% saturation with ammonium sulfate (0.57 g/mL). It was ensured that the ammonium sulfate was completely dissolved before the samples were placed at 4°C overnight. The precipitate (white) was spun down at 15,000 rpm for 20 min and resuspended in 5 mL dialysis buffer (0.15 M NaCl, 0.05 M NaAc, pH 6.0). The dialysis membrane was prepared by boiling in dH_2O for 5 min. The samples were then loaded into the tubing and immersed in additional dialysis buffer and left overnight. After this overnight dialysis, the samples were loaded into a column.

Isoform Analysis

PE isoform separation was conducted through Bio-Rad heparin affinity chromatography. In heparin column, proteins can be specifically and reversibly adsorbed by heparins immobilized on an insoluble support. Different proteins have different affinity with heparin. The binding ability of a particular protein depends on its buffer composition, pH, flow rate, and temperature. Dissociation was carried out by increasing the ionic strength in the buffer with a continuous NaCl gradient. Then, a PE assay was carried out to profile different PE isoforms base on the PE activity and salt dependency.

The Bio-Rad system consisted of an Econo system controller model ES-1, Econo pump model EP-1, Econo UV monitor model EM-1, Econo buffer selector model EV-1, six-port sample injection valve model MV-6, diverter valve model SV-3, and fraction collector model 2128. The column, with a 5-mL bed volume, was equilibrated with buffer A (10 mM Tris–HCl, 10 mM NaCl, pH 7.5). The samples were applied in buffer A and isoforms eluted at a flow rate of 1 mL/min using a linear gradient of NaCl from 10 mM (buffer A) to 300 mM (10 mM Tris–HCl, 300 mM NaCl, pH 7.5). Fractions (75 × 2 mL) were collected and assayed for PE activity using the microtiter plate method. Then, 20 μL of each fraction was placed into wells in a 96-well microtiter plate. A total of 200 μL assay buffer with salt (0.5% citrus pectin, 2 mM Tris–HCl, 150 mM NaCl, 0.002% phenol red, pH 8.0) or without salt (0.5% citrus pectin, 2 mM Tris–HCl, 0.002% phenol red, pH 8.0) was added into each well. The plate was read on a Dynatech MR 5000 microtiter plate reader at 405 nm every 20 min for up to 5 h with 2-s shaking before each reading. Three independent assays have been done to confirm these results.

Immunodot Assay

This assay was conducted based on the method of Willats and Knox (Willats and Knox, 1999). The nitrocellulose membrane was loaded with pectin incubated in 3% (w/v) phosphate-buffered saline (MP/PBS) for 1 h to block all binding sites and was then washed with tap water. The blocked sheet was incubated with monoclonal antibody JIM5 (diluted 20-fold using MP/PBS) for 1.5 h and then rinsed extensively with tap water. The sheet was incubated in secondary antibody [anti-rat IgG-horseradish peroxidase (HRP), Pharmacia], which had been diluted 5000-fold with MP/PBS for 1.5 h and washed with tap water. Finally, antibody binding was determined using the EC-ECL chemiluminescence detection kit for HRP (Geneflow Ltd.). Three independent assays have been done to confirm the results.

Immunolocalization

The tomato pericarp was embedded into Steedman's wax and cut to a thickness of 12 μm using a microtome (HM355 Microm) and collected on polylysine-coated slides. The slides were incubated in 97% (v/v) ethanol for 10 min three times and then rehydrated in 90% (v/v) ethanol for 10 min and in 50% (v/v) ethanol for another 10 min at room temperature (RT). Finally, the slides were washed in dH_2O for 10 min. The water was changed, and the slides were washed for another 90 min.

Non-specific binding sites were blocked by incubation with 3% (w/v) milk protein in MP/PBS for at least 30 min. The slides were incubated with rat monoclonal antibody JIM5 that had been diluted fivefold in MP/PBS for at least 1 h at RT or overnight at 4°C and then washed three times with 1 × PBS with at least 5 min for each wash. The slides were incubated with a 100-fold MP/PBS-diluted secondary antibody [anti-rat-IgG (whole molecule) linked to FITC (Sigma)] for 1 h at RT. The slides were washed three times with PBS with at least 5 min for each wash. The slides were mounted using an antifade reagent Citifluor AF1 (Agar Scientific, Stansted, United Kingdom). Finally, these slides were examined and imaged using a fluorescence microscope (Leica Microsystems). Three biological repeats have been done to confirm this result.

RESULTS

Identification and Analysis of PME Family Genes in Tomato

To identify PME genes in the tomato (*S. lycopersicum*), HMM analysis and BLASTP were performed against the whole genome sequence. After removing repetitive sequences, all identified sequences were reserved and submitted to CDD, Pfam, and SMART to confirm the PME domains. Finally, 57 non-redundant PME proteins were obtained; this number is similar to the number of PME genes identified in *A. thaliana* (66; Arabidopsis Genome Initiative, 2000; Scheler et al., 2015). The 57 identified tomato PME gene family members encode predicted proteins

ranging from 267 to 653 aa residues in length, with an average length of 483 aa, and computed molecular masses of 12.1–69.7 kDa, with an average of 47.2 kDa, respectively. In addition, all predicted PME proteins have pIs between 5.12 and 9.56. According to previous research, PMEs are encoded by a large multigene family that can be classified into two classes: Type I and Type II. All PMEs have a conserved pectin esterase domain (Pfam01095), but only Type I has a PME-inhibitory domain (Pfam04043) (Micheli, 2001). In tomato, 36 PMEs have been identified as Type I and 21 PMEs as Type II. Previous studies have found that the glycosylation of a PME protein affects its enzymatic activity and thermostability. Glycosylation site prediction showed that most PME proteins in the tomato have glycosylation sites ranging from 1 to 12 in number, except for Solyc04g080530 and Solyc07g065350. More details about these PMEs are listed in **Supplementary Table S2**.

Multiple Sequence Alignment and Phylogenetic Analysis of Tomato PME Genes

Through the multiple sequence alignment using DNAMAN (version 6), five highly conserved characteristic sequence segments were identified: Region I, _GxYxE; Region II, _QAVAL; Region III, _QDTL; Region IV, _DFIFG; and Region V, _LGRPW. Furthermore, three CE-8 catalytic residues with D (aspartate) in Region IV and R (arginine) and W (tryptophan) in Region V were found to be conserved in these segments. The putative PMEs which do not contain these catalytic residues have been removed (**Supplementary Figure S1**).

Molecular phylogenetic analysis was conducted using the NJ method, and a phylogenetic tree was constructed using the domain sequences of the 57 tomato PMEs and 66 previously annotated *Arabidopsis* PMEs. The evolutionary history was inferred using the NJ method based on the JTT matrix-based model (Jones et al., 1992). All positions with less than 90% site coverage were eliminated. Evolutionary analyses were conducted in MEGA7 (Kumar et al., 2016). The phylogenetic analysis indicated that the tomato PME could be divided into five groups (**Supplementary Figure S2**). Among these proteins, proteins encoded by 36 tomato PME genes belonged to Type I, and proteins encoded by 21 tomato PME genes belonged to Type II.

Gene Structure and Motif Composition of Tomato PME

Evolutionary research suggests that gene structure diversity is the major force driving the evolution of gene families. To further understand the structural diversity of tomato PME genes, we analyzed the exon–intron organization of the 57 PME genes (**Figure 1**). The analysis revealed that PME genes in the same group usually had similar gene structures. Among tomato PME genes 2, 18, 12, 12, 12, and 1 of these genes contained one, two, three, four, five, and six exons, respectively (**Figure 1A** and **Supplementary Table S3**). Most PMEI domain located in exon 1 and most PME domain from group 1 to group 4 located in exon 1–4. Exon–intron structures of paralogous PME gene pairs were further analyzed. Among these paralogous pairs, the exon number of seven gene pairs exhibited exon–intron variations. Comparing the seven gene pairs, Solyc01g066360/Solyc05g054360, Solyc01g066360/Solyc12g099410, Solyc09g075330/Solyc01g099950, Solyc06g051960/Solyc03g083360, and Solyc01g109740/Solyc04g080530 gained or lost one exon, whereas Solyc06g009180/Solyc09g075330 and Solyc02g080200/Solyc07g064170 gained or lost two exons during the long evolutionary period (**Figure 1A** and **Supplementary Table S3**). These results implied that both exon gain and loss occurred during the evolution of tomato PME genes, which may help explain the functional diversity of closely related PME genes.

Ten motifs with lengths from 6 to 50 aa residues were identified in the 57 tomato PME proteins using the MEME website (**Supplementary Figure S3**). Based on motif analysis, a schematic diagram representing the structure of all tomato PME proteins was constructed (**Figure 1B**). Most PME members in the same group had similar motif distributions. Motif 6 was found to be present in all 57 tomato PME proteins, and Motifs 1, 2, 3, 4, 5, 7, and 8 were also highly conserved in tomato PME genes (**Figure 1B** and **Supplementary Table S4**). Motifs 1, 2, 3, 4, 6, and 7 were identified to encode the PME domain, and Motif 9 and 10 were found to encode the PMEI domain, whereas the remaining motifs did not have functional annotations. Overall, the conservative motif composition and similar gene structure of PME members in the same group strongly support the reliability of the phylogenetic classification.

Chromosomal Location and Gene Duplication Analysis

To investigate PME gene chromosomal distribution in the tomato, a chromosome map was drawn according to genome annotation (**Figure 2**). A total of 57 PME genes were distributed in 12 tomato chromosomes. Chromosome 1 had the largest number of predicted PME genes (9), followed by Chromosomes 2 and 7 (8), and the lowest number of PMEs was found on Chromosomes 4 and 8 (1). In addition, the majority of tomato PME genes were found to be located on the proximate or the distal ends of multiple chromosomes, such as Chromosomes 1, 2, 5, and 7.

Gene duplication events provide raw material for the generation of new genes, which in turn may facilitate the generation of new functions. Therefore, duplication events of tomato PME genes were analyzed in this study (Cannon et al., 2004). As shown in **Figure 2** and **Supplementary Table S5**, 11 pairs of tomato PME genes (20 PME genes) were confirmed to be tandem duplicated genes. However, no tandem duplication events were identified in Chromosome 4, 8, 9, 11, and 12. In addition, 11 segmental duplication events for 18 PME genes were identified using the BLASTP and MCScanX methods (**Figure 3** and **Supplementary Table S5**). These results indicated that both tandem duplication and segmental duplication contributed to the expansion of the tomato PME gene family. It is also interesting to see that more Type I PMEs in both segmental and tandem duplication events, which could explain the expansion of Type I PMEs in tomato genome (**Supplementary Table S5**). To explore the selection pressures acting on this gene family, we calculated

FIGURE 1 | Phylogenetic relationships, conserved motif analysis, and gene structure in PME genes from tomato. **(A)** Exon–intron structure of tomato PME genes. **(B)** The conserved motif distribution of tomato PME proteins.

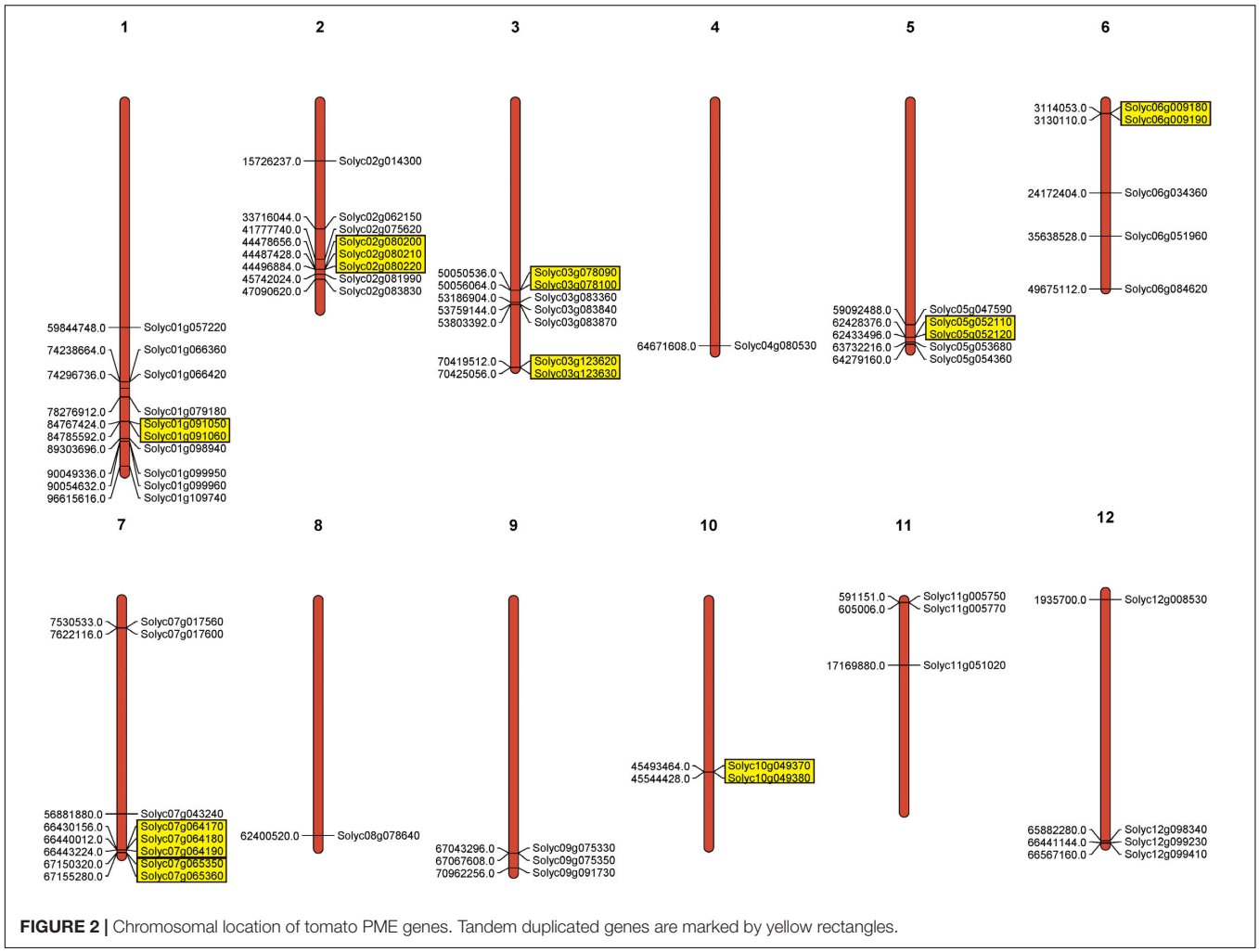

FIGURE 2 | Chromosomal location of tomato PME genes. Tandem duplicated genes are marked by yellow rectangles.

the Ka, Ks, and Ka/Ks ratios of 22 PME gene pairs. As shown in **Supplementary Table S5**, the Ka/Ks values from the five pairs of tomato PME genes (Solyc02g080210/Solyc02g080220, Solyc03g078090/Solyc03g078100, Solyc03g123620/Solyc03g123630, Solyc07g064170/Solyc07g064180, and Solyc10g049370/Solyc10g049380) were greater than 1. These results suggest these tomato PME genes experienced strong positive selective pressure during evolution, which may have caused functional divergence. The divergence time suggest most of the duplication events occurred 30–50 million years ago (**Supplementary Table S5**).

Microsynteny Analysis of Tomato PME Genes

To further identify orthologous genes and infer the evolution history of the tomato PME gene family, we constructed three comparative syntenic maps of tomato associated with three representative species, two dicots (Arabidopsis and peach) and one monocot (rice) (**Figure 4**). A total of 21 orthologous PME gene pairs were identified between tomato and peach, followed by 19 in Arabidopsis and 5 in rice (**Supplementary Table S6**). The total numbers of collinearity region between tomato and the three species, namely Arabidopsis, peach, and rice, were 420, 322, and 151, respectively. We found some orthologous gene pairs between tomato and Arabidopsis/peach that were not found between tomato and rice, such as Solyc01g091060/AT3G60730/Prupe.2G141200, Solyc01g099960/AT3G05620/Prupe.6G318500, Solyc01g109740/AT2G21610/Prupe.1G377100, etc. (**Supplementary Table S6**), indicating these orthologous pairs appeared after the divergence of dicotyledonous and monocotyledonous plants. Additionally, three tomato PME genes (Solyc02g080210, Solyc08g078640, and Solyc09g075330) were identified to have orthologous genes with all other three species, indicating that these orthologous pairs may have already existed before ancestral divergence (**Supplementary Table S6**). In addition, two or more PME genes from Arabidopsis matched one tomato PME gene, such as AT1G53840 and AT3G14300 orthologous to Solyc03g123620; AT1G53830 and AT3G14310 orthologous to Solyc03g123630; and AT1G02810, AT2G47550, and AT4G02330 orthologous to Solyc09g075330, implying that these genes were paralogous gene pairs. The majority of orthologous PME gene pairs had Ka/Ks values less than 1, suggesting that the PME gene family might have experienced mainly purifying selective pressure during

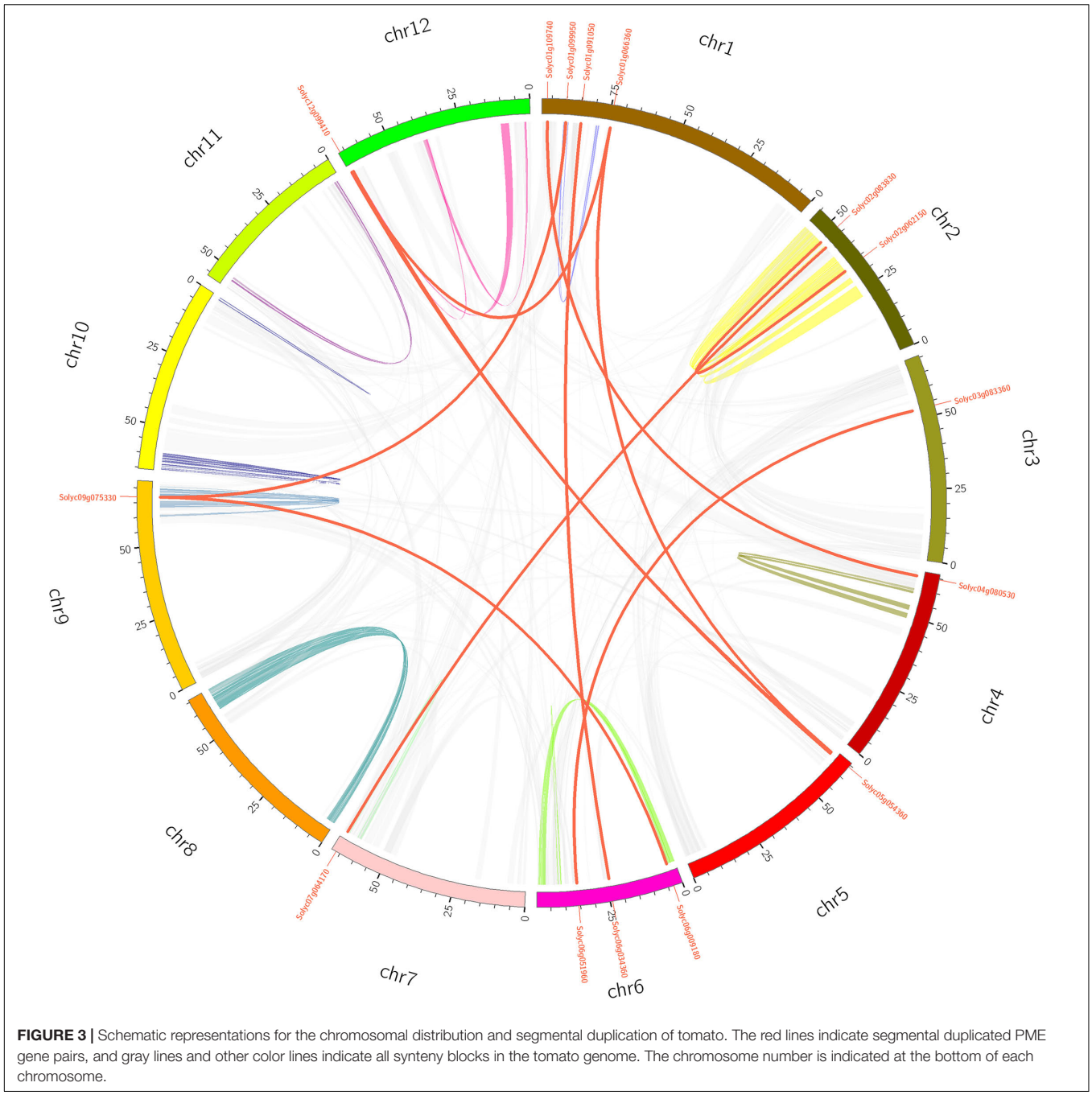

FIGURE 3 | Schematic representations for the chromosomal distribution and segmental duplication of tomato. The red lines indicate segmental duplicated PME gene pairs, and gray lines and other color lines indicate all synteny blocks in the tomato genome. The chromosome number is indicated at the bottom of each chromosome.

evolution. However, positive selection also contributed to the evolution of PME genes (**Supplementary Table S6**).

Identification of PME Genes Exhibiting Ripening-Associated Patterns of Expression

Previous studies have suggested that PME genes play a wide range of roles during plant development, especially during fruit ripening. To gain more insights into PME gene functions, we used transcriptome data (Tomato Genome, 2012) to investigate the expression of tomato PME genes. As shown in **Figure 5A**, the 57 PME genes showed different expression patterns in the flower, bud, leaf, and root. Among the 57 genes, 8 PMEs in Cluster 5 showed ubiquitous expression in all vegetative tissues. In addition, ten PME genes in Cluster 1 and three PMEs (solyc02g081990, solyc02g014300, and solyc09g075330) in Cluster 3 showed the highest transcript accumulation in both the bud and flower and in the root, respectively. Among the 57 PME genes, 27 genes (RPKM > 1) were found to be expressed during fruit development (**Figure 5B**). Nine of the genes in Cluster 3 (solyc03g078100, solyc03g123620, solyc11g005770,

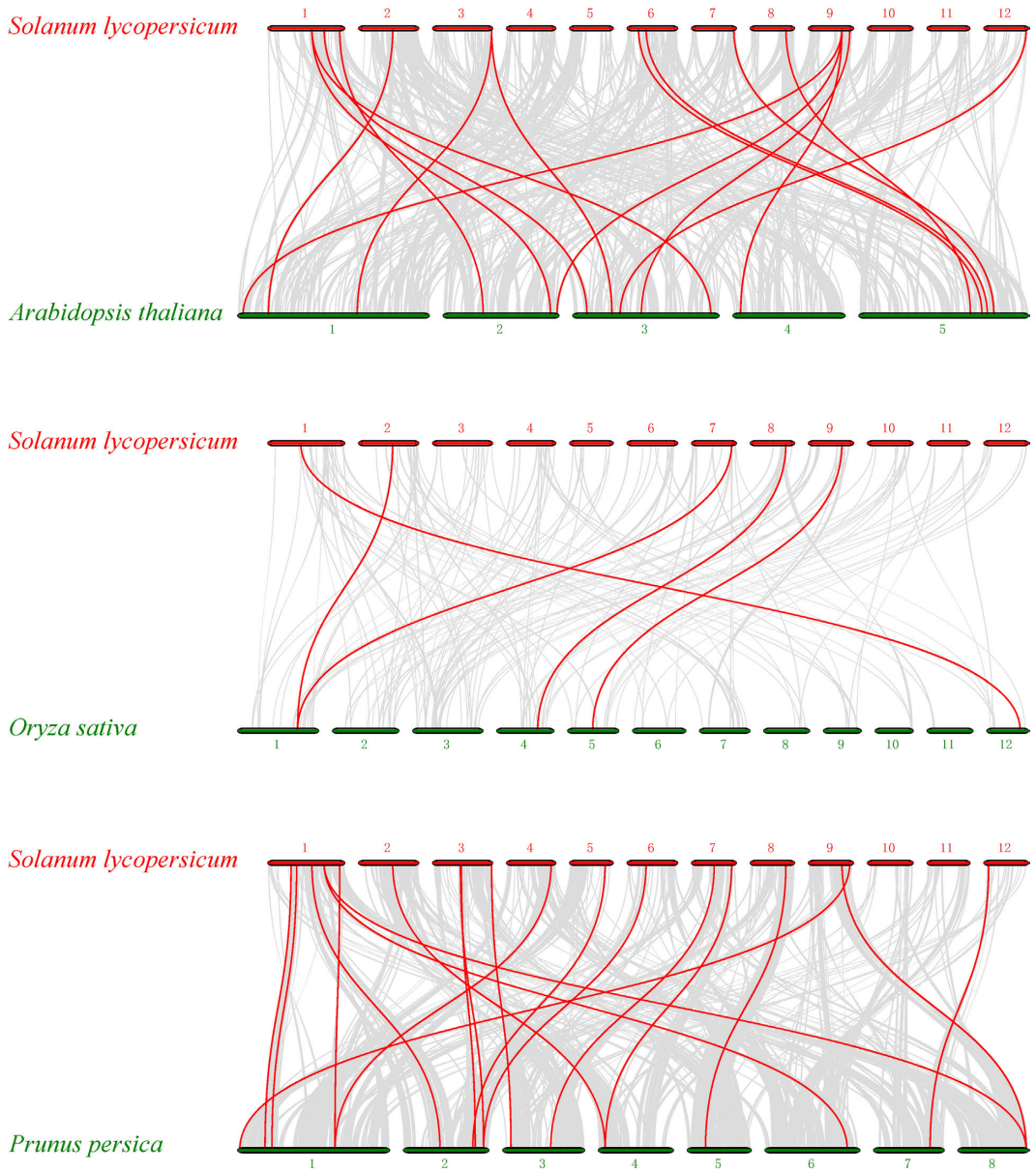

FIGURE 4 | Synteny analysis of PME genes between *Solanum lycopersicum* and three representative plant species. Gray lines in the background indicate the collinear blocks within tomato and other plant genomes, whereas the red lines highlight the syntenic PME gene pairs.

solyc03g083360, solyc07g017600, solyc06g051960, solyc12g008530, solyc06g009190, and solyc03g123630\Pmeu1) showed the highest transcript accumulation during fruit development, three in Cluster 4 (solyc07g064170\PME1.9, solyc07g064180\PME2.1, and solyc07g064190\PME3) during fruit ripening, and one (solyc12g098340) during both fruit developmental and ripening stages. Additionally, some of duplicated gene pairs showed different expression patterns. For example, Solyc02g080200 was highly accumulated in the bud and flower, whereas its duplication gene, Solyc07g064170, was expressed at a high level during fruit ripening, suggesting subfunctionalization after a duplication event.

To further confirm whether the expression of PME genes was influenced by ethylene, nine PME members highly expressed (RPKM > 25) in the ripening stage were selected (Solyc03g123630\Pmeu1, Solyc03g083360, Solyc03g123620, Solyc07g017600, Solyc07g064190/PME2, Solyc12g098340, and Solyc06g009190). Because the three segmental duplication genes of Solyc07g064170, Solyc07g64180, and Solyc07g64190 have very similar sequences that cannot be distinguished through qRT-PCR amplification, Solyc07g64190 is presented as a representative gene in **Figure 6**. It can be noticed that eight out of these nine selected genes belong to Type I PME, except Solyc12g098340 (**Supplementary Table S7**). Among the nine selected genes,

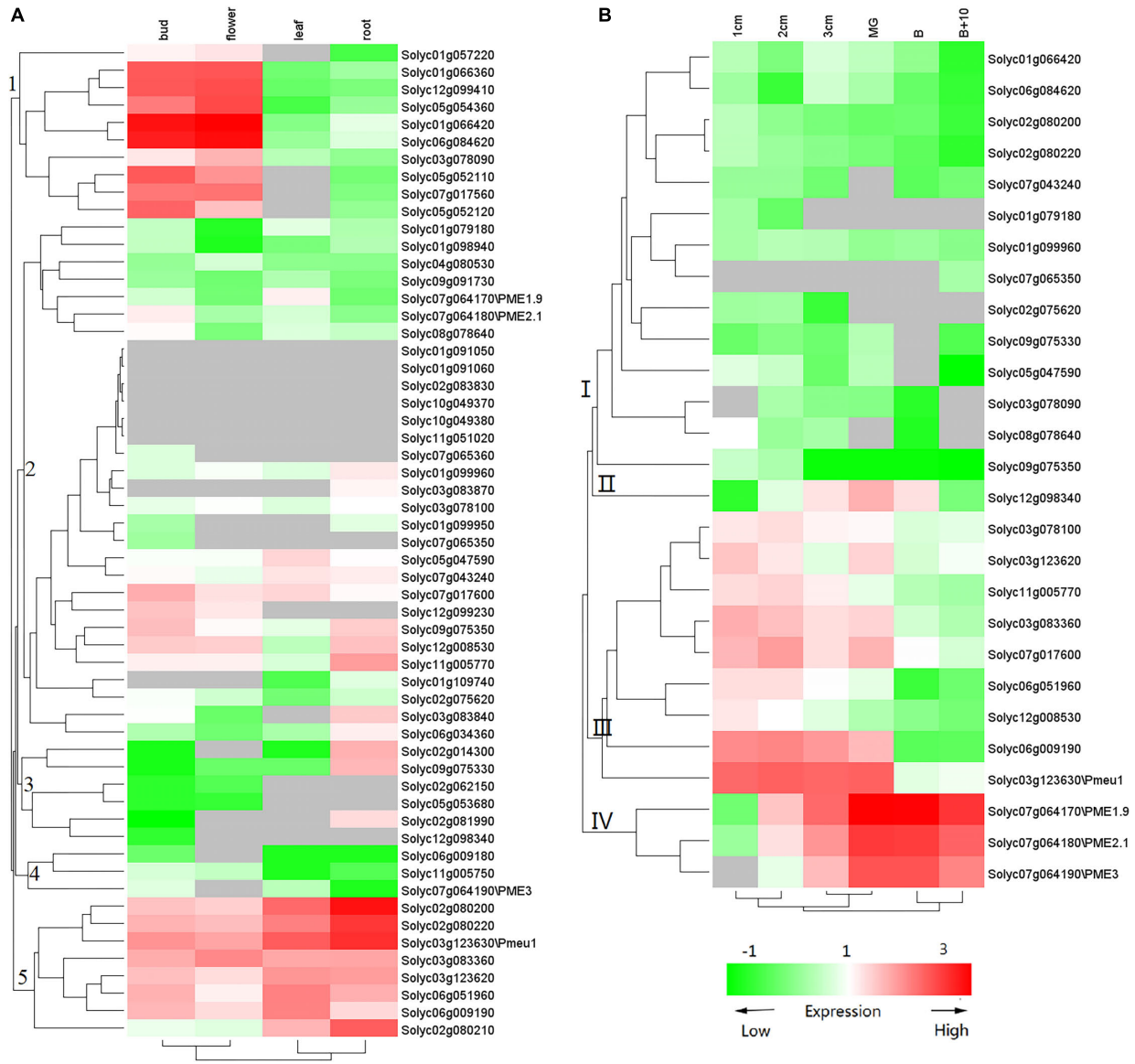

FIGURE 5 | Expression profile of tomato PME genes. **(A)** PME gene expression in vegetative tissues and **(B)** PME gene expression during fruit development. The color of the cell represents transcript abundance: gray cells indicate no transcripts were detected, green-colored boxes denote low levels of expression, and red-colored boxes denote high levels of expression. This experiment was carried out in three biological replicates for each measurement.

the expression of five PME genes (Solyc03g123630\Pmeu1, Solyc03g083360, Solyc07g017600, Solyc07g064190/PME2, and Solyc12g098340) were found to be induced by ethylene. Notably, as a paralogous gene pair, Solyc03g123630\Pmeu1 responded to ethylene, but Solyc03g123620 did not, suggesting its functional diversity after a duplication event.

PE Isoforms in Tomato Fruits, Stems, and Leaves

Total protein was extracted from the MG fruit, stem, and leaf of both wild-type and PE1/PE2 antisense plants and were then profiled by heparin column chromatography. The PE assay was conducted with and without salt (NaCl). In **Figure 7A**, the PE isoform profile obtained from wild-type MG fruit tissue shows three independent isoforms eluting between fractions of 31 to 43, 46 to 61, and 62 to 74, respectively. According to the nomenclature of Tucker and Grierson (1982), these correspond to PE2, PE3, and PE1, respectively. Both PE2 and PE3 activity was salt-independent, whereas PE1 was a salt-dependent isoform (**Supplementary Table S7**). In the fruit of double antisense plants (**Figure 7B**), the peak corresponding to PE2 was almost completely eliminated, PE3 was unaffected, and PE1 was suppressed to a minor peak. Notably, in the corresponding profile without salt, the PE activity of this minor peak was not reduced as it was in the corresponding peak in the wild-type fruit. As

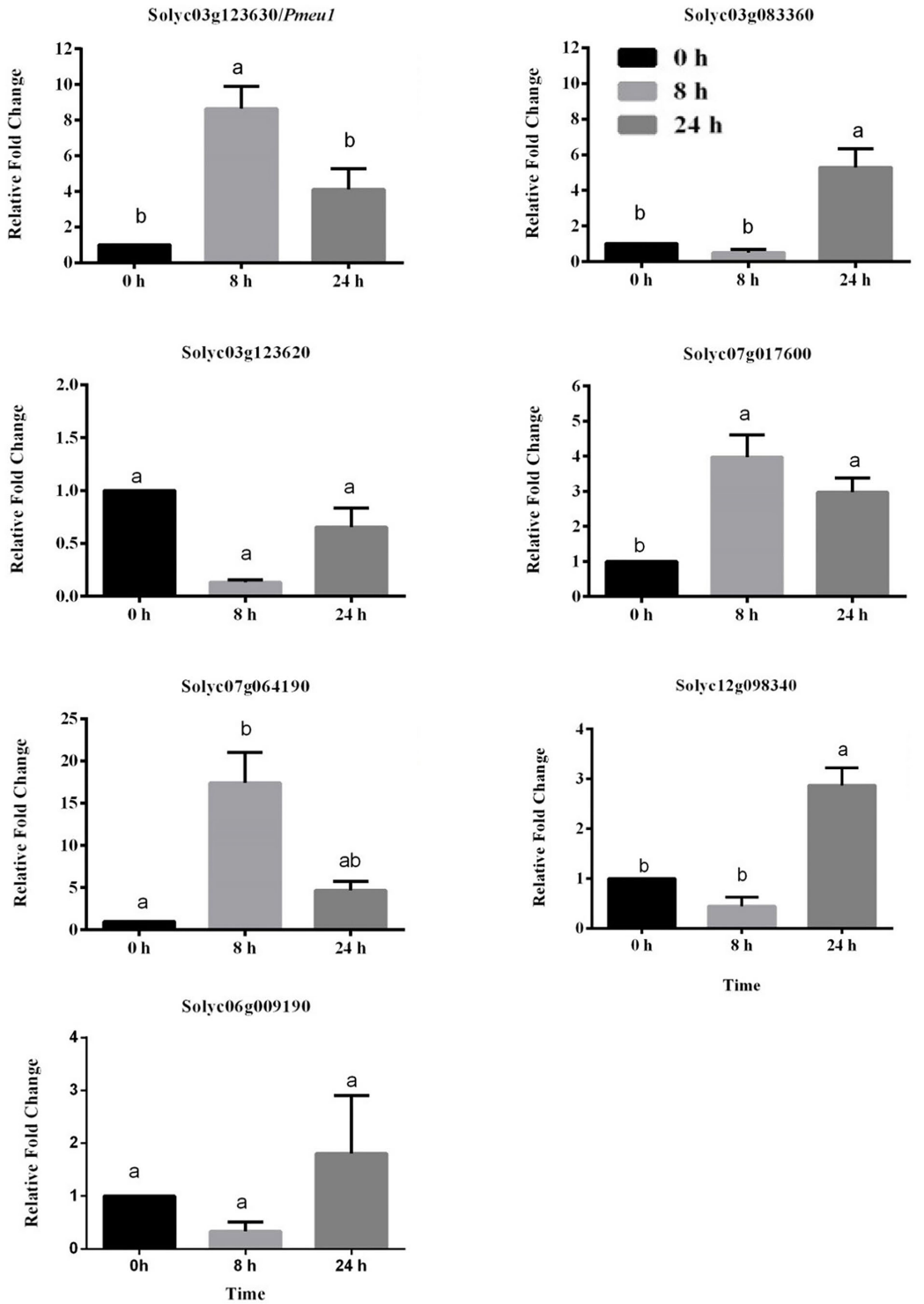

FIGURE 6 | Expression profiles of seven selected tomato PME genes in response to ethylene treatment. Data are the means ± standard error (n = 4). Significant differences ($p < 0.05$) between means are indicated by different small letters.

this activity might result from salt independent PE1 activity or from the activity from an unknown PE, we speculatively annotate this as PE4 (**Figure 7B**). **Figure 7C** shows that the PE activity in the wild-type stem can be resolved into two peaks. According to the elution time and salt dependency, the smaller peak eluted between fraction 41 and 56 was recognized as PE3 and the larger

one eluted from fraction 62 to 76 was identified as PE1. In the double antisense stem (**Figure 7D**), PE3 was unaffected, and the major isoform PE1 was considerably suppressed to reveal a salt-independent peak PE4. As shown in **Figure 7E**, PE activity from the wild-type leaf could be resolved into one small peak representing isoform PE3 and a very large peak from fraction 55 to 76, which contains a shoulder on the left-hand side. Within the larger peak, two independent peaks were observed, indicating different salt dependencies. In the PE1/PE2 double antisense leaf, the isoform peak near fraction 69 was suppressed to smaller residual activity (**Figure 7F**). Combined with the elution time and salt dependency, this peak could be recognized as PE1. The shoulder peak around fractions 59 was salt-dependent and unaffected by the silencing of PE1 and PE2. As this indicates an undescribed isoform, we speculatively annotate this as PE5. Similar to the findings in both the fruit and stem, the small residual peak at fraction 69 was not influenced by salt, which may represent the activity of PE4.

Immunodot Blot and Immunolocalization by Monoclonal Antibody JIM5

To detect the variation of pectin esterification, the monoclonal antibody JIM5 was used to probe the specific epitope in cell wall extracts. As shown in **Figure 8A**, the epitopes of JIM5 were reduced in the PE1/PE2 fruit compared with the wild-type fruit in both Breaker and B + 5 stages, which suggests that PE1 and PE2 may change the HGA esterification pattern in the cell wall during tomato fruit ripening. To determine the HGA structure change in the cell wall, the tomato pericarp from the Breaker fruit of wild-type and PE1/PE2 antisense plants was embedded in Steedman's wax, and the embedded tissue was then sectioned and immunolocalized with the antibody JIM5. As shown in **Figure 8A**, JIM5 epitopes were found to be distributed across the entire wall of the wild-type fruit (**Figures 8B-1,2**). It seemed that, in some regions, the epitope was more prevalent and thus appeared as brighter spots. However, in the fruit of double antisense plants, JIM5 epitopes were mostly concentrated in the corners of intercellular spaces, and a very low signal was detected in other regions of the cell wall (**Figures 8B-3,4**). Compared with the wild-type fruit, epitope binding appeared to be much stronger and uniform in the cell corners of the fruit of PE1/PE2 antisense plants.

DISCUSSION

Pectin methylesterases are widely present in the plant kingdom and play multiple roles in plant development. In this study, 57 non-redundant PME genes from the tomato genome were identified. The number of PME genes in the tomato were higher than that in the monocot *O. sativa* (43) (Jeong et al., 2015) but lower than that in the dicots *Arabidopsis* (66) (Louvet et al., 2006), *Populus* (89) (Geisler-Lee et al., 2006; Pelloux et al., 2007), and *L. usitatissimum* (105) (Pinzon-Latorre and Deyholos, 2013). Sequence comparison revealed that most PMEs contained five highly conserved signature sequences, in which one Asp, one Arg, and one Trp were found to be conserved and crucial for PME function, as suggested by previous studies (Markovic and Janecek, 2004; Pelloux et al., 2007). Phylogenetic analysis indicated that these PME genes could be divided into five groups; the classification is supported by the similar motif composition and gene structure in each group (**Figure 1**), and this finding is also consistent that for Arabidopsis in the study by Louvet et al. (2006).

Many studies have shown that structural diversification of genes plays a key role in the evolution of multigene families and in functional differentiation (Han et al., 2016). In the present study, we found that 57 PME genes contained different numbers of exons and introns, and that exon gain and loss were found in seven closely related paralogous gene pairs, which may explain why PMEs play a wide range of roles during plant development. Motif 9 and motif 10 was identified as the PMEI domain, and it was demonstrated to have a role in preventing the early demethylesterification of pectins in the Golgi apparatus (Bosch and Hepler, 2005). In the tomato phylogenetic tree, the PMEI domain was majorly restricted to Groups 1, 2, 3, and 5 PME genes, implying some specific roles in plant development (**Figure 1**).

In the tomato genome, 57 PME genes were unevenly located across 12 chromosomes. Gene duplication plays a critical role in the expansion of gene families (James et al., 2003; Cannon et al., 2004). It was previously found that both tandem duplication and segmental duplication were the key factors influencing the expansion of gene families (Cao et al., 2016). In this study, a total of 22 duplication events were identified for tomato PME genes. Among of them, 11 gene pairs (18 PME) involved segmental duplication, and 11 gene pairs (20 PME) involved tandem duplication. This result suggests that both segmental and tandem duplication contributed to the expansion of the tomato PME gene family.

Interspecific collinear analysis showed that the numbers of orthologous genes between tomato and peach (21) and between tomato and Arabidopsis (19) were greater than that between tomato and rice (5). This result indicated that a large divergence of the PME gene family after the divergence between monocot and dicot plants in ancient times. In theory, Ka/Ks < 1 indicates purifying or negative selection, Ka/Ks $= 1$ indicates neutral selection, and Ka/Ks > 1 indicates positive selection (Hurst, 2002). In this study, some paralogous and orthologous gene pairs presented Ka/Ks ratios >1, indicating that the PME gene family underwent strong positive selection pressure and tended to acquire new functions in evolution.

In this study, the expression patterns of the 57 PME genes were investigated using transcriptome data. Among them, seven genes (Solyc05g052110, Solyc07g017560, Solyc05g052120, Solyc01g066360, Solyc12g099410, Solyc01g99940, and Solyc05g054360) showed flower- and bud-specific expression, indicating key roles during flower initiation. In Arabidopsis, pollen tube growth was interrupted after one PME gene, VGD1 (At2g47040), was mutated, implying that PME is involved in the flowering process (Pina et al., 2005). Three tomato PMEs (solyc02g81990, solyc02g014300, and solyc09g075330) were found to be specifically expressed in the root, indicating that they may have a function in tomato root development. The role

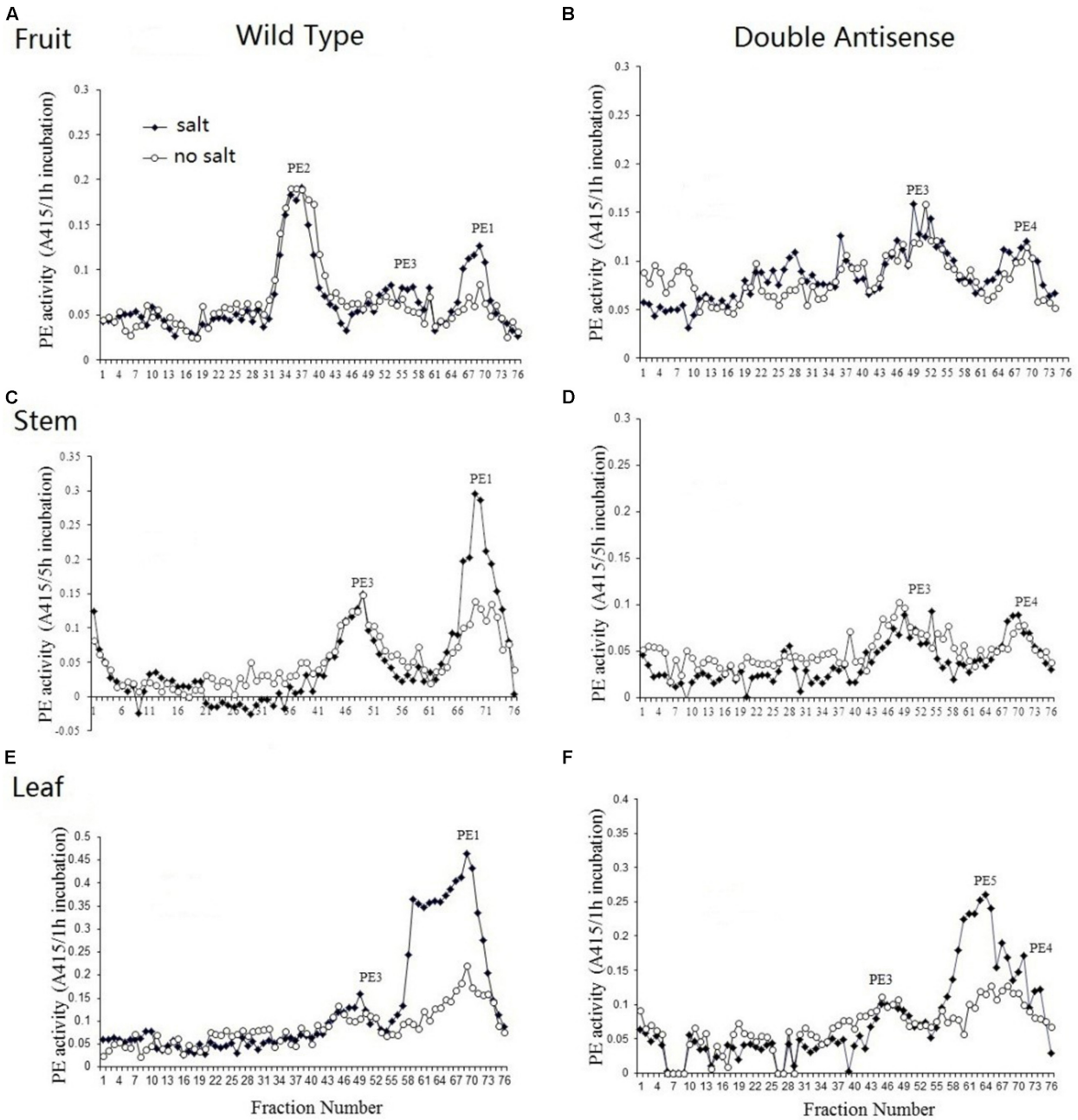

FIGURE 7 | PE isoform profiles from the fruit, stem, and leaf of wild-type and PE1/PE2 double antisense plants. Total PE was extracted from the fruit, stem, and leaf of either wild-type **(A,C,E)** or PE1/PE2 double antisense **(B,D,F)**.

of PME in root elongation has been seen in other plants. For example, an *atpme3* mutant showed decreased PME activity and had a 20% reduction in root length compared with the wild-type, whereas AtPME3 overexpressors showed the opposite phenotype (Hewezi et al., 2008).

Twenty-seven PMEs were identified as fruit-development-related genes, including the previously well characterized solyc03g123630\Pmeu1 (encoding isoform PE1) as well as solyc07g064170\PME1.9, solyc07g064180\PME2.1, and solyc07g064190\PME3 (encoding isoform PE2) (Hall et al., 1993; Phan et al., 2007). Among of them, the expression of five genes (Solyc03g123630\Pmeu1, Solyc03g083360, Solyc07g071600, Solyc07g064170/Solyc07g064180/Solyc07g064190, and Solyc12 g098340) was found to be regulated by ethylene, implying they have important functions in fruit ripening. In the banana (*Musa acuminata*), PME genes also showed ethylene-dependent expression (Dominguez-Puigjaner et al., 1997). Moreover, as paralogous gene pairs, Solyc03g123630\Pmeu1 responded to

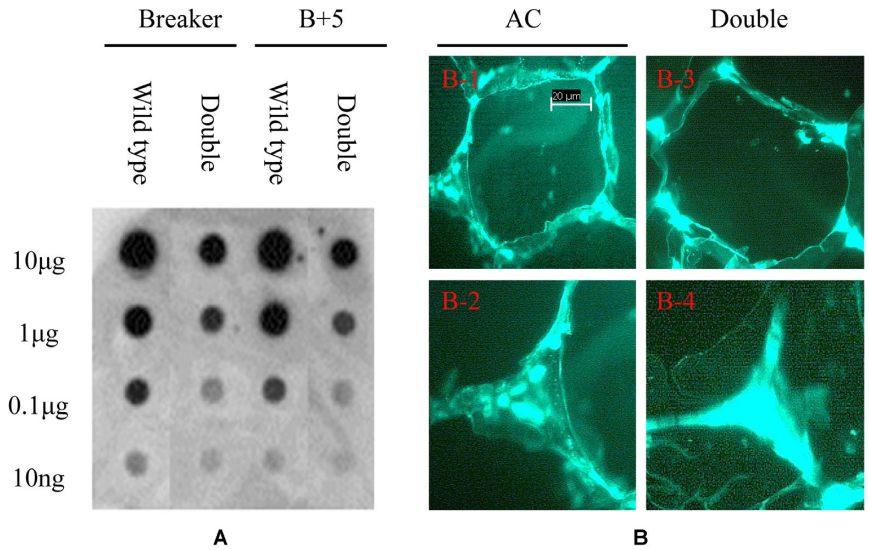

FIGURE 8 | Immunodot blot and immunolocalization analysis of tomato fruit cell wall. Pectin was extracted from tomato wild-type and PE1/PE2 antisense fruit pericarp and loaded onto nitrocellulose membrane for dot blot analysis using monoclonal antibodies of JIM5 **(A)**. Immunolabeling of tomato pericarp with monoclonal antibody JIM5 **(B)**.

ethylene, but Solyc03g123620 did not, suggesting functional differentiation after a duplication event.

According to enzymatic salt dependency, PE isoforms can be classified into two groups: salt-dependent isoforms and salt-independent isoforms (Warrilow et al., 1994; Phan et al., 2007). In the tomato fruit, the major isoforms PE1 and PE2 represent salt-dependent and salt-independent isoforms, respectively (Warrilow et al., 1994; Phan et al., 2007). In this study, PE3 was also proven to be a salt-independent isoform. Using a PE1/PE2 double antisense line, we detected persistent PME activity in the fruit that appeared to be salt-independent, and this can have multiple origins. Either PE1 has some, albeit much reduced, salt independent activity here, or there is another undescribed isoform (speculatively called PE4) which contributes in a minor way to the activity. To date, few PE-related studies have been conducted in vegetative tissue in tomato plants. Here the PE isoform profiles of both the tomato stem and leaf were obtained. The results demonstrated that PE1 is the major isoform in stems and leaves. Interestingly, the analysis of the double antisense plants revealed the contribution of an unknown isoform (speculatively called PE5) activity in leaf extracts. Gaffe et al. (Gaffe et al., 1994) observed two PE isoforms in the tomato stem, both of which showed ubiquitous expression in different tissues and different pIs, which may be equivalent to the PE1 and PE3 isoforms found in the present study. At least three, perhaps even four PME isoforms are active in the tomato fruit, which are the salt-dependent isoform PE1 and the salt independent isoforms PE2, PE3, and potentially PE4. Two or three isoforms have been identified in the tomato leaf: the salt-independent isoforms PE3 and the salt-dependent PE1 and potentially PE5. In addition, in the present study, three isoforms were identified in the tomato stem: the salt-dependent isoform PE1 and salt-independent isoforms PE3 and potentially PE4 (**Supplementary Table S7**). Collectively the observations here suggest that upto five different isoforms might be active across the different plant parts, and that different isoforms are activate in the fruit as compared to the leaves and stems. In addition, previous study have proved that PE1 is encoded by Pmeu1 and isoform PE2 is encoded by three tandem duplication genes of Solyc07g064170/Solyc07g064180/Solyc07g06410 (Hall et al., 1994; Phan et al., 2007). Further investigations by proteomics are required to identify the isoforms of PE3, PE4, and PE5 in future research.

Previous research revealed that only 10% of PME activity remained in the fruit of PE1/PE2 double antisense plants, and ripening-associated pectin de-esterification was almost completely blocked (Wen et al., 2013). JIM5 can recognize a partially and relatively low methyl-esterified HGA epitope (Clausen et al., 2003). As shown in **Figure 8A**, JIM5 epitope reduction was found after downregulating PE1 and PE2 in the tomato Breaker fruit, suggesting that PE1 or PE2 de-esterify HGA before fruit ripening. Through immunolocalization, the low esterified JIM5 epitopes were found to concentrate at cell wall corners and intercellular spaces in the fruit of PE1/PE2 antisense plants; however this phenomenon was not observed in the wild-type fruit. This cell wall structure change may be associated with the faster softening phenotype in the fruit of PE1/PE2 antisense plants (Wen et al., 2013). As mentioned by Jarvis et al. (2003), cell turgor pressure tends to separate adjacent cells. Plant cells resist this separation mainly through adhesion within a cell wall–reinforcing zone located in the cellular junction area. This area is occupied by networks of low-esterified pectic polymers and accumulates high levels of calcium. This pectic network contains at least three types of cross-links to bind the network together, which are calcium bridge links, covalent links through alkali labile esters and amides, and alkali-resistant

covalent links (Guglielmino et al., 1997). Before ripening, the fruits of both PE1/PE2 antisense and wild-type plants showed similar textures (Wen et al., 2013), which could imply that at this stage, covalent links dominate cell adhesion, and calcium bridges contribute very little to it. However, with further ripening, some changes may occur in this area, and the covalent cross-links may be broken. At this point, calcium bridges in this junction area may become the major factor resisting cell separation. PE1 or PE2 could specifically produce block-wise de-esterified pectin in the junction zone that interacts with Ca^{2+} to form calcium pectate gel, resulting in fruits that soften slowly. However, when PE1 and PE2 were suppressed, the calcium bridge structure could no longer be formed. As the covalent cross-links in the network decrease during ripening, PE1/PE2 fruits tend to soften faster.

CONCLUSION

In summary, a total of 57 tomato PME genes were identified and divided into five groups; the classification is supported by the exon–intron structure, conserved motif distribution, and phylogeny. Chromosomal mapping and microsynteny analysis suggested that these PME genes were unevenly distributed in all tomato chromosomes. Both segmental duplication and tandem duplication were found to contribute to PME gene expansion in the tomato genome. Ka/Ks analysis suggested both paralogous and orthologous PME gene pairs experienced strong positive selection during evolution. The gene expression pattern in various tissues suggested that PME may function in organ development and fruit ripening. Three PME genes (Solyc03g083360, Solyc07g071600, and Solyc12g098340) were identified as new candidates for fruit ripening. Immunoassay suggested that isoforms PE1 and PE2 may be involved in pectin structure modification in cell junction areas, which could be associated with tomato fruit softening. In addition, our analysis indicate that two undescribed PE isoforms might be active in leaves and fruits. This study provides useful information for further functional analysis of the PME gene family in the tomato.

DATA AVAILABILITY STATEMENT

The data generated by this study can be found in Figshare using accession number doi: 10.6084/m9.figshare.10007573.v1.

AUTHOR CONTRIBUTIONS

BW conceived and designed the experiments. BW, FZ, XW, and HL performed the experiments. FZ and XW analyzed the data. FZ, XW, and HL contributed reagents, materials, and analysis tools. BW and FZ wrote the manuscript.

FUNDING

This work was supported by the Anhui Natural Science Foundation (No. 1608085MC60), the Key Research Development Program of Anhui Province (No. 201904b11020039), and the National Natural Science Foundation of China (Grant No. 31672167).

ACKNOWLEDGMENTS

This manuscript was edited by Wallace Academic Editing. We thank Dr. Walter Dewitte for his help in manuscript proofreading and enhancement.

SUPPLEMENTARY MATERIAL

The Supplementary Material for this article can be found online at: https://www.frontiersin.org/articles/10.3389/fpls.2020.00238/full#supplementary-material

REFERENCES

Arabidopsis Genome Initiative (2000). Analysis of the genome sequence of the flowering plant *Arabidopsis thaliana*. *Nature* 408, 796–815. doi: 10.1038/35048692

Bailey, T. L., Boden, M., Buske, F. A., Frith, M., Grant, C. E., Clementi, L., et al. (2009). MEME SUITE: tools for motif discovery and searching. *Nucleic Acids Res.* 37, W202–W208. doi: 10.1093/nar/gkp335

Bethke, G., Grundman, R. E., Sreekanta, S., Truman, W., Katagiri, F., and Glazebrook, J. (2014). *Arabidopsis* PECTIN METHYLESTERASEs contribute to immunity against *Pseudomonas syringae*. *Plant Physiol.* 164, 1093–1107. doi: 10.1104/pp.113.227637

Bosch, M., and Hepler, P. K. (2005). Pectin methylesterases and pectin dynamics in pollen tubes. *Plant Cell* 17, 3219–3226. doi: 10.1105/tpc.105.037473

Cannon, S. B., Mitra, A., Baumgarten, A., Young, N. D., and May, G. (2004). The roles of segmental and tandem gene duplication in the evolution of large gene families in *Arabidopsis thaliana*. *BMC Plant Biol.* 4:10. doi: 10.1186/1471-2229-4-10

Cao, Y., Han, Y., Jin, Q., Lin, Y., and Cai, Y. (2016). Comparative genomic analysis of theGRFGenes in Chinese Pear (*Pyrus bretschneideri Rehd*), Poplar (*Populous*), Grape (*Vitis vinifera*), *Arabidopsis* and Rice (*Oryza sativa*). *Front. Plant Sci.* 7:1750. doi: 10.3389/fpls.2016.01750

Chen, M. H., and Citovsky, V. (2003). Systemic movement of a *Tobamovirus* requires host cell pectin methylesterase. *Plant J.* 35, 386–392. doi: 10.1046/j.1365-313x.2003.01818.x

Clausen, M. H., Willats, W. G., and Knox, J. P. (2003). Synthetic methyl hexagalacturonate hapten inhibitors of anti-homogalacturonan monoclonal antibodies LM7, JIM5 and JIM7. *Carbohydr. Res.* 338, 1797–1800. doi: 10.1016/s0008-6215(03)00272-6

Dominguez-Puigjaner, E., LLop, I., Vendrell, M., and Prat, S. (1997). A cDNA clone highly expressed in ripe banana fruit shows homology to pectate lyases. *Plant Physiol.* 114, 1071–1076. doi: 10.1104/pp.114.3.1071

Dorokhov, Y. L., Makinen, K., Frolova, O. Y., Merits, A., Saarinen, J., Kalkkinen, N., et al. (1999). A novel function for a ubiquitous plant enzyme pectin methylesterase: the host-cell receptor for the tobacco mosaic virus movement protein. *FEBS Lett.* 461, 223–228. doi: 10.1016/s0014-5793(99)01447-7

Gaffe, J., Tieman, D. M., and Handa, A. K. (1994). Pectin methylesterase isoforms in tomato (Lycopersicon esculentum) tissues (Effects of expression of a pectin methylesterase antisense gene). *Plant Physiol.* 105, 199–203. doi: 10.1104/pp.105.1.199

Gasteiger, E., Gattiker, A., Hoogland, C., Ivanyi, I., Appel, R. D., and Bairoch, A. (2003). ExPASy: the proteomics server for in-depth protein knowledge and analysis. *Nucleic Acids Res.* 31, 3784–3788. doi: 10.1093/nar/gkg563

Geisler-Lee, J., Geisler, M., Coutinho, P. M., Segerman, B., Nishikubo, N., Takahashi, J., et al. (2006). Poplar carbohydrate-active enzymes. Gene identification and expression analyses. *Plant Physiol.* 140, 946–962. doi: 10.1104/pp.105.072652

Giancaspro, A., Lionetti, V., Giove, S. L., Zito, D., Fabri, E., Reem, N., et al. (2018). Cell wall features transferred from common into durum wheat to improve *Fusarium* head blight resistance. *Plant Sci.* 274, 121–128. doi: 10.1016/j.plantsci.2018.05.016

Gu, Z., Cavalcanti, A., Chen, F. C., Bouman, P., and Li, W. H. (2002). Extent of gene duplication in the genomes of *Drosophila*, nematode, and yeast. *Mol. Biol. Evol.* 19, 256–262. doi: 10.1093/oxfordjournals.molbev.a004079

Guglielmino, N., Liberman, M., Jauneau, A., Vian, B., Catesson, A. M., and Goldberg, R. J. P. (1997). Pectin immunolocalization and calcium visualization in differentiating derivatives from poplar cambium. *Protoplasma* 199, 151–160. doi: 10.1007/bf01294503

Guo, A. Y., Zhu, Q. H., Chen, X., and Luo, J. C. (2007). [GSDS: a gene structure display server]. *Yi Chuan* 29, 1023–1026.

Hall, L. N., Bird, C. R., Picton, S., Tucker, G. A., Seymour, G. B., and Grierson, D. (1994). Molecular characterisation of cDNA clones representing pectin esterase isozymes from tomato. *Plant Mol. Biol.* 25, 313–318. doi: 10.1007/bf00023246

Hall, L. N., Tucker, G. A., Smith, C. J. S., Watson, C. F., Seymour, G. B., Bundick, Y., et al. (1993). Antisense inhibition of pectin esterase gene expression in transgenic tomatoes. *Plant J.* 3, 121–129. doi: 10.1111/j.1365-313x.1993.tb00015.x

Han, Y., Ding, T., Su, B., and Jiang, H. (2016). Genome-wide identification, characterization and expression analysis of the chalcone synthase family in maize. *Int. J. Mol. Sci.* 17:61. doi: 10.3390/ijms17020161

Hewezi, T., Howe, P., Maier, T. R., Hussey, R. S., Mitchum, M. G., Davis, E. L., et al. (2008). Cellulose binding protein from the parasitic nematode *Heterodera schachtii* interacts with *Arabidopsis* pectin methylesterase: cooperative cell wall modification during parasitism. *Plant Cell* 20, 3080–3093. doi: 10.1105/tpc.108.063065

Hu, B., Jin, J., Guo, A. Y., Zhang, H., Luo, J., and Gao, G. (2015). GSDS 2.0: an upgraded gene feature visualization server. *Bioinformatics* 31, 1296–1297. doi: 10.1093/bioinformatics/btu817

Hurst, L. D. (2002). The Ka/Ks ratio: diagnosing the form of sequence evolution. *Trends Genet.* 18, 486–487. doi: 10.1016/s0168-9525(02)02722-1

James, W. K., Robert, B., Angie, H., Webb, M., and David, H. (2003). Evolution's cauldron: duplication, deletion, and rearrangement in the mouse and human genomes. *Proc. Natl. Acad. Sci. U.S.A.* 100, 11484–11489. doi: 10.1073/pnas.1932072100

Jarvis, M. C., Briggs, S. P. H., and Knox, J. P. (2003). Intercellular adhesion and cell separation in plants. *Plant Cell Environ.* 26, 977–989. doi: 10.1046/j.1365-3040.2003.01034.x

Jeong, H. Y., Nguyen, H. P., Eom, S. H., and Lee, C. (2018). Integrative analysis of pectin methylesterase (PME) and PME inhibitors in tomato (Solanum lycopersicum): identification, tissue-specific expression, and biochemical characterization. *Plant Physiol. Biochem.* 132, 557–565. doi: 10.1016/j.plaphy.2018.10.006

Jeong, H. Y., Nguyen, H. P., and Lee, C. (2015). Genome-wide identification and expression analysis of rice pectin methylesterases: implication of functional roles of pectin modification in rice physiology. *J. Plant Physiol.* 183, 23–29. doi: 10.1016/j.jplph.2015.05.001

Jolie, R. P., Duvetter, T., Van Loey, A. M., and Hendrickx, M. E. (2010). Pectin methylesterase and its proteinaceous inhibitor: a review. *Carbohydr. Res.* 345, 2583–2595. doi: 10.1016/j.carres.2010.10.002

Jones, D. T., Taylor, W. R., and Thornton, J. M. (1992). The rapid generation of mutation data matrices from protein sequences. *Comput. Appl. Biosci.* 8, 275–282. doi: 10.1093/bioinformatics/8.3.275

Kumar, S., Stecher, G., and Tamura, K. (2016). MEGA7: molecular evolutionary genetics analysis version 7.0 for bigger datasets. *Mol. Biol. Evol.* 33, 1870–1874. doi: 10.1093/molbev/msw054

Letunic, I., Copley, R. R., Schmidt, S., Ciccarelli, F. D., Doerks, T., Schultz, J., et al. (2004). SMART 4.0: towards genomic data integration. *Nucleic Acids Res.* 32, D142–D144.

Lionetti, V., Cervone, F., and Bellincampi, D. (2012). Methyl esterification of pectin plays a role during plant-pathogen interactions and affects plant resistance to diseases. *J. Plant Physiol.* 169, 1623–1630. doi: 10.1016/j.jplph.2012.05.006

Livak, K. J., and Schmittgen, T. D. (2001). Analysis of relative gene expression data using real-time quantitative PCR and the 2(-Delta Delta C(T)) method. *Methods* 25, 402–408. doi: 10.1006/meth.2001.1262

Louvet, R., Cavel, E., Gutierrez, L., Guenin, S., Roger, D., Gillet, F., et al. (2006). Comprehensive expression profiling of the pectin methylesterase gene family during silique development in *Arabidopsis thaliana*. *Planta* 224, 782–791. doi: 10.1007/s00425-006-0261-9

Markovic, O., and Janecek, S. (2004). Pectin methylesterases: sequence-structural features and phylogenetic relationships. *Carbohydr. Res.* 339, 2281–2295. doi: 10.1016/j.carres.2004.06.023

Micheli, F. (2001). Pectin methylesterases: cell wall enzymes with important roles in plant physiology. *Trends Plant Sci.* 6, 414–419. doi: 10.1016/s1360-1385(01)02045-3

Pelloux, J., Rusterucci, C., and Mellerowicz, E. J. (2007). New insights into pectin methylesterase structure and function. *Trends Plant Sci.* 12, 267–277. doi: 10.1016/j.tplants.2007.04.001

Phan, T. D., Bo, W., West, G., Lycett, G. W., and Tucker, G. A. (2007). Silencing of the major salt-dependent isoform of pectinesterase in tomato alters fruit softening. *Plant Physiol.* 144, 1960–1967. doi: 10.1104/pp.107.096347

Pina, C., Pinto, F., Feijo, J. A., and Becker, J. D. (2005). Gene family analysis of the *Arabidopsis* pollen transcriptome reveals biological implications for cell growth, division control, and gene expression regulation. *Plant Physiol.* 138, 744–756. doi: 10.1104/pp.104.057935

Pinzon-Latorre, D., and Deyholos, M. K. (2013). Characterization and transcript profiling of the pectin methylesterase (PME) and pectin methylesterase inhibitor (PMEI) gene families in flax (*Linum usitatissimum*). *BMC Genomics* 14:742. doi: 10.1186/1471-2164-14-742

Qin, Y. M., and Zhu, Y. X. (2011). How cotton fibers elongate: a tale of linear cell-growth mode. *Curr. Opin. Plant Biol.* 14, 106–111. doi: 10.1016/j.pbi.2010.09.010

Raiola, A., Lionetti, V., Elmaghraby, I., Immerzeel, P., Mellerowicz, E. J., Salvi, G., et al. (2011). Pectin methylesterase is induced in *Arabidopsis* upon infection and is necessary for a successful colonization by necrotrophic pathogens. *Mol. Plant Microbe Interact.* 24, 432–440. doi: 10.1094/MPMI-07-10-0157

Rigano, M. M., Lionetti, V., Raiola, A., Bellincampi, D., and Barone, A. (2018). Pectic enzymes as potential enhancers of ascorbic acid production through the D-galacturonate pathway in Solanaceae. *Plant Sci.* 266, 55–63. doi: 10.1016/j.plantsci.2017.10.013

Scheler, C., Weitbrecht, K., Pearce, S. P., Hampstead, A., Buttner-Mainik, A., Lee, K. J., et al. (2015). Promotion of testa rupture during garden cress germination involves seed compartment-specific expression and activity of pectin methylesterases. *Plant Physiol.* 167, 200–215. doi: 10.1104/pp.114.247429

Sexton, R., and Roberts, J. A. (1982). Cell biology of abscission. *Annu. Rev. Plant Physiol.* 33, 133–162.

Seymour, G. B., Lasslett, Y., and Tucker, G. A. (1987). Differential effects of pectolytic enzymes on tomato polyuronides in vivo and in vitro. *Phytochemistry* 26, 3137–3139. doi: 10.1016/s0031-9422(00)82457-7

Simons, H., and Tucker, G. A. (1999). Simultaneous co-suppression of polygalacturonase and pectinesterase in tomato fruit: inheritance and effect on isoform profiles. *Phytochemistry* 52, 1017–1022. doi: 10.1016/s0031-9422(99)00339-8

Stephenson, M. B., and Hawes, M. C. (1994). Correlation of pectin methylesterase activity in root caps of pea with root border cell separation. *Plant Physiol.* 106, 739–745. doi: 10.1104/pp.106.2.739

Tamura, K., Stecher, G., Peterson, D., Filipski, A., and Kumar, S. (2013). MEGA6: molecular evolutionary genetics analysis version 6.0. *Mol. Biol. Evol.* 30, 2725–2729. doi: 10.1093/molbev/mst197

Tieman, D. M., and Handa, A. K. (1994). Reduction in pectin methylesterase activity modifies tissue integrity and cation levels in ripening tomato (Lycopersicon esculentum Mill.) fruits. *Plant Physiol.* 106, 429–436. doi: 10.1104/pp.106.2.429

Tieman, D. M., Harriman, R. W., Ramamohan, G., and Handa, A. K. (1992). An antisense pectin methylesterase gene alters pectin chemistry and soluble solids in tomato fruit. *Plant Cell* 4, 667–679. doi: 10.1105/tpc.4.6.667

Tomato Genome, C. (2012). The tomato genome sequence provides insights into fleshy fruit evolution. *Nature* 485, 635–641. doi: 10.1038/nature11119

Tucker, G. A., and Grierson, D. (1982). Synthesis of polygalacturonase during tomato fruit ripening. *Planta* 155, 64–67. doi: 1007/BF00402933

Voorrips, R. E. (2002). MapChart: software for the graphical presentation of linkage maps and QTLs. *J. Hered.* 93, 77–78. doi: 10.1093/jhered/93.1.77

Wang, D., Zhang, Y., Zhang, Z., Zhu, J., and Yu, J. (2010). KaKs_calculator 2.0: a toolkit incorporating gamma-series methods and sliding window strategies. *Genomics Proteomics Bioinformatics* 8, 77–80. doi: 10.1016/S1672-0229(10)60008-3

Wang, L., Guo, K., Li, Y., Tu, Y., Hu, H., Wang, B., et al. (2010). Expression profiling and integrative analysis of the CESA/CSL superfamily in rice. *BMC Plant Biol.* 10:282. doi: 10.1186/1471-2229-10-282

Warrilow, A. G., Turner, R. J., and Jones, M. G. (1994). A novel form of pectinesterase in tomato. *Phytochemistry* 35, 863–868. doi: 10.1016/s0031-9422(00)90627-7

Wen, B., Strom, A., Tasker, A., West, G., and Tucker, G. A. (2013). Effect of silencing the two major tomato fruit pectin methylesterase isoforms on cell wall pectin metabolism. *Plant Biol.* 15, 1025–1032. doi: 10.1111/j.1438-8677.2012.00714.x

Willats, W. G., and Knox, J. P. (1999). Immunoprofiling of pectic polysaccharides. *Anal. Biochem.* 268, 143–146. doi: 10.1006/abio.1998.3039

Wu, H. C., Huang, Y. C., Stracovsky, L., and Jinn, T. L. (2017). Pectin methylesterase is required for guard cell function in response to heat. *Plant Signal. Behav.* 12:e1338227. doi: 10.1080/15592324.2017.1338227

Yan, J., He, H., Fang, L., and Zhang, A. (2018). Pectin methylesterase31 positively regulates salt stress tolerance in *Arabidopsis*. *Biochem. Biophys. Res. Commun.* 496, 497–501. doi: 10.1016/j.bbrc.2018.01.025

Yang, S., Zhang, X., Yue, J. X., Tian, D., and Chen, J. Q. (2008). Recent duplications dominate NBS-encoding gene expansion in two woody species. *Mol. Genet. Genomics* 280, 187–198. doi: 10.1007/s00438-008-0355-0

Yue, X., Lin, S., Yu, Y., Huang, L., and Cao, J. (2018). The putative pectin methylesterase gene, BcMF23a, is required for microspore development and pollen tube growth in *Brassica campestris*. *Plant Cell Rep.* 37, 1003–1009. doi: 10.1007/s00299-018-2285-6

Conflict of Interest: The authors declare that the research was conducted in the absence of any commercial or financial relationships that could be construed as a potential conflict of interest.

frontiers in Plant Science

ORIGINAL RESEARCH
published: 14 May 2020
doi: 10.3389/fpls.2020.00584

Hydrogen Sulfide Maintained the Good Appearance and Nutrition in Post-harvest Tomato Fruits by Antagonizing the Effect of Ethylene

Gai-Fang Yao[1†], Chuang Li[1†], Ke-Ke Sun[1†], Jun Tang[2], Zhong-Qin Huang[2], Feng Yang[2], Guan-Gen Huang[1], Lan-Ying Hu[1], Peng Jin[3], Kang-Di Hu[1] and Hua Zhang[1]**

[1] School of Food and Biological Engineering, Hefei University of Technology, Hefei, China, [2] Xuzhou Institute of Agricultural Sciences of the Xuhuai District of Jiangsu Province, Xuzhou, China, [3] Department of Ecology and Environment of Anhui Province, Hefei, China

OPEN ACCESS

Edited by:
Cai-Zhong Jiang,
Crops Pathology and Genetics Research Unit, USDA-ARS, United States

Reviewed by:
María Serrano,
Universidad Miguel Hernández de Elche, Spain
Daniel Alexandre Neuwald,
Competence Centre for Fruit Growing – Lake Constance, Germany

***Correspondence:**
Kang-Di Hu
kangdihu@hfut.edu.cn
Hua Zhang
hzhanglab@hfut.edu.cn

[†] These authors have contributed equally to this work

Specialty section:
This article was submitted to Crop and Product Physiology, a section of the journal Frontiers in Plant Science

Received: 14 February 2020
Accepted: 17 April 2020
Published: 14 May 2020

Citation:
Yao G-F, Li C, Sun K-K, Tang J, Huang Z-Q, Yang F, Huang G-G, Hu L-Y, Jin P, Hu K-D and Zhang H (2020) Hydrogen Sulfide Maintained the Good Appearance and Nutrition in Post-harvest Tomato Fruits by Antagonizing the Effect of Ethylene. Front. Plant Sci. 11:584. doi: 10.3389/fpls.2020.00584

Hydrogen sulfide (H_2S) could act as a versatile signaling molecule in delaying fruit ripening and senescence. Ethylene (C_2H_4) also plays a key role in climacteric fruit ripening, but little attention has been given to its interaction with H_2S in modulating fruit ripening and senescence. To study the role of H_2S treatment on the fruit quality and nutrient metabolism, tomato fruits at white mature stage were treated with ethylene and ethylene plus H_2S. By comparing to C_2H_4 treatment, we found that additional H_2S significantly delayed the color change of tomato fruit, and maintained higher chlorophyll and lower flavonoids during storage. Moreover, H_2S could inhibit the activity of protease, maintained higher levels of nutritional-related metabolites, such as anthocyanin, starch, soluble protein, ascorbic acid by comparing to C_2H_4 treatment. Gene expression analysis showed that additional H_2S attenuated the expression of beta-amylase encoding gene *BAM3*, UDP-glycosyltransferase encoding genes, ethylene-responsive transcription factor *ERF003* and *DOF22*. Furthermore, principal component analysis suggested that starch, titratable acids, and ascorbic acid were important factors for affecting the tomato storage quality, and the correlation analysis further showed that H_2S affected pigments metabolism and the transformation of macromolecular to small molecular metabolites. These results showed that additional H_2S could maintain the better appearance and nutritional quality than C_2H_4 treatment alone, and prolong the storage period of post-harvest tomato fruits.

Keywords: hydrogen sulfide, ethylene, tomato fruits, nutritional quality, post-harvest ripening

INTRODUCTION

Ripening of fleshy fruit is composed of a series of complex and coordinated processes that leading to edible fruit with desirable flavor (Karlova et al., 2014). However, fruit excessive ripening will cause senescence and deterioration during storage, which finally leads to shortened shelf life and reduction in commercial value (Lee et al., 2010). In this process, fruit ripening is accompanied

Abbreviations: C_2H_4, ethylene; CHL, chlorophyllase; CO, carbon monoxide; DAS, day after storage; EDTA, ethylene diamine tetraacetic acid; FW, fresh weight; G–O, green–orange; G–Y, green–yellow; H_2S, hydrogen sulfide; L-R, light red; NO, nitric oxide; O–R, orange–red; PCA, principal component analysis; PPH, pheophytinase; TA, titratable acid; UFGT, UDP glucose: flavonoid-3-*O*-glucosyltransferase.

by profound physiological and transcriptome changes, such as cell wall component degradation, accumulation of sugar and reduction of organic acids, increased volatile compounds, degradation of chlorophyll and accumulation of pigments (Klee and Giovannoni, 2011; Gapper et al., 2013). Ethylene is a gaseous phytohormone that regulates the whole life cycle of plants, including plant growth and development, fruit ripening and organ senescence, plant biotic and abiotic stress, and extensively investigated in a large number of crops (Dubois et al., 2018). Fleshy fruits could be classified as climacteric and non-climacteric which is defined by whether an increase in respiration and concomitant increase in ethylene biosynthesis happened after the start of ripening (Klee and Giovannoni, 2011). In climacteric fruit like tomato, ripening is initiated by ethylene and exogenous ethylene could also promote fruit ripening (Liu et al., 2015). Ethylene coordinates the ripening process and acts in concert with other phytohormones. Chen et al. (2019) reported that exposure to ethylene improved sucrose accumulation in ripening sugarcane. In addition, carotenoid accumulation is modulated by the auxin-ethylene balance during tomato fruit ripening; strawberry fruit ripening was regulated by ABA, IAA, and ethylene (Su et al., 2015; Guo et al., 2018).

Hydrogen sulfide (H_2S) is a small gasotransmitter that plays an important role in diverse plant physiological processes such as plant adaptation to stress conditions, stomatal movement, root development, autophagy and flower senescence (Hancock and Whiteman, 2016). Accumulating evidence reported that H_2S delayed senescence in post-harvest fruits and vegetables, including apple, kiwifruit, broccoli, and strawberry, etc. (Zhang et al., 2011; Hu et al., 2012; Li et al., 2014; Zhu et al., 2014; Zheng et al., 2016). Previous researches reported that H_2S maintains higher metabolites levels in broccoli and strawberry, such as carotenoids, anthocyanin, ascorbic acid, reducing sugars and soluble proteins (Hu et al., 2012; Li et al., 2014). During kiwifruit storage, H_2S played an important role in delaying kiwifruit ripening and senescence and maintaining higher level of titratable acid and ascorbic acid by repression of ethylene production (Zhu et al., 2014). Meanwhile, H_2S could protect lipid from peroxidation by improving antioxidative enzyme activities and decreasing the accumulation of reactive oxygen species (ROS) (Zhu et al., 2014). All the evidence showed that ethylene and H_2S regulate climacteric fruit ripening and senescence, whereas the interaction of H_2S with ethylene in controlling the post-harvest fruit ripening and the nutritional quality are rarely reported.

Tomato (*Solanum lycopersicum*) is one of the most studied fleshy fruit, and it has been assumed as a "functional food" because of the evidence regarding to the reduced risk of cancer and cardiovascular diseases in relationship to its consumption (Giovannetti et al., 2012). Their benefits to human health are primarily associated with the bioactive compounds in fruit such as lycopene, ascorbic acid, tocopherols and polyphenols, carotenoids, anthocyanins (Giovannetti et al., 2012; Vinha et al., 2014). However, tomato is not resistant to storage and prone to rot, thus resulting in economic loss.

In our recent studies, H_2S was found to alleviate tomato fruit ripening by reducing ROS accumulation, and meanwhile ethylene biosynthesis and signaling pathway were inhibited by H_2S (Yao et al., 2018; Hu et al., 2019). Though H_2S has been found to be a senescence regulator in diverse fruits and vegetables, the mechanism of exogenous H_2S in affecting the bioactive compounds of ethylene-induced tomato fruit ripening and senescence is still obscure. In the present research, we tried to explore the effect of H_2S on the mentalism of the bioactive compounds in C_2H_4-induced tomato fruit ripening by comparing to C_2H_4 treatment alone. Tomato fruits of the cultivar "Micro Tom" at white mature stage were fumigated with exogenous C_2H_4 or C_2H_4 plus H_2S, and the bioactive compounds and the expressions of genes involving in nutrient metabolism were investigated during post-harvest storage. Furthermore, PCA, the correlation and the change patterns among the bioactive compounds were analyzed to explore the underlying physiological mechanism.

MATERIALS AND METHODS

Plant Materials and Treatment

Tomato fruits of the cultivar "Micro Tom" were harvested in the man-made glasshouse of School of Food and Biological Engineering, Hefei University of Technology, Anhui province, China. Fruit without pest or mechanical damage were harvested at white mature stage. Random eight fruits were used as one group, and each experiment was composed of three groups. NaHS (purchased from Sigma) was used as the donor of H_2S and ethephon in aqueous solution for C_2H_4 donor. C_2H_4 treatment was proceeded with a 100 mL of 1.0 g/L ethephon aqueous solution. $C_2H_4 + H_2S$ co-treatment was composed of a 150 mL of 0.90 mmol $\cdot$ L^{-1} NaHS aqueous solution and a 100 mL of 1.0 g/L ethephon aqueous solution. The above samples were placed in 3 L sealed containers. Tomato fruits were fumigated by C_2H_4 or C_2H_4 + H_2S for 24 h and the fruits were fumigated by equal amount of distil water. The tomato flesh (without seeds) were sampled every day till 7 days after storage and frozen in liquid N_2 quickly and stored in −80°C refrigerator.

Determination of Color Change of Tomato Fruits

Color change of tomato fruits was measured by a colorimeter (model WSC-100, Japan) as shown in Hu et al. (2012) with some modification. Each tomato fruit at the equatorial part was selected for the determination, and the value of a^*/b^* showed color change of fruit surface.

Determination of Chlorophyll and Carotenoid Contents

Chlorophyll and carotenoid contents of tomato fruits were assayed according to the method of Wellburn (1994). 2.0 ± 0.01 g of fresh tomato sample was ground and extracted by ethanol and 80% acetone solution in a ratio of 1:1 (v/v). The absorbance was measured at 663, 645, and 440 nm. Three replicates were performed for each sample and the results were expressed as mg/g FW (fresh weight).

Determination of Flavonoids, Total Phenols, and Anthocyanin Contents

The flavonoids contents were determined by aluminum chloride colorimetric assay by measuring the absorbance at 510 nm (Li et al., 2014). Rutin was used as the standard for calibration.

Total phenols were assayed following the method of Pirie and Mullins (1976). The total phenols in fruit was determined by spectrophotometer at 280 nm. Gallic acid was used as the standard to make a calibration curve.

Anthocyanin content was extracted and determined according to the protocol described by Lee and Wicker (1991). 2.0 ± 0.01 g of tomato fruits were ground with 10 mL of 0.1% HCl-methanol solution. The absorbance was recorded at 530, 620, and 650 nm and anthocyanin content were expressed as mg/g FW.

Determination of Ascorbic Acid, Titratable Acids, and Reducing Sugar Content

Ascorbic acid was assessed by the indophenol titration method with minor changes (Nath et al., 2011). 5.00 ± 0.01 g of fruit sample was homogenized with 5 mL of 2% oxalic acid followed by centrifugation at 12000 g for 30 min. The supernatant was adjusted to 25 mL with 2% oxalic acid and titrated with 2,6-dichlorophenol-indophenol to a pink color and maintain a pink color in 30 s.

The titratable acid content was determined by the method adapted from Bureau et al. (2009). 5.00 ± 0.01 g of tomato homogenates were mixed with 20 mL distilled water. Then, mixture was used for acid-base neutralization to measure the titratable acid content. The volume of NaOH was recorded to calculate the content of titratable acids.

The content of reducing sugar was assessed according to the method of Miller (1959) with some modifications. 2.00 ± 0.01 g of tomato samples were ground with 5 mL of 0.1M Na-acetate buffer with the enzyme solution (both solutions were preheated at 50°C for 5 min). The absorbance at 540 nm was recorded to measure the content of reducing sugar with glucose as the standard to make a calibration curve. Three replicates were performed for each sample and the results were expressed as mg/g FW (fresh weight).

Determination of the Contents of Soluble Protein and Starch

The content of soluble protein was assayed following the method of Bradford (1976). Absorption of soluble protein was recorded at 595 nm. The content of starch in tomato fruits was determined referring to the method by Zhang et al. (2012). 2.0 g of tomato fruits was homogenized with 3 mL of 80% ethanol solution. The content of starch was determined at 510 nm, and soluble starch was used as the standard for calibration.

Determination of Proteolytic Enzyme and Amylase Activity

For the activity of protease, tomato flesh (2.0 ± 0.01 g) were ground in 5 mL of ice-cold Tris-HCl buffer [50 mM, pH 7.5, included 1 mM EDTA, 15 mM β-mercaptoethanol, and 1% polyvinyl pyrrolidone (PVP)]. The homogenate was centrifuged and then the supernatant was collected for protease activity determination (Reimerdes and Klostermeyer, 1976). Absorbance was recorded at 540 nm, and the activity of protease was quantified as U/g FW.

The activity of amylase was determined according to the method of Staden and Mulaudzi (2000) with some modifications. 2.00 ± 0.01 g of tomato samples were homogenized with 3 mL of citric acid buffer (pH 5.6, 0.1 mM). The homogenate was centrifuged at 12000 *g* for 20 min at 4°C, and the supernatant was placed in a new tube for amylase determination. One unit of enzyme activity was defined as the amount of maltose produced per gram of the sample per min, and the activity of amylase was quantified as U/g FW.

Quantitative Reverse Transcription PCR Analysis

Total RNA from 0.1 g frozen tomato fruit samples was extracted by RNA Extraction Kit (Tiangen, Beijing, China). Then cDNA was synthesized by reverse transcription kit (PrimeScript RT Master Mix, Takara, Kyoto, Japan) and further used for quantitative PCR. The specific primers used for qPCR were listed in **Supplementary Table S1**. The expression of tubulin gene in control tomato was used for the normalization of data.

Statistical Analysis

Statistical analysis was performed using *t*-test in SPSS 22.0. PCA analysis was performed using factor analysis in dimension reduction, and the rotation method was performed by Varimax with Kaiser Normalization. The correlation analysis and the heatmap analysis were performed by Rstudio software. All data are expressed as means ± standard deviations of the values obtained by three independent measurements.

RESULTS

Effect of C_2H_4 and H_2S-C_2H_4 Treatment on Tomato Color Change During Post-harvest Storage

The color change of tomato fruit during the post-harvest storage period was shown in **Figure 1A**. It is clearly showed that all the tomato fruits are at green–yellow (G–Y, ∼30% yellow skin) period on the 0th day. A part of C_2H_4-induced tomatoes is at green–orange (G–O, ∼50% orange skin) period on the 1st and 2nd day, but tomato fruits are almost at G–Y period by C_2H_4 + H_2S co-treatment. All C_2H_4-induced tomatoes turn to orange–red (O–R, > 90% orange or red skin) from the day 3 to day 5. Meanwhile, some tomatoes are still at G–O period in C_2H_4-H_2S co-treatment. On days 6 and 7, all C_2H_4-induced tomato fruits are at the light red (L-R, fully orange or red skin) period, but a part of tomatoes are still at O–R period in C_2H_4-H_2S co-treatment.

As shown in **Figure 1B**, the change of color was expressed with a^*/b^* value. During the whole storage period, the a^*/b^* value of the two treatment groups showed an upward trend,

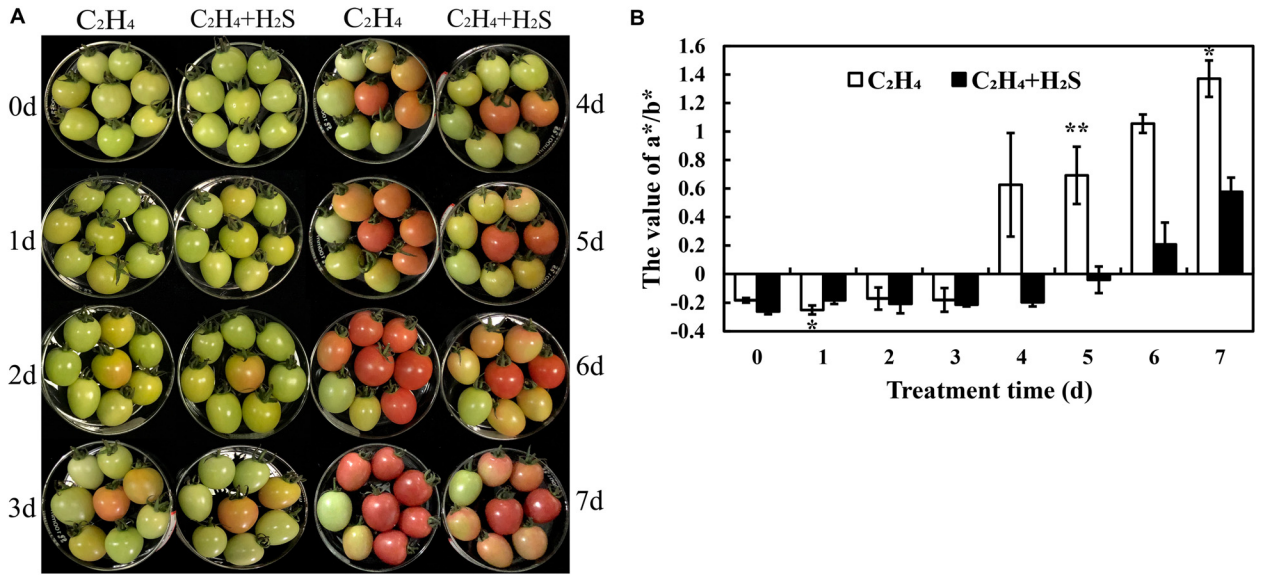

FIGURE 1 | The phenotypic change of post-harvest tomato fruits with C_2H_4 or C_2H_4-H_2S treatment. **(A)** The phenotypic change of post-harvest tomato fruits. **(B)** The color parameter a*/b* value changes with C_2H_4 or C_2H_4-H_2S treatment during tomato post-harvest storage. a* value represents a range from magenta to green, and b* value represents a range from yellow to blue. Values are the means ± SD (n = 3). The experiments and following ones were carried out at room temperature and 85-90% relative humidity. The symbols * and ** stand for significant difference between C_2H_4 and C_2H_4-H_2S at $p < 0.05$ and $p < 0.01$, respectively.

while the a*/b* value of the H_2S plus ethylene treatment group remained at a lower level compared with ethylene treatment alone. Thus, additional H_2S treatment can slow the change of tomato color and delay the ripening of tomato fruit during post-harvest storage.

H_2S Regulated the Metabolism of Chlorophyll, Anthocyanin, Flavonoids, Carotenoid, Total Phenols in Ethylene-Treated Tomato Fruits

To further understand the mechanism of H_2S in alleviating color change of tomato fruits, we determined the contents of chlorophyll, anthocyanin, flavonoids, carotenoid, and total phenols. Total chlorophyll content was composed of chlorophyll a and chlorophyll b. As shown in **Figure 2A**, chlorophyll content in C_2H_4 fumigated tomato increased and reached the peak at the 2st day followed by a gradual decrease until 7th DAS. In contrast, chlorophyll increased and reached the highest level at 3 DAS with C_2H_4-H_2S treatment. Thus, chlorophyll sustained a higher level with C_2H_4-H_2S co-treatment than those of C_2H_4 treatment and reached a significant difference on 6th and 7th day ($p < 0.01$ or $p < 0.05$). Meanwhile, the change trend of chlorophyll a and chlorophyll b was the similar to total chlorophyll (**Figures 2B,C**). The contents of chlorophyll a and chlorophyll b in C_2H_4 treatment always sustained a significantly lower level than that of C_2H_4-H_2S co-treatment at 6 and 7 DAS ($p < 0.01$ or $p < 0.05$).

Figure 3A shows that anthocyanins increased and peaked at 4 DAS followed by a rapid decrease in C_2H_4 treatment, while in C_2H_4-H_2S co-treatment, anthocyanins increased steadily in the first 4 days and remained stable on the day 6 and day 7, and sustained a significantly higher level of anthocyanin at 6 and 7 DAS ($p < 0.05$).

Figure 3B showed the change of carotenoid content in tomato fruit during storage. The carotenoid content was increased firstly, then decreased and then increased with the extension of storage period in C_2H_4-H_2S and C_2H_4 treatment. Comparing with C_2H_4 treatment, carotenoid content remained at a higher level from day 2 to day 4 in C_2H_4-H_2S co-treatment.

As shown in **Figure 3C**, flavonoids increased gradually in both C_2H_4 and C_2H_4-H_2S treatments until 4 DAS followed by a decrease. The content of flavonoids in the C_2H_4 treatment increased and reached the highest level on the day 3, then began to decrease until 7 DAS. The content of flavonoids in the C_2H_4-H_2S treatment decreased from the 2nd day, and was significantly lower than the C_2H_4 treatment at 3 and 4 DAS ($p < 0.01$).

In general, **Figure 3D** showed that total phenols increased steadily during the early storage time. It increased at first, but decreased at 3 DAS, then gradually increased and then tended to be stable in C_2H_4 treatment. Similar trends were observed in C_2H_4-H_2S co-treatment, but decreased at 4 DAS.

Changes of Amylase Activity, Protease Activity, Contents of Starch and Soluble Protein Between C_2H_4-H_2S and C_2H_4 Treatment

To compare the effects of H_2S treatment on C_2H_4-induced tomato fruit quality, amylase activity, protease activity, the content of starch and soluble protein were measured. **Figure 4A** showed the changes of amylase activity in tomato fruit. It

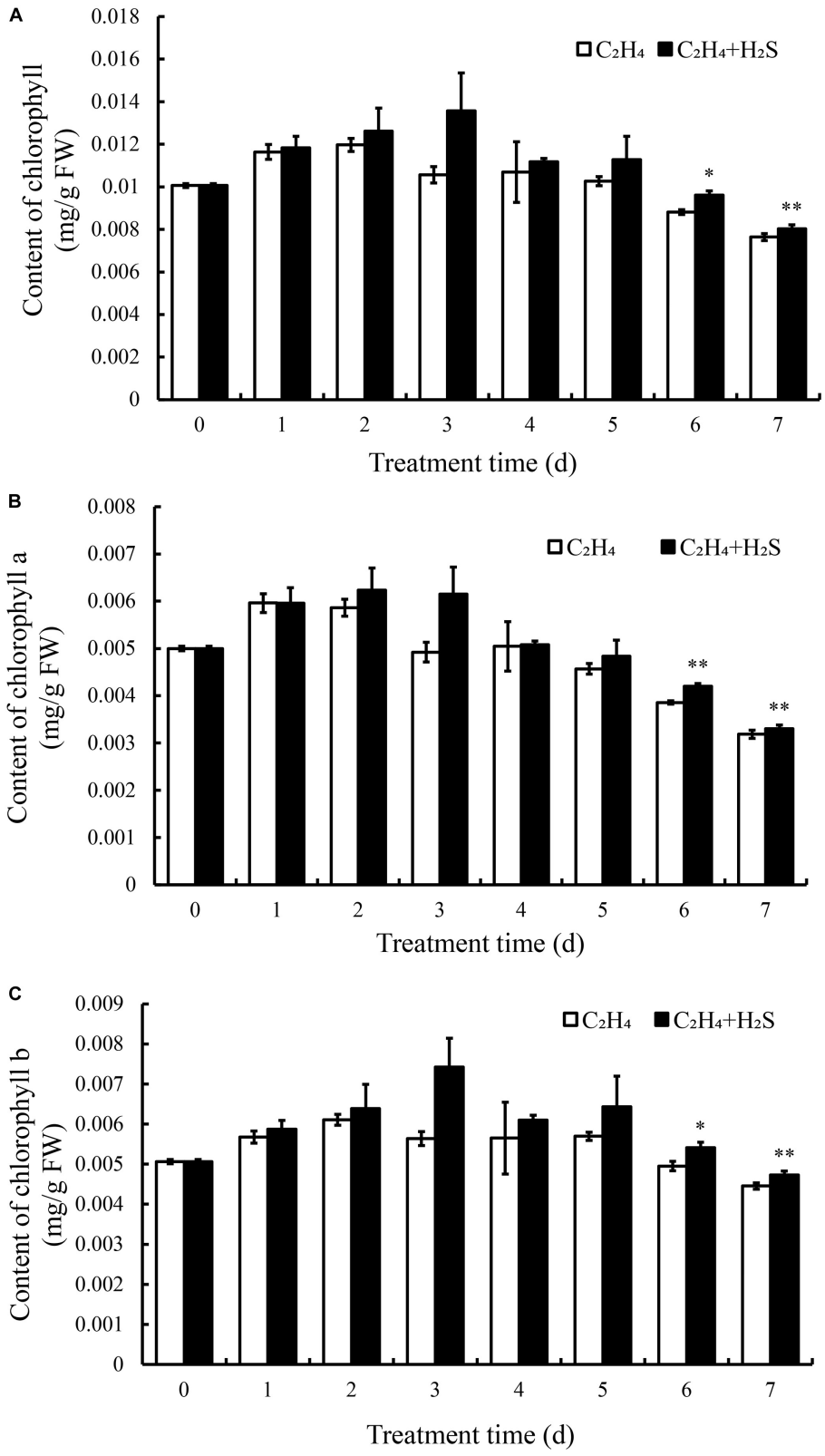

FIGURE 2 | Effects of C_2H_4 and C_2H_4-H_2S on the contents of total chlorophyll **(A)**, chlorophyll a **(B)**, chlorophyll b **(C)** in post-harvest tomato. Data are presented as means ± SD ($n = 3$). * and ** in this figure and following ones stand for a significant difference between C_2H_4 treatment and C_2H_4-H_2S co-treatment at $p < 0.05$ and $p < 0.01$, respectively.

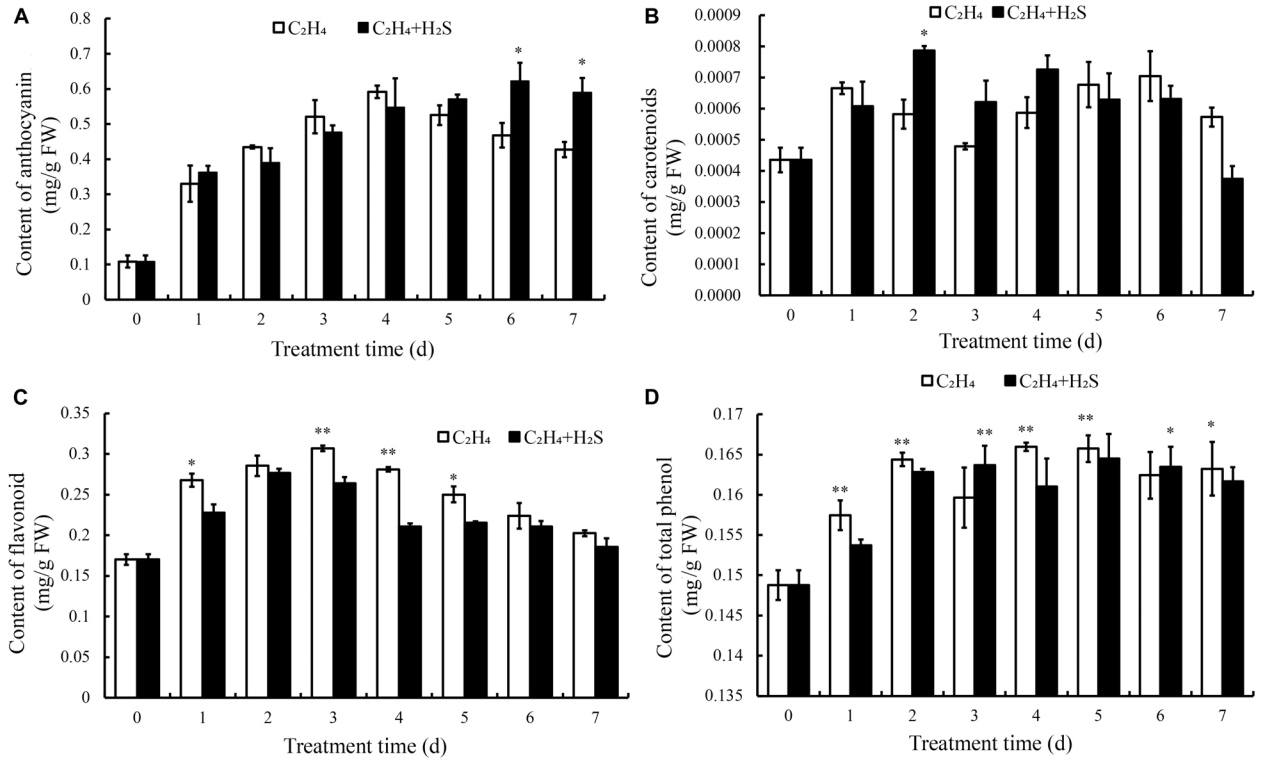

FIGURE 3 | Effect of C_2H_4 and C_2H_4-H_2S on the contents of anthocyanin **(A)**, flavonoids **(B)**, carotenoid **(C)**, total phenols **(D)**. Data are presented as means ± SD ($n = 3$). The symbols * and ** stand for significant difference between C_2H_4 and C_2H_4-H_2S at $p < 0.05$ and $p < 0.01$, respectively.

increased and reached the highest level at 3 DAS and then decreased with the storage time in C_2H_4 and C_2H_4-H_2S co-treatment. As shown in **Figure 4B**, protease activity was steadily increased in both treatments during the storage. C_2H_4-H_2S co-treatment maintained significant lower level of protease activity from 3 to 7 DAS except day 5 compared with C_2H_4 treatment.

The change of starch content was shown in **Figure 4C**. In general, with the extension of storage period, the starch content decreased rapidly. The content of starch in C_2H_4-H_2S co-treatment decreased relatively slowly, and maintained a significantly higher level on 4 DAS ($p < 0.05$). The change of soluble protein was shown in **Figure 4D**. The content of soluble protein increased in the first 3 days of the two treatments. Compared with the C_2H_4 treatment, C_2H_4-H_2S co-treatment sustained a significantly higher level of soluble protein content from day 3 to day 7 ($p < 0.01$ or $p < 0.05$), suggesting that H_2S could alleviate the degradation of protein in tomato fruit during storage.

Effect of H_2S on the Contents of Reducing Sugar, Titratable Acid (TA) and Ascorbic Acid, the Ratio of the Reducing Sugar to Titratable Acids

The change of reducing sugar in tomato fruit is shown in **Figure 5A**. The contents of reducing sugar showed a downward trend in the two treatment groups. Reducing sugar contents in the C_2H_4-H_2S co-treatment had higher level from 2 to 7 days than that those of C_2H_4 treatment. **Figure 5B** showed that TA content decreased gradually in the two treatments. The C_2H_4-H_2S co-treatment sustained a significantly lower level of TA than C_2H_4 treatment from 1 to 6 days ($p < 0.01$ or $p < 0.05$).

The sweetness and acidity of the fruit are the important indicators for evaluating the flavor. As shown in **Figure 5C**, in C_2H_4 treatment, the ratio decreased slightly till 4 DAS, then increased gradually. Meanwhile, the ratio sustained a higher level in the C_2H_4-H_2S co-treatment on 2, 3, 6 DAS.

Ascorbic acid is an important nutrient for tomato fruits. As shown in **Figure 5D**, ascorbic acid contents in both treatments increased gradually and peaked on 4 DAS followed by a decrease. However, there is no significant differences between the two treatments.

Role of H_2S on the Transcription of Metabolism and Ripening Related Genes

As shown in **Figure 6A**, the transcript level of beta-amylase encoding gene *BAM3* increased gradually till day 5 in ethylene-treated tomatoes, whereas ethylene + H_2S treatment induced the expression of *BAM3* on day 1 and reduced the expression on day 5. **Figures 6B,C** showed the changes of UDP glucose: flavonoid-3-O-glucosyltransferase encoding genes *UFGT73* and *UFGT5* during tomato storage, respectively. The expression of *UFGT73* fluctuated and H_2S induced lower transcript level on

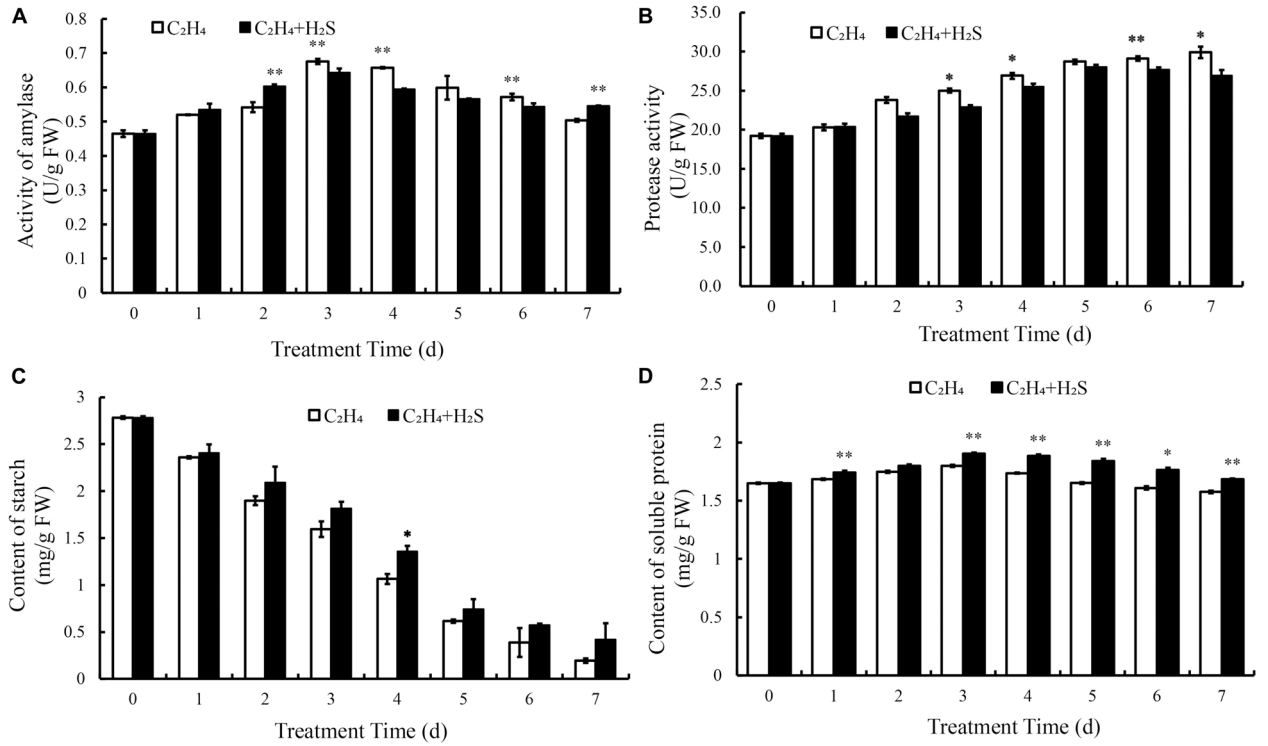

FIGURE 4 | Effect of C_2H_4 and C_2H_4-H_2S on activity of amylase **(A)**, protease activity **(B)**, content of starch **(C)** and content of soluble protein **(D)**. Data are presented as means ± SD (n = 3). The symbols * and ** stand for significant difference between C_2H_4 and C_2H_4-H_2S at $p < 0.05$ and $p < 0.01$, respectively.

day 5. However, H_2S enhanced the expression of *UFGT5* on day 1 while attenuated the expression on day 5 in comparison to C_2H_4 treatment. The transcription of several ripening related transcription factor *ERF003*, *DOF22* and *WRKY51* were also analyzed and shown in **Figures 6D–F**, respectively. Generally, *ERF003* expression showed an increasing trend during storage in C_2H_4 group. The increase of *ERF003* expression on day 5 was significantly inhibited by additional H_2S treatment, though H_2S induced a mild increase of *ERF003* expression on days 1 and 3. Besides, C_2H_4 treatment induced higher expression of *DOF22* on day 1 followed by a decrease, whereas the increase in *DOF22* expression was significantly attenuated by additional H_2S treatment. An increase in *WRKY51* expression was observed in both treatments on day 1. Additional H_2S was found to inhibit the expression of *WRKY51* on day 5 and reverse trend was observed on day 3. Thus, the modulation of metabolism and ripening related gene expression by H_2S may contribute to changes in nutrient metabolism.

PCA Analysis, Correlation Analysis, and Heatmap of the Changes in Bioactive Substances in Tomato Fruits

Principal component analysis analysis was performed in **Table 1** and shown in **Figure 7**. The contribution rate of PC1, PC2, and PC3 was 47.64, 38.42, and 6.3%, respectively. In PC1, TA, protease activity and starch were the main factors. In PC2, flavonoid, chlorophyll b, and amylase activity were the main factors, while, in PC3, ascorbic acid was the main factor.

Correlation analysis of various bioactive substances are shown in **Figure 8A**. Starch and reducing sugar showed a significant negative correlation with ascorbic acid, total phenols, and anthocyanin. Meanwhile, starch and reducing sugar had a significant positive correlation with titratable acid and chlorophyll. Chlorophyll (including chlorophyll a, chlorophyll b) showed a positive correlation with flavonoids, carotenoids, TA, whereas had a negatively correlation with anthocyanins. From the **Figure 8A**, it can be clearly seen that carotenoids have significant color differences in the C_2H_4 treatment and C_2H_4 + H_2S co-treatment, indicating that under the conditions of ethylene fumigation, H_2S could significantly enhance correlation of carotenoids with other indicators.

As shown in **Figure 8B**, in general, protease activity, anthocyanins, total phenols, ascorbic acid were gradually increased with the storage time; starch, reducing sugar, titratable acid were gradually decreased. Content of soluble protein, activity of amylase, contents of chlorophyll b and flavonoids were increased firstly, reached the highest level on day 2 or day 3, and then gradually decreased with the storage time. Comparing with C_2H_4 treatment, the content of reducing sugar, content of chlorophyll b, content of chlorophyll reached the highest level in the C_2H_4 + H_2S co-treatment later, indicating that under the conditions of ethylene application, H_2S could slow the degradation of reducing sugar and chlorophyll.

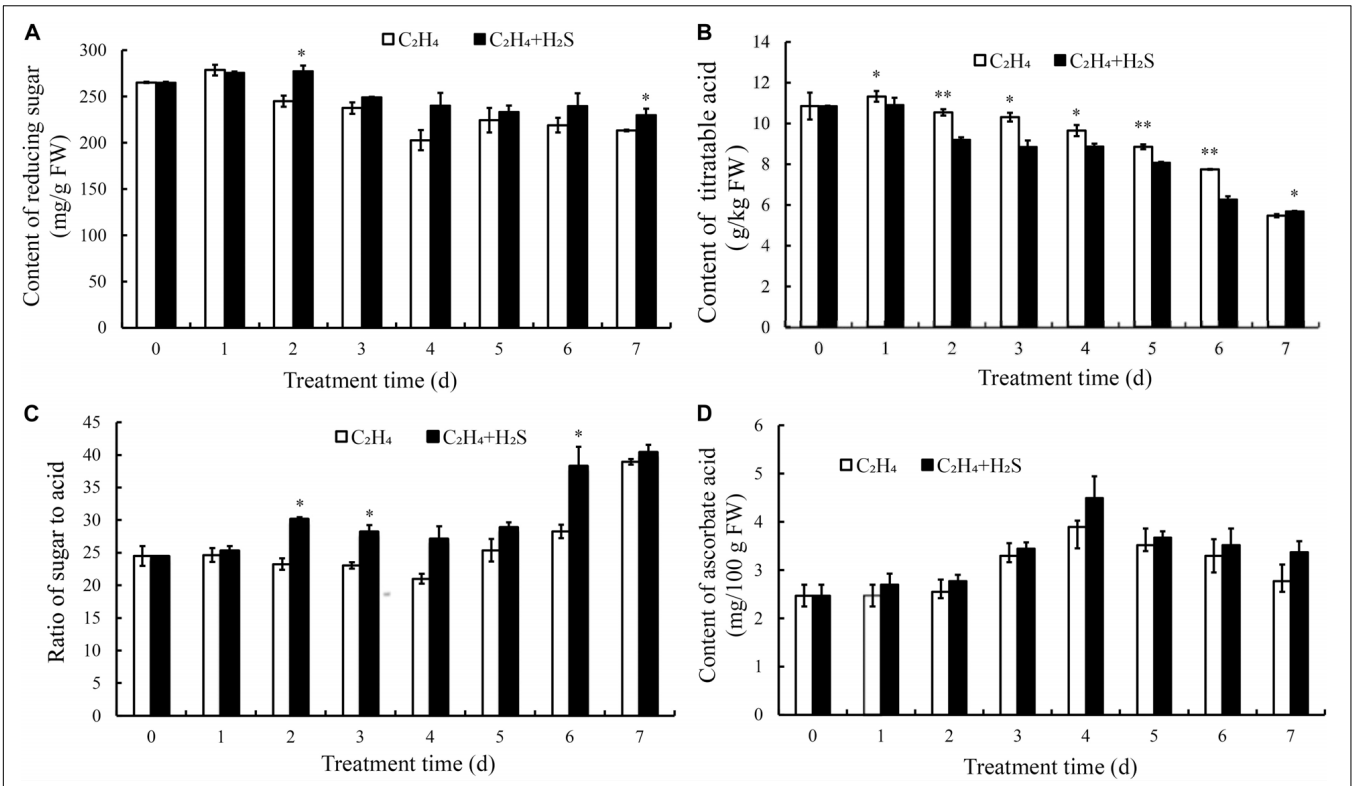

FIGURE 5 | Changes of contents of reducing sugar **(A)**, titratable acid **(B)**, the ratio of sugar to acid **(C)** and ascorbic acid **(D)** in C_2H_4 treatment and C_2H_4-H_2S co-treatment. Data are presented as means ± SD ($n = 3$). The symbols * and ** stand for significant difference between C_2H_4 and C_2H_4-H_2S at $p < 0.05$ and $p < 0.01$, respectively.

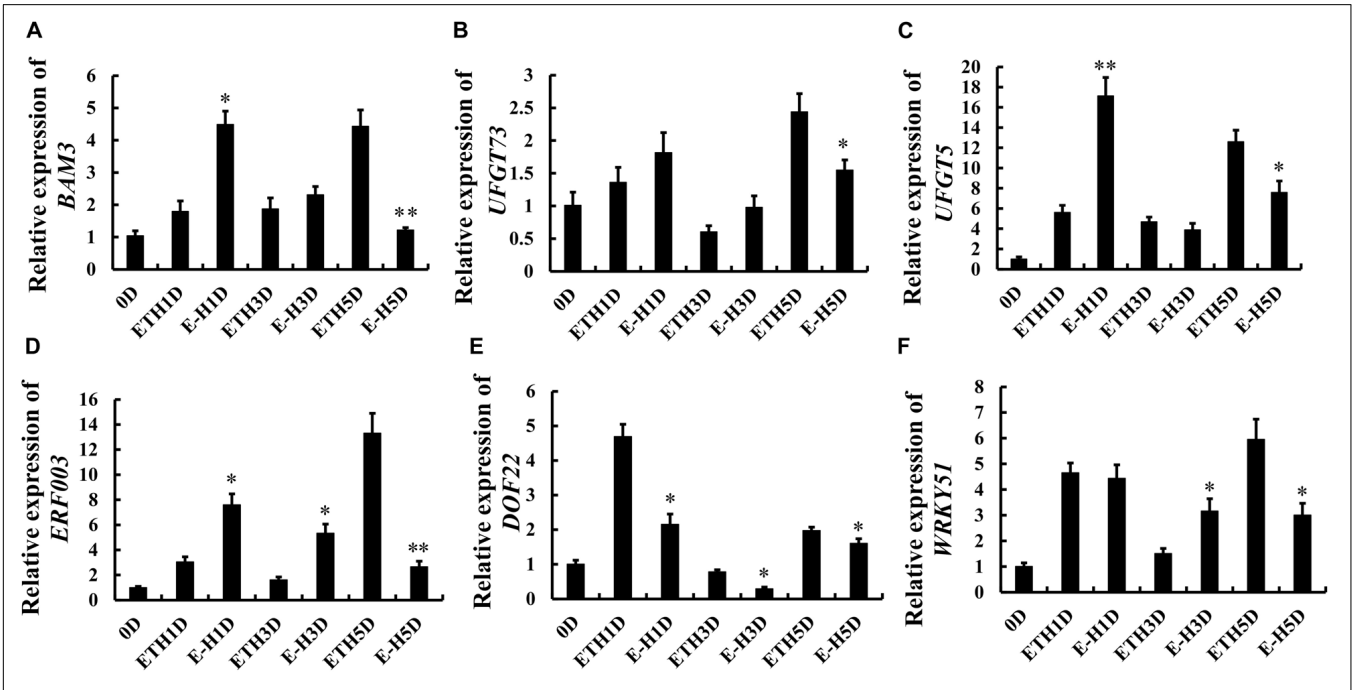

FIGURE 6 | Changes in the gene expression of beta-amylase encoding gene *BAM3* **(A)**, *UFGT73* **(B)**, *UFGT5* **(C)**, ethylene response factor *ERF003* **(D)**, *DOF22* **(E)**, *WRKY51* **(F)** in tomato fruit during storage after C_2H_4 and C_2H_4 + H_2S treatment for 1 day. Error bars indicate standard error ($n = 3$). Asterisks indicate significant differences between C_2H_4 (ETH) and C_2H_4 + H_2S (E-H) co-treated fruit according to the Student's *t*-test (*$p < 0.05$, **$p < 0.01$).

TABLE 1 | The factors score of all the metabolites by principal component analysis in tomato fruits.

Metabolites	Component 1	Component 2	Component 3
Content of titratable acid (C_2H_4 + H_2S)	0.975	0.18	
Protease activity (C_2H_4)	−0.95		0.272
Content of chlorophyll b (C_2H_4 + H_2S)	0.948	0.101	−0.25
Content of starch (C_2H_4 + H_2S)	0.939	0.156	−0.228
Content of titratable acid (C_2H_4)	0.895	0.427	
Content of Anthocyanidin (C_2H_4 + H_2S)	−0.88	0.191	0.276
Protease activity (C_2H_4 + H_2S)	−0.871		0.376
Content of total phenol (C_2H_4 + H_2S)	−0.806	0.535	0.133
Content of chlorophyll a (C_2H_4)	0.796	0.522	−0.109
Content of reducing sugar (C_2H_4)	0.783		−0.537
Content of reducing sugar (C_2H_4 + H_2S)	0.776	0.252	−0.529
Content of total phenol (C_2H_4)	−0.697	0.427	0.237
Content of chlorophyll (C_2H_4)	0.69	0.645	
Content of Anthocyanidin (C_2H_4)	−0.633	0.581	0.445
Content of flavonoid (C_2H_4 + H_2S)		0.952	−0.274
Content of flavonoid (C_2H_4)		0.95	0.143
Content of chlorophyll b (C_2H_4 + H_2S)		0.93	0.195
Activity of amylase (C_2H_4 + H_2S)	−0.37	0.904	0.15
Content of chlorophyll (C_2H_4 + H_2S)	0.411	0.895	
Content of soluble protein (C_2H_4)	0.378	0.876	0.172
Content of soluble protein (C_2H_4 + H_2S)	−0.169	0.83	0.522
Content of chlorophyll b (C_2H_4)	0.436	0.798	
Content of carotenoids (C_2H_4 + H_2S)	0.111	0.767	0.191
Content of chlorophyll a (C_2H_4 + H_2S)	0.633	0.761	−0.124
Activity of amylase (C_2H_4)	−0.268	0.702	0.631
Content of ascorbic acid (C_2H_4)	−0.408	0.259	0.865
Content of ascorbic acid (C_2H_4 + H_2S)	−0.516	0.19	0.81
Content of carotenoids (C_2H_4)	−0.39		

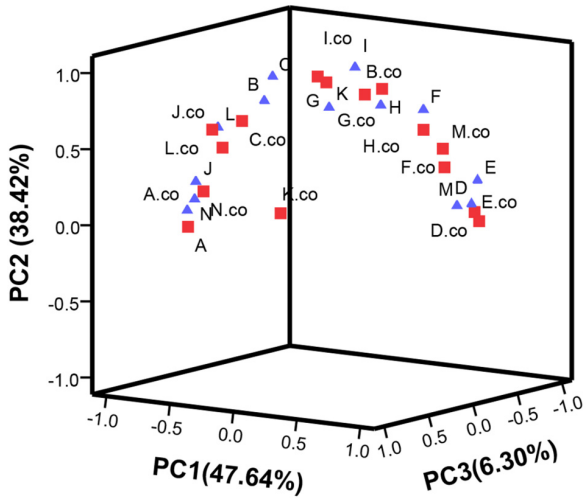

FIGURE 7 | Principal component analysis the main metabolites of post-harvest tomato fruits. PC1∼PC3 were respectively represented the contribution rate of principal components. C_2H_4 treatment groups were marked as "co" and square, C_2H_4-H_2S treatment groups were marked by triangle. Metabolites are expressed by A∼N. (A) Protease activity, (B) Soluble protein, (C) Activity of amylase, (D) Starch content, (E) Reducing sugar, (F) Chlorophyll a, (G) Chlorophyll b, (H) Chlorophyll, (I) flavonoid, (J) anthocyanins, (K) Carotenoids, (L) Total phenol, (M) Titratable acid, (N) Ascorbic acid. Data represent the normalized mean values of three independent biological replicates.

DISCUSSION

Ethylene, a gaseous hormone with a simple structure, regulates many processes of plant growth and development, including root hair formation, flowering, the senescence and abscission of fruit and leaf, etc. (Dugardeyn and Van Der Straeten, 2008). In the ripening of climacteric fruits, ethylene biosynthesis system 2 called "autocatalytic synthesis" accounts for massive ethylene production (Bapat et al., 2010). Besides, exogenous application of ethylene will hasten ripening process by initiating a signaling cascade. Researchers have developed different means to slowing down post-ripening process in fleshy fruit by genetic engineering or ethylene inhibitor (Bapat et al., 2010). H_2S, with the odor of rotten eggs, has been found to participate in varied physiological processes in both animal and plant after the discovery of the physiological roles of nitric oxide (NO) and carbon monoxide (CO) (Rochette and Vergely, 2008). In plants, H_2S has been revealed as a crucial regulator in multiple physiological processes, including seed germination, root morphogenesis, photosynthesis, and flower senescence (Zhang et al., 2008, 2009, 2010, 2011). Recently, it was reported that H_2S could induce changes in transcriptome and inhibit ethylene production, delay the ripening and senescence of kiwifruits and maintain higher contents of nutrients during storage (Zhu et al., 2014; Lin et al., 2020). Moreover, H_2S delayed the loss of chlorophyll and respiration in leafy vegetables by inhibiting ethylene production and action (Ubeed et al., 2017).

In this study, the antagonizing effect of C_2H_4 and H_2S on various bioactive substances were estimated in tomato fruits during the post-harvest storage. Color is an important characteristic that reflects the ripening stage of tomato fruit. It has shown that the color change of fruits is closely related to chlorophyll, carotenoids and anthocyanins. In our experiments, as shown in **Figures 2A–C**, comparing with C_2H_4 treatment, C_2H_4-H_2S co-treatment sustained a higher level of chlorophyll and anthocyanin during storage period, but remained a lower level of flavonoid. The similar phenomenon was reported in broccoli, water spinach as well as other

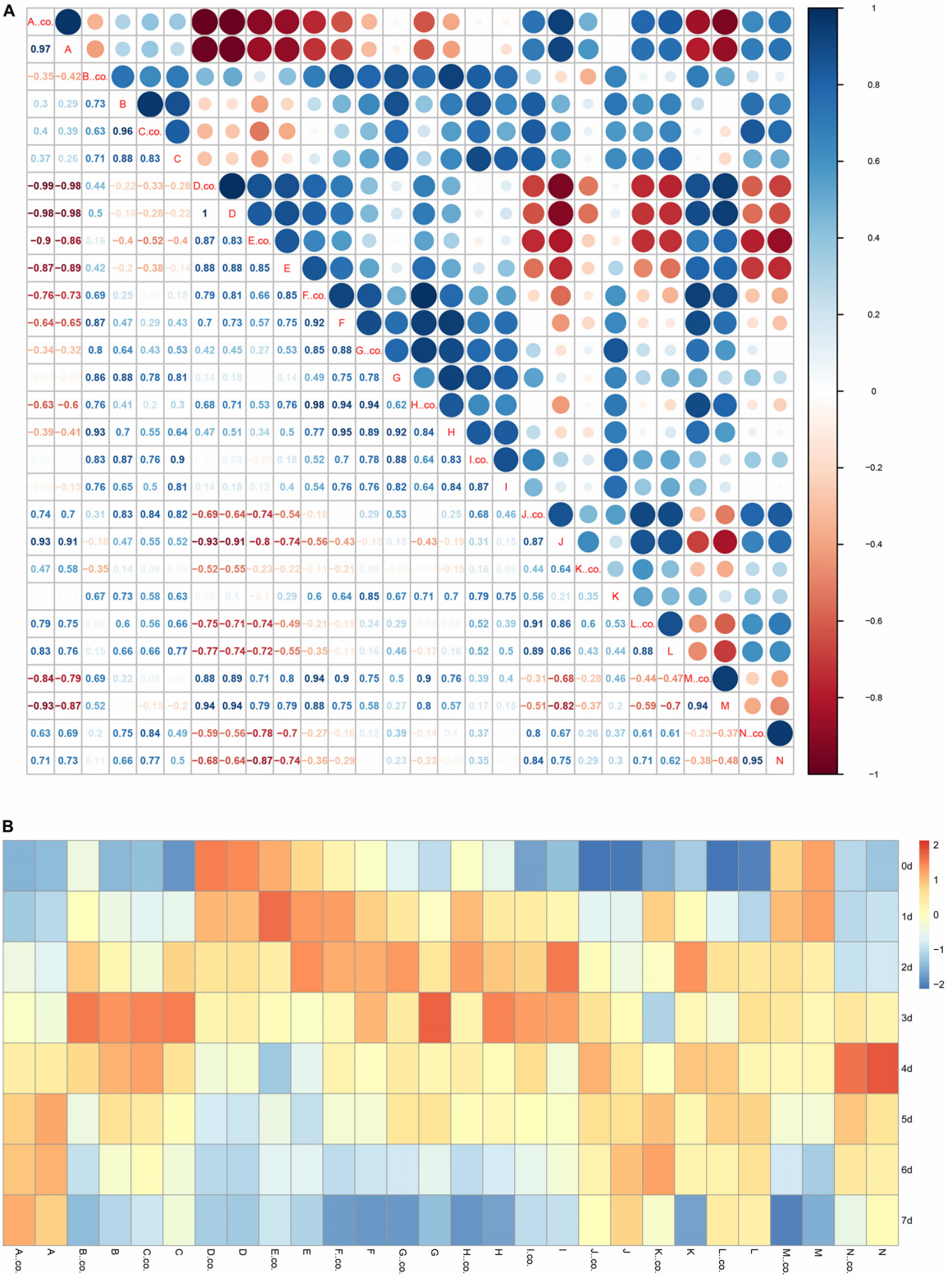

FIGURE 8 | Correlation analysis **(A)** and the heatmap **(B)** among the parameters of bioactive compounds. **(A)** The correlation analysis the relationship among bioactive compounds. Correlation coefficient was analyzed using R scripts. **(B)** The heatmap analyzed the change of bioactive compounds in the storage periods of tomato fruit. co- indicated control group (C_2H_4), co-treatment group no marked. (A) Protease activity, (B) Soluble protein, (C) Activity of amylase, (D) Starch content, (E) Reducing sugar, (F) Chlorophyll a, (G) Chlorophyll b, (H) Chlorophyll, (I) flavonoid, (J) anthocyanins, (K) Carotenoids, (L) Total phenol, (M) Titratable acid, (N) Ascorbic acid.

living plants (Li et al., 2014; Hu et al., 2015). Correlation analysis showed that chlorophyll has a positive correlation with flavonoids, carotenoids, however, has a negative correlated with anthocyanins (**Figure 8A**). The shift of the pigments reflects the tomato ripening stage, which provides a good basis for assessing fruit ripening. However, H_2S could delay the color changes of tomato and slow the ripening process of tomato fruit. Moreover, H_2S was closely associated with chlorophyll degradation and anthocyanin biosynthesis. It was reported chlorophyllase (CHL) and pheophytinase (PPH) are required in chlorophyll degradation (Schelbert et al., 2009). Moreover, UDP glucose: flavonoid-3-*O*-glucosyltransferase (UFGT) catalyzes anthocyanidins to glucosylated anthocyanins in litchi during fruit coloration (Zhao et al., 2012). In the present research, we found that H_2S up-regulated the expression of *UFGT5* in the early stage of storage which may contribute to accumulated anthocyanin in H_2S-treated tomato fruits. However, the regulating role of H_2S on CHL/PPH in delaying ripening and senescence still needs further study.

H_2S can maintain the well-appearance of post-harvest broccoli and meanwhile higher nutrient contents, such as, ascorbic acid, reducing sugar and soluble protein than C_2H_4 treatment (Li et al., 2014). In the present study, ascorbic acid, reducing sugar, soluble protein and starch were also determined in tomato during post-harvest storage. As shown in **Figures 4C,D**, **5A,D**, tomato fruit with C_2H_4-H_2S co-treatment could sustain higher level of ascorbic acid, reducing sugar and soluble protein, starch than C_2H_4 treatment. In PCA analysis, soluble protein, starch and TA, amylase activity and ascorbic acid were the main factors, which could significantly affect tomato fruit quality during post-harvest storage. Thus, H_2S can alleviate the decreases in ascorbic acid, reducing sugar, soluble protein and starch, strongly supporting the role of H_2S in alleviating the senescence of tomato fruits. RT-qPCR result showed that the expression of beta-amylase encoding gene *BAM3* at late storage stage was inhibited by H_2S treatment. Recently, it is reported that starch degradation was regulated by an ethylene responsive C2H2-type zinc finger transcription factor *AdDof3* in kiwifruit ripening and senescence (Zhang et al., 2018), thereby providing a cue to research the molecular mechanism of H_2S in tomato fruit quality during storage.

Sugar content was the best criteria for evaluating the maturity of the fruit. The ratio of sugar/acid is an index which affects fruit flavor quality. In this study, H_2S could maintain higher level of reducing sugar from 2 to 7 DAS and ascorbic acid contents than those of C_2H_4 treatment (**Figures 5A,D**). It was showed that reducing sugar has an obviously negative correlation with ascorbic acid (**Figure 8A**). Meanwhile, phenolic compounds are second metabolites in many fruits and well-known for their antioxidant potential, and their role in prevention of heart diseases, inflammation, and reducing the incidence of cancer and diabetes (Kaur and Kapoor, 2001). Previous report suggested a strong correlation between total antioxidant activity and total phenolic content (Macoris et al., 2012). The total phenols have a negative correlation with reducing sugar (**Figure 8A**). The results showed that H_2S can effectively inhibit the decrease of reducing sugar and ascorbic acid, indicating that H_2S contributed to improved antioxidant capacity to extend post-harvest storage period.

In our study, we demonstrated the indispensable role of H_2S in delaying ripening and senescence of tomato fruits during the storage period. Our results showed H_2S could maintained higher levels of metabolites, such as chlorophyll, starch, soluble protein and ascorbic acid. It implied that H_2S might be an endogenous signal which regulated the ripening and senescence of post-harvest fruits by repression of the effect of ethylene.

DATA AVAILABILITY STATEMENT

The raw data supporting the conclusions of this article will be made available by the authors, without undue reservation, to any qualified researcher.

AUTHOR CONTRIBUTIONS

G-FY, CL, K-KS, K-DH, and HZ conceived and designed the experiments. G-FY, CL, K-KS, G-GH, Z-QH, PJ, and JT performed the experiments. G-FY, CL, FY, and L-YH analyzed the data. G-FY, CL, PJ, and K-DH wrote the manuscript. G-FY, K-DH, and HZ interpreted the data and revised the manuscript.

FUNDING

This work was supported by the National Natural Science Foundation of China (31970312, 31970200, 31901993, 31670278, and 31872078), the Natural Science Foundations of Anhui Province (1908085MC72), the Key Research and Development Program of Anhui Province (201904a06020031), and the Earmarked Fund for the China Agriculture Research System (CARS-10-B1).

SUPPLEMENTARY MATERIAL

The Supplementary Material for this article can be found online at: https://www.frontiersin.org/articles/10.3389/fpls.2020.00584/full#supplementary-material

REFERENCES

Bapat, V. A., Trivedi, P. K., Ghosh, A., Sane, V. A., Ganapathi, T. R., and Nath, P. (2010). Ripening of fleshy fruit: molecular insight and the role of ethylene. *Biotechnol Adv.* 28, 94–107. doi: 10.1016/j.biotechadv.2009.10.002

Bradford, M. M. (1976). A rapid and sensitive method for the quantitation of microgram quantities of protein utilizing the principle of protein-dye binding. *Anal. Biochem.* 72, 248–254. doi: 10.1006/abio.1976.9999

Bureau, S., Ruiz, D., Reich, M., Gouble, B., Bertrand, D., Audergon, J. M., et al. (2009). Application of ATR-FTIR for a rapid and simultaneous determination of sugars and organic acids in apricot fruit. *Food Chem.* 115, 1133–1140.

Chen, Z., Qin, C., Wang, M., Liao, F., Liao, Q., Liu, X., et al. (2019). Ethylene-mediated improvement in sucrose accumulation in ripening sugarcane involves

increased sink strength. *BMC Plant Biol.* 19:285. doi: 10.1186/s12870-019-1882-z

Dubois, M., Van den Broeck, L., and Inzé, D. (2018). The pivotal role of ethylene in plant growth. *Trends Plant Sci.* 23, 311–323. doi: 10.1016/j.tplants.2018.01.003

Dugardeyn, J., and Van Der Straeten, D. (2008). Ethylene: fine-tuning plant growth and development by stimulation and inhibition of elongation. *Plant Sci.* 175, 59–70.

Gapper, N. E., McQuinn, R. P., and Giovannoni, J. J. (2013). Molecular and genetic regulation of fruit ripening. *Plant Mol. Biol.* 82, 575–591. doi: 10.1007/s11103-013-0050-3

Giovannetti, M., Avio, L., Barale, R., Ceccarelli, N., Cristofani, R., Iezzi, A., et al. (2012). Nutraceutical value and safety of tomato fruits produced by mycorrhizal plants. *Br. J. Nutr.* 107, 242–251. doi: 10.1017/S000711451100290X

Guo, J., Wang, S., Yu, X., Dong, R., Li, Y., Mei, X., et al. (2018). Polyamines regulate strawberry fruit ripening by abscisic acid, auxin, and ethylene. *Plant Physiol.* 177, 339–351. doi: 10.1104/pp.18.00245

Hancock, J. T., and Whiteman, M. (2016). Hydrogen sulfide signaling: interactions with nitric oxide and reactive oxygen species. *Ann. N. Y. Acad. Sci.* 1365, 5–14.

Hu, H., Liu, D., Li, P., and Shen, W. (2015). Hydrogen sulfide delays leaf yellowing of stored water spinach (*Ipomoea aquatica*) during dark-induced senescence by delaying chlorophyll breakdown, maintaining energy status and increasing antioxidative capacity. *Postharvest Biol. Technol.* 108, 8–20.

Hu, K. D., Zhang, X. Y., Wang, S. S., Tang, J., Yang, F., Huang, Z. Q., et al. (2019). Hydrogen sulfide inhibits fruit softening by regulating ethylene synthesis and signaling pathway in tomato (*Solanum lycopersicum*). *HortScience* 54, 1824–1830.

Hu, L. Y., Hu, S. L., Wu, J., Li, Y. H., Zheng, J. L., Wei, Z. J., et al. (2012). Hydrogen sulfide prolongs postharvest shelf life of strawberry and plays an antioxidative role in fruits. *J. Agric. Food Chem.* 60, 8684–8693. doi: 10.1021/jf300728h

Karlova, R., Chapman, N., David, K., Angenent, G. C., Seymour, G. B., and de Maagd, R. A. (2014). Transcriptional control of fleshy fruit development and ripening. *J. Exp. Bot.* 65, 4527–4541. doi: 10.1093/jxb/eru316

Kaur, C., and Kapoor, H. C. (2001). Antioxidants in fruits and vegetables: the millennium's health. *Int. J. Food Sci. Technol.* 36, 703–725.

Klee, H. J., and Giovannoni, J. J. (2011). Genetics and control of tomato fruit ripening and quality attributes. *Annu. Rev. Genet.* 45, 41–59. doi: 10.1146/annurev-genet-110410-132507

Lee, H. S., and Wicker, L. (1991). Anthocyanin pigments in the skin of lychee fruit. *J. Food Sci.* 56, 466–468.

Lee, L., Arul, J., Lencki, R., and Castaigne, F. (2010). A review on modified atmosphere packaging and preservation of fresh fruits and vegetables: physiological basis and practical aspects—part I. *Packag. Technol. Sci.* 2010, 315–331.

Li, S. P., Hu, K. D., Hu, L. Y., Li, Y. H., Jiang, A. M., Xiao, F., et al. (2014). Hydrogen sulfide alleviates postharvest senescence of broccoli by modulating antioxidant defense and senescence-related gene expression. *J. Agric. Food Chem.* 62, 1119–1129. doi: 10.1021/jf4047122

Lin, X., Yang, R., Dou, Y., Zhang, W., Du, H., Zhu, L., et al. (2020). Transcriptome analysis reveals delaying of the ripening and cell-wall degradation of kiwifruit by hydrogen sulfide. *J. Sci. Food Agric.* 100, 2280–2287. doi: 10.1002/jsfa.10260

Liu, M., Pirrello, J., Chervin, C., Roustan, J. P., and Bouzayen, M. (2015). Ethylene control of fruit ripening: revisiting the complex network of transcriptional regulation. *Plant Physiol.* 169, 2380–2390.

Macoris, M. S., Marchi, D. R., Janzantti, N. S., and Monteiro, M. (2012). The influence of ripening stage and cultivation system on the total antioxidant activity and total phenolic compounds of yellow passion fruit pulp. *J. Sci. Food Agric.* 92, 1886–1891. doi: 10.1002/jsfa.5556

Miller, G. L. (1959). Use of dinitrosalicylic acid reagent for determination of reducing sugar. *Anal. Chem.* 31, 426–428.

Nath, A., Bagchi, B., Misra, L. K., and Deka, B. C. (2011). Changes in postharvest phytochemical qualities of broccoli florets during ambient and refrigerated storage. *Food Chem.* 127, 1510–1514.

Pirie, A., and Mullins, M. G. (1976). Changes in anthocyanin and phenolics content of grapevine leaf and fruit tissues treated with sucrose, nitrate and abscisic acid. *Plant Physiol.* 58, 468–472. doi: 10.1104/pp.58.4.468

Reimerdes, E. H., and Klostermeyer, H. (1976). Determination of proteolytic activities on casein substrates. *Methods Enzymol.* 45, 26–28.

Rochette, L., and Vergely, C. (2008). Hydrogen sulfide (H2S), an endogenous gas with odor of rotten eggs might be a cardiovascular function regulator. *Ann. Cardiol. Angeiolo.* 57, 136–138. doi: 10.1016/j.ancard.2008.02.014

Schelbert, S., Aubry, S., Burla, B., Agne, B., Kessler, F., Krupinska, K., et al. (2009). Pheophytin pheophorbide hydrolase (pheophytinase) is involved in chlorophyll breakdown during leaf senescence in *Arabidopsis*. *Plant Cell* 21, 767–785. doi: 10.1105/tpc.108.064089

Staden, J. F. V., and Mulaudzi, L. V. (2000). Flow injection spectrophotometric assay of α-amylase activity. *Anal. Chim. Acta.* 421, 19–25.

Su, L., Diretto, G., Purgatto, E., Danoun, S., Zouine, M., Li, Z., et al. (2015). Carotenoid accumulation during tomato fruit ripening is modulated by the auxin-ethylene balance. *BMC Plant Biol.* 15:114. doi: 10.1186/s12870-015-0495-4

Ubeed, H. M. S. A., Wills, R. B. H., Bowyer, M. C., Vuong, Q. V., and Golding, J. B. (2017). Interaction of exogenous hydrogen sulphide and ethylene on senescence of green leafy vegetables. *Postharvest Biol. Technol.* 133, 81–87.

Vinha, A. F., Barreira, S. V., Costa, A. S., Alves, R. C., and Oliveira, M. B. (2014). Organic versus conventional tomatoes: influence on physicochemical parameters, bioactive compounds and sensorial attributes. *Food Chem. Toxicol.* 67, 139–144. doi: 10.1016/j.fct.2014.02.018

Wellburn, A. R. (1994). The spectral determination of chlorophylls a, and b, as well as total carotenoids, using various solvents with spectrophotometers of different resolution. *J. Plant Physiol.* 144, 307–313.

Yao, G. F., Wei, Z. Z., Li, T. T., Tang, J., Huang, Z. Q., Yang, F., et al. (2018). Modulation of enhanced antioxidant activity by hydrogen sulfide antagonizing ethylene in tomato fruit ripening. *J. Agri. Food Chem.* 66, 10380–10387. doi: 10.1021/acs.jafc.8b03951

Zhang, A. D., Wang, W. Q., Tong, Y., Li, M. J., Grierson, D., Ferguson, I., et al. (2018). Transcriptome analysis identifies a zinc finger protein regulating starch degradation in kiwifruit. *Plant Physiol.* 178, 850–863. doi: 10.1104/pp.18.00427

Zhang, H., Dou, W., Jiang, C. X., Wei, Z. J., Liu, J., and Jones, R. L. (2010). Hydrogen sulfide stimulates β-amylase activity during early stages of wheat grain germination. *Plant Signal Behav.* 5, 1031–1033.

Zhang, H., Hu, L. Y., Hu, K. D., He, Y. D., Wang, S. H., and Luo, J. P. (2008). Hydrogen sulfide promotes wheat seed germination and alleviates oxidative damage against copper stress. *J. Integr. Plant Biol.* 50, 1518–1529. doi: 10.1111/j.1744-7909.2008.00769.x

Zhang, H., Hu, S. L., Zhang, Z. J., Hu, L. Y., Jiang, C. X., Wei, Z. J., et al. (2011). Hydrogen sulfide acts as a regulator of flower senescence in plants. *Postharvest Biol. Technol.* 60, 251–257.

Zhang, H., Tang, J., Liu, X. P., Wang, Y., Yu, W., Peng, W. Y., et al. (2009). Hydrogen sulfide promotes root organogenesis in *Ipomoea batatas*. *Salix matsudana* and *Glycine max*. J. Integr. Plant Biol. 51, 1086–1094. doi: 10.1111/j.1744-7909.2009.00885.x

Zhang, L., Li, S., Liu, X., Song, C., and Liu, X. (2012). Effects of ethephon on physicochemical and quality properties of kiwifruit during ripening. *Postharvest Biol. Technol.* 65, 69–75.

Zhao, Z. C., Hu, G. B., Hu, F. C., Wang, H. C., Yang, Z. Y., and Lai, B. (2012). The UDP glucose: flavonoid-3-glucosyltransferase, gene regulates anthocyanin biosynthesis in litchi (*Litchi chinesis* Sonn.) *during fruit coloration*. *Mol. Biol. Rep.* 39, 6409–6415. doi: 10.1007/s11033-011-1303-3

Zheng, J. L., Hu, L. Y., Hu, K. D., Wu, J., Yang, F., and Zhang, H. (2016). Hydrogen sulfide alleviates senescence of fresh-cut apple by regulating antioxidant defense system and senescence-related gene expression. *HortScience* 51, 152–158.

Zhu, L. Q., Wang, W., Shi, J. Y., Zhang, W., Shen, Y., Du, H., et al. (2014). Hydrogen sulfide extends the postharvest life and enhances antioxidant activity of kiwifruit during storage. *J. Sci. Food Agric.* 94, 2699–2704. doi: 10.1002/jsfa.6613

Conflict of Interest: The authors declare that the research was conducted in the absence of any commercial or financial relationships that could be construed as a potential conflict of interest.

frontiers in Plant Science

ORIGINAL RESEARCH
published: 20 May 2020
doi: 10.3389/fpls.2020.00543

Exogenous Nitric Oxide Enhances Disease Resistance by Nitrosylation and Inhibition of *S*-Nitrosoglutathione Reductase in Peach Fruit

Zifei Yu[1†], Jixuan Cao[1†], Shuhua Zhu[2], Lili Zhang[2], Yong Peng[1] and Jingying Shi[1*]*

[1] Key Laboratory of Food Processing Technology and Quality Control in Shandong Province, College of Food Science and Engineering, Shandong Agricultural University, Tai'an, China, [2] College of Chemistry and Material Science, Shandong Agricultural University, Tai'an, China

OPEN ACCESS

Edited by:
Cai-Zhong Jiang, Crops Pathology and Genetics Research Unit, USDA-ARS, United States

Reviewed by:
David Obenland, San Joaquin Valley Agricultural Sciences Center, United States
Mirko Zaffagnini, University of Bologna, Italy

***Correspondence:**
Yong Peng
pengyongxyz@sina.com
Jingying Shi
jyshi80@163.com

† These authors have contributed equally to this work

Specialty section:
This article was submitted to Crop and Product Physiology, a section of the journal Frontiers in Plant Science

Received: *31 January 2020*
Accepted: *09 April 2020*
Published: *20 May 2020*

Citation:
Yu Z, Cao J, Zhu S, Zhang L, Peng Y and Shi J (2020) Exogenous Nitric Oxide Enhances Disease Resistance by Nitrosylation and Inhibition of S-Nitrosoglutathione Reductase in Peach Fruit. Front. Plant Sci. 11:543. doi: 10.3389/fpls.2020.00543

Nitric oxide (NO), a signaling molecule, participates in defense responses during plant–pathogen interactions. *S*-Nitrosoglutathione (GSNO) is found to be an active intracellular NO storage center and regulated by *S*-nitrosoglutathione reductase (GSNOR) in plants. However, the role of GSNOR in NO-induced disease resistance is not clear. In this research, the effects of NO and GSNOR inhibitor (N6022) on the defense response of harvested peach fruit to *Monilinia fructicola* infection were investigated. It was found that the disease incidence and lesion diameter of peach fruits were markedly ($P < 0.05$) reduced by NO and GSNOR inhibitor. However, the expression of *GSNOR* was significantly inhibited ($P < 0.05$) by NO only during 2–6 h. Analyses using iodo-TMT tags to detect the nitrosylation sites of GSNOR revealed that the sulfhydryl group of the 85-cysteine site was nitrosylated after NO treatment in peach fruit at 6 and 12 h, suggesting that exogenous NO enhances disease resistance via initial inhibition of gene expression and the *S*-nitrosylation of GSNOR, thereby inhibiting GSNOR activity. Moreover, NO and GSNOR inhibitor enhanced the expression of systemic acquired resistance (SAR)-related genes, such as pathogenesis-related gene 1 (*PR1*), nonexpressor of *PR1* (*NPR1*), and TGACG-binding factor 1 (*TGA1*). These results demonstrated that *S*-nitrosylation of GSNOR protein and inhibition of GSNOR activity contributed to the enhanced disease resistance in fruit.

Keywords: *Prunus persica*, nitric oxide, *S*-nitrosoglutathione reductase, brown rot, nitrosylation

INTRODUCTION

Peach [*Prunus persica* (L.) Batsch] fruit is rich in nutrients that provide favorable growth conditions for pathogenic bacteria. In addition, due to the high temperature and environmental humidity during the picking period of the peach fruit, the infection and growth of pathogenic bacteria are accelerated, causing a large amount of decay of the peach fruit, resulting in huge economic losses. Brown rot caused by *Monilinia fructicola* is severely destructive to stone fruits, involving in cherries, plums, and peaches (Hu et al., 2011).

At present, cold storage and chemical fungicides are widely used to inhibit brown rot development of peach fruit. Studies have shown that cold storage can effectively control

M. fructicola disease by delaying spore germination (Sommer, 1985). However, peach fruit is very sensitive to low temperature, resulting in chilling injury during cold storage. Chemical fungicides can inhibit brown rot (Adaskaveg et al., 2005), but long-term use of chemicals may induce several problems such as fungicide resistance, chemicals residues on fruits, and environmental pollution. Therefore, the development of safe and effective methods is necessary to control brown rot in stone fruit.

Induced resistance based on biotic or abiotic activation of certain cellular defense responses is considered a sustainable strategy to inhibit pathogen invasion and reduce postharvest decay (Romanazzi et al., 2016). Nitric oxide (NO) is an active molecule with high fat solubility that can diffuse rapidly through the cell membrane. NO is also a gaseous radical. NO and NO-derived molecules are collectively referred to as reactive nitrogen species (RNS) (Corpas et al., 2007). Less is known about the role of NO-derived molecules in the interactions of plants with pathogens (Chaki et al., 2009). However, the function of NO as an important RNS in plants has been extensively studied (Corpas et al., 2007; Besson-Bard et al., 2008). NO is involved in various physiological processes in plants, including seed germination, growth, development, maturation, senescence, and stress response (Arasimowicz and Floryszak-Wieczorek, 2007). Moreover, during plant–pathogen interactions, NO participates in defense responses (Romero-Puertas et al., 2004). Salicylic acid (SA)-mediated activation of signaling pathways is an important manifestation of NO-induced resistance in plants (Domingos et al., 2015). Studies have shown that exogenous NO treatment has obvious inhibitory effects on pathogens including *Penicillium expansum*, *Botrytis cinerea*, and *Colletotrichum gloeosporioides* of postharvest fruits (Zheng et al., 2011; Lai et al., 2014; Hu et al., 2019). However, mechanisms of disease resistance induced by NO in harvested peach fruit are not well understood.

Stamler (1994) first proposed the concept of protein nitrosylation modification, that is, the NO group is covalently bonded to the cysteine (Cys) residue of the protein to produce *S*-nitrosothiol (SNO). Nitrosylation can influence the structure, activity, and function of target proteins (Stamler et al., 2001; Chen et al., 2006), thereby affecting the corresponding signal transduction pathways in the cell. Numerous studies confirm that *S*-nitrosylation plays a wide range of roles in different pathological and physiological processes (Hess and Stamler, 2012). Recently, it is found that NO may accomplish long distance signal transduction by protein nitrosylation in plants (Skelly and Loake, 2013; Kulik et al., 2015). *S*-nitrosoglutathione reductase (GSNOR), classified as the alcohol dehydrogenase family, which exists in all species from bacteria to humans, is an important regulatory protein in NO turnover (Liu et al., 2001). Feechan et al. (2005) found that GSNOR, associated with protein nitrosylation in *Arabidopsis*, plays a critical role in disease resistance. GSNOR has attracted more and more attention as an important regulator of nitrosylation of proteins.

S-Nitrosoglutathione (GSNO) is a storage site for the biological activity of NO. GSNOR regulates the levels of GSNO and other *S*-nitrosothiols (SNOs) and protein nitrosylation in eukaryotic cells (Liu et al., 2001). As a key factor in plant disease resistance response, GSNOR causes changes in intracellular redox status by regulating GSNO content, which in turn leads to *S*-nitrosylation of defense-related proteins (Sakamoto et al., 2002; Dìaz et al., 2003; Lee et al., 2008). Post-translational modification of these proteins can cause different defense responses in plants (Rustérucci et al., 2007; Kwon et al., 2012). However, the study of GSNOR in post-harvest fruits has not been reported. Therefore, it is of great significance to elucidate the role of GSNOR in the disease resistance of post-harvest peach fruit.

MATERIALS AND METHODS

Fruit Materials and Treatments

Peach fruit (cultivar "Zhonghuashoutao") were collected from Yiyuan, Shandong Province, China, and selected for uniform size and no mechanical damage. According to previous methods, peach fruit were soaked in either deionized water (served as control), NO solution (15 μmol L^{-1}; diluted with a saturated NO solution made from NO gas), or GSNOR inhibitor [N6022, bought on MCE official website (MedChemExpress)[1]] solution (60 μmol L^{-1}), respectively, for 20 min and dried at room temperature (Gu et al., 2014). A 3 mm × 3 mm × 3 mm wounded site was made on each fruit and inoculated with 20 μl of 1 × 10^5 spores ml^{-1} of brown rot spore suspension. Then, the fruits were stored in a constant temperature and humidity chamber [23°C, 85–90% relative humidity (RH)] to observe the disease development in peach fruit. The disease incidence and lesion diameter were measured at 48 and 72 h, respectively. Six repetitions are set for each treatment, and each repetition contained 30 peaches. Samples of three peach fruits at each time point were taken out from each repetition and cut into small pieces. Then, the pieces were frozen with liquid nitrogen, grinded into power, and stored at −80°C. Moreover, samples of three fruits of each repetition were taken at 0, 6, 12, 24, 48, and 72 h for RNA and protein extraction, enzyme assay, and the content of SNOs, GSNO, glutathione of reduced state (GSH), glutathione disulfide (GSSG), and endogenous NO measurement.

Measurement of GSNOR and GR Activity in Different Treated Peach Fruit

Glutathione reductase (GR) activity was measured according to Knorzer et al. (1996). One half gram peach powder was homogenized in 4 ml of 50 mM phosphate-buffered saline (PBS) [pH 7.0, containing 20% (*v*/*v*) glycerol, 2 mM DL-dithiothreitol (DTT), 2 mM ethylene diamine tetraacetic acid (EDTA), 2% polyvinylpyrrolidone (PVP)]. The supernatant obtained after centrifugation at 20,000 × *g* for 30 min at 4°C was used to determine the enzyme activity. The reaction system included 100 μl supernatant, 3 ml reaction liquid [pH 7.5, containing 50 mM Tris–HCl, 0.5 mM GSSG, 5 mM $MgCl_2$, and 0.2 mM reduced nicotinamide adenine dinucleotide phosphate (NADPH)]. The changes in absorbance at 340 nm were determined.

S-nitrosoglutathione reductase activity was measured following the means of Sakamoto et al. (2002). One half gram

[1]https://www.medchemexpress.cn/

peach powder was extracted with 3 ml assay mixture containing 50 mM HEPES (pH 8.0), 20% (*v*/*v*) glycerol, 10 mM $MgCl_2$, 1 mM EDTA, 1 mM ethylene glycol-bis(2-aminoethylether)-N,N,N′,N′-tetraacetic acid (EGTA), 1 mM benzamidine, and 1 mM ε-aminocaproic acid at 4°C and then centrifuged at 16,000 × *g* for 15 min. Three hundred microliters of supernatant was incubated in 3 ml assay mixture containing 20 mM Tris–HCl (pH 8.0), 0.5 mM EDTA, and 0.2 mM NADH, and the GSNO was mixed to a final concentration of 400 mM to initiate the reaction.

Measurement of SNOs and NO Levels in Differently Treated Peach Fruits

The SNO content was measured according to Frungillo et al. (2013) with some modifications. One half gram peach powder was homogenized in 4 ml of 100 mM phosphate buffer (pH 7.2, containing 100 mM EDTA, 100 mM EGTA), after which centrifugation was carried out at 20,000 × *g* for 30 min at 4°C to obtain the supernatant. One milliliter supernatant was reacted with solution I [containing 1% sulfanilamide, 0.1% *N*-(1-naphthyl) ethylene-diamino dihydrochoride] or solution II [containing 1% sulfanilamide, 0.1% *N*-(1-naphthyl) ethylene-diamino dihydrochoride, 2 mM $HgCl_2$] in a ratio of 1:1. After incubating in the dark for 10 min, the reaction solution was centrifuged at 12,000 × *g* for 5 min. The SNO content in plants was quantified by determining the absorbance difference between solutions II and I at 540 nm. The absorbance at 540 nm was determined using different concentrations of GSNO instead of the enzyme solution, and a standard curve was prepared. The content of SNOs in the plants was calculated according to the value of the standard curve.

The NO content was performed according to the means of Shi et al. (2015). One half gram peach powder was extracted in 3 ml 50 mM glacial acetic acid buffer [pH 3.6, containing 4% (*w*/*v*) zinc acetate], then centrifuged at 10,000 × *g* for 15 min at 4°C. Equal volumes of extraction and Griess reagent (Sigma-Aldrich, St Louis, United States) were mixed and reacted at 25°C for 30 min. The optical density (OD) value at 540 nm was determined.

Measurement of the Content of Endogenous GSNO, GSSG, and GSH in Peach Fruit

The contents of GSNO, GSSG, and GSH were measured according to Hodges and Forney (2000) with minor modifications. One half gram peach powder was dissolved with 5 ml of 5% (*w*/*v*) 5-sulfosalicylic acid and then centrifuged at 12,000 × *g* for 15 min at 4°C. Solution A (containing 100 mM $Na_2HPO_4{\cdot}7H_2O$, 40 mM $Na_2HPO_4{\cdot}H_2O$, 1.8 mM 5,5′-dithiobis-(2-nitrobenzoic acid) (DTNB), 15 mM EDTA, and 0.04% (*w*/*v*) bovine serum albumin (BSA)] and solution B (including 1.0 mM EDTA, 50 mM imidazole, and 0.02% (*w*/*v*) BSA] were prepared and then adjusted to pH 7.2. The GSNO content was measured by mixing 800 μl solution A, 640 μl solution B, 800 μl of 1:25 dilution of extract in 0.5 M K_2HPO_4 buffer (pH 7.0), and 160 μl of 3.0 mM NADPH. The changes in the OD value of the mixed solution at 412 nm were recorded. The GSH content was measured by adding 300 μl of 10 U mol^{-1} glutathione reductase (GR) (100 U) to the above reaction system for 1 min, and the change of OD value at 412 nm for 5 min was measured. The measurement method of GSSG was as follows. 1.0 ml extract was diluted into 1:10 in 0.5 M K_2HPO_4 buffer (pH 6.5, containing 20 μl 2-vinylpyridine) at 25°C for 1 h. Then, 400 μl of solution A and 320 μl of solution B was added, and the change in OD value was determined at 412 nm. The standard curve of GSNO, GSSG, and GSH was prepared, and the content of GSNO, GSSG, and GSH in the sample was calculated according to the standard curve.

Transcript Analyses of *GR*, *GSNOR*, and Defense-Related Gene Expression by Real-Time Quantitative PCR

Total RNA extraction was conducted from samples at various time intervals. One hundred milligrams of the sample was taken, and the RNAprep Pure Polysaccharide Polyphenol Plant Total RNA extraction kit (DP441) produced by Tiangen (Shanghai, China) was used for extraction of the total RNA. The CWBIO HiFiScript cDNA Synthesis Kit (CW2596) was use to synthesize complementary DNA (cDNA) by incubating at 42°C for 50 min, then at 85°C for 5 min. The primers of *GR*, *GSNOR*, *PR1*, *NPR1*, and *TGA1* were designed based on their genetic sequences (**Table 1**). *TEF2* (TC3544) and *tubulin-α* (DY650410) from peach fruit were used as reference genes (Tong et al., 2009). Real-time (RT-PCR) was performed using of the CWBIO UltraSYBR Mixture (CW0957) kit with reaction volumes of 25 μl.

Nitrosylation Site Detection

Some experimental methods involved in the detection of nitrosation sites mainly refer to Gong and Shi (2019) and Xie et al. (2016) with slight modifications. The experimental methods and steps were as follows.

Protein Extraction From Peach Fruit

The peach fruit treated with NO, inoculated with *M. fructicola* then stored for 4, 6, 12, and 24 h, was ground into powder in liquid nitrogen. The sample with lysis buffer [including 8 M urea, 100 mM triethylammonium bicarbonate buffer (TEAB, Sigma-Aldrich, St Louis, MI, United States),

TABLE 1 | Primers used for real-time qPCR analysis.

Gene name	Primer sequences	Tm (°C)	Product size (bp)
GR	F: CCTTCAATCTGGGCTGTA	55	158
	R: ATTGGTGGCTGGGAAA		
GSNOR	F: TGTTCATGATGTTAGTGTTGCG	58	121
	R: TGATTCTACTTTTGCCGTGTTC		
PR1	F: TCTAACACTTGTGCCGATGAC	58	126
	R: ATAGTTGCACCCGATGAAGG		
NPR1	F: CAGATGATGTGAACTTGTGAA	55	71
	R: GTAAGCCGCAGCATAATG		
TGA1	F: GCCTCAGCATCAATGATAGTTG	58	105
	R: TGCTTCTTGGTCATACTTGCTA		

50 mM Iodoacetamide (IAM, Sigma-Aldrich, St Louis, MI, United States), 1% Protease Inhibitor Cocktail (Merck Millipore, Billerica, MA, United States), and 1% Triton X-100] added was sonicated three times on ice. The lysate was incubated at room temperature without light for 30 min, and then, centrifugation was performed at 20,000 × *g* at 4°C for 10 min to remove the remaining debris. Finally, cold 20% TCA was used to precipitate the protein at −20°C for 2 h. The precipitate obtained by centrifugation was washed three times with cold acetone. HES buffer [50 mM TEAB, 1 mM EDTA, and 0.1% sodium dodecyl sulfate (SDS)] was used to redissolve the protein. The protein concentration was measured according to the instructions of the BCA kit (Beyotime Biotechnology, Shanghai, China).

Iodo-TMT Labeling

One milligram protein per treatment was redissolved in 1 ml HES buffer and processed with the iodo-TMT kit (Thermo Fisher Scientific, Waltham, MA, United States). In short, iodo-TMT reagent dissolved in 10 μl MS grade methanol was mixed to the redissolved protein solution; then, 20 μl of 1 M sodium ascorbate was added and mixed briefly. The mixed solution was incubated in the dark at 37°C for 2 h. The reaction was quenched by the addition of 40 μl of 0.5 M DTT (20 mM final concentration) and incubated in darkness at 37°C for 15 min.

Trypsin Digestion

Six volumes of prechilled (−20°C) acetone were used to precipitate the mixed labeled protein at −20°C for at least 2 h and then centrifuged to discard the supernatant. The protein precipitate was dissolved in 8 M urea after washing with cold acetone three times. The protein solution after reduction with 5 mM DTT for 30 min at 56°C was alkylated with 11 mM IAM for 15 min at room temperature without light. The protein samples were diluted with 100 mM TEAB, and the final urea concentration was below 2 M. Trypsin was added at a trypsin-to-protein mass ratio of 1:50 overnight, and a second digestion was performed at a mass ratio of 1:100 trypsin to protein for 4 h. Strata X C18 SPE column (Phenomenex, Torrance, CA, United States) was used for desalting of trypsin-digested peptides. Finally, the peptide was dried under vacuum.

HPLC Fractionation

Fractionation of the samples was carried out by high pH reverse-phase HPLC (EASY-nLC 1000, Thermo Fisher Scientific, Waltham, MA, United States) applying 300 Extend C18 column (5 μM particles, 4.6 mM ID, and 250 mM length; Agilent Technologies, Santa Clara, CA, United States). First, the peptides were dissociated into 80 fractions with a gradient of 2–60% acetonitrile (ACN) in 10 mM NH_4HCO_3 (pH 10) over 80 min. Then, the peptides were combined into four fractions and vacuum dried.

Affinity Enrichment

Tryptic peptides were dissolved in TBS buffer (pH 7.5, 150 mM NaCl, 250 mM Tris–HCl) and incubated with prewashed anti-TMT antibody beads (Thermo Fisher Scientific, Waltham, MA, United States) at 4°C overnight to enrich cysteine nitrosylation peptides The beads were cleaned once with disinfected deionized water after three times with TBS buffer. The peptide bound to the beads was eluted with elution buffer (0.4% TFA, 50% ACN). The eluted peptides were mixed and vacuum dried. The peptides obtained after C18 ZipTips (Millipore, Boston, MA, United States) washing were analyzed by liquid chromatography tandem mass spectrometry (LC-MS/MS).

LC-MS/MS Analysis

Refer to the means of Yang et al. (2018) with minor modifications. The peptides were resuspended in solvent A (containing 0.1% FA and 2% ACN) and separated using an EASY-nLC 1000 UPLC system (Thermo Fisher Scientific, Waltham, MA, United States). The gradient of solvent B (containing 0.1% FA and 98% ACN) included an increase from 6 to 25% over 26 min, 25 to 40% in 8 min, and climbing to 80% in 3 min, then remaining at 80% for the last 3 min. The flowrate was maintained at 400 nl min^{-1}. The peptides were injected into the NSI source for ionization and then analyzed using tandem mass spectrometry (MS/MS) on an Q Exactive™ Plus (Thermo Fisher Scientific, Waltham, MA, United States) coupled online to the ultraperformance liquid chromatography (UPLC).

Statistical Analysis

The MaxQuant search engine (v.1.5.2.8) was used to analysis the resulting MS/MS data. The UniProtKB *Prunus persica* (sequences: 28234. Version: 2016.5.30) database was connected to the reverse decoy database to search for tandem mass spectra. IodoTMT-6plex was selected as the quantification method. The fold-change threshold was set when peptides with quantitative ratios over 1.2 or under 1/1.2 are considered significant. Intensive bioinformatic analyses were then carried out to annotate those quantifiable lysine acetylated targets in response to NO solution treatment, including Gene Ontology (GO) annotation, subcellular localization, Kyoto Encyclopedia of Genes and Genomes (KEGG) pathway annotation, etc. Based on the results, further studies following the quantitative cysteine nitrosylation analysis were suggested. Three repetitions were used in nitrosylation measurement. The compilation and mapping of experimental data were performed using Microsoft Excel 2013 and Sigma Plot 10.0 software. IBM SPSS version 20.0 was used for statistical analysis, and significant ($P < 0.05$) level test was performed using least significant difference (LSD) test.

RESULTS

Effect of NO and GSNOR Inhibitor on Disease Incidence and Lesion Diameter of Peach Fruit Inoculated With *M. fructicola*

The disease incidence and lesion diameter of peach fruit inoculated with *M. fructicola* were significantly ($P < 0.05$) suppressed by NO and GSNOR inhibitor (N6022), and the inhibitory effect of GSONR inhibitor on *M. fructicola* was better than that of NO solution treatment (**Figure 1**). At 36 h, the disease incidence of the control fruit was approximately 15%, and

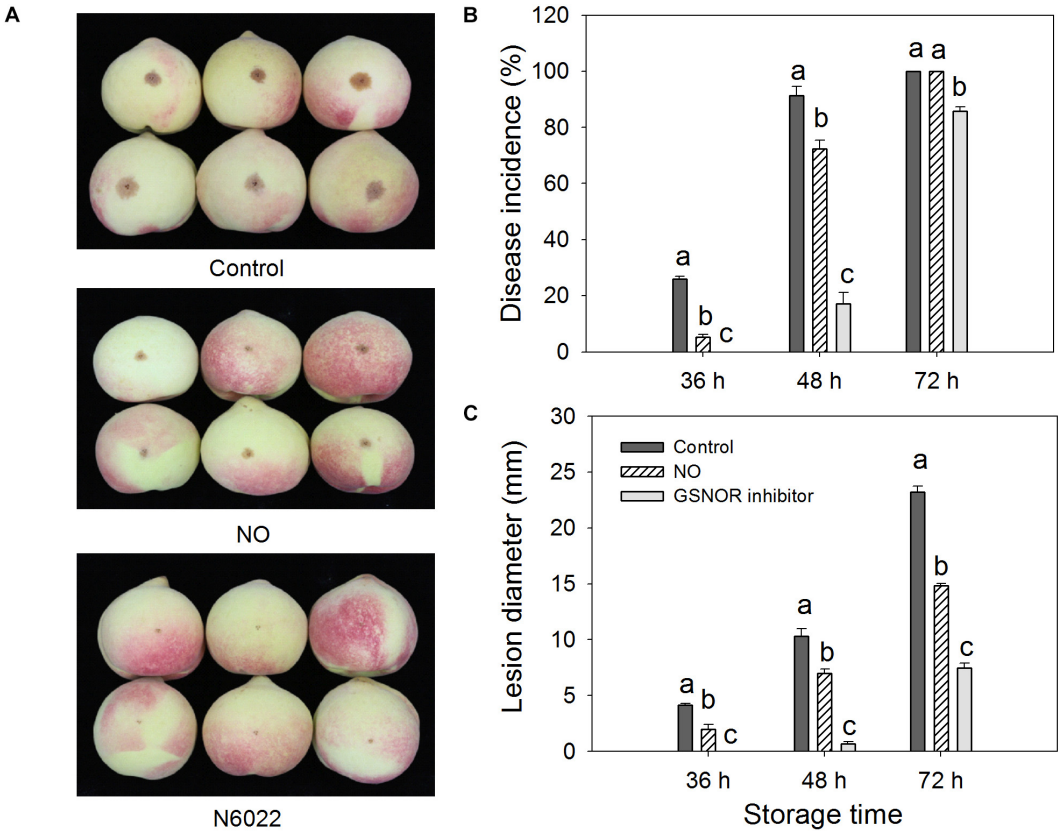

FIGURE 1 | Effect of nitric oxide (NO) or *S*-nitrosoglutathione reductase (GSNOR) inhibitor treatment on the **(A)** disease development (at 48 h after inoculation), **(B)** disease incidence, and **(C)** lesion diameter of peach fruit after inoculation with *M. fructicola* spore suspension (1×10^5 spores ml^{-1}) and then stored at 23°C. Bars represent standard deviations of the means ($n = 6$). Different letters represent significant differences ($p < 0.05$) according to least significant difference (LSD) test.

the average lesion diameter was 2.3 mm, however, the disease symptom was not present on GSNOR inhibitor-treated fruit. During the investigated period, the lesion development on NO-treated or GSNOR inhibitor-treated fruit was lower than that on the control (**Figure 1A**). Moreover, 36 and 48 h, the NO and GSNOR inhibitor-treated fruit exhibited significantly ($P < 0.05$) lower disease incidence than the control (**Figure 1B**). The lesion diameter on the control fruit was 2.1, 1.5, and 1.6 times of NO-treated fruit, and even at 72 h, the lesion diameter on the control fruit was almost 3.1 times that of GSNOR inhibitor-treated peach fruit (**Figure 1C**). These results indicate that treatment with NO and GSNOR inhibitor reduces disease incidence and the extent of lesions. GSNOR inhibitor was the most effective at inhibiting brown rot development.

Effect of NO and GSNOR Inhibitor on the Activity and Gene Expression of GR and GSNOR in Peach Fruit

The activity and gene expression of GR and GSNOR were measured in peach fruit after inoculation with *M. fructicola* (**Figure 2**). Compared with the control, NO and GSNOR inhibitor obviously ($P < 0.05$) enhanced the activity of GR. The enhancement effect of NO on GR activity was very obvious at 6–24 h, but the GR activity was slightly different from the control at 48 and 72 h. The effect of GSNOR inhibitor on GR activity was more obvious than that of NO and GR activity, showing a downward trend at 0–72 h (**Figure 2A**). The activity of GSNOR showed a tendency of increase first and then decrease. Both NO and N6022 inhibited the activity of GSNOR, and the inhibitory effect of N6022 treatment was stronger than that of NO treatment (**Figure 2B**). Furthermore, higher levels of *GR* expression were observed in both NO-treated and GSNOR inhibitor-treated fruit than the control (**Figure 2C**). *GSNOR* expression in peach fruit treated with NO and GSNOR inhibitor was obviously ($P < 0.05$) lower than the control at 2–6 h. The expression of *GSNOR* in all three treatments stabilized at 12 h. GSNOR inhibitors have the most marked inhibitory effect on *GSNOR* gene expression (**Figure 2D**).

Determination of the S-Nitrosylation Site of GSNOR in Peach Fruit After Treated With NO

Nitric oxide-treated and non-treated peach fruits inoculated with *M. fructicola* were quantitatively measured for nitrosylation using iodo-TMT tags. The sulfydryl in Cys-85 of GSNOR was identified as an *S*-nitrosylated residue in peach fruit treated with NO at 6

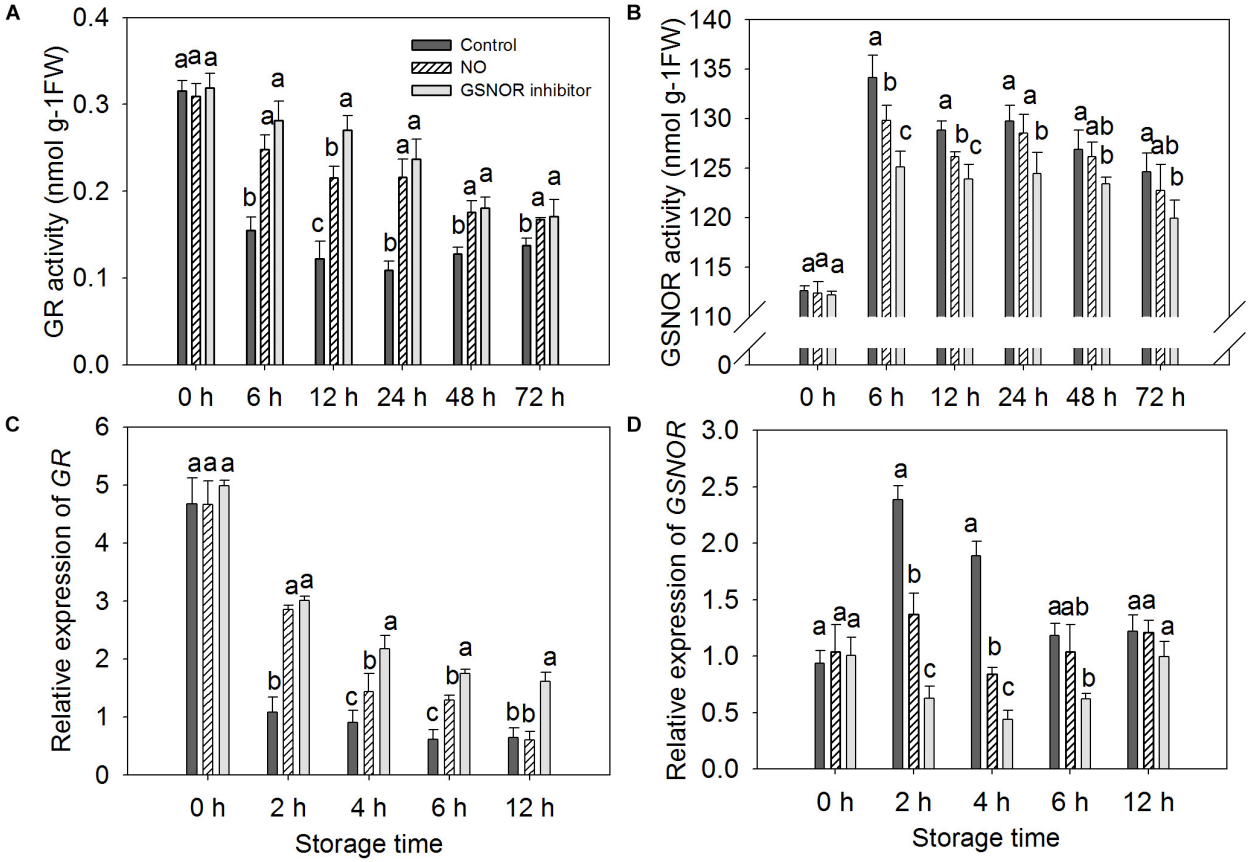

FIGURE 2 | Effect of nitric oxide (NO) or *S*-nitrosoglutathione reductase (GSNOR) inhibitor treatment on the activity of **(A)** glutathione reductase (GR) and **(B)** GSNOR and the **(C)** gene expression of *GR* and **(D)** *GSNOR* of peach fruit storage at 23°C. Vertical bars represent the standard deviation of the means (n = 6). Different letters represent significant differences ($P < 0.05$) according to least significant difference (LSD) test.

and 12 h (**Figure 3A**). The peptide sequences of nitrosylation was KILYTALCHTDAYTWGGKD. To get the 3D structural model of GSNOR, find the GSNOR (M5VJ61) information page on the UniProt official website and click M5VJ61 under "Structure" (**Figure 3B**). From the structure of the model, GSNOR is a dimer containing two subunits, and its ligands include two zinc ion and two nicotinamide adenine dinucleotide.

The content of endogenous NO and SNOs increased from 0 to 12 h and then decreased in both treated and the control fruit from 12 to 48. At 72 h, the content increased slightly but did not change much. The change in endogenous NO content is similar to SNOs (**Figure 4**). Treatment with NO and GSNOR inhibitor increased the levels of SNOs and NO in peach fruit compared to the control (**Figures 4A,B**). GSNOR inhibitor treatment had a stronger effect on the content of SNOs and NO than exogenous NO treatment.

Effect of Different Treatments on the Content of GSH, GSSG, and GSNO

The level of GSH increased from 0 to 72 h in the treated fruit. However, GSH levels in control fruits increased from 0 to 48 h and decreased at 72 h (**Figure 5A**). GSNOR inhibitor treatment enhanced GSH level maximum, NO treatment was the second, and the GSH level of the control peach fruit was relatively low (**Figure 5A**). The change in GSSG content is opposite to that of GSH. GSSG content showed a downward trend within 0–48 h after inoculation with *M. fructicola*. The GSSG content of the control fruits increased at 72 h, but a decrease in GSSG levels was still found in the treated peach fruit (**Figure 5B**). The level of GSNO increased significantly at 0–6 h, and then decreased. It can be seen from the figure that NO and GSNOR inhibitor treatment could obviously ($P < 0.05$) increase the level of GSNO during 0–24 h. However, GSNO content in the three treatment fruits had no significant difference ($P > 0.05$) at 48 h. At 72 h, the content of GSNO in peach fruits treated with GSNOR inhibitor was higher than the other two groups (**Figure 5C**).

Effect of NO and GSNOR Inhibitor on the Expression of Several Defense-Related Genes in Peach Fruit

The expressions of three defense-related genes in peaches pretreated with NO and GSNOR inhibitor were investigated by RT-PCR. NO and GSNOR inhibitor increased the expression levels of *PR1*, *NPR1*, and *TGA1* genes (**Figure 6**). The expression

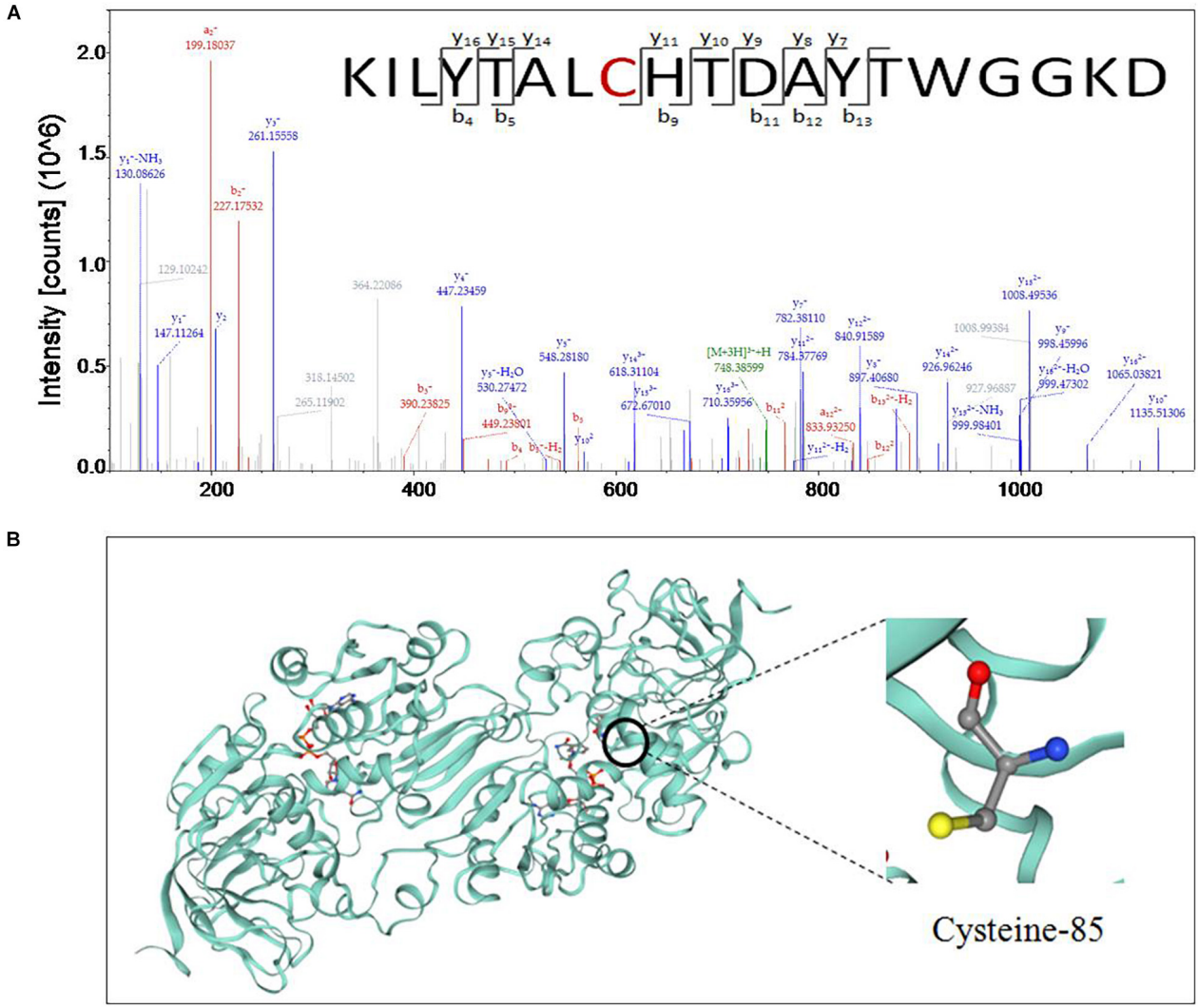

FIGURE 3 | (A) Cys-85 of *S*-nitrosoglutathione reductase (GSNOR) was identified as an *S*-nitrosylated residue by site-specific proteomic mass spectrometry, and **(B)** 3D structure model of GSNOR protein of peach was predicted in Uniprot. Illustrated in the figure is the cysteine located at position 85 of the amino acid sequence.

trend of *PR1* was similar to that of *NPR1*, gradually increasing during 0–48 h. It decreases when it reaches the maximum at 48 h (**Figures 6A,B**). The expression level of *TGA1* in the control fruit was relatively stable, but NO and GSNOR inhibitor significantly ($P < 0.05$) induced *TGA1* gene expression from 24 to 72 h (**Figure 6C**).

DISCUSSION

Nitric oxide involves participating in plant responses to biotic and abiotic stresses as an important signaling molecule (Mur et al., 2006; Carreras and Poderoso, 2007). It is reported that NO has a direct and effective inhibitory effect on a variety of microorganisms (Schairer et al., 2012). However, in our previous studies, low concentration of NO solution could effectively restrict disease development but had no significant inhibition against *M. fructicola in vitro* (Gu et al., 2014). In recent years, more and more studies have shown that NO has obvious inhibitory effects on post-harvest diseases. Treatment of tomato fruit with L-arginine, a precursor of NO, inhibits the expansion of lesion diameter caused by *B. cinerea* (Zheng et al., 2011). In apple fruit, NO donor sodium nitroprusside (SNP) treatment could inhibit virulence of *P. expansum*, causing obviously lower disease incidence and smaller lesion diameter compared to the water treatment (Lai et al., 2014). Hu et al. (2019) showed that NO could significantly increase the resistance of pitaya fruit to *C. gloeosporioides* after harvest, which is consistent with the results observed on the present result in peach fruit.

The pyrrole group located in N6022 is an efficient GSNOR inhibitor with potent inhibitory ability (Sun et al., 2011). The inhibitory effect of N6022 on GSNOR activity has been shown to be safe and effective in animal models of asthma and

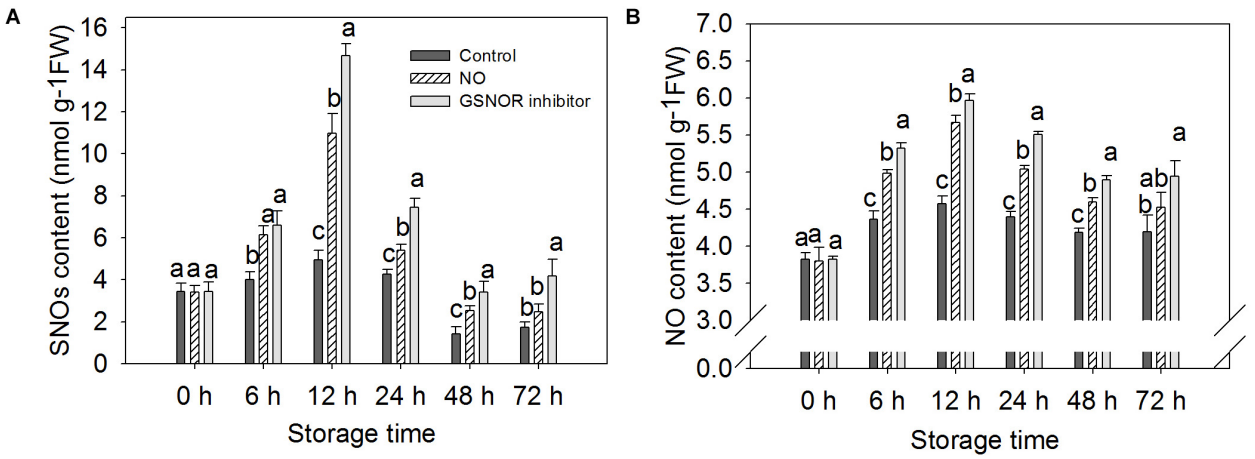

FIGURE 4 | Effect of nitric oxide (NO) or *S*-nitrosoglutathione reductase (GSNOR) inhibitor treatment on the content of **(A)** SNOs and **(B)** NO of peach fruit storage at 23°C. Vertical bars represent the standard deviation of the means ($n = 6$). Different letters represent significant differences ($P < 0.05$) according to least significant difference (LSD) test.

inflammatory disease. As a tight bonding inhibitor, N6022 is currently under application for early clinical research in humans (Green et al., 2012). However, it has not been used in postharvest fruits. The present results show that the GSNOR inhibitor N6022 reduces disease incidence significantly ($P < 0.05$) and enhances the resistance of peach fruit to brown rot while reducing the activity of GSNOR of peaches.

S-nitrosoglutathione reductase regulates the levels of GSNO and SNOs in eukaryotic cells by specifically recognizing and degrading GSNO that can be decomposed into GSSG and ammonia (NH3) (Liu et al., 2001). As the most abundant of endogenous intracellular SNOs, GSNO is considered as a potential NO storage site or transport center in the cell (Butler and Rhodes, 1997; Mayer et al., 1998; Liu et al., 2001). It can transfer NO to the target protein to change the function of the protein (Liu et al., 2001). The present results show that NO-treated fruit had markedly ($P < 0.05$) higher content of GSNO than the control, which contributed to promoting the nitrosylation of the target protein of GSNOR (**Figures 3A**, **5C**). Studies have shown that when plants are infected with pathogenic bacteria, the content of SNOs will increase, suggesting that SNOs play a vital role in signal transduction and host defense (Feechan et al., 2005; Chaki et al., 2009). The present results showed that the content of SNOs increased at 0–12 h, and both NO and GSNOR inhibitor treatments promoted the production of SNOs, which was helpful for the improvement of disease resistance of peach fruit (**Figure 4A**). It is reported that the concentration of NO in the cells increased, and NO could bound to GSH to form GSNO under stress conditions (Liu et al., 2001). Under the catalysis of GR, the oxidized form of glutathione (GSSG) can be readily converted to the reduced state (GSH). GSH is a major intracellular antioxidant that eliminates reactive oxygen species (ROS) (Macdonald et al., 2003). GR maintains a high GSH/GSSG ratio by reducing GSSG to play a key role in the antioxidant defense process (Foyer and Noctor, 2005; Patel and Patra, 2015). The present result showed that exogenous NO and N6022 treatments promoted the degradation of GSSG by increasing the activity of GR, thereby increasing the content of GSH, thus improving the antioxidant capacity of peach fruit.

The accumulation of endogenous NO after inoculation of *Rhizoctonia solani* in cucumber plant may be due to a decrease in GSNOR activity (Nawrocka et al., 2019). Our study also found the content of endogenous NO increased when GSNOR activity was inhibited by exogenous NO and GSNOR inhibitor (**Figure 4B**). Romero-Puertas et al. (2008) has identified some *S*-nitrosylated proteins in *Arabidopsis thaliana* during defense response of the plant, which shows that protein nitrosylation plays an indispensable role in the process of defense reaction. Our nitrosylation modification analysis showed that the GSNOR protein in the NO-treated peach fruit was nitrosylated, which indicates that exogenous NO may participate in the disease resistance response by nitrosylation modification of this protein. As GSNOR inhibitor or NO treatment reduced the activity of GSNOR in peach fruit, the degrading activity of GSNOR on GSNO declined, which leads to GSNO and other SNOs accumulation in peach fruit. Studies have shown that nitrosation of cysteine results in reduced GSNOR activity in *Arabidopsis*, budding yeast, and humans (Guerra et al., 2016). Similar results were shown in this research. Therefore, it can be speculated that NO induces nitrosylation of cysteine-85 in GSNOR, which results in lower GSNOR activity in peach fruit. Lee et al. (2008) found that transcriptional levels or protein abundance levels of GSNOR was not significantly ($P < 0.05$) regulated under stress conditions in *Arabidopsis*, suggesting that some mean of redox regulation via cysteine modification may be a mechanism to control its activity. This study indicated that the relative gene expression of *GSNOR* in the NO-treated peach fruit was not markedly ($P > 0.05$) different from the control after 6 h, but the GSNOR activity was markedly ($P < 0.05$) inhibited (**Figure 2**). Therefore, the nitrosylation of GSNOR may be another main regulation mode

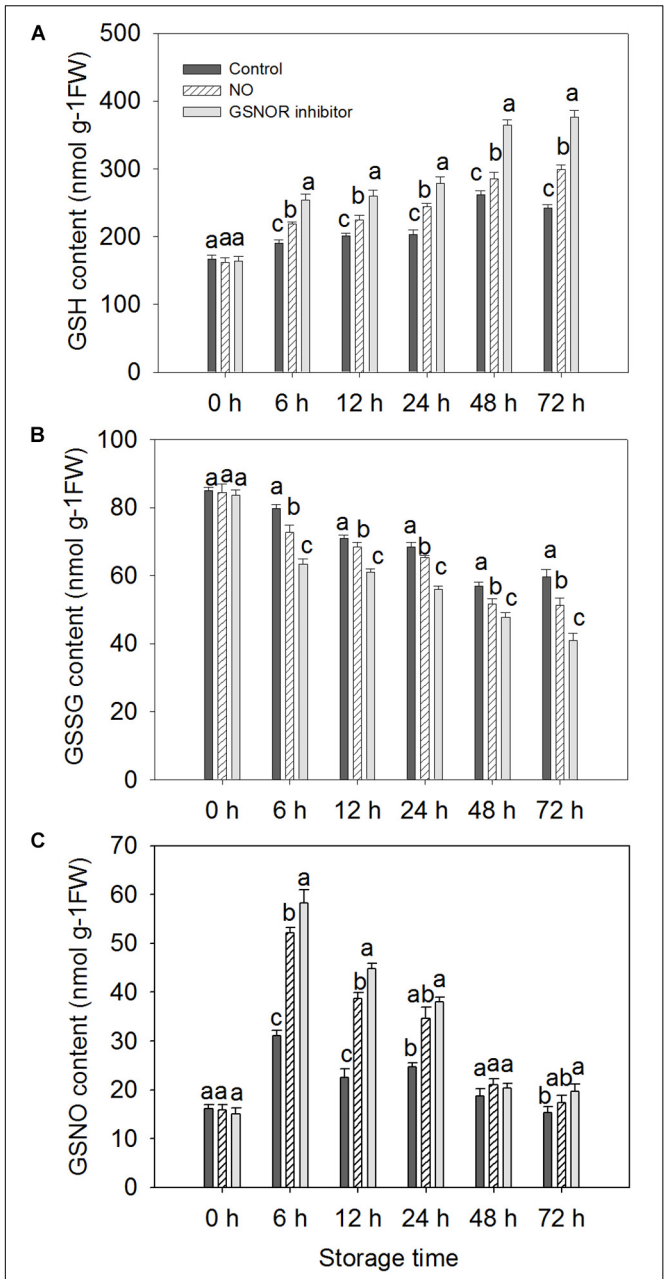

FIGURE 5 | Effect of nitric oxide (NO) or *S*-nitrosoglutathione reductase (GSNOR) inhibitor treatment on the level of **(A)** GSH, **(B)** GSSG, and **(C)** GSNO of peach fruit during storage at 23°C. Vertical bars represent the standard deviation of the means (n = 6). Different letters represent significant differences ($P < 0.05$) according to least significant difference (LSD) test.

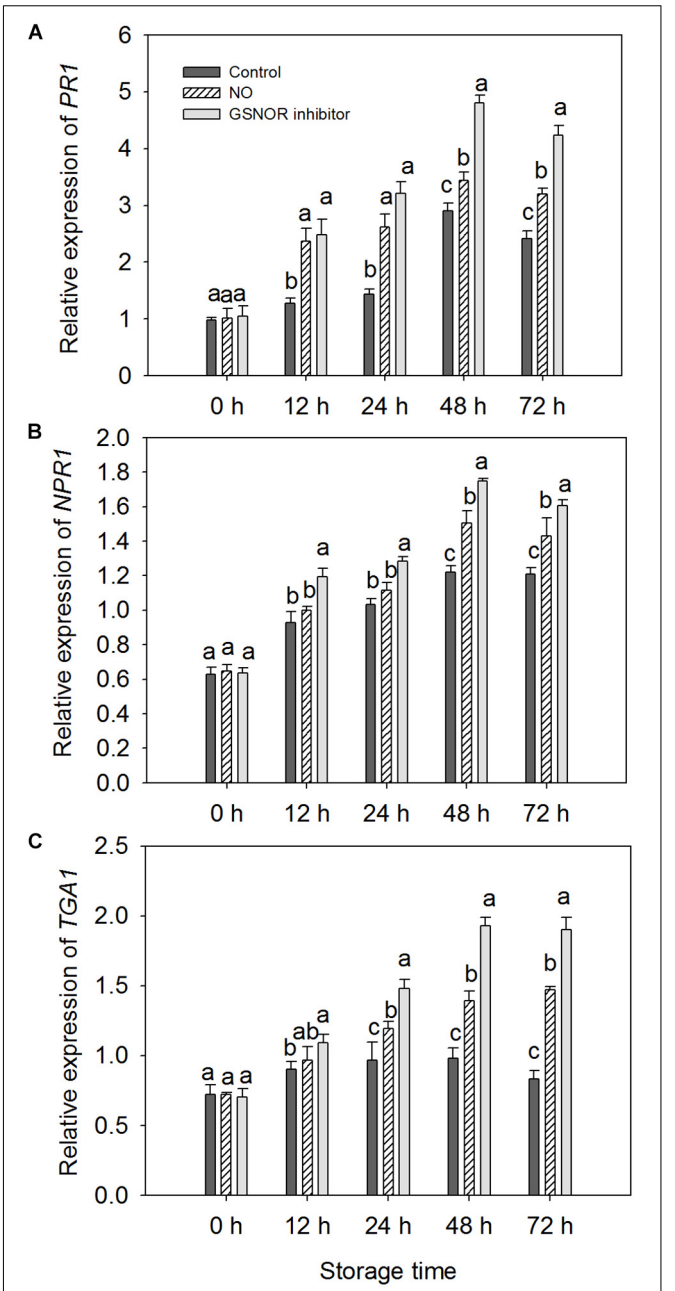

FIGURE 6 | Effects of nitric oxide (NO) or *S*-nitrosoglutathione reductase (GSNOR) inhibitor treatment on **(A)** *PR1*, **(B)** *NPR1*, and **(C)** *TGA1* gene expression, determined by real-time qPCR. All experiments were run in triplicate with different complementary DNAs (cDNAs) synthesized from six biological replicates. Vertical bars represent the standard deviation of the means (n = 6). Different letters represent significant differences ($P < 0.05$) according to least significant difference (LSD) test.

besides the transcriptional control that occurred to its enzyme activity changes.

S-nitrosoglutathione reductase is a highly conserved protein rich in cysteine. Through analysis, it is found that the GSNOR homology between peach and *Arabidopsis* reached 84.17% (**Supplementary Figure S1**). Xu et al. (2013) analyzed the structure of *Arabidopsis* GSNOR protein and found that Cys-10, Cys-271, and Cys-370 of AtGSNOR are solvent accessible and can provide conditions for post-translational modification. In addition, it was suggested that these three residues may be conserved

in regulating the activity of GSNOR. Moreover, Cys-10, Cys-271, and Cys-370 of AtGSNOR have been identified as *S*-nitrosylated residues (Guerra et al., 2016; Zhan et al., 2018). However, Cys-85 of GSNOR of peach was found to be an *S*-nitrosylated residues in our identification results. Sequence analysis of GSNOR revealed that Cys-85 corresponds to Cys-47 in *Arabidopsis thaliana*, *Antrodia camphorata*, and tomato (**Supplementary Figures S2, S3**). At the same time, Cys-85 residue was also found to be conserved in other plant GSNORs. Huang et al. (2009) found that Cys-47 of *A. camphorata* is closely related to the enzyme activity of GSNOR. This further indicates the possible role of Cys-85 nitrosylation in the control of protein activity.

Pathogenesis-related gene 1 was first identified from *Nicotiana tabacum* infected with tobacco mosaic virus (TMV) in the 1970s (Van Loon and Van Kammen, 1970). After that, similar *PR1* proteins from many species of both mono- and dicotyledonous plants have been reported successively (Ohshima et al., 1987; Tornero et al., 1997; Maleck et al., 2000; Liu and Xue, 2006; Mitsuhara et al., 2008). Studies have confirmed that *PR1* is capable to protect plants against abiotic stress (Rauscher et al., 1999; Cutt et al., 1989). Klessig et al. (2000) demonstrated that NO can participate in the induction of *PR1* gene expression. Inhibition of *Arabidopsis GSNOR1* expression enhances *Arabidopsis* resistance to *Peronospora parasitica* and promotes systemic acquired resistance (SAR) and *PR1* expression (Rustérucci et al., 2007). Our research has yielded similar results, which indicates that GSNOR may have the parallel role in post-harvest fruits. Gene expression of *PR1* is upregulated when GSNOR is inhibited by NO and GSNOR inhibitors. NPR1 and TGA1 are pivotal redox-controlled regulators of SAR in plants. NO could promote the ability of NPR1 to increase DNA binding activity of TGA1 (Lindermayr et al., 2010). When the SA-mediated defense response is activated, changes in intracellular redox status will lead to the revivification of NPR1 to its active monomeric form. The *NPR1* monomers interacts with the reduced form of TGA1 to promote the binding of TGA1 to the activation sequence-1 (as-1) element of the promoter region of defense proteins. Studies have confirmed that this interaction promotes the DNA combing activity of TGA1 to the as-1 of the *PR-1* gene to motivate its expression (Després et al., 2003; Pieterse and Van Loon, 2004; Lindermayr et al., 2010). Lindermayr et al. (2010) showed that GSNO protects TGA1 from oxygen-mediated modifications and promotes the combing of TGA1 to the as-1 when NPR1 is present. From our results, it can be seen that both NO and GSNOR inhibitor treatment increased the content of GSNO and endogenous NO, and the expressions of *NPR1* and *TGA1* were obviously higher than the control. Therefore, treatment of peach fruit by NO and GSNOR inhibitors may promote SAR by activating the SA signaling pathway, thereby improving the disease resistance of peach fruit.

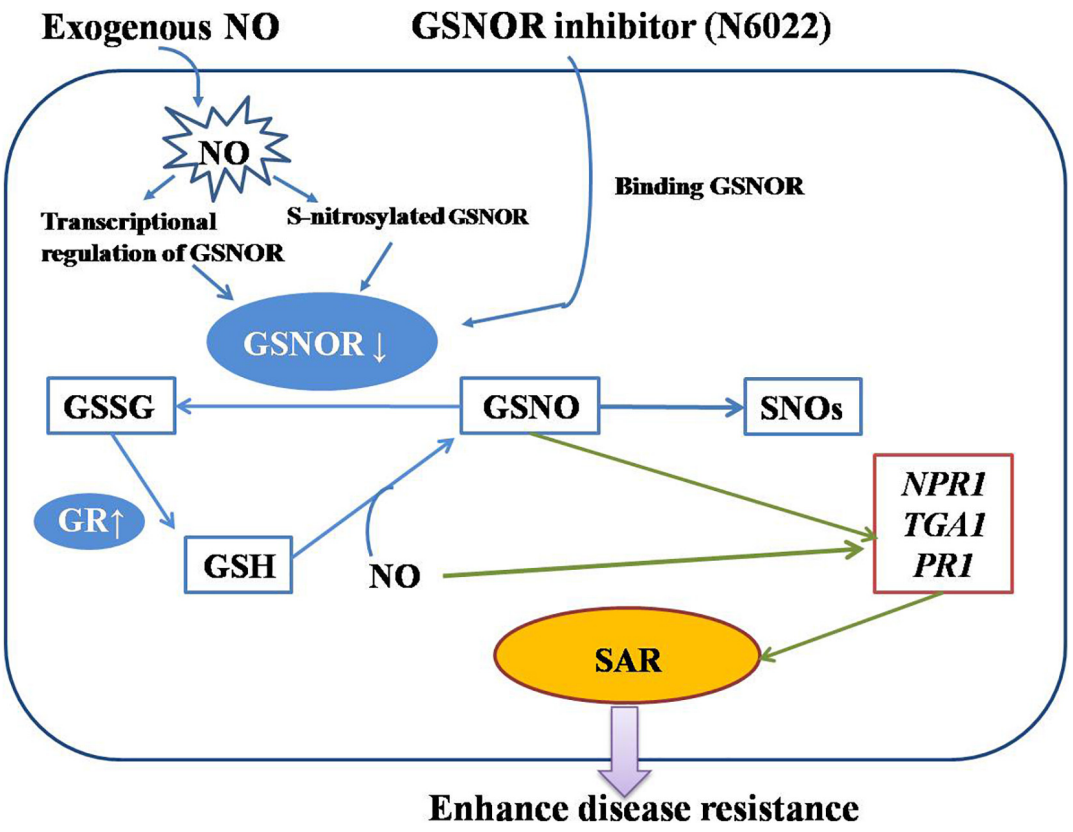

FIGURE 7 | A diagram of the action mechanism of exogenous nitric oxide (NO) and N6022 on improving disease resistance of peach fruits made according to our research.

S-nitrosoglutathione reductase is critical for GSNO and SNOs homeostasis, as well as protecting against nitrosative stress. GSNOR activity is also a major regulator of intracellular GSNO and SNO levels, playing a key role in regulating plant resistance (Liu et al., 2001; Lindermayr et al., 2006). Salicylic acid (SA), as an immune activator in plants, is controlled by *GSNOR1* in its synthesis and signaling transduction, so the regulation of GSNOR activity is closely related to plant disease resistance (Feechan et al., 2005; Malik et al., 2011). In this study, GSNOR inhibitor N6022 was used for soaking postharvest peach fruits that were later inoculated with *M. fructicola*. It was found that N6022 could significantly ($P < 0.05$) inhibit the disease spot development of peach fruit. Moreover, the expression of *GSNOR* was decreased while the expression of *PR1* was significantly increased, and the content of endogenous SNOs and glutathione (GSH) in fruits was increased. The results indicate that partial inhibition of GSNOR activity can lead to increase in intracellular SNOs levels, accumulation of GSH, and enhancement of fruit defense capacity.

Plant defense response is a complex network involving the transmission of multiple hormones and signaling molecules. Our research mainly revealed an important defense mechanism for GSNOR to regulate the level of nitrosation and promote the production of SAR by regulating the levels of GSNO and NO (**Figure 7**). This provides a new orientation for probing the defense mechanism of peach fruit against *M. fructicola* and lays a foundation for in-depth research on the function of GSNOR in harvested fruit. However, it is unclear whether other signaling pathways have an effect on this mechanism, which requires more extensive research.

CONCLUSION

In conclusion, the results of this study point to the key role of GSNOR in the potential molecular mechanisms of peach fruit resistant to brown rot stress. Studies have found that NO and N6022 have a good inhibitory effect on peach fruit brown rot. They inhibit the GSNOR activity and cause the accumulation of SNO, GSNO, and endogenous NO in peach fruit, and increase the GSH accumulation through enhancing GR activity, leading to the enhancement of antioxidant and defense capabilities of peach fruit. In addition, NO and N6022 activate the SA signaling pathway by promoting the expression of SAR-related genes (such as *PR1*, *NPR1*, and *TGA1*), which are also important components of peach fruit defense mechanism. Interestingly, Cys-85 residue of GSNOR was identified as an *S*-nitrosylated residue in the NO-treated peach fruit. This has not been reported in heretofore studies. It is speculated that this may be related to GSNOR enzyme activity, but further research is needed to support this conclusion. Collectively, presented data uncover that inhibition of GSNOR activity has a positive role in peach fruit response to *M. fructicola* infection.

DATA AVAILABILITY STATEMENT

The raw data supporting the conclusions of this article will be made available by the authors, without undue reservation, to any qualified researcher.

AUTHOR CONTRIBUTIONS

JS designed the experiments. ZY and JC conducted the experiments and analyzed the data. ZY conceived the manuscript. JS, YP, LZ, and SZ provided the valuable advice and revised the manuscript.

FUNDING

The work was supported by the Projects of National Natural Science Foundation of China (31570688) and Funds of Shandong "Double Tops" Program (SYT2017XTTD04).

SUPPLEMENTARY MATERIAL

The Supplementary Material for this article can be found online at: https://www.frontiersin.org/articles/10.3389/fpls.2020.00543/full#supplementary-material

REFERENCES

Adaskaveg, J. E., Forster, H., Gubler, W. D., Teviotdale, B. L., and Thompson, D. F. (2005). Reduced-risk fungicides help manage brown rot and other fungal diseases of stone fruit. *Calif. Agric.* 59, 109–114. doi: 10.3733/ca.v059n02p109

Arasimowicz, M., and Floryszak-Wieczorek, J. (2007). Nitric oxide as a bioactive signaling molecule in plant stress responses. *Plant Sci.* 172, 876–887. doi: 10.1016/j.plantsci.2007.02.005

Besson-Bard, A., Pugin, A., and Wendehenne, D. (2008). New insights into nitric oxide signaling in plants. *Annu. Rev. Plant Biol.* 59, 21–39. doi: 10.1146/annurev.arplant.59.032607.092830

Butler, A. R., and Rhodes, P. (1997). Chemistry, analysis, and biological roles of *S*-Nitrosothiols. *Anal. Biochem.* 249, 1–9. doi: 10.1006/abio.1997.2129

Carreras, M. C., and Poderoso, J. J. (2007). Mitochondrial nitric oxide in the signaling of cell integrated responses. *Am. J. Physiol. Cell. Physiol.* 292, C1569–C1580. doi: 10.1152/ajpcell.00248.2006

Chaki, M., Fernandez-Ocana, A. M., Valderrama, R., Carreras, A., Esteban, F. J., Luque, F., et al. (2009). Involvement of reactive nitrogen and oxygen species (RNS and ROS) in sunflower-mildew interaction. *Plant Cell. Physiol.* 50, 665–679. doi: 10.1093/pcp/pcp039

Chen, C., Huang, B., Han, P. W., and Duan, S. J. (2006). *S*-nitrosation: the prototypic redox-based post-translational modification of proteins. *Prog. Biochem. Biophys.* 33, 609–615.

Corpas, F. J., Carreras, A., Valderrama, R., Chaki, M., Palma, J. M., del Río, L. A., et al. (2007). Reactive nitrogen species and nitrosative stress in plants. *Plant Stress* 1, 37–41.

Cutt, J. R., Harpster, M. H., Dixon, D. C., Carr, J. P., Dunsmuir, P., and Klessig, D. F. (1989). Disease response to tobacco mosaic virus in transgenic tobacco plants that constitutively express the pathogenesis-related *PR1b* gene. *Virology* 173, 89–97. doi: 10.1016/0042-6822(89)90224-9

Després, C., Chubak, C., Rochon, A., Clark, R., Bethune, T., Desveaux, D., et al. (2003). The *Arabidopsis* NPR1 disease resistance protein is a novel cofactor that

confers redox regulation of DNA binding activity to the basic domain/leucine zipper transcription factor TGA1. *Plant Cell* 15, 2181–2191. doi: 10.1105/tpc.012849

Dìaz, M., Achkor, H., Titarenko, E., and Martìnez, M. C. (2003). The gene encoding glutathione-dependent formaldehyde dehydrogenase/GSNO reductase is responsive to wounding, jasmonic acid and salicylic acid. *FEBS Lett.* 543, 136–139. doi: 10.1016/s0014-5793(03)00426-5

Domingos, P., Prado, A., Wong, A., Gehring, C., and Feijo, J. (2015). Nitric oxide: a multitasked signaling gas in plant. *Mol. Plant* 8, 506–520. doi: 10.1016/j.molp.2014.12.010

Feechan, A., Kwon, E. J., Yun, B. W., Wang, Y., Pallas, J. A., and Loake, G. J. (2005). A central role for *S*-nitrosothiols in plant disease resistance. *Proc. Natl. Acad. Sci. U.S.A.* 102, 8054–8059. doi: 10.1073/pnas.0501456102

Foyer, C. H., and Noctor, G. (2005). Oxidant and antioxidant signaling in plants: a re-evaluation of the concept of oxidative stress in a physiological context. *Plant Cell Environ.* 28, 1056–1071. doi: 10.1111/j.1365-3040.2005.01327.x

Frungillo, L., De Oliveira, J. F. P., Saviani, E. E., Oliveira, H. C., Martínez, M. C., and Salgado, I. (2013). Modulation of mitochondrial activity by *S*-nitrosoglutathione reductase in *Arabidopsis thaliana* transgenic cell lines. *Biochim. Biophys. Acta* 1827, 239–247. doi: 10.1016/j.bbabio.2012.11.011

Gong, B., and Shi, Q. H. (2019). Identifying S-nitrosylated proteins and unraveling S-nitrosoglutathione reductase-modulated sodic alkaline stress tolerance in *Solanum lycopersicum* L. *Plant Physiol. Biochem.* 142, 84–93. doi: 10.1016/j.plaphy.2019.06.020

Green, L. S., Chun, L. E., Patton, A. K., Sun, X. C., Rosenthal, G. J., and Richards, J. P. (2012). Mechanism of inhibition for N6022, a first-in-class drug targeting *S*-Nitrosoglutathione reductase. *Biochemistry* 51, 2157–2168. doi: 10.1021/bi201785u

Gu, R. X., Zhu, S. H., Zhou, J., Liu, N., and Shi, J. Y. (2014). Inhibition on brown rot disease and induction of defence response in harvested peach fruit by nitric oxide solution. *Eur. J. Plant Pathol.* 139, 369–378. doi: 10.1007/s10658-014-0393-x

Guerra, D., Ballard, K., Truebridge, I., and Vierling, E. (2016). *S*-Nitrosation of conserved cysteines modulates activity and stability of *S*-Nitrosoglutathione reductase (GSNOR). *Biochemistry* 55, 2452–2464. doi: 10.1021/acs.biochem.5b01373

Hess, D. T., and Stamler, J. S. (2012). Regulation by *S*-nitrosylation of protein post-translational modification. *J. Biol. Chem.* 287, 4411–4418. doi: 10.1074/jbc.r111.285742

Hodges, D. M., and Forney, C. F. (2000). The effects of ethylene, depressed oxygen and elevated carbon dioxide on antioxidant profiles of senescing spinach leaves. *J. Exp. Bot.* 51, 645–655. doi: 10.1093/jexbot/51.344.645

Hu, M. J., Cox, K. D., Schnabel, G., Luo, C. X., and Redfield, R. J. (2011). *Monilinia* species causing brown rot of peach in china. *PLoS One* 6:e24990. doi: 10.1371/journal.pone.0024990

Hu, M. J., Zhu, Y. Y., Liu, G. S., Gao, Z. Y., Li, M., Su, Z. H., et al. (2019). Inhibition on anthracnose and induction of defense response by nitric oxide in pitaya fruit. *Sci. Hortic.* 245, 224–230. doi: 10.1016/j.scienta.2018.10.030

Huang, C. Y., Ken, C. F., Wen, L., and Lin, C. T. (2009). An enzyme possessing both glutathione-dependent formaldehyde dehydrogenase and s-nitrosoglutathione reductase from antrodia camphorata. *Food Chem.* 112, 795–802. doi: 10.1016/j.foodchem.2008.06.031

Klessig, D. F., Durner, J., Noad, R., Navarre, D. A., Wendehenne, D., Kumar, D., et al. (2000). Nitric oxide and salicylic acid signaling in plant defense. *Proc. Natl. Acad. Sci.* 97, 8849–8855. doi: 10.1073/pnas.97.16.8849

Knorzer, O. C., Durner, J., and Boger, P. (1996). Alterations in the antioxidative system of suspension-cultured soybean cells (Glycine max) induced by oxidative stress. *Physiol. Plant.* 97, 388–396. doi: 10.1034/j.1399-3054.1996.970225.x

Kulik, A., Noirot, E., Grandperret, V., Bourque, S., Fromentin, J., Salloignon, P., et al. (2015). Interplays between nitric oxide and reactive oxygen species in cryptogein signaling. *Plant Cell Environ.* 38, 331–343. doi: 10.1111/pce.12295

Kwon, E., Feechan, A., Yun, B. W., Hwang, B. H., Pallas, J. A., Kang, J. G., et al. (2012). *AtGSNOR1* function is required for multiple developmental programs in *Arabidopsis*. *Planta* 236, 887–900. doi: 10.1007/s00425-012-1697-8

Lai, T. F., Chen, Y., Li, B. Q., Qin, G. Z., and Tian, S. P. (2014). Mechanism of *Penicillium expansum* in response to exogenous nitric oxide based on proteomics analysis. *J. Proteomics* 103, 47–56. doi: 10.1016/j.jprot.2014.03.012

Lee, U., Wie, C., Fernandez, B. O., Feelisch, M., and Vierling, E. (2008). Modulation of nitrosative stress by *S*-nitrosoglutathione reductase is critical for thermotolerance and plant growth in *Arabidopsis*. *Plant Cell* 20, 786–802. doi: 10.1105/tpc.107.052647

Lindermayr, C., Saalbach, G., Bahnweg, G., and Durner, J. (2006). Differential inhibition of *Arabidopsis* methionine adenosyl transferases by protein *S*-nitrosylation. *J. Biol. Chem.* 281, 4285–4291. doi: 10.1074/jbc.M511635200

Lindermayr, C., Sell, S., Müller, B., Leister, D., and Durner, J. (2010). Redox regulation of the NPR1-TGA1 system of *Arabidopsis thaliana* by nitric oxide. *Plant Cell* 22, 2894–2907. doi: 10.1105/tpc.109.066464

Liu, L. M., Hausladen, A., Zeng, M., Que, L., Heitman, J., and Stamler, J. S. (2001). A metabolic enzyme for *S*-nitrosothiol conserved from bacteria to humans. *Nature* 410, 490–494. doi: 10.1038/35068596

Liu, Q. P., and Xue, Q. Z. (2006). Computational identification of novel PR-1-type genes in *Oryza sativa*. *J. Genet.* 85, 193–198. doi: 10.1007/bf02935330

Macdonald, J., Galley, H. F., and Webster, N. R. (2003). Oxidative stress and gene expression in sepsis. *Br. J. Anaesth.* 90, 221–232. doi: 10.1093/bja/aeg034

Maleck, K., Levine, A., Eulgem, T., Morgan, A., and Dietrich, R. A. (2000). The transcriptome of *Arabidopsis thaliana* during systemic acquired resistance. *Nature* 26, 403–410. doi: 10.1038/82521

Malik, S. I., Hussain, A., Yun, B. W., Spoel, S. H., and Loake, G. J. (2011). GSNOR-mediated de-nitrosylation in the plant defence response. *Plant Sci.* 181, 540–544. doi: 10.1016/j.plantsci.2011.04.004

Mayer, B., Pfeiffer, S., Schrammel, A., Koesling, D., Schmidt, K., and Brunner, F. (1998). A new pathway of nitric oxide/cyclic GMP signaling involving *S*-Nitrosoglutathione. *J. Biol. Chem.* 273, 3264–3270. doi: 10.1074/jbc.273.6.3264

Mitsuhara, I., Iwai, T., Seo, S., Yanagawa, Y., Kawahigasi, H., Hirose, S., et al. (2008). Characteristic expression of twelve rice *PR1* family genes in response to pathogen infection, wounding, and defense-related signal compounds (121/180). *Mol. Genet. Genomics* 279, 415–427. doi: 10.1007/s00438-008-0322-9

Mur, L. A. J., Carver, T. L. W., and Prats, E. (2006). NO way to live; the various roles of nitric oxide in plant-pathogen interactions. *J. Exp. Bot.* 57, 489–505. doi: 10.1093/jxb/erj052

Nawrocka, J., Gromek, A., and Małolepsza, U. (2019). Nitric oxide as a beneficial signaling molecule in *Trichoderma atroviride* TRS25-induced systemic defense responses of cucumber plants against *Rhizoctonia solani*. *Front. Plant Sci.* 10:421. doi: 10.3389/fpls.2019.00421

Ohshima, M., Matsuoka, M., Yamamoto, N., Tanaka, Y., Kano-Murakami, Y., Ozeki, Y., et al. (1987). Nucleotide sequence of the *PR-1* gene of *Nicotiana tabacum*. *FEBS Lett.* 225, 243–246. doi: 10.1016/0014-5793(87)81166-3

Patel, A., and Patra, D. D. (2015). Effect of tannery sludge amended soil on glutathione activity of four aromatic crops: *Tagetes minuta*, *Pelargonium graveolens*, *Ocimum basilicum* and *Mentha spicata*. *Ecol. Eng.* 81, 348–352. doi: 10.1016/j.ecoleng.2015.04.070

Pieterse, C. M., and Van Loon, L. C. (2004). NPR1: the spider in the web of induced resistance signaling pathways. *Curr. Opin. Plant Biol.* 7, 456–464. doi: 10.1016/j.pbi.2004.05.006

Rauscher, M., Adám, A. L., Wirtz, S., Guggenheim, R., Mendgen, K., and Deising, H. B. (1999). PR-1 protein inhibits the differentiation of rust infection hyphae in leaves of acquired resistant broad bean. *Plant J. Cell Mol. Biol.* 19, 625–633. doi: 10.1046/j.1365-313x.1999.00545.x

Romanazzi, G., Sanzani, S. M., Bi, Y., Tian, S. P., Gutiérrez Martínez, P., and Alkan, N. (2016). Induced resistance to control postharvest decay of fruit and vegetables. *Postharvest Biol. Technol.* 122, 82–94.

Romero-Puertas, M. C., Campostrini, N., Mattè, A., Righetti, P. G., and Dr, M. D. P. (2008). Proteomic analysis of *S*-nitrosylated proteins in *Arabidopsis thaliana* undergoing hypersensitive response. *Proteomics* 8, 1459–1469. doi: 10.1002/pmic.200700536

Romero-Puertas, M. C., Perazzolli, M., Zago, E. D., and Delledonne, M. (2004). Nitric oxide signalling functions in plant–pathogen interactions. *Cell. Microbiol.* 6, 795–803. doi: 10.1111/j.1462-5822.2004.00428.x

Rustérucci, C., Espunya, M. C., Díaz, M., Chabannes, M., and Martínez, M. C. (2007). *S*-nitrosoglutathione reductase affords protection against pathogens in

Arabidopsis, both locally and systemically. *Plant Physiol.* 143, 1282–1292. doi: 10.1104/pp.106.091686

Sakamoto, A., Ueda, M., and Morikawa, H. (2002). *Arabidopsis* glutathione dependent formaldehyde dehydrogenase is an *S*-nitrosoglutathione reductase. *FEBS Lett.* 515, 20–24. doi: 10.1016/s0014-5793(02)02414-6

Schairer, D. O., Chouake, J. S., Nosanchuk, J. D., and Friedman, A. J. (2012). The potential of nitric oxide releasing therapies as antimicrobial agents. *Virulence* 3, 271–279. doi: 10.4161/viru.20328

Shi, J. Y., Liu, N., Gu, R. X., Zhu, L. Q., Zhang, C., Wang, Q. G., et al. (2015). Signals induced by exogenous nitric oxide and their role in controlling brown rot disease caused by *Monilinia fructicola* in postharvest peach fruit. *J. Gen. Plant Pathol.* 81, 68–76. doi: 10.1007/s10327-014-0562-y

Skelly, M. J., and Loake, G. (2013). Synthesis of redox-active molecules and their signalling functions during the expression of plant disease resistance. *Antioxid. Redox Signal.* 19, 990–997. doi: 10.1089/ars.2013.5429

Sommer, N. F. (1985). Role of controlled environments in suppression of postharvest diseases. *Can. J. Plant Pathol.* 7, 331–339.

Stamler, J. S. (1994). Redox signaling: nitrosylation and related target interactions of nitric oxide. *Cell* 78, 931–936. doi: 10.1016/0092-8674(94)90269-0

Stamler, J. S., Lamas, S., and Fang, F. C. (2001). Nitrosylation: the prototypic redox-based signaling mechanism. *Cell* 106, 675–683. doi: 10.1016/s0092-8674(01)00495-0

Sun, X. C., Wasley, J. W., Qiu, J., Blonder, J. P., Stout, A. M., Green, L. S., et al. (2011). Discovery of *S*-nitrosoglutathione reductase inhibitors: potential agents for the treatment of asthma and other inflammatory diseases. *ACS Med. Chem. Lett.* 2, 402–406. doi: 10.1021/ml200045s

Tong, Z. G., Gao, Z. H., Wang, F., Zhou, J., and Zhang, Z. (2009). Selection of reliable reference genes for gene expression studies in peach using real-time PCR. *BMC Mol. Biol.* 10:71. doi: 10.1186/1471-2199-10-71

Tornero, P., Gadea, J., Conejero, V., and Vera, P. (1997). Two *PR-1* genes from tomato are differentially regulated and reveal a novel mode of expression for a pathogenesis-related gene during the hypersensitive response and development. *Mol. Plant Microbe Interact.* 10, 624–634. doi: 10.1094/MPMI.1997.10.5.624

Van Loon, L. C., and Van Kammen, A. (1970). Polyacrylamide disc electrophoresis of the soluble leaf proteins from *Nicotiana tabacum* var. 'Samsun' and 'Samsun NN'. II. Changes in protein constitution after infection with Tobacco mosaic virus. *Virology* 40, 199–211. doi: 10.1016/0042-6822(70)90395-8

Xie, L. X., Wang, G. R., Yu, Z. X., Zhou, M. L., Li, Q. M., Huang, H. R., et al. (2016). Proteome-wide lysine glutarylation profiling of the mycobacterium tuberculosis h37rv. *J. Proteome Res.* 15, 1379–1385. doi: 10.1021/acs.jproteome.5b00917

Xu, S., Guerra, D., Lee, U., and Vierling, E. (2013). S-nitrosoglutathione reductases are low-copy number, cysteine-rich proteins in plants that control multiple developmental and defense responses in *Arabidopsis*. *Front. Plant Sci.* 4:430. doi: 10.3389/fpls.2013.00430

Yang, F., Feng, L., Liu, Q., Wu, X., and Yang, W. (2018). Effect of interactions between light intensity and red-to- far-red ratio on the photosynthesis of soybean leaves under shade condition. *Environ. Exp. Bot.* 150, 79–87. doi: 10.1016/j.envexpbot.2018.03.008

Zhan, N., Wang, C., Chen, L. C., Yang, H. J., Feng, J., Gong, X. Q., et al. (2018). S -nitrosylation targets gsno reductase for selective autophagy during hypoxia responses in plants. *Mol. Cell* 71, 142–154. doi: 10.1016/j.molcel.2018.05.024

Zheng, Y., Sheng, J. P., Zhao, R. R., Zhang, J., Lv, S. N., Liu, L. Y., et al. (2011). Preharvest L-arginine treatment induced postharvest disease resistance to *Botrysis cinerea* in tomato fruits. *J. Agric. Food Chem.* 59, 6543–6549. doi: 10.1021/jf2000053

Conflict of Interest: The authors declare that the research was conducted in the absence of any commercial or financial relationships that could be construed as a potential conflict of interest.

frontiers in Plant Science

ORIGINAL RESEARCH
published: 30 June 2020
doi: 10.3389/fpls.2020.00975

Ethylene and *RIPENING INHIBITOR* Modulate Expression of *SlHSP17.7A, B* Class I Small Heat Shock Protein Genes During Tomato Fruit Ripening

Rakesh K. Upadhyay[1], *Mark L. Tucker*[2] *and Autar K. Mattoo*[1]*

[1] *Sustainable Agricultural Systems Laboratory, The Henry A. Wallace Beltsville Agricultural Research Center, United States Department of Agriculture-ARS, Beltsville, MD, United States,* [2] *Soybean Genomics and Improvement Laboratory, The Henry A. Wallace Beltsville Agricultural Research Center, United States Department of Agriculture-ARS, Beltsville, MD, United States*

OPEN ACCESS

Edited by:
Carolina Andrea Torres, Washington State University, United States

Reviewed by:
Julia Vrebalov, Boyce Thompson Institute, United States
Niranjan Chakraborty, National Institute of Plant Genome Research (NIPGR), India

***Correspondence:**
Autar K. Mattoo
autar.mattoo@usda.gov

Specialty section:
This article was submitted to Crop and Product Physiology, a section of the journal Frontiers in Plant Science

Received: *15 April 2020*
Accepted: *16 June 2020*
Published: *30 June 2020*

Citation:
Upadhyay RK, Tucker ML and Mattoo AK (2020) Ethylene and RIPENING INHIBITOR Modulate Expression of SlHSP17.7A, B Class I Small Heat Shock Protein Genes During Tomato Fruit Ripening. Front. Plant Sci. 11:975. doi: 10.3389/fpls.2020.00975

Heat shock proteins (HSPs) are ubiquitous and highly conserved in nature. Heat stress upregulates their gene expression and now it is known that they are also developmentally regulated. We have studied regulation of small HSP genes during ripening of tomato fruit. In this study, we identify two small HSP genes, *SlHSP17.7A* and *SlHSP17.7B*, localized on tomato Chr.6 and Chr.9, respectively. Each gene encodes proteins constituting 154 amino acids and has characteristic domains as in other sHSP genes. We found that *SlHSP17.7A* and *SlHSP17.7B* gene expression is low in the vegetative tissues as compared to that in the fruit. These sHSP genes are characteristically expressed in a fruit-ripening fashion, being upregulated during the ripening transition of mature green to breaker stage. Their expression patterns mirror that of the rate-limiting ethylene biosynthesis gene ACC (1-aminocyclopropane-1-carboxylic acid) synthase, *SlACS2,* and its regulator *SlMADS-RIN*. Exogenous application of ethylene to either mature green tomato fruit or tomato leaves suppressed the expression of both the *SlHSP17.7A, B* genes. Notably and characteristically, a transgenic tomato line silenced for *SlACS2* gene and whose fruits produce ~50% less ethylene *in vivo*, had higher expression of both the *sHSP* genes at the fruit ripening transition stages [breaker (BR) and BR+3] than the control fruit. Moreover, differential gene expression of *SlHSP17.7A versus SlHSP17.7B* gene was apparent in the tomato ripening mutants—*rin/rin*, *nor/nor*, and *Nr/Nr*, with the expression of *SlHSP17.7A* being significantly reduced but that of *SlHSP17.7B* significantly upregulated as compared to the wild type (WT). These data indicate that ethylene negatively regulates transcriptional abundance of both these sHSPs. Transient overexpression of the ripening regulator *SlMADS-RIN* in WT and ACS2-AS mature green tomato fruits suppressed the expression of *SlHSP17.7A* but not that of *SlHSP17.7B*. Thus, ethylene directly or in tune with *SlMADS-RIN* regulates the transcript abundance of both these sHSP genes.

Keywords: gene expression, ethylene, 1-MCP, *SlMADS-RIN*, *small heat shock protein genes*, tomato, tomato ripening mutants

INTRODUCTION

Heat shock proteins (HSPs) are ubiquitous in nature and highly conserved in living organisms (Plesofsky-Vig et al., 1992; Waters and Vierling, 1999; Kappé et al., 2002; Franck et al., 2004; Fu et al., 2006; Aevermann and Waters, 2008; Waters, 2013). They are prominent in cells/tissues exposed to elevated temperatures (Sun et al., 2002; Waters, 2013; Zhang et al., 2015) as well as to chilling temperatures (Ré et al., 2016). HSPs are classified based on their molecular weight, namely, HSP100s, HSP90s, HSP70s, HSP60s, HSP20s and small HSPs (sHSPs) (Waters, 2013). sHSPs constitute low molecular weight proteins that function as molecular chaperones critical for protein folding and prevention of irreversible protein aggregation (Becker and Craig, 1994; Hartl, 1996; Liberek et al., 2008; Giorno et al., 2010; Tyedmers et al., 2010; Waters, 2013). In addition to sHSPs being prominently expressed during heat shock response in plants, it is now known that some are expressed in unstressed cells as well and are, therefore, involved in processes other than heat stress (Tyedmers et al., 2010; Waters, 2013). For example, in plants, they are upregulated during ripening initiation of tomato fruit (Goyal et al., 2012; Shukla et al., 2017) and may also protect ripe tomato fruits against chilling injury (Ré et al., 2016).

Ethylene regulates plant processes such as fruit ripening independently as well as in conjunction with other hormones and molecules (Fluhr and Mattoo, 1996; Giovannoni et al., 2017; Mattoo and Upadhyay, 2019). Ethylene directly or indirectly promotes transcription/translation of numerous ripening-related genes, including those associated with cell wall breakdown, carotenoid biosynthesis, aroma development, pigment accumulation, fruit softening, and flavor (Gray et al., 1994; Barry and Giovannoni, 2007; Klee and Giovannoni, 2011). Tomato is one of the models for dissection of ethylene-mediated regulation of genes during fruit ripening, facilitated by the availability of nonripening tomato lines, such as *ripening-inhibitor (rin/rin)*, *nonripening (nor/nor)*, and *never-ripe (Nr/Nr),* in which ethylene production is compromised (Mattoo and Vickery, 1977; Oeller et al., 1991; Picton et al., 1993; Wilkinson et al., 1995; Hackett et al., 2000; Alexander and Grierson, 2002; Moore et al., 2002; Vrebalov, 2002; Giovannoni, 2007; Razdan and Mattoo, 2007). Of these mutants, *ripening-inhibitor* (*rin*) mutation encodes a MADS-box transcription factor *SlMADS-RIN* that regulates genes involved in fruit ripening (Ng and Yanofsky, 2001; Vrebalov, 2002; Hileman et al., 2006; Martel et al., 2011; Fujisawa et al., 2013).

Tomato genome harbors five members of class I sHSP genes (Goyal et al., 2012; Yu et al., 2016; Shukla et al., 2017). The involvement of sHSPs in fruit biology became apparent by earlier studies which demonstrated *VISCOSITY 1* (*VIS1*) as a regulator of pectin depolymerization affecting juice viscosity of tomato fruit (Ramakrishna et al., 2003) while *HSP21* was shown to stabilize photosystem II of photosynthesis against oxidative stress in addition to promoting color change during tomato fruit ripening (Neta-Sharir et al., 2005). More recently, a unique intron-less cluster of three sHSP chaperone genes, *SlHSP17.6*, *SlHSP20.0* and *SlHSP20.1*, was shown to be resident on the short arm of chromosome 6 and found differentially expressed during tomato fruit ripening (Goyal et al., 2012). Further, it was shown that ethylene suppresses the transcription of the latter tomato sHSP gene cluster during the transition of mature green stage to ripening initiation and involves SlMADS-RIN box protein (Shukla et al., 2017).

Here we identify, characterize and present transcriptional regulation of two novel duplicated members of class I sHSPs in tomato, *SlHSP17.7A* and *SlHSP17.7B*, during fruit ripening. Further, expression of *SlHSP17.7A* gene was found minimal in the isogenic ripening mutants of Alisa Craig—*rin/rin*, *nor/nor*, and *Nr/Nr*, while that of *SlHSP17.7B* was higher in these mutants. We also utilized an ethylene-deficient tomato line to demonstrate that ethylene biosynthesis directly and/or indirectly regulates the expression of sHSP genes in tomato.

MATERIALS AND METHODS

Plant Materials, Transgenic Tomato Lines, and Sample Collection

Wild-type tomato (*Solanum lycopersicum* cv. Ailsa Craig) and its near isogenic mutant lines—*ripening-inhibitor (rin/rin)*, *nonripening (nor/nor)* and *never-ripe (Nr/Nr)*—and previously characterized ACC synthase 2 (*ACS2*)-silenced transgenic line (ACS2-AS) together with its azygous/wild-type control tomato (WT-Ohio8245) (Mehta et al., 2002; Sobolev et al., 2014) were employed for the studies presented here. sHSP gene expression was quantified at distinct ripening stages: mature green (-5BR), breaker (BR), pink (breaker+3), and red ripe (breaker+7). All these genotypes were grown in a temperature-controlled greenhouse under natural light conditions. Vegetative tissues, leaf, stem, flower, and roots, were collected from 1-month-old wild-type Ailsa Craig tomato plants. *For seedling collection*, 8- to 10-day-old 50-germinated seeds in triplicates with two cotyledons were immediately frozen in liquid nitrogen and stored at −80°C until used. *For development studies*, fruits tagged at anthesis (DPA: days post anthesis) were collected at 8 DPA (developmental stage 1), 15 DPA (developmental stage 2), and 22 DPA (developmental stage 3). *For ripening studies*, tomato fruits at 5 days before breaker (-)5BR —equivalent to mature green (MG) stage, breaker (BR) and red ripe stage [8 days after breaker (BR+8)] were collected. Fruits from the WT-Ohio8245 were harvested at (-)5BR, (MG), BR, and BR+8 stages. Pericarp tissue excised from harvested fruits was immediately frozen in liquid nitrogen and stored at −80°C until used (Mehta et al., 2002). A minimum of 3 biological replicates were used for each experiment.

Identification, Sequence Alignment and Phylogenetic Analysis of SlHSP17.7A and SlHSP17.7B

Two novel ripening-specific genes *SlHSP17.7A* (NM_001279116.2/ Solyc06g076520.1) and *SlHSP17.7B* (XM_015231817.1/ Solyc09g015020.1) were identified by utilizing prior information on the following genes: *SlHSP17.6* (AY150039/Solyc06g076540.1.1), *SlHSP20.0* (AJ225048/Solyc06g076570.1.1), and *SlHSP20.1* (AJ225046/Solyc06g076560.1.1) (Goyal et al., 2012; Shukla et al., 2017). The latter tomato HSPs were used as query sequences for BLAST P search in gene bank (https://blast.ncbi.nlm.nih.gov) as

well as with BLAST P program in tomato genome [International Tomato Genome Sequencing Consortium (SGN; solgenomics.net) database, version ITAG 2.4] to look for similar sequences. ExPASy bioinformatics resource (https://www.expasy.org) portal was used for the prediction of molecular weight and isoelectric point (PI). Individual domains in the protein sequences were identified and manually highlighted. Multiple sequence alignment was performed using MUSCLE program (http://www.ebi.ac.uk/Tools/msa) and primers were designed using Primer3 program (http://bioinfo.ut.ee/primer3-0.4.0/). Forty-two similar sequences were extracted from tomato genome database to generate the phylogeny among tomato sHSPs (Goyal et al., 2012; Paul et al., 2016; Yu et al., 2016; Shukla et al., 2017; **Supplementary Table 1**). The phylogenetic tree was constructed by maximum likelihood method based on JTT matrix model with 1000 boot strap values using Mega 7 program (Kumar et al., 2016). The analysis involved 42 amino acid sequences. All positions with less than 95% site coverage were eliminated. For qRT-PCR analysis, forward primer was made from 3′ coding DNA sequence while reverse primer was designed from 3′ UTR due to sequence degeneracy within the five closely related class I tomato HSP members. Primer sequences used in qRT-PCR along with their gene bank accessions and SGN identity numbers are listed in **Supplementary Table 2**.

Exogenous Ethylene and 1-Methylcyclopropene Treatments

Mature green [MG/(-)5BR] tomato fruits from WT-Ohio8245 control and ACS2-AS transgenic lines were treated with 25 ppm ethylene or 2 ppm 1-Methylcyclopropene (1-MCP) (AgroFresh, Goyal et al., 2012 Collegeville, PA, USA) in triplicate from three independent biological replicates (Shukla et al., 2017). A third set of fruits left in the open air was considered as a control for the experiment. Treated and control fruit were collected at 0, 12, and 24 h of treatment. Ethylene (25 ppm) treatment of 8–10 fully expanded leaves from mature WT-Ailsa Craig plants was carried out for 0, 24, 48, 72, and 96 h in the dark at 25°C. Samples were removed at the indicated time points and immediately flash frozen at −80°C until used.

Total RNA Extraction, cDNA Synthesis, and Quantitative Real-Time PCR (qRT-PCR)

Total RNA was extracted from 100 mg of each sample using Plant RNeasy kit according to manufacturer's instructions (Qiagen). Isolated RNA was first subjected to RNase-free DNase (Qiagen) treatment to eliminate genomic DNA contamination and then purified using a RNeasy Mini Kit (Qiagen). RNA samples with an $A_{260/280}$ ratio of 1.8–2 were electrophoresed on agarose gels to ensure the presence of intact rRNA bands (Goyal et al., 2012). Methods for cDNA synthesis and qRT-PCR were essentially as described previously (Bustin et al., 2009; Shukla et al., 2017; Upadhyay et al., 2017). Relative gene expression was quantified according to $2^{-\Delta\Delta CT}$ method (Livak and Schmittgen, 2001). Tomato genes *SlTIP41* and *SlUBI3* were used as standard housekeeping genes to normalize the expression of target genes (Expósito-Rodríguez et al., 2008; Mascia et al., 2010). For relative expression data, the threshold cycle (C_T) values for all the genes of interest (C_T of GOI) were normalized to the geometric mean C_T value obtained from the two tomato reference genes (C_T tom Refs) as ΔCT = (CT of GOI) − (geometric mean CT of *SlTIP41* and *SlUBI3*) (Vandesompele et al., 2002). For fruit ripening studies, mature green/(-)5BR was taken as a calibrator to calculate the $2^{-\Delta\Delta CT}$ for relative gene expression values. Primer efficiency was calculated for each primer pair as: efficiency=10^(-1/slope). Primer pairs with primer efficiency above 90% were used for the study. qRT-PCR data represent average ± standard deviation from a minimum of three independent biological replicates for each gene.

In Silico Analysis of *SlHSP17.7A* and *SlHSP17.7B* Promoters for Predicting *cis*-Elements

International Tomato Genome Sequencing Consortium (SGN; solgenomics.net) database (version ITAG 2.4) was used to extract promoter region sequences (≈ 2 kb of the 5′ upstream region of the start codon) of *SlHSP17.7A* and *SlHSP17.7B* genes. Plant CARE relational database (Lescot et al., 2002) and PLACE (the plant-*cis*-acting regulatory DNA elements) database (Higo et al., 1999) were used for plant *cis*-element searches in both the gene promoters (**Supplementary Tables 3** and **4**).

Overexpression, Construct Preparation, and Agro-Injection of Tomato Fruits for Transient Expression Analysis

For overexpression, *SlMADS-RIN* coding sequence was amplified from breaker stage cDNA and then cloned into the pENTR/D-TOPO donor vector (Invitrogen). It was further subcloned into the pK2GW7 gateway plant destination vector to generate a plasmid-designated as pK2GW7-SlMADS-RIN-OE, and then transformed into agrobacterium GV3101pmp90RK strains. Mature green fruits from wild-type and ethylene-deficient genotypes were chosen for agroinfiltration and subsequent expression analysis. Agrobacterium culture carrying pK2GW7-SlMADS-RIN-OE was grown overnight at 28°C in Luria-Bertani (Sigma) medium with selective antibiotics (gentamycin, rifampicin and kanamycin). Primary culture (500 µl) was then transferred to a 50-ml modified induction medium (2 mM $MgSO_4$, 20 mM acetosyringone, 10 mM MES, pH 5.6) plus antibiotics, and grown overnight until optical density reached 1.0. The culture was centrifuged at 8,000 rpm for 5 min, resuspended in the infiltration medium (10 mM $MgCl_2$, 10 mM MES, 200 mM acetosyringone, pH 5.6), and incubated at room temperature with gentle agitation (50 rpm) for a minimum of 2 h. Tomato agro-injection was done as described earlier (Orzaez et al., 2006). Briefly, 3–4 mature green tomato fruits from each genotype were infiltrated using a 2-ml syringe with needle (BD Biosciences). Needle was introduced to a depth of 3 to 4 mm into the fruit tissue through the stylar apex, and the infiltrated solution was gently injected into the fruit. The total volume of solution injected varied with the size of the mature green tomato fruit, from 600 µl to 1 ml. The completely infiltrated fruits were used for the experiments. Thereafter, fruits were harvested after 72–96 h of infiltration. RNA from agro-injected fruit samples was isolated and used to make cDNA as described previously (Shukla et al., 2017). cDNA was diluted 10-fold for qRT-PCR

analysis. pK2GW7-*SlMADS-RIN* infiltrated fruits and control fruits infiltrated with infiltration medium were analyzed for the accumulation of *SlMADS-RIN*, *SlACS2* and both *sHSP* gene transcripts.

Data Analysis and Statistics

Statistical analysis was carried out using Graph Pad (version Prism 8.0) and P values < 0.05 treated as statistically significant as described previously (Upadhyay and Mattoo, 2018). Significant differences between fruit ripening stages were calculated by separately comparing mature green/(-)5BR stage with breaker (BR), breaker+3 (BR+3), and breaker+8 (BR+8) stages for each gene. Similarly, significant differences between wild-type and ripening stages of mutants were calculated by comparing BR, BR+3 and BR+8 stages of *AC/AC* with respective stages of *rin/rin*, *nor/nor*, and *Nr/Nr*. Significant changes for *SlHSP17.7* transcripts in the *in vitro* ethylene suppression experiment were calculated by comparing air and ethylene treated samples at 12 and 24 h.

RESULTS

Identification and Phylogenetic Analysis of Tomato *SlHSP17.7A, B* Class I HSP Genes

Bioinformatics analysis carried out as described in the Materials and Methods section revealed two novel class I intron-less sHSP genes which are organized similarly to a cluster of three sHSP genes described previously (Goyal et al., 2012). The two novel proteins were named SlHSP17.7A (Solyc06g076520.1.1) and SlHSP17.7B (Solyc09g015020.1.1), respectively. While this work was in progress, two genome-wide studies identified HSP20-related gene family in tomato (Paul et al., 2016; Yu et al., 2016). These studies indicated that *SlHSP17.7A* was housed on chromosome 6, and its close relative was identified as *SlHSP17.7B* housed on chromosome 9 of tomato. *SlHSP17.7A* gene (NM_001279116.2) constitutes 798 nucleotides with a coding DNA sequence (CDS) of 495 nucleotides with 127 nucleotides of 5′ UTR and 206 nucleotides of 3′ UTR. It encodes a functional protein of 154 amino acids, with a predicted molecular weight of 17,735.12 Daltons and PI 5.84 (**Figure 1A**). Like the *SlHSP17.7A* gene, the *SlHSP17.7B* gene (XM_015231817.1) constitutes 813 nucleotides with a coding DNA sequence (CDS) of 495 nucleotides along with 176 nucleotides of 5′ UTR and 172 nucleotides of 3′ UTR. The *SlHSP17.7B* CDS encodes a functional protein of 154 amino acids, with a predicted molecular weight of 17,662.01 Daltons and PI 5.84 (**Figure 1A**). The gene bank sequences for *SlHSP17.7A* (NM_001279116.2) and *SlHSP17.7B* (XM_015231817.1) were annotated with both untranslated regions (UTRs) while SGN sequence for *SlHSP17.7A* (Solyc06g076520.1) has yet to be annotated for positioning the 5′ and 3′ UTRs. Further, neither *SlHSP17.7A* (NM_001279116.2), (submitted in gene bank, Fray et al., 1990), nor *SlHSP17.7 B* (XM_015231817.1) have been so far characterized.

Alignment of protein sequences revealed that both the SlHSP17.7A and SlHAP17.7B proteins differ from the other three close homologs, SlHSP17.6, SlHSP20.0 and SlHSP20.1, at 14 amino acid positions (namely, 14, 16, 27, 29, 34, 35, 36, 41, 62, 76, 98, 102, 124, and 146) (N→C) (**Figure 1B**). To decode evolutionary relationship among tomato sHSPs, a total of 42 protein sequences were extracted from SGN database and were exclusively annotated as small HSP proteins in tomato genome (Goyal et al., 2012; Yu et al., 2016) to construct a phylogenetic tree using MEGA7 program (**Figure 2**). The sequences separated into 3 major groups/clades. Both the SlHSP17.7A and SlHAP17.7B proteins constitute to clade I along with other members of this cluster, viz., SlHSP17.6, SlHSP20.0 and SlHSP21.0 (Shukla et al., 2017).

Fruit Ripening-Specific Expression of *SlHSP17.7A* and *SlHSP17.7B* Is Synergistic With Upregulation of *SlMADS-RIN* and *SlACS2* Gene Transcripts

We extracted available transcriptome data (*S. lycopersicum* cv. Heinz) from International Tomato Genome Sequencing Consortium (SGN; solgenomics.net) database (version ITAG 2.4) in order to determine the relative transcript abundances for *SlHSP17.7A*, *SlHSP17.7B, SlMADS-RIN* and *SlACS2* during plant development and tomato fruit ripening (**Figure 3A**). Gene transcripts of all these four are upregulated during ripening with the abundance of each gene transcripts increasing from MG/(-)5BR to BR stage [5.8-fold for *SlHSP17.7A,* 5.7-fold for *SlHSP17.7B,* 10.7-fold for *SlACS2*, and 49.3-fold for *SlMADS-RIN*] and yet more abundant at the BR+10 stage [8.9-fold for *SlHSP17.7A,* 9.4-fold for *SlHSP17.7B,* 24.1-fold for *SlACS2*, and 102.9-fold for *SlMADS-RIN*] (**Figure 3B**). Their RPKM counts followed an increasing trend with *SlHSP17.7A* > *SlHSP17.7B* > *SlMADS*-RIN > *SlACS2*, which indicates that the relative expression of *SlHSP17.7A* was highest among the four genes tested. In terms of fold change from mature green to ripening stages, *SlMADS-RIN* transcripts were highly expressed, followed by *SlACS2* > *SlHSP17.7B* > *SlHSP17.7A*. The transcriptome data for *SlHSP17.7* genes expression was validated by qRT-PCR analysis of RNA from vegetative tissues (root, stem, leaf, flower and seedling) (**Figure 4A**) and fruit developmental/ripening stages of Ailsa Craig (**Figures 4B, C**). Overall, the expression of *SlHSP17.7A* and *B* genes was found low in the vegetative tissues and during fruit development as compared to that during fruit ripening progression. Both sHSPs were similarly expressed in the stem while in leaf, flower and seedling tissues expression of *SlHSP17.7B* was significantly lower (P < 0.001) compared to that of *SlHSP17.7A* (**Figure 4A**).

During fruit ripening both the sHSP genes were upregulated as is known for the ripening regulators *SlACS2* and *SlMADS-RIN*. In Ailsa Craig, *SlHSP17.7A* expression was 40.63-fold higher at BR stage, increasing significantly (P < 0.001) to 61.56-fold at BR+3 stage, and decreased thereafter to 35-fold as compared to MG (-)5BR fruit (**Figure 4B**). In comparison, *SlHSP17.7B* expression was 1.8-fold higher at BR stage (P > 0.01), increasing to 2.3-fold (P < .001) at BR+3 and 2.27-fold (P < .01) at BR+8 stage compared to the MG/(-)5BR fruit (**Figure 4C**). Notably, *SlACS2* expression in Ailsa Craig fruit increased from 18 thousand-fold at the BR stage to 25 thousand-fold (P <0.001) at the BR+8 stage as compared to the MG/(-)5BR fruit (**Figure 4D**). Similarly, *SlMADS-RIN*

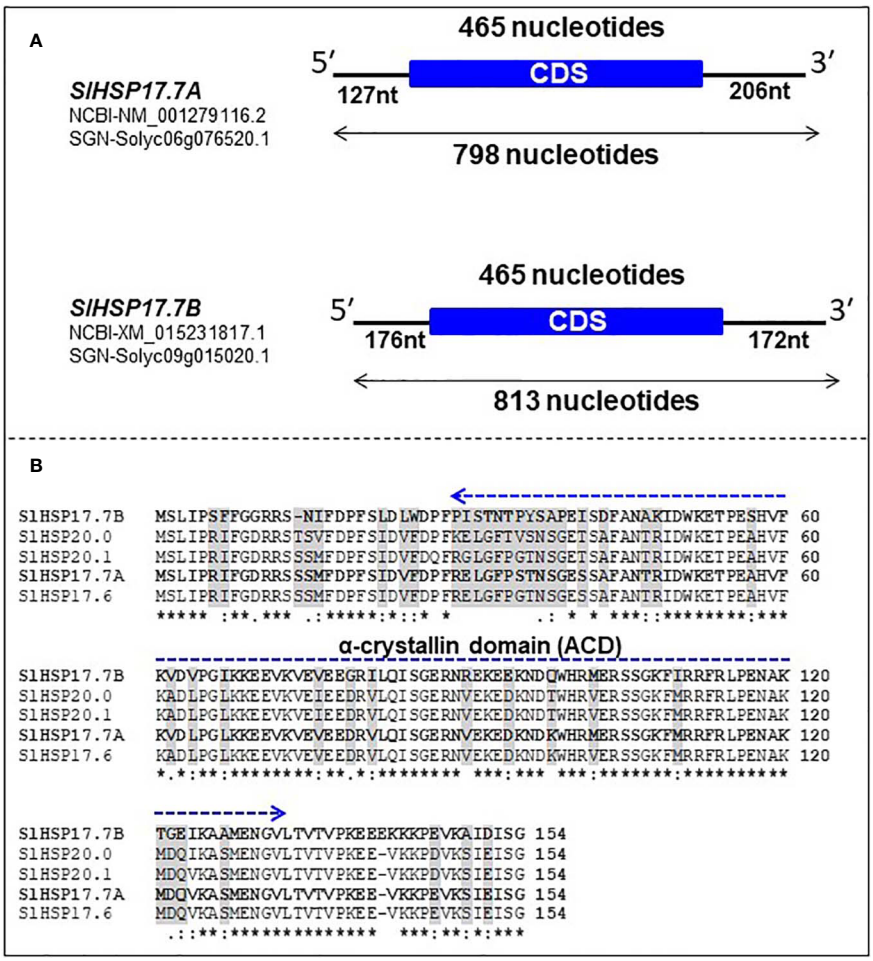

FIGURE 1 | Organization, alignment and phylogeny of *SlHSP17.7A* and *SlHSP17.7B* genes. **(A)** Schematic representation of heat shock protein (*HSP*) genes with coding DNA sequence (CDS) and untranslated regions (UTRs). *SlHSP17.7A* gene (NM_001279116.2/Solyc06g076520.1) is made of 798 nucleotides with a CDS of 465 nucleotides, and 127 nucleotides of 5′ UTR, and 206 nucleotides of 3′ UTR. The *SlHSP17.7* CDS encodes a functional protein of 154 amino acids. Similarly, *SlHSP17.7B* gene (XM_015231817.1/Solyc09g015020.1) is made of 813 nucleotides with CDS of 465 nucleotides, and 176 nucleotides of 5′ UTR and 172 nucleotides of 3′ UTR. The *SlHSP17.7B* CDS encodes a functional protein of 154 amino acids. **(B)** Alignment of *SlHSP17.7A* and *SlHSP17.7B* to their closest homologs *SlHSP17.6*, *SlHSP20.0* and *SlHSP20.1*—different key conserved amino acid positions are shown. The characteristic conserved α-crystallin domain (ACD) is highlighted by dark blue line. Conserved residues are denoted by asterisks.

expression increased from 26 thousand-fold (P <0.001) at the BR stage to 43 thousand-fold (P <0.001) at the BR+8 stage as compared to the MG/(-)5BR fruit (**Figure 4E**). Similar high expression dynamics of *SlACS2* and *SlMADS-RIN* genes are known (Martel et al., 2011).

Differential Accumulation of *SlHSP17.7A* and *SlHSP17.7B* Gene Transcripts in Alisa Craig Versus Ohio 8245 During Ripening

Ripening-regulated expression of *SlHSP17.7A* and *SlHSP17.7B* genes in Ailsa Craig was notably higher than in the Ohio 8245 variety (**Figures 5A, B**). Expression of *SlHSP17.7A* in Ailsa Craig fruit was 40.97-fold higher at BR stage, further increased by 64.87-fold at BR+3, and decreased thereafter to 35.65-fold at BR +8 compared to that at MG/(-)5BR. In comparison, *SlHSP17.7A* transcript expression in Ohio8245 genotype was notably much lower with a 3.7-fold increase at the BR stage, increasing further to 7.3-fold at BR+3 and 4.5-fold at BR+8 relative to that at MG/(-)5BR stage (**Figure 5A**). The expression of *sHSP17.7B* in Ailsa Craig and Ohio8245 fruits during ripening was not as dramatically different as that found for *SlHSP17.7A* gene above. In Ailsa Craig fruit stages, expression of *sHSP17.7B* was 1.63-fold at BR, 2.18-fold at BR+3 and 2.20-fold at BR+8 stages as compared to that in the MG/(-)5BR fruit. Likewise, in Ohio 8245 fruit stages, a moderate sequential increase in *SlHSP17.7* transcript expression was 1.26-fold at BR, 1.5-fold at BR+3 and 3.6-fold at BR+8 stages as compared to MG/(-)5BR stage (**Figure 5B**). Thus, the expression levels of these sHSP genes vary to different degrees in the two tomato varieties; however, in both varieties, the two genes are upregulated during fruit ripening.

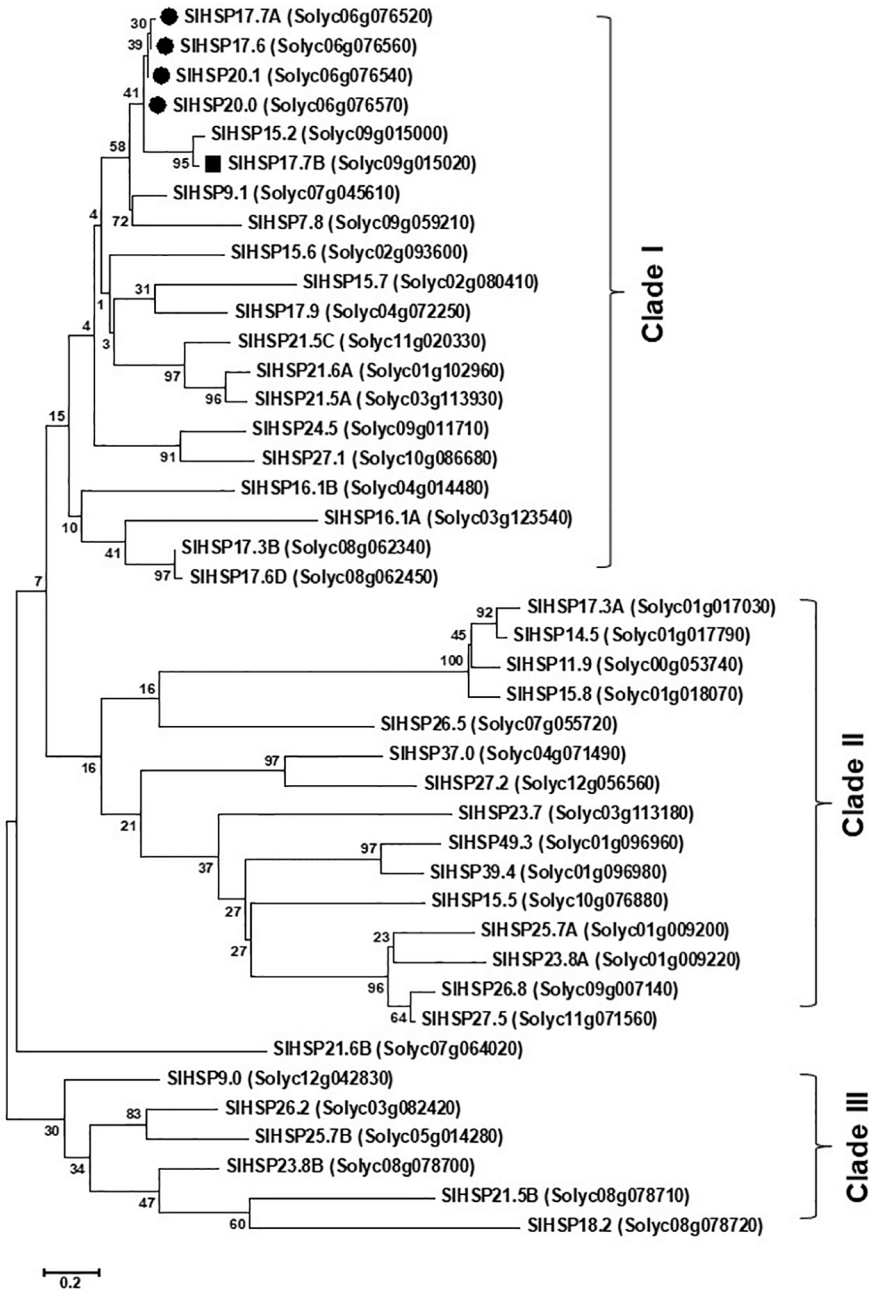

FIGURE 2 | Phylogeny relatedness of SlHSP17.7A and SlHSP17.7B with other known proteins. The phylogenetic tree was constructed by maximum likelihood method with 1,000 boot strap values. Poisson model with complete deletion was employed during construction of the tree. The tree is drawn to scale, with branch lengths measured in the number of substitutions per site (Kumar et al., 2016). Forty two small heat shock proteins (HSPs) from tomato fell into two major groups, I and II. Group I was further segregated into "A" and "B" subgroups while group II was segregated into "C" and "D" subclades. *SlHSP21.5C* did not fall in any of the major groups. Subclade 'A' of group I consisted of small class I heat shock proteins namely, *SlHSP17.6*, *20.0*, and *20.1* (Goyal et al., 2012; Shukla et al., 2017) and the newly identified *SlHSP17.7A* and *SlHSP17.7B*.

Transcriptome data for *Solanum lycopersicum* Heinz and *Solanum pimpinellifolium* from tomato expression database also indicated that HSP expression greatly depends on the tomato genotype. However, a consistent ripening-induced expression of *SlHSP17.7A, B* genes is observed irrespective of genotypes (**Figures 5C, D**). This also reflects a functional conservation of these genes during evolution irrespective of gain in fruit size between S. *lycopersicum* vs. S. *pimpinellifolium*.

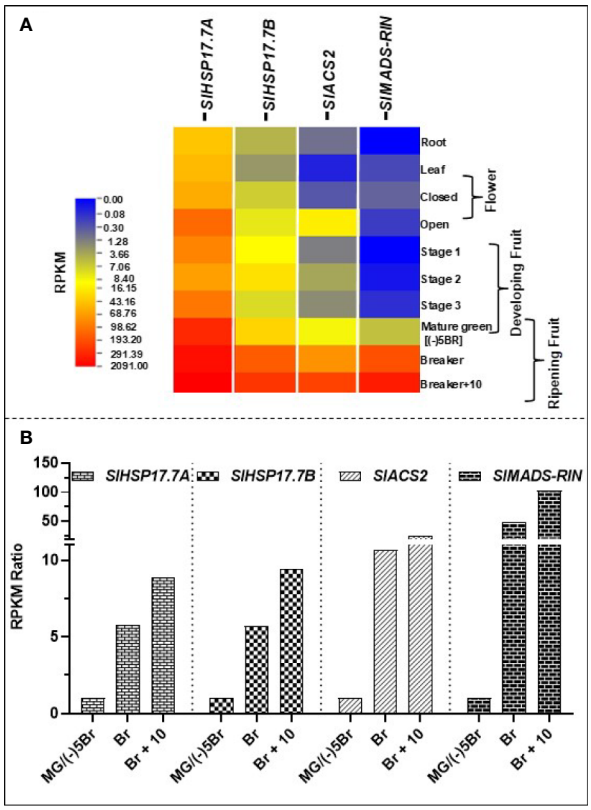

FIGURE 3 | Transcriptome analysis of *SlHSP17.7* transcripts in wild-type *S. lycopersicum* cv. Heinz tomato during fruit ripening. **(A)** RPKM values for the *SlHSP17.7A*, *SlHSP17.7B SlACT2*, and *SlRIN* genes in tomato during plant growth, devepolment and fruit ripening [root, leaf, bud, flower, 3 fruit developmental stages, mature green (MG), breaker (BR), and red ripe (BR+10)] were derived from RNA-seq data from the SGN database (*S. lycopersicum* cv. Heinz) as described in the materials and methods section. **(B)** Mature green stage/(-)5BR was used as calibrator to reveal ripening-specific changes in gene expression. Fold change for each gene was calculated by dividing the RPKM values of (-)5BR stage to BR and BR +8 stages. Ripening-induced gene expression seen for *SlHSP17.7A* and *SlHSP17.7B* was corroborated with the expression of climacteric ethylene regulator *SlACS2* and *SlMADS-RIN*.

Ethylene Inhibits *SlHSP17.7A, B* Expression in a Time-Dependent Manner in Fruit and Leaf Tissues

To discern if ethylene treatment of fruit modulates the expression of these two sHSP genes, we held the Ohio8245 MG/(-)5BR fruits separately in either air (control), ethylene or in the presence of 1-MCP an inhibitor of ethylene signaling (**Figure 6**). Fruits held in ethylene atmosphere for 12 and 24 h were found to be suppressed for the expression of both *SlHSP17.7A* and *SlHSP17.7B* genes ($P < 0.001$). However, it took 24 h before the fruits held in 1-MCP were found to be suppressed in *SlHSP17.7A* expression (**Figure 6**). Notably, 1-MCP-treated tomato fruit had higher expression levels of *SlHSP17.7B* gene at 12 and 24 h as compared to air control. We also determined if ethylene-mediated suppression of these two sHSPs occurs also in leaves. Both the gene transcripts were found suppressed for a longer duration in tomato leaves incubated in the ethylene atmosphere (**Supplementary Figure 1**). This demonstrates that ethylene mediated transient suppression of both these sHSP transcripts occurs in both fruit and leaf tissues.

Ripening Mutants Are Compromised in *SlHSP17.7A* Expression but *SlHSP17.7B* Expression Is Differentially Elevated During Ripening as Compared to the Wild Type

Expression of *SlHSP17.7A* and *SlHSP17.7B* genes was also quantified in the near isogenic nonripening mutant lines - *ripening-inhibitor (rin/rin)*, *nonripening (nor/nor)*, and *Never-ripe (Nr/Nr)* at similar age/ripening as the WT-Ailsa Craig (**Figure 7**). *SlHSP17.7A* transcript abundance was significantly impacted in the *rin/rin* and *nor/nor* mutants during the progression of ripening as compared to the WT-Ailsa Craig (**Figure 7A**). Similar was the case with *Nr/Nr* mutant fruit except that *SlHSP17.7A* transcript abundance was significantly higher at BR and BR+3 than in *nor/nor* and *rin/rin* mutants vis a vis WT-Ailsa Craig fruit (**Figure 7A**). An opposite trend in the expression of *SlHSP17.7B* gene in the three mutant lines was apparent as compared to WT. *SlHSP17.7B* gene expression remained high in mutants as ripening progressed (in *rin/rin*: 2.5-fold higher at BR and Br+8; in *nor/nor*: 5 to 6-fold higher at

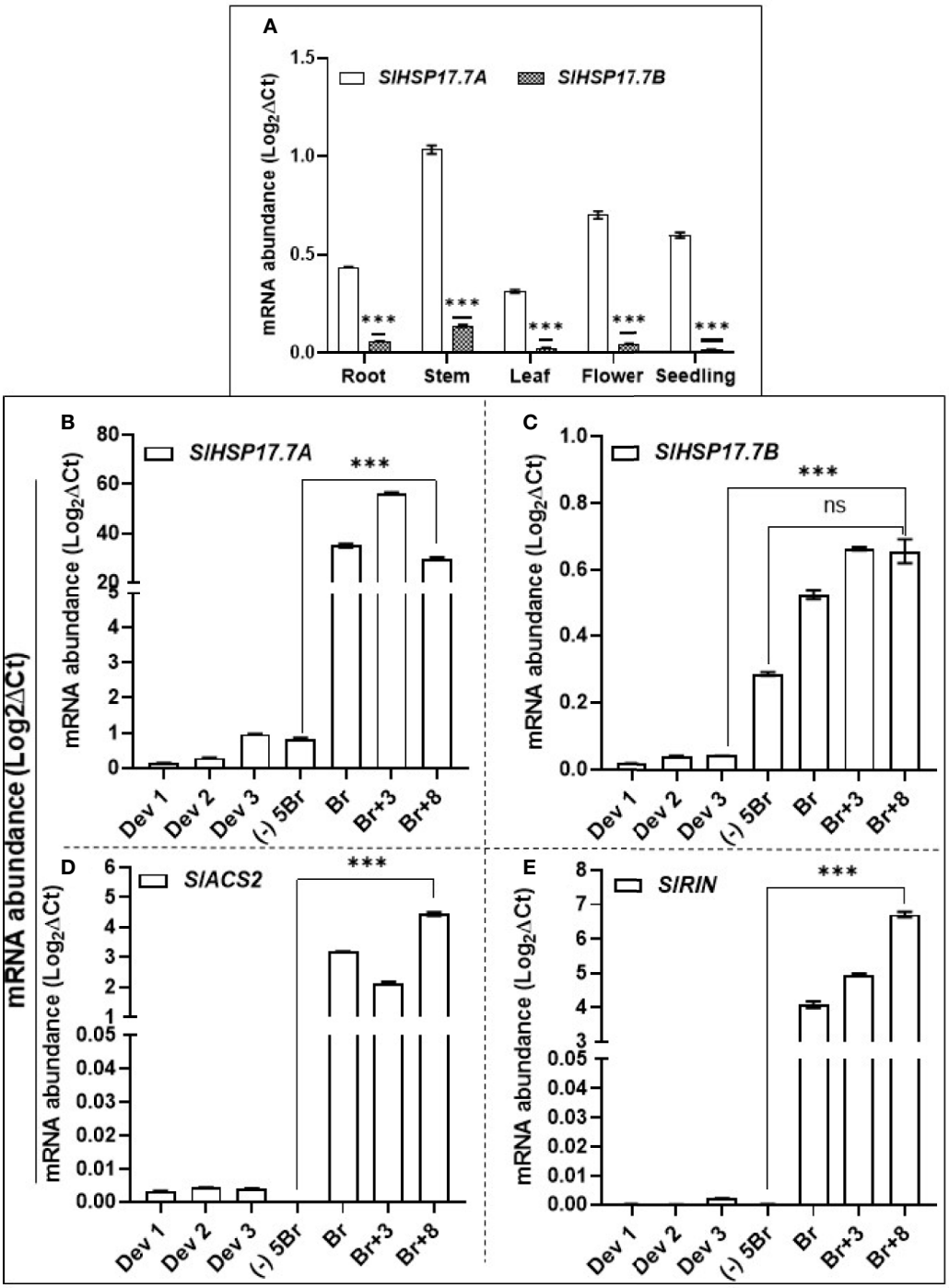

FIGURE 4 | Quantitative real-time PCR (qRT-PCR) of *SlHSP17.7A, SlHSP17.7B, SlACS2 and SlMADS-RIN* genes in different tissues of wild-type *S. lycopersicum* cv. Ailsa Craig. RNA was isolated from root, stem, leaf, flower, seedling tissue and from fruit developmental and ripening stages. Leaf and stem samples were from 1-month old tomato plants; flowers were sampled from 3-month old plant; young seedlings were harvested from 8- to 10-day-old germinated seeds while for fruit harvesting stages Ailsa Craig plants were tagged at anthesis and fruits harvested at 8DPA (DPA = days post anthesis) (Dev 1), 15DPA (Dev 2), 22DPA (Dev 3) and ripening stages [(-)5BR, BR, BR+3, BR+8]. **(A)** Expression of *SlHSP17.7A* and *SlHSP17.7B* genes in vegetative tissue; **(B)** expression of *SlHSP17.7A* and **(C)** *SlHSP17.7B* during fruit development and ripening; **(D)** expression of *SlACS2* and **(E)** *SlMADS-RIN* during fruit development and ripening. *SlTIP41* and *SlUBI3* genes were used to normalize the expression of the target genes (Expósito-Rodríguez et al., 2008; Mascia et al., 2010). Error bars indicate standard deviation from a minimum of three biological replicates. Asterisks indicate statistically significant differences, *P < 0.05, **P < 0.01, ***P < 0.001 and ****P < 0.0001 (see Materials and Methods). ns, not significant.

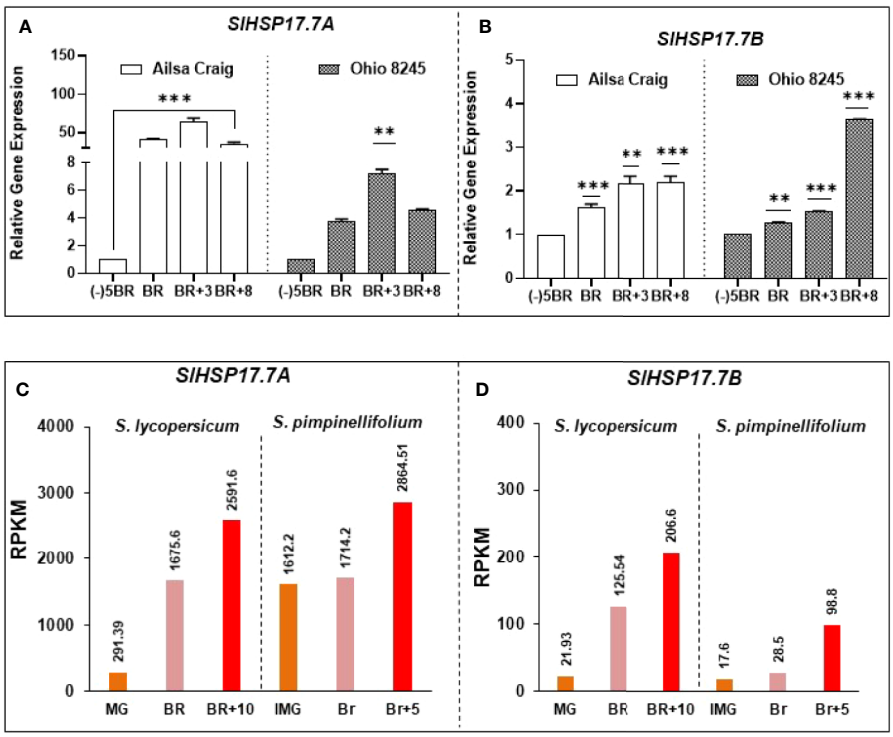

FIGURE 5 | Differential expression of *SlHSP17.7A and SlHSP17.7B* genes in two modern tomato varieties as well as in two different genotypes. Tomato (*S. lycopersicum*) var. Ailsa Craig and Ohio 8245 fruits from various ripening stages were harvested as described in the Materials and Methods section. Both **(A)** *SlHSP17.7A* and **(B)** *SlHSP17.7B* genes showed differential expression during ripening. Variety-based abundance was also determined. Calibrator used for quantitative real-time PCR (qRT-PCR) calculations was (-)5BR stage. *SlTIP41* and *SlUBI3* genes were used to normalize the expression of target genes as described in the legend to **Figure 3**. Three biological replicates were used from each variety. A minimum of three fruits (n=3) were used for RNA isolation for each biological replicate. Transcriptome data for *Solanum lycopersicum* Heinz and *Solanum pimpinellifolium* fruit ripening stages for *SlHSP17.7A* and *B*, obtained from tomato expression database, show fold difference variation among genotypes with a functionally conserved ripening-induced nature of both HSPs **(C, D)**.

BR and BR+3 but lower at BR+8 stage; in *Nr/Nr:* 2-fold higher at BR and BR+3 stages but lower at BR+8) in comparison to the same ripening period of the WT-Ailsa Craig fruits (**Figure 7B**).

Since these tomato mutants are nonripening in nature and deficient in ethylene biosynthesis and perception, any deviation in their expression from wild type would be considered as ripening-specific and ethylene dependent. These results indicate that while *SlHSP17.7A* has ripening-specific expression, expression of *SlHSP17.7B* is not limited or regulated by ripening.

Differential Regulation of *SlHSP17.7* and *SlMADS-RIN* Expression in ACS2 Gene-Silenced Transgenic Tomato

To differentiate ethylene regulation of the two sHSP genes and of *SlMADS-RIN,* we employed our previously characterized transgenic tomato line ACS2-AS silenced for ACS2 gene which produces 50% less ethylene than the wild type (Sobolev et al., 2014). Expression of both, *SlHSP17.7*A and *SlHSP17.7B* genes, was upregulated only at the breaker stage compared to the azygous control line; however, this upregulation was many-fold evident in the *SlHSP17.7B* gene right from breaker stage to BR+8 stage (**Figures 8A, B**). Interestingly, the ACS2-AS ethylene-deficient line was also found to be compromised in the expression of the ripening-regulator *SlMADS-RIN* gene (**Figures 8C, D**). These data invoke ethylene as a negative regulator of the two sHSPs and, likely, the *SlMADS-RIN* gene.

In Silico Analysis of the *SlHSP17.7A, B* Gene Promoters and Identification of Various *cis*-Elements

We also analyzed the 2 Kb upstream 5′ putative promoter regions of the two tomato *SlHSPs* genes for the presence of ethylene-related cis-elements ERE (ethylene response elements) and RIN binding 'CArG' box *cis*-elements using PLACE (Higo et al., 1999) and Plant Care (Lescot et al., 2002) databases. Several binding sites responsive to hormonal and environmental signals were found in the promoter of both the HSP genes (**Supplementary Tables 3** and **4**). Notably, two 'CArG' binding *cis*-elements in the promoters of each gene were found. The *SlHSP17.7A* promoter was decorated with one "atypical" [C(A/T)$_8$G] motif type at -29 and other "possible" [C(C/T)(A/T)$_6$(A/G)G] motif type at -1841 position (**Supplementary Table 3**). Similarly, *SlHSP17.7B* gene promoter was found decorated with both "atypical" [C(A/T)$_8$G] motif types at -633 and at -1067 positions (**Supplementary Table 4**). Previously, CArG motifs have been shown to be target binding sites for *SlMADS-RIN* transcription factor to regulate fruit ripening

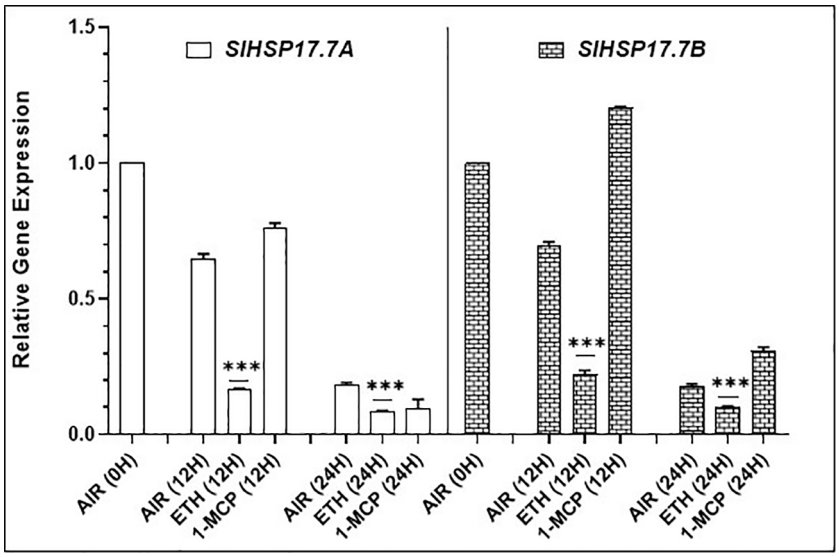

FIGURE 6 | Effects of ethylene (ETH) and 1-methylcyclopropene (1-MCP) treatments on the expression of *SlHSP17.7A* and *SlHSP17.7B* genes. Wild-type (WT) (Ohio8245) fruits at (-)5BR/mature green stage were treated with either 25 ppm ethylene, 2 ppm 1-MCP, or left in air. Samples were then harvested at 0, 12 and 24 h, total RNA was isolated and expression of *SlHSP17.7A* and *SlHSP17.7B* genes was quantified. Error bars indicate standard deviation from a minimum of three replicates. *SlTIP41* and *SlUBI3* genes were used to normalize the expression of the target genes as described in the legend to **Figure 3**. Statistical differences [*P ≤ 0.05, **P ≤ 0.01, ***P ≤ 0.001, and ****P ≤ 0.0001] are indicated.

genes (Martel et al., 2011; Fujisawa et al., 2013; Shukla et al., 2017). The presence of CArG motifs in *SlHSP17.7A* and *SlHSP17.7B* gene promoters suggests that *SlMADS-RIN* transcription factor may bind these *cis*-elements and regulate expression of HSPs during fruit ripening.

Transient Overexpression of *SlMADS-RIN* Transcription Factor Reveals Differential Expression of *SlHSP17.7A* and *SlHSP17.7B* Genes in WT Versus ACS2-AS Tomato Line

Tomato fruits were infiltrated with pK2GW7-*SlMADS-RIN*-OE construct and, after 72–96 h of incubation period, infiltrated fruits were analyzed for the abundance of *SlMADS-RIN* and *SlACS2* transcripts as described in the methods section. Transcripts of both *SlMADS-RIN* and *SlACS2* were found upregulated, which indicated successful activation of *SlACS2* gene (3-fold; $P < 0.01$) by *SlMADS-RIN* transcription factor (**Figure 8E**). To check if *SlMADS-RIN* mediates suppression or activation of the two sHSPs, this cDNA was analyzed for the status of both the HSP genes. Interestingly, *SlHSP17.7A* expression was significantly suppressed (P=0.0023), and the *SlHSP17.7B* transcripts were activated but not to an extent to be statistically significant.

Finally, we also agro-injected the ACS2-AS transgenic tomato line (with low ethylene background) with the pK2GW7-*SlMADS-RIN*-OE construct. This experiment revealed a lower transcript abundance of *SlHSP17.7A* (P=0.0069); however, the *SlHSP17.7B* transcripts also were downregulated but not to a level to be statistically significant (**Figure 8F**). These results demonstrate that *SlHSP17.7A* transcripts are suppressed by *SlMADS-RIN* in different genetic backgrounds. These results are in tune with the previous findings where *SlMADS-RIN* was shown to regulate some genes in both ethylene-dependent and independent manner, reminiscent of the existence of negative as well as positive regulation of tomato genes during the transition of mature green fruit into ripening progression (Fujisawa et al., 2013).

DISCUSSION

Two novel class I small HSP genes (*SlHSP17.7A* and *SlHSP17.7B*) were identified in tomato and their transcriptional regulation was found to be mediated by the plant hormone ethylene. Both the sHSP genes share sequence similarities with other tomato class I small HSPs sequences (Goyal et al., 2012; Paul et al., 2016; Yu et al., 2016; Shukla et al., 2017). However, they are localized in different chromosomes in tomato, *SlHSP17.7A* gene is localized to chr. 6 in a tandem repeated manner with a previously characterized cluster of three small HSP genes *SlHSP17.6*, *SlHSP20.0* and *SlHSP20.1* (Goyal et al., 2012; Shukla et al., 2017). However, the *SlHSP17.7B* gene is resident on chr. 9 but shares a close homology to *SlHSP17.7A*. Both the s*HSP* genes are ripening-specific with minimal expression in the vegetative tissues; moreover, the *SlHSP17.7B* transcripts were observed at the developmental stage 3 of tomato fruit, a stage earlier than the mature green fruit. These two sHSPs can be further differentiated by their expression patterns in the ethylene-deficient tomato mutants (*rin/rin*, *nor/nor*, and *Nr/Nr*), with *SlHSP17.7A* gene expression characteristically impaired in these mutants while *SlHSP17.7B* gene is abundantly expressed in them.

A mutation in the ripening-regulator MADS-RIN protein prevents the tomato ripening mutants, particularly *rin*, from

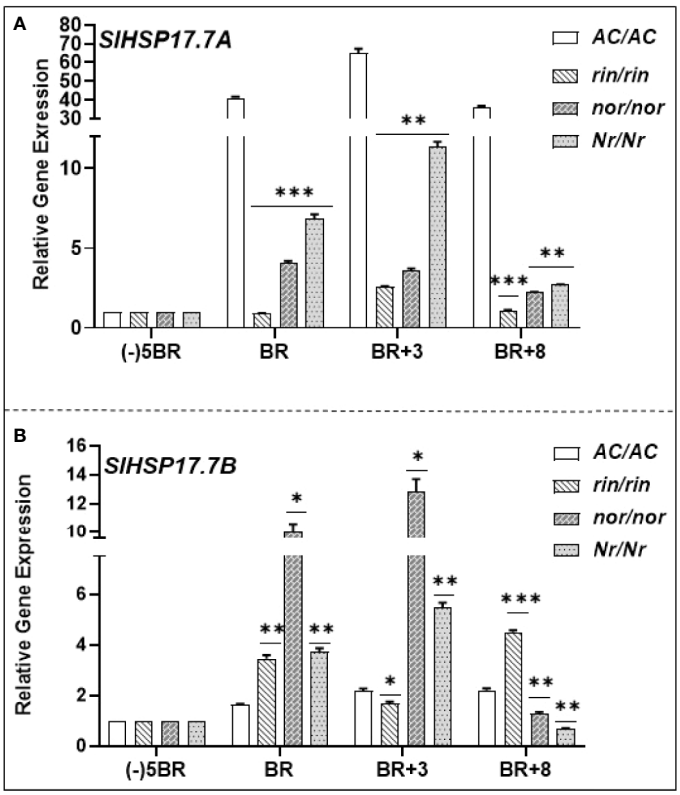

FIGURE 7 | Expression patterns of **(A)** *SlHSP17.7A* and **(B)** *SlHSP17.7B* genes in nonripening tomato mutants. Fruits from wild-type tomato (*S. lycopersicum*) var. Ailsa Craig (*AC/AC*) and its ripening mutants (*rin/rin*, *nor/nor*, and *Nr/Nr*) were harvested as described in Materials and Methods section. quantitative real-time PCR (qRT-PCR) analysis, calibrator used for qRT-PCR calculations, and normalization of expression were the same as described in the legends to **Figure 5**. Statistical differences [*P ±0.05, **P ≤ 0.01, ***P ≤ 0.001, and ****P ≤ 0.0001] are indicated.

ripening (Vrebalov, 2002) since MADS-RIN protein regulates the expression of ethylene biosynthesis genes *ACS2* and *ACS4* during fruit ripening (Cara and Giovannoni, 2008; Martel et al., 2011). This is also apparent from the data presented here showing that the *SlMADS-RIN* transcription is in congruence with the expression patterns of *SlACS2*. In this regard, our *in silico* analysis revealed that the promoters of both the *SlHSP17.7A* and *SlHSP17.7B* genes harbor at least two *MADS-RIN* binding *cis*-elements (**Supplementary Tables 3** and **4**), the CArG motif (Ito et al., 2008; Fujisawa et al., 2011; Zhong et al., 2013). Similar CArG motifs has been shown in promoters of other genes by previous workers. For example, CArG motif at position −1841 (CAAAAAAAAG) in gene promoter of *SlHSP17.7A* has been previously identified in Solyc04g082420 promoter as potential direct target of RIN transcription factor (Fujisawa et al., 2013). While, CArG motifs in *SlHSP17.7B* promoter at position −633 (CTTAAATATG) and −1067 (CATTAATTTG) has been previously shown as direct target of RIN in Solyc01g104050 and Solyc09g065030 gene promoters, respectively (Fujisawa et al., 2013). This further strengthen a possibility of RIN transcription factor binding with CArG motifs present in HSP gene promoters. Thus, we envisioned an interaction of RIN with promoter elements of the two sHSPs and tested this hypothesis *via* transient expression of RIN in WT and ethylene-deficient tomato line. Significant suppression was apparent for *SlHSP17.7A* gene but not the *SlHSP17.7B*. Thus, *SlMADS-RIN* may be a negative regulator of *SlHSP17.7A* gene.

Together, these data reinforce the view that some small HSPs regulate fruit ripening in tomato. Thus, ethylene and transcription of class-1 sHSP genes seem interlinked in tomato, particularly at the initial phase of fruit ripening. These findings also corroborate the suggestion put forward earlier that observation of ripening induced expression of some HSP ESTs (Fei et al., 2004) and another class-I s*HSP21* gene may be crucial for progression of fruit ripening (Neta-Sharir et al., 2005). This indicates that additional factor(s) are involved in inducing these sHSP genes during fruit ripening. Our data showing that ethylene-treated tomato leaf is suppressed in the expression of *SlHSP17.7* gene suggests that this regulation occurs in both tissues, fruit and leaf. tissue independent.

We opine that ethylene suppression of *SlHSP* genes at the onset of fruit ripening when ethylene synthesis is initiated may be an indigenous regulation slated to enable fruit ripening to proceed uninterruptedly. Interestingly, transient suppression of both *SlHSP17.7A* and *SlHSP17.7B* genes by exogenous ethylene was more robust in the ethylene-deficient ACS2-AS genotype. Since ACS2-AS transgenic line produces only 50% of ethylene relative to its control suggests that a certain threshold

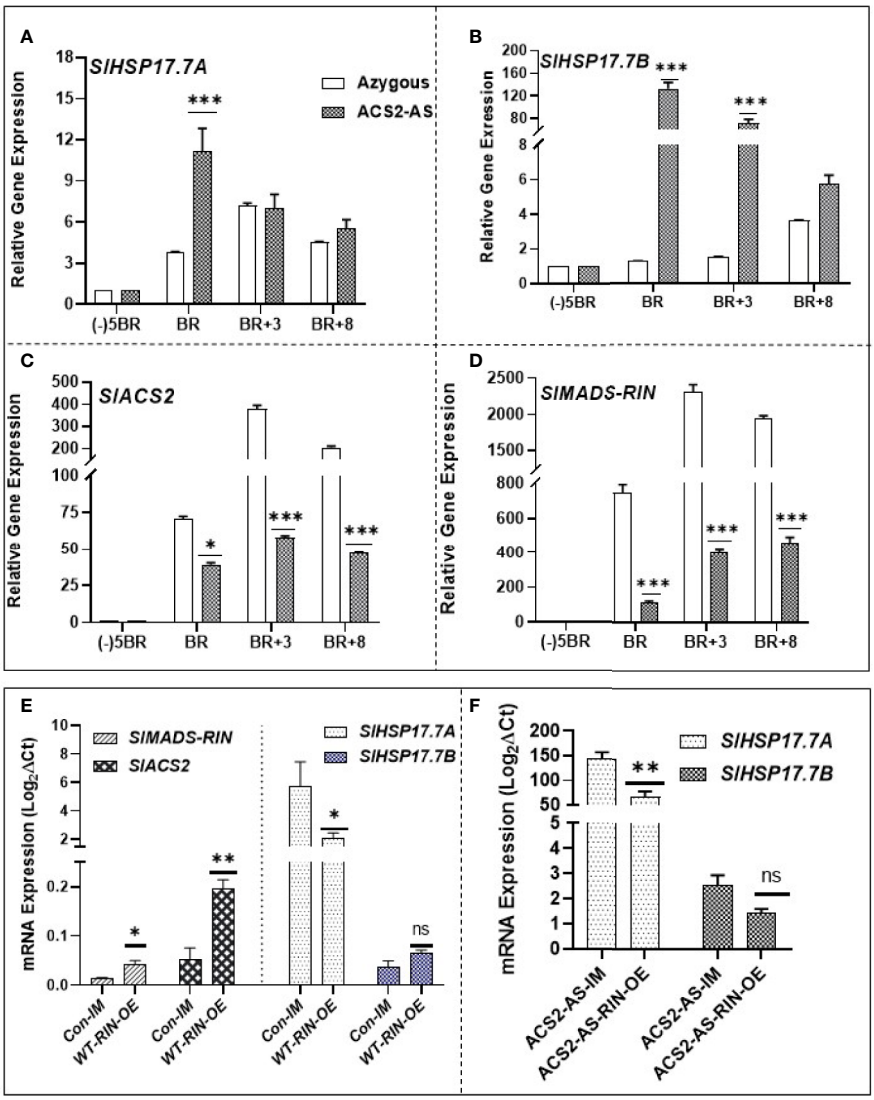

FIGURE 8 | Expression dynamics of *SlHSP17.7A*, *SlHSP17.7B*, and *SlMADS-RIN* during fruit ripening of ACC synthase 2 (*SlACS2*)-silenced tomato transgenic line (ACS2-AS) and the azygous/wild-type control lines (WT-Ohio8245) and RIN agroinjection. Fruit at different ripening stages were harvested from ACS2-AS and azygous control plants. RNA was isolated and expression levels of **(A)** SlHSP17.7A; **(B)** SlHSP17.7B; **(C)** SlACS2; **(D)** SlRIN were determined by qRT-PCR analysis. **(E)** Wild-type mature green tomato fruits were infiltrated with agrobacterium culture carrying RIN overexpression construct as described in the Materials and Methods Section. Fruits injected with only the infiltration medium were taken as control. RNA was isolated from infiltrated fruits and cDNA was prepared. Expression studies were done for *SlACS2, SlMADS-RIN*, *SlHSP17.7A*, *and SlHSP17.7B.* **(F)** Similar methodology as in (A) was repeated for ACS2-AS tomato and expression of *SlHSP17.7A* and *SlHSP17.7B* was determined. Error bars indicate standard deviation from a minimum of three replicates for each data point and statistical differences [*P ≤ 0.05, **P ≤ 0.01, ***P ≤ 0.001 and ****P ≤ 0.0001] are indicated.

of ethylene is necessary to achieve robust suppression of *SlHSP17.7* transcripts.

Our previous work on SlHSP17.6, 20.0, and 20.1 showed that transient suppression of these genes during fruit ripening transition is regulated by SlMADS-RIN-mediated and ethylene-dependent pathway (Shukla et al., 2017). Here, we demonstrated that *SlHSP17.7A* follows a similar kind of transcription regulation as the other members of this cluster (Goyal et al., 2012). However, *SlHSP17.8B* gene seems to be regulated by some other, as yet unknown transcriptional regulator different from SlMADS-RIN. However, in regard to regulation by ethylene both of these sHSPs are similarly suppressed by exogenous ethylene and their expression is highly upregulated at breaker stage in the ACS2-AS transgenic background tomato, a situation where SlMADS-RIN transcripts were found to be very low.

Notably, our results that demonstrated low SlMADS-RIN expression during fruit ripening in the ACS2-AS transgenic line deficient in ethylene by 50% suggest that (i) ethylene is required to induce SlMADS-RIN transcripts directly or/and (ii) an unknown ethylene-dependent regulator is necessary to induce

SlMADS-RIN during fruit ripening transition. These results suggest the need for a reevaluation of the role of SlMADS-RIN as the master regulator of fruit ripening which is also recently studied by different groups (Ito et al., 2017; Wang et al., 2020). Although, this was not the primary focus of this study but our primary results indicate that still ethylene is upstream to RIN, albeit this hypothesis needs rigorous experimentation. Further functional genomics studies are needed to characterize *in planta* the promoter of the two *SlHSP17.7* genes. Novel transgenic approaches can shed further light on specific role(s) of small HSPs in fruit physiology and ripening.

Differential gene expression in duplicated sHSP genes has been linked to homeostasis maintenance and their likely role(s) in responses to different stresses (Arce et al., 2018). Since HSP roles include protein folding, chaperone function and other, they are deemed essential for refolding proteins under abiotic stress situations (Murakami et al., 2004; Wang et al., 2004). Clearly, their committed role(s) in plant life and fruit ripening as presented here need to be followed further.

DATA AVAILABILITY STATEMENT

The raw data supporting the conclusions of this article will be made available by the authors, without undue reservation.

AUTHOR CONTRIBUTIONS

Conceived and designed the study: RU and AM. Performed the experiments: RU. Ethylene treatment of fruits and leaves: RU and MT. Analyzed the final data: RU and AM. Reagents availability: AM. Facilitated the research: AM. Wrote the paper: RU. Finalized the paper: AM.

FUNDING

This research was supported by an USDA-ARS intramural Project No. 8042-21000-143-00D (PI. AM). Mention of trade names or commercial products in this publication is solely for the purpose of providing specific information and does not imply recommendation or endorsement by the U.S. Department of Agriculture.

SUPPLEMENTARY MATERIAL

The Supplementary Material for this article can be found online at: https://www.frontiersin.org/articles/10.3389/fpls.2020.00975/full#supplementary-material

REFERENCES

Aevermann, B. D., and Waters, E. R. (2008). A comparative genomic analysis of the small heat shock proteins in *Caenorhabditis elegans* and *briggsae*. *Genetica* 133, 307–319. doi: 10.1007/s10709-007-9215-9

Alexander, L., and Grierson, D. (2002). Ethylene biosynthesis and action in tomato: a model for climacteric fruit ripening. *J. Exp. Bot.* 53, 2039–2055. doi: 10.1093/jxb/erf072

Arce, D., Spetale, F., Krsticevic, F., Cacchiarelli, P., Las-Rivas, J. D., Ponce, S., et al. (2018). Regulatory motifs found in the small heat shock protein (sHSP) gene family in tomato. *BMC Genomics* 19, 860. doi: 10.1186/s12864-018-5190-z

Barry, C. S., and Giovannoni, J. J. (2007). Ethylene and fruit ripening. *J. Plant Growth Regul.* 26, 143–159. doi: 10.1007/s00344-007-9002-y

Becker, J., and Craig, E. A. (1994). Heat-shock proteins as molecular chaperones. *Eur. J. Biochem.* 219, 11–23. doi: 10.1111/j.1432-1033.1994

Bustin, S. A., Benes, V., Garson, J. A., Hellemans, J., Huggett, J., Kubista, M., et al. (2009). The MIQE guidelines: minimum information for publication of quantitative real-time PCR experiments. *Clin. Chem.* 55, 611–622. doi: 10.1373/clinchem

Cara, B., and Giovannoni, J. J. (2008). Molecular biology of ethylene during tomato fruit development and maturation. *Plant Sci.* 175, 106–113. doi: 10.1016/j

Expósito-Rodríguez, M., Borges, A. A., Borges-Pérez, A., and Pérez, J. A. (2008). Selection of internal control genes for quantitative real-time RT-PCR studies during tomato development process. *BMC Plant Biol.* 8, 131. doi: 10.1186/1471-2229-8-131

Fei, Z. J., Tang, X., Alba, R. M., White, J. A., Ronning, C. M., Martin, G. B., et al. (2004). Comprehensive EST analysis of tomato and comparative genomics of fruit ripening. *Plant J.* 40, 47–59. doi: 10.1111/j.1365-313X.2004.02188.x

Fluhr, R., and Mattoo, A. K. (1996). Ethylene — Biosynthesis and perception. *CRC Crit. Rev. Plant Sci.* 15, 479–523. doi: 10.1080/07352689609382368

Franck, E., Madsen, O., van Rheede, T., Ricard, G., Huynen, M. A., and de Jong, W. W. (2004). Evolutionary diversity of vertebrate small heat shock proteins. *J. Mol. Evol.* 59, 792–805. doi: 10.1007/s00239-004-0013-z

Fray, R. G., Lycett, G. W., and Grierson, D. (1990). Nucleotide sequence of a heat-shock and ripening-related cDNA from tomato. *Nucleic Acids Res.* 18, 7148. doi: 10.1093/nar/18.23.7148

Fu, X., Jiao, W., and Chang, Z. (2006). Phylogenetic and biochemical studies reveal a potential evolutionary origin of small heat shock proteins of animals from bacterial class. *A. J. Mol. Evol.* 62, 257–266. doi: 10.1007/s00239-005-0076-5

Fujisawa, M., Nakano, T., and Ito, Y. (2011). Identification of potential target genes for the tomato fruit-ripening regulator RIN by chromatin immunoprecipitation. *BMC Plant Biol.* 11, 26. doi: 10.1186/1471-2229-11-26

Fujisawa, M., Nakano, T., Shima, Y., and Ito, Y. (2013). A large-scale identification of direct targets of the tomato MADS box transcription factor RIPENING INHIBITOR reveals the regulation of fruit ripening. *Plant Cell* 25, 371–386. doi: 10.1105/tpc.112.108118

Giorno, F., Wolters-Arts, M., Grillo, S., Scharf, K. D., Vriezen, W. H., and Mariani, C. (2010). Developmental and heat stress-regulated expression of HsfA2 and small heat shock proteins in tomato anthers. *J. Exp. Bot.* 61, 453–462. doi: 10.1093/jxb/erp316

Giovannoni, J., Nguyen, C., Ampofo, B., Zhong, S., and Fei, Z. (2017). The epigenome and transcriptional dynamics of fruit ripening. *Ann. Rev. Plant Biol.* 68, 61–84. doi: 10.1146/annurev-arplant-042916-040906

Giovannoni, J. J. (2007). Fruit ripening mutants yield insights into ripening control. *Curr. Opin. Plant Biol.* 10, 283–289. doi: 10.1016/j.pbi

Goyal, R. K., Kumar, V., Shukla, V., Mattoo, R., Liu, Y., Chung, S. H., et al. (2012). Features of a unique intron-less cluster of class I small heat shock protein genes in tandem with box C/D snoRNA genes on chromosome 6 in tomato (*Solanum lycopersicum*). *Planta* 235, 453–471. doi: 10.1007/s00425-011-1518-5

Gray, J. E., Picton, S., Giovannoni, J. J., and Grierson, D. (1994). The use of transgenic and naturally occurring mutants to understand and manipulate tomato fruit ripening. *Plant Cell Environ.* 17, 557–571. doi: 10.1111/j.1365-3040

Hackett, R. M., Ho, C. W., Lin, Z., Foote, H. C., Fray, R. G., and Grierson, D. (2000). Antisense inhibition of the *Nr* gene restores normal ripening to the tomato Never-ripe mutant, consistent with the ethylene receptor-inhibition model. *Plant Physiol.* 124, 1079–1086. doi: 10.1104/pp.124.3.1079

Hartl, F. U. (1996). Molecular chaperones in cellular protein folding. *Nature* 381, 571–579. doi: 10.1038/381571a0

Higo, K., Ugawa, Y., Iwamoto, M., and Korenaga, T. (1999). Plant cis-acting regulatory DNA elements (PLACE) database: 1999. *Nucleic Acids Res.* 27, 297–300. doi: 10.1093/nar/27.1.297

Hileman, L. C., Sundstrom, J. F., Litt, A., Chen, M., Shumba, T., and Irish, V. F. (2006). Molecular and phylogenetic analyses of the MADS-box gene family in tomato. *Mol. Biol. Evol.* 23, 2245–2258. doi: 10.1093/molbev/msl095

Ito, Y., Kitagawa, M., Ihashi, N., Yabe, K., Kimbara, J., Yasuda, J., et al. (2008). DNA-binding specificity, transcriptional activation potential, and the *rin* mutation effect for the tomato fruit-ripening regulator RIN. *Plant J.* 55, 212–223. doi: 10.1111/j.1365-313X

Ito, Y., Nishizawa-Yokoi, A., Endo, M., Mikami, M., Shima, Y., Nakamura, N., et al. (2017). Re-evaluation of the rin mutation and the role of RIN in the induction of tomato ripening. *Nat. Plants* 3, 866–874.

Kappé, G., Leunissen, J. A. M., and de Jong, W. W. (2002). Evolution and diversity of prokaryotic small heat shock proteins. *Small Stress Proteins* 28, 1–17. doi: 10.1007/978-3-642-56348-5_1

Klee, H. J., and Giovannoni, J. J. (2011). Genetics and control of tomato fruit ripening and quality attributes. *Annu. Rev. Genet.* 45, 41–59. doi: 10.1146/annurev-genet-110410-132507

Kumar, S., Stecher, G., and Tamura, K. (2016). MEGA7: Molecular Evolutionary Genetics Analysis version 7.0 for bigger datasets. *Mol. Biol. Evol.* 33, 1870–1874. doi: 10.1093/molbev/msw054

Lescot, M., Déhais, P., Thijs, G., Marchal, K., Moreau, Y., Van de Peer, Y., et al. (2002). PlantCARE, a database of plant cis-acting regulatory elements and a portal to tools for in silico analysis of promoter sequences. *Nucleic Acids Res.* 30, 325–327. doi: 10.1093/nar/30.1.325

Liberek, K., Lewandowska, A., and Zietkiewicz, S. (2008). Chaperones in control of protein disaggregation. *EMBO J.* 27, 328–335. doi: 10.1038/sj.emboj

Livak, K. J., and Schmittgen, T. D. (2001). Analysis of relative gene expression data using real time quantitative PCR and the $2^{-\Delta\Delta CT}$ method. *Methods* 25, 402–408. doi: 10.1006/meth.2001.1262

Martel, C., Vrebalov, J., Tafelmeyer, P., and Giovannoni, J. J. (2011). The tomato MADS-box transcription factor RIPENING INHIBITOR interacts with promoters involved in numerous ripening processes in a COLORLESS NONRIPENING-dependent manner. *Plant Physiol.* 157, 1568–1579. doi: 10.1104/pp.111.181107

Mascia, T., Santovito, E., Gallitelli, D., and Cillo, F. (2010). Evaluation of reference genes for quantitative reverse-transcription polymerase chain reaction normalization in infected tomato plants. *Mol. Plant Pathol.* 11, 805–816. doi: 10.1111/j.1364-3703.2010

Mattoo, A. K., and Upadhyay, R. K. (2019). "Plant hormones: Some glimpses on biosynthesis, signaling networks, and crosstalk," in *Sensory Biology of Plants*. Ed. S. Sopory (Singapore: Springer), 227–246. doi: 10.1007/978-981-13-8922-1_9

Mattoo, A. K., and Vickery, R. S. (1977). Subcellular distributions of isoenzymes in fruits of a normal cultivar of tomato and of the *rin* mutant at two stages of development. *Plant Physiol.* 60, 496–498. doi: 10.1104/pp.60.4.496

Mehta, R. A., Cassol, T., Li, N., Ali, N., Handa, A. K., and Mattoo, A. K. (2002). Engineered polyamine accumulation in tomato enhances phytonutrient content, juice quality, and vine life. *Nat. Biotechnol.* 20, 613–618. doi: 10.1038/nbt0602-613

Moore, S., Vrebalov, J., Payton, P., and Giovannoni, J. (2002). Use of genomics tools to isolate key ripening genes and analyse fruit maturation in tomato. *J. Exp. Bot.* 53, 2023–2030. doi: 10.1093/jxb/erf057

Murakami, T., Matsuba, S., Funatsuki, H., Kawaguchi, K., Saruyama, H., Tanida, M., et al. (2004). Over-expression of a small heat shock protein, sHSP17.7, confers both heat tolerance and UV-B resistance to rice plants. *Mol. Breed.* 13, 165–175. doi: 10.1023/B:MOLB.0000018764.30795.c1

Neta-Sharir, I., Isaacson, T., Lurie, S., and Weiss, D. (2005). Dual role for tomato heat shock protein 21: protecting photosystem II from oxidative stress and promoting color changes during fruit maturation. *Plant Cell* 17, 1829–1838. doi: 10.1105/tpc.105.031914

Ng, M., and Yanofsky, M. F. (2001). Function and evolution of the plant MADS-box gene family. *Nat. Rev. Genet.* 2, 186–195. doi: 10.1038/35056041

Oeller, P. W., Lu, M. W., Taylor, L. P., Pike, D. A., and Theologis, A. (1991). Reversible inhibition of tomato fruit senescence by antisense RNA. *Science* 254, 437–439. doi: 10.1126/science.1925603

Orzaez, D., Mirabel, S., Wieland, W. H., and Granell, A. (2006). Agroinjection of Tomato Fruits. A tool for rapid functional analysis of transgenes directly in fruit. *Plant Physiol.* 140, 3–11. doi: 10.1104/pp.105.068221

Paul, A., Rao, S., and Mathur, S. (2016). The α-Crystallin Domain Containing Genes: Identification, phylogeny and expression profiling in abiotic stress, phytohormone response and development in Tomato (*Solanum lycopersicum*). *Front. Plant Sci.* 7, 426. doi: 10.3389/fpls.2016.00426

Picton, S., Barton, S. L., Bouzayen, M., Hamilton, A. J., and Grierson, D. (1993). Altered fruit ripening and leaf senescence in tomatoes expressing an antisense ethylene-forming enzyme transgene. *Plant J.* 3, 469–481. doi: 10.1111/j.1365-313X.1993.tb00167.x

Plesofsky-Vig, N., Vig, J., and Brambl, R. (1992). Phylogeny of the α crystallin-related heat shock proteins. *J. Mol. Evol.* 35, 537–545. doi: 10.1007/BF00160214

Ré, M. D., Gonzalez, C., Escobar, M. R., Sossi, M. L., Valle, E. M., and Boggio, S. B. (2016). Small heat shock proteins and the postharvest chilling tolerance of tomato fruit. *Physiol. Plant* 159, 148–160. doi: 10.1111/ppl.12491

Ramakrishna, W., Deng, Z., Ding, C., Handa, A. K., and Ozminkowski, R. H. J. (2003). A novel small heat shock protein gene, *vis1*, contributes to pectin depolymerization and juice viscosity in tomato fruit. *Plant Physiol.* 131, 725–735. doi: 10.1104/pp.012401

Razdan, M. K., and Mattoo, A. K. (2007). "Genetic improvement of Solanaceous crops," in *Tomato*, vol. 2. (Enfield, UK: Science Publishers, Inc.). doi: 10.1017/S0014479707005443

Shukla, V., Upadhyay, R. K., Tucker, M. L., Giovannoni, J. J., Rudrabhatla, S. V., and Mattoo, A. K. (2017). Transient regulation of three clustered tomato class-I small heat-shock chaperone genes by ethylene is mediated by *SlMADS-RIN* transcription factor. *Sci. Rep.* 7, 6474. doi: 10.1038/s41598-017-06622-0

Sobolev, A. P., Neelam, A., Fatima, T., Shukla, V., Handa, A. K., and Mattoo, A. K. (2014). Genetic introgression of ethylene-suppressed transgenic tomatoes with higher-polyamines trait overcomes many unintended effects due to reduced ethylene on the primary metabolome. *Front. Plant Sci.* 5, 632. doi: 10.3389/fpls.2014.00632

Sun, W., Van Montagu, M., and Verbruggen, N. (2002). Small heat shock proteins and stress tolerance in plants. *Biochim. Biophys. Acta* 1577, 1–9. doi: 10.1016/S0167-4781(02)00417-7

Tyedmers, J., Mogk, A., and Bukau, B. (2010). Cellular strategies for controlling protein aggregation. *Nat. Rev. Mol. Cell Biol.* 11, 777–788. doi: 10.1038/nrm2993

Upadhyay, R. K., and Mattoo, A. K. (2018). Genome-wide identification of tomato (Solanum lycopersicum L.) lipoxygenases coupled with expression profiles during plant development and in response to methyl-jasmonate and wounding. *J. Plant Physiol.* 231, 318–328. doi: 10.1016/j.jplph.2018.10.001.

Upadhyay, R. K., Gupta, A., Soni, D., Garg, R., Pathre, U. V., Nath, P., et al. (2017). Ectopic expression of a tomato DREB gene affects several ABA processes and influences plant growth and root architecture in an age-dependent manner. *J. Plant Physiol.* 214, 97–107. doi: 10.1016/j.jplph.2017.04.004

Vandesompele, J., De Preter, K., Pattyn, i., Poppe, B., Van Roy, N., De Paepe, A., et al. (2002). Accurate normalization of real-time quantitative RT-PCR data by geometric averaging of multiple internal control genes. *Genome Biol.* 3, 34–41. doi: 10.1186/gb-2002-3-7-research0034

Vrebalov, J. (2002). A MADS-Box gene necessary for fruit ripening at the tomato ripening-inhibitor (*rin*) locus. *Science* 296, 343–346. doi: 10.1126/science.1068181

Wang, W., Vinocur, B., Shoseyov, O., and Altman, A. (2004). Role of plant heat-shock proteins and molecular chaperones in the abiotic stress response. *Trends Plant Sci.* 9, 244–252. doi: 10.1016/j.tplants.2004.03.006

Wang, R., Angenent, G. C., Seymour, G., and de Maagd, R. A. (2020). Revisiting the role of master regulators in tomato ripening. *Trends Plant Sci.* 25, 291–301. doi: 10.1016/j.tplants.2019.11.005

Waters, E. R., and Vierling, E. (1999). Chloroplast small heat shock proteins: evidence for atypical evolution of an organelle-localized protein. *Proc. Natl. Acad. Sci. U.S.A.* 96, 14394–14399. doi: 10.1073/pnas.96.25.14394

Waters, E. R. (2013). The evolution, function, structure, and expression of the plant sHSPs. *J. Exp. Bot.* 64, 391–403. doi: 10.1093/jxb/ers355

Wilkinson, J. Q., Lanahan, M. B., Yen, H., Giovannoni, J. J., and Klee, H. J. (1995). An ethylene-inducible component of signal transduction encoded by never-ripe. *Science* 270, 14–16. doi: 10.1126/science.270.5243.1807

Yu, J., Cheng, Y., Feng, K., Ruan, M., Ye, Q., Wang, R., et al. (2016). Genome-wide identification and expression profiling of tomato Hsp20 Gene family in response to biotic and abiotic stresses. *Front. Plant Sci.* 7, 1215. doi: 10.3389/fpls.2016.01215

Zhang, J., Chen, H., Wang, H., Li, B., Yi, Y., Kong, F., et al. (2015). Constitutive expression of a tomato small heat shock protein gene *LeHSP21* improves tolerance to high-temperature stress by enhancing antioxidation capacity in tobacco. *Plant Mol. Biol. Rpt* 34, 399–409. doi: 10.1007/s11105-015-0925-3

Zhong, S., Fei, Z., Chen, Y.-R., Zheng, Y., Huang, M., Vrebalov, J., et al. (2013). Single-base resolution methylomes of tomato fruit development reveal epigenome modifications associated with ripening. *Nat. Biotechnol.* 31, 154–159. doi: 10.1038/nbt.2462

Conflict of Interest: The authors declare that the research was conducted in the absence of any commercial or financial relationships that could be construed as a potential conflict of interest.

frontiers in Plant Science

ORIGINAL RESEARCH
published: 01 July 2020
doi: 10.3389/fpls.2020.00668

The Effects of Salicylic Acid and Its Derivatives on Increasing Pomegranate Fruit Quality and Bioactive Compounds at Harvest and During Storage

*María E. García-Pastor[1], Pedro J. Zapata[1], Salvador Castillo[1], Domingo Martínez-Romero[1], Fabián Guillén[1], Daniel Valero[1] and María Serrano[2]**

[1] Department of Agro-Food Technology, University Miguel Hernández, Orihuela, Spain, [2] Department of Applied Biology, University Miguel Hernández, Orihuela, Spain

OPEN ACCESS

Edited by:
Cai-Zhong Jiang, Crops Pathology and Genetics Research Unit, USDA-ARS, United States

Reviewed by:
Francisco Garcia-Sanchez, Spanish National Research Council, Spain
Valerio Cristofori, University of Tuscia, Italy

***Correspondence:**
María Serrano
m.serrano@umh.es

Specialty section:
This article was submitted to Crop and Product Physiology, a section of the journal Frontiers in Plant Science

Received: 11 March 2020
Accepted: 29 April 2020
Published: 01 July 2020

Citation:
García-Pastor ME, Zapata PJ, Castillo S, Martínez-Romero D, Guillén F, Valero D and Serrano M (2020) The Effects of Salicylic Acid and Its Derivatives on Increasing Pomegranate Fruit Quality and Bioactive Compounds at Harvest and During Storage. Front. Plant Sci. 11:668. doi: 10.3389/fpls.2020.00668

In the present research two experiments were performed to evaluate the effect of pre-harvest salicylic acid (SA), acetyl salicylic acid (ASA), and methyl salicylate (MeSa), applied as a foliar spray to pomegranate "Mollar de Elche," on crop yield, fruit quality parameters, and bioactive compounds at harvest and during storage. In the 2017 experiment, trees were treated with SA, ASA, and MeSa at 1, 5, and 10 mM and a higher crop yield (kg tree^{-1} and number of harvested fruit tree^{-1}) and quality parameters (firmness, aril color, and individual sugars and organic acids) at harvest were obtained, as well as a higher concentration of phenolics, anthocyanins, and ascorbic acid. The best results were achieved with 10 mM dose of the three assayed compounds, which was chosen for the 2018 experiment, and results for crop yield and fruit quality attributes were confirmed. These quality traits and the concentration of phenolics, anthocyanins, and ascorbic acid were maintained at higher levels in pomegranate fruit from treated trees than in controls during prolonged storage at 10°C. In addition, the effects of salicylate treatments on increasing total and individual anthocyanin concentration in pomegranate arils led to arils with a deeper red color (**Graphical Abstract**) and, in turn, fruit that would be more appreciated in the international market. This fact, together with the increased crop yield, would contribute to the increased profit of this crop. Thus, pre-harvest treatment with salicylates, and especially SA at 10 mM concentration, could be a safe, natural, and new tool to improve fruit quality and its content on antioxidant compounds with health beneficial effects (namely, ascorbic acid, phenolics, and anthocyanins) at harvest and during storage.

Keywords: ***Punica granatum*** **L, acetyl salicylic acid, methyl salicylate, anthocyanins, phenolics, ascorbic acid, sugars, organic acids**

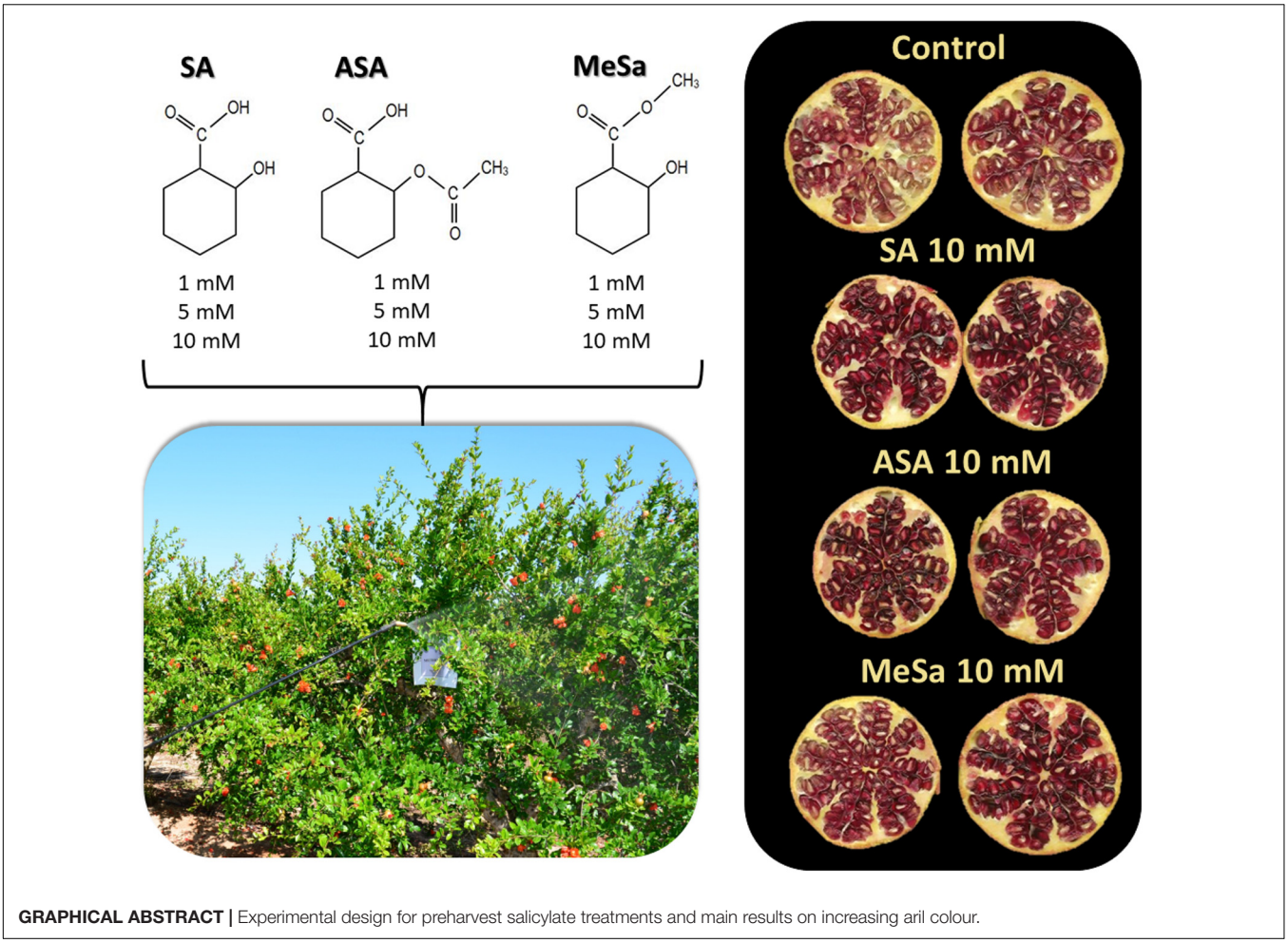

GRAPHICAL ABSTRACT | Experimental design for preharvest salicylate treatments and main results on increasing aril colour.

INTRODUCTION

Pomegranate is one of the oldest known edible fruits, associated with ancient civilizations in the Middle East. It was originated in the area nowadays occupied by Iran and Afghanistan and from this area it was spread to India, China, Turkey, Egypt, Tunisia, Morocco, and Spain (Pareek et al., 2015). Spain is the major producer and exporting country of pomegranate fruit in the European Union, with a production area of 3,567 ha and a production of 65,165 t in 2017 (MAGRAMA, 2017). The edible portion of pomegranate are the arils, which consist of around 80% juice and 20% seed (Cristofori et al., 2011) and the fruit can be consumed as fresh fruit or used to prepare juices, canned beverages, jellies, jams, and flavorings and colorings for drinks (Valero et al., 2014).

Pomegranate fruit quality depends largely on fruit size, skin color, and absence of visual defects, such as sunburn, growth cracks, cuts, bruises, and decay, as well as on aril color, sugar and acid content, and the presence of small and soft seeds. In Spain, "Mollar de Elche" is the most cultivated pomegranate cultivar which is very appreciated by consumers due to its high concentration of sugars, low acidity, and its barely discernible seeds, since they are very small and soft and can be easily eaten (Nuncio-Jáuregui et al., 2014). On the other hand, pomegranate has been used in the folk medicine of many countries from ancient times, and its beneficial effects against several diseases, such as atherosclerosis, inflammatory and infective-mediated diseases, Alzheimer, diabetes, infarct brain ischemia, and several types of cancer, have been reported recently and attributed to its phenolic compounds and anthocyanins (Faria and Calhau, 2011; Ismail et al., 2012; Asgary et al., 2017; Panth et al., 2017). Nevertheless, the phytochemical composition of pomegranate fruit is affected by several factors, such as genotype, area of cultivation, environmental conditions, and agronomic management, among others. Thus, six different anthocyanins, namely, cyanidin-3,5-diglucoside, pelargonidin-3,5-diglucoside, delphinidin-3,5-diglucoside, cyanidin-3-glucoside, pelargonidin-3-glucoside, and delphinidin-3-glucoside, were identified in a wide range of Italian pomegranate cultivars, although their concentrations were different depending on cultivars, as well as other phenolic compounds (Fanali et al., 2016; Russo et al., 2018). Great variations on total and individual phenolic and anthocyanin concentrations were also found by Zaouay et al. (2012) in thirteen Tunisian cultivars. However, "Mollar de Elche" cultivar does not have a high anthocyanin content as compared with other worldwide-known cultivars such as "Wonderful" and,

in turn, its arils are only slightly red-colored and the skin has a cream-pink color (Li et al., 2015; Pareek et al., 2015; Cano-Lamadrid et al., 2018). This fact makes it difficult for this cultivar to reach international markets. Thus, treatments to increase the coloration of the skin and arils of "Mollar de Elche" pomegranate would lead to its increased commercialization in international markets as well as its antioxidant properties and health beneficial effects. In this sense, it has been reported that water restrictions applied in summer (during the linear phase of fruit growth) led to an increase in aril anthocyanin content (Bartual et al., 2015), as well as treatment with methyl jasmonate during on-tree pomegranate fruit development (García-Pastor et al., 2020).

Salicylic acid (SA) and its derivatives, acetyl salicylic acid (ASA) and methyl salicylate (MeSa), are plant hormones that play important roles in a wide range of physiological processes, from seed germination to flowering and fruit ripening, although the most studied roles have been their effects on inducing plant defense systems against different biotic and abiotic stresses (Tiwari et al., 2017; Koo et al., 2020). It has been reported that postharvest treatments with salicylates reduce decay and chilling injury in a wide range of fruits, and improve other quality properties, such as appearance, texture, and nutritional compounds (Asghari and Aghdam, 2010; Glowacz and Ree, 2015). Thus, SA, ASA, or MeSa applied as postharvest treatments resulted in higher quality attributes in apricots (Wang et al., 2015) and increased the content on anthocyanins and other bioactive compounds in blood oranges (Habibi et al., 2020), sweet cherries (Valero et al., 2011), kiwifruit (Zhang et al., 2003), mango (Ding et al., 2007), sugar apples (Mo et al., 2008), and peaches (Tareen et al., 2012), with additional effects on delaying the postharvest ripening process. On the other hand, the application of these salicylates during fruit development on trees has been reported to improve fruit quality parameters at harvest. Thus, SA treatment at 0.1 and 0.2 mM of vine (at veraison stage) increased anthocyanin content in berries (Oraei et al., 2019) and SA, ASA, or MeSa treatments (0.5, 1, and 2 mM) applied at three key points of fruit development enhanced sugars, organic acids, and antioxidant compounds in plums at harvest and after storage (Martínez-Esplá et al., 2017, 2018) as well as in sweet cherries (Giménez et al., 2014, 2015, 2017; Valverde et al., 2015). In these previous papers, a delay on the postharvest ripening process was also observed, which was attributed to the increased concentration of antioxidant compounds and the activity of antioxidant enzymes.

Specifically, in pomegranate SA, ASA, and MeSa postharvest treatments reduced chilling injury (CI) and maintained fruit quality and higher levels of total antioxidant compounds, such as anthocyanins, phenolics, or ascorbic acid (Sayyari et al., 2009, 2011a,b). Accordingly, postharvest 2 mM SA treatment in combination with a controlled atmosphere storage delayed quality losses and extended the storage life of "Hicazna" pomegranates (Koyuncu et al., 2019). In addition, 0.25 mM ASA treatment of pomegranate arils reduced browning and maintained higher concentrations of phenolics and anthocyanins during storage (Dokhanieh et al., 2016). As a preharvest treatment, just one previous paper is available in which 1 mM SA treatment reduced bacterial blight, a devastating pomegranate disease caused by *Xanthomonas axonopodis pv. Punicae* (Lalithya et al., 2017). However, there are no previous reports regarding the effect of pre-harvest treatments of pomegranate trees with SA, ASA, or MeSa on fruit growth and ripening, as well as on fruit quality attributes at harvest, which was the main goal of the present research. In addition, it was hypothesized that an increase on anthocyanin content would occur as a consequence of these treatments, according to results on other fruit species obtained in previous reports, as commented above.

MATERIALS AND METHODS

Plant Material and Experimental Design

The experiments (2017 and 2018) were performed in a commercial orchard of 'Mollar de Elche' pomegranate trees (10,11 years-old), planted at 6 × 5 m, located in Elche, south of Alicante, Spain (UTMX: 694006.000 UTMY: 4234860.000). Climatic conditions in the crop field were: a semi-arid Mediterranean climate, with mean annual temperatures of 19.28 and 18.97°C for 2017 and 2018, respectively; maximum temperatures in summer, from June to September, of 31.62 and 31.42 for 2017 and 2018, respectively; and accumulated rainfall of 238.32 and 270.19 mm for 2017 and 2018, respectively[1]. Soil was composed of sand, silt, and clay at 30, 34, and 36%, respectively, and had a pH of 7.8. Irrigation was carried out by using a drip irrigation system with eight emitters per tree, each delivering 4 L h^{-1} as follows. April: two watering cycles of 1 h per week; May, June, July, August, and September: two watering cycles of 2 h per week; and October: one watering cycle of 1 h. The irrigation water used had an electrical conductivity ca. 3 dS m^{-1}. Fertilization was applied in the irrigation system at 160/80/160 kg ha^{-1} nitrogen/phosphorus/potassium (N/P/K) ratio. Pruning and thinning were carried out during the experiments according to standard cultural practices for pomegranate. In 2017 experiment, three blocks or replicates (of three trees each) were selected, totally at random, for treatments: SA, ASA, and MeSA at 1, 5, and 10 mM and control. Treatments were performed by foliar spray application of 3 L of freshly prepared SA, ASA, or MeSa (Sigma Aldrich, Madrid) solutions, containing 1 mL L^{-1} Tween-20 (a polyoxyethylene sorbitol ester, acting as a non-ionic detergent). Control trees were sprayed with distilled water containing 1 mL L^{-1} Tween-20. Dates of treatments were set by taking into account the harvest dates of this cultivar in similar growing conditions in previous seasons, so that the first treatment was applied before the skin color changes and the last one 4 days before the first harvest, according to previous reports (García-Pastor et al., 2020). Dates of treatments in 2017 were: 3rd July, 2nd August, 1st September, and 2nd October. In the 2018 experiment, treatments were SA, ASA, or MeSa at 10 mM concentration and control, which were applied as in the 2017 experiment but instead using five trees for each of the three blocks or replicates. Dates of treatments were: 10th July, 10th August, 11th September, and 11th October. For both

[1]http://riegos.ivia.es/datos-meteorologicos

years, each block or replicate for each treatment was set in a row, leaving an untreated tree between each block and an untreated row between each treated row in order to avoid treatment cross effects. In addition, at least one tree without treatment was left in each row to avoid edge effect.

Fruits were harvested according to commercial criteria based on fruit size (8.5–9.0 cm of diameter and weight of 325–350 g), skin color (cream-light pink), and total soluble solids (TSS) content characteristic of this cultivar (more than 15°Brix). In both years, fruits were picked on two dates, separated by 20 days, due to the heterogeneous fruit on-tree ripening process. On both harvest dates, the yield (kg tree^{-1} and number of fruits tree^{-1}) were determined. In the 2017 experiment, five fruits from the first picking, homogenous in size and color and without visual defects, were selected from each replicate and treatment and immediately transferred to the laboratory for analytical determinations. In the 2018 experiment, four lots of five fruits also homogenous in size and color and without visual defects were chosen at random for each replicate and treatment, immediately transferred to the laboratory, and stored for 0 (day 0), 30, 60, and 90 days at 10°C and at a relative humidity of 85–90%. For each sampling date during storage, one lot was taken at random for each replicate and treatment.

Fruit Yield, Respiration Rate and Qualitative Traits

Yield, expressed as kg tree^{-1} and number of fruit tree^{-1}, was measured at two harvest dates and growing seasons. Then, fruit mass (g) and the percentage of fruits harvested at the first picking were calculated. Results were expressed as the mean ± SE. The weight of each pomegranate lot was measured at day 0 and after each storage period, and weight loss was expressed as a percentage with respect to initial weight. To quantify respiration rate, each fruit lot was hermetically sealed in a 3 L jar for 30 min. After that, 1 mL from the holder atmosphere was withdrawn with a syringe and injected into a Shimadzu TM 14A gas chromatograph (Kyoto, Japan) equipped with a thermal conductivity detector under the chromatographic conditions previously described (Sayyari et al., 2011b).Respiration rate was expressed as g of CO_2 released by kg^{-1} s^{-1}.

Fruit firmness was measured individually in each of the five fruits of each replicate by using a TX-XT2i Texture Analyzer (Stable Mycrosystems, Godalming, United Kingdom) which applied a force to achieve a 3% deformation of the fruit diameter. Results were expressed as the relation between the applied force and the traveled distance (kN m^{-1}) and are the mean ± SE.

Skin and aril color were measured by digital image analysis. Photographs of the pomegranates were captured using a digital camera (Nikon D3400) in a light box with black background. The setup conditions of the camera were as follows: light provided by two LEDs of color temperature of 5600 K, flash speed of 1/5 s, ISO-200, focal opening (f) 20, and length 35 mm. For skin color measure, one image of the front and another of the back side of the five fruits of each of the three replicates for each treatment were captured, saved as JPEG file, and analyzed by using the software ImageJ v1.52a (NIH Image, National Institutes of Health, Bethesda, United States). The CIELab model was used to calculate Hue angle (arctg b*/a*) according to García et al. (2017). Pomegranate fruits were cut by the equatorial plane and aril color was measured by taking photographs of the cut surface as indicated above. After that, arils of the five pomegranates of each replicate were combined to obtain a homogeneous sample for each replicate in which the following parameters were measured. Titratable acidity (TA) was determined in duplicate in each sample, by using 1 mL of diluted juice (in 25 mL distilled H_2O), obtained from 30 g of pomegranate arils, which was automatically titrated (785 DMP Titrino, Metrohm) with 0.1 N NaOH up to pH 8.1, and the results were expressed as g malic acid equivalent kg^{-1} in fresh weight basis. Total soluble solids (TSS) were measured in duplicate in the same juice by using a digital refractometer (Atago PR-101, Atago Co., Ltd., Tokyo, Japan) at 20°C and expressed as g kg^{-1} in fresh weight basis. After that, the aril samples were stored at −25°C until the following determinations were performed.

Total Phenolics, Total Anthocyanin, and Total Antioxidant Activity Quantification

To extract phenolic compounds, 5 g of arils were homogenized with 10 mL of water: methanol (2:8, v/v) containing 2 mM NaF by using a homogenizer (Ultraturrax, T18 basic, IKA, Berlin, Germany) for 30 s. The extracts were centrifuged at 10,000 *g* for 10 min at 4°C and the supernatant was used to quantify total phenolics (in duplicate in each extract) by using the Folin-Ciocalteu reagent as previously described by Sayyari et al. (2011a). The results were expressed as g gallic acid equivalent (GAE) kg^{-1} and are the mean ± SE of three replicates. For anthocyanin extraction, 5 g of arils were homogenized as above in 15 mL of methanol: formic acid: water (79:1:20, v/v/v) and then centrifuged at 10,000 *g* for 10 min at 4°C. The absorbance at 520 nm was measured in the supernatant (in duplicate for each sample) and total anthocyanin content (TAC) was expressed as g kg^{-1} of cyanidin 3-*O*-glucoside equivalents (Cyn 3-gluc, molar absorption coefficient of 23,900 L cm^{-1} mol^{-1} and molecular weight of 449.2 g mol^{-1}). To measure total antioxidant activity (TAA), 5 g of arils were homogenized in 10 mL of 50 mM phosphate buffer pH = 7.8 and 5 mL of ethyl acetate as indicated above. The homogenate was centrifuged at 10,000 *g* for 15 min at 4°C and the upper and lower fractions were used to quantify lipophilic (L-TAA) and hydrophilic total antioxidant activity (H-TAA), respectively. H-TAA and L-TAA were determined in duplicate in each extract as previously described (Sayyari et al., 2011a), in a reaction mixture containing 2,20-azino-bis-(3-ethylbenzothiazoline-6-sulfonic acid) diammonium salt (ABTS), horseradish peroxidase enzyme, and its oxidant substrate (hydrogen peroxide), in which $ABTS^+$ radicals are generated and monitored at 730 nm. The decrease in absorbance after adding the pomegranate extract was proportional to TAA of the sample which was calculated by using a calibration curve made with Trolox [(R)-(+)-6-hydroxy- 2, 5, 7, 8-tetramethyl-croman-2-carboxylic acid] (0–20 nmol) from Sigma Aldrich (Madrid, Spain), and results are expressed as g of Trolox Equivalent (TE) kg^{-1} and are the mean ± SE of three replicates.

Individual Anthocyanin Quantification

The extracts obtained for total anthocyanin quantification described previously were filtered through a 0.45 μm PVDF filter (Millex HV13, Millipore, Bedford, MA, United States) and then individual anthocyanins were identified by liquid chromatography coupled to mass spectrometry (HPLC-DAD-ESI/MSn) by using an Agilent HPLC1100 series machine equipped with a photodiode array detector and a mass detector in series (Agilent Technologies, Waldbronn, Germany), as previously reported (Martínez-Esplá et al., 2014). To quantify individual anthocyanins, two samples of each extract were injected into a HPLC system (Agilent HPLC 1200 Infinity series) working with the chromatographic conditions previously reported (Martínez-Esplá et al., 2014). Chromatograms were recorded at 520 nm and quantification was performed by using calibration curves carried out with cyanidin 3-*O*-glucoside (Cyn 3-gluc), cyanidin 3,5-*O*-di-glucoside (Cyn 3,5-di-gluc), pelargonidin 3-*O*-glucoside (Plg 3-gluc), and pelargonidin 3,5-*O*-di-glucoside (Plg 3,5-di-gluc) (Sigma-Aldrich, Germany). Delphinidin 3-*O*-glucoside (Dlp 3-gluc) and delphinidin 3,5-*O*-di-glucoside (Dlp 3,5-di-gluc) were quantified as Cyn 3-gluc equivalents. Results were expressed as mg kg^{-1} fresh weight (mean ± SE of three replicates).

Ascorbic Acid (AA), Dehydroascorbic Acid (DHA), and Total Vitamin C Quantification

Ascorbic (AA) and dehydroascorbic (DHA) acids were measured according to Peña-Estévez et al. (2016). Briefly, 5 g of frozen arils were homogenized with 5 mL of methanol: water (5:95) containing 0.1 mM citric acid, 0.05 mM ethylenediamine tetraacetic acid disodium salt, and 4 mM NaF for 30 s on an Ultraturrax, T18 basic, IKA, Berlin, Germany. Then, the extract was filtered through a four-layer cheesecloth, the pH was adjusted to 2.35–2.40 with 2 N ClH, and centrifuged at 10,000 *g* for 15 min at 4°C. The supernatant was purified through a methanol-activated C18 cartridge (Sep-Pak cartridges C18, Waters, Dublin, Ireland) and filtered through a 0.45 μm PFTE filter. For DHA derivatization, 750 μL of extract were mixed with 250 μL of 7.7 M 1,2-phenylenediamine in an HPLC amber vial. The mixture was allowed to react for 37 min and then 20 μL were injected onto a Luna (250 mm × 4.6 mm, 5 μm particle size) C18 column (Phenomenex, Macclesfield, United Kingdom) with a C18 security guard (4.0 mm × 3.0 mm) cartridge system (Phenomenex, Macclesfield, United Kingdom) using a HPLC system (Agilent HPLC 1200 Infinity series). The mobile phase was 50 mM KH_2PO_4 containing 5 mM hexadecyl trimethyl ammonium bromide and 5% methanol (pH 4.59) with isocratic flow of 1 mL min^{-1}. Absorbance was recorded at 261 nm for AA (Rt = 9.4 min) and at 348 nm for DHA (Rt = 4.5 min) and they were quantified by comparison with AA and DHA standards areas (Sigma-Aldrich, Germany). The results (mean ± SE) were expressed as g kg^{-1} fresh weight.

Individual Sugars and Organic Acids Content

To measure sugars and organic acids, 5 g of the aril sample of each replicate were extracted with 5 mL of 0.5% phosphoric acid and the supernatant was filtered through 0.45 μm Millipore filter and injected in duplicate into a HPLC system (Hewlett-Packard HPLC series 1100). The elution system consisted of 0.1% phosphoric acid running isocratically at 0.5 mL min^{-1} through a Supelco column (Supelcogel C-610H, 30 cm 7.8 mm, Supelco Park, Bellefonte, United States). Organic acids were detected by absorbance at 210 nm and sugars by refractive index detector and quantified by using standard curves of pure sugars and organic acids (Sigma-Aldrich, Germany). Results were expressed as g kg^{-1} fresh weight and are the mean ± SE of three replicates.

Statistical Analysis

Results are expressed as mean ± SE of three replicates. Data for the analytical determinations were subjected to analysis of variance (ANOVA) being sources of variation treatment for the 2017 experiment and storage time and treatment for the 2018 experiment. Mean comparisons were performed using HSD Tukey's test to examine if differences between control and treated fruit were significant at $P < 0.05$. All analyses were performed with SPSS software package v. 17.0 for Windows.

RESULTS

Crop Yield

SA treatments of pomegranate trees during the development of pomegranate fruit increased crop yield in a dose-dependent way, the effect being significant ($P < 0.05$) with 5 and 10 mM. Thus, the yield in the 2017 experiment, expressed as kg $tree^{-1}$, was 37.75 ± 3.28 in control trees and 51.08 ± 6.52 in those treated with 10 mM SA. Yield was also increased by MeSa treatments although no significant differences were observed among 1, 5, and 10 mM doses. These increases were due to the higher number of fruits harvested from each tree, while fruit mass was not affected by treatment. However, ASA treatments did not have a significant effect ($P < 0.05$) on crop yield, neither on kg $tree^{-1}$ nor on number of fruit $tree^{-1}$ (**Table 1**). These results were confirmed in the 2018 experiment, in which 10 mM dose was applied for SA, ASA, and MeSa treatments (**Table 1**). The percentage of fruits that were harvested in the first picking date was 55.32 ± 3.18% in control fruits which was increased, in a dependent-concentration manner, by SA and ASA treatments, with ca 90% of total fruit being harvested at the first picking date on SA and ASA 10 mM treated fruits. However, the percentage of fruits picked at the first picking date on trees treated with MeSa, either at 1, 5, or 10 mM concentration, was similar to those of non-treated trees (**Table 1**).

Fruit Quality Parameters and Bioactive Compounds at Harvest

Fruit quality parameters, such as firmness, TA, and skin and aril color, at harvest, were improved by all salicylate treatments in the 2017 experiment. Thus, fruit firmness and TA were significantly

TABLE 1 | Effects of preharvest salicylic acid (SA at 1, 5, and 10 mM), acetyl salicylic acid (ASA at 1, 5, and 10 mM), and methyl salicylate (MeSa at 1, 5, and 10 mM) treatments on pomegranate crop yield (kg tree^{-1} and number of fruit tree^{-1}), fruit mass, and% of fruits harvested in the first picking date in the 2017 and 2018 experiments.

	kg tree^{-1}	Fruits tree^{-1}	Fruit mass (g)	% first pick
2017 experiment				
Control	37.54 ± 3.28 a	110.96 ± 7.17 a	338.3 ± 9.54 a	55.32 ± 3.18 a
SA 1	41.45 ± 3.14 ab	123.8 ± 5.2 ab	334.8 ± 9.27 a	49.61 ± 2.65 a
SA 5	45.59 ± 4.29 bc	135.6 ± 6.1 bc	336.2 ± 7.48 a	81.87 ± 2.77 c
SA 10	51.08 ± 3.52 c	141.8 ± 5.7 c	352.9 ± 11.8 a	88.48 ± 3.18 d
ASA 1	42.62 ± 3.56 ab	127.8 ± 4.6 b	333.5 ± 12.8 a	63.17 ± 1.11 b
ASA 5	39.70 ± 3.58 a	117.21 ± 6.6 a	338.7 ± 10.3 a	84.67 ± 4.14 cd
ASA 10	42.39 ± 2.08 ab	124.9 ± 3.74 ab	339.2 ± 12.1 a	88.84 ± 3.64 d
MeSa 1	50.90 ± 3.78 c	142.0 ± 6.4 c	358.0 ± 9.89 a	54.63 ± 5.51 a
MeSa 5	50.43 ± 2.74 c	152.6 ± 9.57 c	330.5 ± 15.3 a	50.28 ± 4.70 a
MeSa 10	50.39 ± 2.66 c	151.0 ± 7.8 c	333.8 ± 16.2 a	49.69 ± 4.61 a
2018 experiment				
Control	43.42 ± 4.06 a	119.6 ± 9.28 a	362.9 ± 11.1 a	55.21 ± 4.22 a
SA 10	51.39 ± 2.90 b	145.7 ± 8.82 b	352.8 ± 9.81 a	65.67 ± 3.70 b
ASA 10	41.41 ± 3.99 a	118.7 ± 8.03 a	348.9 ± 13.3 a	64.59 ± 3.80 b
MeSa 10	55.96 ± 4.70 b	150.0 ± 13.6 b	372.9 ± 7.75 a	47.91 ± 3.96 a

Within a column, different letters show significant differences ($P < 0.05$) among treatments.

higher ($P < 0.05$) in all SA, ASA, and MeSa treated fruits than in controls, the effects being, in general, dose-dependent and higher for SA and ASA treatments than for MeSa (**Figures 1A,C**). On the contrary, Hue angle in skin and arils was significantly ($P < 0.05$) lower in all treated fruits with respect to control ones (**Figures 1B,D**), which show a deep red color of both skin and arils as a consequence of treatments, although no significant differences were observed among treatments. TSS at harvest were 158.5 ± 1.0 g kg^{-1} in arils control fruits and significantly ($P < 0.05$) higher in 10 mM SA, ASA, and MeSa treated ones, 173.8 ± 0.7, 168.9 ± 0.9, and 169.7 ± 1.2 g kg^{-1}, respectively, while no significant effects were observed for salicylate treatments at 1 and 5 mM (data not shown).

In 2017, SA, ASA, and MeSa treatments also induced a significant ($P < 0.05$) increase in total phenolics and anthocyanin concentrations in pomegranate arils, which was higher as increased the applied dose (**Figures 2A,B**). A similar trend was observed for H-TAA, the highest increase being observed on arils of 10 mM SA treated fruits (**Figure 2C**). However, for L-TAA the effects of salicylate treatments were not so evident, since it was significantly ($P < 0.05$) increased only by SA and ASA 10 mM treatments (**Figure 2D**). Taking into account the results obtained in the 2017 experiment, SA, ASA, and MeSa treatments were applied at 10 mM in 2018 and fruits were used for the storage experiment.

Evolution of Pomegranate Quality Parameters and Respiration Rate During Storage

Weight loss increased along storage time, reaching final values of 9.42 ± 0.43% in control fruits and significantly ($P < 0.05$) lower 5.90 ± 0.49, 7.02 ± 0.36, and 7.88 ± 0.58% in fruits from SA, ASA, and MeSa treated ones, respectively (**Supplementary Figure S1A**). Respiration rate at harvest was 86.36 ± 1.14 g kg^{-1} s^{-1} in control fruit and this was significantly ($P < 0.05$) higher than those from SA treated trees (76.30 ± 2.52 g kg^{-1} s^{-1}).However, no significant differences were observed between control and ASA or MeSa treated fruit. Respiration rate decreased sharply during storage from day 0 to day 30 and then more slowly after that, and it was lower in SA treated fruits than in controls during the whole storage time (**Supplementary Figure S1B**).

Fruit firmness at harvest was significantly ($P < 0.05$) increased by SA and ASA treatments, from values of 15.89 ± 0.74 kN m^{-1} in control fruit to 18.46 ± 0.46 and 18.88 ± 0.74 kN m^{-1} in those treated with SA and ASA, respectively, confirming the results obtained in the 2017 experiment. During storage, fruit firmness decreased in control and treated fruits, although final firmness levels after 90 days of storage at 10°C remained significantly higher ($P < 0.05$) in fruits from treated trees than in controls (**Supplementary Figure S2A**). With respect to arils color, lower values of Hue angle were measured at harvest in fruits from SA, ASA, and MeSa treated trees. Hue angle of arils decreased during storage, although values of control fruits were always higher than those of treated ones (**Supplementary Figure S2B**). These results indicated that the aril red color increased as a consequence of salicylate treatments, either at harvest or during storage for 90 days, as can be observed in **Supplementary Figure S3**. Fructose was the major sugar in pomegranate arils, followed by glucose, and both sugars were significantly ($P < 0.05$) increased by salicylate treatments, while sucrose was found at a very low concentration without significant differences attributed to treatments (**Figure 3A**). Organic acids were also increased by salicylate treatments, the highest increase

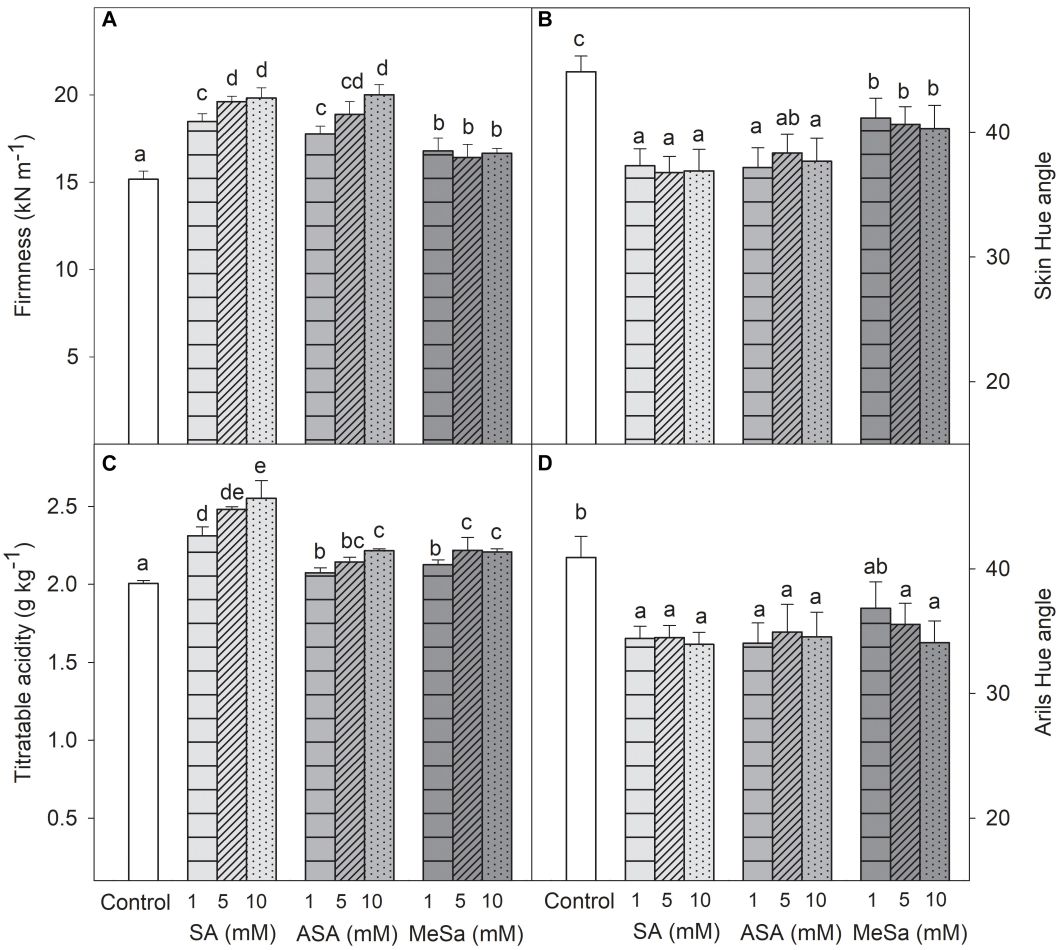

FIGURE 1 | Fruit firmness **(A)**, skin color (Hue angle) **(B)**, titratable acidity **(C)**, and arils color (Hue angle) **(D)** in pomegranate from control and salicylic acid (SA), acetyl salicylic acid (ASA), and methyl salicylate (MeSa) treated fruits at harvest, in the 2017 experiment. Data are the mean ± SE. Different letters show significant differences ($P < 0.05$) among treatments.

being found in the major organic acid, malic acid, by SA treatment (**Figure 3B**).

Bioactive Compounds and Antioxidant Activity During Storage

In the 2018 experiment, SA, ASA, and MeSa treatments at 10 mM led to arils with increased concentrations of total phenolics and total anthocyanins at harvest time (**Figures 4A,B**), in agreement with results from the 2017 experiment. Total phenolic concentration increased during storage in pomegranate arils for all treatments, the major increases being found during the first month of storage. At the last sampling date, phenolic concentration was 1.22 ± 0.04 g kg^{-1} in arils from control fruit, and significantly higher ($P < 0.05$), in those from SA, ASA, and MeSa treated ones, at 1.54 ± 0.04, 1.42 ± 0.03, and 1.30 ± 0.04 g kg^{-1}, respectively (**Figure 4A**). For total anthocyanin concentration, values at harvest were significantly higher ($P < 0.05$) in arils from treated fruits than in those from controls, without significant differences among SA, ASA, or MeSa treatments. Anthocyanin concentration also increased during the whole storage period and was higher in arils from all treated fruits than in controls, the highest increase being found in arils of SA and ASA treated fruits (**Figure 4B**). Individual anthocyanin concentration was measured at day 0 in the arils from control and treated fruits. In all aril samples a similar anthocyanin profile was found, Cyn 3-gluc being the major anthocyanin (62.29 ± 4.58 mg kg^{-1} in control fruit), followed by Dlp 3-gluc, Plg 3-gluc, Cyn 3,5-di-gluc, and Dlp 3,5-di-gluc while Plg 3,5-di-gluc was found at a very low concentration (**Figure 5**). It is worth noting that all individual anthocyanins, except those found at very low concentrations, were increased as a consequence of salicylate treatments, although no significant differences were observed between SA, ASA, and MeSa treatments.

Similar trends than those for phenolic and anthocyanin content was observed for H-TAA in the arils, which increased during storage, especially in fruits from SA treated trees, while similar increases were found in arils from ASA and MeSa treatments, although they were significantly higher than in arils from control fruits (**Figure 6A**). However, L-TAA showed very

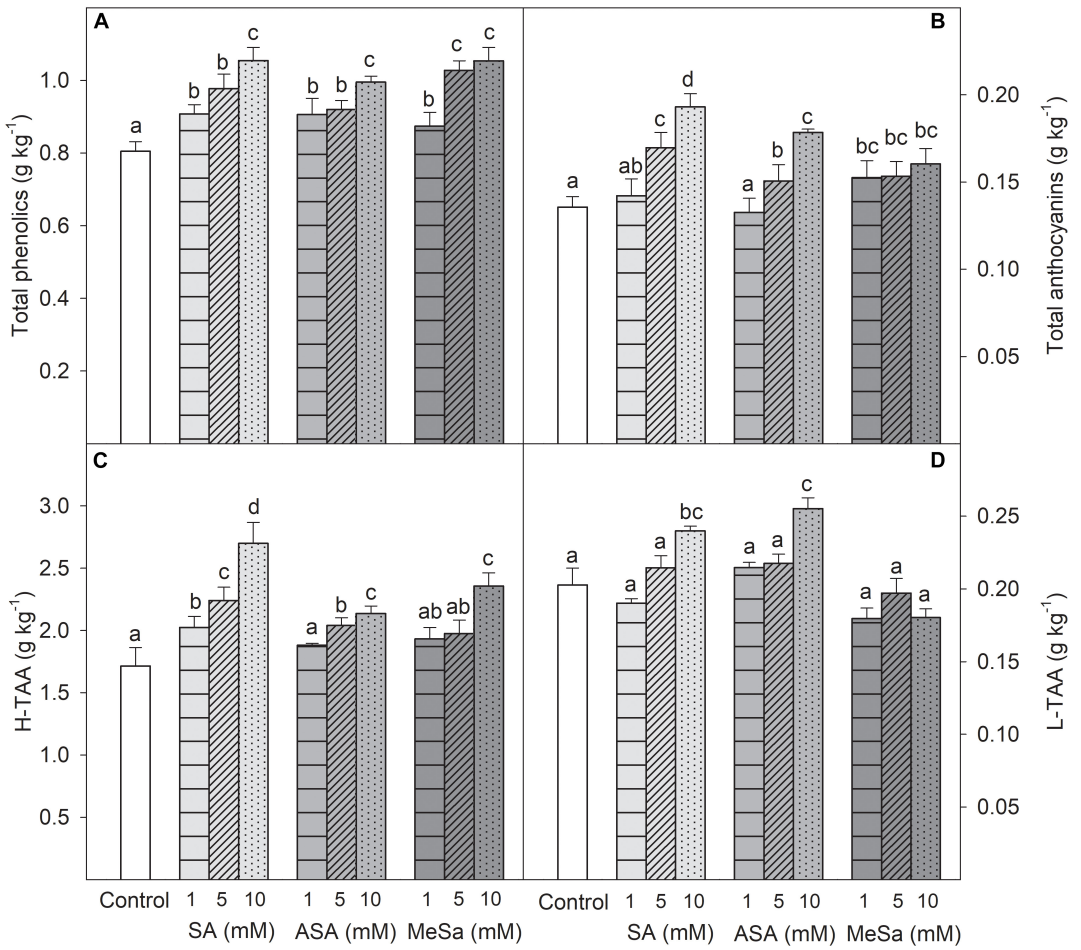

FIGURE 2 | Total phenolic concentration **(A)**, total anthocyanin concentration **(B)**, total hydrophilic antioxidant activity (H-TAA) **(C)**, and total lipophilic antioxidant activity (L-TAA) **(D)** in arils of pomegranate from control and salicylic acid (SA), acetyl salicylic acid (ASA), and methyl salicylate (MeSa) treated fruits at harvest, in the 2017 experiment. Data are the mean ± SE. Different letters show significant differences ($P < 0.05$) among treatments.

low values as compared with H-TAA, its increase during storage was small and differences between control and treated fruits were only significant at the last two sampling dates (**Figure 6B**).

Ascorbic acid content was significantly ($P < 0.05$) increased due to salicylate treatments, with values at harvest of 0.055 ± 0.008 g kg^{-1} in arils of control fruit, 0.086 ± 0.009 g kg^{-1} in those treated with MeSa, and 0.130 ± 0.008 and 0.123 ± 0.003 g kg^{-1} in arils of SA and ASA treated fruits. During storage, AA acid concentration decreased in all treatments, although higher values were found in arils of all treated fruits than in controls during the whole storage time, with final values of 0.019 ± 0.003 g kg^{-1} in control fruit and between 0.067 and 0.082 g kg^{-1} in treated ones (**Figure 7A**). DHA concentration at harvest was also significantly increased ($P < 0.05$) by salicylate treatments and maintained at higher levels during storage, although the effects were not as pronounced as in ascorbic acid (**Figure 7B**). Total vitamin C, calculated as the sum of AA plus DHA, followed a similar trend, with significantly higher values ($P < 0.05$) in treated than in control fruits, at harvest and along the whole storage time (**Figure 7C**).

DISCUSSION

Crop management, and especially water availability, during pomegranate fruit development has been reported to affect fruit ripening, quality, and phytochemical content (Galindo et al., 2014). In the present experiments, climatic conditions were similar for 2017 and 2018 and control and salicylate treated trees were under similar climatic and agronomic conditions. Thus, differences among control and treated trees on yield, fruit ripening, and quality attributes would be due just to the effects of treatments. Results showed that SA, ASA, and MeSa treatments increased crop yield due to an increase in the number of fruits that were harvested from each tree, which had a similar mass, independently of the applied treatment. The increase in fruit number by salicylate treatments could be due to: (i) an increased flowering rate, (ii) an increased rate

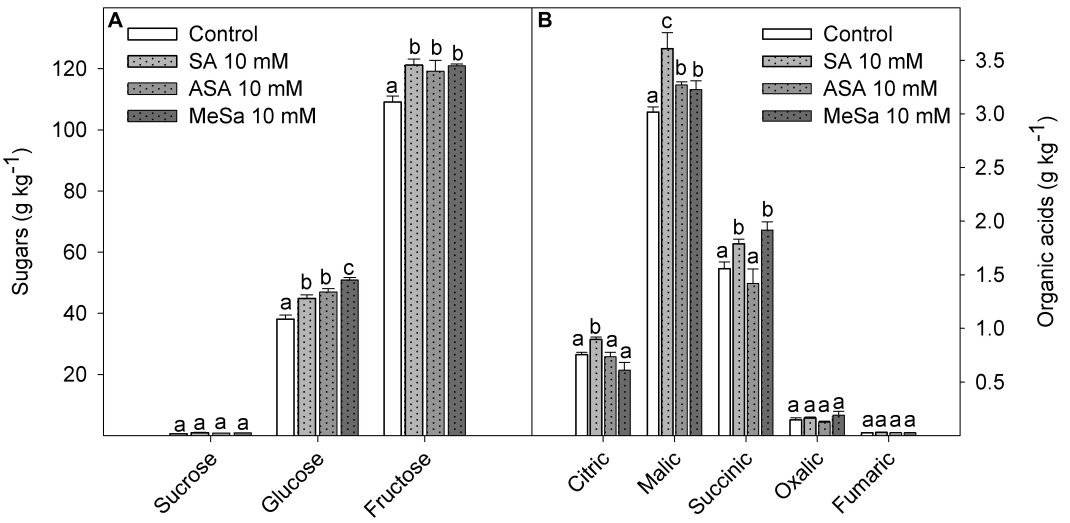

FIGURE 3 | Concentration of major individual sugars **(A)** and organic acids **(B)** in arils of pomegranate from control and salicylic acid (SA), acetyl salicylic acid (ASA), and methyl salicylate (MeSa) treated fruits at harvest, in the 2018 experiment. Data are the mean ± SE. Different letters show significant differences ($P < 0.05$) among treatments for each individual sugar and organic acid.

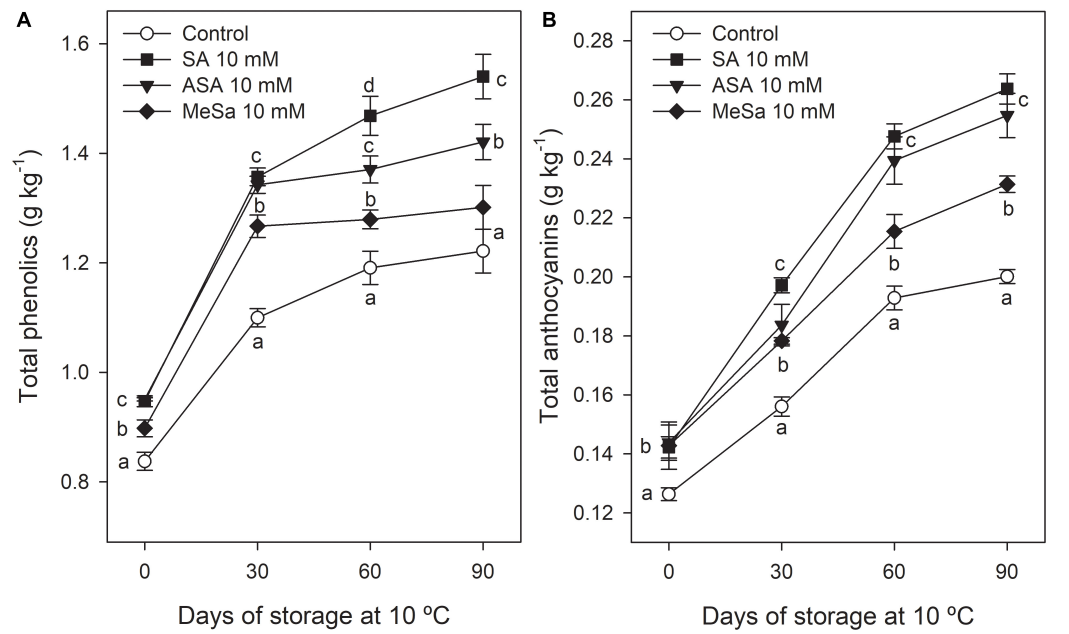

FIGURE 4 | Total phenolic **(A)** and anthocyanin **(B)** concentration in arils of pomegranate from control and salicylic acid (SA), acetyl salicylic acid (ASA), and methyl salicylate (MeSa) treated fruits during storage at 10°C, in the 2018 experiment. Data are the mean ± SE. Different letters show significant differences ($P < 0.05$) among treatments for each sampling date.

of set fruits, or (iii) a decrease in fruit abscission. However, in our experiments, treatments were performed when fruit had reached ca 30% of their final size so that flowering or fruit set were not affected and the increase in fruit number was due to the reduction of fruit abscission that naturally occurs during the fruit developmental process. Accordingly, an increase in plum tree yield has been recently reported as a consequence of salicylate treatments, although it was due to increased fruit mass but not fruit number (Martínez-Esplá et al., 2018). Moreover, significant increases in total yield and cluster weight of 'Flame Seedless' table grapes were observed as a consequence of vine treatment with a foliar spray of 1.5 or 2.0 mM SA (Champa et al., 2015). These results prove that treatment with salicylates increases net photo-assimilate production in plants and/or the sink strength of developing fruits. In fact, foliar application of SA to ginger plants increased leaves' chlorophyll content,

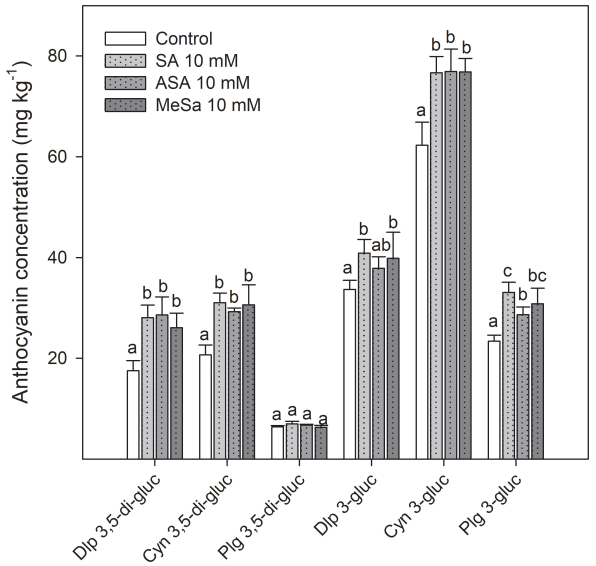

FIGURE 5 | Concentration of delphinidin 3,5-di-*O*-glucoside (Dlp 3,5-di-gluc), cyanidin 3,5-di-*O*-glucoside (Cyn 3,5-di-gluc), pelargonidin 3,5-di-*O*-glucoside (Plg 3,5-di-gluc), delphinidin 3-*O*-glucoside (Dlp 3-gluc), cyanidin 3-*O*-glucoside (Cyn 3-gluc), and pelargonidin 3-*O*-glucoside (Plg 3-gluc) in arils of pomegranate from control and salicylic acid (SA), acetyl salicylic acid (ASA), and methyl salicylate (MeSa) treated fruits at harvest, in the 2018 experiment. Data are the mean ± SE. Different letters show significant differences ($P < 0.05$) among treatments for each individual anthocyanin.

photosynthetic rate, and total dry weight (Ghasemzadeh and Jaafar, 2013). Moreover, an increase in Rubisco activity and total yield by SA treatment were also reported in maize and mustard plants (Fariduddin et al., 2003; Elgamaal and Maswada, 2013). However, the recent results also show an effect on reducing the abscission of pomegranate fruit. Accordingly, Helaly et al. (2018) found a higher percentage of fruit retention and crop yield on two mango cultivars for three consecutive years as a consequence of SA treatments. These effects were attributed to the role of SA activating growth and the nutritional state of trees due to an increase in fresh and dry weight and chlorophyll, carotenoid, and sugar concentration in leaves, showing an effect on enhancing net photosynthesis on tree. In addition, given the pivotal role of SA on increasing tree tolerance to environmental stresses (Tiwari et al., 2017; Koo et al., 2020), its effect allowing pomegranate tress to overcome drought and high temperature stresses during summer seasons in the Spain Southeast cannot be discarded. In fact, maximum mean temperatures in summer, from June to September, were very high in the field crop, ca. 31.5°C in both years. On the other hand, it is worth noting that the percentage of fruits harvested in the first picking date was higher in 5 and 10 mM treated trees and in all ASA treated ones than in controls (**Table 1**). These results show that the on-tree ripening process was accelerated by SA and ASA treatments, especially when applied at 10 mM concentration since all trees (control and treated) were located on the same farm and under similar agronomic and environmental conditions, and pomegranate fruits were harvested upon reaching their commercial ripening stage, according to their size and skin color. This effect could be attributed to an increase of net photosynthesis and/or sink strength induced by treatment with salicylates previously commented (Fariduddin et al., 2003; Elgamaal and Maswada, 2013; Ghasemzadeh and Jaafar, 2013). This is important to point out the rule showing an inverse relationship between tree fruit

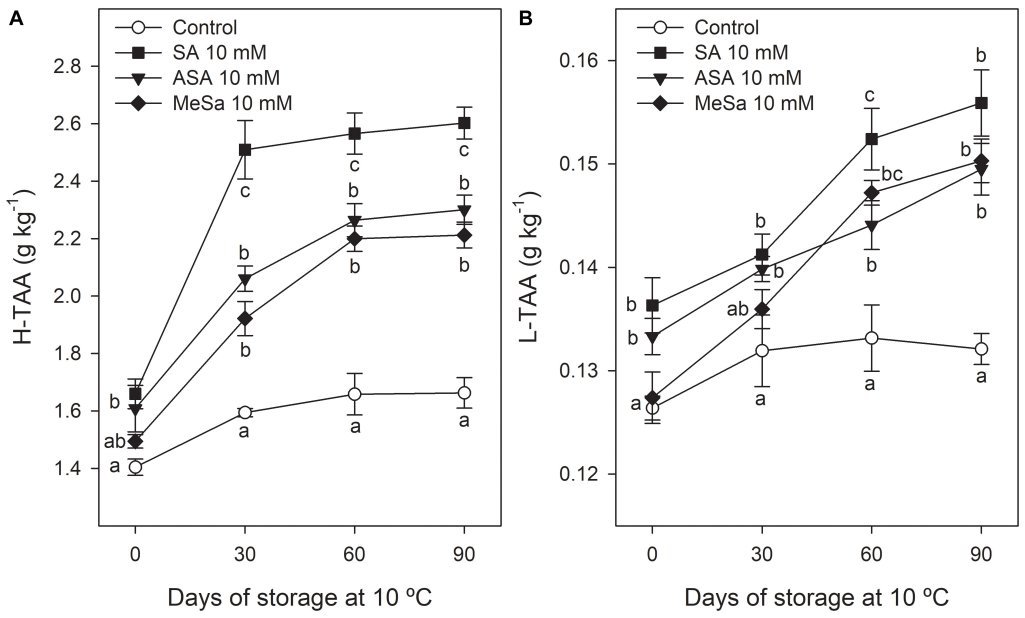

FIGURE 6 | Total hydrophilic antioxidant activity (H-TAA) **(A)** and total lipophilic antioxidant activity (L-TAA) **(B)** in arils of pomegranate from control and salicylic acid (SA), acetyl salicylic acid (ASA), and methyl salicylate (MeSa) treated fruits during storage at 10°C, in the 2018 experiment. Data are the mean ± SE. Different letters show significant differences ($P < 0.05$) among treatments for each sampling date.

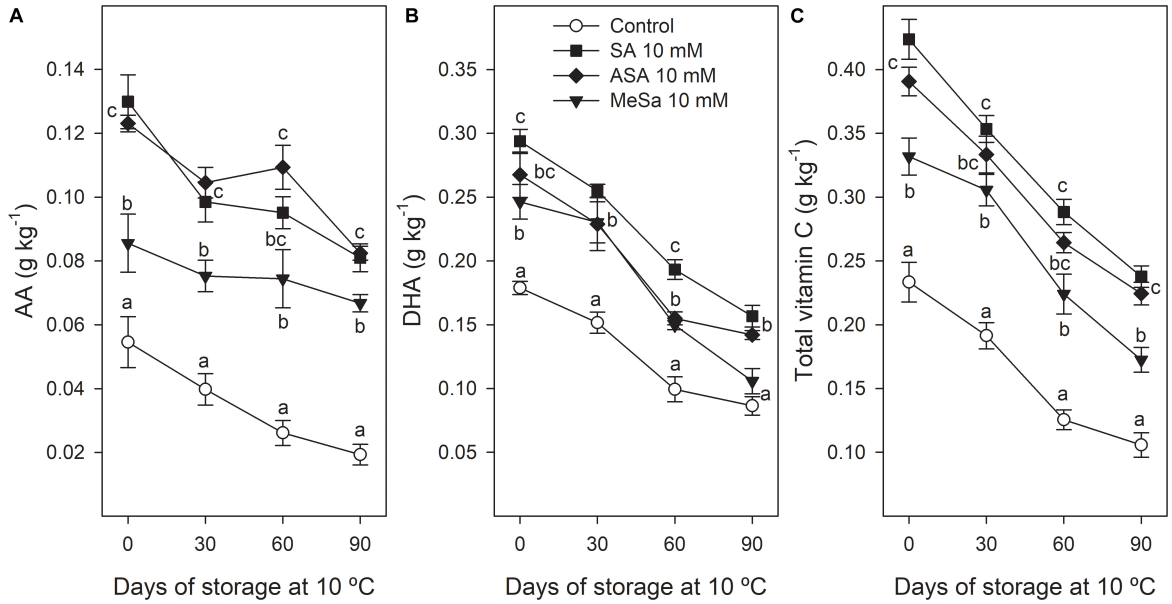

FIGURE 7 | Ascorbic acid (AA) **(A)**, dehydroascorbic acid (DHA) **(B)**, and vitamin C **(C)** in arils of pomegranate from control and salicylic acid (SA), acetyl salicylic acid (ASA), and methyl salicylate (MeSa) treated fruits during storage at 10°C, in the 2018 experiment. Data are the mean ± SE. Different letters show significant differences ($P < 0.05$) among treatments for each sampling date.

load and fruit quality. In this experiment, despite that, the number of fruits was higher in treated trees but the fruit quality was not decreased.

Fruit firmness, TA, TSS, and skin and aril color are indicators of pomegranate fruit quality (Nuncio-Jáuregui et al., 2014; Valero et al., 2014; Pareek et al., 2015). Then, the higher firmness, TSS, and TA and the lower skin and aril Hue angle values found at harvest in the pomegranates of treated trees show that they had higher quality attributes than controls. It is worth noting that the major sugars, fructose and glucose, and the major organic acid, malic acid, were found at higher concentrations in arils of treated fruit than in control (**Figure 3A**). This sugar profile is in agreement with previous reports on 'Mollar de Elche' and other sweet pomegranate cultivars, while in sour cultivars the major organic acid is citric acid (Nuncio-Jáuregui et al., 2014; Cano-Lamadrid et al., 2018). In addition, increases in weight losses (**Supplementary Figure S1**) and decreases in firmness (**Supplementary Figure S2A**) and arils Hue angle (**Supplementary Figure S2B**) show the normal evolution of the postharvest ripening process in "Mollar de Elche" and other pomegranate cultivars (Sayyari et al., 2011a, 2016; García-Pastor et al., 2020), which were delayed by pre-harvest salicylate treatments. Accordingly, the evolution of the postharvest ripening process was delayed in two sweet cherry cultivars by pre-harvest treatments with SA, ASA, and MeSa leading to maintenance of fruit quality parameters (Valverde et al., 2015; Giménez et al., 2017). In this non-climacteric fruit species, as well as in plum (Martínez-Esplá et al., 2017), which is a climacteric fruit, the effect of salicylate preharvest treatments on delaying the postharvest ripening process was attributed to an increase on the concentration of antioxidant compounds and the activity of the antioxidant enzymes. The enhance of these antioxidant systems could lead to efficient scavenging of reactive oxygen species (ROS) which are generated during fruit ripening, a process considered as a functionally modified protracted form of senescence (Hodges et al., 2004).

Pomegranate fruits are a rich source of bioactive compounds, such as phenolics, including anthocyanins and other complex flavonoids and hydrolyzable tannins, and ascorbic acid, as compared with other fruits of the Mediterranean diet, although they are found at different concentrations depending on cultivar, cultural practices, and environmental conditions (Mphahlele et al., 2014; Li et al., 2015; Attanayake et al., 2018). These bioactive compounds have antioxidant properties which are responsible for the beneficial health effects attributed to pomegranate fruit consumption (Faria and Calhau, 2011; Asgary et al., 2017; Panth et al., 2017). Results of the present research show that pre-harvest treatments with salicylates increased total phenolic compound and total and individual anthocyanin concentrations, as well as ascorbic acid, leading to increases in H-TAA. These effects of salicylate treatments on increasing antioxidant compounds were significant at harvest and were maintained during long term storage (**Figures 2A,B,C**, **4A,B**, **5**, **6A**, **7A**) showing that pre-harvest treatment with salicylates would provide the fruit with increased beneficial health effects for human consumption. In fact, it has been claimed that these hydrophilic compounds are responsible for the antioxidant properties of a wide range of fresh fruit species (Valero and Serrano, 2010; Valverde et al., 2015; Martínez-Esplá et al., 2018). This statement is supported by the present results which show that H-TAA was 10-fold higher than L-TAA and strongly correlated $r^2 = 0.827$ ($y = 1.726x–0.120$) and $r^2 = 0.753$ ($y = 7.929x + 0.439$) with total phenolic and total

anthocyanin content, respectively, by taking into account data of all treatment and sampling dates of the 2018 storage experiment.

On the other hand, it is worth noting that AA concentration in pomegranate arils decreased during storage, which is a general trend previously reported in other fruit species such as kiwifruit (Yang et al., 2016), peaches (Falagán et al., 2016) and even in "Hicaznar" (Koyuncu et al., 2019) and "Mridula" (Barman et al., 2014) pomegranate cultivars. However, AA concentration was higher on arils of pomegranates from treated trees than in controls, at harvest and along the storage process. Accordingly, postharvest SA treatment at 2 mM delayed the decrease in AA during storage at 2°C + 2 days at 20°C in "Malas Saveh" pomegranate (Sayyari et al., 2009), as well as in "Malase Yazd" pomegranate, especially if SA dipping treatment was applied as a hot solution (Dokhanieh et al., 2016). This effect could be attributed to an increase in the GR/APX system activity, to lower activity of ascorbic acid oxidase activity (AAO), and/or to higher reducing sugar (glucose and fructose) accumulation. It has been reported that AA is oxidized to DHA by AAO during storage, leading to increases in DHA in a wide range of fresh fruits (Mazurek and Pankiewicz, 2012), including kiwifruit (Yang et al., 2016). However, in the present experiment, DHA decreased in pomegranate arils during storage (**Figure 7B**), as has been reported to occur in peaches (Falagán et al., 2016). Nevertheless, DHA concentration was maintained at higher levels in salicylate treated fruits than in controls, leading to higher concentration in vitamin C (**Figure 7C**), which is an important effect of salicylate treatments on the nutritional value of pomegranate, along with the enhancing of its antioxidant properties.

No previous reports are available in the literature regarding the effect of pre-harvest salicylate treatments on increasing phenolic and anthocyanin content in pomegranate fruit, although some papers exist on other fruits for comparative purposes. In this sense, SA, ASA, and MeSA applied as pre-harvest treatments on sweet cherry and plum trees increased fruit total phenolic and anthocyanin concentrations at harvest with respect to controls, and these differences were maintained during cold storage (Giménez et al., 2014, 2015, 2017; Martínez-Esplá et al., 2018). Accordingly, SA pre-harvest treatments of vine led to higher levels of these bioactive compounds in table grape "Flame Seedless" at harvest and during postharvest storage (Champa et al., 2015). On pomegranate fruits, postharvest treatments with SA, ASA, or MeSA have been reported to maintain total phenolics, anthocyanins, and antioxidant activity at higher levels than in control fruit during cold storage (Sayyari et al., 2011a,b) as well as SA and ASA on sweet cherry (Valero et al., 2011), and SA on cornelian cherry fruit (Dokhanieh et al., 2013) and apricot (Wang et al., 2015). These enhancements were attributed to an increase in the activity of phenylalanine ammonia lyase (PAL), which is the main enzyme involved in the biosynthetic phenolic pathway. Accordingly, dipping of pomegranate arils with SA maintained higher anthocyanin and phenolic concentrations during storage, the effect being higher if SA dipping was performed at 45 than at 25°C and also attributed to the enhanced activity of PAL (Dokhanieh et al., 2016).

CONCLUSION

Overall results show that, in the 2017 and 2018 experiments, salicylate pre-harvest treatments of pomegranate trees increased crop yield (kg tree^{-1} and number of harvested fruit tree^{-1}) and fruit quality parameters at harvest, such as firmness, aril color, and individual sugar and organic acid contents. Moreover, aril content on bioactive compounds, such as phenolics, anthocyanins, and ascorbic acid, was also increased by salicylate treatments. The quality traits and the concentration of bioactive compounds were maintained at higher levels in pomegranate fruit from treated trees than in controls during prolonged storage at 10°C. It is worth noting the effects of these treatments on increasing total and individual anthocyanin concentration in pomegranate arils which reached a deeper red color and, in turn, would be more appreciated in the international market, all these effects contributing to increasing the profit of this crop. Thus, pre-harvest treatment with salicylates, and especially SA at 10 mM, could be a safe and natural new tool to improve pomegranate fruit quality and their content on antioxidant compounds with beneficial health effects, at harvest and during storage.

DATA AVAILABILITY STATEMENT

All datasets generated for this study are included in the article/**Supplementary Material**.

AUTHOR CONTRIBUTIONS

DV and MS conceived and designed the work in association with other authors. SC, PZ, and DM-R performed the field treatments. MG-P performed most of the analytical determination in collaboration with the other authors. MS and DV analyzed the data and wrote the manuscript. All authors approved the final version of the manuscript.

FUNDING

This work has been funded by Spanish Ministry of Economy and Competitiveness through Projects AGL2015-63986R and RTI2018-099664-B-100 and European Commission with FEDER funds.

ACKNOWLEDGMENTS

The authors thank Miguel Hernández University for Ph.D. scholarship of MG-P (grant number 1541/16).

SUPPLEMENTARY MATERIAL

The Supplementary Material for this article can be found online at: https://www.frontiersin.org/articles/10.3389/fpls.2020.00668/full#supplementary-material

FIGURE S1 | Weight loss **(A)** and respiration rate **(B)** in arils of pomegranate from control and salicylic acid (SA), acetyl salicylic acid (ASA), and methyl salicylate (MeSa) treated fruits during storage at 10°C, in the 2018 experiment. Data are the mean ± SE. Different letters show significant differences ($P < 0.05$) among treatments for each sampling date.

FIGURE S2 | Fruit firmness **(A)** and aril color (Hue angle) **(B)** in pomegranate from control and salicylic acid (SA), acetyl salicylic acid (ASA), and methyl salicylate (MeSa) treated fruits during storage at 10°C, in the 2018 experiment. Data are the mean ± SE. Different letters show significant differences ($P < 0.05$) among treatments for each sampling date.

FIGURE S3 | Pictures of the cut surface of pomegranate from control and salicylic acid (SA), acetyl salicylic acid (ASA), and methyl salicylate (MeSa) treated fruits at harvest **(A)** and after 90 days of storage at 10°C **(B)**, in the 2018 experiment. Pictures represent one of the three replicates for each treatment.

REFERENCES

Asgary, S., Keshvari, M., Sahebkar, A., and Sarrafzadegan, N. (2017). Pomegranate consumption and blood pressure: a review. *Curr. Pharm. Des.* 23, 1042–1050. doi: 10.2174/1381612822666161010103339

Asghari, M., and Aghdam, M. S. (2010). Impact of salicylic acid on post-harvest physiology of horticultural crops. *Trends Food Sci. Technol.* 21, 502–509. doi: 10.1016/j.tifs.2010.07.009

Attanayake, R., Eeswaran, R., Rajapaksha, R., Weerakkody, P., and Bandaranayake, P. C. G. (2018). Biochemical composition and expression of anthocyanin biosynthetic genes of a yellow peeled and pinkish ariled pomegranate (*Punica granatum* L.) cultivar are differentially regulated in response to agro-climatic conditions. *J. Agric. Food Chem.* 66, 8761–8771. doi: 10.1021/acs.jafc.8b02909

Barman, K., Asrey, R., Pal, R. K., Kaur, C., and Jha, S. K. (2014). Influence of putrescine and carnauba wax on functional and sensory quality of pomegranate (*Punica granatum* L.) fruits during storage. *J. Food Sci. Technol.* 51, 111–117. doi: 10.1007/s13197-011-0483-0

Bartual, J., Pérez-Gago, M. B., Pomares, F., Palou, L., and Intrigliolo, D. S. (2015). Nutrient status and irrigation management affect anthocyanins in 'Mollar de Elche' pomegranate. *Acta Hortic.* 1106, 85–92. doi: 10.17660/ActaHortic.2015.1106.14

Cano-Lamadrid, M., Galindo, A., Collado-González, J., Rodríguez, P., Cruz, Z. N., Legua, P., et al. (2018). Influence of deficit irrigation and crop load on the yield and fruit quality in Wonderful and Mollar de Elche pomegranates. *J. Sci. Food Agric.* 98, 3098–3108. doi: 10.1002/jsfa.8810

Champa, W. A. H., Gill, M. I. S., Mahajan, B. V. C., and Arora, N. K. (2015). Preharvest salicylic acid treatments to improve quality and postharvest life of table grapes (*Vitis vinifera* L.) cv. Flame Seedless. *J. Food Sci. Technol.* 52, 3607–3616. doi: 10.1007/s13197-014-1422-7

Cristofori, V., Caruso, D., Latini, G., Dell'Agli, M., Cammilli, C., Rugini, E., et al. (2011). Fruit quality of pomegranate (*Punica granatum* L.) autochonous varieties.*Eur. Food Res. Technol.* 232, 397–403. doi: 10.1007/s00217-010-1390-8

Ding, Z. S., Tian, S. P., Zheng, X. L., Zhou, Z. W., and Xu, Y. (2007). Responses of reactive oxygen metabolism and quality in mango fruit to exogenous oxalic acid or salicylic acid under chilling temperature stress. *Physiol. Plant.* 30, 112–121. doi: 10.1111/j.1399-3054.2007.00893.x

Dokhanieh, A. Y., Aghdam, M. S., Fard, J. R., and Hassanpour, H. (2013). Postharvest salicylic acid treatment enhances antioxidant potential of cornelian cherry fruit. *Sci. Hortic.* 154, 31–36. doi: 10.1016/j.scienta.2013.01.025

Dokhanieh, A. Y., Aghdam, M. S., and Sarcheshmeh, M. A. A. (2016). Impact of postharvest hot salicylic acid treatment on aril browning and nutritional quality in fresh-cut pomegranate. *Hortic. Environ. Biotechnol.* 57, 378–384. doi: 10.1007/s13580-016-0087-8

Elgamaal, A. A., and Maswada, H. F. (2013). Response of three yellow maize hybrids to exogenous salicylic acid under two irrigation intervals. *Asian J. Crop Sci.* 5, 264–274. doi: 10.3923/ajcs.2013.264.274

Falagán, N., Artés, F., Gómez, P. A., Artés-Hernández, F., Conejero, W., and Aguayo, E. (2016). Deficit irrigation strategies enhance health-promoting compounds through the intensification of specific enzymes in early peaches. *J. Sci. Food Agric.* 96, 1803–1813. doi: 10.1002/jsfa.7290

Fanali, C., Belluomo, M. G., Cirilli, M., Cristofori, V., Zecchini, M., Cacciola, F., et al. (2016). Antioxidant activity evaluation and HPLC-photodiode array/MS polyphenols analysis of pomegranate juice from selected Italian cultivars: a comparative study. *Electrophoresis* 37, 1947–1955. doi: 10.1002/elps.201500501

Faria, A., and Calhau, C. (2011). The bioactivity of pomegranate: impact on health and disease. *Crit. Rev. Food Sci. Nutr.* 51, 626–634. doi: 10.1080/10408391003748100

Fariduddin, Q., Hayat, S., and Ahmad, A. (2003). Salicylic acid influences net photosynthetic rate, carboxylation efficiency, nitrate reductase activity and seed yield in *Brassica juncea*. *Photosynthetica* 41, 281–284. doi: 10.1023/B:PHOT.0000011962.05991.6c

Galindo, A., Calín-Sánchez, A., Collado-González, J., Ordoño, S., Hernández, F., Torrecillas, A., et al. (2014). Phytochemical and quality attributes of pomegranate fruits for juice consumption as affected by ripening stage and deficit irrigation. *J. Sci. Food Agric.* 94, 2259–2265. doi: 10.1002/jsfa.6551

García, C. J., García-Villalba, R., Gil, M. I., and Tomas-Barberán, F. A. (2017). LC-MS untargeted metabolomics to explain the signal metabolites inducing browning in fresh-cut lettuce. *J. Agric. Food Chem.* 65, 4526–4535. doi: 10.1021/acs.jafc.7b01667

García-Pastor, M. E., Serrano, M., Guillén, F., Giménez, M. J., Martínez-Romero, D., Valero, D., et al. (2020). Preharvest application of methyl jasmonate increases crop yield, fruit quality and bioactive compounds in pomegranate 'Mollar de Elche' at harvest and during postharvest storage. *J. Sci. Food Agric.* 100, 145–153. doi: 10.1002/jsfa.10007

Ghasemzadeh, A., and Jaafar, H. Z. E. (2013). Interactive effect of salicylic acid on some physiological features and antioxidant enzymes activity in ginger (*Zingiber officinale* Roscoe). *Molecules* 18, 5965–5979. doi: 10.3390/molecules18055965

Giménez, M. J., Serrano, M., Valverde, J. M., Martínez-Romero, D., Castillo, S., Valero, D., et al. (2017). Preharvest salicylic acid and acetylsalicylic acid treatments preserve quality and enhance antioxidant systems during postharvest storage of sweet cherry cultivars. *J. Sci. Food Agric.* 97, 1220–1228. doi: 10.1002/jsfa.7853

Giménez, M. J., Valverde, J. M., Valero, D., Díaz-Mula, H. M., Zapata, P. J., Serrano, M., et al. (2015). Methyl salicylate treatments of sweet cherry trees improve fruit quality at harvest and during storage. *Sci. Hortic.* 197, 665–673. doi: 10.1016/j.scienta.2015.10.033

Giménez, M. J., Valverde, J. M., Valero, D., Guillén, F., Martínez-Romero, D., Serrano, M., et al. (2014). Quality and antioxidant properties on sweet cherries as affected by preharvest salicylic and acetylsalicylic acids treatments. *Food Chem.* 160, 226–232. doi: 10.1016/j.foodchem.2014.03.107

Glowacz, M., and Ree, D. (2015). Using jasmonates and salicylates to reduce losses within the fruit supply chain. *Eur. Food Res. Technol.* 242, 143–156. doi: 10.1007/s00217-015-2527-6

Habibi, F., Ramezanian, A., Guillén, F., Serrano, M., and Valero, D. (2020). Blood oranges maintain bioactive compounds and nutritional quality by postharvest treatments with γ-aminobutyric acid, methyl jasmonate or methyl salicylate during cold storage. *Food Chem.* 306:125634. doi: 10.1016/j.foodchem.2019.125634

Helaly, M. N., El-Sheery, N. I., El-Hoseiny, H., Rastogi, A., Kalaji, H. M., and Zabochnicka-Świątek, M. (2018). Impact of treated wastewater and salicylic acid on physiological performance, malformation and yield of two mango cultivars. *Sci. Hortic.* 233, 159–177. doi: 10.1016/j.scienta.2018.01.001

Hodges, D. M., Lester, G. E., Munro, K. D., and Toivonen, P. M. A. (2004). Oxidative stress: importance for postharvest quality. *HortScience* 39, 924–929. doi: 10.21273/HORTSCI.39.5.924

Ismail, T., Sestili, P., and Akhtar, S. (2012). Pomegranate peel and fruit extracts: a review of potential anti-inflammatory and anti-infective effects. *J. Etnopharmacol.* 143, 397–405. doi: 10.1016/j.jep.2012.07.004

Koo, Y. M., Heo, A. Y., and Choi, H. W. (2020). Salicylic acid as a safe plant protector and growth regulator. *Plant Pathol. J.* 36, 1–10. doi: 10.5423/PPJ.RW.12.2019.0295

Koyuncu, M. A., Erbas, D., Onursal, C. E., Secmen, T., Guneyli, A., and Sevinc Uzumcu, S. (2019). Postharvest treatments of salicylic acid, oxalic acid and

putrescine influences bioactive compounds and quality of pomegranate during controlled atmosphere storage. *J. Food Sci. Technol.* 56, 350–359. doi: 10.1007/s13197-018-3495-1

Lalithya, K. A., Manjunatha, G., Raju, B., Kulkarni, M. S., and Lokesh, V. (2017). Plant growth regulators and signal molecules enhance resistance against bacterial blight disease of pomegranate. *J. Phytopathol.* 165, 727–736. doi: 10.1111/jph.12612

Li, X., Wasila, H., Liu, L., Yuan, T., Gao, Z., Zhao, B., et al. (2015). Physicochemical characteristics, polyphenol compositions and antioxidant potential of pomegranate juices from 10 Chinese cultivars and the environmental factors analysis. *Food Chem.* 175, 575–584. doi: 10.1016/j.foodchem.2014.12.003

MAGRAMA (2017). *Ministry of Agriculture, Fisheries and Food*. Available online at: https://www.mapa.gob.es/es/estadistica/temas/estadisticas-agrarias/agricultura/superficies-producciones-anuales-cultivos/ (accessed January 30, 2020).

Martínez-Esplá, A., Serrano, M., Valero, D., Martínez-Romero, D., Castillo, S., and Zapata, P. J. (2017). Enhancement of antioxidant systems and storability of two plum cultivars by preharvest treatments with salicylates. *Int. J. Mol. Sci.* 18:1911. doi: 10.3390/ijms18091911

Martínez-Esplá, A., Zapata, P. J., Castillo, S., Guillén, F., Martínez-Romero, D., Valero, D., et al. (2014). Preharvest application of methyl jasmonate (MeJA) in two plum cultivars. 1. Improvement of fruit growth and quality attributes at harvest. *Postharvest Biol. Technol.* 98, 98–105. doi: 10.1016/j.postharvbio.2014.07.011

Martínez-Esplá, A., Zapata, P. J., Valero, D., Martínez-Romero, D., Díaz-Mula, H. M., and Serrano, M. (2018). Preharvest treatments with salicylates enhance nutrient and antioxidant compounds in plum at harvest and after storage. *J. Sci. Food Agric.* 98, 2742–2750. doi: 10.1002/jsfa.8770

Mazurek, A., and Pankiewicz, U. (2012). Changes of dehydroascorbic acid content in relation to total content of vitamin C in selected fruits and vegetables [Zmiany zawartości kwasu dehydro-l-askorbinowego w stosunku do całkowitej zawartości witaminy C w wybranych owocach i warzywach]. *Acta Sci. Pol Hortoru* 11, 169–177.

Mo, Y., Gong, D., Liang, G., Han, R., Xie, J., and Li, W. (2008). Enhanced preservation effects of sugar apple fruits by salicylic acid treatment during post-harvest storage. *J. Sci. Food Agric.* 88, 2693–2699. doi: 10.1002/jsfa.3395

Mphahlele, R. R., Fawole, O. A., Stander, M. A., and Opara, U. L. (2014). Preharvest and postharvest factors influencing bioactive compounds in pomegranate (*Punica granatum* L.) - A review. *Sci. Hortic.* 178, 114–123. doi: 10.1016/j.scienta.2014.08.010

Nuncio-Jáuregui, N., Calín-Sánchez, A., Carbonell-Barrachina, A., and Hernández, F. (2014). Changes in quality parameters, proline, antioxidant activity and color of pomegranate (*Punica granatum* L.) as affected by fruit position within tree, cultivar and ripening stage. *Sci. Hortic.* 165, 181–189. doi: 10.1016/j.scienta.2013.11.021

Oraei, M., Panahirad, S., Zaare-Nahandi, F., and Gohari, G. (2019). Pre-véraison treatment of salicylic acid to enhance anthocyanin content of grape (*Vitis vinifera* L.) berries. *J. Sci. Food Agric.* 99, 5946–5952. doi: 10.1002/jsfa.9869

Panth, N., Manandhar, B., and Paudel, K. R. (2017). Anticancer activity of *Punica granatum* (pomegranate): a review. *Phytother. Res.* 31, 568–578. doi: 10.1002/ptr.5784

Pareek, S., Valero, D., and Serrano, M. (2015). Postharvest biology and technology of pomegranate. *J. Sci. Food Agric.* 95, 2360–2379. doi: 10.1002/jsfa.7069

Peña-Estévez, M. E., Artés-Hernández, F., Artés, F., Aguayo, E., Martínez-Hernández, G. B., Galindo, A., et al. (2016). Quality changes of pomegranate arils throughout shelf life affected by deficit irrigation and pre-processing storage. *Food Chem.* 209, 302–311. doi: 10.1016/j.foodchem.2016.04.054

Russo, M., Fanali, C., Tripodo, G., Dugo, P., Muleo, R., Lugo, L., et al. (2018). Analysis of phenolic compounds in different parts of pomegranate (*Punica granatum*) fruit by HPLC-PDA-ESI/MS and evaluation of their antioxidant activity: application to different Italian varieties. *Anal. Bioanal. Chem.* 410, 3507–3520. doi: 10.1007/s00216-018-0854-8

Sayyari, M., Aghdam, M. S., Salehi, F., and Ghanbari, F. (2016). Salicyloyl chitosan alleviates chilling injury and maintains antioxidant capacity of pomegranate fruits during cold storage. *Sci. Hortic.* 211, 110–117. doi: 10.1016/j.scienta.2016.08.015

Sayyari, M., Babalar, M., Kalantari, S., Martínez-Romero, D., Guillén, F., Serrano, M., et al. (2011a). Vapour treatments with methyl salicylate or methyl jasmonate alleviated chilling injury and enhanced antioxidant potential during postharvest storage of pomegranates. *Food Chem.* 124, 964–970. doi: 10.1016/j.foodchem.2010.07.036

Sayyari, M., Babalar, M., Kalantari, S., Serrano, M., and Valero, D. (2009). Effect of salicylic acid treatment on reducing chilling injury in stored pomegranates. *Postharvest Biol. Technol.* 53, 152–154. doi: 10.1016/j.postharvbio.2009.03.005

Sayyari, M., Castillo, S., Valero, D., Díaz-Mula, H. M., and Serrano, M. (2011b). Acetyl salicylic acid alleviates chilling injury and maintains nutritive and bioactive compounds and antioxidant activity during postharvest storage of pomegranates. *Postharvest Biol. Technol.* 60, 136–142. doi: 10.1016/j.postharvbio.2010.12.012

Tareen, M. J., Abbasi, N. A., and Hafiz, I. A. (2012). Postharvest application of salicylic acid enhanced antioxidant enzyme activity and maintained quality of peach cv. "Flordaking" fruit during storage. *Sci. Hortic.* 142, 221–228. doi: 10.1016/j.scienta.2012.04.027

Tiwari, S., Lata, C., Chauhan, P. S., Prasad, V., and Prasad, M. (2017). A functional genomic perspective on drought signalling and its crosstalk with phytohormone-mediated signalling pathways in plants. *Curr. Genomics* 18, 469–482. doi: 10.2174/1389202918666170605083319

Valero, D., and Serrano, M., (2010). *Postharvest Biology and Technology for Preserving Fruit Quality*. Boca Raton, FL: CRC-Taylor & Francis Group. doi: 10.1201/9781439802670

Valero, D., Díaz-Mula, H. M., Zapata, P. J., Castillo, S., Guillén, F., Martínez-Romero, D., et al. (2011). Postharvest treatments with salicylic acid, acetylsalicylic acid or oxalic acid delayed ripening and enhanced bioactive compounds and antioxidant capacity in sweet cherry. *J. Agric. Food Chem.* 59, 5483–5489. doi: 10.1021/jf200873j

Valero, D., Mirdehghan, S. H., Sayyari, M., and Serrano, M. (2014). "Vapor treatments, chilling, storage, and antioxidants in pomegranates," in *Processing and Impact on Active Components in Food*, ed. V.R. Preedy (Cambridge, MA: Academic Press). 189–196. doi: 10.1016/b978-0-12-404699-3.00023-8

Valverde, J. M., Giménez, M. J., Guillén, F., Valero, D., Martínez-Romero, D., and Serrano, M. (2015). Methyl salicylate treatments of sweet cherry trees increase antioxidant systems in fruit at harvest and during storage. *Postharvest Biol. Technol.* 109, 106–113. doi: 10.1016/j.postharvbio.2015.06.011

Wang, Z., Ma, L., Zhang, X., Xu, L., Cao, J., and Jiang, W. (2015). The effect of exogenous salicylic acid on antioxidant activity, bioactive compounds and antioxidant system in apricot fruit. *Sci. Hortic.* 181, 113–120. doi: 10.1016/j.scienta.2014.10.055

Yang, Q., Wang, F., and Rao, J. (2016). Effect of putrescine treatment on chilling injury, fatty acid composition and antioxidant system in kiwifruit. *PLoS One* 11:e0162159. doi: 10.1371/journal.pone.0162159

Zaouay, F., Mena, P., Garcia-Viguera, C., and Mars, M. (2012). Antioxidant activity and physico-chemical properties of Tunisian grown pomegranate (*Punica granatum* L.) cultivars. *Ind. Crop. Prod.* 40, 81–89. doi: 10.1016/j.indcrop.2012.02.045

Zhang, Y., Chen, K., Zhang, S., and Ferguson, I. (2003). The role of salicylic acid in postharvest ripening of kiwifruit. *Postharvest Biol. Technol.* 28, 67–74. doi: 10.1016/S0925-5214(02)00172-2

Conflict of Interest: The authors declare that the research was conducted in the absence of any commercial or financial relationships that could be construed as a potential conflict of interest.

frontiers in Plant Science

REVIEW
published: 28 August 2020
doi: 10.3389/fpls.2020.564917

Sugar Signaling During Fruit Ripening

Sara Durán-Soria†, Delphine M. Pott†, Sonia Osorio and José G. Vallarino**

Departamento de Biología Molecular y Bioquímica, Instituto de Hortofruticultura Subtropical y Mediterránea "La Mayora", Universidad de Málaga – Consejo Superior de Investigaciones Científicas (IHSM-UMA-CSIC), Málaga, Spain

Sugars play a key role in fruit quality, as they directly influence taste, and thus consumer acceptance. Carbohydrates are the main resources needed by the plant for carbon and energy supply and have been suggested to be involved in all the important developmental processes, including embryogenesis, seed germination, stress responses, and vegetative and reproductive growth. Recently, considerable progresses have been made in understanding regulation of fruit ripening mechanisms, based on the role of ethylene, auxins, abscisic acid, gibberellins, or jasmonic acid, in both climacteric and non-climacteric fruits. However, the role of sugar and its associated molecular network with hormones in the control of fruit development and ripening is still poorly understood. In this review, we focus on sugar signaling mechanisms described up to date in fruits, describing their involvement in ripening-associated processes, such as pigments accumulation, and their association with hormone transduction pathways, as well as their role in stress-related responses.

Keywords: sucrose, sugars, signaling, ripening, hormones, pigments, stress, fruit

OPEN ACCESS

Edited by:
Carolina Andrea Torres, Washington State University, United States

Reviewed by:
Zhanwu Dai, Chinese Academy of Sciences, China
Yong Xu, Beijing Academy of Agriculture and Forestry Sciences, China

****Correspondence:***
Sonia Osorio
sosorio@uma.es
José G. Vallarino
vallarino@uma.es

†These authors have contributed equally to this work

Specialty section:
This article was submitted to Crop and Product Physiology, a section of the journal Frontiers in Plant Science

Received: *22 May 2020*
Accepted: *13 August 2020*
Published: *28 August 2020*

Citation:
Durán-Soria S, Pott DM, Osorio S and Vallarino JG (2020) Sugar Signaling During Fruit Ripening. Front. Plant Sci. 11:564917. doi: 10.3389/fpls.2020.564917

INTRODUCTION

Sugars are the main structural components of plant tissues, providing energy and carbon building blocks for growth and reproduction. In particular, fruit and seed development, crucial processes for global crop production, depends on the transport of photoassimilates through the phloem and assimilation from source to sink tissues (Ruan et al., 2012; Liu et al., 2013). Numerous studies, including metabolomic-driven approaches, have reported sugar content behavior during fruit growth and ripening, as soluble sugar accumulation determines fruit sweetness at harvest, an essential parameter of fruit quality (Deluc et al., 2007; Lombardo et al., 2011; Osorio et al., 2012; Vallarino et al., 2018). Furthermore, several studies pointed out that both sucrose and the main hexoses (glucose and fructose) originated from sucrose degradation, are involved in signaling and regulation of plant development (Ruan, 2012; Xu et al., 2012; Tognetti et al., 2013). Indeed, sugars may control in a direct or indirect way several processes, including photosynthesis, nitrogen uptake, defense mechanism, hormone balance, or secondary metabolism (Smeekens et al., 2010; Lecourieux et al., 2014). This control is mainly exerted by regulating gene expression, affecting mRNA stability or protein translation/stability (Koch, 1996; Wiese et al., 2004). Plants have developed mechanisms by which they perceive sugar fluxes, known as sugar sensing, and by which they control sugar-mediated responses, allowing them to adapt their activity at the cellular level based on sugar status and maintain homeostasis (Lecourieux et al., 2014).

Sugar Metabolism in the Fruit

Sucrose is the major fixed carbon (C) form of carbohydrates for long-distance transport through the phloem from leaves sources to non-photosynthetic sink organs, including developing fruits (Julius et al., 2017). Once sucrose reaches the sink cells, sucrose is hydrolyzed by sucrose synthases or invertases into fructose and glucose, which help maintaining sink strength. Sucrose synthases are mainly involved in the synthesis of carbohydrate polymers, i.e. starch or cellulose, or in the generation of energy, necessary for the production of a myriad of compounds which help fruit development and seed dispersal (Braun et al., 2014).

Invertases are classified into three groups based on their subcellular localization: cytoplasmic invertases (CIN), vacuolar invertases (VIN), and cell wall invertases (CWIN) (Li et al., 2012). Invertases play a regulatory role in plant growth and development, and VIN and CWIN are also involved in biotic and abiotic stress responses, connecting sucrose and hexose signaling with stress adaptation (Li et al., 2012; Li et al., 2016). Apart from their roles in stress responses, which evidences in fruits will be discussed further in this review, invertases and sucrose synthases are key factors determining the growth of bulky sinks (Xu et al., 2012). As an example, *LIN5* gene, which encodes a CWIN in tomato, is considered one of the main enzymes affecting sugar uptake into the fruit (Fridman et al., 2004; Baxter et al., 2005; Zanor et al., 2009; Vallarino et al., 2017). In addition, CWIN activity increases during ovary-to-fruit transition, possibly to facility phloem unloading and to produce a glucose signal, which positively regulate cell division and thus, fruit set (Palmer et al., 2015).

Sugar Transporters

Sugar transport is highly regulated and several transporters are involved in sucrose export from photosynthetic cells, phloem loading and unloading. Additionally, once in the fruits, part of the sucrose-derived hexose pool is also transported to the vacuole as a strategy to maintain sink strength (Lemoine et al., 2013; Liu et al., 2013; Lecourieux et al., 2014). These transporters can be divided into three main families: sucrose (SUT), monosaccharide (MST), and sugar will eventually be exported (SWEET) transporters (Julius et al., 2017; Jeena et al., 2019).

Both SWEET and SUT proteins are involved in phloem loading; while SWEET transporters act as facilitated diffusers, transporting sugars across membrane down a concentration gradient (Chen et al., 2010; Chen et al., 2012). SUTs are sucrose/proton symporters, using stored energy to drive active sucrose movement (Gaxiola et al., 2007). Phloem unloading in developing fruits can occur apoplasmically into cell wall matrix, as described in apples, or symplasmically through plasmodesmata in recipient cells (Wang and Ruan, 2013; Braun et al., 2014). In some fruits, such as tomato, both apoplasmic and symplasmic unloading take place and is under developmental control (Braun et al., 2014). In this process, sucrose effluxers, such as SWEET or SUT proteins, are involved in export sucrose from phloem, and sucrose or hexose influxers uptake sugars to the recipient sink cells. In apoplasmic unloading, the co-expression of cell wall invertases, which convert sucrose to hexoses, with MST generally occurs (Ruan et al., 1997; Jin et al., 2009). Once in the cell, other transporters belonging to the MST, SUT, and SWEET families, carry sucrose, fructose, and glucose into the vacuole, where most sugars are stored (Wormit et al., 2006; Aluri and Büttner, 2007; Cheng et al., 2018). In particular, members from the MST family, namely tonoplast sugar/monosaccharide transporters (TST/TMT), have been described to be involved in this process in high-sugar storage organs, such as sugar beet roots or melon and watermelon fruits (Hedrich et al., 2015; Cheng et al., 2018; Ren et al., 2018). *Arabidopsis* genome contains three isoforms of *TMT*; it was reported that *TMT1* expression increased during grape berry development (Terrier et al., 2005), and the study of Afoufa-Bastien et al. (2010) suggests that both TMT1 and TMT2 could play a role during fruit ripening. A recent study reported that the overexpression of watermelon *ClTST2* is positively correlated with sugar accumulation during fruit ripening in watermelon, and its regulation by a sugar-induced transcription factor (TF) will be discussed in another section of this review (Ren et al., 2018).

Sugar Signaling in the Fruit

In most species, sucrose is the main form of long-distance transported sugars through the plant; additionally, it can also initiate signaling pathways and affect gene expression, even if a specific receptor has not been found yet. The ability of sugars as regulators of gene expression has been long known, and glucose has been reported to regulate cell division (Smeekens et al., 2010; Wang et al., 2014; Palmer et al., 2015), while sucrose is involved in the accumulation of reserves during embryogenesis (Borisjuk et al., 2002; Borisjuk et al., 2003). Sucrose participation in signaling has been long known as demonstrated by Maas et al. (1990), who described how it can inhibit maize *Shrunken* gene promotor or by Wenzler et al. (1989) and Jefferson et al. (1990), which showed that *patatin-1* promoter was specifically induced by sucrose in potato tubers. More recently, Wiese et al. (2004) observed that sucrose induces the repression of a basic region leucine zipper (*AtbZIP*) transcription factor (TF) in *Arabidopsis*, while other sugars such as glucose and fructose have no effect (Kanayama, 2017). Additionally, other bZIP-sucrose sensitive TFs have been discovered, such as *CAREB1* in carrot, which is sensitive to both sucrose and abscisic acid (ABA) (Guan et al., 2009; Wind et al., 2010). Regarding fruit, it was verified that hexose transporter genes involved in sugar metabolism, were induced by sucrose, and that their promotor contains sucrose-responsive motifs or "sucrose box" (Çakir et al., 2003; Jia et al., 2016). For instance, *VvHT1* gene, which encodes a monosaccharide transporter in grape, contains two sugar boxes and is regulated by several sugars, including sucrose, glucose, and palatinose (Atanassova et al., 2003).

Furthermore, sugar and hormones crosstalk has already been described in plant development (Eveland and Jackson, 2012). However, most studies have focused on seeds and early plant development, and very few on sugar signaling role during fruit ripening. It is more recently that sugars have been associated with key processes related to fruit ripening, such as pigment

accumulation, and their regulating roles in this complex process, alone or in a crosstalk with hormone signaling (Jia et al., 2013; Liu et al., 2013; Li et al., 2016), are discussed below.

SUGAR SIGNALING IN FRUIT DEVELOPMENT AND RIPENING AND ITS CROSSTALK WITH HORMONES

Sucrose

Several studies have confirmed that sugar (and especially sucrose) metabolism is a key process in fruit development, promoting both its own accumulation and driving ripening events (Ruan et al., 2012; Tognetti et al., 2013). Indeed, a high correlation between endogenous sucrose and ripening phase changes has been observed in orange fruits (Wu et al., 2014). Similarly, late ripening has been observed when the concentration of sucrose in orange spontaneous mutant decreased (Zhang Y. J. et al., 2014). Exogenous sucrose treatment also improves strawberry ripening, accelerating the coloration of the fruit and allowing it to reach the ripe stage earlier (Jia et al., 2011; Jia et al., 2013; Luo et al., 2019). As well, the effect of exogenous sucrose in harvested tomatoes at the green mature stage by accelerating ripening and postharvest processes in the fruits has been described (Li et al., 2016).

Sucrose controls genes involved in sugar metabolism, such as the expression of starch biosynthetic enzymes, starch synthase and β-amylase (Nakamura et al., 1991; Wang et al., 2001). The investigation of Li et al. (2002) showed that in tomato fruit sucrose induced the expression of *ApL3*, which encodes an ADP-glucose phosphorylase, a key regulatory enzyme in starch biosynthesis. *CIN* genes, which are implicated in sucrose degradation and have a fundamental role in the maintenance of sugar homeostasis in the cytoplasm, are also regulated by sucrose itself, as demonstrated in tomato fruits (Ruan et al., 2010; Li et al., 2016). Furthermore, exogenous sucrose treatment in tomato fruits resulted in the downregulation of an invertase inhibitor gene (*INVINH1*). *CIN6*, unlike most sucrose breakdown genes, is downregulated when sucrose increases (Li et al., 2016). Interestingly, increased sucrose degradation by overexpressing *CIN* or *LIN5* genes did not enhance glucose and fructose levels, and seems to confirm that sucrose acts, at least partially, independently of hexose-derived signals in certain signaling pathways (Albacete et al., 2014; Li et al., 2016). Another proof of sucrose regulator role during ripening is its interaction in tomato with the MADS-box TF *RIN*. *RIN* is a global regulator of fruit ripening, well studied in this fruit (Ng and Yanofsky, 2001; Vrebalov et al., 2002; Giovannoni, 2007; Osorio et al., 2012); interestingly, Qin et al. (2016) observed that several genes involved in sugar metabolism, were differentially expressed in the *rin* mutant compared to Aisla Craig tomato wild type fruits. In particular, lower VIN expression was observed in the *RIN*-silenced fruits, while a VIN inhibitor (*SlVIF*) showed higher expression. Interestingly, in *SlVIF*-silenced lines, *RIN* expression was affected and the green to red transition of the fruits was retarded in comparison with wild-type and *SlVIF*-overexpressed lines (Qin et al., 2016). Concomitant with the impact on color change, *SlVIF* silencing results in diminished ethylene production, and in the alteration of transcript/protein profiles involved in fruit maturation, suggesting a key role of this invertase inhibitor in controlling tomato ripening (Qin et al., 2016).

Sucrose transport, from leaves sources to sink organs is more important than *de novo* synthesis in the fruit (Hackel et al., 2006; Jia et al., 2013). Thus, regulation of SUT transporters is an important factor which demonstrates the role of endogenous sucrose in fruit development and ripening. In this way, *SUT1* silencing clearly reduces sucrose concentration in the fruit, delaying strawberry and citrus ripening (Jia et al., 2013; Wu et al., 2014). In apple, cytochrome B5 has been proposed as a possible sucrose sensor, since it interacts with MdSUT1 and MdSOT6, a sorbitol transporter (Fan et al., 2009). Another suggested sucrose sensor is SUT2, which may couple sucrose sensing with G protein and thus mediate sugar regulation on the expression of genes involved in fruit development (Barker et al., 2000; Wind et al., 2010). Alternatively, sucrose could be transformed into glucose and fructose, and these sugars would be responsible to regulate gene expression (Rolland et al., 2006; Zhang Y. J. et al., 2014). However, it was recently demonstrated that the downregulation of the genes involved in the catalysis of sucrose into fructose and glucose, *i.e.* α-glucosidase and invertase, did not affect the expression of *SUT2* (Luo et al., 2019). Furthermore, no significant differences were observed in the expression of *LeSUT1*, *LeSUT2*, and *LeSUT4* when sucrose (25 μl, 500 mM) were injected into the pedicle of tomato fruit recently harvested (Li et al., 2016). Hexokinase (HXK), a very important enzyme for monosaccharide metabolism, has also been proposed as a possible sugar receptor. Indeed, HXK1 can form a complex with a vacuolar H^+-ATPase and the 19S subunit of the proteasome, that directly modulates the expression of target genes (Cho et al., 2006). While most SUT transporters are localized in plasma membrane, some members of SUTII subfamily were found associated with vacuole membrane and their overexpression results in increased sucrose accumulation in this organelle (Ma et al., 2017; Ma et al., 2019; Peng et al., 2020). Surprisingly, a negative correlation between apple tonoplast *MdSut4.1* expression and sucrose accumulation was observed, and was confirmed by transient overexpression in strawberry fruit, suggesting a function in sucrose remobilization out of the vacuole (Schneider et al., 2012; Peng et al., 2020). Taken together, these observations could propose MdSUT4.1 as a key component of the regulation of apple fruit sugar accumulation.

Recently, the study of Ren et al. (2018) shows that watermelon genome contains three *TST* orthologs, being *ClTST2* the principal sugar transporter into vacuoles. *SUSIWM1*, a sugar-induced TF, binds to a SURE element, located in a region of *ClTST2* promoter, and induces *ClTST2* expression stimulating sugar loading and storage into vacuoles of watermelon fruit cells (Ren et al., 2018). Interestingly, SURE elements were described in potato to be localized in promoters of genes regulated by sucrose (Grierson et al., 1994), suggesting that sugar storage in vacuoles during fruit ripening, mediated by TST2 transporters, is controlled by sucrose itself. Three *TST* genes were also found in melon genome, and

CmTST2 presents the highest correlation with sugar accumulation during fruit ripening (Cheng et al., 2018). Stable overexpression of *CmTST2* in melon and cucumber plants allowed to establish the role of this transporter in sugar accumulation during fruit ripening, as ripe overexpressed fruits contained higher levels of fructose, glucose, and sucrose, compared to control fruits (Cheng et al., 2018). Moreover, *TST2* gene was transiently overexpressed in strawberry fruit and, as a result, the fruits presented a lower concentration of cytosolic sugar, due to an increased rate in sucrose introduction into the vacuole. More interestingly, strawberry ripening was delayed in the transient-overexpressed fruits, compared to the control, possibly as the consequence of sugar signaling involvement in this physiological process (Cheng et al., 2018). *CmTST1* expression is very high during the early stage of melon fruit development, and then decreased rapidly, concomitant with glucose and fructose accumulation pattern in this fruit, suggesting a role of this ortholog in hexose storage in the vacuole. It is worth noting that sugar-responsive elements were identified in the promotor region of the three *CmTST* genes (Cheng et al., 2018). In this sense, the functions and characteristics of tonoplast transporters in fleshy fruits and their involvement in ripening need more research.

Sucrose also regulates anthocyanin and carotenoid biosynthesis, two groups of secondary metabolites involved in fruit coloration, and will be detailed in other sections of this review. Experiments have recently been conducted to demonstrate that the role of sucrose in ripening is not due to its degradation into fructose and glucose. Indeed, Jia et al. (2013, 2017); demonstrated that turanose, a non-metabolizable sucrose analogue, has the same effect than sucrose on the expression of ripening genes in grape and strawberry.

Trehalose-6-Phosphate: Its Dual Function in Sucrose Sensing and Its Regulation

In addition to the aforementioned main sugars present in the fruit, ***i.e.*** fructose, glucose, and sucrose, some minor sugars, such as trehalose-6-phosphate, an intermediate in the disaccharide trehalose metabolism, have been proposed as a signal for carbon availability and homeostasis, and could play an essential role in both plant development and abiotic stress tolerance (Yadav et al., 2014; Kretzschmar et al., 2015; Nuccio et al., 2015). In particular, it was demonstrated that trehalose-6-phosphate levels in different plant tissues was positively correlated with sucrose content, and that the addition of sucrose or sugars which can be metabolized to this disaccharide, was able to induce a fast rise in trehalose-6-phosphate content, suggesting that the latter is a specific signal monitoring sucrose status (Debast et al., 2011; Martínez-Barajas et al., 2011; Nunes et al., 2013; Yadav et al., 2014; Zhang et al., 2015; Figueroa and Lunn, 2016). Furthermore, as the correlation between sucrose and trehalose-6-phosphate was conserved in *Arabidopsis* plants which constitutively expressed the *E. coli* ***trehalose-6-phosphate synthase*** or ***trehalose-6-phosphate phosphatase***, involved in trehalose-6-phosphate synthesis and catabolism, respectively, it could be concluded that trehalose-6-phosphate is both a signal of sucrose availability and a negative feedback regulator of sucrose content, maintaining it in a closely controlled range (Yadav et al., 2014; Figueroa and Lunn, 2016).

Trehalose-6-phosphate is thought to act through the action of the sucrose non-fermenting-related kinase-1 (SnRK1) pathway, even if the exact molecular mechanism by which they interact is still imprecise (Delatte et al., 2011; Ponnu et al., 2011; Figueroa and Lunn, 2016). SnRKs are kinase proteins involved in signal transduction of carbon and nitrogen, being key regulators and sensors in plant carbohydrate metabolism (Emanuelle et al., 2016). Regarding fruit set and development, a study in cucumber suggests that trehalose-6-phosphate and SnRK1-mediated pathways are involved in "first-fruit inhibition," a phenomenon in which first fruit set has an inhibitory effect on the growth of subsequent fruits (Zhang et al., 2015). Indeed, high trehalose-6-phosphate levels and low SnRK1 activity in the peduncle of the first fruit may participate in increasing sink strength, by modulating the expression of *CsAGA1*, an alpha-galactosidase, which catalyzes the hydrolysis of stachyose, the main carbohydrate transport form in cucumber, to sucrose (Zhang et al., 2015).

Wang et al. (2012) was the first study to show that the heterologous overexpression of *SnRK1* from *Malus hupehensis* in Sy12f tomato can promote fruit ripening by increasing both starch and soluble sugars. In addition, the fruits of *MhSnRK1* overexpressed plants displayed early ripening. Furthermore, these fruits showed greater diameter. Increased carbon metabolism in the leaves could explain the higher available carbon in the fruits stored as starch and soluble sugars (Wang et al., 2012). A second study overexpressing *Prunus persica* SNF1-related kinase α subunit (*PpSnRK1α*) in Sy12f tomato allowed to go deeper in understanding the molecular mechanism by which SnRK1 regulates fruit ripening (Yu et al., 2018). By yeast-two-hybrid experiment and BiFC assay, positive interaction was detected between PpSnRK1α and RIN. Furthermore, in *PpSnRK1α* overexpressing fruits, *RIN* expression, together with the levels of other TFs directly controlled by RIN, were enhanced, suggesting a regulation by SnRK1 both at the post- and transcriptional level (Yu et al., 2018).

FaSnRK1α overexpression and silencing in Miaoxiang 7 strawberry confirmed its importance in fruit ripening, by accelerating and delaying it, respectively. In addition, FaSnRK1α was seen to increase sucrose content in the fruit, by controlling the expression of genes involved in its transport and metabolism (Luo J. et al., 2020). The physical interaction between FaSnRK1α and several enzymes involved in sucrose hydrolysis and synthesis, including the sucrose phosphate synthase FaSPS3, which has been directly associated with sucrose accumulation during strawberry fruit ripening, was also demonstrated by yeast two-hybrid (Wei et al., 2018; Luo J. et al., 2020).

The relation between trehalose-6-phosphate and SnRK1 protein seems to be conserved in species that transport other sugars than sucrose. Kiwifruits transport both sucrose and the trisaccharide planteose through the phloem to heterotrophic tissues (Boldingh et al., 2015). Under carbon starvation, the low levels of trehalose-6-phosphate in Zes006 kiwifruit removed the inhibition on SnRK1, which initiates the signaling of low-energy status (Delatte et al., 2011; Nardozza et al., 2020).

Even if trehalose-6-phosphate acts as a signal and regulator of sucrose levels in plants, the nexus between both sugars is still not

so well understood, and a possible role in fruit ripening has not yet been clearly established. For example, a study in Cabernet Sauvignon grape during berry development did not observe a clear correlation between sucrose or hexoses and trehalose-6-phosphate levels (Dai et al., 2013). A possible explanation for this lack of direct correlation could be the accumulation in different organelles—vacuole for sugars, cytosol for trehalose-6-phosphate. However, by building a metabolite-metabolite correlation network, Dai et al. (2013) demonstrated that trehalose-6-phosphate was the most connected compound in the network, suggesting its participation in multiple metabolic pathways. Interestingly, a strong and positive correlation was observed between trehalose-6-phosphate and sorbitol content during Gala apple fruit development (Zhang W. et al., 2017). Sorbitol, instead of sucrose, is the main transported sugar from leaves to sink tissues in some economically important crop species belonging to the Rosaceae family, such as apples or pears, and is mainly found in the cytosol of the sink cells (Rennie and Turgeon, 2009; Shangguan et al., 2014). Furthermore, trehalose-6-phosphate levels are negatively correlated with sucrose and other sugars during apple fruit ripening, and positively correlated with sucrose in sorbitol-limited fruits (obtained by thinning), indicating that sucrose may be regulated by a specific pathway which acts only under abnormal growth situation, such as carbon starvation (Zhang W. et al., 2017). In addition, sorbitol:trehalose-6-phosphate ratio was strongly linked to starch content and correlated with glucose, one of the two main products of starch degradation, which occurs in the later stages of apple ripening (Zhang W. et al., 2017). Even if the relation between trehalose-6-phosphate and starch content needs further confirmation, it could nevertheless outline the possible role of this sugar in starch breakdown during fruit development, as previously described in potato tubers by Kolbe et al. (2005).

UDP-Sugars

UDP-sugars are an activated form of sugars which act as donors for different biosynthetic reactions. Although little evidence exists at the present time, a possible role in plant signaling has been suggested based on studies in animals, which outlined a role for uridine-5' disphosphate-glucose (UDPG) as an extracellular signaling molecule, that is sensed by G-protein-coupled receptors (Chambers et al., 2000; Harden et al., 2010; Lazarowski and Harden, 2015). Additionally, as sucrose, a known signaling molecule in plant, is rapidly split into glucose, UDPG, and fructose, a potential role of these breakdown products in sugar signaling cannot be ruled out (Hummel et al., 2009). Furthermore, the lack of identified sucrose receptor might imply a signaling function of its breakdown products (Janse van Rensburg and Van den Ende, 2018). However, as UDPG is directly related to the concentration of sucrose, and therefore, to the accumulation of glucose, fructose, and trehalose-6-phosphate, it cannot be ruled out that UDPG can cause an imbalance in the levels of other metabolites involved in signaling instead of being a signaling sugar itself. Deeper studies on the possible signaling role of UDPG seems nevertheless necessary, as UDPG function in plant growth and development is well described, and a recent study suggests that UDPG enhances biomass accumulation in sugarcane because of its rapid conversion to sucrose (Wai et al., 2017). UDPG pyrophosphorylase, an enzyme involved in UDPG formation and which is differentially expressed under stress conditions (Ciereszko et al., 2001; Meng et al., 2007), has been shown to be a regulator of programmed cell death (Janse van Rensburg and Van den Ende, 2018; Xiao et al., 2018). A very recent study has suggested that UDPG might have an important role in the induction of reactive oxygen species generation and lesion mimics in rice (Xiao et al., 2018), nevertheless, further studies are required to understand this process and the possible role of UDPG or any other UDP-sugar in plant signaling and fruit ripening.

Sucrose and Abscisic Acid

The function of ethylene in climacteric fruit ripening has been long known, however, in non-climacteric fruits, ABA seems to play a more important role (Jia et al., 2016). Indeed, ABA increases during orange ripening and promotes fruit color formation (Rodrigo et al., 2006), while in strawberry, another non-climacteric fruit, ABA modulates growth and softening, as well as the synthesis of anthocyanins and volatiles compounds (Jia et al., 2011), whereas ethylene role is more limited (Chervin et al., 2004; Trainotti et al., 2005; Merchante et al., 2013; Jia et al., 2016). Furthermore, in early tomato development, a climacteric fruit, the peak of ABA precedes the peak of ethylene, suggesting that both hormones promote together fruit ripening (Li et al., 2016).

An idea that is becoming more and more expanded is that sugar signaling and ABA are involved in a crosstalk which regulates fruit ripening, being this interaction especially evident in non-climacteric fruits (**Figure 1**; Gambetta et al., 2010; Cherian et al., 2014). A recent model in apple plant established the role of ABA in promoting soluble sugar accumulation, by activating the expression of genes involved in sugar transport, such as *MdSUT2*, and starch degradation. As a consequence, ABA signaling contributes greatly to enhance sweetness, a very important trait for fruit quality (Ma et al., 2017). Furthermore, other studies focused on the interaction between ABA and sucrose signaling in promoting ripening-associated processes. Indeed, it was recently described that treatments with exogenous ABA and sucrose greatly accelerate strawberry and grape fruits ripening, being the effect obtained much more intense than with either sucrose or ABA alone (Jia et al., 2016; Jia et al., 2017; Luo Y. et al., 2020). Grapes were collected and treated with different concentrations of ABA and sucrose (100 μM ABA and 16 mM sucrose) (Jia et al., 2017) and green-stage strawberries were sprayed with 95 μM ABA and 100 mM sucrose, and collected fully ripe (Luo Y. et al., 2020). Differentially expressed genes have been observed between the three aforementioned treatments (ABA, sucrose and ABA + sucrose), suggesting that the differences are due to the synergistic action between ABA and sucrose, and not due to the additive effects of two independent routes (Luo Y. et al., 2020). In particular, recent studies have reported that this interaction between ABA and sucrose exerts control on the synthesis of anthocyanins in strawberry fruit (Jia et al., 2016) and starch in maize (Huang et al., 2016). During peach ripening, a crucial connection was outlined between ABA

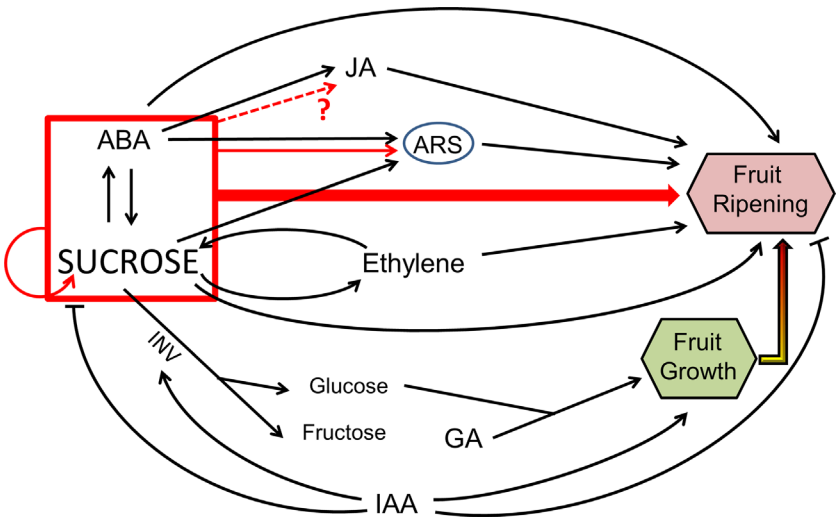

FIGURE 1 | General schema of sugar signaling and its crosstalk with hormones. In the first stages of fruit development IAA and GA promote cell expansion and elongation, meanwhile IAA represses sucrose accumulation and stimulates its degradation by invertase (INV) into glucose and fructose, which are also necessary for fruit growth. During ripening, sucrose can activate several genes which enhanced ABA, ethylene, and JA levels, as well as ASR genes, thus promoting fruit ripening processes; in addition, sucrose by itself can promote fruit ripening too. Red lines symbolize a synergetic action between sucrose and ABA. This model is inspired in Jia et al., 2013; Wu et al., 2014; Zhang Y. J. et al., 2014; Zhang Y. et al., 2014; Jia et al., 2016, and Murayama et al., 2015.

and sucrose, admitting a possible crosstalk between the two signaling molecules (Falchi et al., 2013). Furthermore, other studies in citrus fruit suggest that sucrose could be a key regulatory molecule of ripening, together with the phytohormones ABA, ethylene, and jasmonic acid (JA) (Wu et al., 2014; Zhang Y. J. et al., 2014). Indeed, ABA, ethylene, and sucrose pathways were clearly different between a spontaneous late-ripening mutant and wild type orange, as shown by the significant differences in the levels of these three metabolites. However, there is still need to clarify which is the most important factor responsible for the delay in ripening observed in the spontaneous mutant (Wu et al., 2014).

In addition, sucrose and ABA could concurrently regulate the expression of some genes during fruit development, including genes involved in sugar metabolism and accumulation. For example, sucrose and ABA induce sucrose synthase activity in rice (Tang et al., 2009), although more studies are needed to understand the molecular mechanisms of this process. Another study in Cabernet Sauvignon grape focused on the effect of sugar status on the expression of genes in grape berry cell suspension. Following a transcriptomic approach, Lecourieux et al. (2010) observed that the expression of a *glycogen synthase kinase3*, *VvSK1*, was enhanced both by ABA and exogenous sucrose, underlining the intercommunication between sugars and hormone signaling pathways. The overexpression of *VvSK1* in cell suspension enhanced the expression of some MST and as a consequence, increased the levels of soluble sugars in the cell (Lecourieux et al., 2010). In grape berries, *VvSK1* expression increased after the veraison stage, concomitant with sugar and ABA levels, suggesting that sugar could regulate fruit sugar content by modulating VvSK1 action (Lecourieux et al., 2014).

ASR (ABA stress ripening) belongs to a gene family which encodes small basic proteins induced by ABA, abiotic stresses and during fruit ripening. The expression of *ASR* genes has been reported in several fruits, such as tomato (Iusem et al., 1993), pomelo (Canel et al., 1995), apricot (Mbeguie-A-Mbeguie et al., 1997), and grape (Çakir et al., 2003). The first evidence about ASR physiological function in sugar and ABA signaling pathways was found by Çakir et al. (2003). Indeed, they observed in grape cell suspension grown in medium supplemented with sucrose alone (58 mM) or with sucrose and ABA (10 μM) that expression of a grape *ASR* gene (*VvMSA*), which is upregulated during grape fruit ripening, was inducible by sucrose, and also this induction was enhanced in presence of ABA. It was later established that *ASR* was also involved in the crosstalk between ABA and sucrose during ripening, as its expression could also be induced by these hormone and sugar during tomato, peach, and strawberry fruit maturation (Chen et al., 2011; Jiaxing et al., 2018). *ASR* expression in tomato and strawberry pointed out a role in fruit ripening and was also induced by ABA and sucrose, in two different pathways, which can work independently or together (Jia et al., 2016). Indeed, sucrose and ABA inhibitor nordihydroguaiaretic acid treatment induced *ASR* expression, while nordihydroguaiaretic acid alone did not induce it, suggesting that sucrose can act separately from the hormone response (Jia et al., 2016).

Transient overexpression of peach *ASR* gene in tomato fruits resulted in changes in cell wall degradation and pigment synthesis, confirming ASR role in promoting fruit ripening, as observed in overexpression and silencing experiments in tomato and strawberry fruits (Jia et al., 2016; Jiaxing et al., 2018). In fact, Jia et al. (2016) suggested that *ASR* acts as a switch, controlling ripening-related genes in response to activation by ABA and/or sucrose. Furthermore, ASR may also act as a transcription factor, as suggested by Çakir et al. (2003), which showed that it could

bind two sugar-responsive elements (sugar boxes) present in the promotor region of *VvHT1*, enhancing the expression of this hexose transporter. Peach *ASR* gene was also able to bind the unique *hexose transporter* gene present in this species, confirming its role as TF, acting in response to ABA and sucrose signaling, which cooperatively regulated its transcription (Jiaxing et al., 2018). *Hexose transporter* gene induction by *ASR* was also confirmed in tomato and strawberry, and, as expected, was enhanced by sucrose, ABA, or sucrose + ABA (Jia et al., 2016).

Besides the synergistic effect that ABA and sucrose shows during fruit ripening, it seems that sucrose is also involved in enhancing ABA levels (**Figure 1**). Jia et al. (2011, 2013); observed an increase in the level of ABA after glucose and sucrose treatments, accelerating strawberry fruit ripening, being sucrose effect more pronounced. As a consequence of this observation, this sugar has been proposed to induce the expression of key genes involved in ABA biosynthetic pathway, such as 9-cis-epoxycarotenid dioxygenase (*NCED*) and beta-glucosidase (*BG*) (Jia et al., 2013). A recent investigation confirmed that ABA (95 μM) and sucrose (100 μM) treatments resulted in the overexpression of *FaNCED1* and *FaNCED2* in sprayed strawberry fruit (Luo et al., 2019). Nevertheless, it is worth noting that in the absence of ABA, sucrose treatment had no effect on the expression of *FaNCED*, even if it was able to significantly upregulated the expression of *FaBG*. Taken together, these data suggest that sucrose level can modulate ABA content in strawberry fruit (Luo et al., 2019).

Silencing of the E1 component subunit alpha of the pyruvate dehydrogenase, involved in glucose metabolism and in the conversion of pyruvate to acetyl-CoA, has been reported to inhibit glycolysis, and accelerate ripening in strawberry, as a consequence of ATP and respiration repression (Wang et al., 2017). Luo Y. et al. (2020) suggested that this inhibition of glycolysis is an important factor for ripening and could be induced by ABA and sucrose, supported by the observation that *GAPDH*, another key enzyme in glycolysis, was downregulated after treatment with ABA and sucrose in strawberry fruit. Furthermore, they proposed that hydrogen peroxide (H_2O_2) could affect the synergetic action of ABA/sucrose showing a short inhibition of glycolysis during strawberry fruit ripening, as the levels of endogenous H_2O_2 was induced by ABA, sucrose, and ABA + sucrose treatments. Enhanced H_2O_2 level is an indication of oxidative stress, which may inactivate GAPDH, resulting in a shift of the carbon flux from glycolysis towards the pentose phosphate pathway to generate reducing equivalents (Krüger et al., 2011). Interestingly when strawberry fruits were treated with reduced glutathion, an important antioxidant, H_2O_2 content was decreased and an important delay in fruit coloration was also observed, confirming the role of H_2O_2 in connecting ABA, sucrose, and fruit ripening (Luo Y. et al., 2020).

Sucrose and Other Hormones

Ethylene has long been known for its function in fruit ripening, being the key hormone controlling this process in climacteric fruits (Giovannoni, 2007). It has already been reported that ethylene promotes sucrose accumulation in several fruits (Chervin et al., 2006; Choudhury et al., 2009; Farcuh et al., 2018), but it has also been observed that sucrose can also stimulate ethylene biosynthesis, promoting the postharvest ripening of tomato and kiwifruits (**Figure 1**; Li et al., 2016; Fei et al., 2020). Sucrose was able to enhance the expression of ethylene receptor (*ETR*) genes, *SlETR3 and SlETR4*, and ethylene signaling in tomato fruit (Li et al., 2016). In detached kiwifruits, exogenous application of sucrose induced an increase in the expression levels of two ethylene biosynthetic genes (Fei et al., 2020). Furthermore, *ETR* showed higher expression at the onset of tomato, grape, apple, and clementine ripening coincidently to the start of sugar accumulation, although the causal relation between both events remains to be further investigated (Chen et al., 2018). However, taken together, these findings may suggest the existence of a hub between ethylene and sucrose for fruit ripening control.

In early stages of fruit development, auxins play a key role in preventing fruit abscission, which will be induced by ethylene when the fruit is ripe (Murayama et al., 2015). In young fruits, auxins accumulate in the peduncle to avoid abscission, and thus allow sucrose transport to sink cells where it is usually degraded by CWIN. As a consequence, the resulting glucose inhibits programmed cell death, and thus promotes fruit development (Ruan, 2012). In addition, it was suggested that auxin accumulates during early stages of fruit development which promotes cell division and represses genes involved in ripening-associated processes (Medina-Puche et al., 2016). Jia et al. (2017) observed that ABA, sucrose, and auxin had an integrated regulation during grape berry ripening; indeed, apart from the synergetic action of ABA/sucrose previously commented, a negative influence of the auxin indole acetic acid on sugar accumulation was observed (**Figure 1**; Jia et al., 2017). Jia et al. (2016) showed that indole acetic acid inhibited the expression of sugar-accumulated genes during strawberry and tomato fruit ripening. Furthermore, overexpression of the auxin response factor *SlARF6* and downregulation of *SlARF4* resulted in increased soluble sugar content in tomato fruits, as a consequence of enhanced photosynthetic activity. Enhanced levels of sucrose in tomato fruits further impact starch synthesis, for which a crosstalk between auxin and sucrose metabolism at the early stages of fruit development cannot be ruled out (Sagar et al., 2013; Yuan et al., 2019).

A link between gibberellic acid (GA), fruit ripening, and sugar signaling has also been outlined, as mentioned later in this review for anthocyanin synthesis (Li et al., 2014). GA is involved in fruit development, in particular in cell division and expansion, which may depend on a complex network between GA and glucose signaling, as described in barley embryos (Perata et al., 1997). Exogenous application of GA on Cabernet Sauvignon grape cell culture was able to relieve the hexokinase-dependent repression of glucose on *CWIN* expression, suggesting a coupling between the hexose and the hormone transduction pathways to control berry development (Zhang Y. et al., 2014). In addition, transient silencing of *FaGAMYB*, a MYB TF regulated by GA, outlines the connection between GA, ABA, and sucrose pathways during Camarosa strawberry fruit ripening. Indeed, *FaGAMYB*-silenced

fruits showed both sucrose and ABA decreased levels, suggesting that GA signaling may act upstream of the ABA- and sucrose-dependent ripening processes (Vallarino et al., 2015).

Sucrose and ABA treatments could also separately induce the expression of two genes involved in JA synthesis in strawberry (Jia et al., 2016). This hormone is positively affected by ABA and promotes fruit-ripening processes in a possible crosstalk with this latter and sucrose (**Figure 1**; Jia et al., 2016). However, in some climacteric fruits, JA seems to act as an inhibitor of ethylene biosynthesis pathways, thereby delaying fruit ripening, as observed in apples and pears (Kondo et al., 2000; Nham et al., 2017; Lindo-García et al., 2020). More studies are needed to fully understand the role of JA in fruit ripening and to confirm the putative existence of any crosstalk with sugars.

SUCROSE PROMOTES ANTHOCYANIN AND CAROTENOID SYNTHESIS DURING FRUIT RIPENING

One of the common traits of fleshy fruit ripening is the synthesis and accumulation of metabolites which function is to increase their palatability to seed dispersers (Pott et al., 2019). Some of these compounds are pigments, conferring bright and appealing colous to ripe fruits. An important group of colorful molecules synthesized during ripening are anthocyanins, which accumulate in vacuoles, conferring red, purple, pink, or blue colors to fruits such as strawberries, blueberries, eggplants, grapes, or apples (Petrussa et al., 2013). They are polyphenol molecules belonging to the flavonoid class and synthesized through the phenylpropanoid pathway, and which metabolism and regulation have been widely studied, both for their important roles *in planta* and in the human diet (Vogt, 2010; Fraser and Chapple, 2011; Hassan and Mathesius, 2012; Petrussa et al., 2013; Giampieri et al., 2015; Pott et al., 2019). In particular, their biosynthesis is mediated in higher plants through a ternary conserved complex (MBW complex), formed by R2R3-MYB, basic helix-loop-helix (bHLH) and WD40-repeat proteins, which regulates the expression of the pathway structural genes (Xie et al., 2016).

Interestingly, sucrose treatment in *Arabidopsis* was able to up-regulate several biosynthetic genes of the flavonoid/anthocyanin pathway and also to induce the expression of *MYB75/PAP1* TF, involved in this class of pigments biosynthesis. These results were concomitant with the observed increase levels of anthocyanins in mutants with enhanced content in soluble sugars and starch (Lloyd and Zakhleniuk, 2004; Teng et al., 2005; Solfanelli et al., 2006). Furthermore, the interplay between sucrose and ABA brought to light the role of sugars in anthocyanin synthesis during strawberry fruit ripening (Jia et al., 2013; Jia et al., 2016; Luo et al., 2019). However, it seems that sugar alone, without the presence of exogenous ABA is sufficient to trigger anthocyanin synthesis, as described in grape berries (Dai et al., 2014; Olivares et al., 2017). Indeed, sucrose application (90 mM applied with a hand-held sprayer) on Crimson Seedless grape berries 13 days after veraison increased anthocyanin accumulation, quickening the development of fruit skin color, where these pigments are found. Even if the effect was less accentuated than with ABA or ABA + sucrose treatments, sucrose application could be an easy handling, low-cost strategy to promote earlier harvests (Olivares et al., 2017).

Studies in grape suspension cells have allowed to understand better the mechanisms by which sugars promote anthocyanins, and to establish which are the sugars involved in anthocyanin synthesis. An early study in Gamay Fréaux cell suspension showed that sucrose (100–150 mM), glucose (150 mM), and fructose (150 mM) were able to enhance anthocyanin content, and that neither mannitol nor sorbitol induced pigment accumulation, suggesting that the sugar effect was not osmotic (Larronde et al., 1998). By applying fructose, glucose, sucrose, or different glucose analogs to sliced Cabernet Sauvignon grape disks, Zheng et al. (2009) could conclude that only sugars that can serve as substrates for hexokinase (HXK) are able to affect anthocyanin accumulation, as previously found in Gamay Fréaux cell suspension (Vitrac et al., 2000). These results suggest that HXK may act as a sensor for sugar signaling in grape cells, as suggested previously by Cho et al. (2006) in *Arabidopsis*, and consequently activate anthocyanin synthesis. HXK mechanism in modulating anthocyanin content was further studied in apple. Indeed, the activation of apple HXK1 by phosphorylation under high glucose condition allows to stabilize basic helix-loop-helix TF *MdbHLH3*, a part of the regulatory complex controlling anthocyanin synthesis at the transcription level (**Figure 2**). The HXK1-mediated anthocyanin accumulation in apple peel depends on *MdHLH3*, and was confirmed by transient expression assay in the fruit (Hu et al., 2016).

Apart from HXK role in sugar signaling for anthocyanin synthesis, the function of SnRK1 protein was put forward in *Arabidopsis* and apple calli (Baena-González et al., 2007; Liu et al., 2017). While 1% sucrose promoted anthocyanin accumulation in apple calli overexpressing *MdSnRK1.1*, higher concentration of this sugar (12%) showed inhibition. In this sense, the proposed model under low sucrose level, MdSnRK1.1 interacts with MdJAZ18, a repressor in jasmonate signaling pathway, and induces its degradation. As MdJAZ18 interacts with MdbHLH3, its degradation allows MdbHLH3 to activate anthocyanin biosynthesis (**Figure 2**; Liu et al., 2017). Furthermore, a link between JA, GA, and sucrose signaling pathways, fine-tuning anthocyanin accumulation was established in *Arabidopsis* by Li et al. (2014) and Xie et al. (2016). In particular, DELLA proteins, key GA signaling negative regulators, have been identified as components of sucrose signaling, as GA-mediated degradation of RGA, one of the five DELLA proteins found in *Arabidopsis*, was inhibited in seedlings grown with 100 mM sucrose (Li et al., 2014). It was later established that DELLA proteins, in GA absence, favored anthocyanin accumulation by sequestering the anthocyanin repressors JAZs and MYBL2, allowing the formation of an active MBW complex (Qi et al., 2014; Xie et al., 2016). While anthocyanin synthesis by the mechanisms involving JA, GA-DELLA and sugar signaling could be explained as a plant response to abiotic stresses (Tarkowski and Van den

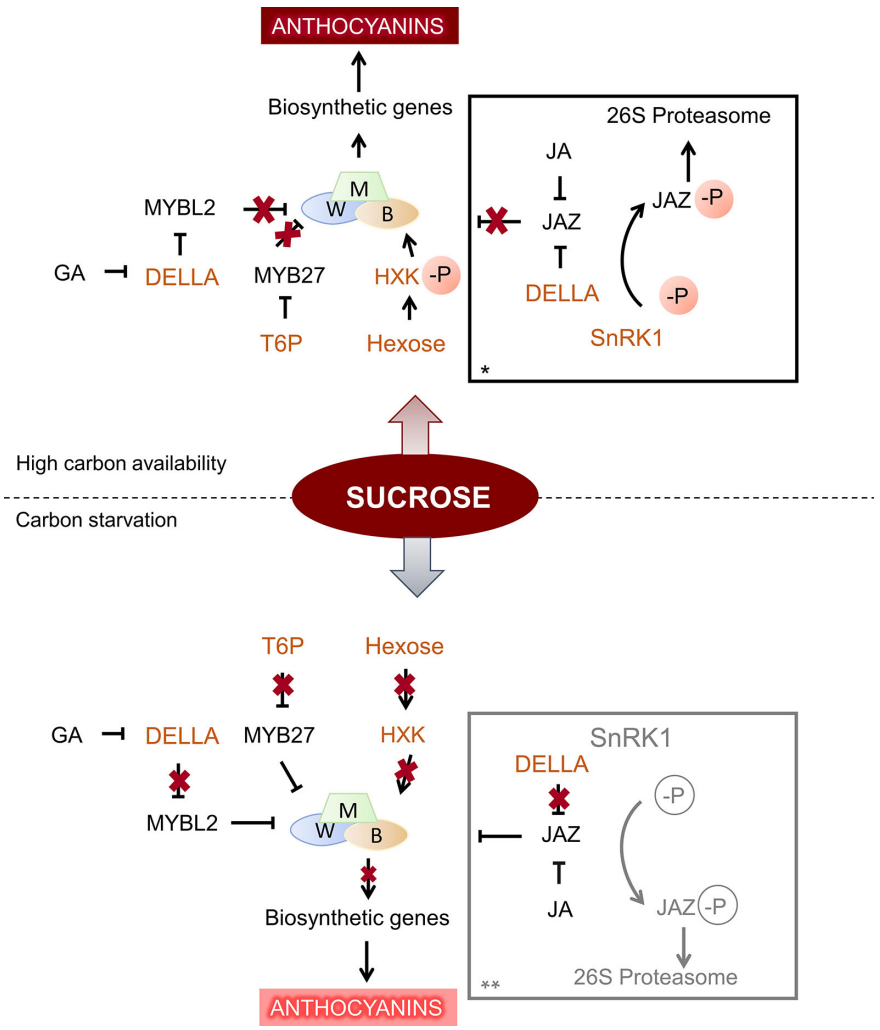

FIGURE 2 | General schema of sugar signaling in anthocyanin synthesis, under high and low carbon conditions. Components of sugar signaling cascade are shown in orange. When there is a high supply of sucrose, hexokinase (HXK) is phosphorylated and activates *bHLH3* (B) transcription factor, part of the MBW complex, which promotes anthocyanin synthesis by its action upon downstream biosynthetic genes. In addition, high levels of trehalose-6-phosphate (T6P) represses *MYB27*, a general repressor of anthocyanin synthesis, leading to increased anthocyanin content showed in darker hues (Hu et al., 2016; Nardozza et al., 2020). DELLA protein degradation is also repressed under sucrose treatment, and favors anthocyanin accumulation by sequestering JAZs and MYBL2 repressors (Li et al., 2014; Qi et al., 2014; Xie et al., 2016). Under carbon starvation, HXK is no more phosphorylated, and thus does not activate *bHLH3* (B). In addition, low T6P level removes the repression upon *MYB27*, resulting in lower anthocyanin accumulation, represented in paler tone. In addition, lower DELLA stability under low sucrose and its degradation mediated by GA releases its effect upon MYBL2 and JAZ repressors (Li et al., 2014). * Under a specific range of sucrose (under sucrose oversupply, this process is inhibited, possibly by T6P repression over SnRK1), SnRK1 induces the phosphorylation of JAZ18, promoting its degradation through the 26 proteasome. JAZ18 repression upon *bHLH3* (B) is removed, allowing the MBW complex to activate downstream biosynthetic genes for anthocyanin accumulation (Liu et al., 2017). ** No data are available about SnRK1 effect under sucrose starvation (shown in gray).

Ende, 2015; Zhang Y. et al., 2017; Wingler et al., 2020), its role in pigment accumulation during fruit ripening still remains to be determined.

Other studies outlined the effect of sugar treatment on the expression of structural genes of the flavonoid pathway. Using Gamay Red cell culture, Gollop et al. (2001, 2002); observed that the expression of *dihydroflavonol-4-reductase* and *leucoanthocyanidin dioxygenase*, two genes involved in anthocyanin pathway, were up-regulated by sucrose. Sugars were also able to increase transcript and proteins levels of flavanone 3-hydroxylase, a crucial enzyme regulating the bifurcation between the flavonol and anthocyanin branches within the flavonoid pathway (Zheng et al., 2009). In Barbera grape suspension cells, the up-regulation of different structural genes of the general phenylpropanoid pathway led to an increase in polyphenols, not restricted to the anthocyanin class, but including also other flavonoids, such as catechins, and stilbenes (Ferri et al., 2011).

Interestingly, sugar effect on pigment accumulation seems to be anthocyanin-specific, as suggested in intact Cabernet Sauvignon grape berries cultivated *in vitro* (Dai et al., 2014).

Red grape berries usually accumulate five different classes of anthocyanins, cyanidin and petunidin derivatives, which confer red colors and peonidin, delphinidin, and malvidin compounds, responsible for blue hues (Liang et al., 2008). Sixty days after starting the *in vitro* culture, the delphinidin- to cyanidin-derived compounds ratio increased concomitant with sucrose, glucose, or fructose concentration. This ratio is known to depend on berry developmental stage (Falginella et al., 2012) and on the ratio of expression of two enzymes, the flavonoid 3',5'-hydroxylase and the flavonoid 3'-hydroxylase, which drive metabolic fluxes toward delphinidin and cyanidin anthocyanins, respectively (Castellarin et al., 2006). Transcriptomic analysis pointed out that the ratio between the two enzymes, flavonoid 3',5'-hydroxylase/flavonoid 3'-hydroxylase, was increased by higher glucose concentration in the culture medium (Dai et al., 2014). Furthermore, *in vitro* berries transcriptomic analysis highlighted that anthocyanin content enhancement by sugars results from important changes in the expression of both regulatory and structural genes of the phenylpropanoid pathways by signal reprogramming. In particular, the expression of a putative *UDP-glucose:anthocyanin 3-O-glucosyltransferase*, was up-regulated and could play a key role in anthocyanin increase, also considered a major control point in the synthesis of these compounds (Boss et al., 1996; Dai et al., 2014).

Sugar's effect on anthocyanin regulation is not restricted to grape berries or apples. Indeed, carbon starvation in Zes006 red kiwifruit affected fruit development as well as anthocyanin concentration by affecting key structural genes of the anthocyanin pathway (Nardozza et al., 2020). Here, the authors proposed a model in which anthocyanin level modulation under carbon starvation involved trehalose-6 phosphate (**Figure 2**). Comparing anthocyanin and main sugar levels (sucrose, fructose, glucose, and sorbitol) in different varieties of apricot, a strong correlation was observed between both groups of compounds, but only in red-blushed varieties, which accumulates higher content of cyanidin derivatives (Huang et al., 2019). In Chinese bayberry fruits, a correlation between soluble sugars and anthocyanin levels were also observed in Dongkui and Biqi varieties (Shi et al., 2014). Zhao et al. (2017) identified a sucrose synthase gene, *FaSS1*, in Beinongxiang strawberry, which down-regulation led to a significant delay in fruit ripening, as well as a decrease in anthocyanin content. However, sucrose effect on anthocyanin accumulation do not appear to be universal among fruit-bearing species. Indeed, the immersion of pre- and postharvest bilberry fruits in glucose and sucrose solution (200 mM) did not induce anthocyanin biosynthesis (Karppinen et al., 2018).

As sucrose treatment has been recently proposed as a postharvest strategy to maintain fruit and vegetables quality traits, its effect (50, 270, and 500 mM) on strawberry was also evaluated (Li et al., 2019; Siebeneichler et al., 2020). While exogenous sucrose treatment increases internal glucose and fructose, the effect on pigment accumulation seems more anthocyanin-specific. Indeed, from the two main anthocyanin classes found in strawberry, only pelargonidin-derived compounds were increased, while no changes were observed in cyanidin-derived pigments (Li et al., 2019). This differential effect on anthocyanin content could be explained by the fact that exogenous sucrose application up-regulated the expression of all structural genes of the flavonoid pathway, with the exception of the *flavonoid 3'-hydroxylase*, which, as mentioned above, drive the metabolic flux to the synthesis of cyanidin-derived anthocyanins (Castellarin et al., 2006). However, the exact role of sucrose treatment in anthocyanin accumulation during fruit postharvest remains to be determined, as a function as mere metabolic substrate cannot be ruled out (Siebeneichler et al., 2020).

Carotenoids are another class of important pigments, which accumulate during fruit ripening and are responsible for the bright yellow and red tones of many ripe fruits, including tomato, watermelon or citrus (Sun et al., 2018). Carotenoids are tetraterpenoid compounds, which synthesis takes place through the methyleryhtritol 4-phosphate pathway (Eisenreich et al., 2004). Interestingly, they also provide precursors for ABA synthesis, and are essential components of the human diet (Sun et al., 2018). A first study in Okitsu mandarin outlined that sucrose supplementation in the peel accelerated the conversion of chloroplasts to chromoplasts, which characteristic is the massive accumulation of carotenoids, during citrus ripening, and thus promoting color break (Iglesias et al., 2001). Addition of ethylene, known to mediate chlorophyll degradation and thus color change, to sucrose-treated mandarin epicarps had no additive effect, therefore, it was suggested that both signaling molecules are components of the same pathway or share common transductor elements (Iglesias et al., 2001). The effect of exogenous sucrose on carotenoid accumulation was evaluated using mature green Aisla Craig tomato pericarp discs (Télef et al., 2006). Only lycopene and phytoene were enhanced under sucrose treatment, while no significant differences were observed in other carotenoids. However, it was also established that sucrose is not vital to induce carotenoid synthesis and requires ethylene signaling (Télef et al., 2006). Furthermore, upregulation of *phytoene synthase* (*PSY*) gene by sucrose, the enzyme catalyzing the first committed step of carotenoid synthesis, has been proposed to positively affect ABA levels, concomitant with the evidences discussed in the previous section (**Figure 3**; Falchi et al., 2013). PSY catalyzed the first committed step of carotenoid synthesis and is considered a major control point of the pathway. Télef et al. (2006) demonstrated that sugar treatment in tomato pericarp discs accelerated the accumulation of *PSY1* mRNA, while no effect was observed on other enzymes of the pathway. Mandarin, orange, and lemon juice sacs cultured *in vitro* also allowed to observe the promotion of carotenoid accumulation by sucrose treatment, and *PSY* upregulation (Zhang et al., 2012). However, the molecular mechanism by which sucrose regulates carotenoid metabolism at the transcriptional level is still unknown.

A recent study in watermelon established a possible molecular connection between sugar (glucose) signaling and carotenoid accumulation (Zhang J. et al., 2017). Indeed, a phosphate transporter, ClPHT4;2 was identified in chromoplast membranes, and which expression during fruit ripening was associated with carotenoid accumulation in the fruit flesh. *ClPHT4;2* expression is modulated by two bZIP TF, ClbZIP1 and ClbZIP2, which in turn are regulated both by sugar and ABA signaling pathways (**Figure 3**;

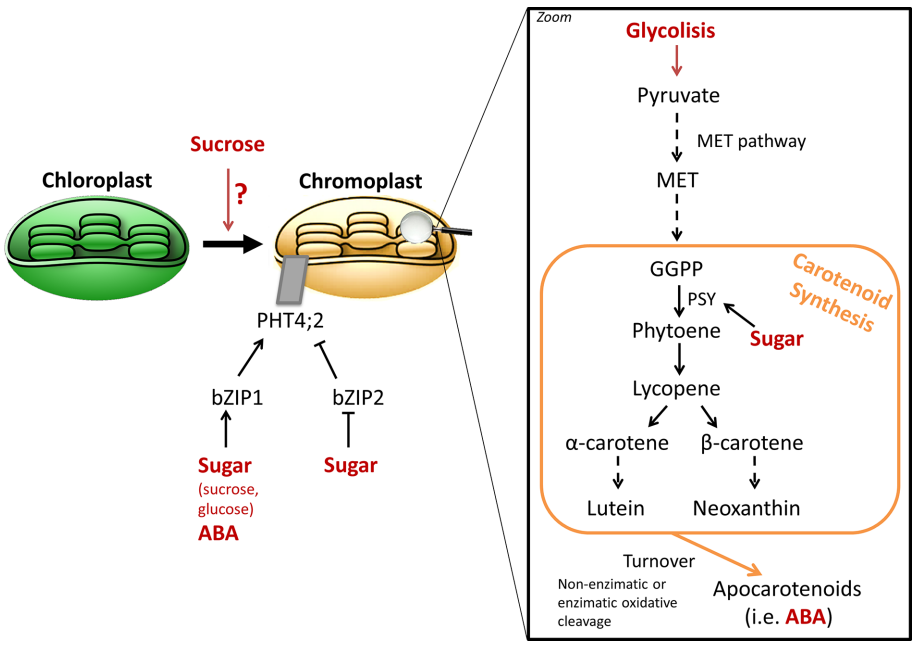

FIGURE 3 | General schema of sugar signaling in carotenoid synthesis. Several evidences highlight the relationship between sugar content and carotenogenesis (Zhang et al., 2017; Heng et al., 2019). While sucrose appears to be involved chromoplast differentiation (Iglesias et al., 2001; Fanciullino et al., 2014), the molecular cascade remains unknown. Modulation of *ClPHT4;2* expression through bZIP TF, which in turn are regulated by sugars and ABA, has been described to be involved in carotenoid accumulation during domesticated watermelon ripening (Zhang et al., 2017). While sugar catabolism can fuel carotenoid biosynthetic pathway by providing precursor building blocks through glycolysis, a regulating role over the pathway seems to exist, as demonstrated by the effect upon *phytoene synthase* (PSY) expression (Télef et al., 2006). In addition, sugar effect on carotenoid synthesis may also impact its crosstalk with ABA, as carotenoid turnover yields apocarotenoids, which serve as ABA precursors.

Zhang J. et al., 2017). In fact, the authors of the study proposed a model in which ABA and sugars increase *ClPHT4;2* expression by the binding of ClbZIP1 TF to motifs "ABA and osmotic stress response elements" present in the promotor sequence. On the opposite, the absence of these *cis*-elements in wild watermelon lines would not modulate *ClPHT4;2* expression, which remains low along ripening, and may explain the pale color of the non-domesticated watermelon accessions. This association between sugars, carotenoid, and *ClPHT4;2* gene expression is of particular interest, as it outlined a regulatory relation between carbohydrates and pigments during the evolution of domesticated watermelon from uncolored and non-sweet wild progenitors (Zhang J. et al., 2017; Ren et al., 2018).

A combination of proteomic and metabolomic approaches outlined that carotenogenesis ***in planta*** in banana pulp is associated with enhanced soluble sugar content and carbohydrate metabolism (Heng et al., 2019). On one hand, it cannot be ruled out that pigment accumulation is favored by sucrose degradation and a higher glycolytic activity to fuel the carotenoid biosynthetic pathway, as it has been observed in transgenic maize and golden rice (**Figure 3**; Decourcelle et al., 2015; Gayen et al., 2016). On the other hand, a plausible role for sugar signaling in plastid development and the integration of carbon and redox status, which in turn depends strongly on sugar metabolism, to regulate carotenoid synthesis was suggested by Fanciullino et al. (2014). However, the components of the signaling cascades linking sugars to plastid formation and carotenoid accumulation are still missing (Fanciullino et al., 2014; Heng et al., 2019).

SUGAR SIGNALING IS INVOLVED IN ABIOTIC AND BIOTIC STRESS RESPONSES DURING FRUIT DEVELOPMENT

During the last decades, consequences of global warming, *i.e.* increased abiotic stresses on plants, are challenging crop productivity (Rampino et al., 2012). In this sense, fruit and seed development involves key processes for global production, and those have been described to be particularly sensitive to heat or drought stresses. It known that abiotic stress during early reproductive organ formation leads to abnormal growth and fruit abortion (Thakur et al., 2010). Several evidence outlined the role of sugars as signaling molecules in abiotic stress responses in plant (Ruan et al., 2010; Ruan, 2012; Ruan, 2014). The little information available to date for sugar transduction pathways in responses to abiotic stresses during fruit development and ripening is reviewed in the next paragraphs.

Sucrose import to the fruit, together with invertase activity are especially susceptible to abiotic stresses; CWIN and VIN activities have been linked to ovary abortion under drought in maize (McLaughlin and Boyer, 2004). In Moneymaker tomato, RNAi-mediated silencing a flower and fruit specific CWIN gene, *LIN5*, had negative consequences on the reproductive organs, by

increasing fruit abortion, reducing fruit size and seed number per plant (Zanor et al., 2009). While the higher rate of fruit abortion has been directly correlated with low sucrose content in the ovary tissue in many species (McLaughlin and Boyer, 2004), the aberrant fruit phenotypes are probably the result of altered hormonal balance in the silenced tomato lines, as a consequence of the crosstalk between sugars and hormones (Zanor et al., 2009). On the opposite, silencing the expression of its inhibitor (*INVINH1*) leads to an enhanced CWIN activity, which in turn positively impacts fruit and seed development (Jin et al., 2009). Furthermore, increased CWIN activity through *INVINH1* silencing enhanced sucrose import and allowed to sustain tomato fruit set under long-term moderate heat stress (28/20°C, day/night) (Liu et al., 2016). CWIN protective effect was most likely achieved by providing energy for the synthesis of heat stress TFs and heat shock proteins, which are key mechanisms for heat tolerance, or by favoring auxin synthesis, a key hormone impacting fruit set. In addition, Liu et al. (2016) also corroborated that increased CWIN activity results in an inhibition of programmed cell death both under long-term moderate and short-term severe heat stresses, in an oxidative independent- and dependent-response, respectively. Interestingly, a recent study in XF-2 tomato plants suggests that high CWIN activity is also requires for cold tolerance. Indeed, *INVINH1* silencing results in enhanced chilling resistance (Xu et al., 2017).

By comparing CWIN, VIN, sugar import and sucrose synthase activities in heat-tolerant and heat-sensitive tomato lines under optimal (25°/20° day/night) and heat-stress conditions (5° above normal), Li et al. (2012) showed that not only CWIN (LIN7) but also VIN may be involved in heat tolerance in tomato reproductive organs, as their activities were higher in the former genotype young fruits. In addition, heat-tolerant plants showed a higher fruit to vegetative biomass ratio than susceptible lines, without significant changes in photosynthesis efficiency, suggesting that the former lines have a higher phloem import rate. Finally, and in agreement with the results obtained by CWIN overexpression (Liu et al., 2016), the expression of a *PLDa1*, a programmed cell death marker was found to be higher in the heat-sensible tomato plants, and could be related to invertase activities. Indeed, based on studies in maize (McLaughlin and Boyer, 2004; Boyer and McLaughlin, 2007), it is reasonable to hypothesize that the higher amounts of hexoses generated by invertase activity in heat-tolerant genotype can suppress the expression of *PLDa1*, and probably other programmed cell death-related genes (Li et al., 2012). Taken together, the results discussed here seem to confirm the role of invertases in connecting sugar signaling and fruit heat tolerance.

In addition, impairment of sugar metabolism in tomato is also observed under high salinity, resulting in decreased sink strength and activity, and thus fruit yield (Albacete et al., 2014). Heterologous overexpression of *CIN1*, a cell wall invertase gene, under the control of a putative fruit promotor was able to decrease the negative impact of salinity on yield, showing also altered hormonal levels (*i.e.* increased content of indole acetic acid [an auxin], *trans*-zeatin [a cytokinin], and ABA and decreased concentration of 1-aminocyclopropane-1-carboxylic acid, the precursor of ethylene). The interplay between CIN1 and hormones remains still to be further clarify, but it appears that it promotes fruit set by inducing cell division and expansion, and adjusts sink strength to sugar availability (Albacete et al., 2014).

Apart from the role of sucrose and hexoses described in heat stress responses, accumulation of the sugar alcohol galactinol was observed in Cabernet Sauvignon grape berries under heat stress (Pillet et al., 2012). As no induction of the raffinose family oligosaccharide pathway was observed, in which galactinol production is the first committed step, it was suggested that galactinol could act as a signal metabolite under grape heat stress, in order to trigger adaptive responses (Pillet et al., 2012).

Other hints towards the role of sugar signaling in abiotic or biotic fruit stress tolerance were found in the possible role of some SWEET transporters (Chen et al., 2010; Chong et al., 2014; Miao et al., 2017; Lu et al., 2019). The heterologous expression of apple *MdSWEET17* in Tianjinbaiguo tomato induced fructose accumulation in the fruits. Additionally, the resistance of the transgenic plants to drought was increased, suggesting that fructose signaling may be involved in stress tolerance (Lu et al., 2019). Interaction and co-expression network analysis outlined the strong transcriptional response of some SWEET transporters in early Baxi Jiao banana fruit development and under abiotic/biotic stresses, suggesting an enhanced sugar transport under environmental pressure (Miao et al., 2017).

Sugar signaling seems to be also affected under biotic stress, as described in grape berries (Vega et al., 2011; Chong et al., 2014). Glucose transporter *VvSWEET4* is strongly induced in response to the necrotrophic fungus *Botrytris cinerea* (Chong et al., 2014). While a possible explanation of this up-regulation would be the manipulation of the host resources, *i.e.* sugars, by the pathogen, an alternative hypothesis would be the possible function of VvSWEET4 in plant cell death. Indeed, *Arabidopsis* mutants for *SWEET4* were found to be more resistant to *B. cinerea* and to show reduced cell death, which is required by the fungus to infect the host (van Kan, 2006). In Cabernet Sauvignon berries infected with Grapevine leaf-roll-associated virus-3, the expression of genes implicated in sugar metabolism and transport was decreased, concomitant with reduced accumulation of fructose and glucose. Possibly as a consequence of sugar content decrease, the infection by the virus also induced a reduction in anthocyanin content and in the transcript levels of several structural and regulatory genes of the anthocyanin pathway (Vega et al., 2011).

CONCLUSION

Carbohydrates are the main components of plant tissues, being needed both for their structural role and energy obtaining. However, very little is still known about the transduction pathways which convert them into signaling molecules, allowing the plant to monitor sugar status to optimize growth and development, including fruit set and ripening. Here we reviewed the role of sugars, alone or in a crosstalk with hormone signaling pathway, in controlling important events in fruit ripening, such as the accumulation of health-promoting pigments. Furthermore, we highlighted the need for a deeper understanding of the regulatory mechanisms underlying sugar and hormone connection in controlling fruit set, growth, and

ripening, as this will permit to have a better control on crop yield and productivity, an urgent issue due to overpopulation and global warming.

AUTHOR CONTRIBUTIONS

All authors contributed to the article and approved the submitted version.

FUNDING

This work was supported through grants RTI2018-099797-B-100 (Ministerio de Ciencia, Innovación y Universidades, Spain) and UMA18-FEDERJA-179 (FEDER-Junta Andalucía). In addition, we acknowledge partial funding by the European Union's H2020 Programme (GoodBerry; grant number 679303). SD-S and SO acknowledge the support by Plan Propio from University of Malaga.

REFERENCES

Afoufa-Bastien, D., Medici, A., Jeauffre, J., Coutos-Thévenot, P., Lemoine, R., Atanassova, R., et al. (2010). The Vitis vinifera sugar transporter gene family: Phylogenetic overview and macroarray expression profiling. *BMC Plant Biol.* 10:245. doi: 10.1186/1471-2229-10-245

Albacete, A., Cantero-Navarro, E., Balibrea, M. E., Großkinsky, D. K., De La Cruz González, M., Martínez-Andújar, C., et al. (2014). Hormonal and metabolic regulation of tomato fruit sink activity and yield under salinity. *J. Exp. Bot.* 65, 6081–6095. doi: 10.1093/jxb/eru347

Aluri, S., and Büttner, M. (2007). Identification and functional expression of the Arabidopsis thaliana vacuolar glucose transporter 1 and its role in seed germination and flowering. *Proc. Natl. Acad. Sci. U. S. A.* 104, 2537–2542. doi: 10.1073/pnas.0610278104

Atanassova, R., Leterrier, M., Gaillard, C., Agasse, A., Sagot, E., Coutos-Thévenot, P., et al. (2003). Sugar-regulated expression of a putative hexose transport gene in grape. *Plant Physiol.* 131, 326–334. doi: 10.1104/pp.009522

Baena-González, E., Rolland, F., Thevelein, J. M., and Sheen, J. (2007). A central integrator of transcription networks in plant stress and energy signalling. *Nature* 448, 938–942. doi: 10.1038/nature06069

Barker, L., Kühn, C., Weise, A., Schulz, A., Gebhardt, C., Hirner, B., et al. (2000). SUT2, a putative sucrose sensor in sieve elements. *Plant Cell* 12, 1153–1164. doi: 10.1105/tpc.12.7.1153

Baxter, C. J., Carrari, F., Bauke, A., Overy, S., Hill, S. A., Quick, P. W., et al. (2005). Fruit carbohydrate metabolism in an introgression line of tomato with increased fruit soluble solids. *Plant Cell Physiol.* 46, 425–437. doi: 10.1093/pcp/pci040

Boldingh, H., Richardson, A., Minchin, P., and MacRae, E. (2015). Planteose is a major sugar translocated in Actinidia arguta "Hortgem Tahi." *Sci. Hortic. (Amsterdam).* 193, 261–268. doi: 10.1016/j.scienta.2015.07.009

Borisjuk, L., Walenta, S., Rolletschek, H., Mueller-Klieser, W., Wobus, U., and Weber, H. (2002). Spatial analysis of plant metabolism: Sucrose imaging within Vicia faba cotyledons reveals specific developmental patterns. *Plant J.* 29, 521–530. doi: 10.1046/j.1365-313x.2002.01222.x

Borisjuk, L., Rolletschek, H., Wobus, U., and Weber, H. (2003). Differentiation of legume cotyledons as related to metabolic gradients and assimilate transport into seeds. *J. Exp. Bot.* 54, 503–512. doi: 10.1093/jxb/erg051

Boss, P. K., Davies, C., and Robinson, S. P. (1996). Analysis of the expression of anthocyanin pathway genes. *Plant Physiol.* 111, 1059–1066. doi: 10.1104/pp.111.4.1059

Boyer, J. S., and McLaughlin, J. E. (2007). Functional reversion to identify controlling genes in multigenic responses: Analysis of floral abortion. *J. Exp. Bot.* 58, 267–277. doi: 10.1093/jxb/erl177

Braun, D. M., Wang, L., and Ruan, Y. L. (2014). Understanding and manipulating sucrose phloem loading, unloading, metabolism, and signalling to enhance crop yield and food security. *J. Exp. Bot.* 65, 1713–1735. doi: 10.1093/jxb/ert416

Çakir, B., Agasse, A., Gaillard, C., Saumonneau, A., Delrot, S., and Atanassova, R. (2003). A grape ASR protein involved in sugar and abscisic acid signaling. *Plant Cell* 15, 2165–2180. doi: 10.1105/tpc.013854

Canel, C., Bailey-Serres, J. N., and Roose, M. L. (1995). Pummelo fruit transcript homologous to ripening-induced genes. *Plant Physiol.* 108, 1323–1324. doi: 10.1104/pp.108.3.1323

Castellarin, S. D., Di Gaspero, G., Marconi, R., Nonis, A., Peterlunger, E., Paillard, S., et al. (2006). Colour variation in red grapevines (Vitis vinifera L.): Genomic organisation, expression of flavonoid 3′-hydroxylase, flavonoid 3′,5′-hydroxylase genes and related metabolite profiling of red cyanidin-/blue delphinidin-based anthocyanins in berry skin. *BMC Genomics* 7, 1–17. doi: 10.1186/1471-2164-7-12

Chambers, J. K., Macdonald, L. E., Sarau, H. M., Ames, R. S., Freeman, K., Foley, J. J., et al. (2000). A G protein-coupled receptor for UDP-glucose. *J. Biol. Chem.* 275, 10767–10771. doi: 10.1074/jbc.275.15.10767

Chen, L. Q., Hou, B. H., Lalonde, S., Takanaga, H., Hartung, M. L., Qu, X. Q., et al. (2010). Sugar transporters for intercellular exchange and nutrition of pathogens. *Nature* 468, 527–532. doi: 10.1038/nature09606

Chen, J., Liu, D.j., Jiang, Y.m., Zhao, M.l., Shan, W., Kuang, J.f., et al. (2011). Molecular characterization of a strawberry faasr gene in relation to fruit ripening. *PloS One* 6, e24649. doi: 10.1371/journal.pone.0024649

Chen, L.-Q., Qu, X.-Q., Hou, B.-H., Sosso, D., Osorio, S., Fernie, A. R., et al. (2012). Sucrose efflux mediated by SWEET proteins as a key step for phloem transport. *Science* 335, 207–211. doi: 10.1126/science.1213351

Chen, Y., Grimplet, J., David, K., Castellarin, S. D., Terol, J., Wong, D. C. J., et al. (2018). Ethylene receptors and related proteins in climacteric and non-climacteric fruits. *Plant Sci.* 276, 63–72. doi: 10.1016/j.plantsci.2018.07.012

Cheng, J., Wen, S., Xiao, S., Lu, B., Ma, M., and Bie, Z. (2018). Overexpression of the tonoplast sugar transporter CmTST2 in melon fruit increases sugar accumulation. *J. Exp. Bot.* 69, 511–523. doi: 10.1093/jxb/erx440

Cherian, S., Figueroa, C. R., and Nair, H. (2014).). "Movers and shakers" in the regulation of fruit ripening: A cross-dissection of climacteric versus non-climacteric fruit. *J. Exp. Bot.* 65, 4705–4722. doi: 10.1093/jxb/eru280

Chervin, C., El-Kereamy, A., Roustan, J. P., Latché, A., Lamon, J., and Bouzayen, M. (2004). Ethylene seems required for the berry development and ripening in grape, a non-climacteric fruit. *Plant Sci.* 167, 1301–1305. doi: 10.1016/j.plantsci.2004.06.026

Chervin, C., Terrier, N., Ageorges, A., Ribes, F., and Kuapunyakoon, T. (2006). Influence of ethylene on sucrose accumulation in grape berry. *Am. J. Enol. Vitic.* 57, 511–513.

Cho, Y. H., Yoo, S. D., and Sheen, J. (2006). Regulatory Functions of nuclear hexokinase1 complex in glucose signaling. *Cell* 127, 579–589. doi: 10.1016/j.cell.2006.09.028

Chong, J., Piron, M. C., Meyer, S., Merdinoglu, D., Bertsch, C., and Mestre, P. (2014). The SWEET family of sugar transporters in grapevine: *VvSWEET4* is involved in the interaction with *Botrytis cinerea*. *J. Exp. Bot.* 65, 6589–6601. doi: 10.1093/jxb/eru375

Choudhury, S. R., Roy, S., and Sengupta, D. N. (2009). A comparative study of cultivar differences in sucrose phosphate synthase gene expression and sucrose formation during banana fruit ripening. *Postharvest Biol. Technol.* 54, 15–24. doi: 10.1016/j.postharvbio.2009.05.003

Ciereszko, I., Johansson, H., and Kleczkowski, L. A. (2001). Sucrose and light regulation of a cold-inducible UDP-glucose pyrophosphorylase gene via a hexokinase-independent and abscisic acid-insensitive pathway in Arabidopsis. *Biochem. J.* 354, 67–72. doi: 10.1042/0264-6021:3540067

Dai, Z. W., Léon, C., Feil, R., Lunn, J. E., Delrot, S., and Gomès, E. (2013). Metabolic profiling reveals coordinated switches in primary carbohydrate metabolism in grape berry (*Vitis vinifera* L.), a non-climacteric fleshy fruit. *J. Exp. Bot.* 64, 1345–1355. doi: 10.1093/jxb/ers396

Dai, Z. W., Meddar, M., Renaud, C., Merlin, I., Hilbert, G., Delro, S., et al. (2014). Long-term in vitro culture of grape berries and its application to assess the effects of sugar supply on anthocyanin accumulation. *J. Exp. Bot.* 65, 4665–4677. doi: 10.1093/jxb/ert489

Debast, S., Nunes-Nesi, A., Hajirezaei, M. R., Hofmann, J., Sonnewald, U., Fernie, A. R., et al. (2011). Altering trehalose-6-phosphate content in transgenic potato tubers affects tuber growth and alters responsiveness to hormones during sprouting. *Plant Physiol.* 156, 1754–1771. doi: 10.1104/pp.111.179903

Decourcelle, M., Perez-fons, L., Baulande, S., Steiger, S., Couvelard, L., Hem, S., et al. (2015). Combined transcript , proteome , and metabolite analysis of transgenic maize seeds engineered for enhanced carotenoid synthesis reveals pleotropic effects in core metabolism. *J. Exp. Bot.* 66, 3141–3150. doi: 10.1093/jxb/erv120

Delatte, T. L., Sedijani, P., Kondou, Y., Matsui, M., de Jong, G. J., Somsen, G. W., et al. (2011). Growth arrest by trehalose-6-phosphate: An astonishing case of primary metabolite control over growth by way of the SnRK1 signaling pathway. *Plant Physiol.* 157, 160–174. doi: 10.1104/pp.111.180422

Deluc, L. G., Grimplet, J., Wheatley, M. D., Tillett, R. L., Quilici, D. R., Osborne, C., et al. (2007). Transcriptomic and metabolite analyses of Cabernet Sauvignon grape berry development. *BMC Genomics* 8, 1–42. doi: 10.1186/1471-2164-8-429

Eisenreich, W., Bacher, A., Arigoni, D., and Rohdich, F. (2004). Biosynthesis of isoprenoids via the non-mevalonate pathway. *Cell. Mol. Life Sci.* 61, 1401–1426. doi: 10.1007/s00018-004-3381-z

Emanuelle, S., Doblin, M. S., Stapleton, D.II, Bacic, A., and Gooley, P. R. (2016). Molecular insights into the enigmatic metabolic regulator, SnRK1. *Trends Plant Sci.* 21, 341–353. doi: 10.1016/j.tplants.2015.11.001

Eveland, A. L., and Jackson, D. P. (2012). Sugars, signalling, and plant development. *J. Exp. Bot.* 63, 3367–3377. doi: 10.1093/jxb/err379

Falchi, R., Zanon, L., De Marco, F., Nonis, A., Pfeiffer, A., and Vizzotto, G. (2013). Tissue-specific and developmental expression pattern of abscisic acid biosynthetic genes in peach fruit: Possible role of the hormone in the coordinated growth of seed and mesocarp. *J. Plant Growth Regul.* 32, 519–532. doi: 10.1007/s00344-013-9318-8

Falginella, L., Di Gaspero, G., and Castellarin, S. D. (2012). Expression of flavonoid genes in the red grape berry of "Alicante Bouschet" varies with the histological distribution of anthocyanins and their chemical composition. *Planta* 236, 1037–1051. doi: 10.1007/s00425-012-1658-2

Fan, R. C., Peng, C. C., Xu, Y. H., Wang, X. F., Li, Y., Shang, Y., et al. (2009). Apple sucrose transporter SUT1 and sorbitol transporter SOT6 interact with cytochrome b5 to regulate their affinity for substrate sugars. *Plant Physiol.* 150, 1880–1901. doi: 10.1104/pp.109.141374

Fanciullino, A. L., Bidel, L. P. R., and Urban, L. (2014). Carotenoid responses to environmental stimuli: Integrating redox and carbon controls into a fruit model. *Plant Cell Environ.* 37, 273–289. doi: 10.1111/pce.12153

Farcuh, M., Rivero, R. M., Sadka, A., and Blumwald, E. (2018). Ethylene regulation of sugar metabolism in climacteric and non-climacteric plums. *Postharvest Biol. Technol.* 139, 20–30. doi: 10.1016/j.postharvbio.2018.01.012

Fei, L., Yuan, X., Chen, C., Wan, C., Fu, Y., Chen, J., et al. (2020). Exogenous application of sucrose promotes postharvest ripening of kiwifruit. *Agronomy* 10:245. doi: 10.3390/agronomy10020245

Ferri, M., Righetti, L., and Tassoni, A. (2011). Increasing sucrose concentrations promote phenylpropanoid biosynthesis in grapevine cell cultures. *J. Plant Physiol.* 168, 189–195. doi: 10.1016/j.jplph.2010.06.027

Figueroa, C. M., and Lunn, J. E. (2016). A tale of two sugars: Trehalose 6-phosphate and sucrose. *Plant Physiol.* 172, 7–27. doi: 10.1104/pp.16.00417

Fraser, C. M., and Chapple, C. (2011). The phenylpropanoid pathway in Arabidopsis. *Arab. B.* 9, e0152. doi: 10.1199/tab.0152

Fridman, E., Carrari, F., Sheng, Y., Fernie, A., and Zamir, D. (2004). Zooming in on a quantitative trait for tomato yield using interspecific introgressions. *Science* 305, 1786–1789. doi: 10.1126/science.1101666

Gambetta, G. A., Matthews, M. A., Shaghasi, T. H., McElrone, A. J., and Castellarin, S. D. (2010). Sugar and abscisic acid signaling orthologs are activated at the onset of ripening in grape. *Planta* 232, 219–234. doi: 10.1007/s00425-010-1165-2

Gaxiola, R. A., Palmgren, M. G., and Schumacher, K. (2007). Plant proton pumps. *FEBS Lett.* 581, 2204–2214. doi: 10.1016/j.febslet.2007.03.050

Gayen, D., Ghosh, S., Paul, S., Sarkar, S. N., Datta, S. K., and Datta, K. (2016). Metabolic regulation of carotenoid-enriched golden rice line. *Front. Plant Sci.* 7:1622. doi: 10.3389/fpls.2016.01622

Giampieri, F., Forbes-Hernandez, T. Y., Gasparrini, M., Alvarez-Suarez, J. M., Afrin, S., Bompadre, S., et al. (2015). Strawberry as a health promoter: an evidence based review. *Food Funct.* 6, 1386–1398. doi: 10.1039/c5fo00147a

Giovannoni, J. J. (2007). Fruit ripening mutants yield insights into ripening control. *Curr. Opin. Plant Biol.* 10, 283–289. doi: 10.1016/j.pbi.2007.04.008

Gollop, R., Farhi, S., and Perl, A. (2001). Regulation of the leucoanthocyanidin dioxygenase gene expression in vitis vinifera. *Plant Sci.* 161, 579–588. doi: 10.1016/S0168-9452(01)00445-9

Gollop, R., Even, S., Colova-Tsolova, V., and Perl, A. (2002). Expression of the grape dihydroflavonol reductase gene and analysis of its promoter region. *J. Exp. Bot.* 53, 1397–1409. doi: 10.1093/jxb/53.373.1397

Grierson, C., Du, J.-S., De Torres Zabala, M., Beggs, K., Smith, C., Holdsworth, M., et al. (1994). Separate cis sequences and trans factors direct metabolic and developmental regulation of a potato tuber storage protein gene. *Plant J.* 5, 815–826. doi: 10.1046/j.1365-313X.1994.5060815.x

Guan, Y., Ren, H., Xie, H., Ma, Z., and Chen, F. (2009). Identification and characterization of bZIP-type transcription factors involved in carrot (Daucus carota L.) somatic embryogenesis. *Plant J.* 60, 207–217. doi: 10.1111/j.1365-313X.2009.03948.x

Hackel, A., Schauer, N., Carrari, F., Fernie, A. R., Grimm, B., and Kühn, C. (2006). Sucrose transporter LeSUT1 and LeSUT2 inhibition affects tomato fruit development in different ways. *Plant J.* 45, 180–192. doi: 10.1111/j.1365-313X.2005.02572.x

Harden, T. K., Sesma, J.II, Fricks, I. P., and Lazarowski, E. R. (2010). Signalling and pharmacological properties of the P2Y14 receptor. *Acta Physiol.* 199, 149–160. doi: 10.1111/j.1748-1716.2010.02116.x

Hassan, S., and Mathesius, U. (2012). The role of flavonoids in root-rhizosphere signalling: Opportunities and challenges for improving plant-microbe interactions. *J. Exp. Bot.* 63, 3429–3444. doi: 10.1093/jxb/err430

Hedrich, R., Sauer, N., and Neuhaus, H. E. (2015). Sugar transport across the plant vacuolar membrane: Nature and regulation of carrier proteins. *Curr. Opin. Plant Biol.* 25, 63–70. doi: 10.1016/j.pbi.2015.04.008

Heng, Z., Sheng, O., Huang, W., Zhang, S., Fernie, A. R., Motorykin, I., et al. (2019). Integrated proteomic and metabolomic analysis suggests high rates of glycolysis are likely required to support high carotenoid accumulation in banana pulp. *Food Chem.* 297:125016. doi: 10.1016/j.foodchem.2019.125016

Hu, D. G., Sun, C. H., Zhang, Q. Y., An, J. P., You, C. X., and Hao, Y. J. (2016). Glucose sensor MdHXK1 phosphorylates and stabilizes MdbHLH3 to promote anthocyanin biosynthesis in apple. *PloS Genet.* 12, 1–27. doi: 10.1371/journal.pgen.1006273

Huang, H., Xie, S., Xiao, Q., Wei, B., Zheng, L., Wang, Y., et al. (2016). Sucrose and ABA regulate starch biosynthesis in maize through a novel transcription factor, ZmEREB156. *Sci. Rep.* 10:27590. doi: 10.1038/srep27590

Huang, Z., Wang, Q., Xia, L., Hui, J., Li, J., Feng, Y., et al. (2019). Preliminarily exploring of the association between sugars and anthocyanin accumulation in apricot fruit during ripening. *Sci. Hortic. (Amsterdam).* 248, 112–117. doi: 10.1016/j.scienta.2019.01.012

Hummel, M., Rahmani, F., Smeekens, S., and Hanson, J. (2009). Sucrose-mediated translational control. *Ann. Bot.* 104, 1–7. doi: 10.1093/aob/mcp086

Iglesias, D. J., Tadeo, F. R., Legaz, F., Primo-Millo, E., and Talon, M. (2001). In vivo sucrose stimulation of colour change in citrus fruit epicarps: Interactions between nutritional and hormonal signals. *Physiol. Plant* 112, 244–250. doi: 10.1034/j.1399-3054.2001.1120213.x

Iusem, N. D., Bartholomew, D. M., Hitz, W. D., and Scolnik, P. A. (1993). Tomato (*Lycopersicon esculentum*) transcript induced by water deficit and ripening. *Plant Physiol.* 102, 1353–1354. doi: 10.1104/pp.102.4.1353

Janse van Rensburg, H. C., and Van den Ende, W. (2018). UDP-glucose: A potential signaling molecule in plants? *Front. Plant Sci.* 8, 2230. doi: 10.3389/fpls.2017.02230

Jeena, G. S., Kumar, S., and Shukla, R. K. (2019). Structure, evolution and diverse physiological roles of SWEET sugar transporters in plants. *Plant Mol. Biol.* 100, 351–365. doi: 10.1007/s11103-019-00872-4

Jefferson, R., Goldsbrough, A., and Bevan, M. (1990). Transcriptional regulation of a patatin-1 gene in potato. *Plant Mol. Biol.* 14, 995–1006. doi: 10.1007/BF00019396

Jia, H.-F., Chai, Y.-M., Li, C.-L., Lu, D., Luo, J.-J., Qin, L., et al. (2011). Abscisic acid plays an important role in the regulation of strawberry fruit ripening. *Plant Physiol.* 157, 188–199. doi: 10.1104/pp.111.177311

Jia, H., Wang, Y., Sun, M., Li, B., Han, Y., Zhao, Y., et al. (2013). Sucrose functions as a signal involved in the regulation of strawberry fruit development and ripening. *New Phytol.* 198, 453–465. doi: 10.1111/nph.12176

Jia, H., Jiu, S., Zhang, C., Wang, C., Tariq, P., Liu, Z., et al. (2016). Abscisic acid and sucrose regulate tomato and strawberry fruit ripening through the abscisic

acid-stress-ripening transcription factor. *Plant Biotechnol. J.* 14, 2045–2065. doi: 10.1111/pbi.12563

Jia, H., Xie, Z., Wang, C., Shangguan, L., Qian, N., Cui, M., et al. (2017). Abscisic acid, sucrose, and auxin coordinately regulate berry ripening process of the Fujiminori grape. *Funct. Integr. Genomics* 17, 441–457. doi: 10.1007/s10142-017-0546-z

Jiaxing, W., Feng, H., Weibing, J., and Haoming, C. (2018). Functional analysis of abscisic acid-stress ripening transcription factor in *Prunus persica* f. atropurpurea. *J. Plant Growth Regul.* 37, 85–100. doi: 10.1007/s00344-017-9695-5

Jin, Y., Ni, D. A., and Ruan, Y. L. (2009). Posttranslational elevation of cell wall invertase activity by silencing its inhibitor in tomato delays leaf senescence and increases seed weight and fruit hexose Level. *Plant Cell* 21, 2072–2089. doi: 10.1105/tpc.108.063719

Julius, B. T., Leach, K. A., Tran, T. M., Mertz, R. A., and Braun, D. M. (2017). Sugar transporters in plants: New insights and discoveries. *Plant Cell Physiol.* 58, 1442–1460. doi: 10.1093/pcp/pcx090

Kanayama, Y. (2017). Sugar metabolism and fruit development in the tomato. *Hortic. J.* 86, 417–425. doi: 10.2503/hortj.OKD-IR01

Karppinen, K., Tegelberg, P., Häggman, H., and Jaakola, L. (2018). Abscisic acid regulates anthocyanin biosynthesis and gene expression associated with cell wall modification in ripening bilberry (vaccinium myrtillus l.) fruits. *Front. Plant Sci.* 9, 1259. doi: 10.3389/fpls.2018.01259

Koch, K. E. (1996). Carbohydrate-modulated gene expression in plants. *Annu. Rev. Plant Physiol. Plant Mol. Biol.* 47, 509–540. doi: 10.1146/annurev.arplant.47.1.509

Kolbe, A., Tiessen, A., Schluepmann, H., Paul, M., Ulrich, S., and Geigenberger, P. (2005). Trehalose 6-phosphate regulates starch synthesis via posttranslational redox activation of ADP-glucose pyrophosphorylase. *Proc. Natl. Acad. Sci. U. S. A.* 102, 11118–11123. doi: 10.1073/pnas.0503410102

Kondo, S., Tomiyama, A., and Seto, H. (2000). Changes of endogenous jasmonic acid and methyl jasmonate in apples and sweet cherries during fruit development. *J. Am. Soc Hortic. Sci.* 125, 282–287. doi: 10.21273/jashs.125.3.282

Kretzschmar, T., Pelayo, M. A. F., Trijatmiko, K. R., Gabunada, L. F. M., Alam, R., Jimenez, R., et al. (2015). A trehalose-6-phosphate phosphatase enhances anaerobic germination tolerance in rice. *Nat. Plants* 1, 1–5. doi: 10.1038/nplants.2015.124

Krüger, A., Grüning, N. M., Wamelink, M. M. C., Kerick, M., Kirpy, A., Parkhomchuk, D., et al. (2011). The pentose phosphate pathway is a metabolic redox sensor and regulates transcription during the antioxidant response. *Antioxid. Redox Signal.* 15, 311–324. doi: 10.1089/ars.2010.3797

Larronde, F., Krisa, S., Decendit, A., Chèze, C., Deffieux, G., and Mérillon, J. M. (1998). Regulation of polyphenol production in Vitis vinifera cell suspension cultures by sugars. *Plant Cell Rep.* 17, 946–950. doi: 10.1007/s002990050515

Lazarowski, E. R., and Harden, T. K. (2015). UDP-sugars as extracellular signaling molecules: Cellular and physiologic consequences of P2Y14 receptor activation. *Mol. Pharmacol.* 88, 151–160. doi: 10.1124/mol.115.098756

Lecourieux, F., Lecourieux, D., Vignault, C., and Delrot, S. (2010). A sugar-inducible protein kinase, VvSK1, regulates hexose transport and sugar accumulation in grapevine cells. *Plant Physiol.* 152, 1096–1106. doi: 10.1104/pp.109.149138

Lecourieux, F., Kappel, C., Lecourieux, D., Serrano, A., Torres, E., Arce-Johnson, P., et al. (2014). An update on sugar transport and signalling in grapevine. *J. Exp. Bot.* 65, 821–832. doi: 10.1093/jxb/ert394

Lemoine, R., La Camera, S., Atanassova, R., Dédaldéchamp, F., Allario, T., Pourtau, N., et al. (2013). Source-to-sink transport of sugar and regulation by environmental factors. *Front. Plant Sci.* 4:272. doi: 10.3389/fpls.2013.00272

Li, X., Xing, J., Gianfagna, T. J., and Janes, H. W. (2002). Sucrose regulation of ADP-glucose pyrophosphorylase subunit genes transcript levels in leaves and fruits. *Plant Sci.* 162, 239–244. doi: 10.1016/S0168-9452(01)00565-9

Li, Z., Palmer, W. M., Martin, A. P., Wang, R., Rainsford, F., Jin, Y., et al. (2012). High invertase activity in tomato reproductive organs correlates with enhanced sucrose import into, and heat tolerance of, young fruit. *J. Exp. Bot.* 63, 1155–1166. doi: 10.1093/jxb/err329

Li, Y., Van Den Ende, W., and Rolland, F. (2014). Sucrose induction of anthocyanin biosynthesis is mediated by DELLA. *Mol. Plant* 7, 570–572. doi: 10.1093/mp/sst161

Li, D., Mou, W., Wang, Y., Li, L., Mao, L., Ying, T., et al. (2016). Exogenous sucrose treatment accelerates postharvest tomato fruit ripening through the influence on its metabolism and enhancing ethylene biosynthesis and signaling. *Acta Physiol. Plant* 38, 225. doi: 10.1007/s11738-016-2240-5

Li, D., Zhang, X., Xu, Y., Li, L., Aghdam, M. S., and Luo, Z. (2019). Effect of exogenous sucrose on anthocyanin synthesis in postharvest strawberry fruit. *Food Chem.* 289, 112–120. doi: 10.1016/j.foodchem.2019.03.042

Liang, Z., Wu, B., Fan, P., Yang, C., Duan, W., Zheng, X., et al. (2008). Anthocyanin composition and content in grape berry skin in Vitis germplasm. *Food Chem.* 111, 837–844. doi: 10.1016/j.foodchem.2008.04.069

Lindo-García, V., Muñoz, P., Larrigaudière, C., Munné-Bosch, S., and Giné-Bordonaba, J. (2020). Interplay between hormones and assimilates during pear development and ripening and its relationship with the fruit postharvest behaviour. *Plant Sci.* 291, 110339. doi: 10.1016/j.plantsci.2019.110339

Liu, Y. H., Offler, C. E., and Ruan, Y. L. (2013). Regulation of fruit and seed response to heat and drought by sugars as nutrients and signals. *Front. Plant Sci.* 4:282. doi: 10.3389/fpls.2013.00282

Liu, Y. H., Offler, C. E., and Ruan, Y. L. (2016). Cell wall invertase promotes fruit set under heat stress by suppressing ROS-independent cell death. *Plant Physiol.* 172, 163–180. doi: 10.1104/pp.16.00959

Liu, X. J., An, X. H., Liu, X., Hu, D. G., Wang, X. F., You, C. X., et al. (2017). MdSnRK1.1 interacts with MdJAZ18 to regulate sucrose-induced anthocyanin and proanthocyanidin accumulation in apple. *J. Exp. Bot.* 68, 2977–2990. doi: 10.1093/jxb/erx150

Lloyd, J. C., and Zakhleniuk, O. V. (2004). Responses of primary and secondary metabolism to sugar accumulation revealed by microarray expression analysis of the Arabidopsis mutant, pho3. *J. Exp. Bot.* 55, 1221–1230. doi: 10.1093/jxb/erh143

Lombardo, V. A., Osorio, S., Borsani, J., Lauxmann, M. A., Bustamante, C. A., Budde, C. O., et al. (2011). Metabolic profiling during peach fruit development and ripening reveals the metabolic networks that underpin each developmental stage. *Plant Physiol.* 157, 1696–1710. doi: 10.1104/pp.111.186064

Lu, J., Sun, M.h., Ma, Q.j., Kang, H., Liu, Y.j., Hao, Y.j., et al. (2019). MdSWEET17, a sugar transporter in apple, enhances drought tolerance in tomato. *J. Integr. Agric.* 18, 2041–2051. doi: 10.1016/S2095-3119(19)62695-X

Luo, Y., Lin, Y., Mo, F., Ge, C., Jiang, L., Zhang, Y., et al. (2019). Sucrose promotes strawberry fruit ripening and affects ripening-related processes. *Int. J. Genomics* 2019. doi: 10.1155/2019/9203057

Luo, J., Peng, F., Zhang, S., Xiao, Y., and Zhang, Y. (2020). The protein kinase FaSnRK1α regulates sucrose accumulation in strawberry fruits. *Plant Physiol. Biochem.* 151, 369–377. doi: 10.1016/j.plaphy.2020.03.044

Luo, Y., Ge, C., Ling, Y., Mo, F., Yang, M., Jiang, L., et al. (2020). ABA and sucrose co-regulate strawberry fruit ripening and show inhibition of glycolysis. *Mol. Genet. Genomics* 295, 421–438. doi: 10.1007/s00438-019-01629-w

Ma, Q. J., Sun, M. H., Lu, J., Liu, Y. J., Hu, D. G., and Hao, Y. J. (2017). Transcription factor AREB2 is involved in soluble sugar accumulation by activating sugar transporter and amylase genes1. *Plant Physiol.* 174, 2348–2362. doi: 10.1104/pp.17.00502

Ma, Q. J., Sun, M. H., Lu, J., Kang, H., You, C. X., and Hao, Y. J. (2019). An apple sucrose transporter MdSUT2.2 is a phosphorylation target for protein kinase MdCIPK22 in response to drought. *Plant Biotechnol. J.* 17, 625–637. doi: 10.1111/pbi.13003

Maas, C., Schaal, S., and Werr, W. (1990). A feedback control element near the transcription start site of the maize Shrunken gene determines promoter activity. *EMBO J.* 9, 3447–3452. doi: 10.1002/j.1460-2075.1990.tb07552.x

Martínez-Barajas, E., Delatte, T., Schluepmann, H., de Jong, G. J., Somsen, G. W., Nunes, C., et al. (2011). Wheat grain development is characterized by remarkable trehalose 6-phosphate accumulation pregrain filling: Tissue distribution and relationship to SNF1-related protein kinase1 activity. *Plant Physiol.* 156, 373–381. doi: 10.1104/pp.111.174524

Mbeguie-A-Mbeguie, D., Gomez, R.-M., and Fils-Lycaon, B. (1997). Molecular cloning and nucleotide sequence of a protein from apricot fruit (accession No. U82760) homologous to LEC14B protein isolated from Lithospermum gene expression during fruit ripening (PGR 97– 161). *Plant Physiol.* 115, 1287–1289. doi: 10.1104/pp.115.3.1287

McLaughlin, J. E., and Boyer, J. S. (2004). Sugar-responsive gene expression, invertase activity, and senescence in aborting maize ovaries at low water potentials. *Ann. Bot.* 94, 675–689. doi: 10.1093/aob/mch193

Medina-Puche, L., Blanco-Portales, R., Molina-Hidalgo, F. J., Cumplido-Laso, G., García-Caparrós, N., Moyano-Cañete, E., et al. (2016). Extensive transcriptomic studies on the roles played by abscisic acid and auxins in the development and ripening of strawberry fruits. *Funct. Integr. Genomics* 16, 671–692. doi: 10.1007/s10142-016-0510-3

Meng, M., Geisler, M., Johansson, H., Mellerowicz, E. J., Karpinski, S., and Kleczkowski, L. A. (2007). Differential tissue/organ-dependent expression of two sucrose- and cold-responsive genes for UDP-glucose pyrophosphorylase in Populus. *Gene* 389, 186–195. doi: 10.1016/j.gene.2006.11.006

Merchante, C., Vallarino, J. G., Osorio, S., Aragüez, I., Villarreal, N., Ariza, M. T., et al. (2013). Ethylene is involved in strawberry fruit ripening in an organ-specific manner. *J. Exp. Bot.* 64, 4421–4439. doi: 10.1093/jxb/ert257

Miao, H., Sun, P., Liu, Q., Miao, Y., Liu, J., Zhang, K., et al. (2017). Genome-wide analyses of SWEET family proteins reveal involvement in fruit development and abiotic/biotic stress responses in banana. *Sci. Rep.* 7, 1–15. doi: 10.1038/s41598-017-03872-w

Murayama, H., Sai, M., Oikawa, A., and Itai, A. (2015). Inhibitory factors that affect the ripening of pear fruit on the tree. *Hortic. J.* 84, 14–20. doi: 10.2503/hortj.MI-015

Nakamura, K., Ohto, M. A., Yoshida, N., and Nakamura, K. (1991). Sucrose-induced accumulation of β-amylase occurs concomitant with the accumulation of starch and sporamin in leaf-petiole cuttings of sweet potato. *Plant Physiol.* 96, 902–909. doi: 10.1104/pp.96.3.902

Nardozza, S., Boldingh, H. L., Kashuba, M. P., Feil, R., Jones, D., Thrimawithana, A. H., et al. (2020). Carbon starvation reduces carbohydrate and anthocyanin accumulation in red-fleshed fruit via trehalose 6-phosphate and MYB27. *Plant Cell Environ.* 43, 819–835. doi: 10.1111/pce.13699

Ng, M., and Yanofsky, M. F. (2001). Function and evolution of the plant MADS-box gene family. *Nat. Rev. Genet.* 2, 186–195. doi: 10.1038/35056041

Nham, N. T., Macnish, A. J., Zakharov, F., and Mitcham, E. J. (2017). 'Bartlett' pear fruit (*Pyrus communis* L.) ripening regulation by low temperatures involves genes associated with jasmonic acid, cold response, and transcription factors. *Plant Sci.* 260, 8–18. doi: 10.1016/j.plantsci.2017.03.008

Nuccio, M. L., Wu, J., Mowers, R., Zhou, H. P., Meghji, M., Primavesi, L. F., et al. (2015). Expression of trehalose-6-phosphate phosphatase in maize ears improves yield in well-watered and drought conditions. *Nat. Biotechnol.* 33, 862–869. doi: 10.1038/nbt.3277

Nunes, C., O'Hara, L. E., Primavesi, L. F., Delatte, T. L., Schluepmann, H., Somsen, G. W., et al. (2013). The trehalose 6-phosphate/snRK1. signaling pathway primes growth recovery following relief of sink limitation. *Plant Physiol.* 162, 1720–1732. doi: 10.1104/pp.113.220657

Olivares, D., Contreras, C., Muñoz, V., Rivera, S., González-Agüero, M., Retamales, J., et al. (2017). Relationship among color development, anthocyanin and pigment-related gene expression in 'Crimson Seedless' grapes treated with abscisic acid and sucrose. *Plant Physiol. Biochem.* 115, 286–297. doi: 10.1016/j.plaphy.2017.04.007

Osorio, S., Alba, R., Nikoloski, Z., Kochevenko, A., Fernie, A. R., and Giovannoni, J. J. (2012). Integrative comparative analyses of transcript and metabolite profiles from pepper and tomato ripening and development stages uncovers species-specific patterns of network regulatory behavior. *Plant Physiol.* 159, 1713–1729. doi: 10.1104/pp.112.199711

Palmer, W. M., Ru, L., Jin, Y., Patrick, J. W., and Ruan, Y. L. (2015). Tomato ovary-to-fruit transition is characterized by a spatial shift of mrnas for cell wall invertase and its inhibitor with the encoded proteins localized to sieve elements. *Mol. Plant* 8, 315–328. doi: 10.1016/j.molp.2014.12.019

Peng, Q., Cai, Y., Lai, E., Nakamura, M., Liao, L., Zheng, B., et al. (2020). The sucrose transporter MdSUT4.1 participates in the regulation of fruit sugar accumulation in apple. *BMC Plant Biol.* 20, 4–5. doi: 10.1186/s12870-020-02406-3

Perata, P., Matsukura, C., Vernieri, P., and Yamaguchi, J. (1997). Sugar repression of a gibberellin-dependent signaling pathway in barley embryos. *Plant Cell* 9, 2197–2208. doi: 10.1105/tpc.9.12.2197

Petrussa, E., Braidot, E., Zancani, M., Peresson, C., Bertolini, A., Patui, S., et al. (2013). Plant flavonoids-biosynthesis, transport and involvement in stress responses. *Int. J. Mol. Sci.* 14, 14950–14973. doi: 10.3390/ijms140714950

Pillet, J., Egert, A., Pieri, P., Lecourieux, F., Kappel, C., Charon, J., et al. (2012). VvGOLS1 and VvHsfA2 are involved in the heat stress responses in grapevine berries. *Plant Cell Physiol.* 53, 1776–1792. doi: 10.1093/pcp/pcs121

Ponnu, J., Wahl, V., and Schmid, M. (2011). Trehalose-6-phosphate: Connecting plant metabolism and development. *Front. Plant Sci.* 2, 70. doi: 10.3389/fpls.2011.00070

Pott, D. M., Osorio, S., and Vallarino, J. G. (2019). From central to specialized metabolism: An overview of some secondary compounds derived from the primary metabolism for their role in conferring nutritional and organoleptic characteristics to fruit. *Front. Plant Sci.* 10, 835. doi: 10.3389/fpls.2019.00835

Qi, T., Huang, H., Wu, D., Yan, J., Qi, Y., Song, S., et al. (2014). Arabidopsis DELLA and JAZ proteins bind the WD-Repeat/ bHLH/MYB complex to modulate gibberellin and jasmonate signaling synergy. *Plant Cell* 26, 1118–1133. doi: 10.1105/tpc.113.121731

Qin, G., Zhu, Z., Wang, W., Cai, J., Chen, Y., Li, L., et al. (2016). A tomato vacuolar invertase inhibitor mediates sucrose metabolism and influences fruit ripening. *Plant Physiol.* 172, 1596–1611. doi: 10.1104/pp.16.01269

Rampino, P., Mita, G., Fasano, P., Borrelli, G. M., Aprile, A., Dalessandro, G., et al. (2012). Novel durum wheat genes up-regulated in response to a combination of heat and drought stress. *Plant Physiol. Biochem.* 56, 72–78. doi: 10.1016/j.plaphy.2012.04.006

Ren, Y., Guo, S., Zhang, J., He, H., Sun, H., Tian, S., et al. (2018). A tonoplast sugar transporter underlies a sugar accumulation QTL in watermelon. *Plant Physiol.* 176, 836–850. doi: 10.1104/pp.17.01290

Rennie, E. A., and Turgeon, R. (2009). A comprehensive picture of phloem loading strategies. *Proc. Natl. Acad. Sci. U. S. A.* 106, 14162–14167. doi: 10.1073/pnas.0902279106

Rodrigo, M. J., Alquezar, B., and Zacarías, L. (2006). Cloning and characterization of two 9-cis-epoxycarotenoid dioxygenase genes, differentially regulated during fruit maturation and under stress conditions, from orange (Citrus sinensis L. Osbeck). *J. Exp. Bot.* 57, 633–643. doi: 10.1093/jxb/erj048

Rolland, F., Baena-Gonzalez, E., and Sheen, J. (2006). Sugar sensing and signaling in plants: conserved and novel mechanisms. *Annu. Rev. Plant Biol.* 57, 675–709. doi: 10.1146/annurev.arplant.57.032905.105441

Ruan, Y. L., Chourey, P. S., Delmer, D. P., and Perez-Grau, L. (1997). The differential expression of sucrose synthase in relation to diverse patterns of carbon partitioning in developing cotton seed. *Plant Physiol.* 115, 375–385. doi: 10.1104/pp.115.2.375

Ruan, Y. L., Jin, Y., Yang, Y. J., Li, G. J., and Boyer, J. S. (2010). Sugar input, metabolism, and signaling mediated by invertase: Roles in development, yield potential, and response to drought and heat. *Mol. Plant* 3, 942–955. doi: 10.1093/mp/ssq044

Ruan, Y. L., Patrick, J. W., Bouzayen, M., Osorio, S., and Fernie, A. R. (2012). Molecular regulation of seed and fruit set. *Trends Plant Sci.* 17, 656–665. doi: 10.1016/j.tplants.2012.06.005

Ruan, Y. L. (2012). Signaling role of sucrose metabolism in development. *Mol. Plant* 5, 763–765. doi: 10.1093/mp/sss046

Ruan, Y.-L. (2014). Sucrose metabolism: gateway to diverse carbon use and sugar signaling. *Annu. Rev. Plant Biol.* 65, 33–67. doi: 10.1146/annurev-arplant-050213-040251

Sagar, M., Chervin, C., Mila, I., Hao, Y., Roustan, J. P., Benichou, M., et al. (2013). SlARF4, an auxin response factor involved in the control of sugar metabolism during tomato fruit development. *Plant Physiol.* 161, 1362–1374. doi: 10.1104/pp.113.213843

Schneider, S., Hulpke, S., Schulz, A., Yaron, I., Höll, J., Imlau, A., et al. (2012). Vacuoles release sucrose via tonoplast-localised SUC4-type transporters. *Plant Biol.* 14, 325–336. doi: 10.1111/j.1438-8677.2011.00506.x

Shangguan, L., Song, C., Leng, X., Kayesh, E., Sun, X., and Fang, J. (2014). Mining and comparison of the genes encoding the key enzymes involved in sugar biosynthesis in apple, grape, and sweet orange. *Sci. Hortic. (Amsterdam).* 165, 311–318. doi: 10.1016/j.scienta.2013.11.026

Shi, L., Cao, S., Shao, J., Chen, W., Zheng, Y., Jiang, Y., et al. (2014). Relationship between sucrose metabolism and anthocyanin biosynthesis during ripening in chinese bayberry fruit. *J. Agric. Food Chem.* 62, 10522–10528. doi: 10.1021/jf503317k

Siebeneichler, T. J., Crizel, R. L., Camozatto, G. H., Paim, B. T., da Silva Messias, R., Rombaldi, C. V., et al. (2020). The postharvest ripening of strawberry fruits induced by abscisic acid and sucrose differs from their in vivo ripening. *Food Chem.* 317, 126407. doi: 10.1016/j.foodchem.2020.126407

Smeekens, S., Ma, J., Hanson, J., and Rolland, F. (2010). Sugar signals and molecular networks controlling plant growth. *Curr. Opin. Plant Biol.* 13, 273–278. doi: 10.1016/j.pbi.2009.12.002

Solfanelli, C., Poggi, A., Loreti, E., Alpi, A., and Perata, P. (2006). Sucrose-specific induction of the anthocyanin biosynthetic pathway in Arabidopsis. *Plant Physiol.* 140, 637–646. doi: 10.1104/pp.105.072579.the

Sun, T., Yuan, H., Cao, H., Yazdani, M., Tadmor, Y., and Li, L. (2018). Carotenoid metabolism in plants: The Role of Plastids. *Mol. Plant* 11, 58–74. doi: 10.1016/j.molp.2017.09.010

Tang, T., Xie, H., Wang, Y., Lü, B., and Liang, J. (2009). The effect of sucrose and abscisic acid interaction on sucrose synthase and its relationship to grain filling of rice (Oryza sativa L.). *J. Exp. Bot.* 60, 2641–2652. doi: 10.1093/jxb/erp114

Tarkowski, Ł.P., and Van den Ende, W. (2015). Cold tolerance triggered by soluble sugars: A multifaceted countermeasure. *Front. Plant Sci.* 6, 203. doi: 10.3389/fpls.2015.00203

Télef, N., Stammitti-Bert, L., Mortain-Bertrand, A., Maucourt, M., Carde, J. P., Rolin, D., et al. (2006). Sucrose deficiency delays lycopene accumulation in tomato fruit pericarp discs. *Plant Mol. Biol.* 62, 453–469. doi: 10.1007/s11103-006-9033-y

Teng, S., Keurentjes, J., Bentsink, L., Koornneef, M., and Smeekens, S. (2005). Sucrose-specific induction of anthocyanin biosynthesis in Arabidopsis requires the MYB75/PAP1 gene. *Plant Physiol.* 139, 1840–1852. doi: 10.1104/pp.105.066688

Terrier, N., Glissant, D., Grimplet, J., Barrieu, F., Abbal, P., Couture, C., et al. (2005). Isogene specific oligo arrays reveal multifaceted changes in gene expression during grape berry (Vitis vinifera L.) development. *Planta* 222, 832–847. doi: 10.1007/s00425-005-0017-y

Thakur, P., Kumar, S., Malik, J. A., Berger, J. D., and Nayyar, H. (2010). Cold stress effects on reproductive development in grain crops: An overview. *Environ. Exp. Bot.* 67, 429–443. doi: 10.1016/j.envexpbot.2009.09.004

Tognetti, J. A., Pontis, H. G., and Martínez-Noël, G. M. A. (2013). Sucrose signaling in plants: A world yet to be explored. *Plant Signal. Behav.* 8, e23316. doi: 10.4161/psb.23316

Trainotti, L., Pavanello, A., and Casadoro, G. (2005). Different ethylene receptors show an increased expression during the ripening of strawberries: Does such an increment imply a role for ethylene in the ripening of these non-climacteric fruits? *J. Exp. Bot.* 56, 2037–2046. doi: 10.1093/jxb/eri202

Vallarino, J. G., Osorio, S., Bombarely, A., Casañal, A., Cruz-Rus, E., Sánchez-Sevilla, J. F., et al. (2015). Central role of FaGAMYB in the transition of the strawberry receptacle from development to ripening. *New Phytol.* 208, 482–496. doi: 10.1111/nph.13463

Vallarino, J. G., Yeats, T. H., Maximova, E., Rose, J. K., Fernie, A. R., and Osorio, S. (2017). Postharvest changes in LIN5-down-regulated plants suggest a role for sugar deficiency in cuticle metabolism during ripening. *Phytochemistry* 142, 11–20. doi: 10.1016/j.phytochem.2017.06.007

Vallarino, J. G., de Abreu e Lima, F., Soria, C., Tong, H., Pott, D. M., Willmitzer, L., et al. (2018). Genetic diversity of strawberry germplasm using metabolomic biomarkers. *Sci. Rep.* 8, 14386. doi: 10.1038/s41598-018-32212-9

van Kan, J. A. L. (2006). Licensed to kill: the lifestyle of a necrotrophic plant pathogen. *Trends Plant Sci.* 11, 247–253. doi: 10.1016/j.tplants.2006.03.005

Vega, A., Gutiérrez, R. A., Peña-Neira, A., Cramer, G. R., and Arce-Johnson, P. (2011). Compatible GLRaV-3 viral infections affect berry ripening decreasing sugar accumulation and anthocyanin biosynthesis in Vitis vinifera. *Plant Mol. Biol.* 77, 261–274. doi: 10.1007/s11103-011-9807-8

Vitrac, X., Larronde, F., Krisa, S., Decendit, A., Deffieux, G., and Mérillon, J. M. (2000). Sugar sensing and Ca2+-calmodulin requirement in Vitis vinifera cells producing anthocyanins. *Phytochemistry* 53, 659–665. doi: 10.1016/S0031-9422(99)00620-2

Vogt, T. (2010). Phenylpropanoid biosynthesis. *Mol. Plant* 3, 2–20. doi: 10.1093/mp/ssp106

Vrebalov, J., Ruezinsky, D., Padmanabhan, V., White, R., Drake, R., Schuch, W., et al. (2002). A MADS-Box gene necessary for fruit ripening at the tomato ripening-inhibitor (Rin). *Science* 296, 343–346. doi: 10.1126/science.1068181

Wai, C. M., Zhang, J., Jones, T. C., Nagai, C., and Ming, R. (2017). Cell wall metabolism and hexose allocation contribute to biomass accumulation in high yielding extreme segregants of a Saccharum interspecific F2 population. *BMC Genomics* 18, 773. doi: 10.1186/s12864-017-4158-8

Wang, L., and Ruan, Y. L. (2013). Regulation of cell division and expansion by sugar and auxin signaling. *Front. Plant Sci.* 4:163. doi: 10.3389/fpls.2013.00163

Wang, S. J., Yeh, K. W., and Tsai, C. Y. (2001). Regulation of starch granule-bound starch synthase I gene expression by circadian clock and sucrose in the source tissue of sweet potato. *Plant Sci.* 161, 635–644. doi: 10.1016/S0168-9452(01)00449-6

Wang, X., Peng, F., Li, M., Yang, L., and Li, G. (2012). Expression of a heterologous SnRK1 in tomato increases carbon assimilation, nitrogen uptake and modifies fruit development. *J. Plant Physiol.* 169, 1173–1182. doi: 10.1016/j.jplph.2012.04.013

Wang, L., Cook, A., Patrick, J. W., Chen, X. Y., and Ruan, Y. L. (2014). Silencing the vacuolar invertase gene GhVIN1 blocks cotton fiber initiation from the ovule epidermis, probably by suppressing a cohort of regulatory genes via sugar signaling. *Plant J.* 78, 686–696. doi: 10.1111/tpj.12512

Wang, Q. H., Zhao, C., Zhang, M., Li, Y. Z., Shen, Y. Y., and Guo, J. X. (2017). Transcriptome analysis around the onset of strawberry fruit ripening uncovers an important role of oxidative phosphorylation in ripening. *Sci. Rep.* 14, 41477. doi: 10.1038/srep41477

Wei, L., Mao, W., Jia, M., Xing, S., Ali, U., Zhao, Y., et al. (2018). FaMYB44.2, a transcriptional repressor, negatively regulates sucrose accumulation in strawberry receptacles through interplay with FaMYB10. *J. Exp. Bot.* 69, 4805–4820. doi: 10.1093/jxb/ery249

Wenzler, H., Mignery, G., Fisher, L., and Park, W. (1989). Sucrose-regulated expression of a chimeric potato tuber gene in leaves of transgenic tobacco plants. *Plant Mol. Biol.* 13, 347–354. doi: 10.1007/BF00015546

Wiese, A., Elzinga, N., Wobbes, B., and Smeekens, S. (2004). A Conserved upstream open reading frame mediates sucrose-induced repression of translation. *Plant Cell* 16, 1717–1729. doi: 10.1105/tpc.019349.Rolland

Wind, J., Smeekens, S., and Hanson, J. (2010). Sucrose: Metabolite and signaling molecule. *Phytochemistry* 71, 1610–1614. doi: 10.1016/j.phytochem.2010.07.007

Wingler, A., Tijero, V., Müller, M., Yuan, B., and Munné-Bosch, S. (2020). Interactions between sucrose and jasmonate signalling in the response to cold stress. *BMC Plant Biol.* 20, 1–13. doi: 10.1186/s12870-020-02376-6

Wormit, A., Trentmann, O., Feifer, I., Lohr, C., Tjaden, J., Meyer, S., et al. (2006). Molecular identification and physiological characterization of a novel monosaccharide transporter from Arabidopsis involved in vacuolar sugar transport. *Plant Cell* 18, 3476–3490. doi: 10.1105/tpc.106.047290

Wu, J., Xu, Z., Zhang, Y., Chai, L., Yi, H., and Deng, X. (2014). An integrative analysis of the transcriptome and proteome of the pulp of a spontaneous late-ripening sweet orange mutant and its wild type improves our understanding of fruit ripening in citrus. *J. Exp. Bot.* 65, 1651–1671. doi: 10.1093/jxb/eru044

Xiao, G., Zhou, J., Lu, X., Huang, R., and Zhang, H. (2018). Excessive UDPG resulting from the mutation of UAP1 causes programmed cell death by triggering reactive oxygen species accumulation and caspase-like activity in rice. *New Phytol.* 217, 332–343. doi: 10.1111/nph.14818

Xie, Y., Tan, H., Ma, Z., and Huang, J. (2016). DELLA proteins promote anthocyanin biosynthesis via sequestering MYBL2 and JAZ suppressors of the MYB/bHLH/WD40 complex in Arabidopsis thaliana. *Mol. Plant* 9, 711–721. doi: 10.1016/j.molp.2016.01.014

Xu, S. M., Brill, E., Llewellyn, D. J., Furbank, R. T., and Ruan, Y. L. (2012). Overexpression of a potato sucrose Synthase gene in cotton accelerates leaf expansion, reduces seed abortion, and enhances fiber production. *Mol. Plant* 5, 430–441. doi: 10.1093/mp/ssr090

Xu, X., Hu, Q., Yang, W., and Jin, Y. (2017). The roles of call wall invertase inhibitor in regulating chilling tolerance in tomato. *BMC Plant Biol.* 17, 1–13. doi: 10.1186/s12870-017-1145-9

Yadav, U. P., Ivakov, A., Feil, R., Duan, G. Y., Walther, D., Giavalisco, P., et al. (2014). The sucrose-trehalose 6-phosphate (Tre6P) nexus: Specificity and mechanisms of sucrose signalling by. *J. Exp. Bot.* 65, 1051–1068. doi: 10.1093/jxb/ert457

Yu, W., Peng, F., Xiao, Y., Wang, G., and Luo, J. (2018). Overexpression of PpSnRK1α in tomato promotes fruit ripening by enhancing RIPENING INHIBITOR regulation pathway. *Front. Plant Sci.* 871, 1856. doi: 10.3389/fpls.2018.01856

Yuan, Y., Xu, X., Gong, Z., Tang, Y., Wu, M., Yan, F., et al. (2019). Auxin response factor 6A regulates photosynthesis, sugar accumulation, and fruit development in tomato. *Hortic. Res.* 6, 85. doi: 10.1038/s41438-019-0167-x

Zanor, M.II, Osorio, S., Nunes-Nesi, A., Carrari, F., Lohse, M., Usadel, B., et al. (2009). RNA interference of LIN5 in tomato confirms its role in controlling brix content, uncovers the influence of sugars on the levels of fruit hormones, and demonstrates the importance of sucrose cleavage for normal fruit development and fertility. *Plant Physiol.* 150, 1204–1218. doi: 10.1104/pp.109.136598

Zhang, L., Ma, G., Kato, M., Yamawaki, K., Takagi, T., Kiriiwa, Y., et al. (2012). Regulation of carotenoid accumulation and the expression of carotenoid metabolic genes in citrus juice sacs in vitro. *J. Exp. Bot.* 63, 871–886. doi: 10.1093/jxb/err318

Zhang, Y. J., Wang, X. J., Wu, J. X., Chen, S. Y., Chen, H., Chai, L. J., et al. (2014). Comparative transcriptome analyses between a spontaneous late-ripening sweet orange mutant and its wild type suggest the functions of ABA, sucrose and JA during citrus fruit ripening. *PloS One* 9, 1–27. doi: 10.1371/journal.pone.0116056

Zhang, Y., Zhen, L., Tan, X., Li, L., and Wang, X. (2014). The involvement of hexokinase in the coordinated regulation of glucose and gibberellin on cell wall invertase and sucrose synthesis in grape berry. *Mol. Biol. Rep.* 41, 7899–7910. doi: 10.1007/s11033-014-3683-7

Zhang, Z. P., Deng, Y., Song, X., and Miao, M. (2015). Trehalose-6-phosphate and SNF1-related protein kinase 1 are involved in the first-fruit inhibition of cucumber. *J. Plant Physiol.* 177, 110–120. doi: 10.1016/j.jplph.2014.09.009

Zhang, J., Guo, S., Ren, Y., Zhang, H., Gong, G., Zhou, M., et al. (2017). High-level expression of a novel chromoplast phosphate transporter ClPHT4;2 is required for flesh color development in watermelon. *New Phytol.* 213, 1208–1221. doi: 10.1111/nph.14257

Zhang, W., Lunn, J. E., Feil, R., Wang, Y., Zhao, J., Tao, H., et al. (2017). Trehalose 6-phosphate signal is closely related to sorbitol in apple (Malus domestica Borkh. Cv. Gala). *Biol. Open* 6, 260–268. doi: 10.1242/bio.022301

Zhang, Y., Liu, Z., Liu, J., Lin, S., Wang, J., Lin, W., et al. (2017). GA-DELLA pathway is involved in regulation of nitrogen deficiency-induced anthocyanin accumulation. *Plant Cell Rep.* 36, 557–569. doi: 10.1007/s00299-017-2102-7

Zhao, C., Hua, L. N., Liu, X. F., Li, Y. Z., Shen, Y. Y., and Guo, J. X. (2017). Sucrose synthase FaSS1 plays an important role in the regulation of strawberry fruit ripening. *Plant Growth Regul.* 81, 175–181. doi: 10.1007/s10725-016-0189-4

Zheng, Y., Tian, L., Liu, H., Pan, Q., Zhan, J., and Huang, W. (2009). Sugars induce anthocyanin accumulation and flavanone 3-hydroxylase expression in grape berries. *Plant Growth Regul.* 58, 251–260. doi: 10.1007/s10725-009-9373-0

Conflict of Interest: The authors declare that the submitted work was carried out in the absence of any commercial or financial relationships that could be construed as a potential conflict of interest.

frontiers in Plant Science

ORIGINAL RESEARCH
published: 09 September 2020
doi: 10.3389/fpls.2020.543747

Auxin Response Factor 2A Is Part of the Regulatory Network Mediating Fruit Ripening Through Auxin-Ethylene Crosstalk in Durian

Gholamreza Khaksar[1] *and Supaart Sirikantaramas*[1,2]*

[1] Molecular Crop Research Unit, Department of Biochemistry, Faculty of Science, Chulalongkorn University, Bangkok, Thailand, [2] Omics Sciences and Bioinformatics Center, Chulalongkorn University, Bangkok, Thailand

Fruit ripening is a highly coordinated developmental process driven by a complex hormonal network. Ethylene is the main regulator of climacteric fruit ripening. However, a putative role of other key phytohormones in this process cannot be excluded. We previously observed an increasing level of auxin during the post-harvest ripening of the durian fruit, which occurred concomitantly with the rise in the climacteric ethylene biosynthesis. Herein, we connect the key auxin signaling component, auxin response factors (ARFs), with the regulatory network that controls fruit ripening in durian through the identification and functional characterization of a candidate ripening-associated ARF. Our transcriptome-wide analysis identified 15 ARF members in durian (*DzARF*s), out of which 12 were expressed in the fruit pulp. Most of these *DzARF*s showed a differential expression, but *DzARF2A* had a marked ripening-associated expression pattern during post-harvest ripening in Monthong, a commercial durian cultivar from Thailand. Phylogenetic analysis of DzARF2A based on its tomato orthologue predicted a role in ripening through the regulation of ethylene biosynthesis. Transient expression of *DzARF2A* in *Nicotiana benthamiana* leaves significantly upregulated the expression levels of ethylene biosynthetic genes, pointing to a ripening-associated role of DzARF2A through the transcriptional regulation of ethylene biosynthesis. Dual-luciferase reporter assay determined that DzARF2A trans-activates durian ethylene biosynthetic genes. We previously reported significantly higher auxin level during post-harvest ripening in a fast-ripening cultivar (Chanee) compared to a slow-ripening one (Monthong). *DzARF2A* expression was significantly higher during post-harvest ripening in the fast-ripening cultivars (Chanee and Phuangmanee) compared to that of the slow-ripening ones (Monthong and Kanyao). Thus, higher auxin level could upregulate the expression of *DzARF2A* during ripening of a fast-ripening cultivar. The auxin-induced expression of *DzARF2A* confirmed its responsiveness to exogenous auxin treatment in a dose-dependent manner, suggesting an auxin-mediated role of DzARF2A in fruit ripening. We suggest that high *DzARF2A* expression would activate ARF2A-mediated transcription of ethylene biosynthetic genes, leading to increased climacteric ethylene biosynthesis (auxin-ethylene crosstalk) and faster ripening. Hence, we demonstrated DzARF2A as a

OPEN ACCESS

Edited by:
Carlos R. Figueroa, University of Talca, Chile

Reviewed by:
Jian-ye Chen, South China Agricultural University, China
Antonio Chalfun-Junior, Universidade Federal de Lavras, Brazil

***Correspondence:**
Supaart Sirikantaramas
supaart.s@chula.ac.th

Specialty section:
This article was submitted to Crop and Product Physiology, a section of the journal Frontiers in Plant Science

Received: *18 March 2020*
Accepted: *24 August 2020*
Published: *09 September 2020*

Citation:
Khaksar G and Sirikantaramas S (2020) Auxin Response Factor 2A Is Part of the Regulatory Network Mediating Fruit Ripening Through Auxin-Ethylene Crosstalk in Durian. Front. Plant Sci. 11:543747. doi: 10.3389/fpls.2020.543747

new component of the regulatory network possibly mediating durian fruit ripening through transcriptional regulation of ethylene biosynthetic genes.

Keywords: auxin, auxin response factor, durian, ethylene, fruit ripening, transcriptional regulation

INTRODUCTION

Fruit ripening is a genetically programmed and coordinated developmental process involving dramatic physiological transformations, some of which include changes in the aroma, texture, color, and nutritional value of the flesh (Alexander and Grierson, 2002; Adams-Phillips et al., 2004). This process is controlled by transcriptional regulatory networks with transcription factors (TFs) acting as pivotal regulators. Depending on the mechanism, the ripening of fleshy fruits can be divided into climacteric and non-climacteric ripening (Lelievre et al., 1997). Climacteric ripening is associated with an autocatalytic increase in ethylene biosynthesis and the key role played by ethylene in this process (as the main trigger of fruit ripening) has been well documented (Barry et al., 2000). Consistently, various genes involved in ethylene biosynthesis and signaling were shown to be vital for ripening (Ayub et al., 1996; Xie et al., 2006; Wang et al., 2009), but the involvement of other plant hormones in this process (together with ethylene) seems also likely. The possibility that fruit ripening is regulated by a complex hormonal network has already been formulated and suggested by the existing literature. Auxin (IAA; indole-3-acetic acid) is a crucial phytohormone which regulates numerous aspects of plant growth and development (Woodward and Bartel, 2005), including ripening (Jones et al., 2002). Along with significant increases in the climacteric ethylene, elevated auxin levels of have also been detected during the ripening of tomato (Gillaspy et al., 1993), peach (Miller et al., 1987), and durian (Khaksar et al., 2019), suggesting a possible ripening-associated role of auxin. Auxin response factor (ARF) TFs represent the core of auxin signaling. These proteins mediate the auxin-dependent gene expression *via* binding to the auxin response elements (AuxREs; TGTCTC), located in the promoter regions of the auxin responsive genes, in a dose-dependent manner (Hagen and Guilfoyle, 2002). ARFs are generally characterized by a highly conserved DNA binding domain (DBD) at their N terminus. They also contain a middle region, responsible for the transactivation or repression of target genes and a carboxyl-terminal dimerization domain (CTD) that is involved in the protein-protein interactions (Guilfoyle and Hagen, 2007; Guilfoyle and Hagen, 2012; Nanao et al., 2014; Guilfoyle, 2015). The domain architecture of ARFs is known to play a key role in their specificity. Since the identification and characterization of the first Arabidopsis *ARF* (*AtARF1*) (Ulmasov et al., 1997), numerous studies have identified members of the ARF gene family in plant species, such as tomato (Kumar et al., 2011), rice (Wang et al., 2007), Medicago (Shen et al., 2015), banana (Hu et al., 2015), apple (Luo et al., 2014), maize (Xing et al., 2011), chickpea (Singh et al., 2017), physic nut (Tang et al., 2018), grape (Wan et al., 2014), and papaya (Liu et al., 2015). Functional characterization of some ARFs based on the phenotypes of the loss-of-function and gain-of-function mutants have also been carried out. For instance, the Arabidopsis *arf1* and *arf2* mutants showed abnormal abscission of the floral organs (Ellis et al., 2005), while mutation in the *AtARF7* gene diminished hypocotyl response to blue light and auxin (Harper et al., 2000). The *AtARF8* loss-of-function mutation, on the other hand, impaired hypocotyl elongation and auxin homeostasis (Goetz et al., 2006), while the tomato *SlARF3* was found to participate in the formation of trichomes and epidermal cells (Zhang et al., 2015). In addition to their roles in plant growth and development, ARFs are also involved in the responses to abiotic stressors. *OsARF16*, for example, has been found to participate in the adaptive response to phosphate starvation in rice (Shen et al., 2013), while another member (*OsARF12*) has been found to play role in iron homeostasis (Qi et al., 2013). Although the links between ARFs and plant growth and development have been extensively studied, our actual knowledge regarding the possible roles of ARFs in fruit ripening remains poorly understood and limited only to a few studies in tomato and papaya. In tomato, the *SlARF2A* and *SlARF2B* (two *ARF2* paralogs) displayed a ripening-associated expression pattern. Down-regulation of either *SlARF2A* or *SlARF2B* led to ripening defects, while the *arf2a/arf2b* double mutation resulted in a severe inhibition of the ripening process (Hao et al., 2015). Moreover, a significant decrease in the climacteric ethylene biosynthesis and the expression levels of ethylene biosynthetic genes was observed in the *SlARF2AB-RNAi* fruits (Hao et al., 2015). Breitel et al. (2016) identified *SlARF2A*, an auxin signaling component that controls ripening. They found *SlARF2A* expression to be ripening-regulated and responsive to exogenous ethylene and auxin treatments. In papaya, Liu et al. (2015) profiled the expression pattern of 11 *ARF*s (*CpARF*s) during the different fruit developmental stages and found that the expression of most *CpARF*s underwent significant changes with ripening. Specifically, the expression of *CpARF1* and *CpARF2* increased, while that of *CpARF7* and *CpARF11* decreased.

Durian (*Durio zibethinus* Murr.) is a tropical fruit crop of rising economy value endemic to Southeast Asia, with an ever-growing popularity on the international market. Durian is distinctive for its strong and unique odor and formidable spiny husk. With over 200 existing cultivars, Thailand is the top durian exporter across the Southeast Asian region. However, only a few of these cultivars are commercially cultivated and in high demand both locally and on the international market. These include Monthong (*D. zibethinus* Murr. cv. "Monthong"), Chanee (*D. zibethinus* Murr. cv. "Chanee"), Phuangmanee (*D. zibethinus* Murr. cv. "Phuangmanee"), and Kanyao (*D. zibethinus* Murr. cv. "Kanyao"). Among these, Monthong—due to its mild odor and creamy texture—is of great interest (Pinsorn et al., 2018). Notably, these cultivars harbor different post-harvest ripening behaviors; Monthong and Kanyao are slow-ripening cultivars that need around 5 days to fully ripen after being harvested at mature stage. Chanee and Phuangmanee, on the other hand, are fast-ripening

cultivars that ripen 3 days after harvesting at mature stage. Durian is a climacteric fruit that has a strikingly limited shelf life after harvesting. Hence, the fast and slow ripening processes are agronomic traits of great economic importance for agricultural industry. Offering durian fruit with a pleasant flavor and nutritional value, while also harboring longer shelf life remains a challenge for the industry. Over recent decades, investigations have focused on extending shelf life. However, our actual knowledge on the molecular mechanisms underlying the ripening process is still limited, especially with regard to fast- and slow-ripening cultivars. In our previous study, we observed an increasing level of auxin production during the post-harvest ripening of the durian fruit in both Monthong and Chanee cultivars, suggesting a ripening-associated role of auxin during fruit ripening (Khaksar et al., 2019). Here, considering the major role of ARFs in the auxin signaling pathway, we performed a transcriptome-wide analysis on the durian genome and identified 15 members of the ARF gene family. Comprehensive gene expression profiling of the durian *ARF*s (*DzARF*s) during the post-harvest ripening revealed significant differential expression of some *ARF*s and suggested putative ripening-associated ones. We then functionally characterized a candidate ripening-associated TF (DzAFR2A). Our findings positioned DzARF2A as a key component of the regulatory network behind the post-harvest ripening of the durian. To our knowledge, this is the first report on the identification and characterization of the ARF gene family in this fruit. Findings from this study can be further exploited towards the development of molecular markers for breeding new durian varieties with longer shelf lives.

MATERIALS AND METHODS

Plant Materials and Treatments

Durian (*Durio zibethinus* Murr.) cv. Monthong, Chanee, and Phuangmanee were collected from commercial durian plantations located in the eastern part of Thailand. Fruit samples having similar size and weight (~3–4 kg each) were harvested at mature stage which occurs at 90 days (for Chanee and Phuangmanee) and 105 days (for Monthong) after anthesis. Samples were kept at room temperature (30°C) until peeling. For these cultivars, three types of samples during post-harvest ripening (unripe, midripe, and ripe) were used. For unripe samples, fruits harvested at the mature stage of all three cultivars were kept at room temperature for one day and then peeled. For midripe samples, fruits harvested at the mature stage were kept at room temperature for two days (for Chanee and Phuangmanee) and three days (for Monthong) and then peeled. For ripe samples, fruits harvested at the mature stage were kept at room temperature for three days (for Chanee and Phuangmanee) and five days (for Monthong) and then peeled. In this study, another cultivar called Kanyao was also used. However, for Kanyao cultivar, we only had access to the ripe fruit which was bought at the ripe stage and peeled. After peeling, two of the central pulps were collected from each fruit sample, following the method described in Pinsorn et al. (2018). To ensure samples of the different cultivars were compared at the same ripening stage, the first pulp was collected along with a seed, and was used to measure fruit firmness with a texture analyzer following our previous study (Khaksar et al., 2019). Midripe and ripe pulps had a mean [± standard deviation (SD)] firmness of 3.4 ± 0.81 and 1.55 ± 0.45 N, respectively in all cultivars. After this test, the second pulp was collected without a seed, immediately frozen in liquid nitrogen, and stored at -80°C for RNA extraction.

To further validate the putative ripening-associated *DzARF*s in Monthong cultivar, three different ripening treatments were applied as follows: natural, ethephon-induced, and 1-methylcyclopropene (1-MCP)-delayed ripening. Durian samples were collected at mature stage and treated with either ethephon (48% 2-chloroethylphosphonic acid; Alpha Agro Tech Co., Ltd., Thailand) or 1-MCP (0.19% 1-MCP tablet; BioLene Co., Ltd., China) for ethephon-induced and 1-MCP-delayed ripening, respectively following the method described in our previous study (Khaksar et al., 2019). After treatments, control and treated samples were kept at room temperature (30°C) until the ethephon-induced samples ripened. As soon as ethephon-treated samples ripened, all samples from the other ripening conditions were peeled. Two central pulps were collected from each sample and processed as mentioned previously. In this study, for each type of sample (unripe, midripe, and ripe, as well as natural ripening, ethephon-induced ripening, and 1-MCP-delayed ripening) of each cultivar, three independent biological replicates were used. Each biological replicate is one durian fruit harvested from a separate tree.

For transient expression of *DzAFR2A* in *Nicotiana benthamiana* leaves, *N. benthamiana* seeds were sown in pots containing peat moss and were grown under controlled conditions (temperature 25°C and 16/8 h light/dark photoperiod; artificial light of 4,500 Lux). Two-week-old seedlings were transplanted individually into pots and were grown under similar conditions.

For exogenous auxin treatment, young leaves of Monthong cultivar were soaked in different concentrations (10, 20, and 40 μM) of indole-3-acetic acid (IAA) (Duchefa Biochemie, The Netherlands) for 1 and 2 h. As control, leaves were soaked in distilled water without IAA. For reverse transcription quantitative polymerase chain reaction (RT-qPCR) analysis, leaves were immediately frozen in liquid nitrogen and stored at -80°C until total RNA extraction.

Transcriptome-Wide Identification and Tissue-Specific Expression Analysis of Durian *ARF*s

In order to obtain the assembled transcriptome data, Illumina sequencing reads from RNA-Seq study of durian (Musang King cultivar) were retrieved from a public repository database (SRA, Sequence Read Archive) with the following accession numbers: SRX3188225 (root tissue), SRX3188222 (stem tissue), SRX3188226 (leaf tissue), and SRX3188223 (aril/pulp tissue). To obtain the *de novo* assembled transcriptome, we followed the

method described in our previous study (Khaksar et al., 2019). We then followed Hidden Markov Model (HMM) search to identify ARF gene family members. First, we obtained the ARF conserved domain (PF06507) from the Pfam protein database (http://pfam.xfam.org) and used as a query to search against the assembled transcriptome database using the HMMER software (http://hmmer.org/) following e-value cut-off $\leq 1e^{-5}$. This approach enabled us to identify 15 non-redundant ARF gene family members. Further, the amino acid sequences of durian ARFs (DzARFs) were checked in SMART database for the presence of the ARF domain. The expression levels of *DzARF*s in different tissues, including root, stem, leaf, and aril (pulp) were analyzed using the *de novo* assembled transcriptome. Abundance estimation tool in Trinity package was used to align the input reads to the *de novo* assembled transcriptome to obtain raw counts of each contig. The raw read counts were then merged in a single read count matrix which was then normalized to generate a Trimmed Mean of M-values (TMM) normalized matrix. For generating heatmap, the normalized total read counts were used as queries in MetaboAnalyst 4.0, an open source R-based program (Chong et al., 2018). For the heatmap construction, the values were sum normalized, log2 transformed and autoscaled.

Phylogenetic Analysis

To study evolutionary relationships among DzARFs and ARFs from Arabidopsis and tomato, a neighbor-joining (NJ) phylogenetic tree was constructed with 1,000 bootstrap replicates using MEGA X software (with a JTT model and pairwise gap deletion) by aligning their full-length protein sequences (Kumar et al., 2018).

Prediction of Conserved Motifs and Gene Structure

MEME program (http://meme-suite.org) was used for identification of the conserved motifs (Bailey et al., 2009) with the following parameter settings: motif length = 6–100; motif sites = 2–120; maximum number of motifs = 10; and the distribution of one single motif was "any number of repetitions". Exon/intron organization of the durian ARF genes was determined using Gene Structure Display Server 2.0 (with default parameters) (http://gsds.cbi.pku.edu.cn).

RT-qPCR Analysis

Total RNA isolation from durian fruit pulp samples was carried out using PureLink Plant RNA Reagent (Thermo Fisher Scientific™) following the manufacturer's instructions. Genomic DNA was removed with DNase I (Thermo Fisher Scientific™) treatment. The quality and quantity of RNA samples were examined using agarose gel electrophoresis and an Eppendorf BioPhotometer D30 with A260/280 and A260/230 ratios between 1.8 to 2.0 and 2.0 to 2.2, respectively following the standard guidelines described in Bustin et al. (2009). For reverse transcription, one microgram of total RNA was used to generate cDNA using a RevertAid First Strand cDNA Synthesis Kit (Thermo Fisher Scientific™), following the manufacturer's recommended protocol and the standard guidelines of reverse transcription described in Bustin et al. (2009). Primer 3 online (http://primer3.ut.ee/) was used to design the primers used in this study which are presented in **Supplementary Table S1**. To measure the transcript levels of *DzARF*s at three stages (unripe, midripe, and ripe) during post-harvest ripening of Monthong and compare the expression level of candidate ripening-associated *DzARF* among different cultivars, RT-qPCR was performed. The PCR reaction was performed in a total volume of 10 µl containing 1 µl of diluted cDNA (1 ng of cDNA), 5 µl of 2x QPCR Green Master Mix LRox (biotechrabbit, Berlin, Germany), and 200 nM of each gene-specific primer. A CFX95 Real-time System (Bio-Rad Laboratories Inc., California, USA) was used under the following conditions: initial activation at 95°C for 3 min, followed by 40 cycles of denaturation at 95°C for 15 s, then annealing at 58–60°C for 30 s, and finally extension at 72°C for 20 s. Three independent biological replicates were used for each RT-qPCR experiment. The elongation factor 1 alpha (*EF-1α*; XM_022889169.1) and actin (*ACT*; XM_022897008.1) genes of durian were selected as reference genes for the normalization of RT-qPCR data according to our in-house transcriptome data of durian fruit from different cultivars which confirmed the invariant expression levels of *EF-1α* and *ACT* under different experimental conditions. In addition, to further confirm this, we used Genorm software (Vandesompele et al., 2002) to check the stability of our reference genes (see **Supplementary Table S1** for primers).

Statistical analysis of RT-qPCR data was carried out using the method described in Steibel et al. (2009) which consists of the analysis of cycles to threshold values (Ct) for the target and reference genes according to a linear mixed model [Model I of the report of Steibel et al. (2009)]. Treatments, genes, and their interactions were the fixed factors whereas the obtained Ct values comprised the dependent variables of the model. Samples were the random effects of the model. The normalization of RT-qPCR expression data was carried out using normalization factors; the geometric mean of the two reference genes calculated with Genorm software (Vandesompele et al., 2002). For graphical illustration, the expression data are presented as fold change ($2^{-\Delta\Delta Ct}$) (Livak and Schmittgen, 2001). $P < 0.05$ was considered statistically significant. R programming language (https://www.R-project.org/) was used for the analysis.

Transient Expression of *DzARF2A* in *N. benthamiana* Leaf

The full-length cDNA of *DzARF2A* was amplified from the cDNA of Monthong cultivar (at midripe stage) using Phusion Hot Start II High-Fidelity DNA Polymerase (Thermo Fisher Scientific, Waltham, MA, USA) (primers are listed in **Supplementary Table S2**). After that, the PCR amplicon was inserted into the entry vector pDONR207 using Gateway® BP Clonase® II (Thermo Fisher Scientific, Waltham, MA, USA). After sequencing, *DzARF2A*

in Monthong cultivar was confirmed to be identical to the *DzARF2A* in Musang King cultivar (XM_022883347.1). From the resultant pDONR207-*DzARF2A*, the putative *DzARF2A* was inserted in to the pGWB2 expression vector using Gateway® LR Clonase® II (Thermo Fisher Scientific, Waltham, MA, USA) to produce pGWB2-*DzARF2A*. The resulting pGWB2-*DzARF2A* as well as pGWB2-*GFP* (control) were individually introduced into the *Agrobacterium tumefaciens* strain GV3101 by electroporation. The positive *A. tumefaciens* colony harbouring each construct was further grown in 25 ml of LB broth containing 25 mg L^{-1} gentamycin and 25 mg L^{-1} rifampicin with shaking at 250 rpm overnight at 30°C. Cells were harvested by centrifugation at 4,000×g for 10 min and resuspended in MM buffer (10 mM MES and 10 mM $MgCl_2$, pH 5.6) to reach an optical density of 0.6 (OD_{600}). For the agroinfiltration experiment, the agrobacterium solution containing either pGWB2-*DzARF2A* or pGWB2-*GFP* (control) was mixed with the agrobacterium solution harbouring the gene encoding the silencing inhibitor protein p19 at a ratio of 1:1. Then, acetosyringone was added at a concentration of 100 mg L^{-1} and the mixture was incubated at room temperature for 3 h under dark conditions. Then, the solution was infiltrated into the abaxial surface of three individual leaves per plant using a needleless 1 ml syringe. Three independent biological replicates (three 4-week-old plants) were used for each construct at each timepoint. At three and five days after infiltration, samples of the infiltrated leaves were collected, frozen in liquid nitrogen and ground into a fine powder with a mortar and pestle. This powder was then used for RNA isolation and cDNA synthesis. The cDNA was further used as the template for RT-qPCR analysis. The elongation factor 1 alpha (*EF-1α*; XM_016613715.1) and actin (*ACT*; XM_016618072.1) genes of *Nicotiana* were used as reference genes for the normalization of RT-qPCR data. In order to design primers for *N. benthamiana* ethylene biosynthetic genes, the *Nicotiana tabacum* genome [i.e., 1-aminocyclopropane-1-carboxylic acid (ACC) synthase; *ACS* (NM_001326261.2) and ACC oxidase; *ACO* (NM_001325823.1)] were used to blast against the genome sequence of *N. benthamiana* (SGN *Nicotiana benthamiana* ftp site; https://solgenomics.net/organism/Nicotiana_benthamiana/genome). Primers are listed in **Supplementary Table S2**. The 2000-bp upstream promoter regions of these genes were scanned for the auxin response elements (AuxREs; TGTCTC) using the online tool PLACE (http://www.dna.affrc.go.jp/) (Liu et al., 2017).

Dual-Luciferase Reporter Assay

To examine the binding activity of DzARF2A to the promoters of ethylene biosynthetic genes, dual-luciferase assay was performed following the method described in Feng et al. (2016). Briefly, genomic DNA was extracted from durian leaves using the cetyltrimethyl ammonium bromide (CTAB)-based method according to Abdel-Latif and Osman (2017). The 2,000-bp promoter regions of ethylene biosynthetic genes of durian; *DzACS* (XM_022901720.1) and *DzACO* (XM_022903265.1) were amplified using the primers listed in **Supplementary Table S2** and cloned into the pGreenII 0800-LUC double-reporter vector (Hellens et al., 2005). For generating the effector construct, the coding sequence of *DzARF2A* was cloned into the pGWB2 expression vector. *A. tumefaciens* (GV3101) harbouring each of the reporter or effector constructs were then co-infiltrated into *N. benthamiana* leaves. After three days, firefly (LUC) and *Renilla* (REN) luciferase activities were measured by a dual-luciferase reporter assay system (Promega, E1910) according to the manufacturer's instructions on a Tecan Infinite 200 PRO microplate reader (TECAN) and the relative LUC/REN ratios were calculated. Four independent biological replicates were used.

RESULTS

Transcriptome-Wide Identification of *ARF*s in Durian

Based on the bioinformatics analysis of the publicly available transcriptomic data from different tissues (stem, root, leaf, and pulp) of the durian cv. Musang King, we identified 15 genes encoding putative ARFs (**Table 1**). The deduced DzARFs ranged

TABLE 1 | List of *DzARF* genes identified by a transcriptome-wide analysis.

Gene name	ORF length (bp)	Protein ID	Protein length (aa)	Molecular weight (KDa)	Isoelectric point (pI)
ARF1	2010	XP_022716380.1	669	74.24	5.64
ARF2A	2556	XP_022739082.1	851	94.35	6.11
ARF2B	2136	XP_022758097.1	711	80.24	7.55
ARF3	2211	XP_022724470.1	736	80.35	6.65
ARF4	2391	XP_022752446.1	796	88.04	6.33
ARF5A	2691	XP_022772671.1	896	98.90	5.10
ARF5B	2844	XP_022769144.1	947	104.32	5.21
ARF6	2706	XP_022720240.1	901	99.72	6.10
ARF7	3429	XP_022732351.1	1142	128.00	6.08
ARF8	2406	XP_022759400.1	801	88.88	5.92
ARF9	2097	XP_022721637.1	698	77.90	6.10
ARF10	2133	XP_022730470.1	710	78.29	8.50
ARF17	1731	XP_022746581.1	576	63.65	5.47
ARF18	2127	XP_022752863.1	708	77.77	8.46
ARF19	3342	XP_022729004.1	1113	123.10	6.25

from 576 (ARF17) to 1142 (ARF7) amino acids in length and varied from 63.65 (ARF17) to 128.00 (ARF7) kDa in molecular weight. Their isoelectric points were between 5.10 (ARF5A) and 8.50 (ARF10), suggesting that they could function in various microenvironments.

Phylogenetic Analysis

To examine the evolutionary relationships between DzARFs and the previously-reported ARFs from the model plants Arabidopsis and tomato, we constructed a NJ phylogenetic tree based on the full-length amino acid sequence similarity and topology of 23 Arabidopsis ARFs (AtARFs) and 18 tomato ARFs (SlARFs), by aligning their full-length protein sequences with 1,000 bootstrap replicates using MEGA X. Our phylogenetic analysis classified DzARFs into three major clades (A, B, and C), which were further classified into 12 subclades (A1, A2, B1, B2, B3, C1, C2, C3, C4, C5, C6, and C7) (**Figure 1A**). Subclades C2, C6, and C7 lacked any DzARFs and harbored AtARFs and/or SlARFs. Group C6 was the biggest subclade and was comprised of eight members, whereas groups C2 and C7 were the smallest ones and harbored only two members in each group.

Multiple Sequence Alignment, Determination of Conserved Motifs and Gene Structure Analysis

Multiple peptide sequence alignment of DzARFs revealed a highly conserved DBD of around 80 amino acids at the N-terminal region (**Figure 1B**). Moreover, these DzARFs contained a middle region that functions as a transcriptional activation or repression domain and a CTD responsible for the protein-protein interactions. Notably, we also identified an unknown domain located at the early N-terminal region of the DzARF protein sequences (**Figure 1B**). Moreover, our *in silico* analyses revealed the presence of a conserved putative mono-partite nuclear localization signal (NLS) at the end of the DBD of all DzARFs which confirmed their localization to the nucleus (**Figure 1B**). Our observation is in line with previous studies which have well documented the occurrence of NLS in members of the ARF TF family (Shen et al., 2010; Yu et al., 2014; Niu et al., 2018; Diao et al., 2020).

By using MEME, we analyzed the protein sequence features of DzARFs and identified at least 10 conserved motifs (**Supplementary Figure S1**). Among these, two novel motifs (1 and 2) were associated with the N-terminal unknown domain. Motifs 3, 4, and 5 were found to be associated with the DBD. The ARF domain corresponded to motifs 6, 7, and 8 and the CTD corresponded to motifs 9 and 10. Notably, the DzARFs in the phylogenetic tree harbored similar motif organization and clustered together (**Supplementary Figure S1**). We also analyzed the exon-intron organization of *DzARF*s and found no introns within the *DzARF*s (**Supplementary Figure S2**). This observation was similar to members of the Dof gene family in durian (*DzDof*s), which harbored no introns (Khaksar et al., 2019).

Tissue-Specific Expression of *DzARF*s

We analyzed the publicly available transcriptomic data on the different tissues (stem, root, leaf, and pulp) from durian cv. Musang King and observed that 12 out of the 15 *DzARF*s (*DzARF1*, *DzARF2A*, *DzARF2B*, *DzARF3*, *DzARF5A*, *DzARF5B*, *DzARF6*, *DzARF7*, *DzARF8*, *DzARF10*, *DzARF17*, and *DzARF19*) were expressed in the fruit pulp (**Figure 2**). This suggests a possible role of these *DzARF*s in the post-harvest ripening of the durian fruit. The three remaining *DzARF*s, including *DzARF4*, *DzARF9*, and *DzARF18* were expressed in other tissues, but not in the fruit pulp (**Figure 2**), suggesting that their roles in fruit ripening seem unlikely.

Differential Expression of the *DzARF*s During Post-Harvest Ripening of Durian cv. Monthong

We used RT-qPCR to verify the expression patterns of *DzARF*s in three stages of the post-harvest ripening (unripe, midripe, and ripe) and identified 12 pulp-expressed *DzARF*s that were similar to those found in the Musang King cultivar. Notably, eight out of these 12 *DzARF*s (*DzARF2A*, *DzARF2B*, *DzARF3*, *DzARF5A*, *DzARF5B*, *DzARF6*, *DzARF7*, and *DzARF19*) harbored a ripening-associated expression pattern and were considered as putative ripening-associated TFs. The expression levels of the remaining four *DzARF*s (*DzARF1*, *DzARF8*, *DzARF10*, and *DzARF17*) did not vary significantly over the course of post-harvest ripening (**Figure 3**) and therefore these four *DzARF*s were not considered as ripening-associated TFs. Among the eight ripening-associated *DzARF* candidates, the *DzARF2A* and *DzARF19* transcripts were up-, while the *DzARF2B*, *DzARF3*, *DzARF5A*, *DzARF5B*, *DzARF6*, and *DzARF7* transcripts were down-regulated during post-harvest ripening. The expression levels of these eight putative ripening-associated *DzARF*s were further investigated under ethylene treatment.

Validating Transcript Levels of Putative Ripening-Associated *DzARF*s Under Three Different Ripening Conditions

Since ethylene plays a key role in climacteric fruit ripening, we analyzed the expression levels of the eight putative ripening-associated *DzARF*s under three different ripening conditions: ethephon-induced, natural, and 1-methylcyclopropane (1-MCP)-delayed ripening. Among these, the expression levels of *DzARF2A* and *DzARF19* were significantly induced under ethephon and suppressed under 1-MCP treatment, compared to those under natural ripening (control). However, the expression levels of *DzARF3* and *DzARF6* were significantly induced by 1-MCP and suppressed by ethephon relative to the control (**Figure 4**). Taken together, these results provide compelling evidence on the ripening-associated roles of these four DzARFs during post-harvest ripening in the durian fruit. Notably, the expression levels of *DzARF2B*, *DzARF5A*, and *DzARF5B* did not vary significantly under ethephon and 1-MCP treatments (compared to the control), so they were not considered as ripening-associated TFs. *DzARF7*, on the other hand, was not expressed under any examined condition, and thus it was also not considered as a ripening-associated TF. Among the validated ripening-associated *DzARF*s, *DzARF2A* displayed a dramatic increase of transcript accumulation under

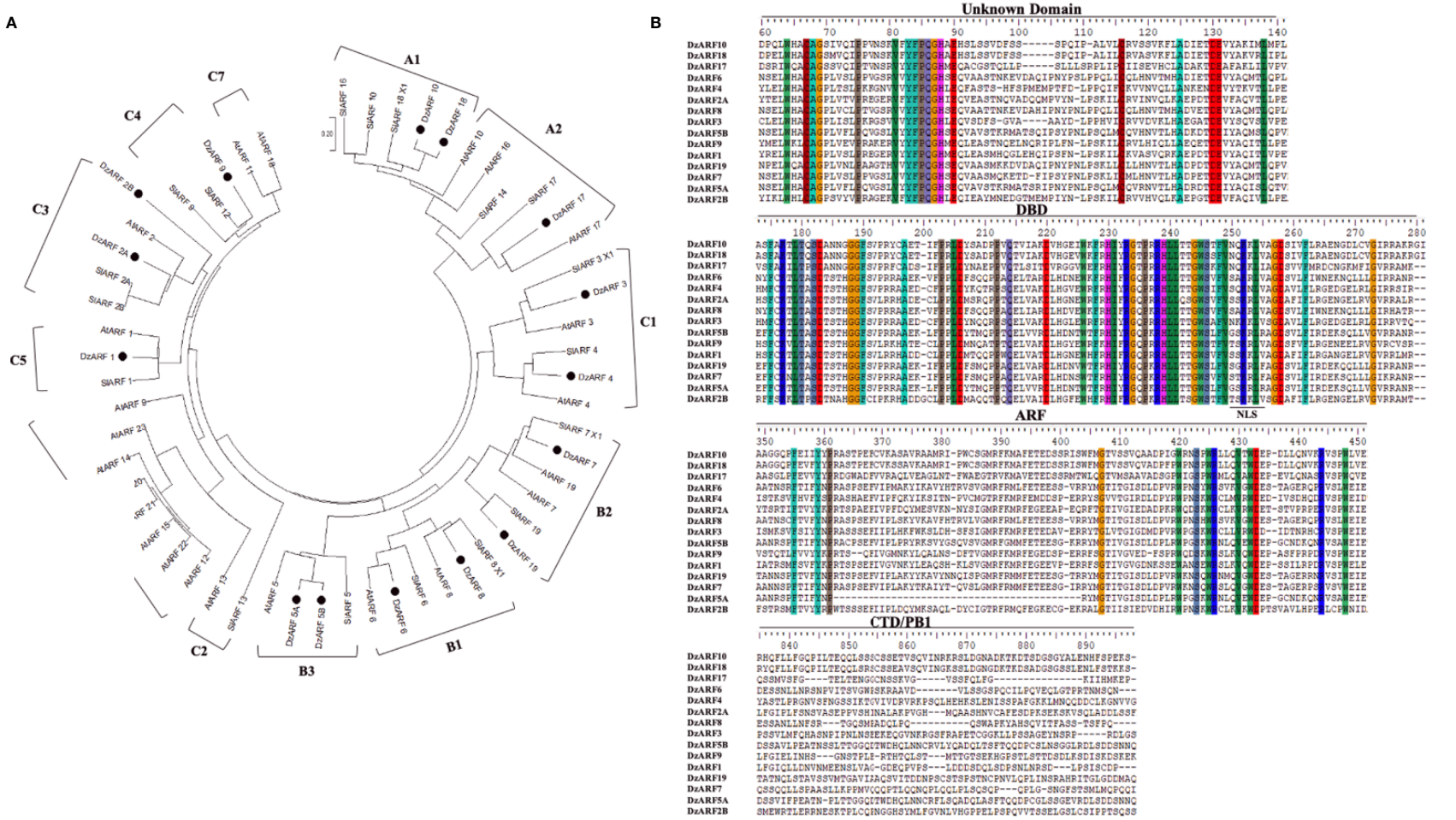

FIGURE 1 | Phylogenetic tree and multiple sequence alignment of the amino acid sequences of the DzARFs. **(A)** The deduced full-length protein sequences of durian ARFs (DzARFs) were aligned with *Arabidopsis thaliana* (AtARFs) and *Solanum lycopersicum* (SlARFs) protein sequences to construct the phylogenetic tree using MEGA X software and the neighbor-joining method (with 1,000 bootstrap replicates, a JTT model and pairwise gap deletion using a bootstrap test of phylogeny with the minimum evolution test and default parameters). **(B)** Multiple sequence alignment analysis was carried out using ClutalW. Identical amino acids are highlighted by color. Only important domains are presented (DBD, DNA binding domain; ARF, auxin response factor domain; CTD/PB1, carboxyl-terminal dimerization/Phox and Bem 1 domain). A nuclear localization signal (NLS) was identified at the end of DBD in all DzARFs.

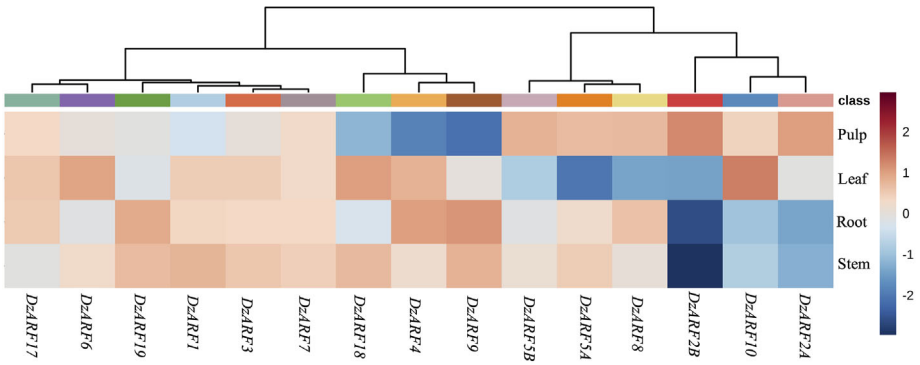

FIGURE 2 | Tissue-specific expression profile of *DzARF*s in Musang King cultivar at ripe stage. The publicly available Illumina RNA-seq data were used to analyze the expression levels of *DzARF*s in root, stem, leaf, and fruit pulp tissues. The higher expression for each gene was presented in red; otherwise, blue was used. Heatmap was generated using MetaboAnalyst 4.0, an open source R-based program. Data were sum normalized, log transformed, and auto scaled.

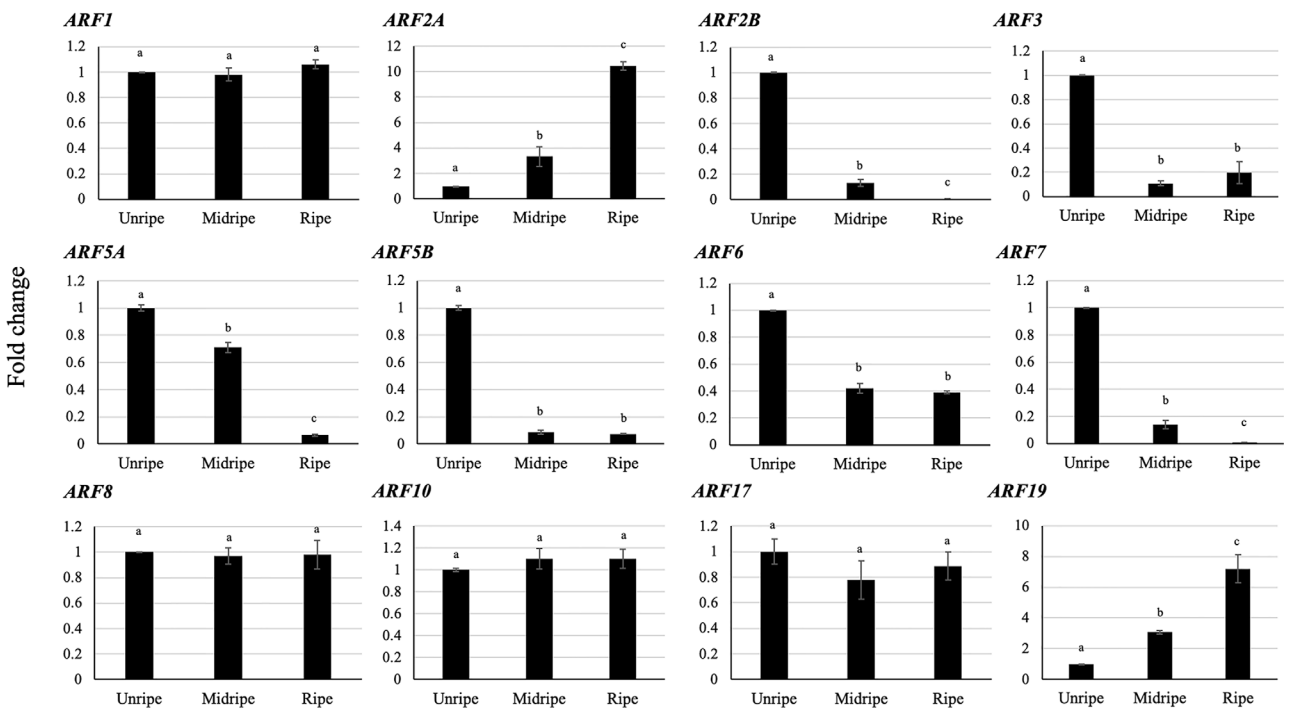

FIGURE 3 | Fold changes in expression levels of *DzARF*s at three different stages (unripe, midripe, and ripe) during post-harvest ripening of durian fruit (Monthong cultivar). The relative gene expression levels were calculated by using the $2^{-\Delta\Delta Ct}$ method and levels were normalized by the geometric mean of reference genes and the unripe stage as control. Three independent biological replicates were used. Bars with different letters show significant differences ($P < 0.05$).

ethephon treatment and it was expressed increasingly during the post-harvest ripening of the durian fruit, suggesting a potential role as a transcriptional activator of ripening. This marked ripening-associated expression pattern of *DzARF2A* prompted its functional characterization to gain a better understanding of its physiological significance during fruit ripening in durian.

According to our phylogenetic analysis, DzARF2A was paired with ARF2 from tomato (SlARF2A and 2B) in subclade C3 (**Figure 1A**). Therefore, SlARF2A seemed to be DzARF2A's closest tomato orthologue. Since down-regulation of *SlARF2A* resulted in ripening defects, decreased levels of climacteric ethylene production, and a decreased expression of the ethylene

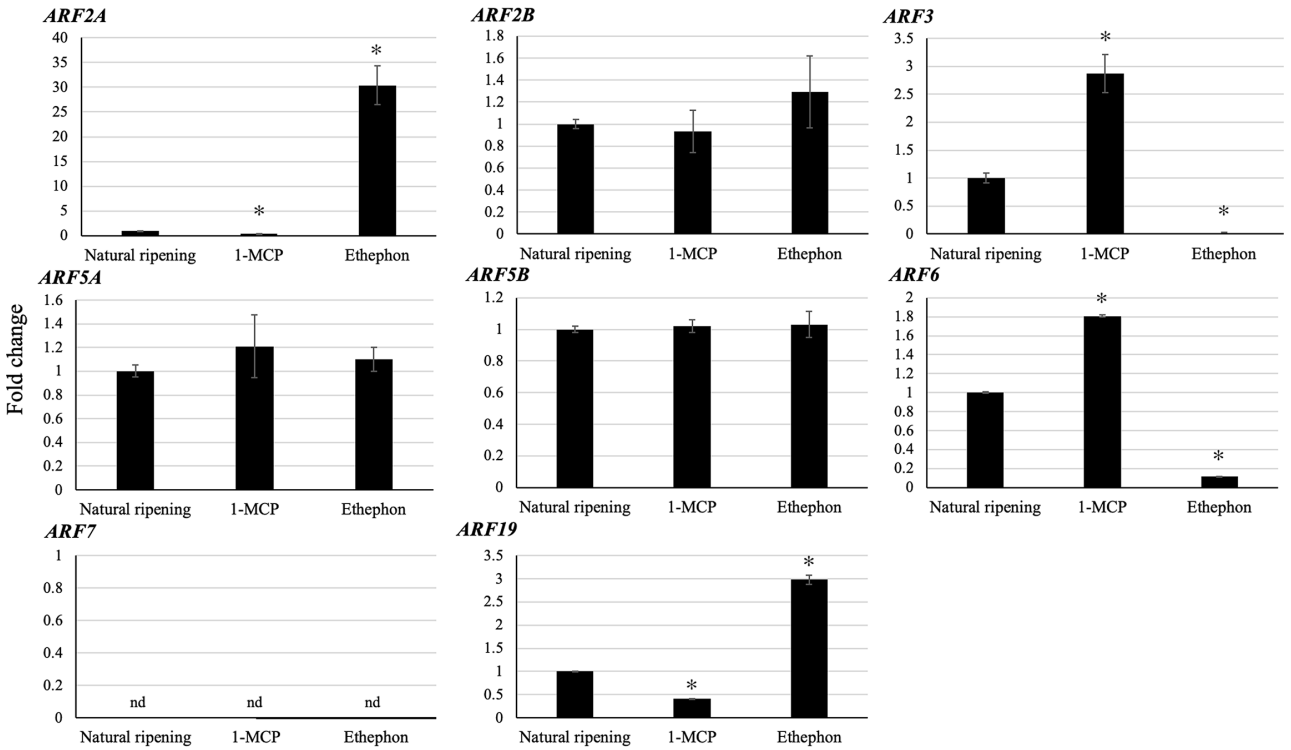

FIGURE 4 | Fold changes in expression levels of eight candidate ripening-associated *DzARF*s under three different ripening conditions. The relative expression levels of candidate ripening-associated *DzARF*s were quantified under three different ripening conditions; natural (control), ethylene-induced, and 1-MCP-delayed ripening by using the $2^{-\Delta\Delta Ct}$ method and levels were normalized by the geometric mean of reference genes and the natural ripening condition as control. Three independent biological replicates were used. An asterisk (*) above the bar indicates a significant difference ($P < 0.05$) (nd = not detected).

biosynthetic genes in tomato (Hao et al., 2015), it raised the possibility of a similar role by DzARF2A in the transcriptional regulation of ethylene biosynthetic genes during fruit ripening in durian.

Transient Expression of *DzARF2A* in *Nicotiana benthamiana*

To gain insights into the *in planta* function of DzARF2A during the post-harvest ripening of durian, we transiently expressed it in *N. benthamiana* leaves. We found a significantly higher expression levels of ethylene biosynthetic genes (*NbACS* and *NbACO*) in the leaves infiltrated with *DzARF2A* compared to the control at day 3 and 5 post-infiltration (**Figure 5A**). In addition, our *in silico* analyses of the 2-kb promoter regions located upstream of the translation start site of *NbACS* and *NbACO* confirmed the existence of cis-regulatory binding sites (TGTCTC) for ARFs (**Supplementary Figure S3**). Notably, the 2-kb upstream region of the transcription start site should cover the putative promoter region of a gene (Jo and Choi, 2019; Liu et al., 2020). We compared the expression levels of *DzARF2A*, *NbACS*, and *NbACO* in the *DzARF2A*-infiltrated leaves between day 3 and 5 and found a strong positive correlation between the expression levels of *DzARF2A* and ethylene biosynthetic genes (**Figure 5A**). Taken together, our results strengthen the possible ripening-associated role of DzARF2A during durian fruit ripening through the transcriptional regulation of ethylene biosynthetic genes. To further confirm this role, the transcriptional activity of DzARF2A was investigated using dual-luciferase reporter assay.

In Vivo Transcriptional Activity of DzARF2A

We performed dual-luciferase assay to evaluate the transcriptional activity of DzARF2A *in vivo*. Our effector plasmid contained the *DzARF2A* under the control of a CaMV35S promoter (pGWB2-*DzARF2A*) whereas our double-reporter vector harbored an internal control REN driven by the CaMV35S promoter and LUC driven by the 2000-bp promoter region of *ACS* (pGreenII-pro*DzACS*) or *ACO* (pGreenII-pro*DzACO*) (**Supplementary Figure S4**). The relative LUC/REN ratios in the leaves co-expressing both effector (pGWB2-*DzARF2A*) and reporter (pGreenII-pro*DzACS* or pGreenII-pro*DzACO*) constructs were compared to the control leaves co-infiltrated with pGWB2-*GFP* and reporter (pGreenII-pro*DzACS* or pGreenII-pro*DzACO*) plasmids. As shown in **Figure 5B**, compared to the control, the co-expression of DzARF2A with each of the two promoters significantly increased the relative LUC/REN ratio, suggesting that DzARF2A trans-activates ethylene biosynthetic genes.

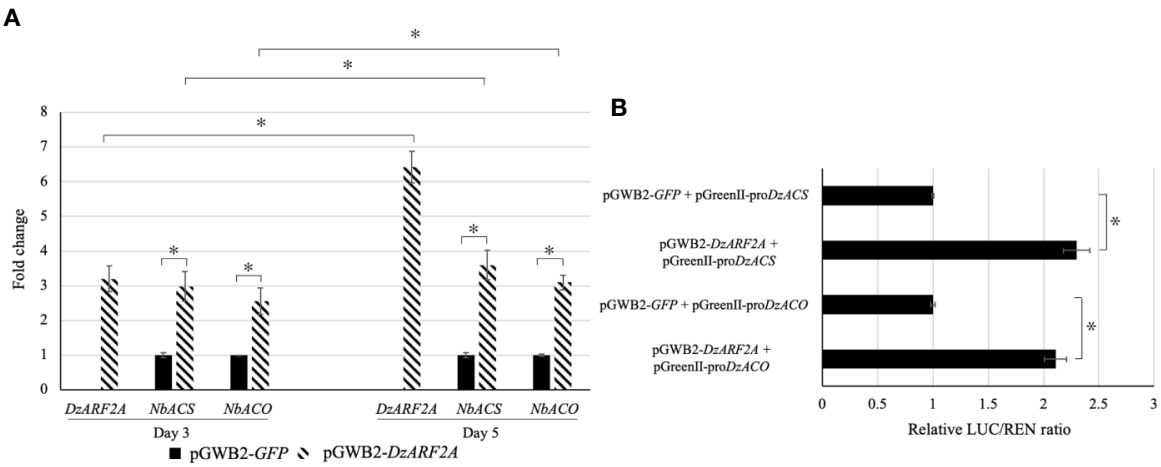

FIGURE 5 | Fold changes in expression levels of *DzARF2A* and ethylene biosynthetic genes in *Nicotiana benthamiana* leaves transiently expressing *DzARF2A* and *in vivo* transcriptional activity of DzARF2A in *N. benthamiana* leaves. **(A)** The relative expression levels of *DzARF2A* and ethylene biosynthetic genes from *N. benthamiana*; ACC synthase (*NbACS*) and ACC oxidase (*NbACO*) were measured in *N. benthamiana* leaves infiltrated with pGWB2-*DzARF2A* (treatment) and pGWB2-*GFP* (control) at three and five days after infiltration by using the $2^{-\Delta\Delta Ct}$ method. The levels were then normalized by the geometric mean of reference genes and the pGWB2-*GFP* as control. Three independent biological replicates were used. An asterisk (*) above the bars indicates a significant difference ($P < 0.05$). In the *DzARF2A*-infiltrated leaves, comparisons were also made between day 3 and day 5. An asterisk (*) above the bars indicates a significant difference between day 3 and day 5 ($P < 0.05$). **(B)** After three days of infiltration, firefly luciferase (LUC) and *Renilla* luciferase (REN) activities were measured and presented as relative LUC/REN ratio. The LUC/REN ratio in the control leaves co-infiltrated with the pGWB2-*GFP* and pGreenII-pro*DzACS* or pGreenII-pro*DzACO* was set as 1 and was used as a calibrator. Error bars represent means ± standard deviations (SD) among four independent biological replicates. An asterisk (*) above the bars indicates a significant difference compared to the control (Student's *t*-test, $P < 0.05$).

Expression Level of Candidate Ripening-Associated *DzARF2A* Among Different Cultivars

It was our great interest to investigate any possible correlation between the expression level of candidate ripening-associated *DzARF2A* during ripening and the ripening behaviors of different durian cultivars. Therefore, we analyzed the expression level of *DzARF2A* in four cultivars; two fast-post-harvest ripening (Chanee and Phuangmanee) and two slow-post-harvest ripening (Monthong and Kanyao) cultivars. We observed a significantly higher expression level of *DzARF2A* in the fast-ripening cultivars compared to the slow-ripening ones (**Figure 6** and **Supplementary Figure S5**). This higher *DzARF2A* expression could therefore enhance the climacteric ethylene biosynthesis through the transcriptional regulation of ethylene biosynthetic genes and thus contribute to the faster ripening of Chanee and Phuangmanee, compared to the Monthong and Kanyao cultivars.

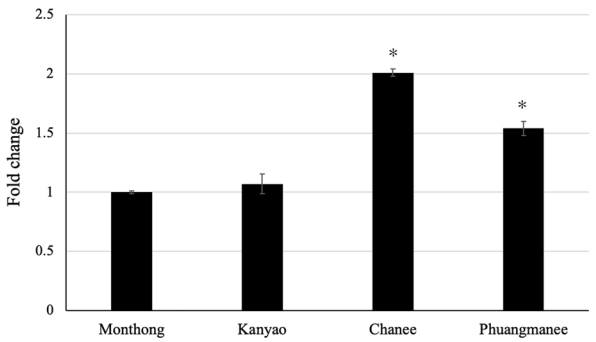

FIGURE 6 | Fold changes in expression level of *DzARF2A* at ripe stage of different durian cultivars. The relative expression level of *DzARF2A* was analyzed in fruit pulps of two fast-ripening (Chanee and Phuangmanee) and two slow-ripening (Monthong and kanyao) cultivars at ripe stage by using the $2^{-\Delta\Delta Ct}$ method and levels were normalized by the geometric mean of reference genes and the Monthong cultivar as control. Three independent biological replicates were used. An asterisk (*) above the bar indicates a significant difference ($P < 0.05$).

Expression Level of *DzARF2A* Under Exogenous Auxin Treatment

In our previous study, we observed an increasing level of auxin during fruit ripening in both Monthong and Chanee cultivars with a significantly higher auxin level in Chanee compared to Monthong (Khaksar et al., 2019). This observation highlighted the possible ripening-associated role of auxin during durian fruit ripening and prompted us to further investigate whether there is a positive correlation between auxin levels and *DzARF2A* expression. Accordingly, we aimed to investigate the auxin inducibility of *DzARF2A* expression. Indeed, the accumulation of *DzARF2A* transcript was induced by exogenous auxin in the leaves of Monthong cultivar. We observed a significantly higher transcript abundance of *DzARF2A* in the leaves with increasing concentration of auxin and expression was significantly higher

than that of the control (mock treatment) (**Figure 7**). Among the three auxin treatments (10, 20, and 40 μMu), exogenous auxin treatment at 40 μM elicited the highest expression of *DzARF2A* (**Figure 7**). Notably, auxin-induced expression of *DzARF2A* also depended on induction time and the highest expression level occurred at 40 μM after 2 h auxin exposure (**Figure 7**). This finding confirmed the auxin responsiveness of *DzARF2A* in a dose- and time-dependent manner. Moreover, it strengthened the possibility that DzARF2A could mediate the post-harvest ripening of durian fruit in harmony with auxin.

We found an increasing expression of *DzARF2A* in the leaves treated with different concentrations of exogenous auxin for 2 h. To further examine any correlation between the expression levels of *DzARF2A* and ethylene biosynthetic genes of durian, we profiled the expression levels of *DzACS* and *DzACO* in those leaves. The expression levels of *DzACS* and *DzACO* were positively correlated with increase in the expression level of *DzARF2A* (**Supplementary Figure S6**), consistent with our observation in *N. benthamiana* leaves (**Figure 5A**).

DISCUSSION

Fruit ripening is described as a well-orchestrated coordination of several steps, marked by major physiological and biochemical changes, and regulated by a complex hormonal network. Ethylene is regarded as the major regulator of climacteric fruit ripening. However, without minimizing the role of ethylene, the putative role of other phytohormones in regulating the climacteric ripening process remains elusive. Auxin, the most ubiquitous hormone in plants, is a crucial phytohormone involved in the regulation of various growth and developmental processes.

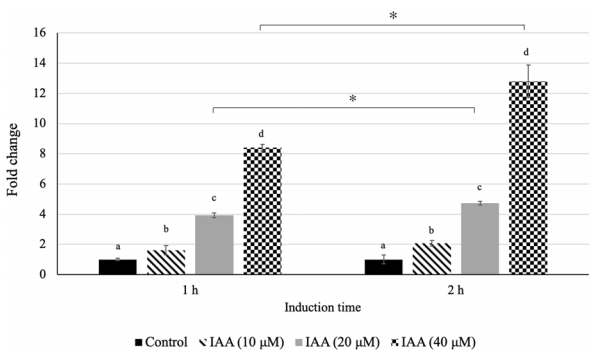

FIGURE 7 | Auxin responsiveness of *DzARF2A*. Fold changes in expression level of *DzARF2A* in young leaves of Monthong cultivar treated with 0 (control), 10, 20, and 40 μM IAA for 1 and 2 h were calculated by using the $2^{-\Delta\Delta Ct}$ method and levels were normalized by the geometric mean of reference genes and the control samples (0 μM IAA). Three independent biological replicates were used for each condition at each timepoint. Different letters indicate significant differences ($P < 0.05$). Comparisons were also made for each condition between the two timepoints; an asterisk (*) above the bars indicates a significant difference for that condition between 1 and 2 h ($P < 0.05$).

In recent years, an increasing body of evidence has pointed towards a possible ripening-associated role of auxin in climacteric fruit ripening, with a number of emerging studies in peach, tomato, and durian. Auxin signaling is known to regulate the expression of early/primary auxin response genes through ARFs. Previous studies have already identified members of the ARF family in crops with economic values (Wang et al., 2007; Kumar et al., 2011; Xing et al., 2011; Luo et al., 2014; Wan et al., 2014; Shen et al., 2015; Hu et al., 2015; Liu et al., 2015; Singh et al., 2017; Tang et al., 2018). According to the Plant Transcription Factor Database (http://planttfdb.cbi.pku.edu.cn), 4,578 members of the ARF gene family exist in the genomes of different plant species in varying numbers; papaya (10), tomato (22), Arabidopsis (37), banana (50), and durian (77). Even though genetic and molecular studies have begun documenting the important roles of ARF gene family members in several aspects of plant growth and development, such as AtARF1, AtARF2, AtARF7, and AtARF8 in Arabidopsis and SlARF3 of tomato, the actual knowledge on the role of ARFs in fruit ripening remains strikingly limited. Durian is a typical climacteric fruit with restricted shelf life after the initiation of ripening. This limits the handling and transportation of the fruit, which can cause significant economic losses to both farmers and consumers. Therefore, a deeper understanding of the molecular mechanisms behind ripening and the different ripening behaviors of durian cultivars (e.g., fast and slow post-harvest ripening) is critical to improve their post-harvest life. Our transcriptome-wide analysis of durian (Musang King cultivar) identified 15 non-redundant members of the ARF gene family. Out of these, our gene expression analysis identified 12 fruit pulp-expressed *DzARF*s during the post-harvest ripening of the Monthong cultivar, from which eight *ARF*s harbored ripening-associated expression patterns (**Figure 3**). The expression levels of these putative ripening-associated *DzARF*s were further examined under three different ripening conditions. The expression levels of *DzARF2A* and *DzARF19* were induced under ethephon and suppressed under 1-MCP (**Figure 4**). The expression of these ethylene-induced *DzARF*s showed an increasing trend during the post-harvest ripening of durian and are speculated to act as transcriptional activators of ripening. Similar to our observation, Hao et al. (2015) identified a member of the ARF gene family in tomato (SlARF2A) which was ethylene-induced and acted as a transcriptional activator of ripening. In contrast, the expression levels of *DzARF3* and *DzARF6* were significantly suppressed under ethylene but induced under 1-MCP and showed a decreasing trend during ripening. According to our knowledge, this is the first report on the inducing effect of 1-MCP on the expression of an ARF gene. Since the inhibition of ethylene biosynthesis (Kieber et al., 1993; Tatsuki and Endo, 2006) and signaling (Hall et al., 2000) by 1-MCP is well documented, a plausible explanation for the upregulation of *DzARF3* and *DzARF6* by 1-MCP through the inhibition of ethylene biosynthesis and signaling is possible since the expression of these two genes was negatively regulated by ethylene. Thus, these two ethylene-repressed *DzARF*s possibly act as transcriptional repressors of ripening. A similar observation was made in our previous study, where we identified both ethylene-induced and ethylene-repressed Dof TFs in durian (Khaksar et al., 2019).

From the validated ripening-associated and ethylene-induced *DzARF*s, the dramatic increase in the expression level of *DzARF2A* under ethylene and its significantly higher expression level during fruit ripening, compared to that of *DzARF19* (**Figure 2**), motivated us to characterize it further. Transient expression of *DzARF2A* in *N. benthamiana* leaves significantly upregulated the expression levels of the ethylene biosynthetic genes (*NbACS* and *NbACO*) (**Figure 5A**), confirming the transcriptional regulation of these genes by DzARF2A. This observation is in line with the results of previous studies on *ARF2*. Specifically, the expression of *ACS* genes was downregulated in the Arabidopsis *arf2* mutant (Okushima et al., 2005) and Hao et al. (2015) showed that tomato fruits under-expressing *SlARF2A/B* produced less climacteric ethylene and exhibited a dramatic down-regulation of the ethylene biosynthetic genes. Our *in silico* analyses of the *ACS* and *ACO* promoter regions from durian and *N. benthamiana* revealed the existence of cis-regulatory binding sites (TGTCTC) that are needed to interact with ARFs (**Supplementary Figures S7** and **S3**). Using dual-luciferase reporter assay, we then confirmed the transcriptional activation ability of DzARF2A (**Figure 5B**). Taken together, these observations strengthen the possible role of DzARF2A in the regulation of fruit ripening through the transcriptional regulation of ethylene biosynthetic genes in durian.

In our previous study, we profiled the expression levels of ethylene biosynthetic genes (*DzACS* and *DzACO*) during durian fruit ripening of Monthong and Chanee cultivars. Both genes were found to express increasingly over the course of ripening in both cultivars (Khaksar et al., 2019). Notably, the increasing expression levels of *DzACS* and *DzACO* were consistent with the expression level of *DzARF2A* during ripening. In addition, we observed significantly higher expression levels of *DzACS* and *DzACO* during post-harvest ripening in Chanee (a fast-ripening cultivar), compared to Monthong (a slow-ripening cultivar) (Khaksar et al., 2019). This observation prompted us to further examine any possible correlation between the expression levels of *DzARF2A* and ethylene biosynthetic genes during durian fruit ripening. We observed a strong positive correlation between the expression levels of *DzARF2A* and ethylene biosynthetic genes (**Figure 5A** and **Supplementary Figure S6**). Moreover, the expression level of *DzARF2A* was positively correlated with the faster post-harvest ripening of durian fruit (**Figure 6**). Thus, higher *DzARF2A* expression would upregulate climacteric ethylene biosynthesis and lead to a faster ripening of the fast-ripening cultivars (Chanee and Phuangmanee) compared to those of the slow-ripening ones (Monthong and Kanyao). To the best of our knowledge, this is the first report on the role of a ripening-associated TF that positively regulates the post-harvest ripening of a climacteric fruit in a cultivar-dependent manner; in other words, the higher the *DzARF2A* expression (in fast-ripening cultivars), the faster the ripening. It has been postulated that the regulatory network mediating fast- and slow-ripening cultivars would involve not only DzARF2A and ethylene as master regulators, but also other TFs and hormones. We observed an exogenous auxin-induced expression pattern of *DzARF2A* in a concentration-dependent manner (**Figure 7**), which was similar to that of *SlARF2A* in tomato (Breitel et al., 2016) and *CpARF2* of papaya (Liu et al., 2015), suggesting that *ARF2* has an evolutionarily conserved function in regulating fruit ripening. Thus, the auxin responsiveness of *ARF2* in these climacteric fruits strengthened the active involvement of auxin during climacteric fruit ripening.

In our previous study, we observed an increasing level of auxin during ripening in both Monthong and Chanee cultivars and a significantly higher auxin level during post-harvest ripening in Chanee over Monthong. This phenomenon coincided with the significantly higher expression levels of auxin biosynthetic genes in Chanee compared to those of Monthong (Khaksar et al., 2019). In addition, we identified the cultivar-dependent DzDof2.2, a member of the Dof TF family, which was expressed at a significantly higher level during ripening in Chanee compared to Monthong. Functional characterization of *DzDof2.2* suggested its role in controlling fruit ripening through the transcriptional regulation of the auxin biosynthetic genes (Khaksar et al., 2019). Based on these previous findings and the results of our current study, DzARF2A might act jointly with DzDof2.2 in a regulatory network to control post-harvest ripening in durian. In the fast-ripening cultivars, higher *DzDof2.2* expression would enhance auxin biosynthesis. Higher auxin level would consequently upregulate the expression of *DzARF2A* and activate the ARF2A-mediated transcription of ethylene biosynthetic genes, leading to a higher climacteric ethylene biosynthesis (auxin-ethylene crosstalk) and faster ripening.

The present study documents for the first time a regulatory network that controls fast and slow post-harvest ripening in different cultivars of a climacteric fruit, in which DzARF2A interconnects signals from ethylene and auxin to fine-tune and to coordinate the initiation of ripening. The relationship between ethylene and auxin in plant growth, development, and fruit senescence has been previously documented (Iqbal et al., 2017). In addition, Bleecker and Kende (2000) pointed out that auxin can stimulate climacteric ethylene biosynthesis through its inductive action on the expression of ethylene biosynthetic genes. Besides the already known role of auxin to induce climacteric ethylene synthesis and thereby to influence ripening, the assumption that auxin would play a direct role during climacteric ripening, even though previously formulated, due to the lack of clear experimental evidence is still somewhat uncertain. A study by El-Sharkawy et al. (2016) suggested a possibly direct role of auxin in plum fruit ripening through the upregulation of several genes encoding cell-wall metabolism-related proteins. However, the intriguing question about which ripening-associated genes could be auxin responsive remains open and needs further investigation.

Often, different TFs control the expression of a particular gene and the fine-tuning of these different TFs occurs through the formation of enhanceosome or repressosome complexes that affect protein–protein and protein–DNA interactions (Martinez and Rao, 2012). Various ripening-associated TFs have been investigated. However, only a few studies have indicated their involvement in fruit ripening, such as the studies in tomato

(Shima et al., 2013; Fujisawa et al., 2014) and in banana (Feng et al., 2016). To the best of our knowledge, there has only been one study that reported a possible ARF interactor in the regulation of ripening. Breitel et al. (2016) identified the ASR1 (ABA STRESS RIPENING-INDUCED 1) protein as a putative ARF2A interactor in tomato fruit. They suggested the possibility that these two proteins could be coordinating the interaction between ethylene and ABA during tomato ripening. The possible interaction between DzARF2A and other TFs, such as DzDof2.2 in controlling fruit ripening in durian could be the subject of a further investigation.

In summary, out of the 15 identified *DzARF*s, 12 were expressed in the fruit pulp. Gene expression analysis revealed differential expression of the fruit pulp-expressed *DzARF*s during post-harvest ripening in the Monthong cultivar. A total of eight *DzARF*s harbored a ripening-associated expression pattern, suggesting a potential role in fruit ripening. Among those, the appealing ripening-associated expression pattern of *DzARF2A* prompted its further functional characterization and confirmed its role in ripening through binding to the promoters of ethylene biosynthetic genes and transcriptionally regulating their expression levels. We observed a positive correlation between the expression level of *DzARF2A* and ripening speed in the fast-ripening cultivars (Chanee and Phuangmanee). Taken together, our results propose DzARF2A as a component of the regulatory network underlying fruit ripening in durian. Thus, the present study on durian suggests another layer in the complex regulatory networks behind fruit ripening and it strengthens the concept that the ripening process relies on the interplay between different transcription factors and hormones. Further functional analysis of DzARF2A in fruits would provide more insights into its ripening-associated role during durian fruit ripening.

DATA AVAILABILITY STATEMENT

The datasets presented in this study can be found in online repositories. Illumina sequencing reads from RNA-Seq study of durian (Musang King cultivar) were retrieved from a public repository database (SRA, Sequence Read Archive) with the following accession numbers: SRX3188225 (root tissue), SRX3188222 (stem tissue), SRX3188226 (leaf tissue), and SRX3188223 (aril/pulp tissue).

AUTHOR CONTRIBUTIONS

SS conceived the research. GK performed the experiments. GK and SS designed the experiments, analyzed the data, and wrote the manuscript. All authors contributed to the article and approved the submitted version.

FUNDING

This research is supported by the Thailand Research Fund (RSA6080021) and Chulalongkorn University (GRU 6203023003-1) (to SS).

ACKNOWLEDGMENTS

This research is supported by Ratchadapisek Somphot Fund for Postdoctoral Fellowship, Chulalongkorn University (to GK). We sincerely thank Tsuyoshi Nakagawa (Shimane University, Japan) for providing the Gateway® expression vector pGWB2, Sophien Kamoun (Sainsbury Laboratory, UK) for providing *A. tumefaciens* GV3101 carrying pJL3:p19, Roger P Hellens (HortResearch, Mt Albert Research Centre, New Zealand) for providing pGreenII 0800-LUC double-reporter vector, Lalida Sangpong for assisting in plant material collection, and Pinnapat Pinsorn and Kittiya Tantisuwanichkul for assisting in genomic DNA extraction.

SUPPLEMENTARY MATERIAL

The Supplementary Material for this article can be found online at: https://www.frontiersin.org/articles/10.3389/fpls.2020.543747/full#supplementary-material

REFERENCES

Abdel-Latif, A., and Osman, G. (2017). Comparison of three genomic DNA extraction methods to obtain high DNA quality from maize. *Plant Methods* 13, 1.

Adams-Phillips, L., Barry, C., and Giovannoni, J. (2004). Signal transduction systems regulating fruit ripening. *Trends Plant Sci.* 9, 331–338.

Alexander, L., and Grierson, D. (2002). Ethylene biosynthesis and action in tomato: a model for climacteric fruit ripening. *J. Exp. Bot.* 53, 2039–2055.

Ayub, R., Guis, M., Ben Amor, M., Gillot, L., Roustan, J. P., Latché, A., et al. (1996). Expression of ACC oxidase antisense gene inhibits ripening of cantaloupe melon fruits. *Nat. Bitechnol.* 14, 862–866.

Bailey, T. L., Boden, M., Buske, F. A., Frith, M., Grant, C. E., Clementi, L., et al. (2009). "MEME SUITE: tools for motif discovery and searching". *Nucleic Acids Res.* 37, 202–208.

Barry, C. S., Llop-Tous, M.II, and Grierson, D. (2000). The regulation of 1-aminocyclopropane-1-carboxylic acid synthase gene expression during the transition from system-1 to system-2 ethylene synthesis in tomato. *Plant Physiol.* 123, 979–986.

Bleecker, A. B., and Kende, H. (2000). Ethylene: a gaseous signal molecule in plants. *Ann. Rev. Cell Dev. Biol.* 16, 1–18.

Breitel, D. A., Chappell-Maor, L., Meir, S., Panizel, I., Puig, C. P., Hao, Y., et al. (2016). AUXIN RESPONSE FACTOR 2 intersects hormonal signals in the regulation of tomato fruit ripening. *PloS Genet.* 12, e1005903.

Bustin, S. A., Benes, V., Garson, J. A., Hellemans, J., Huggett, J., Kubista, M., et al. (2009). The MIQE guidelines: minimum information for publication of quantitative real-time PCR experiments. *Clin. Chem.* 55, 611–622.

Chong, J., Soufan, O., Li, C., Caraus, I., Li, S., Bourque, G., et al. (2018). MetaboAnalyst 4.0: towards more transparent and integrative metabolomics analysis. *Nucleic Acids Res.* 46, 486–494.

Diao, D., Hu, X., Guan, D., Wang, W., Yang, H., and Liu, Y. (2020). Genome-wide identification of the ARF (auxin response factor) gene family in peach and their expression analysis. *Mol. Biol. Rep.* 47, 4331–4344.

Ellis, C. M., Nagpal, P., Young, J. C., Hagen, G., Guilfoyle, T. J., and Reed, J. W. (2005). AUXIN RESPONSE FACTOR1 and AUXIN RESPONSE FACTOR2 regulate senescence and floral organ abscission in Arabidopsis thaliana. *Development* 132, 4563–4574.

El-Sharkawy, I., Sherif, S., Qubbaj, T., Sullivan, A. J., and Jayasankar, S. (2016). Stimulated auxin levels enhance plum fruit ripening, but limit shelf-life characteristics. *Postharvest Biol. Tec.* 112, 215–223.

Feng, B. H., Han, Y. C., Xiao, Y. Y., Kuang, J. F., Fan, Z. Q., Chen, J. Y., et al. (2016). The banana fruit Dof transcription factor MaDof23 acts as a repressor and interacts with MaERF9 in regulating ripening-related genes. *J. Exp. Bot.* 67, 2263–2275.

Fujisawa, M., Shima, Y., Nakagawa, H., Kitagawa, M., Kimbara, J., Nakano, T., et al. (2014). Transcriptional regulation of fruit ripening by tomato FRUITFULL homologs and associated MADS box proteins. *Plant Cell.* 26, 89–101.

Gillaspy, G., Ben-David, H., and Gruissem, W. (1993). Fruits: a develop- mental perspective. *Plant Cell.* 5, 1439–1451.

Goetz, M., Vivian-Smith, A., Johnson, S. D., and Koltunow, A. M. (2006). AUXIN RESPONSE FACTOR8 is a negative regulator of fruit initiation in Arabidopsis. *Plant Cell.* 18, 1873–1886.

Guilfoyle, T. J., and Hagen, G. (2007). Auxin response factors. *Curr. Opin. Plant Biol.* 10, 453–460.

Guilfoyle, T. J., and Hagen, G. (2012). Getting a grasp on domain III/IV responsible for auxin response factor–IAA protein interactions. *Plant Sci.* 190, 82–88.

Guilfoyle, T. J. (2015). The PB1 domain in auxin response factor and Aux/IAA proteins: a versatile protein interaction module in the auxin response. *Plant Cell* 27, 33–43.

Hagen, G., and Guilfoyle, T. (2002). Auxin-responsive gene expression: genes, promoters and regulatory factors. *Plant Mol. Biol.* 49, 373–385.

Hall, A. E., Findell, J. L., Schaller, G. E., Sisler, E. C., and Bleecker, A. B. (2000). Ethylene perception by the ERS1 protein in Arabidopsis. *Plant Physiol.* 123, 1449–1457.

Hao, Y., Hu, G., Breitel, D., Liu, M., Mila, I., Frasse, P., et al. (2015). Auxin Response Factor SlARF2 Is an Essential Component of the Regulatory Mechanism Controlling Fruit Ripening in Tomato. *PloS Genet.* 11, e1005649.

Harper, R. M., Stowe-Evans, E. L., Luesse, D. R., Muto, H., Tatematsu, K., Watahiki, M. K., et al. (2000). The NPH4 locus encodes the auxin response factor ARF7, a conditional regulator of differential growth in aerial Arabidopsis tissue. *Plant Cell.* 12, 757–770.

Hellens, R., Allan, A., Friel, E., Bolitho, K., Grafton, K., Templeton, M., et al. (2005). Transient expression vectors for functional genomics, quantification of promoter activity and RNA silencing in plants. *Plant Methods* 1, 13.

Hu, W., Zuo, J., Hou, X., Yan, Y., Wei, Y., Liu, J., et al. (2015). The auxin response factor gene family in banana: genome-wide identification and expression analyses during development, ripening, and abiotic stress. *Front. Plant Sci.* 6, 742.

Iqbal, N., Khan, N. A., Ferrante, A., Trivellini, A., Francini, A., and Khan, M.II (2017). Ethylene Role in Plant Growth, Development and Senescence: Interaction with Other Phytohormones. *Front. Plant Sci.* 8, 475.

Jo, S. S., and Choi, S. S. (2019). Enrichment of rare alleles within epigenetic chromatin marks in the first intron. *Genomics Inform.* 17, e9.

Jones, B., Frasse, P., Olmos, E., Zegzouti, H., Li, Z. G., Latché, A., et al. (2002). Down-regulation of DR12, an auxin- response-factor homolog, in the tomato results in a pleiotropic phenotype including dark green and blotchy ripening fruit. *Plant J.* 32, 603–613.

Khaksar, G., Sangchay, W., Pinsorn, P., Sangpong, L., and Sirikantaramas, S. (2019). Genome-wide analysis of the Dof gene family in durian reveals fruit ripening-associated and cultivar-dependent Dof transcription factors. *Sci. Rep.* 9, 12109.

Kieber, J. J., Rothenberg, M., Roman, G., Feldmann, K. A., and Ecker, J. R. (1993). CTR1, a negative regulator of the ethylene response pathway in Arabidopsis, encodes a member of the Raf family of protein kinases. *Cell* 72, 427–441.

Kumar, R., Tyagi, A. K., and Sharma, A. K. (2011). Genome-wide analysis of auxin response factor (ARF) gene family from tomato and analysis of their role in flower and fruit development. *Mol. Gen. Genet.* 285, 245–260.

Kumar, S., Stecher, G., Li, M., Knyaz, C., and Tamura, K. (2018). MEGA X: Molecular evolutionary genetics analysis across computing platforms. *Mol. Biol. Evol.* 35, 1547–1549.

Lelievre, J.-M., Latche, A., Jones, B., Bouzayen, M., and Pech, J.-C. (1997). Ethylene and fruit ripening. *Physiol. Plant* 101, 727–739.

Liu, K., Yuan, C., Li, H., Lin, W., Yang, Y., Shen, C., et al. (2015). Genome-wide identification and characterization of auxin response factor (ARF) family genes related to flower and fruit development in papaya (*Carica papaya* L.). *BMC Genomics* 16, 901.

Liu, K., Yuan, C., Feng, S., Zhong, S., Li, H., Zhong, J., et al. (2017). Genome-wide analysis and characterization of Aux/IAA family genes related to fruit ripening in papaya (*Carica papaya* L.). *BMC Genomics* 18, 351.

Liu, P., Wang, S., Wang, X., Yang, X., Li, Q., Wang, C., et al. (2020). Genome-wide characterization of two-component system (TCS) genes in melon (*Cucumis melo* L.). *Plant Physiol. Biochem* 151, 197–213.

Livak, K. J., and Schmittgen, T. D. (2001). Analysis of relative gene expression data using real-time quantitative PCR and the 2(-Delta Delta C(T)) Method. *Methods* 4, 402–408.

Luo, X. C., Sun, M. H., Rui, X. U., Shu, H. R., Wang, J. W., and Zhang, S. Z. (2014). Genome wide identification and expression analysis of the ARF gene family in apple. *J. Genet.* 93, 785–797.

Martinez, G. J., and Rao, A. (2012). Immunology. Cooperative transcription factor complexes in control. *Science* 338, 891–892.

Miller, A. N., Walsh, C. S., and Cohen, J. D. (1987). Measurement of indole- 3-acetic acid in peach fruits (*Prunus persica* L. Batsch cv. Redhaven) during development. *Plant Physiol.* 84, 491–494.

Nanao, M. H., Vinos-Poyo, T., Brunoud, G., Thévenon, E., Mazzoleni, M., Mast, D., et al. (2014). Structural basis for oligomerization of auxin transcriptional regulators. *Nat. Commun.* 5, 3617.

Niu, J., Bi, Q., Deng, S., Chen, H., Yu, H., Wang, L., et al. (2018). Identification of AUXIN RESPONSE FACTOR gene family from *Prunus sibirica* and its expression analysis during mesocarp and kernel development. *BMC Plant Biol.* 18, 21.

Okushima, Y., Mitina, I., Quach, H., and Theologis, A. (2005). AUXIN RESPONSE FACTOR 2 (ARF2): a pleiotropic developmental regulator. *Plant J.* 43, 29–46.

Pinsorn, P., Oikawa, A., Watanabe, M., Sasaki, R., Ngamchuachit, P., Hoefgen, R., et al. (2018). Metabolic variation in the pulps of two durian cultivars: Unraveling the metabolites that contribute to the flavor. *Food Chem.* 268, 118–125.

Qi, Y., Wang, S., Shen, C., Zhang, S., Chen, Y., Xu, Y., et al. (2013). OsARF12, a transcription activator on auxin response gene, regulates root elongation and affects iron accumulation in rice (*Oryza sativa*). *New Phytol.* 193, 109–120.

Shen, C., Wang, S., Bai, Y., Wu, Y., Zhang, S., Chen, M., et al. (2010). Functional analysis of the structural domain of ARF proteins in rice (*Oryza sativa* L.). *J. Exp. Bot.* 61, 3971–3981.

Shen, C., Wang, S., Zhang, S., Xu, Y., Qian, Q., Qi, Y., et al. (2013). OsARF16, a transcription factor, is required for auxin and phosphate starvation response in rice (*Oryza sativa* L.). *Plant Cell Environ.* 36, 607–620.

Shen, C., Yue, R., Sun., T., Zhang, L., Xu, L., Tie, S., et al. (2015). Genome-wide identification and expression analysis of auxin response factor gene family in *Medicago truncatula*. *Front. Plant Sci.* 6, 73.

Shima, Y., Kitagawa, M., Fujisawa, M., Nakano, T., Kato, H., Kimbara, J., et al. (2013). Tomato FRUITFULL homologues act in fruit ripening via forming MADS-box transcription factor complexes with RIN. *Plant Mol. Biol.* 82, 427–438.

Singh, V. K., Rajkumar, M. S., Garg, R., and Jain, M. (2017). Genome-wide identification and co-expression network analysis provide insights into the roles of auxin response factor gene family in chickpea. *Sci. Rep.* 7, 10895.

Steibel, J. P., Poletto, R., Coussens, P. M., and Rosa, G. J. M. (2009). A powerful and flexible linear mixed model framework for the analysis of relative quantification RT-PCR data. *Genomics* 94, 146–152.

Tang, Y., Bao, X., Liu, K., Wang, J., Zhang, J., Feng, Y., et al. (2018). Genome-wide identification and expression profiling of the auxin response factor (ARF) gene family in physic nut. *PloS One* 13, e0201024.

Tatsuki, M., and Endo, A. (2006). Analyses of expression patterns of ethylene receptor genes in apple (*Malus domestica* Borkh.) fruits treated with or without 1-methylcyclopropene (1-MCP). *J. Japan Soc Hortic. Sci.* 75, 481–487.

Ulmasov, T., Hagen, G., and Guilfoyle, T. J. (1997). ARF1, a transcription factor that binds to auxin response elements. *Science* 276, 1865–1868.

Vandesompele, J., De Preter, K., Pattyn, F., Poppe, B., Van Roy, N., De Paepe, A., et al. (2002). Accurate normalization of real-time quantitative RT- PCR data by geometric averaging of multiple internal control genes. *Genome Biol.* 3, RESEARCH0034.

Wan, S., Li, W., Zhu, Y., Liu, Z., Huang, W., and Zhan, J. (2014). Genome-wide identification, characterization and expression analysis of the auxin response factor gene family in *Vitis vinifera*. *Plant Cell Rep.* 33, 1365–1375.

Wang, D., Pei, K., Fu, Y., Sun, Z., Li, S., Liu, H., et al. (2007). Genome-wide analysis of the auxin response factors (ARF) gene family in rice (*Oryza sativa*). *Gene* 394, 13–24.

Wang, A., Yamakake, J., Kudo, H., Wakasa, Y., Hatsuyama, Y., Igarashi, M., et al. (2009). Null mutation of the *MdACS3* gene, coding for a ripening-specific 1-aminocyclopropane-1-carboxylate synthase, leads to long shelf life in apple fruit. *Plant Physiol.* 151, 391–399.

Woodward, A. W., and Bartel, B. (2005). Auxin, regulation, action, and interaction. *Ann. Bot.* 95, 707–735.

Xie, Y. H., Zhu, B. Z., Yang, X. L., Zhang, H. X., Fu, D. Q., Zhu, H. L., et al. (2006). Delay of post-harvest ripening and senescence of tomato fruit through virus-induced *LeACS2* gene silencing. *Postharvest Biol. Technol.* 42, 8–15.

Xing, H., Pudake, R. N., Guo, G., Xing, G., Hu, Z., Zhang, Y., et al. (2011). Genome-wide identification and expression profiling of auxin response factor (ARF) gene family in maize. *BMC Genomics* 12, 178.

Yu, H., Soler, M., Mila, I., San Clemente, H., Savelli, B., Dunand, C., et al. (2014). Genome-wide characterization and expression profiling of the AUXIN RESPONSE FACTOR (ARF) gene family in *Eucalyptus grandis*. *PloS One* 9, e108906.

Zhang, X., Yan, F., Tang, Y., Yuan, Y., Deng, W., and Li, Z. (2015). Auxin response gene SlARF3 plays multiple roles in tomato development and is involved in the formation of epidermal cells and trichomes. *Plant Cell Physiol.* 56, 2110–2124.

Conflict of Interest: The authors declare that the research was conducted in the absence of any commercial or financial relationships that could be construed as a potential conflict of interest.

frontiers in Plant Science

REVIEW
published: 27 October 2020
doi: 10.3389/fpls.2020.543958

Beyond Ethylene: New Insights Regarding the Role of Alternative Oxidase in the Respiratory Climacteric

Seanna Hewitt[1,2] *and Amit Dhingra*[1,2]*

[1]*Molecular Plant Sciences Program, Washington State University, Pullman, WA, United States,* [2]*Department of Horticulture, Washington State University, Pullman, WA, United States*

Climacteric fruits are characterized by a dramatic increase in autocatalytic ethylene production that is accompanied by a spike in respiration at the onset of ripening. The change in the mode of ethylene production from autoinhibitory to autostimulatory is known as the System 1 (S1) to System 2 (S2) transition. Existing physiological models explain the basic and overarching genetic, hormonal, and transcriptional regulatory mechanisms governing the S1 to S2 transition of climacteric fruit. However, the links between ethylene and respiration, the two main factors that characterize the respiratory climacteric, have not been examined in detail at the molecular level. Results of recent studies indicate that the alternative oxidase (AOX) respiratory pathway may play an essential role in mediating cross-talk between ethylene response, carbon metabolism, ATP production, and ROS signaling during climacteric ripening. New genomic, metabolic, and epigenetic information sheds light on the interconnectedness of ripening metabolic pathways, necessitating an expansion of the current, ethylene-centric physiological models. Understanding points at which ripening responses can be manipulated may reveal key, species- and cultivar-specific targets for regulation of ripening, enabling superior strategies for reducing postharvest wastage.

Keywords: alternative oxidase, fruit, ethylene, respiration, climacteric ripening, glyoxylic acid, tricarboxylic acid cycle, metabolism

OPEN ACCESS

Edited by:
Noam Alkan, Agricultural Research Organization (ARO), Israel

Reviewed by:
Bram Van De Poel, KU Leuven, Belgium
Carlos H. Crisosto, University of California, Davis, United States

***Correspondence:**
Amit Dhingra
adhingra@wsu.edu

Specialty section:
This article was submitted to Crop and Product Physiology, a section of the journal Frontiers in Plant Science

Received: *08 April 2020*
Accepted: *24 September 2020*
Published: *27 October 2020*

Citation:
Hewitt S and Dhingra A (2020) Beyond Ethylene: New Insights Regarding the Role of Alternative Oxidase in the Respiratory Climacteric. Front. Plant Sci. 11:543958. doi: 10.3389/fpls.2020.543958

INTRODUCTION

Ripening of fruit involves a symphony of transcriptionally and hormonally controlled processes that result in the accumulation of sugars, reduction in acidity, development of aroma, and nutritional profiles (McAtee et al., 2013; Cherian et al., 2014). The ripening process has been under continual manipulation both as a result of natural selection for improved seed dispersal as well as human domestication via the selection of desirable organoleptic properties (Giovannoni, 2004; Liu M. et al., 2015).

Fleshy fruits fall into one of two broadly defined ripening categories, climacteric and nonclimacteric, based on their respiratory profile as well as the manner in which they produce the phytohormone ethylene (Seymour et al., 2012). Nonclimacteric fruits respire and produce ethylene at basal levels throughout fruit maturation and senescence. This mode of ethylene production is termed System 1 (S1) ethylene production. Nonclimacteric fruits, including cherries,

berries, and citrus, are harvested ripe and do not exhibit increasing levels of ethylene production during ripening, although in a few cultivars, ripening may be accelerated through exogenous application of ethylene or ethylene-producing compounds, such as ethrel (Barry et al., 2000; Barry and Giovannoni, 2007; Chen et al., 2018). In contrast, ripening in climacteric fruits, such as apple, pear, banana, papaya, avocado, mango, and tomato, is characterized by a burst of respiration accompanied by a substantial increase in ethylene biosynthesis as fruit transitions from S1 to System 2 (S2) ethylene production (**Figure 1**; Osorio et al., 2013b; Chen et al., 2018). The synchronization of the hallmark respiratory rise with autocatalytic ethylene production forms the basis for the modern understanding of climacteric ripening (Lelièvre et al., 1997; Cara and Giovannoni, 2008). Because of this distinct ripening physiology, climacteric fruits can be harvested unripe and ripened off the tree or vine (Seymour et al., 2013a; Hiwasa-Tanase and Ezura, 2014). Following the respiratory climacteric, ripening proceeds rapidly and irreversibly, which presents additional challenges to the storage and preservation of climacteric fruit after harvest (Jogdand et al., 2017). While the concept of two distinct ripening categories is simple in theory, the reality is far more complex, with certain fruits displaying variable phenotypes (Paul et al., 2012). Interestingly, some cultivars within the same species display differences in ripening profiles; such is the case for, peach, plum, melon, and Chinese pear (Yamane et al., 2007; Minas et al., 2015; Saladié et al., 2015; Farcuh et al., 2018). This is clearly exemplified in Japanese plum (*Prunus salicina* Lindl.), where a nonclimacteric cultivar and an ethylene-responsive, suppressed-climacteric cultivar were both found to be derived from independent bud sport mutations in a single climacteric plum variety (Minas et al., 2015). This discovery suggests that

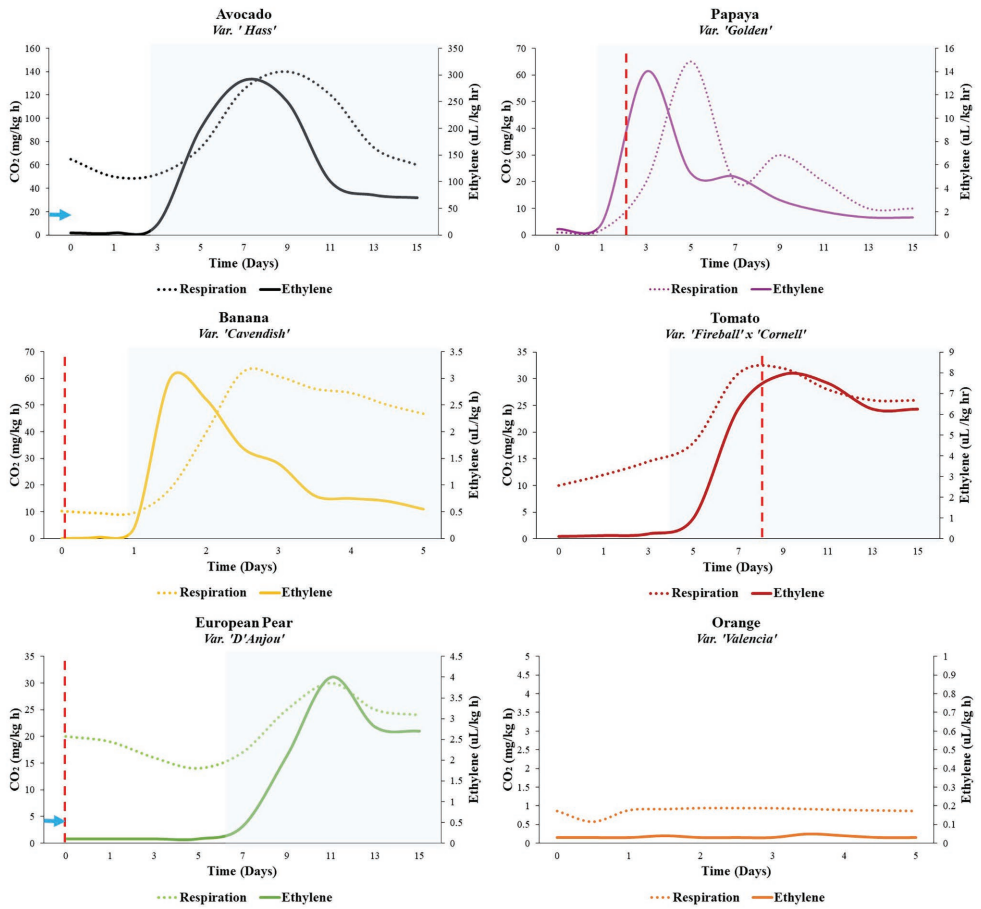

FIGURE 1 | Ripening profiles of five climacteric fruits and one nonclimactic fruit. Rates of ethylene production and respiration are indicated by the solid and dotted lines, respectively. At the 0-day time point, fruits were unripe but assumed to have reached physiological maturity and 100% ripening competency. Some fruits require cold conditioning in order to achieve ripening competency (e.g., European pear, 15–90 days, 0–10°C) (solid blue arrow). Other fruits can be induced to ripen more quickly through appropriate cold storage (e.g., avocado, 14 days, 5–10°C; dashed blue arrow; Eaks, 1983). Expression and activity of alternative oxidase (AOX) have been implicated in preclimacteric and/or climacteric stages of some fruits (e.g., European pear, papaya, banana, and tomato; Woodward et al., 2009; Oliveira et al., 2015; Hendrickson et al., 2019; Hewitt et al., 2020b). Peak AOX expression, as indicated in the cited studies, is indicated by vertical dashed red lines. The transition from white to shaded background represents the transition from S1 to S2 ethylene (preclimacteric to climacteric shift). General respiration and ethylene profiles for each fruit were adapted from the following studies: avocado (Eaks, 1983), banana (McMurchie et al., 1972), European pear (Wang and Mellenthin, 1972), papaya (Fabi et al., 2007), tomato (Herner and Sink, 1973), orange (McMurchie et al., 1972).

the basis for the distinction between climacteric versus nonclimacteric ripening is highly specific at the genetic level. Furthermore, such systems provide natural models that could facilitate study of the biological basis for climacteric and nonclimacteric ripening (Kim H. -Y. et al., 2015; Minas et al., 2015; Fernandez i Marti et al., 2018).

Transcriptional and phytohormonal regulation of ethylene-dependent ripening have been reviewed extensively (Cherian et al., 2014; Karlova et al., 2014; Kumar et al., 2014; Chen et al., 2018). In contrast to climacteric fruit, the regulatory network involved in nonclimacteric ripening has been much less studied. Nevertheless, it is known that abscisic acid (ABA) and polyamines, rather than ethylene, play essential roles in ripening in nonclimacteric fruits (Li et al., 2011; Jia et al., 2016a). Studies in strawberry and tomato indicate that the split between climacteric and nonclimacteric ripening responses lies in the way that S-adenosyl-L-methionine (SAM) is preferentially utilized as a precursor to ethylene or as a substrate for polyamine biosynthesis (Van de Poel et al., 2013; Lasanajak et al., 2014; Guo et al., 2018). Decarboxylation of SAM by decarboxylase (SAMDC) represents the rate-limiting step in polyamine biosynthesis (Handa and Mattoo, 2010; Seymour et al., 2013b; Cherian et al., 2014). Moreover, transgenic expression of a yeast SAMDC in tomato results in preferential shunting of substrate into the polyamine biosynthesis pathway, rather than the ethylene biosynthesis pathway (Lasanajak et al., 2014). In addition to increased flux through the polyamine biosynthesis pathway, overexpression of SAMDC in strawberry leads to spermine and spermidine-mediated increase in expression of positive regulators of ABA biosynthesis and signaling (Guo et al., 2018). Signaling components downstream of ABA receptors are believed to induce changes in the expression of genes associated with pigment development and sugar metabolism (Li et al., 2011).

Through the exploration of the underlying genetic factors of ripening of both climacteric and nonclimacteric fruit in model systems, foundations have been laid for evaluation of ripening processes in nonmodel fruits exhibiting deviations from the standard profiles. Not surprisingly, manipulation of environmental factors, genetic factors, and use of chemical inhibitors like 1-methylcyclopropene (1-MCP) to inhibit ripening result in developmental patterns that do not follow the classical model of ethylene response and signaling (Watkins, 2006, 2015; Tatsuki et al., 2007; Chiriboga et al., 2013). Mechanisms for blockage and/or bypass of the concerted steps in classical ethylene biosynthesis are beginning to be elucidated as more studies examine how genetic manipulation or stimulation via temperature or chemical application affect ripening (Klee and Giovannoni, 2011; Hewitt et al., 2020a,b). Furthermore, as molecular biology, transcriptomics, and epigenetic analysis tools have rapidly advanced, new insights have been gained into some of the master regulators of ripening acting upstream and/or independently of ethylene (Liu R. et al., 2015; Giovannoni et al., 2017).

The alternative oxidase (AOX) respiratory pathway has recently garnered interest as a potential target for ripening manipulation (Hendrickson et al., 2019; Hewitt et al., 2020a,b). This review will explore AOX as a branch point for variation from the classical model of climacteric ripening, which may be affected by physiological or chemical perturbations in metabolism, transcriptional regulatory elements, and epigenetic signatures regulating fruit ripening. Understanding these variations is expected to inform novel strategies to reduce postharvest waste while improving marketability of fruit efficiently.

Reexamining the Classical Model for Ethylene-Dependent Ripening

Early knowledge of the role of ethylene in the ripening process made components of ethylene biosynthesis and transduction some of the first targets for ripening control in model systems such as tomato (*Solanum lycopersicum*) (Barry and Giovannoni, 2007; Klee and Giovannoni, 2011; Liu M. et al., 2015; Mattoo and White, 2018). Resulting as a side product of methionine cycling (Yang and Hoffman, 1984), ethylene biosynthesis begins with the conversion of L-methionine into SAM. SAM is then converted into 5'-methylthioadenosine (MTA) and 1-aminocyclopropane carboxylate (ACC) via ACC synthase (ACS). ACC is subsequently converted into ethylene by 1-aminocyclopropane carboxylate oxidase (ACO). ACC, long known for its role as the immediate precursor to ethylene, has recently been investigated for its potential role in ethylene-independent regulation of growth (Polko and Kieber, 2019; Vanderstraeten et al., 2019). Following successful perception of ethylene, the hormone signal is transduced via a series of messengers to the nucleus where ethylene-responsive transcription factors (ERFs) activate downstream ripening-associated genes involved in cell wall softening, starch to sugar conversion, aroma production, and changes in pigmentation, among numerous other changes (Seymour et al., 2012; Osorio et al., 2013a; Cherian et al., 2014; Gao et al., 2020).

While ethylene is important in ripening, the associated hormone perception and signaling pathways do not operate in isolation (McAtee et al., 2013); they may be dependent on other processes or manipulated by altering preripening conditions (**Figure 2**). Some fruits require a period of cold temperature exposure, known as "conditioning," in order for ripening to commence (Hartmann et al., 1987). European pear (*Pyrus communis*), for example, must undergo between 15 and 90 days (depending on the cultivar) of conditioning at 0–10°C to activate the S2 autocatalytic ethylene biosynthesis (Villalobos-Acuna and Mitcham, 2008; Hendrickson et al., 2019; **Figure 1**). Other fruits do not require conditioning to ripen but can be induced to ripen more quickly through appropriate cold storage regimes. Kiwifruit subjected to cold conditioning, upon transfer to room temperature, respires faster, and softens appreciably in comparison to fruits subjected to ethylene preconditioning alone (Ritenour et al., 1999). In 'Hass' avocado, for example, exposure to moderate chilling temperatures of 5–10°C for 2 weeks results in the early onset of the respiratory climacteric by 2–7 days in comparison with control fruits stored at 20°C, without any negative impacts. However, longer storage and colder storage temperatures result in a reduced climacteric response and development of symptoms of chilling injury in avocado (Eaks, 1983).

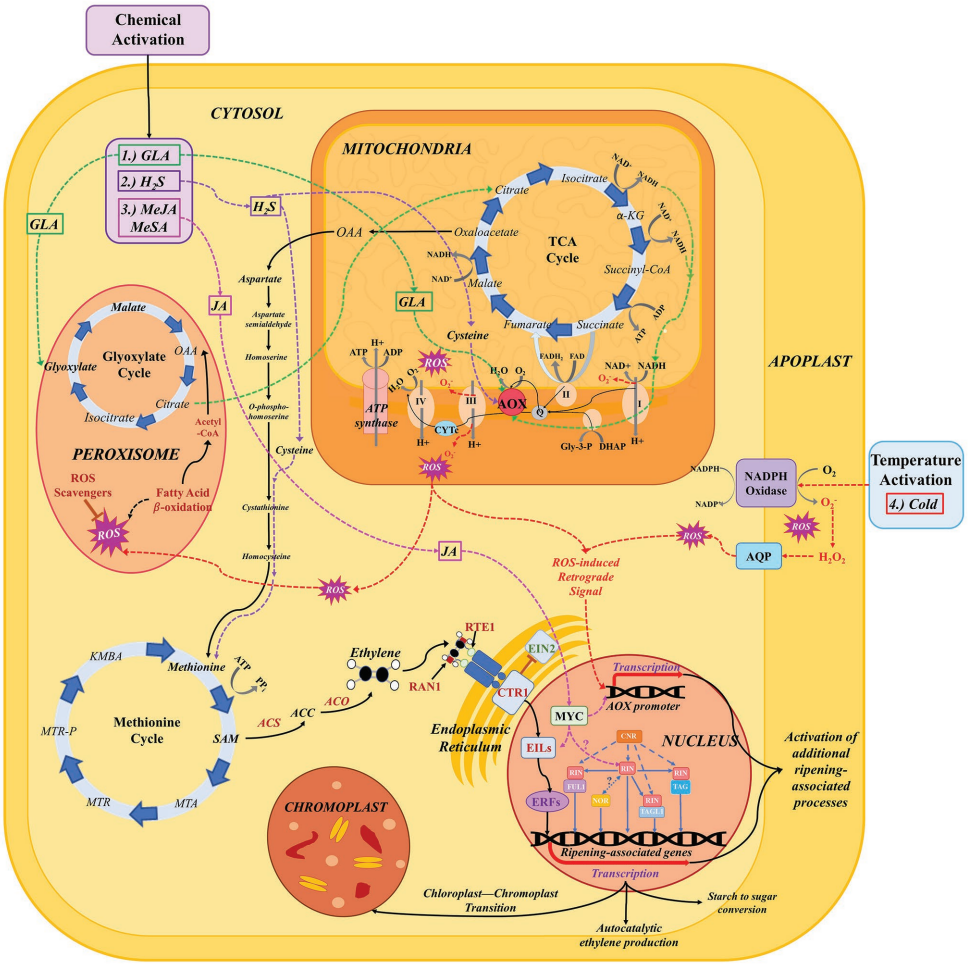

FIGURE 2 | The network of pathways involved in respiration, ethylene biosynthesis, and signaling, and ROS production and signaling during the ripening process. Pathways implicated in the stimulation of AOX expression or activity are indicated by dashed, colored lines. (1) Glyoxylic acid (GLA; green): GLA has been shown to directly activate AOX *in vivo* via interaction with the two cysteine residues that gate the protein (Umbach et al., 2006). *In vivo*, exogenous GLA application is hypothesized to lead to increased flux through the glyoxylate cycle and, consequently, the TCA cycle (Hewitt et al., 2020a). The latter leads to increased accumulation of NADH, resulting in increased flux of electrons through the cytochrome c (CYTc) pathway and consequent activation of AOX to prevent CYTc overreduction (Calderwood and Kopriva, 2014). (2) Hydrogen sulfide (H_2S; purple): sulfides accumulate in the cytoplasm as a result of exogenous treatment with H_2S; these can be converted to the amino acid cysteine (Calderwood and Kopriva, 2014). Cysteine, in turn, may directly modulate the activity of the AOX protein in response to stress or developmental changes in cellular redox state (Jia et al., 2016b; Dhingra and Hendrickson, 2017). (3) Methyl Jasmonate (MeJA; pink): exogenous treatment with MeJA leads to increased flux through the jasmonic acid biosynthesis pathway and accumulation of JA. JA has been shown to activate MYC, a transcription factor (TF) that enhances the function of ethylene signaling factors, particularly EIN/EIL family TFs, leading to an enhanced ethylene response (Shinshi, 2008; Kim J. et al., 2015). It has also been hypothesized that JA can directly influence AOX gene expression, possibly via a similar mechanism, with MYC acting alone or as a complex with other transcription factors to target promoter regions of AOX family genes (Fung et al., 2006). In addition to MYC, JA may regulate additional TFs like RIN, NOR, and cold-induced TFs that target ripening-associated genes (Czapski and Saniewski, 1992; Nham et al., 2017). (4) Cold (red): low temperature causes activation of respiratory burst oxidases (NADPH oxidases) embedded in the cell membrane, which produce superoxide that is then converted to hydrogen peroxide (Marino et al., 2012). Continued stimulation of NADPH oxidases leads to accumulation of ROS in the apoplast; these ROS can then be transferred into the cytosol via aquaporin channels (Qi et al., 2017). When redox state is disrupted, both cytosolic ROS and ROS produced in the mitochondria by the CYTc pathway transmit signals to the nucleus to mediate gene expression changes (including activation of AOX; Li et al., 2013).

Recent independent studies, as well as reviews, have indicated that such modifications to the classical climacteric ripening implicate several pathways that operate concomitantly with ethylene biosynthesis and perception, including AOX respiration, signaling by reactive oxygen species (ROS), and pathways that may be triggered by changes in epigenetic signatures (Perotti et al., 2014; Kumar et al., 2016; Farinati et al., 2017; Bucher et al., 2018; Hendrickson et al., 2019; Hewitt et al., 2020b). New advances in genome editing have provided further insight regarding potential sites for variation in ripening, as manipulation of upstream transcriptional regulators (Ito et al., 2017) leads to alterations in fruit texture, photoperiodic response, and posttranscriptional regulation of ripening-related genetic elements (Martín-Pizarro and Posé, 2018). Understanding the

way in which other key pathways may interact with ethylene biosynthesis and response during ripening will lend important insight into how control of ripening in various fruits can be fine tuned to increase predictability and marketability.

A Novel Role for AOX in Fruit Ripening

The hallmark aspect of climacteric ripening is the respiratory rise that occurs prior to the S1–S2 ethylene transition, in which an initially gradual increase in carbon dioxide evolution is followed by a heightened burst in respiratory activity during the ripening climacteric (Hiwasa-Tanase and Ezura, 2014; Colombié et al., 2017). The respiratory climacteric has been extensively documented in terms of physiology and biochemistry in a number of fruits (Hulme et al., 1963; Krishnamurthy and Subramanyam, 1970; Salminen and Young, 1975; Hartmann et al., 1987; Andrews, 1995; Hadfield et al., 1995). While early studies were foundational to the understanding and characterization of climacteric ripening with respect to total respiration, greater examination of the genetic and biochemical underpinnings of the respiratory climacteric in a variety of systems is needed.

Climacteric respiration represents the combined activity of several mitochondrial pathways that differentially direct electron transport, leading to several possible energetic fates. The first is the cytochrome c (CYTc) pathway. CYTc operates as a result of a proton gradient generated in the mitochondrial intermembrane space and concludes in the production of cellular energy currency via ATP synthase. In plants, CYTc activity also facilitates cellular detoxification via the synthesis of antioxidant compounds, namely, ascorbic acid (Welchen and Gonzalez, 2016; Fenech et al., 2019). The final step in ascorbic acid production is catalyzed by l-galactono-1,4-lactone dehydrogenase (GLDH), an enzyme that also plays a role in the assembly of respiratory complex I and serves as an electron donor to CYTc in the synthesis of ascorbic acid (Millar et al., 2003; Schimmeyer et al., 2016; Welchen and Gonzalez, 2016). Thus, when antioxidant production is high, electron flux through the CYTc pathway is correspondingly increased. Furthermore, when flux through the CYTc pathway is at maximum capacity due to high cellular respiratory demands, the alternative oxidase (AOX) pathway provides a secondary avenue for electron flux, thereby preventing overreduction of the mitochondrial electron transport chain. Unlike CYTc, AOX is insensitive to cyanide-containing compounds, allowing for viability when normal respiratory activity is inhibited (Wagner and Moore, 1997; Rogov and Zvyagilskaya, 2015).

Additionally, expression of AOX can also be modulated via retrograde mitochondrial signaling in response to reactive oxygen species (ROS) or metabolic disruption (Dojcinovic et al., 2005; Li et al., 2013). Because of this, AOX expression has been used both as an indicator of stress and as a metric to infer the energetic and metabolic status of plant biological systems during development (Saha et al., 2016). In almost all plants, AOX proteins are encoded by a small nuclear multigene family, which consists of two gene subfamilies: AOX1 and AOX2 (Polidoros et al., 2009).

The transition from S1 to S2 ethylene biosynthesis involves numerous metabolic changes, which may occur simultaneously or in series, that require a great deal of regulation and feedback mechanisms to ensure that ripening occurs properly. There is increasing evidence, including respiratory partitioning studies, supporting a role of AOX in the modulation of respiration at various stages around the time of climacteric via induction of S2 ethylene, which thereby influences the development of ripening-associated phenotypes downstream (**Figure 1**; Considine et al., 2001; Xu et al., 2012; Ng et al., 2014; Perotti et al., 2014; Hendrickson et al., 2019).

Activation of AOX During Ripening

In several fruits, AOX expression and/or activity has been characterized at the preclimacteric and climacteric stages of fruit development and ripening (**Figure 1**). Banana, a comparatively fast-ripening fruit, displays elevated preclimacteric expression of AOX at the mature green stage (Woodward et al., 2009), while in papaya, AOX expression peaks between the onset of S2 ethylene and the climacteric peak. In tomato and apple, expression reaches a maximum around the same time as the climacteric peak, indicating that the climacteric rise in these fruits can be partially attributed to the increased capacity for mitochondrial oxidation (Duque and Arrabaça, 1999; Xu et al., 2012; Oliveira et al., 2015). In mango, interestingly, AOX peaks after the climacteric, contributing to oxidation during fruit senescence rather than ripening (Considine et al., 2001).

Furthermore, in some fruits, both climacteric and nonclimacteric, AOX activation can be achieved via cold temperature or chemical stimulation (**Figure 2**). In zucchini and sweet pepper, cold-induced activation of AOX results in the mitigation of chilling injury (Aghdam, 2013; Hu et al., 2014; Carvajal et al., 2015). Recently, it was demonstrated that completion of cold conditioning, facilitating the S1–S2 transition, in European pear coincides with preclimacteric maxima in AOX transcript accumulation (Hendrickson et al., 2019; Dhingra et al., 2020; Hewitt et al., 2020b).

In a subsequent study, chemical genomics approaches to further target AOX in pear fruit led to the discovery of glyoxylic acid (GLA) as a chemical activator of both AOX and ripening (Dhingra et al., 2020; Hewitt et al., 2020a). GLA has been shown to directly activate AOX *in vivo* via interaction with the two cysteine residues that gate the protein (Umbach et al., 2006). Furthermore, transcriptomic characterization of expressed genes in response to GLA implicates the AOX pathway and glyoxylate cycle in a more extensive ripening network wherein exogenous GLA application results in increased flux through the glyoxylate cycle and TCA cycles, the latter of which leads to accumulation of NADH (Hewitt et al., 2020a). This, in turn, results in increased flux of electrons through the CYTc pathway and consequent activation of AOX to prevent CYTc overreduction (**Figure 2**; Hewitt et al., 2020a,b). In addition to GLA, there is evidence for activation and differential regulation of AOX protein isoforms by TCA cycle intermediates (Selinski et al., 2018). The results of these studies provide information necessary to develop and test "cocktails" of TCA/GLA cycle metabolites that could result in optimal activation of alternative respiration in the context of fruit ripening regulation when applied exogenously to preclimacteric fruit postharvest.

Hydrogen sulfide (H_2S), though a known phytotoxin, in minuscule doses can enhance alternative pathway respiration and inhibit ROS production (Hu et al., 2012; Luo et al., 2015; Li et al., 2016; Ziogas et al., 2018). Exogenous treatment with H_2S leads to the accumulation of sulfides in the cytoplasm, some of which are directly converted to the amino acid cysteine (Calderwood and Kopriva, 2014). Cysteine, in turn, may directly modulate the activity of the AOX protein in response to stress or developmental changes in cellular redox state (Jia et al., 2016b). Additional studies have demonstrated the activation of AOX and ripening in response to H_2S treatment. In 'Bartlett' and 'D'Anjou' pears, H_2S facilitated a bypass of normal cold conditioning requirements for ripening, and treated fruit demonstrated increased ethylene evolution, heightened respiratory rate, and activated *AOX* expression (Dhingra and Hendrickson, 2017). In hawthorn fruit, H_2S application mitigated chilling injury, which is linked to increased AOX activity and antioxidant capacity (Aghdam et al., 2018).

Application of metabolism-regulatory hormones methyl salicylate (MeSA) and methyl jasmonate (MeJA) results in increased expression of AOX, correlating with a reduction in chilling injury in sweet pepper. JA is a known activator of MYC, a transcription factor that enhances the function of ethylene signaling factors, particularly within the EIN/EIL family, thus leading to enhanced ethylene responses (Shinshi, 2008; Kim J. et al., 2015). It has also been hypothesized that JA can directly influence *AOX* gene expression (Fung et al., 2006) via a similar mechanism, with MYC acting alone or in complex with other transcription factors to target promoter regions of *AOX* family genes (**Figure 2**). In addition to MYC, JA may regulate additional TFs like RIN, NOR, and cold-induced TFs that target ripening-associated genes (Czapski and Saniewski, 1992; Nham et al., 2017; Li et al., 2018).

Together, these findings reveal interesting insights into chemical and hormonal events that operate in an ethylene-independent space during climacteric ripening, as well as how ripening can be better regulated as a result of this information. Novel discoveries presented in recent studies, which complement and expand upon the foundational knowledge of the role of AOX in ripening, have laid the framework for several exciting hypotheses. First, knowledge of how AOX expression can be induced may provide an avenue for development and testing of ripening strategies in fruits whose respiratory profiles are affected by temperature. Furthermore, knowledge of how temperature preconditioning may mitigate chilling injury via AOX stimulation could allow for improved management practices of papaya, avocado, banana, mango, zucchini, and other temperature-sensitive fruits during storage (Lederman et al., 1997; Aghdam, 2013; Carvajal et al., 2015; Luo et al., 2015; Valenzuela et al., 2017).

Molecular and Metabolic Links Between Respiration and Ethylene

It is clear, based on the simultaneity and interdependency of responses, that respiration and ethylene are physiologically correlated during climacteric ripening—climacteric rise in respiration is accompanied by a spike in autocatalytic ethylene production, and blocking ethylene perception prevents respiration from increasing further (Hiwasa-Tanase and Ezura, 2014; Watkins, 2015). While elucidating the precise connections between the two pathways will require more genetic and metabolic work, the results of several studies point toward crosstalk between ethylene and respiration and implicate AOX expression and signaling by ROS in this connection (Sewelam et al., 2016).

In tomato, 1-MCP treatment reduces transcript levels of *AOX1a* (Xu et al., 2012); the simultaneous inhibition of ethylene response and maintenance of respiration at low levels by 1-MCP indicates a relationship between ethylene, the respiratory climacteric, and AOX at the molecular level. The activity of AOX and biosynthesis of ethylene are directly dependent upon flux through CYTc and the availability of ATP. RNA interference studies in tomato reveal a modulatory role of *AOX* in ethylene production, as ACS4 activity in *AOX-RNAi* plants is significantly lower than in wildtype (WT) plants (Xu et al., 2012). Reduced activity of ethylene biosynthetic enzymes when *AOX* is silenced could be due to a decrease in precursors for ethylene production. For example, the methionine cycle, and therefore ethylene biosynthesis, is dependent upon ATP generation via respiration (Mattoo and White, 2018). Specifically, methionine is converted to the immediate precursor to ACC, SAM, in an ATP-dependent reaction catalyzed by SAM synthetase (**Figure 2**; Yang and Hoffman, 1984). During ripening, AOX could allow for heightened carbon flux through glycolysis and the TCA cycle; this would prevent overreduction of the ubiquinone pool, increase oxidation of NADH, and accelerate carbon turnover, resulting in the production of large amounts of ATP that could be used for S2 ethylene and other ripening-associated metabolic processes. Moreover, a recent report of a link between the TCA and methionine metabolism (and consequently, ethylene metabolism) via NADH oxidation lends further support to this concept (Lozoya et al., 2018).

In cucumber, brassinosteroids were reported to induce ethylene responses and ROS, the collective activities of which resulted in stimulation of AOX and activation of downstream abiotic stress responses (Wei et al., 2015). ROS, which are produced in the mitochondria during respiration and accumulate in the apoplast as a result of abiotic stimulation of respiratory burst oxidase (NADPH oxidase) homologs, were historically thought of in terms of their toxicity to plants in high concentrations; however, their critical roles in response to perturbations in cellular redox state have become clearer in recent years (Jimenez et al., 2002; Marino et al., 2012; Vaahtera et al., 2013; El-Maarouf-Bouteau et al., 2015; Kumar et al., 2016; Noctor et al., 2018; Decros et al., 2019). During fruit maturation, ROS accumulation peaks once at the start of ripening (presumably the start of the respiratory climacteric) and again at overripening, around the time of harvest maturity (Muñoz and Munné-Bosch, 2018). This accumulation may coincide with the activation of AOX in certain species (**Figure 1**). In *Arabidopsis*, ethylene-induced signaling by hydrogen peroxide (H_2O_2), a form of ROS, was shown to activate AOX in response to cold temperatures (Wang et al., 2010, 2012). It has been suggested that such temperature-induced transcriptional changes in AOX occur via ROS derived from NADPH oxidase activity

(Vanlerberghe, 2013; McDonald and Vanlerberghe, 2018). These NADPH oxidases produce O_2^-, which is converted to H_2O_2, in the apoplast. These ROS are translocated to the cytoplasm via aquaporin channels (Qi et al., 2017). The influx of apoplastic ROS, along with additional species produced in the mitochondria, serves to activate nuclear-targeted redox signals, which elicit antioxidative responses and alteration in metabolic processes (Suzuki et al., 2011; Marino et al., 2012; McDonald and Vanlerberghe, 2018; Chu-Puga et al., 2019; **Figure 2**). Such ROS-induced retrograde signaling leads to modulation of AOX expression, as has been shown in potato and pea. It has been hypothesized that in this way, ROS may facilitate crosstalk between respiration and ethylene via AOX activation in fruit ripening (Marti et al., 2009; Hewitt et al., 2020b; Hua et al., 2020).

Taken together, these results indicate that an interplay between different components of several metabolic signaling pathways is responsible for initial AOX activation. Furthermore, the activity of both ethylene and alternative respiratory pathways may be self-perpetuating by means of an autostimulatory feedback loop involving ROS (Wei et al., 2015). While AOX serves as a mechanism to prevent overreduction of the CYTc pathway, it is possible that overstimulation of AOX via external perturbations (e.g., chemical or temperature) in fruit prior to the S2 transition induces a vacuum effect, drawing the glycolytic pathway and TCA cycle into action to deliver more reducing power, thereby initiating CYTc pathway respiratory activity. For example, in *Arabidopsis* and tomato, *aox* mutants displayed disrupted accumulation of primary respiratory metabolites, which affect development (Xu et al., 2012; Jiang et al., 2019). The same may be true of AOX impairment in fruit. Understanding the regulation of the respiratory climacteric and how crosstalk between ethylene and AOX is facilitated may require a look at the transcriptional regulators of these responses.

Transcriptional Regulation Modulates Both Ethylene and Respiratory Responses

Within the last decade, the importance of transcriptional regulation of ripening response has become more evident. During ripening, signals from upstream transcription factors (which may be activated by environmental or intrinsic triggers) facilitate a cascade of downstream signaling activity (Cherian et al., 2014; Gao et al., 2020). In fruits, this signaling activity leads to increased respiration, cell wall softening, and changes in the production of pigments, volatiles, starch, and sugar content, and phytonutrient metabolite content—these processes are all characteristic of ripening, with respiration and biosynthesis of ethylene particularly relevant to climacteric ripening (Seymour et al., 2013a; Karlova et al., 2014). Among some of the most important transcriptional regulators during ripening are ripening inhibitor (RIN), colorless non-ripening (CNR), tomato Agamous 1 (TAG1), tomato Agamous-like 1 (TAGL1), fruitful 1 and 2 (FUL1 and 2), and non-ripening (NOR); all of these are involved in a complex and interconnected regulatory network that ultimately leads to fruit ripening and the aforementioned ripening-associated qualities (**Figure 2**; Seymour et al., 2013a; Fujisawa et al., 2014; Datta and Bora, 2019). The availability of mutants targeting the aforementioned ripening regulators in tomato allows for study of consequences of ripening perturbation at the regulatory level. Many studies have demonstrated the detrimental effects of mutations in these key transcriptional regulators on ethylene production and signaling, which are expected to have further downstream respiratory consequences via the avenues for the interpathway crosstalk discussed in the previous section.

Because of its resultant complete inhibition of ripening in tomato, the *rin* mutation has become one of the most iconic ripening-associated mutations in studies of climacteric fruit. *Rin* mutant tomatoes fail to mature beyond the green-ripe stage and do not exhibit the characteristic ripening climacteric of wild-type fruit (Vrebalov et al., 2002). Commercial varieties of tomato, heterozygous for the *rin* mutation, have been introduced to the market and have displayed increased shelf life with little noticeable alteration to the desired flavor profile (Garg et al., 2008). Chromatin immunoprecipitation studies revealed several direct targets of *RIN*, including the ethylene-biosynthesizing enzyme 1-aminocyclopropene carboxylate oxidase 4 (ACO4) and α-galacturonase (α-gal), an enzyme-associated with cell wall breakdown and fruit softening (Martel et al., 2011; Fujisawa et al., 2012). Furthermore, RIN protein binding sites (CArG box) were identified in the promoter regions of *α-gal* and *ACO4*, and *ACS2* genes (Fujisawa et al., 2012, 2013). Binding to these motifs is facilitated by localized demethylation of associated promoter regions (Li et al., 2017). Expression of ethylene biosynthetic enzymes ACS1 and ACO1 in apple was greatly decreased when expression of various *RIN-like* MADS-box genes was downregulated or silenced (Ireland et al., 2013). Bisulfite sequencing studies revealed that binding sites in the promoter regions of known transcriptional targets of RIN were found to be demethylated, suggesting that demethylation is necessary for RIN binding and development (Zhong et al., 2013). Treatment with the methyltransferase inhibitor 5-azacytidine resulted in fruit that ripened prematurely, further lending support to demethylation of binding sites as a trigger for RIN-activated ripening (Zhong et al., 2013; Liu R. et al., 2015). While the *rin* mutant was classically understood as a loss of function mutant, more recent work suggests that it is actually a gain-of-function mutant that produces a protein that actively represses ripening (Ito et al., 2017). Regardless, it is clear that when RIN is perturbed, ripening does not proceed to completion.

Colorless non-ripening (CNR) transcription factor is a squamosal-promoter binding-like protein, which appears to be necessary for RIN to bind to promoters (Martel et al., 2011; Zhong et al., 2013). With a hypermethylated, heritable promoter that results in reduced transcriptional activity, CNR is a unique example of an epiallele, requiring the activity of a specific chromatin-methylating enzyme, chromomethylase3, for somatic inheritance (Ecker, 2013; Seymour et al., 2013b; Chen et al., 2015). Thus, the CNR transcription factor lends evidence for the role of epigenetics in critical developmental transitions such as those that occur during S1–S2 ethylene production and ripening.

TAG1, TAGL1, and MADS-box transcription factors FUL1 and FUL2 can form complexes with RIN (Shima et al., 2013; Fujisawa et al., 2014). Mutation of these regulatory factors results in fruit with decreased ripening capacity or non-ripening phenotypes (Itkin et al., 2009; Garceau et al., 2017). Another TF among the core set of regulatory elements is the NAC-domain-containing protein at the tomato non-ripening (NOR) locus. NOR mutants fail to ripen in a physiologically similar manner to RIN and TAGL1 mutants. NOR acts upstream of ethylene biosynthesis and, like RIN, appears to bind to promoter regions of genes involved in ethylene biosynthesis, thereby positively regulating ripening (Gao et al., 2018; **Figure 2**). It is unclear whether RIN and NOR interact with one another to stimulate ripening in conjunction. Considering increasing understanding of their regulatory role in ripening, NOR and FUL genes have been recent targets for improving shelf life in tomato fruit (Nguyen and Sim, 2017; Wang et al., 2019).

Recently, the role of AOX has been investigated in NOR, CNR, and RIN mutant fruit (Manning et al., 2006; Xu et al., 2012; Perotti et al., 2014). AOX activity elicits differential effects in each of these mutants, and expression of RIN, CNR, and the ethylene receptor never ripe (NR) has been observed in fruit in which *AOX* is silenced. When *AOX* was inhibited via RNA interference, the expression of these transcriptional regulators decreased (Xu et al., 2012). Because CNR acts upstream of ethylene biosynthesis and the NR receptor acts downstream, this observation suggests that AOX plays a yet uncharacterized role in ripening mediated by transcriptional regulators that affect ethylene biosynthesis, signal transduction, and response (Giovannoni, 2004; Seymour et al., 2013b; Hewitt et al., 2020b). Interestingly, it has been hypothesized that the activation of both NOR and RIN may be linked, either directly or indirectly, to jasmonic acid signaling (Czapski and Saniewski, 1992). As indicated previously, JA is known to enhance transcriptional activation of other ripening-associated processes, including AOX. In addition to JA, the ethylene signaling molecule EIN3/EIL1 is hypothesized to directly activate RIN in tomato, thus serving as an instrumental part of a positive feedback loop resulting in autocatalytic ethylene production (**Figure 2**; Lü et al., 2018), and corresponding to increased consumption of ATP produced from CYTc respiration.

Epigenetic Regulation of Ripening and a Potential Link to the Respiratory Climacteric

Epigenetics refers to the heritable modifications of the genome beyond the physical nucleotide sequence, including DNA methylation and modifications to histone proteins. In contrast, epigenomics refers to all modifications, regardless of heritability (Giovannoni et al., 2017). One of the most commonly studied forms of epigenetic modification is DNA methylation. Methylation status is in constant flux due to the changing environment; therefore, condition-specific methylation status may be used to infer stress conditions, ripening competency, and developmental progress, among other things. Recent evidence suggests that perturbation of mitochondrial function has an effect on epigenetics. At the same time, continued oxidation of NADH serves to counteract the increase in nuclear DNA methylation and maintain cellular homeostasis (Lozoya et al., 2018).

The causes of such perturbations may vary. Temperature is known to be a major factor in alteration of methylation status, and conditioning of fruit requiring chilling to ripen, or to avoid chilling injury, could affect the methylation of promoter regions of key ripening related genes and regulatory transcription factors. With more tools for epigenetic and epigenomic analyses available, including bisulfite sequencing and PacBio long-read sequencing, new insights are being gained into the impact of epigenetic signatures on development and senescence of fruit (Daccord et al., 2017; Xu and Roose, 2020). Understanding how the epigenome governs downstream transcriptional regulation and response is critical to better understanding ripening and senescence.

Chemically induced demethylation of tomato fruit using 5-azacytidine results in early ripening of fruit (Zhong et al., 2013). This finding indicates that the alteration of methylation status is one of the first steps in the regulation of downstream processes associated with ripening. Recent transcriptomic and gene ontology enrichment analysis of cold conditioned 'D'Anjou' and 'Bartlett' pear fruit suggests that both methylation and chromatin modifications may be important for activation of vernalization-associated genes and ripening-associated transcriptional elements, which were activated in conjunction with AOX during prolonged cold temperature exposure (Hewitt et al., 2020b). Interestingly, these two cultivars appear to differentially engage expression of vernalization genes VRN1 and VIN3, which could justify the need for different cold exposure time in different cultivars (Hewitt et al., 2020b). Studying the epigenomic status in light of mutations to key transcription factors, mentioned previously, illuminates the way that DNA methylation and histone modifications in genetic regulatory elements serve to modulate certain aspects of ripening early on in development. Beyond abiotic influences, it is possible that some signal from mature seeds is originally what signals the onset of ripening progression (McAtee et al., 2013). This hypothesis is supported by the recent characterization of enzymes responsible for removing epigenetic signatures to DNA or histones, such as the recently characterized DEMETER-like DNA demethylase gene *SlDML2* in tomato (Liu R. et al., 2015; Zhou et al., 2019). These proteins are particularly highly expressed in the locular tissue surrounding mature seeds in the fruit. In contrast to tomato, a climacteric fruit in which demethylation is an important factor in ripening, nonclimacteric orange fruit was recently reported to exhibit global increases in DNA methylation as ripening progresses (Huang and Liu, 2019). In addition to factors known to directly affect methylation, recent evidence suggests that additional factors, including noncoding RNAs, circular RNAs, and microRNAs, may target genes with specific methylation patterns or abundance to elicit changes in expression (Zuo et al., 2020). The breadth of factors that may contribute to alterations in the epigenome is still being elucidated; however, it is possible that methylation status during ripening is tied to fruits' classifications as climacteric or nonclimacteric. This, in turn, is expected to differentially

impact a wide range of ripening-associated parameters, in addition to ethylene and respiratory profiles.

CONCLUSIONS AND FUTURE PERSPECTIVES

The interplay of ethylene (biosynthesis, signaling, and response) and respiration (CYTc and AOX) have been extensively characterized at the physiological level. Studies conducted within the last several years provide new insights with respect to the connection between these two critical pathways at the molecular and metabolic levels. AOX activity begins to increase during the preclimacteric phase, prior to the S1–S2 ethylene transition, particularly in the context of cold temperature or other external stimuli. This activity may be accompanied by the accumulation of ROS as the CYTc pathway capacity reaches a maximum. At the onset of S2 ethylene stimulation, both ethylene response and alternative pathway respiration appear to be interdependent. Ethylene biosynthesis requires ATP, generated via respiration, and activity of respiratory pathways modulated by ERFs in the nucleus; this is evidenced by the inhibition of ethylene production and respiration by the ethylene receptor antagonist 1-MCP. The commencement of both ethylene and respiration-associated processes is likely due to upstream transcriptional and epigenetic regulators, as well as the signaling activity of ROS generated during increased respiration. Mutants of master transcriptional regulators in tomato have provided a means for the study of their effects on both ethylene production and respiration during ripening. Furthermore, studies have investigated the effects of temperature and chemical manipulation of AOX with the aim to understand ways in which the timing of ripening can be controlled. AOX and related processes represent a new frontier in regulating postharvest ripening and, therefore, better management to reduce fruit wastage and development of postharvest management strategies in different types of fruits.

The ever-growing fields of genomics, transcriptomics, metabolomics, and epigenomics offer high-throughput strategies for extrapolation of important biological function and expression information from large datasets generated in recent ripening experiments (Morozova and Marra, 2008; Banerjee et al., 2019). The relatively new ability to examine plant epigenomes, and most recently the "ripenome" at the level of single nucleotide bases reveals further avenues for understanding epigenetic regulators of the transition from preclimacteric to climacteric, and the subsequent development of species-specific ripening phenotypes (Giovannoni et al., 2017). Advances in gene editing have provided improved tools by which candidate ripening-associated genes, identified using the aforementioned "omics" approaches, can be targeted in a concise way to achieve specific results with limited or no off-target effects. Use of these new approaches will facilitate improved understanding of the array of diverse transcriptional responses, the interaction of associated pathways (including AOX, vernalization-associated, and organic acid metabolic pathways), functional implications of the S1–S2 transition, and interdependent roles of ethylene and respiration in ripening (Nham et al., 2017; Hewitt et al., 2020a,b). Such approaches used independently or in conjunction will facilitate the identification and targeted manipulation of candidate regulators of important ripening and fruit quality-associated characteristics in fruits. This, in turn, could translate to greater storability of fruits after harvest, improved marketability within respective fruit industries, and enhanced consumer satisfaction overall.

AUTHOR CONTRIBUTIONS

SH and AD conceptualized the review. Both the authors contributed to the article and approved the submitted version.

FUNDING

Work in the Dhingra lab in the area of fruit ripening is supported in part by Washington State University Agriculture Center Research Hatch grants WNP00797 and WNP00011 and grant funding from the Fresh and Processed Pear Research Subcommittee to AD. SH acknowledges the support received from ARCS Seattle Chapter and National Institutes of Health/ National Institute of General Medical Sciences through an institutional training grant award T32-GM008336. The contents of this work are solely the responsibility of the authors and do not necessarily represent the official views of the NIGMS or NIH.

REFERENCES

Aghdam, M. S. (2013). Role of alternative oxidase in postharvest stress of fruit and vegetables: chilling injury. *Afr. J. Biotechnol.* 12, 7009–7016.

Aghdam, M. S., Mahmoudi, R., Razavi, F., Rabiei, V., and Soleimani, A. (2018). Hydrogen sulfide treatment confers chilling tolerance in hawthorn fruit during cold storage by triggering endogenous H2S accumulation, enhancing antioxidant enzymes activity and promoting phenols accumulation. *Sci. Hortic.* 238, 264–271. doi: 10.1016/j.scienta.2018.04.063

Andrews, J. (1995). The climacteric respiration rise in attached and detached tomato fruit. *Postharvest Biol. Technol.* 6, 287–292. doi: 10.1016/0925-5214(95)00013-V

Banerjee, R., Kumar, G. V., and Kumar, S. J. (2019). *Omics-based approaches in plant biotechnology*. Hoboken, NJ, USA: John Wiley & Sons.

Barry, C. S., and Giovannoni, J. J. (2007). Ethylene and fruit ripening. *J. Plant Growth Regul.* 26:143. doi: 10.1007/s00344-007-9002-y

Barry, C. S., Llop-Tous, M. I., and Grierson, D. (2000). The regulation of 1-aminocyclopropane-1-carboxylic acid synthase gene expression during the transition from system-1 to system-2 ethylene synthesis in tomato. *Plant Physiol.* 123, 979–986. doi: 10.1104/pp.123.3.979

Bucher, E., Kong, J., Teyssier, E., and Gallusci, P. (2018). "Epigenetic regulations of fleshy fruit development and ripening and their potential applications to breeding strategies" in *Advances in botanical research.* eds. M. Mirouze, E. Bucher and P. Gallusci (Elsevier), 327–360.

Calderwood, A., and Kopriva, S. (2014). Hydrogen sulfide in plants: from dissipation of excess sulfur to signaling molecule. *Nitric Oxide* 41, 72–78. doi: 10.1016/j.niox.2014.02.005

Cara, B., and Giovannoni, J. J. (2008). Molecular biology of ethylene during tomato fruit development and maturation. *Plant Sci.* 175, 106–113. doi: 10.1016/j.plantsci.2008.03.021

Carvajal, F., Palma, F., Jamilena, M., and Garrido, D. (2015). Preconditioning treatment induces chilling tolerance in zucchini fruit improving different physiological mechanisms against cold injury. *Ann. Appl. Biol.* 166, 340–354. doi: 10.1111/aab.12189

Chen, Y., Grimplet, J., David, K., Castellarin, S. D., Terol, J., Wong, D. C., et al. (2018). Ethylene receptors and related proteins in climacteric and non-climacteric fruits. *Plant Sci.* 276, 63–72. doi: 10.1016/j.plantsci.2018.07.012

Chen, W., Kong, J., Qin, C., Yu, S., Tan, J., Chen Y-r, W. C., et al. (2015). Requirement of CHROMOMETHYLASE3 for somatic inheritance of the spontaneous tomato epimutation colourless non-ripening. *Sci. Rep.* 5:9192. doi: 10.1038/srep09192

Cherian, S., Figueroa, C. R., and Nair, H. (2014). 'Movers and shakers' in the regulation of fruit ripening: a cross-dissection of climacteric versus non-climacteric fruit. *J. Exp. Bot.* 65, 4705–4722. doi: 10.1093/jxb/eru280

Chiriboga, M. -A., Saladié, M., Bordonaba, J. G., Recasens, I., Garcia-Mas, J., and Larrigaudière, C. (2013). Effect of cold storage and 1-MCP treatment on ethylene perception, signalling and synthesis: influence on the development of the evergreen behaviour in 'Conference'pears. *Postharvest Biol. Technol.* 86, 212–220. doi: 10.1016/j.postharvbio.2013.07.003

Chu-Puga, Á., González-Gordo, S., Rodríguez-Ruiz, M., Palma, J. M., and Corpas, F. J. (2019). NADPH oxidase (Rboh) activity is up regulated during sweet pepper (*Capsicum annuum* L.) fruit ripening. *Antioxidants* 8:9. doi: 10.3390/antiox8010009

Colombié, S., Beauvoit, B., Nazaret, C., Bénard, C., Vercambre, G., Le Gall, S., et al. (2017). Respiration climacteric in tomato fruits elucidated by constraint-based modelling. *New Phytol.* 213, 1726–1739. doi: 10.1111/nph.14301

Considine, M. J., Daley, D. O., and Whelan, J. (2001). The expression of alternative oxidase and uncoupling protein during fruit ripening in mango. *Plant Physiol.* 126, 1619–1629. doi: 10.1104/pp.126.4.1619

Czapski, J., and Saniewski, M. (1992). Stimulation of ethylene production and ethylene-forming enzyme activity in fruits of the non-ripening nor and rin tomato mutants by methyl jasmonate. *J. Plant Physiol.* 139, 265–268. doi: 10.1111/j.1439-0434.1989.tb00650.x

Daccord, N., Celton, J. -M., Linsmith, G., Becker, C., Choisne, N., Schijlen, E., et al. (2017). High-quality de novo assembly of the apple genome and methylome dynamics of early fruit development. *Nat. Genet.* 49:1099. doi: 10.1038/ng.3886

Datta, H. S., and Bora, S. S. (2019). Physiological approaches for regulation of fruit ripening: a review. *IJCS* 7, 4587–4597.

Decros, G., Baldet, P., Beauvoit, B., Stevens, R., Flandin, A., Colombié, S., et al. (2019). Get the balance right: ROS homeostasis and redox signalling in fruit. *Front. Plant Sci.* 10:1091. doi: 10.3389/fpls.2019.01091

Dhingra, A., and Hendrickson, C. (2017). *Control of ripening and senescence in pre-harvest and post-harvest plants and plant materials by manipulating alternative oxidase activity*. Google Patents.

Dhingra, A., Hendrickson, C., and Hewitt, S. (2020). *Control of ripening and senescence in pre-harvest and post-harvest plants and plant materials by manipulating alternative oxidase activity*. Google Patents.

Dojcinovic, D., Krosting, J., Harris, A. J., Wagner, D. J., and Rhoads, D. M. (2005). Identification of a region of the Arabidopsis AtAOX1a promoter necessary for mitochondrial retrograde regulation of expression. *Plant Mol. Biol.* 58, 159–175. doi: 10.1007/s11103-005-5390-1

Duque, P., and Arrabaça, J. D. (1999). Respiratory metabolism during cold storage of apple fruit. II. Alternative oxidase is induced at the climacteric. *Physiol. Plant.* 107, 24–31. doi: 10.1034/j.1399-3054.1999.100104.x

Eaks, I. L. (1983). Effects of chilling on respiration and ethylene production of 'Hass' avocado fruit at 20°C. *HortScience* 18, 235–237.

Ecker, J. R. (2013). Epigenetic trigger for tomato ripening. *Nat. Biotechnol.* 31, 119–120. doi: 10.1038/nbt.2497

El-Maarouf-Bouteau, H., Sajjad, Y., Bazin, J., Langlade, N., Cristescu, S. M., Balzergue, S., et al. (2015). Reactive oxygen species, abscisic acid and ethylene interact to regulate sunflower seed germination. *Plant Cell Environ.* 38, 364–374. doi: 10.1111/pce.12371

Fabi, J. P., Cordenunsi, B. R., de Mattos Barreto, G. P., Mercadante, A. Z., Lajolo, F. M., and Oliveira do Nascimento, J. R. (2007). Papaya fruit ripening: response to ethylene and 1-methylcyclopropene (1-MCP). *J. Agric. Food Chem.* 55, 6118–6123. doi: 10.1021/jf070903c

Farcuh, M., Rivero, R. M., Sadka, A., and Blumwald, E. (2018). Ethylene regulation of sugar metabolism in climacteric and non-climacteric plums. *Postharvest Biol. Technol.* 139, 20–30. doi: 10.1016/j.postharvbio.2018.01.012

Farinati, S., Rasori, A., Varotto, S., and Bonghi, C. (2017). Rosaceae fruit development, ripening and post-harvest: an epigenetic perspective. *Front. Plant Sci.* 8:1247. doi: 10.3389/fpls.2017.01247

Fenech, M., Amaya, I., Valpuesta, V., and Botella, M. A. (2019). Vitamin C content in fruits: biosynthesis and regulation. *Front. Plant Sci.* 9:2006. doi: 10.3389/fpls.2018.02006

Fernandez i Marti, A., Saski, C. A., Manganaris, G. A., Gasic, K., and Crisosto, C. H. (2018). Genomic sequencing of Japanese plum (*Prunus salicina* Lindl.) mutants provides a new model for Rosaceae fruit ripening studies. *Front. Plant Sci.* 9:21. doi: 10.3389/fpls.2018.00021

Fujisawa, M., Nakano, T., Shima, Y., and Ito, Y. (2013). A large-scale identification of direct targets of the tomato MADS box transcription factor RIPENING INHIBITOR reveals the regulation of fruit ripening. *Plant Cell* 25, 371–386. doi: 10.1105/tpc.112.108118

Fujisawa, M., Shima, Y., Higuchi, N., Nakano, T., Koyama, Y., Kasumi, T., et al. (2012). Direct targets of the tomato-ripening regulator RIN identified by transcriptome and chromatin immunoprecipitation analyses. *Planta* 235, 1107–1122. doi: 10.1034/j.1399-3054.1999.100104.x

Fujisawa, M., Shima, Y., Nakagawa, H., Kitagawa, M., Kimbara, J., Nakano, T., et al. (2014). Transcriptional regulation of fruit ripening by tomato FRUITFULL homologs and associated MADS box proteins. *Plant Cell* 26, 89–101. doi: 10.1105/tpc.113.119453

Fung, R. W., Wang, C. Y., Smith, D. L., Gross, K. C., Tao, Y., and Tian, M. (2006). Characterization of alternative oxidase (AOX) gene expression in response to methyl salicylate and methyl jasmonate pre-treatment and low temperature in tomatoes. *J. Plant Physiol.* 163, 1049–1060. doi: 10.1016/j.jplph.2005.11.003

Gao, Y., Wei, W., Zhao, X., Tan, X., Fan, Z., Zhang, Y., et al. (2018). A NAC transcription factor, NOR-like1, is a new positive regulator of tomato fruit ripening. *Hortic. Res.* 5:75. doi: 10.1038/s41438-018-0111-5

Gao, J., Zhang, Y., Li, Z., and Liu, M. (2020). Role of ethylene response factors (ERFs) in fruit ripening. *Food Qual. Safet.* 4, 15–20. doi: 10.1093/fqsafe/fyz042

Garceau, D. C., Batson, M. K., and Pan, I. L. (2017). Variations on a theme in fruit development: the PLE lineage of MADS-box genes in tomato (TAGL1) and other species. *Planta* 246, 313–321. doi: 10.1007/s00425-017-2725-5

Garg, N., Cheema, D., and Dhatt, A. (2008). Utilization of rin, nor, and alc alleles to extend tomato fruit availability. *Int. J. Veg. Sci.* 14, 41–54. doi: 10.1080/19315260801890526

Giovannoni, J. J. (2004). Genetic regulation of fruit development and ripening. *Plant Cell* 16, S170–S180. doi: 10.1105/tpc.019158

Giovannoni, J., Nguyen, C., Ampofo, B., Zhong, S., and Fei, Z. (2017). The epigenome and transcriptional dynamics of fruit ripening. *Annu. Rev. Plant Biol.* 68, 61–84. doi: 10.1146/annurev-arplant-042916-040906

Guo, J., Wang, S., Yu, X., Dong, R., Li, Y., Mei, X., et al. (2018). Polyamines regulate strawberry fruit ripening by abscisic acid, auxin, and ethylene. *Plant Physiol.* 177, 339–351. doi: 10.1104/pp.18.00245

Hadfield, K. A., Rose, J. K. C., and Bennett, A. B. (1995). The respiratory climacteric is present in Charentais (*Cucumis melo* cv. Reticulatus F1 alpha) melons ripened on or off the plant. *J. Exp. Bot.* 46, 1923–1925.

Handa, A. K., and Mattoo, A. K. (2010). Differential and functional interactions emphasize the multiple roles of polyamines in plants. *Plant Physiol. Biochem.* 48, 540–546. doi: 10.1016/j.plaphy.2010.02.009

Hartmann, C., Drouet, A., and Morin, F. (1987). Ethylene and ripening of apple, pear and cherry fruit. *Plant Physiol. Bioch.* 25, 505–512.

Hendrickson, C., Hewitt, S., Swanson, M. E., Einhorn, T., and Dhingra, A. (2019). Evidence for pre-climacteric activation of AOX transcription during cold-induced conditioning to ripen in European pear (*Pyrus communis* L.). *PLoS One* 14:e0225886. doi: 10.1371/journal.pone.0225886

Herner, R., and Sink, K. (1973). Ethylene production and respiratory behavior of the rin tomato mutant. *Plant Physiol.* 52, 38–42. doi: 10.1104/pp.52.1.38

Hewitt, S. L., Ghogare, R., and Dhingra, A. (2020a). Glyoxylic acid overcomes 1-MCP-induced blockage of fruit ripening in *Pyrus communis* L. var. 'D'Anjou. *Sci. Rep.* 10, 1–14. doi: 10.1101/852954

Hewitt, S. L., Hendrickson, C. A., and Dhingra, A. (2020b). Evidence for the involvement of Vernalization-related genes in the regulation of cold-induced

ripening in 'D'Anjou' and 'Bartlett' pear fruit. *Sci. Rep.* 10:8478. doi: 10.1038/s41598-020-65275-8

Hiwasa-Tanase, K., and Ezura, H. (2014). "Climacteric and non-climacteric ripening" in *Fruit ripening, physiology, signalling and genomics*. eds. P. Nath, M. Bouzayen, A. K. Mattoo and J. C. Pech (CAB International), 1–14.

Hu, L. -Y., Hu, S. -L., Wu, J., Li, Y. -H., Zheng, J. -L., Wei, Z. -J., et al. (2012). Hydrogen sulfide prolongs postharvest shelf life of strawberry and plays an antioxidative role in fruits. *J. Agric. Food Chem.* 60, 8684–8693. doi: 10.1021/jf300728h

Hu, K. -D., Wang, Q., Hu, L. -Y., Gao, S. -P., Wu, J., Li, Y. -H., et al. (2014). Hydrogen sulfide prolongs postharvest storage of fresh-cut pears (*Pyrus pyrifolia*) by alleviation of oxidative damage and inhibition of fungal growth. *PLoS One* 9:e85524. doi: 10.1371/journal.pone.0085524

Hua, D., Duan, J., Ma, M., Li, Z., and Li, H. (2020). Reactive oxygen species induce cyanide-resistant respiration in potato infected by Erwinia carotovora subsp. Carotovora. *J. Plant Physiol.* 246:153132. doi: 10.1073/iti0419116

Huang, H., and Liu, R. (2019). DNA methylation and orange fruit ripening. *PNAS* 116, 1071–1073. doi: 10.1073/iti0419116

Hulme, A., Jones, J., and Wooltorton, L. (1963). The respiration climacteric in apple fruits. *Proc. R. Soc. Lond.* 158, 514–535. doi: 10.1098/rspb.1963.0061

Ireland, H. S., Yao, J. L., Tomes, S., Sutherland, P. W., Nieuwenhuizen, N., Gunaseelan, K., et al. (2013). Apple SEPALLATA1/2-like genes control fruit flesh development and ripening. *Plant J.* 73, 1044–1056. doi: 10.1111/tpj.12094

Itkin, M., Seybold, H., Breitel, D., Rogachev, I., Meir, S., and Aharoni, A. (2009). TOMATO AGAMOUS-LIKE 1 is a component of the fruit ripening regulatory network. *Plant J.* 60, 1081–1095. doi: 10.1111/j.1365-313X.2009.04064.x

Ito, Y., Nishizawa-Yokoi, A., Endo, M., Mikami, M., Shima, Y., Nakamura, N., et al. (2017). Re-evaluation of the rin mutation and the role of RIN in the induction of tomato ripening. *Nat. Plants* 3:866. doi: 10.1038/s41477-017-0041-5

Jia, H., Jiu, S., Zhang, C., Wang, C., Tariq, P., Liu, Z., et al. (2016a). Abscisic acid and sucrose regulate tomato and strawberry fruit ripening through the abscisic acid-stress-ripening transcription factor. *Plant Biotechnol. J.* 14, 2045–2065. doi: 10.1111/pbi.12563

Jia, H., Wang, X., Dou, Y., Liu, D., Si, W., Fang, H., et al. (2016b). Hydrogen sulfide-cysteine cycle system enhances cadmium tolerance through alleviating cadmium-induced oxidative stress and ion toxicity in Arabidopsis roots. *Sci. Rep.* 6, 1–14. doi: 10.1038/srep39702

Jiang, Z., Watanabe, C. K., Miyagi, A., Kawai-Yamada, M., Terashima, I., and Noguchi, K. (2019). Mitochondrial AOX supports redox balance of photosynthetic electron transport, primary metabolite balance, and growth in *Arabidopsis thaliana* under high light. *Int. J. Mol. Sci.* 20:3067. doi: 10.3390/ijms20123067

Jimenez, A., Creissen, G., Kular, B., Firmin, J., Robinson, S., Verhoeyen, M., et al. (2002). Changes in oxidative processes and components of the antioxidant system during tomato fruit ripening. *Planta* 214, 751–758. doi: 10.1007/s004250100667

Jogdand, S., Bhat, S., Misra, K., Kshirsagar, A., and Lal, R. (2017). New promising molecules for ethylene management in fruit crops, 1-MCP and nitric oxide: a review. *IJCS* 5, 434–441.

Karlova, R., Chapman, N., David, K., Angenent, G. C., Seymour, G. B., and de Maagd, R. A. (2014). Transcriptional control of fleshy fruit development and ripening. *J. Exp. Bot.* 65, 4527–4541. doi: 10.1093/jxb/eru316

Kim, J., Chang, C., and Tucker, M. L. (2015). To grow old: regulatory role of ethylene and jasmonic acid in senescence. *Front. Plant Sci.* 6:20. doi: 10.3389/fpls.2015.00020

Kim, H. -Y., Farcuh, M., Cohen, Y., Crisosto, C., Sadka, A., and Blumwald, E. (2015). Non-climacteric ripening and sorbitol homeostasis in plum fruits. *Plant Sci.* 231, 30–39. doi: 10.1016/j.plantsci.2014.11.002

Klee, H. J., and Giovannoni, J. J. (2011). Genetics and control of tomato fruit ripening and quality attributes. *Annu. Rev. Genet.* 45, 41–59. doi: 10.1146/annurev-genet-110410-132507

Krishnamurthy, S., and Subramanyam, H. (1970). Respiratory climacteric and chemical changes in the mango fruit, *Mangifera indica* L. *J. Am. Soc. Hortic. Sci.* 95, 333–337.

Kumar, V., Irfan, M., Ghosh, S., Chakraborty, N., Chakraborty, S., and Datta, A. (2016). Fruit ripening mutants reveal cell metabolism and redox state during ripening. *Protoplasma* 253, 581–594. doi: 10.1007/s00709-015-0836-z

Kumar, R., Khurana, A., and Sharma, A. K. (2014). Role of plant hormones and their interplay in development and ripening of fleshy fruits. *J. Exp. Bot.* 65, 4561–4575. doi: 10.1093/jxb/eru277

Lasanajak, Y., Minocha, R., Minocha, S. C., Goyal, R., Fatima, T., Handa, A. K., et al. (2014). Enhanced flux of substrates into polyamine biosynthesis but not ethylene in tomato fruit engineered with yeast S-adenosylmethionine decarboxylase gene. *Amino Acids* 46, 729–742. doi: 10.1007/s00726-013-1624-8

Lederman, I. E., Zauberman, G., Weksler, A., Rot, I., and Fuchs, Y. (1997). Ethylene-forming capacity during cold storage and chilling injury development in 'Keitt'mango fruit. *Postharvest Biol. Technol.* 10, 107–112. doi: 10.1016/S0925-5214(96)00060-9

Lelièvre, J. M., Latchè, A., Jones, B., Bouzayen, M., and Pech, J. C. (1997). Ethylene and fruit ripening. *Physiol. Plant.* 101, 727–739.

Li, C., Jia, H., Chai, Y., and Shen, Y. (2011). Abscisic acid perception and signaling transduction in strawberry: a model for non-climacteric fruit ripening. *Plant Signal. Behav.* 6, 1950–1953. doi: 10.4161/psb.6.12.18024

Li, C. R., Liang, D. D., Li, J., Duan, Y. B., Li, H., Yang, Y. C., et al. (2013). Unravelling mitochondrial retrograde regulation in the abiotic stress induction of rice ALTERNATIVE OXIDASE 1 genes. *Plant Cell Environ.* 36, 775–788. doi: 10.1111/pce.12013

Li, D., Limwachiranon, J., Li, L., Du, R., and Luo, Z. (2016). Involvement of energy metabolism to chilling tolerance induced by hydrogen sulfide in cold-stored banana fruit. *Food Chem.* 208, 272–278. doi: 10.1016/j.foodchem.2016.03.113

Li, L., Wang, X., Zhang, X., Guo, M., and Liu, T. (2017). Unraveling the target genes of RIN transcription factor during tomato fruit ripening and softening. *J. Sci. Food Agric.* 97, 991–1000. doi: 10.1002/jsfa.7825

Li, S., Xu, H., Ju, Z., Cao, D., Zhu, H., Fu, D., et al. (2018). The RIN-MC fusion of MADS-box transcription factors has transcriptional activity and modulates expression of many ripening genes. *Plant Physiol.* 176, 891–909. doi: 10.1104/pp.17.01449

Liu, R., How-Kit, A., Stammitti, L., Teyssier, E., Rolin, D., Mortain-Bertrand, A., et al. (2015). A DEMETER-like DNA demethylase governs tomato fruit ripening. *Proc. Natl. Acad. Sci.* 112, 10804–10809. doi: 10.1073/pnas.1503362112

Liu, M., Pirrello, J., Chervin, C., Roustan, J. -P., and Bouzayen, M. (2015). Ethylene control of fruit ripening: revisiting the complex network of transcriptional regulation. *Plant Physiol.* 169, 2380–2390. doi: 10.1104/pp.15.01361

Lozoya, O. A., Martinez-Reyes, I., Wang, T., Grenet, D., Bushel, P., Li, J., et al. (2018). Mitochondrial nicotinamide adenine dinucleotide reduced (NADH) oxidation links the tricarboxylic acid (TCA) cycle with methionine metabolism and nuclear DNA methylation. *PLoS Biol.* 16:e2005707. doi: 10.1371/journal.pbio.2005707

Lü, P., Yu, S., Zhu, N., Chen, Y. -R., Zhou, B., Pan, Y., et al. (2018). Genome encode analyses reveal the basis of convergent evolution of fleshy fruit ripening. *Nat. Plants* 4, 784–791. doi: 10.1038/s41477-018-0249-z

Luo, Z., Li, D., Du, R., and Mou, W. (2015). Hydrogen sulfide alleviates chilling injury of banana fruit by enhanced antioxidant system and proline content. *Sci. Hortic.* 183, 144–151. doi: 10.1016/j.scienta.2014.12.021

Manning, K., Tör, M., Poole, M., Hong, Y., Thompson, A. J., King, G. J., et al. (2006). A naturally occurring epigenetic mutation in a gene encoding an SBP-box transcription factor inhibits tomato fruit ripening. *Nat. Genet.* 38, 948–952. doi: 10.1038/ng1841

Marino, D., Dunand, C., Puppo, A., and Pauly, N. (2012). A burst of plant NADPH oxidases. *Trends Plant Sci.* 17, 9–15. doi: 10.1016/j.tplants.2011.10.001

Martel, C., Vrebalov, J., Tafelmeyer, P., and Giovannoni, J. J. (2011). The tomato MADS-box transcription factor RIPENING INHIBITOR interacts with promoters involved in numerous ripening processes in a COLORLESS NONRIPENING-dependent manner. *Plant Physiol.* 157, 1568–1579. doi: 10.1104/pp.111.181107

Marti, M. C., Olmos, E., Calvete, J. J., Diaz, I., Barranco-Medina, S., Whelan, J., et al. (2009). Mitochondrial and nuclear localization of a novel pea thioredoxin: identification of its mitochondrial target proteins. *Plant Physiol.* 150, 646–657. doi: 10.1104/pp.109.138073

Martín-Pizarro, C., and Posé, D. (2018). Genome editing as a tool for fruit ripening manipulation. *Front. Plant Sci.* 9:1415. doi: 10.3389/fpls.2018.01415

Mattoo, A. K., and White, W. B. (2018). "Regulation of ethylene biosynthesis" in *The plant hormone ethylene*. eds. A. K. Mattoo and J. C. Suttle (CRC Press), 21–42.

McAtee, P., Karim, S., Schaffer, R. J., and David, K. (2013). A dynamic interplay between phytohormones is required for fruit development, maturation, and ripening. *Front. Plant Sci.* 4:79. doi: 10.3389/fpls.2013.00079

McDonald, A. E., and Vanlerberghe, G. C. (2018). "The organization and control of plant mitochondrial metabolism" in *Annual Plant Reviews online*. *Vol. 22*. eds. W. C. Plaxton and M. T. McManus (Publisher-Wiley, Annual Plant Reviews online), 290–324.

McMurchie, E., McGlasson, W., and Eaks, I. (1972). Treatment of fruit with propylene gives information about the biogenesis of ethylene. *Nature* 237, 235–236. doi: 10.1038/237235a0

Millar, A. H., Mittova, V., Kiddle, G., Heazlewood, J. L., Bartoli, C. G., Theodoulou, F. L., et al. (2003). Control of ascorbate synthesis by respiration and its implications for stress responses. *Plant Physiol.* 133, 443–447. doi: 10.1104/pp.103.028399

Minas, I. S., Font i Forcada, C., Dangl, G. S., Gradziel, T. M., Dandekar, A. M., and Crisosto, C. H. (2015). Discovery of non-climacteric and suppressed climacteric bud sport mutations originating from a climacteric Japanese plum cultivar (*Prunus salicina* Lindl.). *Front. Plant Sci.* 6:316. doi: 10.3389/fpls.2015.00316

Morozova, O., and Marra, M. A. (2008). Applications of next-generation sequencing technologies in functional genomics. *Genomics* 92, 255–264. doi: 10.1016/j.ygeno.2008.07.001

Muñoz, P., and Munné-Bosch, S. (2018). Photo-oxidative stress during leaf, flower and fruit development. *Plant Physiol.* 176, 1004–1014. doi: 10.1104/pp.17.01127

Ng, S., De Clercq, I., Van Aken, O., Law, S. R., Ivanova, A., Willems, P., et al. (2014). Anterograde and retrograde regulation of nuclear genes encoding mitochondrial proteins during growth, development, and stress. *Mol. Plant* 7, 1075–1093. doi: 10.1093/mp/ssu037

Nguyen, T. T., and Sim, S. -C. (2017). Development of a gene-based marker for the non-ripening (nor) gene in cultivated tomato. *Korean J. Hortic. Sci. Technol.* 110, 618–627. doi: 10.12972/kjhst.20170066

Nham, N. T., Macnish, A. J., Zakharov, F., and Mitcham, E. J. (2017). 'Bartlett'pear fruit (*Pyrus communis* L.) ripening regulation by low temperatures involves genes associated with jasmonic acid, cold response, and transcription factors. *Plant Sci.* 260, 8–18. doi: 10.1016/j.plantsci.2017.03.008

Noctor, G., Reichheld, J. -P., and Foyer, C. H. (2018). "ROS-related redox regulation and signaling in plants" in *Seminars in Cell & Developmental Biology*. *Vol. 80*. (Elsevier, Academic Press), 3–12.

Oliveira, M. G., Mazorra, L. M., Souza, A. F., Silva, G. M. C., Correa, S. F., Santos, W. C., et al. (2015). Involvement of AOX and UCP pathways in the post-harvest ripening of papaya fruits. *J. Plant Physiol.* 189, 42–50. doi: 10.1016/j.jplph.2015.10.001

Osorio, S., Scossa, F., and Fernie, A. (2013a). Molecular regulation of fruit ripening. *Front. Plant Sci.* 4:198. doi: 10.3389/fpls.2013.00198

Osorio, S., Vallarino, J. G., Szecowka, M., Ufaz, S., Tzin, V., Angelovici, R., et al. (2013b). Alteration of the Interconversion of pyruvate and malate in the plastid or cytosol of ripening tomato fruit invokes diverse consequences on sugar but similar effects on cellular organic acid, metabolism, and transitory starch accumulation. *Plant Physiol.* 161, 628–643. doi: 10.1104/pp.112.211094

Paul, V., Pandey, R., and Srivastava, G. (2012). The fading distinctions between classical patterns of ripening in climacteric and non-climacteric fruit and the ubiquity of ethylene-an overview. *J. Food Sci. Technol.* 49, 1–21. doi: 10.1007/s13197-011-0293-4

Perotti, V. E., Moreno, A. S., and Podestá, F. E. (2014). Physiological aspects of fruit ripening: the mitochondrial connection. *Mitochondrion* 17, 1–6. doi: 10.1016/j.mito.2014.04.010

Polidoros, A. N., Mylona, P. V., and Arnholdt-Schmitt, B. (2009). Aox gene structure, transcript variation and expression in plants. *Physiol. Plant.* 137, 342–353. doi: 10.1111/j.1399-3054.2009.01284.x

Polko, J. K., and Kieber, J. J. (2019). 1-Aminocyclopropane 1-carboxylic acid and its emerging role as an ethylene-independent growth regulator. *Front. Plant Sci.* 10:1602. doi: 10.3389/fpls.2019.01602

Qi, J., Wang, J., Gong, Z., and Zhou, J. -M. (2017). Apoplastic ROS signaling in plant immunity. *Curr. Opin. Plant Biol.* 38, 92–100. doi: 10.1016/j.pbi.2017.04.022

Ritenour, M. A., Crisosto, C. H., Garner, D. T., Cheng, G. W., and Zoffoli, J. P. (1999). Temperature, length of cold storage and maturity influence the ripening rate of ethylene-preconditioned kiwifruit. *Postharvest Biol. Technol.* 15, 107–115. doi: 10.1016/S0925-5214(98)00074-X

Rogov, A., and Zvyagilskaya, R. (2015). Physiological role of alternative oxidase (from yeasts to plants). *Biochem. Mosc.* 80, 400–407. doi: 10.1134/S0006297915040021

Saha, B., Borovskii, G., and Panda, S. K. (2016). Alternative oxidase and plant stress tolerance. *Plant Signal. Behav.* 11:e1256530. doi: 10.1080/15592324.2016.1256530

Saladié, M., Cañizares, J., Phillips, M. A., Rodriguez-Concepcion, M., Larrigaudière, C., Gibon, Y., et al. (2015). Comparative transcriptional profiling analysis of developing melon (*Cucumis melo* L.) fruit from climacteric and non-climacteric varieties. *BMC Genomics* 16:440. doi: 10.1186/s12864-015-1649-3

Salminen, S. O., and Young, R. E. (1975). The control properties of phosphofructokinase in relation to the respiratory climacteric in banana fruit. *Plant Physiol.* 55, 45–50. doi: 10.1104/pp.55.1.45

Schimmeyer, J., Bock, R., and Meyer, E. H. (2016). L-Galactono-1, 4-lactone dehydrogenase is an assembly factor of the membrane arm of mitochondrial complex I in Arabidopsis. *Plant Mol. Biol.* 90, 117–126. doi: 10.1007/s11103-015-0400-4

Selinski, J., Hartmann, A., Deckers-Hebestreit, G., Day, D. A., Whelan, J., and Scheibe, R. (2018). Alternative oxidase isoforms are differentially activated by tricarboxylic acid cycle intermediates. *Plant Physiol.* 176, 1423–1432. doi: 10.1104/pp.17.01331

Sewelam, N., Kazan, K., and Schenk, P. M. (2016). Global plant stress signaling: reactive oxygen species at the cross-road. *Front. Plant Sci.* 7:187. doi: 10.3389/fpls.2016.00187

Seymour, G. B., Chapman, N. H., Chew, B. L., and Rose, J. K. (2013a). Regulation of ripening and opportunities for control in tomato and other fruits. *Plant Biotechnol. J.* 11, 269–278. doi: 10.1111/j.1467-7652.2012.00738.x

Seymour, G. B., Taylor, J. E., and Tucker, G. A. (2012). *Biochemistry of fruit ripening*. USA: Springer Science & Business Media.

Seymour, G. B., Tucker, G. A., and Poole, M. (2013b). *Giovann, The molecular biology and biochemistry of fruit ripening*. Ames, Iowa, USA: Wiley Online Library.

Shima, Y., Kitagawa, M., Fujisawa, M., Nakano, T., Kato, H., Kimbara, J., et al. (2013). Tomato FRUITFULL homologues act in fruit ripening via forming MADS-box transcription factor complexes with RIN. *Plant Mol. Biol.* 82, 427–438. doi: 10.1007/s11103-013-0071-y

Shinshi, H. (2008). Ethylene-regulated transcription and crosstalk with jasmonic acid. *Plant Sci.* 175, 18–23. doi: 10.1016/j.plantsci.2008.03.017

Suzuki, N., Miller, G., Morales, J., Shulaev, V., Torres, M. A., and Mittler, R. (2011). Respiratory burst oxidases: the engines of ROS signaling. *Curr. Opin. Plant Biol.* 14, 691–699. doi: 10.1016/j.pbi.2011.07.014

Tatsuki, M., Endo, A., and Ohkawa, H. (2007). Influence of time from harvest to 1-MCP treatment on apple fruit quality and expression of genes for ethylene biosynthesis enzymes and ethylene receptors. *Postharvest Biol. Technol.* 43, 28–35. doi: 10.1016/j.postharvbio.2006.08.010

Umbach, A. L., Ng, V. S., and Siedow, J. N. (2006). Regulation of plant alternative oxidase activity: a tale of two cysteines. *Biochim. Biophys. Acta* 1757, 135–142. doi: 10.1016/j.bbabio.2005.12.005

Vaahtera, L., Brosche, M., Wrzaczek, M., and Kangasjärvi, J. (2013). Specificity in ROS signaling and transcript signatures. *Antioxid. Redox Signal.* 21, 1422–1441. doi: 10.1089/ars.2013.566

Valenzuela, J. L., Manzano, S., Palma, F., Carvajal, F., Garrido, D., and Jamilena, M. (2017). Oxidative stress associated with chilling injury in immature fruit: postharvest technological and biotechnological solutions. *Int. J. Mol. Sci.* 18:1467. doi: 10.3390/ijms18071467

Van de Poel, B., Bulens, I., Oppermann, Y., Hertog, M. L., Nicolai, B. M., Sauter, M., et al. (2013). S-adenosyl-l-methionine usage during climacteric ripening of tomato in relation to ethylene and polyamine biosynthesis and transmethylation capacity. *Physiol. Plant.* 148, 176–188. doi: 10.1111/j.1399-3054.2012.01703.x

Vanderstraeten, L., Depaepe, T., Bertrand, S., and Van Der Straeten, D. (2019). The ethylene precursor ACC affects early vegetative development independently of ethylene signaling. *Front. Plant Sci.* 10:1591. doi: 10.3389/fpls.2019.01591

Vanlerberghe, G. C. (2013). Alternative oxidase: a mitochondrial respiratory pathway to maintain metabolic and signaling homeostasis during abiotic and biotic stress in plants. *Int. J. Mol. Sci.* 14, 6805–6847. doi: 10.3390/ijms14046805

Villalobos-Acuna, M., and Mitcham, E. J. (2008). Ripening of European pears: the chilling dilemma. *Postharvest Biol. Technol.* 49, 187–200. doi: 10.1016/j.postharvbio.2008.03.003

Vrebalov, J., Ruezinsky, D., Padmanabhan, V., White, R., Medrano, D., Drake, R., et al. (2002). A MADS-box gene necessary for fruit ripening at the tomato ripening-inhibitor (rin) locus. *Science* 296, 343–346. doi: 10.1126/science.1068181

Wagner, A. M., and Moore, A. L. (1997). Structure and function of the plant alternative oxidase: its putative role in the oxygen defence mechanism. *Biosci. Rep.* 17, 319–333. doi: 10.1023/a:1027388729586

Wang, R., da Rocha Tavano, E. C., Lammers, M., Martinelli, A. P., Angenent, G. C., and de Maagd, R. A. (2019). Re-evaluation of transcription factor function in tomato fruit development and ripening with CRISPR/Cas9-mutagenesis. *Sci. Rep.* 9, 1–10. doi: 10.1038/s41598-018-38170-6

Wang, H., Huang, J., Liang, X., and Bi, Y. (2012). Involvement of hydrogen peroxide, calcium, and ethylene in the induction of the alternative pathway in chilling-stressed Arabidopsis callus. *Planta* 235, 53–67. doi: 10.1007/s00425-011-1488-7

Wang, H., Liang, X., Huang, J., Zhang, D., Lu, H., Liu, Z., et al. (2010). Involvement of ethylene and hydrogen peroxide in induction of alternative respiratory pathway in salt-treated Arabidopsis calluses. *Plant Cell Physiol.* 51, 1754–1765. doi: 10.1093/pcp/pcq134

Wang, C., and Mellenthin, W. (1972). Internal ethylene levels during ripening and climacteric in Anjou pears. *Plant Physiol.* 50, 311–312. doi: 10.1104/pp.50.2.311

Watkins, C. B. (2006). The use of 1-methylcyclopropene (1-MCP) on fruits and vegetables. *Biotechnol. Adv.* 24, 389–409. doi: 10.1016/j.biotechadv.2006.01.005

Watkins, C. B. (2015). "Advances in the use of 1-MCP" in *Advances in postharvest fruit and vegetable technology.* eds. R. B. H. Willis and J. B. Golding (Boca Raton, FL: CRC Press), 117–145.

Wei, L., Deng, X. -G., Zhu, T., Zheng, T., Li, P. -X., Wu, J. -Q., et al. (2015). Ethylene is involved in brassinosteroids induced alternative respiratory pathway in cucumber (*Cucumis sativus* L.) seedlings response to abiotic stress. *Front. Plant Sci.* 6:982. doi: 10.3389/fpls.2015.00982

Welchen, E., and Gonzalez, D. H. (2016). Cytochrome c, a hub linking energy, redox, stress and signaling pathways in mitochondria and other cell compartments. *Physiol. Plant.* 157, 310–321. doi: 10.1111/ppl.12449

Woodward, E. W., Murphy, C. C., and Heckman, N. (2009). Alternative oxidase identification and capacity in postharvest ripening stages of banana fruit. *J. Undergrad. Chem. Res.* 8:52.

Xu, Q., and Roose, M. L. (2020). "Citrus genomes: from sequence variations to epigenetic modifications" in *The Citrus genome.* eds. A. Gentile, S. La Malfa and Z. Deng (Springer, Cham), 141–165.

Xu, F., Yuan, S., Zhang, D. -W., Lv, X., and Lin, H. -H. (2012). The role of alternative oxidase in tomato fruit ripening and its regulatory interaction with ethylene. *J. Exp. Bot.* 63, 5705–5716. doi: 10.1093/jxb/ers226

Yamane, M., Abe, D., Yasui, S., Yokotani, N., Kimata, W., Ushijima, K., et al. (2007). Differential expression of ethylene biosynthetic genes in climacteric and non-climacteric Chinese pear fruit. *Postharvest Biol. Technol.* 44, 220–227. doi: 10.1016/j.postharvbio.2006.12.010

Yang, S. F., and Hoffman, N. E. (1984). Ethylene biosynthesis and its regulation in higher plants. *Annu. Rev. Plant Physiol.* 35, 155–189. doi: 10.1146/annurev.pp.35.060184.001103

Zhong, S., Fei, Z., Chen, Y. -R., Zheng, Y., Huang, M., Vrebalov, J., et al. (2013). Single-base resolution methylomes of tomato fruit development reveal epigenome modifications associated with ripening. *Nat. Biotechnol.* 31, 154–159. doi: 10.1038/nbt.2462

Zhou, L., Tian, S., and Qin, G. (2019). RNA methylomes reveal the m 6 A-mediated regulation of DNA demethylase gene SlDML2 in tomato fruit ripening. *Genome Biol.* 20, 1–23. doi: 10.1186/s13059-019-1771-7

Ziogas, V., Molassiotis, A., Fotopoulos, V., and Tanou, G. (2018). Hydrogen sulfide: a potent tool in postharvest fruit biology and possible mechanism of action. *Front. Plant Sci.* 9:1375. doi: 10.3389/fpls.2018.01375

Zuo, J., Grierson, D., Courtney, L. T., Wang, Y., Gao, L., Zhao, X., et al. (2020). Relationships between genome methylation, levels of non-coding RNAs, mRNAs and metabolites in ripening tomato fruit. *Plant J.* 103, 980–994. doi: 10.1111/tpj.14778

Conflict of Interest: The authors declare that the research was conducted in the absence of any commercial or financial relationships that could be construed as a potential conflict of interest.

frontiers in Plant Science

ORIGINAL RESEARCH
published: 26 November 2020
doi: 10.3389/fpls.2020.554158

Postharvest Properties of Ultra-Late Maturing Peach Cultivars and Their Attributions to *Melting Flesh* (*M*) Locus: Re-evaluation of *M* Locus in Association With Flesh Texture

Ryohei Nakano[1†], Takashi Kawai[2†], Yosuke Fukamatsu[2‡], Kagari Akita[2], Sakine Watanabe[2], Takahiro Asano[2], Daisuke Takata[3], Mamoru Sato[3], Fumio Fukuda[2] and Koichiro Ushijima[2*]*

[1] *Experimental Farm of Graduate School of Agriculture, Kyoto University, Kizugawa, Kyoto, Japan,* [2] *Graduate School of Environmental and Life Science, Okayama University, Okayama, Japan,* [3] *Faculty of Food and Agricultural Sciences, Fukushima University, Fukushima, Japan*

The postharvest properties of two ultra-late maturing peach cultivars, "Tobihaku" (TH) and "Daijumitsuto" (DJ), were investigated. Fruit were harvested at commercial maturity and held at 25°C. TH exhibited the characteristics of normal melting flesh (MF) peach, including rapid fruit softening associated with appropriate level of endogenous ethylene production In contrast, DJ did not soften at all during 3 weeks experimental period even though considerable ethylene production was observed. Fruit of TH and DJ were treated with 5,000 ppm of propylene, an ethylene analog, continuously for 7 days. TH softened rapidly whereas DJ maintained high flesh firmness in spite of an increase in endogenous ethylene production, suggesting that DJ but not TH lacked the ability to be softened in response to endogenous and exogenous ethylene/propylene. DNA-seq analysis showed that tandem endo-polygalacturonase (*endoPG*) genes located at *melting flesh (M)* locus, *Pp-endoPGM* (*PGM*), and *Pp-endoPGF* (*PGF*), were deleted in DJ. The *endoPG* genes at *M* locus are known to control flesh texture of peach fruit, and it was suggested that the non-softening property of DJ is due to the lack of *endoPG* genes. On the other hand, TH possessed an unidentified *M* haplotype that is involved in determination of MF phenotype. Structural identification of the unknown *M* haplotype, designated as M^0, through comparison with previously reported *M* haplotypes revealed distinct differences between *PGM* on M^0 haplotype (*PGM*-M^0) and *PGM* on other haplotypes (*PGM*-M^1). Peach *M* haplotypes were classified into four main haplotypes: M^0 with *PGM*-M^0; M^1 with both *PGM*-M^1 and *PGF*; M^2 with *PGM*-M^1; and M^3 lacking both *PGM* and *PGF*. Re-evaluation of *M* locus in association with MF/non-melting flesh (NMF) phenotypes in more than 400 accessions by using whole genome shotgun sequencing data on database and/or by PCR genotyping demonstrated that M^0 haplotype was the common haplotype in MF accessions, and M^0 and M^1 haplotypes

OPEN ACCESS

Edited by:
Cai-Zhong Jiang, USDA-ARS, United States

Reviewed by:
Carlos H. Crisosto, University of California, Davis, United States
Macarena Farcuh, University of Maryland, College Park, United States

****Correspondence:***
Fumio Fukuda
ffukuda@okayama-u.ac.jp
Koichiro Ushijima
ushijima@cc.okayama-u.ac.jp

† These authors have contributed equally to this work

‡ Present address:
Yosuke Fukamatsu, Research Institute for Biological Sciences, Okayama Prefectural Technology Center for Agriculture, Forestry, and Fisheries, Okayama, Japan

Specialty section:
This article was submitted to Crop and Product Physiology, a section of the journal Frontiers in Plant Science

Received: *23 April 2020*
Accepted: *28 October 2020*
Published: *26 November 2020*

Citation:
Nakano R, Kawai T, Fukamatsu Y, Akita K, Watanabe S, Asano T, Takata D, Sato M, Fukuda F and Ushijima K (2020) Postharvest Properties of Ultra-Late Maturing Peach Cultivars and Their Attributions to Melting Flesh (M) Locus: Re-evaluation of M Locus in Association With Flesh Texture. Front. Plant Sci. 11:554158. doi: 10.3389/fpls.2020.554158

were dominant over M^2 and M^3 haplotypes and co-dominantly determined the MF trait. It was also assumed on the basis of structural comparison of *M* haplotypes among *Prunus* species that the ancestral haplotype of M^0 diverged from those of the other haplotypes before the speciation of *Prunus persica*.

Keywords: fruit, softening, ethylene, *Prunus persica,* melting flesh locus, endoPG, postharvest

INTRODUCTION

Fruit firmness is an important quality that influences consumer preference, damage during distribution, and shelf life. Studies associated with the decrease in fruit firmness after harvest have been conducted with an eye toward reducing distribution loss and prolonging shelf life and thus, supplying high-quality fruit to consumers (Nimmakayala et al., 2016; Moggia et al., 2017; Tucker et al., 2017; Fernandez et al., 2018; Liu et al., 2018; Carrasco-Valenzuela et al., 2019). Fruit can be classified as climacteric or non-climacteric depending on their respiration and ethylene production patterns during ripening (Biale and Young, 1981). In climacteric fruit, ethylene is acknowledged to play an important role in controlling ripening- and senescence-related phenomena including fruit softening, due to the fact that massive ethylene production commences at the onset of ripening; exogenously applied ethylene and/or ethylene analog, propylene, induces ripening and senescence; ethylene inhibitors retard the progress of fruit ripening and senescence; and mutants and transgenic lines defective in ethylene production ability exhibit suppressed fruit ripening, especially softening (Gapper et al., 2013; Minas et al., 2015; Tucker et al., 2017).

Peach [*Prunus persica* (L.) Batsch] is generally known to belong to the climacteric type and to exhibit dramatic increases in respiration and ethylene production during ripening (Tonutti et al., 1991). In melting flesh (MF) peaches, the increased ethylene stimulates fruit softening principally through cell wall modification (Brummell et al., 2004; Hayama et al., 2006, 2008; Liu et al., 2018). MF peaches are highly perishable, softening rapidly after harvest. The increasing interest in improving peach shelf life has sparked investigations and resulted in findings of peach strains with long shelf lives. Those studies have demonstrated phenotypic variability associated with fruit softening and identified the possible causal genes for peach shelf life, as described below.

Intensively studied peaches that have long shelf lives are the stony-hard (SH) and slow-ripening (SR) peaches (Brecht and Kader, 1984; Haji et al., 2005; Bassi and Monet, 2008). The SH is determined by *Hdhd* gene and fruit with SH flesh bear the *hdhd* genotype (Haji et al., 2005). SH peaches are characterized by the absence of ethylene production and high firmness during postharvest storage, which are caused by the reduced expression of ethylene biosynthesis related gene *PpACS1* encoding 1-aminocyclopropane-1-carboxylic acid synthase (Tatsuki et al., 2006). YUCCA flavin mono-oxygenase gene *PpYUC11*, which is involved in the auxin biosynthesis pathway, has been proposed as a candidate for causal gene for this phenotype (Pan et al., 2015; Tatsuki et al., 2018). SR peaches are known to show delayed maturation on the tree, thereby resulting in late harvest. In SR peaches harvested earlier than the optimum harvest date, flesh firmness decreased slowly (Brecht and Kader, 1984). Its genetic base was characterized and a deletion mutation in a gene encoding the NAC transcription factor was reported to be responsible for the SR phenotype (Eduardo et al., 2015; Nuñez-Lillo et al., 2015; Meneses et al., 2016).

Another peach strain that shows high flesh firmness during postharvest ripening is non-melting flesh (NMF) peaches (Fishman et al., 1993; Yoshioka et al., 2011). Whereas MF peaches soften dramatically and bear melting texture during the final stage of ripening called "melting phase," NMF fruit appear to lack this "melting phase" of softening and remain relatively firm during ripening not only on the tree and but also after harvest (Fishman et al., 1993; Yoshioka et al., 2011). The MF/NMF phenotypes segregate as a single locus (*M*) that is linked tightly to the stone adhesion locus (Bailey and French, 1949; Monet, 1989). MF is dominant over NMF and the recessive allele determines the NMF character (Bailey and French, 1949; Monet, 1989). In NMF peaches, solubilization of cell wall pectin and enzymatic activity and protein accumulation of endo-polygalacturonase (endoPG), a pectin hydrolase, are markedly reduced compared with MF peaches (Pressey and Avants, 1978; Fishman et al., 1993; Lester et al., 1996; Yoshioka et al., 2011). Studies aimed at demonstrating *endoPG(s)* as a candidate gene for *M* locus have shown suppressed or undetectable expression of *endoPG(s)* in NMF peaches and polymorphisms in *endoPG* genes coinciding with MF/NMF phenotypes (Lester et al., 1994, 1996; Callahan et al., 2004; Peace et al., 2005, 2007; Morgutti et al., 2006, 2017; Gu et al., 2016). *M* locus is located at 3.5 cM interval on the bottom of linkage group 4 of the peach map, the position within which a genomic region with clusters of *endoPG* genes exists (Cao et al., 2016; Gu et al., 2016). Two tandem *endoPG* genes in that region, *Pp-endoPGM* (*PGM*) and *Pp-endoPGF* (*PGF*), corresponding to sequences *Prupe.4G262200* in v2.0 of peach genome (*ppa006857m* in v1.0) and *Prupe.4G261900* (*ppa006839m* in v1.0), respectively, were found to be responsible for determining the MF/NMF phenotypes (Gu et al., 2016). Gu et al. (2016) proposed a scenario where *M* locus has three allelic copy number variants of *endoPG* genes designated by H_1 (possessing *PGF* and *PGM*), H_2 (only *PGM*), and H_3 (*null*). Accessions harboring either H_1 and/or H_2 haplotype (H_1H_1, H_1H_2, H_1H_3, H_2H_2, and H_2H_3) exhibit MF phenotype whereas those harboring homozygous recessive H_3 (H_3H_3) show NMF

Abbreviations: *M* locus, Melting flesh locus; MF, melting flesh; NMF, non-melting flesh; SH, stony-hard; SR, slow-ripening; SSC, soluble solids content; endo-PG, endo-polygalacturonase; NADH, nicotinamide adenine dinucleotide dehydrogenase; SRA, sequence read archive; WGS, whole genome shotgun sequencing; SNP, single nucleotide polymorphism; indel, insertion/deletion.

phenotype (Gu et al., 2016). It was also speculated that H_2 is the ancestral haplotype whereas H_1 and H_3 haplotypes are two variants due to the duplication and deletion of *PGM*, respectively, (Gu et al., 2016). However, research on different NMF peach germplasms suggested that mutations in *endoPG* gene(s) could be of more than one type arising from more than one source (Lester et al., 1996; Callahan et al., 2004; Peace et al., 2005; Morgutti et al., 2006, 2017) and some NMF accessions seemed to be incompatible with the model proposed by Gu et al. (2016). Much more comprehensive evaluation of *M* locus in association with flesh textural traits is required. Pursuing *M* locus evolution with much broader genetic resources covering *Prunus* species is also necessary for precise judgment.

Peach is known to have high diversity with regard to not only flesh texture but also fruit maturation date (Elsadr et al., 2019). In Japan, MF peaches reaching maturation stage in early July through September are mainly produced. Recently, because of the increasing demand for fresh peach in late autumn, ultra-late maturing cultivars whose optimum harvest dates are October and November are gathering the attention of growers. However, the postharvest properties of some of these rare cultivars have not yet been characterized.

In this study, first, two postharvest properties, namely, ethylene production and fruit softening, of two extremely late harvest cultivars, "Tobihaku" (TH) and "Daijumitsuto" (DJ), were investigated. It was revealed that TH showed normal MF peach ripening properties, whereas DJ possessed unique properties in that the fruit did not soften at all in spite of significant endogenous ethylene production and exogenous propylene treatment. Second, DNA-seq analysis of these cultivars demonstrated that DJ was a homozygote of an allele lacking *PGM* and *PGF* at *M locus*, whereas TH possessed a previously structurally unidentified haplotype that contained one *endoPG*. Third, accessing database sequences at *M* locus in more than 400 peach accessions and *Prunus* species indicated that the newly identified haplotype was an important allele that distributed widely within MF accessions, determined MF phenotype, and seemed to have been diverse from the other haplotypes before the speciation of *P. persica*. The scenario is discussed in which not three but four allelic variants at *M* locus are associated with the flesh texture and the newly identified haplotype is one of the two dominant determinants of MF texture.

MATERIALS AND METHODS

Plant Materials

Ultra-late maturing peach (*Prunus persica*) cultivars "Tobihaku" (TH) and "Daijumitsuto" (DJ), whose genetic backgrounds are unknown, were examined. TH fruit were harvested on November 7, 2018, the commercial harvest date, from two trees grown in a commercial orchard in Okayama Prefecture located in southwestern Japan. DJ fruit were harvested on October 12, 2018, the commercial harvest date, from two trees grown in the Research Farm of Okayama University. For each cultivar, 26 fruit without any disease and injuries were selected and used for investigation described below. As regards DJ, 16 fruit from a different production area, namely, Fukushima Prefecture, which is located in northeastern Japan, were harvested on October 22, 2018, the commercial harvest date, and 12 fruit without any disease and injuries after transfer to Okayama were used to investigate the effects of growing conditions and harvest maturity. Climate conditions in the peach production areas, which were obtained from the website of the Japan Meteorological Agency[1], are listed in **Supplementary Table S1**. Regardless of cultivar or growing area, fruit were grown under suitable climate conditions for peach production by skilled growers using conventional growing techniques in Japan, including fruit thinning and bagging by the end of June. The fruit were harvested on the basis of skilled growers' visual evaluation using de-greening of fruit ground color as harvest index. It is equivalent to color chip No. 3 (color meter score of L: 76.8, a*: −8.16, b*: 29.7) of de-greening harvest index reported in Yamazaki and Suzuki (1980). After harvest, 16 out of the 26 fruit of TH and DJ harvested from Okayama Prefecture were ripened at 25°C for 3 weeks and ethylene production rate, flesh firmness, soluble solids content (SSC), and juice pH were measured on days 0, 7, 14, and 21 at 25°C. DJ fruit harvested from Fukushima Prefecture were packed carefully in a corrugated cardboard box and transported by vehicle at ambient temperature to Okayama University 2 days after harvest, where 12 fruit without any disease and injuries were ripened at 25°C.

Propylene Treatment

Ten out of 26 fruit of TH and DJ harvested from Okayama Prefecture were used for experiment with continuous propylene treatment. Six fruits per each cultivar, excluding those used for measurement of values at day 0, were treated with 5,000 ppm of propylene, an ethylene analog, continuously for 7 days at 25°C, as described previously (McMurchie et al., 1972; Hiwasa et al., 2004). Ethylene production rates and flesh firmness were measured on treatment days 0, 3, and 7.

Measurement of Ethylene Production Rate, Flesh Firmness, SSC, and Juice pH

Ethylene production rate, flesh firmness, SSC, and juice pH were measured as described previously (Kawai et al., 2018; Nakano et al., 2018). For the measurement of ethylene production rate, individual fruit were incubated in a 1.3 L plastic container at room temperature for 30 min. Headspace gas withdrawn from the container was injected into a gas chromatograph (GC8 CMPF; Shimadzu, Kyoto, Japan) equipped with a flame ionization detector (set at 200°C) and an activated alumina column (ϕ 4 mm × 1 m) set at 80°C. For flesh firmness, the cheek parts of each fruit were cut and peeled, and flesh penetration force was measured using a rheometer (FUDOH RTC Rheometer; RHEOTECH, Tokyo, Japan) with a 3-mm-diameter cylindrical plunger and expressed in Newton per plunger area (N/mm^2). The relationships between the flesh penetration force measured by this system and fruit maturity indexes are listed in **Supplementary Table S2**. SSC and juice pH in the cheek parts of each fruit were measured with a

[1]http://www.jma.go.jp/jma/index.html

refractometer (PR-1; Atago, Tokyo, Japan) and a pH meter (B-712; HORIBA, Kyoto, Japan), respectively.

Statistical Analysis

Three to four fruit were used as biological replicates at each measurement point. In order to evaluate postharvest changing patterns in flesh firmness and ethylene production in different cultivars or production areas under the condition with and without propylene, Tukey's multiple comparison test was conducted after one-way ANOVA. The different letters shown in each figure indicate significant differences among measurement days by Tukey's test ($p < 0.05$).

Mapping WGS Data and Variant Calling

Genomic DNA was isolated from the leaves of DJ, TH, and "Benihakuto" (BH) by Nucleon PhytoPure (Cytiva). DNA-seq analysis was performed by Novogen and 9G data of PE150 reads, corresponding to approx. 30 times coverage, were obtained. We further searched SRA (Sequence Read Archive) database to obtain whole genome shotgun sequencing (WGS) data for doubled haploid "Lovell" (dhLL), "Dr. Davis" (DD), and "Big Top" (BT). Illumina WGS reads were mapped to peach reference genome (ver. 2.0) (Verde et al., 2017) by CLC Genomics Workbench or minimap2 (Li, 2018). SNP, indel, and structural variants were called by CLC Genomics Workbench.

De novo Assembly and Structural Comparison

DNA-seq analysis of BH was further performed by Macrogen to obtain 46G data of PE150 reads, which correspond to approx. 170 times coverage of *P. persica* genome. Illumina reads were assembled by ABySS 2.0 (Jackman et al., 2017). Contigs encompassing *M* locus were detected by Blastn analysis using *PG1*, *PG2*, *PGM/F*, *NADH*, and *F-box* genes, which were located in the *M* locus region, as query. M^0 and M^1 haplotype sequences (see section "Results") were compared by nucmer (Kurtz et al., 2004) and their relationship was drawn by Circos[2]. We generated new reference sequence set "PpREF20 + M0," in which the M^0 haplotype sequence was added to *P. persica* reference genome. Illumina short reads of DJ, TH, BH, dhLL, DD, and BT were mapped to PpREF20 + M0 by minimap2. Coverage was analyzed from BAM file by samtools and drawn by Circos.

Genotyping by PCR

Genomic DNA was extracted from leaves of peach accessions. Genotyping by PCR was conducted with six sets of primers described in **Supplementary Table S3**. PCR was performed with BIOTAQ DNA Polymerase (Bioline, United Kingdom) using the following program: 30–35 cycles at 95°C for 20 s, annealing for 15 s, and extension at 72°C an initial denaturation at 95°C for 3 min, and a final extension at 72°C for 7 min. Annealing temperature and extension time are described under "PCR conditions" in **Supplementary Table S3**. PGM/F products were separated on a 15% acrylamide gel and others were separated on an agarose gel. PCR products were stained with UltraPower DNA Safedye (Gellex International Co., Ltd., Japan).

[2]http://circos.ca

RESULTS

Fruit Ripening Characteristics of Two Ultra-Late Maturing Cultivars

Postharvest changes in ethylene production rate, flesh firmness, SSC, and juice pH were investigated in two ultra-late maturing peach cultivars, TH and DJ. In TH, as much as 22 $nl{\cdot}g^{-1}{\cdot}h^{-1}$ of ethylene was produced at harvest and the amount increased gradually during storage at 25°C (**Figure 1A**). Flesh firmness was 0.7 N/mm^2 at harvest but decreased dramatically to less than 0.2 N/mm^2 by day 7 at 25°C (**Figure 1D**). Thereafter, the decrease became slight until the last day of experiment (day 21). SSC and juice pH did not change remarkably during storage (**Supplementary Figure S1**). In DJ harvested from the Research Farm of Okayama University on October 12, ethylene production rate was almost negligible at harvest. Thereafter, ethylene production rate increased and peaked on day 7, reaching more than 10 $nl{\cdot}g^{-1}{\cdot}h^{-1}$ (**Figure 1B**). Flesh firmness was around 0.85 N/mm^2 at harvest (**Figure 1E**). In spite of considerable ethylene production, flesh firmness showed no significant decrease during storage at 25°C and was almost unchanged until the last day of experiment (day 21). SSC slightly increased during storage, reaching a peak of 18 °Brix on day 14, and juice pH was maintained at around pH 4.0 during storage (**Supplementary Figure S1**).

To confirm that the unique characteristics of DJ were not due to climatic effects and/or misestimated harvest maturity, DJ fruit harvested from a different production area were investigated. In the case of DJ harvested from a commercial orchard in Fukushima Prefecture on October 22, fruit delivered to Okayama University two days after harvest had an ethylene production rate of as high as 5.2 $nl{\cdot}g^{-1}{\cdot}h^{-1}$ and flesh firmness of 0.6 N/mm^2 (**Figures 1C,F**). Substantially high level of ethylene production was maintained during storage at 25°C, scoring 16 $nl{\cdot}g^{-1}{\cdot}h^{-1}$ on day 21. On the other hand, flesh firmness did not change significantly during storage; flesh firmness on day 21 was almost the same as that at harvest. SSC and juice pH did not change remarkably during storage (**Supplementary Figure S1**). **Figure 2** shows DJ fruit on day 14. The external appearance showed no significant deterioration; however, the longitudinal sections showed flesh browning and slight flesh breakdown around the stones.

Different Responses to Exogenous Propylene Treatment of TH and DJ

Although ethylene production rate during storage was higher in TH than DJ, generally speaking, the amount of ethylene produced in DJ is sufficient to induce physiological effects on fruit ripening including flesh softening (Mathooko et al., 2001; Hiwasa et al., 2004; Nishiyama et al., 2007; Hayama et al., 2008; Liu et al., 2018). In order to confirm that the non-softening characteristic of DJ is not due to the low ethylene production rate of this

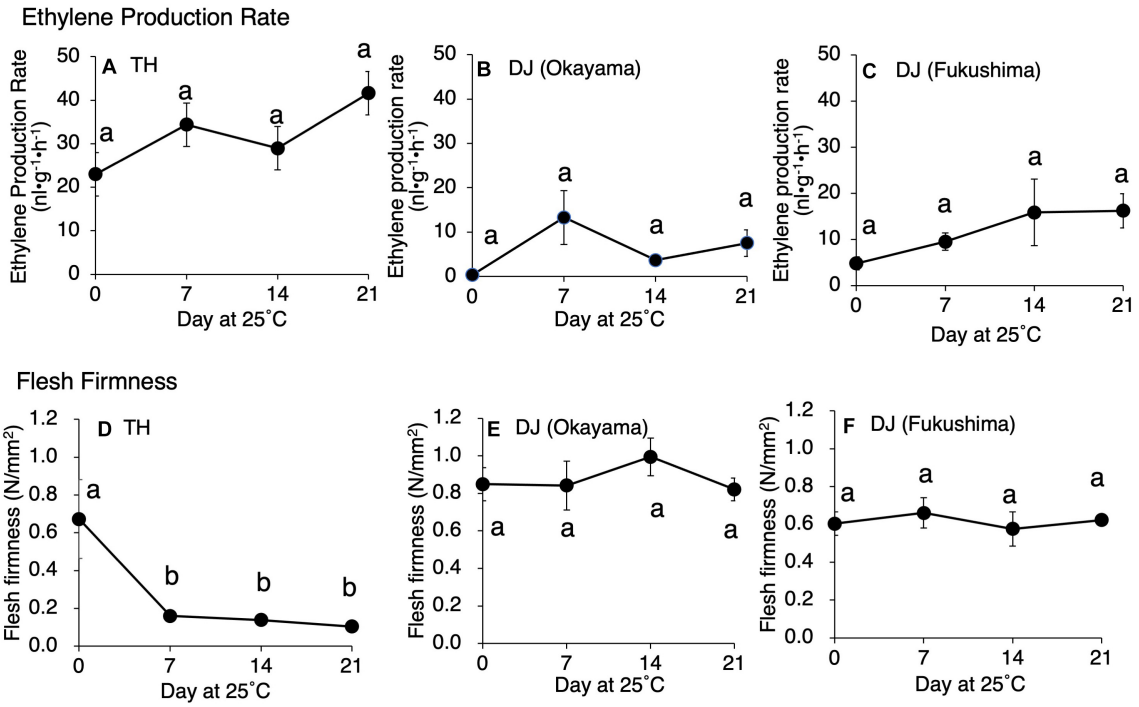

FIGURE 1 | Postharvest changes in **(A–C)** ethylene production rate and **(D–F)** flesh firmness in "Tobihaku" (TH) and "Daijumitsuto" (DJ) fruit grown in Okayama Prefecture and DJ grown in Fukushima Prefecture Japan. In **(A,D)**, TH were harvested on November 7 from a commercial orchard in Okayama Prefecture, Japan and held at 25°C for 21 days. In **(B,E)**, DJ from Okayama were harvested on October 12 from the Research Farm of Okayama University, Japan and held at 25°C for 21 days. In **(C,F)**, DJ from Fukushima were harvested on October 22 from a commercial orchard in Fukushima Prefecture, Japan, followed by 2 days transport at ambient temperature to Okayama University, where fruit were held at 25°C for 21 days. Fruit were harvested at commercial maturity. Each point in **(A,B,D,E)** and in **(C,F)** represents the mean value of three and four fruits, respectively. Vertical bars indicate ± SE (n = 3–4). Statistical analysis was conducted by Tukey's multiple comparison test after one-way ANOVA. Different letters indicate significant differences among measurement days by Tukey's test ($p < 0.05$).

cultivar, TH and DJ were treated with 5,000 ppm of propylene, an ethylene analog, continuously for 7 days. This concentration of propylene is equivalent to 50 ppm of ethylene and is sufficient to induce ethylene response in climacteric fruits (Burg and Burg, 1967; McMurchie et al., 1972). Ethylene production rates of TH and DJ were increased rapidly by the propylene treatment, reaching 45 and 22 nl·g^{-1}·h^{-1} on day 3 of treatment, respectively (**Supplementary Figure S2**). Flesh firmness of TH decreased rapidly whereas that of DJ decreased slightly, and high firmness was maintained in DJ even after 7 days of continuous propylene treatment (**Figure 3**). These results suggest that regardless of the differences in the ethylene production rate, DJ lacked the ability to be softened in response to ethylene.

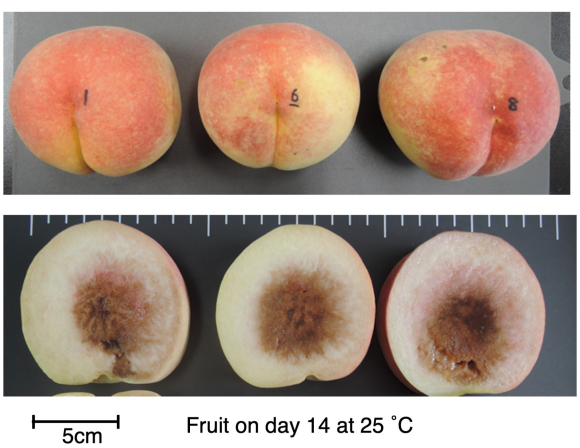

FIGURE 2 | DJ on day 14 at 25°C. Fruit were harvested from a commercial orchard in Fukushima Prefecture and held at 25°C for 21 days, as shown in **Figure 1**. Appearance **(top)** and longitudinal section **(bottom)** of each fruit are shown. Bar indicates 5 cm.

Structural Features of *M* Locus in DJ and TH and an Unidentified Haplotype in TH

M locus is involved in the regulation of peach flesh texture (Bailey and French, 1949; Monet, 1989; Bassi and Monet, 2008). Four polygalacturonase genes, *PG1*, *PG2*, *PGM*, and *PGF*; three *NADHs*; and one *F-box* gene were annotated in the *M* locus region of peach reference genome (**Figure 4A**). Gu et al. (2016) walked the chromosome of three accessions by using PCR based on sequence information of reference genome, and proposed three haplotypes, H_1, H_2, and H_3. The sequence of H_1 haplotype was identical to reference genome, in which tandem duplication of *endoPG* genes, *PGM* and *PGF*, was observed. H_2 haplotype possessed only *PGM* and lacked *PGF*. The 70 kbp

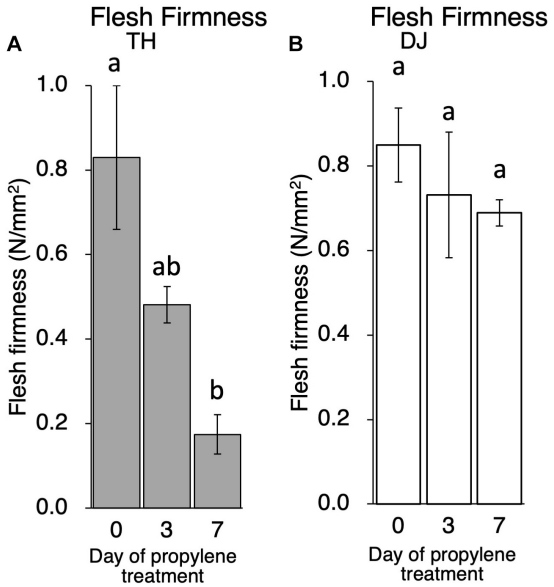

FIGURE 3 | Effect of propylene treatment on postharvest fruit softening in **(A)** TH and **(B)** DJ. Harvested fruit were treated with 5,000 ppm of propylene continuously for 7 days. Flesh firmness was measured on days 0, 3, and 7. For DJ, fruit harvested on October 12 from the Research Farm of Okayama University were used. Each point on day 0, 3 and 7 represents the mean value of four and three fruits, respectively. Vertical bars indicate ± SE (n = 3–4). Statistical analysis was conducted by Tukey's multiple comparison test after one-way ANOVA. Different letters indicate significant differences among measurement days by Tukey's test ($p < 0.05$).

region containing *PG2*, *PGM*, *PGF*, and *NADHs* was deleted in H_3 haplotype. Gu et al. (2016) hypothesized that H_1 and H_2 haplotypes were dominant over H_3 haplotype, *PGM* conferred the melting texture, and *PGF*, which was present only in H_1 haplotype, was involved in freestone phenotype. The lack of both *PGM* and *PGF* in H_3 homozygote could result in the non-melting texture. Further investigations are required to confirm the function of *PGM* in H_2 and H_1 haplotypes and the roles of *PGM* and *PGF* in fruit trait.

WGS of DJ and TH by Illumina was performed to investigate the *M* locus region (19.0–19.1 Mbp of chromosome 4) (**Figure 4**), and the mapping patterns were compared with those of three accessions with different flesh textures: dhLL of MF accession, DD of NMF accession, and BT of MF accession, which is categorized in slow softening peaches (Bassi and Monet, 2008; Ghiani et al., 2011; Morgutti et al., 2017). dhLL, an H_1 homozygote, was used for peach genome sequencing and the reads were mapped uniformly to *M* locus. The reads of DD were also mapped to the entire *M* locus region except the ∼12 kbp region including *PGF* and *NADH1*. No or less reads were mapped to the ∼12 kbp region, indicating that the region was deleted in DD (**Figures 4D,F**). The position and length indicated that the DD deletion unexpectedly corresponded to the region deleted in H_2 haplotype in Gu et al. (2016). The mapping patterns of DJ and TH were not the same as those of dhLL and DD, suggesting that DJ and TH possessed neither H_1 nor H_2 haplotype.

TH and BT showed similar mapping patterns and thus were expected to possess the same haplotypes (**Figure 4**). The DJ mapping results indicated that the genotype of DJ was not identical to those of TH and BT, but the three accessions were expected to share one haplotype. Mapping the pair reads of DJ to peach reference genome revealed many broken pairs around 19,026,186 and 19,096,680 bp (**Figures 4A,B,G**). Only a few reads were mapped between them, except for the many non-specific reads from other chromosomal regions that were mapped between *NADH3* and *NADH2*, the region named M1 insertion in this study (see below). Structural mutation analysis by CLC Genomics Workbench indicated that the region from 19,026,186 to 19,096,680 bp was deleted in DJ, suggesting that DJ is homozygote for the deleted haplotype identical to that reported as H_3 by Gu et al. (2016). Many broken pairs were found at the same position as DJ when mapped with TH and BT pair reads, indicating that one of the two haplotypes was H_3 (**Figures 4A,B,G**). The other haplotype was presumed to be an unidentified novel haplotype that cannot be predicted directly by mapping to reference genome. In TH and BT, SNPs were heterozygous in the outer region of H_3 deletion, whereas they were homologous in the inner region of H_3 deletion (**Figures 4B,G** and **Supplementary Table S4**). All SNPs in this region were homozygous in BH, a Japanese MF accession. In contrast, no SNP was detected in either dhLL or DD. In the region of *PGM* and *PGF*, the coverage of TH, BT, and BH was low and many SNPs and broken pair reads were observed (**Figures 4C,E**). Throughout *M* locus and its surrounding region, SNPs were hardly observed in dhLL, DD, and DJ, whereas many mutations were detected in TH, BT, and BH (**Figure 4** and **Supplementary Table S4**), suggesting the existence of an unidentified haplotype in TH, BT, and BH.

Identification of M^0 Haplotype

Sequence polymorphism and mapping pattern indicated that the sequence and structure of the unidentified haplotype of TH, BT and BH was highly diverged from those of the reference sequence (M^1). We decided to obtain the unidentified haplotype sequence by *de novo* assembly. However, polymorphism shown in the *M* locus of TH had a negative effect on *de novo* assembly. As we found that BH was a homozygote of the unknown haplotype, *de novo* assembly with PE150 reads of BH was conducted and two contigs covering *M* locus were obtained. *PG1*, *PG2*, *PGM*, and *NADH* were located in one of the two contigs. The *F-box* gene was found in another contig. The haplotype composed of the two contigs was defined as M^0 according to the locus name. Haplotypes H_1, H_2, and H_3 in Gu et al. (2016) were renamed M^1, M^2, and M^3, respectively, based on haplotype features, to avoid confusion and define the haplotypes precisely.

When the genome structure of M^0 was compared with M^1 sequence, the region corresponding to *PGF* was not found in M^0 and only one *NADH* was located on M^0 (**Figure 5**). The sequences were conserved among the two haplotypes but M^1 specific sequences were found in the region from *PG2* to *PGM* and the downstream region of *NADH3*. Many non-specific reads were mapped to the region spanning from *NADH3* to *NADH2* of M^1 haplotype, the region corresponding to M1

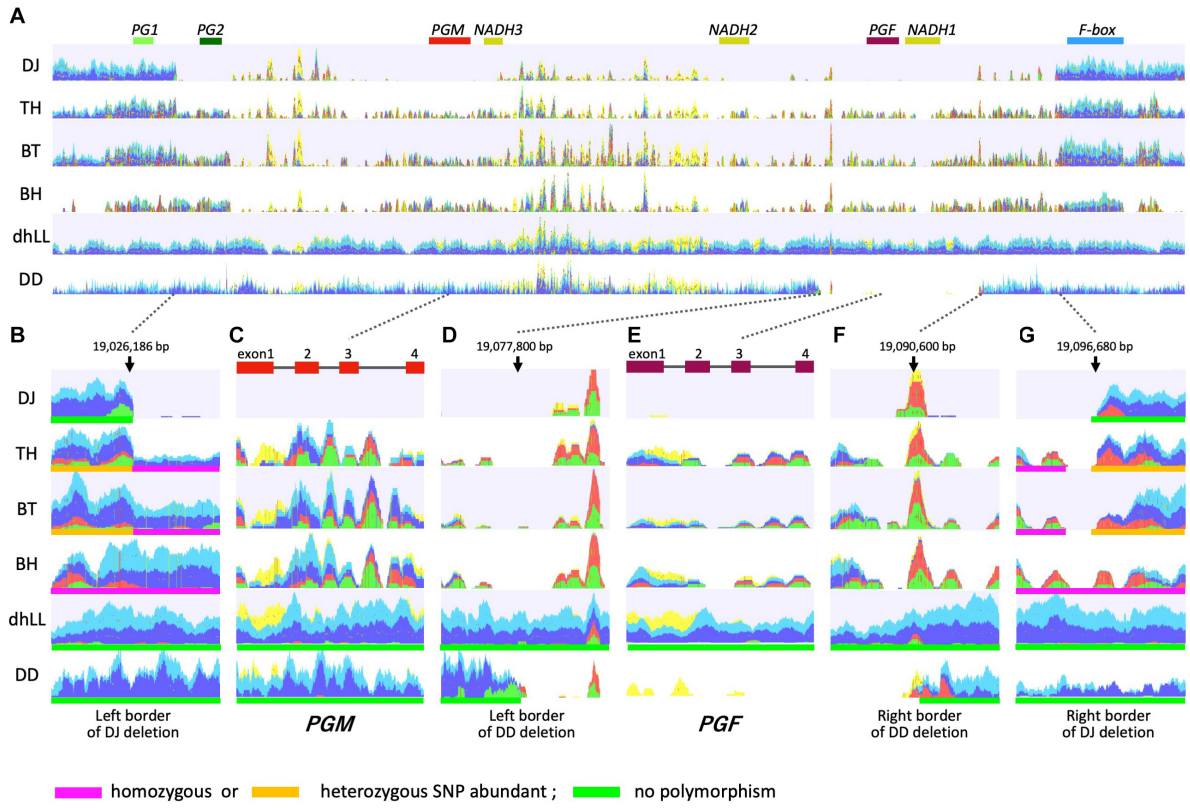

FIGURE 4 | Mapping DNA-seq reads to M^1 haplotype. Illumina short reads of DJ, TH, "Benihakuto" (BH), "Big Top" (BT), "Dr. Davis" (DD), and doubled haploid "Lovell" (dhLL) were mapped to reference genome of *P. persica* (ver 2.0) (Verde et al., 2017) by CLC Genomics Workbench. Properly paired reads that are in the correct orientation and distance are shown in blue and light blue. Green and red reads are broken pairs. Non-specific matches are shown in yellow. **(A)** Overview of mapping graph in the *M* locus region. *PG1* to *F-box* above graph are genes named according to Gu et al. (2016). **(B,G)** show the region around the junction of M3 deletion. **(D,F)** are those of M2 deletion. **(C,E)** are *PGM* and *PGF*, respectively.

insertion described above (**Figures 4**, **5**). The M1 insertion was assumed to be translocated from another chromosomal region and inserted into *NADH* to disrupt it, because both *NADH3* and *NADH2* were partial and their structures appeared to be generated from one *NADH* gene divided at the third intron by the M1 insertion (**Supplementary Figures S3, S4** and NADH3/2 of **Supplementary Figure S5**).

The CDS sequence of *PGM* of M^0 (*PGM*-M^0) showed 99% similarity to those of *PGM* of M^1 (*PGM*-M^1) and *PGF* of M^1. One amino acid substitution between *PGM*-M^0 and *PGM*-M^1 was found at residue 49, where Ser was substituted to Phe in *PGM*-M^1 (**Supplementary Figure S6**). The Ser at residue 49 of *PGM*-M^0 was conserved in other *Prunus* species. Amino acid sequence comparison between *PGM*-M^0 and *PGF* showed substitution of Ser for Thr at residue 269 in PGF, although it was not considered to have a significant effect on the function of the PG protein. The S49F substitution between f and fl alleles was reported by Peace et al. (2005) and Morgutti et al. (2017). However, because they did not perform resequencing analysis, it was not possible to understand the entire structure of the f haplotype and its origin. It was probable that f haplotype was the same as M^0 in this study. We further demonstrated that this M^0 haplotype is not a specific haplotype but a widely found haplotype in various peach accessions, and plays an important role in MF phenotype determination.

DNA-seq reads of BH, TH, DJ, dhLL, DD, and BT were mapped to the reference "PpREF20 + M0," in which the M^0 haplotype sequence was added to peach genome sequence (**Figure 5**). Coverage graphs show that the reads of M^0, M^1, M^2, and M^3 haplotypes could be classified clearly. The reads of BH (M^0M^0) were mapped only to M^0 haplotype and those of dhLL (M^1M^1) were also mapped only to M^1 haplotype. DJ (M^3M^3) and DD (M^2M^2) reads were mapped to M^1 haplotype except for the deleted region, as shown in **Figure 4**. The reads of TH (M^0M^3) and BT (M^0M^3) were mapped to both M^0 and M^1 haplotypes except for M^3 deletion.

Structural Variety of *M* Haplotype Identified by WGS Mapping Patterns and PCR Genotyping

It was demonstrated that WGS data were useful for the precise genotyping of *M* locus. Many WGS data of peach accessions were registered in the SRA database and mapped to "PpREF20 + M0" to identify *M* genotype. We finally predicted *M* genotypes of 412 accessions from the WGS mapping pattern and/or by PCR

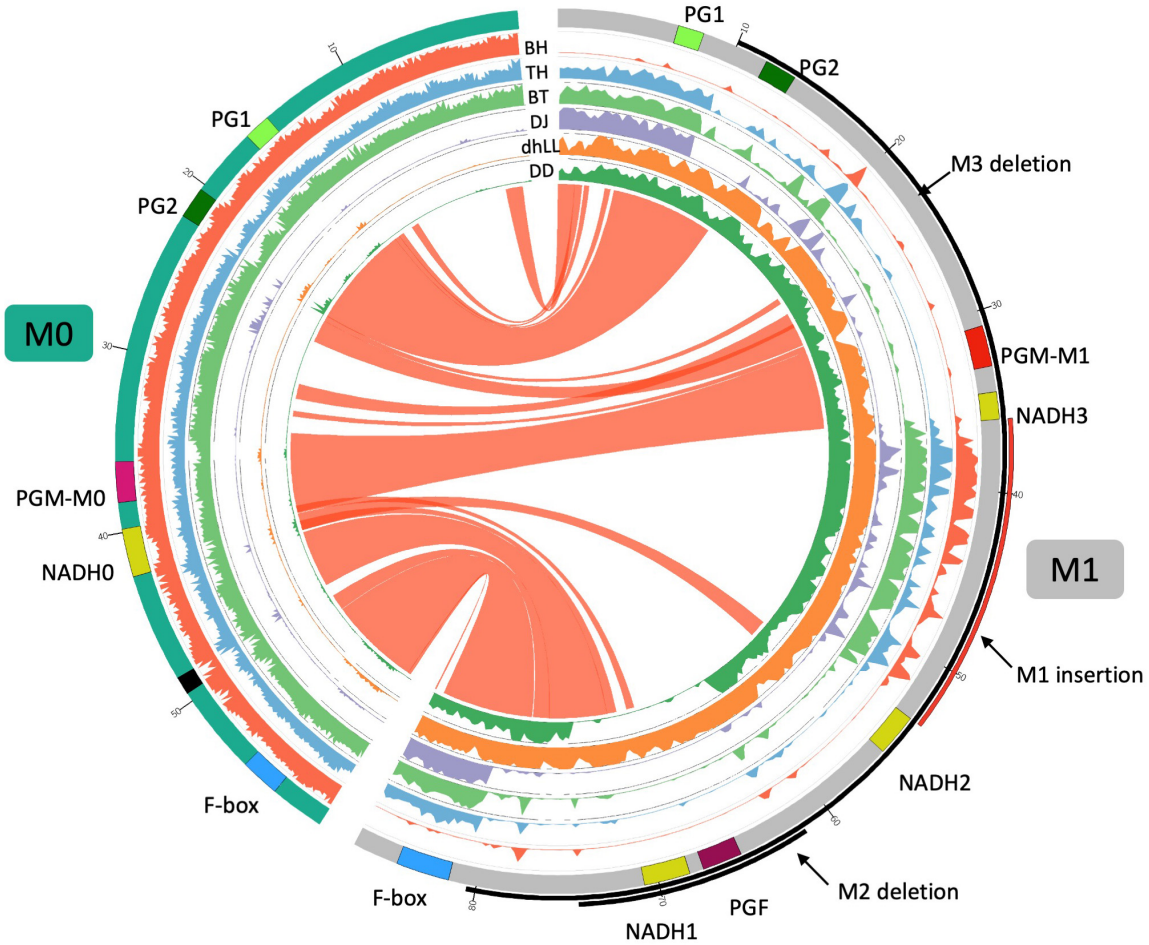

FIGURE 5 | Comparison of M^0 and M^1 haplotypes. Inner six tracks are coverage graphs of DNA-seq reads of BH TH, BT, DJ, dhLL, and DD. Ribbons link similar regions between two haplotypes. M^0 haplotype consists of two contigs connected by N (black in the chromosome track). The nucleotide at 19,016,188 bp of Pp04 chromosome is positioned as + 1 in M^1 haplotype. *PGM* of M^0 haplotype is similar to *PGM* of M^1 but not identical. We named those *PGMs* *PGM-M*^{0} and *PGM-M*^{1}, respectively. *NADH0* is *NADH* of M^0 haplotype and seems to be an intact gene as described in **Supplementary Figures S3–S5**.

genotyping. M^0 and M^1 haplotypes were the most popular in the peach accessions analyzed (**Figure 6** and **Supplementary Table S5**). On the other hand, the frequency of M^2 haplotype was very low. In addition to the four main haplotypes, M^0, M^1, M^2, and M^3, we found variant-type haplotypes and chimeric haplotypes. The former haplotypes exhibited deletion in the region different from those found in M^2 and M^3, whereas the latter haplotypes appeared to be generated by the recombination between M^0 and M^1 (**Figure 6**). In total, 11 haplotypes were structurally identified at *M* locus (**Figure 7**). They were first classified into M^0 to M^3 on the basis of the existence of *PGM-M*^{0}, *PGM-M*^{1}, and *PGF*; the haplotype containing only *PGM-M*^{0} is M^0; the haplotype containing *PGM-M*^{1} and *PGF* was M^1; the haplotype containing only *PGM-M*^{1} was M^2; and the haplotype containing neither *PGM* nor *PGF* was M^3. Furthermore, variants and recombinant types of haplotypes were identified from structural variations and such characters as b, c... or r1, r2... were added to their names, respectively.

Although no significant structural change in gene composition was detected, the sequence variation was found in the accessions with M^0 haplotype, when analyzed on the basis of the mapping patterns of DNA-seq reads of TH. The insertion, whose length was unknown, was found in the 1.8 kbp upstream region of *PGM-M*^{0}, and SNPs were also detected in *PGM-M*^{0}, one of which was located in CDS and led to a synonymous substitution (**Supplementary Figure S7**). It was expected that M^0 was also diversified. However, we regarded both types of M^0 as M^0 in this study because no changes in gene composition (structural feature as haplotype) and no amino acid substitutions were found.

M^0 Haplotype Was Widely Spread Among MF Accessions

We designed primers for PCR genotyping on the basis of the sequence variations at the third intron of *PGM* and *PGF* and the *M* haplotype structural differences (**Figure 8**, **Supplementary Figure S8**, and **Supplementary Table S3**). The structural

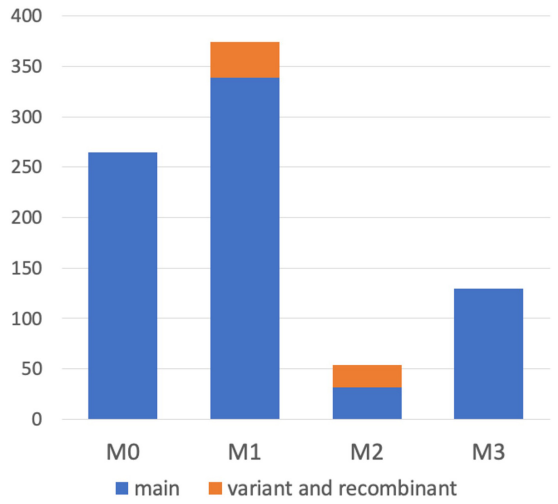

FIGURE 6 | Haplotype frequency at *M* locus in peach accessions. We classified *M* haplotypes into 11 haplotypes (**Figure 7**) in 412 peach accessions, on the basis of the coverage graph patterns and/or PCR genotyping (**Figure 8** and **Supplementary Figure S9**).

variations and the *PGM* and *PGF* compositions of *M* haplotypes identified in this study indicated that the four main haplotypes could be classified using three primer sets, PGM/F, M2D, and M3D. PGM/F primer set detected the indel at the third intron of *PGM* and *PGF*, and three different fragment sizes were amplified (**Figure 8**). The upper fragment was derived from *PGM-M*^{1}, the lower one was from *PGF*, and the middle one was from *PGM-M*^{0}. When the middle fragment was amplified, the accession possessed *M*^{0} haplotype. From *M*^{1} haplotype, both the upper and the lower fragments should be amplified. When the lower fragment was not amplified and only the upper one was amplified, this meant that only *PGM-M*^{1} was amplified, showing that the accession had *M*^{2} haplotype. The genotyping results obtained with the PGM/F primer set could be confirmed by amplification with the M2D primer set that detects the deletion on *M*^{2}. Because no fragment was amplified from *M*^{3} with the PGM/F primer set, the M3D primer set, which amplifies the junction of *M*^{3} deletion, should be useful to identify *M*^{3} haplotype.

The three primer sets were used to genotype 14 accessions. The *M* genotypes of six accessions, "Okubo" (OB), DJ, TH, BH, LL, and "Myojo" (MJ), were predicted from the mapping patterns of WGS data, which were re-confirmed by PCR genotyping. In the other eight accessions, we found inconsistent amplification patterns in "Mochizuki" (MZ) and "Okayama-3" (O3). These two accessions were expected to have *M*^{2} haplotype judging from the result that the PGM/F primer set amplified *PGM-M*^{1} but not *PGF*. However, no amplification was observed in M2D. These results suggested that *M*^{2} haplotype of MZ and O3 was a variant type of *M*^{2}. Indeed, an additional primer set showed that they have *M*^{2b} (**Supplementary Figure S9**).

"Hakuto" (HT), a progeny of "Chinese Cling" (CC), was mainly used as germplasm for MF peach breeding in Japan

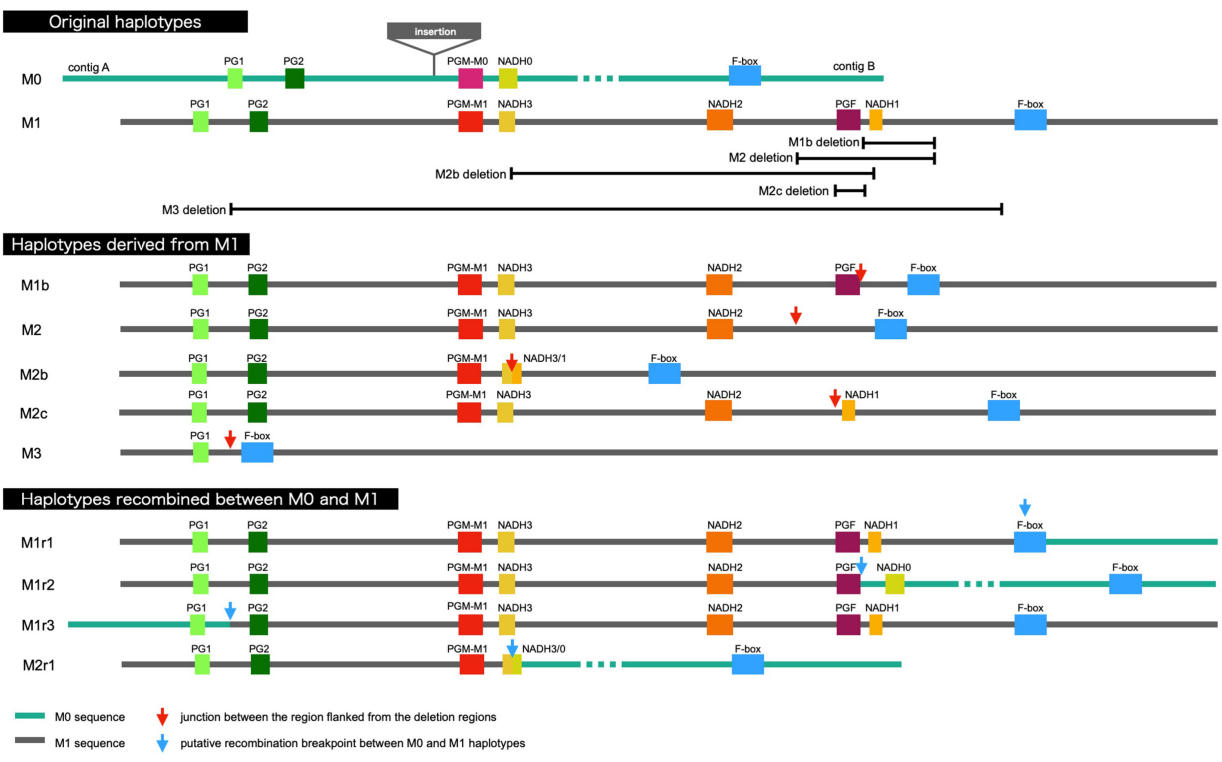

FIGURE 7 | Schematic representation of *M* haplotypes of peach.

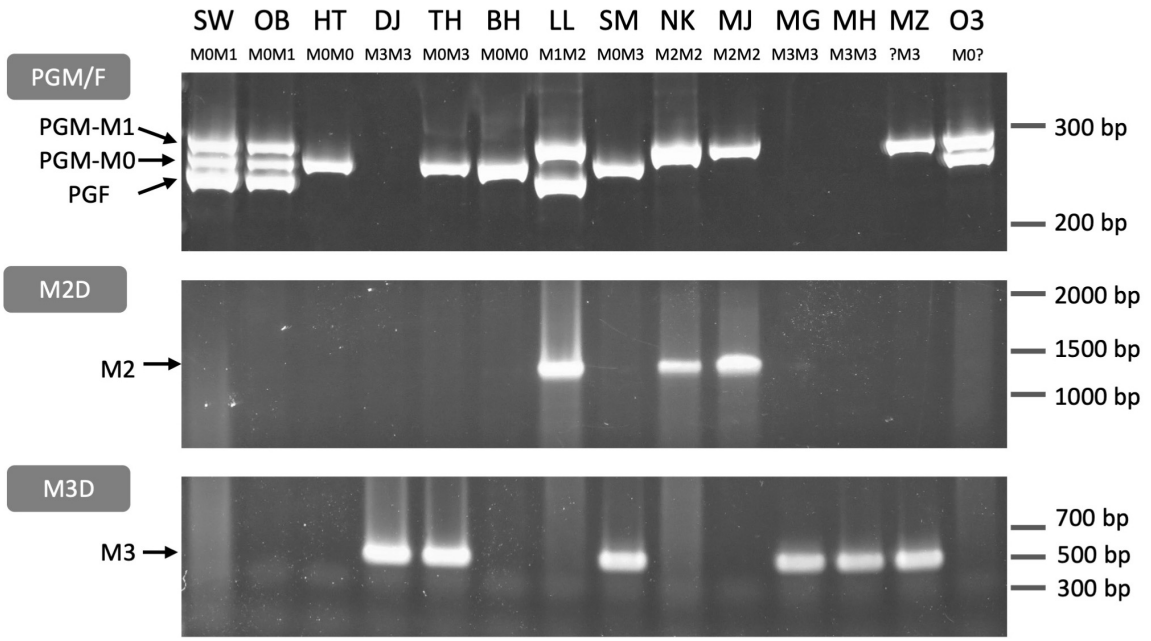

FIGURE 8 | PCR genotyping of *M* locus. Three primer sets PGM/F, M2D, and M3D (**Supplementary Figure S8** and **Supplementary Table S3**) were used to distinguish *M* haplotypes. PGM/F and M2D/M3D fragments were separated on an acrylamide gel and an agarose gel, respectively. PGM/F primer set amplified three fragments derived from *PGM-M*^{1}, *PGM-M*^{0}, and *PGF*, respectively. M2D and M3D detected *M*^{2} and *M*^{3} haplotypes, respectively. All genotypes under each cultivar name except MZ and O3 were identified from these fragment patterns (see **Supplementary Figure S8**). SW, SunagoWase; OB, Okubo; HT, Hakuto; DJ, Daijumitsuto; TH, Tobihaku; BH, BeniHakuto; LL, Lovell; SM, ShimizuHakuto; NK, Nishiki; MJ, Myojo; MG, Meigetsu; MH, Meiho; MZ, Mochizuki; O3, Okayama-3.

(**Supplementary Figure S10A**; Yamamoto et al., 2003a,b). PCR genotyping showed that HT was a homozygote of M^0, indicating the possibility that M^0 haplotype had been spread among Japanese peaches. All the major Japanese cultivars tested in this study were found to have M^0 haplotype (**Supplementary Figure S10B**). All cultivars except OB and "ShimizuHakuto" (SM) were homozygotes of M^0. SM was a typical MF cultivar in Japan (Yamamoto et al., 2003b), and its genotype was M^0M^3, the same as that of TH (**Figure 8**).

M^2 and *M*^{3} Could Confer NMF Phenotype

DJ was an M^3 homozygote and did not have *PGM* and *PGF*. Thirty seven M^3 homozygotes were identified in this study. Flesh textural phenotypes of 16 out of 37 accessions were reported, and 12 accessions were reported as NMF except those whose flesh texture was only reported as **Supplementary Data** in Cao et al. (2016) (**Table 1**). This may support our conclusion that M^3 haplotype was likely involved in the determination of non-softening postharvest property in DJ. M^2 haplotype, in which only *PGM-M*^{1} was located, also appeared to confer the NMF phenotype, unlike M^0 and M^1 haplotypes. In this study, we found 22 homozygotes for M^2 including variant types, 11 of which had fruit textural report(s), and all 11 were reported as NMF (see reference in **Table 1**). Only NJF16 accession had M^2M^3 combination as well as phenotype report. NJF16 was reported to be NMF peach (Clark and Finn, 2010). MZ was $M^{2b}M^3$ that had only *PGM-M*^{1} as confirmed by PCR genotyping, and is a well-known Japanese NMF cultivar (Yoshioka et al., 2011). All together, these findings suggest that *PGM-M*^{1} may not be functional. On the other hand, *PGM-M*^{0} and *PGF* seemed to confer the MF phenotype dominantly because flesh texture of M^0M^2 ("Tsukuba 86"), M^0M^{2b} (O3), M^0M^3 (TH, SM, BT, and CC), M^1M^2 (LL), and M^1M^3 ["Georgia Bell" (GB)] was MF (**Table 1**). "Early Gold" (EG) was identified as M^1M^1 on the basis of the mapping pattern of reads from the SRA database (**Supplementary Table S6**), despite that the flesh texture was considered NMF (Yoshida, 1981). We suspected that the reads of EG registered in SRA were confused with those of the other accessions. This is because "Nishiki" (NK) (M^2M^2), an NMF accession, was the parent of EG (Yoshida, 1981) and one of EG haplotypes was supposed to be M^2.

M Locus Structure in *Prunus* Species

The structure of *M* locus was identified from reference genome sequences of other *Prunus* species, including *P. mira*, *P. kansuensis*, almond (*P. dulcis*), apricot (*P. armeniaca*), Japanese apricot (*P. mume*), sweet cherry (*P. avium*), and Yoshino cherry (*P.* x *yedoensis*; called "Sakura" in Japan), and compared with the four main haplotypes of peach structurally identified in this study (**Figure 9** and **Supplementary Figure S11**). *PGM* and *PGF* were found in the "Lauranne" genome (PdLN) of almond, which belongs to subgenus *Amygdalus* together with peach, indicating that the PdLN *M* haplotype was similar to peach M^1 haplotype. As shown in M^1 of peach, *NADH* located downstream of *PGM* in PdLN was broken by an insertion

TABLE 1 | Flesh texture of M^2 or M^3 homozygotes and heterozygotes.

Cultivar	Haplotype	*PGM-M*^{0}	*PGM-M*^{1}	*PGF*	Flesh texture	References
M2 homozygote						
Dr. Davis	M2M2	No	Yes	No	Non-melting	Peace et al., 2005
Phillips	M2M2	No	Yes	No	Non-melting	Cao et al., 2016 Old canning peach cultivar (Davis, 1937), Some progenies were non-melting (Wang and Lu, 1992; Font i Forcada et al., 2013)
Oro A	M2M2	No	Yes	No	Non-melting	Morgutti et al., 2017
Carson	M2M2	No	Yes	No	Non-melting	Infante et al., 2011; Font i Forcada et al., 2013
NJC105	M2M2	No	Yes	No	Non-melting	Pan et al., 2015
Myojo	M2M2	No	Yes	No	Non-melting	Gu et al., 2016
Nishiki	M2M2	No	Yes	No	Non-melting	Haji et al., 2005. Parent of Early Gold (Yoshida, 1981)
Loadel	M2M2	No	Yes	No	Non-melting	Font i Forcada et al., 2013
G. Klamt	M2M2	No	Yes	No	Non-melting	Font i Forcada et al., 2013
Everts	M2M2	No	Yes	No	Non-melting	Font i Forcada et al., 2013
Golden Queen	M2bM2b	No	Yes	No	Non-melting	Font i Forcada et al., 2013
M3 homozygote						
Daijumitsuto	M3M3	No	No	No	Non-melting	This study
Dawangzhuang Huang Tao	M3M3	No	No	No	Non-melting	Cao et al., 2016
Maria Serena	M3M3	No	No	No	Non-melting	Font i Forcada et al., 2013
Long 1-2-4	M3M3	No	No	No	Non-melting	Yoon et al., 2006
NJC77	M3M3	No	No	No	Non-melting	Pan et al., 2015
NJC47	M3M3	No	No	No	Non-melting	Pan et al., 2015
Meiho	M3M3	No	No	No	Non-melting	Personal communication
Ying Zui Tao	M3M3	No	No	No	Non-melting	Cao et al., 2016
Xi Jiao 1	M3M3	No	No	No	Non-melting	Cao et al., 2016
Yu Bai	M3M3	No	No	No	Non-melting	Zhang et al., 2019
Rou Pan Tao	M3M3	No	No	No	Non-melting	Yoon et al., 2006
Zhang Huang 9	M3M3	No	No	No	Non-melting	Cao et al., 2016
Fen Ling Chong	M3M3	No	No	No	Melting	Cao et al., 2016
Mai Huang Pan Tao	M3M3	No	No	No	Melting	Cao et al., 2016
Tsukuba 85#	M3M3	No	No	No	Melting	Cao et al., 2016
Zhong You Pan Tao 2	M3M3	No	No	No	Melting	Cao et al., 2016
Heterozygote						
Mochizuki	M2bM3	No	Yes	No	Non-melting	Yoshioka et al., 2011
NJF16	M2M3	No	Yes	No	Non-melting	Clark and Finn, 2010
Okayama-3	M0M2b	Yes	Yes	No	Melting	Cao et al., 2016. A germplasm for canning cultivar breeding (Yoshida, 1981)
Tsukuba 86	M0M2	Yes	Yes	No	Melting	Cao et al., 2016
Big Top	M0M3	Yes	No	No	Melting	Bassi and Monet, 2008. Flesh softening was very slow
Tobihaku	M0M3	Yes	No	No	Melting	This study
Chinese Cling	M0M3	Yes	No	No	Melting	Pan et al., 2015
Shimizu Hakuto	M0M3	Yes	No	No	Melting	Gu et al., 2016
Lovell*	M1M2	No	Yes	Yes	Melting	Some progenies were non-melting (Font i Forcada et al., 2013)
Georgia Bell	M1M3	No	Yes	Yes	Melting	Some progenies** were non-melting (Peace et al., 2005)

*Twenty-two M2 homozygotes, including variant and recombinant types, and 37 M3 ones were found in this study. Accessions whose flesh texture was reported are listed in this table.*This "Lovell" was not doubled haploid used for genome sequencing.**Includes offspring from self-pollination and cross of "Dr. Davis" and "Georgia Bell."*

sequence, although this insertion sequence was not similar to the M1 insertion. *F-box* and *NADH* were pseudogenes, probably due to multiple genome rearrangements occurring in almond "Texas" genome (PdTX). One *endoPG* was found in addition to *PG1* and *PG2*, and it was expected to be *PGF*, because *PGFs* in PdLN and PdTX shared amino acid substitutions specific to them and genomic sequence similarity was found not only in the gene region, but also in the intergenic region

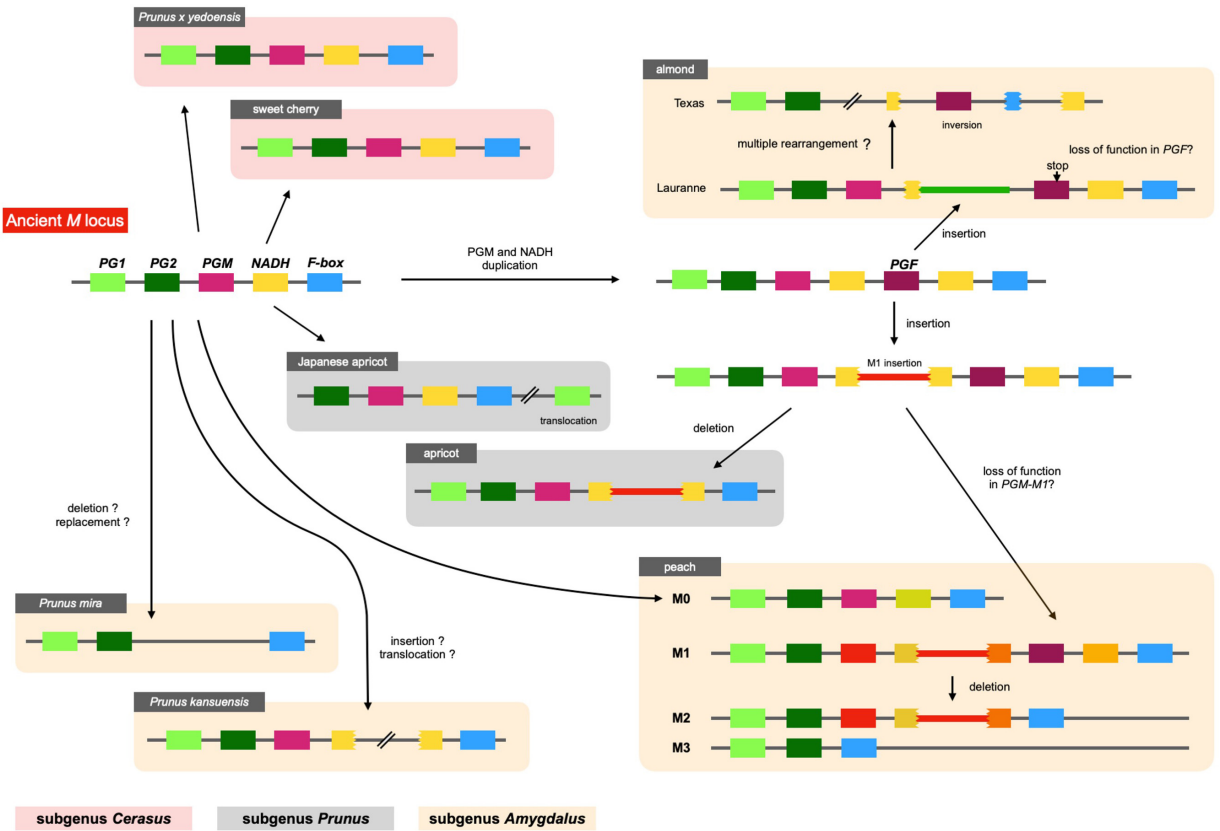

FIGURE 9 | Diversification of *M* haplotypes in genus *Prunus*. We investigated *M* loci of *Prunus* species by Blastn analysis using their reference genomes. Five genes, *PG1, PG2, PGM, NADH,* and *F-box* genes, were shared among *Prunus* and speculated to be located at an ancient *M* haplotype. The structure of the ancient haplotype was conserved in peach M^0, *P. kansuensis*, Japanese apricot, sweet cherry, and *P.* x *yedoensis*. No *PGM* and *NADH* were observed in *P. mira*. M^1 type structure, which possessed *PGF* or M1 insertion, was found in peach M^1 and *M* haplotypes of almond and apricot. This haplotype was speculated to diverge from ancient haplotype by duplication of *PGM* (and *NADH*), followed by M^1 or almond insertion, which disrupted *NADH* gene located downstream of *PGM*.

flanking them. A frameshift mutation was found in *PdLN-PGF*, indicating that *PdLN-PGF* did not function. The absence of this mutation in PdTX suggests that the mutation in *PdLN-PGF* occurred after the haplotype diverged. No tandem duplications of *PGM*, *PGF*, and M1 insertions were observed in *P. mira* or *P. kansuensis*. *NADH* appeared to be a fragmented structure in *P. kansuensis*, but because disrupted exons were located at different contigs in the draft genome, their actual relationship was unclear. *PGM*, *PGF*, and *NADH* were not present in *P. mira* genome.

In subgenus *Amygdalus*, the M1 insertion was found only in peach. However, a sequence similar to the M1 insertion was found in apricot of subgenus *Prunus*. The insertion also disrupted *NADH*, which was located downstream of *PGM*. These findings implied that the two insertions originated from the same event (haplotype), and that this insertion event occurred before the divergence of subgenera *Amygdalus* and *Prunus*. A structure similar to M^0 was found in Japanese apricot (*P. mume*) of subgenus *Prunus*. *PG2*, *PGM*, intact *NADH*, and *F-box* were clustered in *P. mume* haplotype, but *PG1* was translocated to the downstream region to *M* locus. Sweet cherry and Yoshino cherry belong to subgenus *Cerasus*, which is far from subgenus *Amygdalus* (Chin et al., 2014). Their *M* haplotype structure and gene composition were similar to those of peach M^0 haplotype.

DISCUSSION

Different Postharvest Properties of TH and DJ

In this study, first, the postharvest properties of ultra-late maturing peach cultivars TH and DJ were investigated. Generally, peach is considered to be a climacteric fruit in which ripening-related phenomena, such as accelerated endogenous ethylene biosynthesis and fruit softening, were reported to be controlled by ethylene (Liguori et al., 2004; Hayama et al., 2006; Liu et al., 2018). TH exhibited the characteristics of normal MF peach fruit, including rapid fruit softening leading to MF texture associated with appropriate level of endogenous ethylene production. In contrast, DJ did not soften at all even though significant ethylene production was observed. From their sugar contents and pH-values at day 0, it was confirmed that DJ fruit used in this study were not harvested at too early maturity

stage to be ripen normally (**Supplementary Figure S1**). It seemed that DJ possessed the ability to produce ripening-related ethylene but lacked the ability to be softened in response to the ethylene. The lack of softening ability in response to ethylene in DJ was supported by the continuous propylene treatment. Propylene, instead of ethylene, treatment has been used to monitor endogenous ethylene production in parallel to other ripening-related changes (McMurchie et al., 1972). As much as 5,000 ppm of propylene was used for treatment in this study. According to previous reports, this concentration of propylene is equivalent to 50 ppm of ethylene and is sufficient to induce ethylene response in climacteric fruits (Burg and Burg, 1967; McMurchie et al., 1972). Indeed, in peach fruit treated with 500–5,000 ppm of propylene, induction of autocatalytic ethylene production and dramatic fruit softening were reported (Yoshioka et al., 2010; Liu et al., 2018). In this study, DJ exhibited only a slight decrease in flesh firmness and maintained almost similar firmness to that at harvest even after 7 days of continuous propylene treatment. As TH showed dramatic softening by the propylene treatment, it is suggested that the propylene treatment in this study is capable of inducing ethylene response in peach and that DJ has a non-softening characteristic in response to both endogenous and exogenous ethylene/propylene.

Involvement of *M* Locus in Determining Different Postharvest Properties of DJ and TH

The genetic background of DJ and TH and its relationships with other cultivars having long storability and/or shelf lives are unknown. One of the peach strains reported to have a long shelf life is SH peach (Haji et al., 2005). SH peaches, however, are characterized by the absence of ethylene production (Tatsuki et al., 2006). It is reported that ethylene sensing is normal in SH peaches and the fruit soften rapidly with exogenous ethylene or propylene treatment (Haji et al., 2003; Yoshioka et al., 2010), in contrast to DJ. A similar ripening characteristic observed in DJ has been reported in early harvest fruit of SR peaches (Brecht and Kader, 1984). In SR peaches harvested at an earlier date than the optimum harvest date, autocatalytic ethylene production was induced with or without propylene treatment whereas flesh firmness decreased quite slowly. However, DJ is phenotypically different from SR peaches in that it bears large fruit with red coloration, as shown in **Figure 2**, whereas SR fruit do not show normal ripening in terms of fruit size and coloration (Giné-Bordonaba et al., 2020). In agreement with these phenotypical differences between DJ and SH and/or SR peaches, the genomic sequences of DJ and TH did not exhibit any significant differences and/or mutations in the candidate causal genes for these specific strains, *YUCCA flavin mono-oxygenase* (Pan et al., 2015; Tatsuki et al., 2018) and *NAC transcription factor* (Eduardo et al., 2015; Nuñez-Lillo et al., 2015; Meneses et al., 2016) genes (data not shown).

On the other hand, significant differences between DJ and TH were found with regard to genomic sequences at *M* locus, which has been reported to control MF and NMF textures (Bassi and Monet, 2008; Gu et al., 2016). *M* locus is composed of two tandem *endoPG* genes, *PGM* and *PGF* (Gu et al., 2016). Resequencing analysis revealed that DJ is a homozygote of the haplotype that lacks both *PGM* and *PGF*, designated as M^3 in this study, whereas TH is a heterozygote of M^3 and a structurally uncharacterized haplotype that possesses *PGM* (*PGM*-M^0) but not *PGF*, designated as M^0 in this study (**Figures 4**, **5**). Many reports have demonstrated that high level of enzymatic activity, protein accumulation, and gene expression of endoPG are observed only in MF, and supported the involvement of endoPG in the determination of the flesh texture (reviewed in Bassi and Monet, 2008). Thus, it is considered that DJ is a member of NMF peaches. NMF peaches are known to be firm at maturity and to soften slowly during ripening without melting. Different from DJ, it was reported that softening progressed steadily during postharvest ripening in NMF peaches (Fishman et al., 1993; Yoshioka et al., 2011) and thus, the possible involvement of a number of factors in the non-softening property of DJ other than the lack of *endoPG* genes cannot be excluded. Nevertheless, it was indicated that the non-softening postharvest property of DJ is attributed to the lack of *endoPG* genes at *M* locus. The rapid softening property of TH is due to the presence of newly characterized M^0 haplotype (*PGM*-M^0 gene) in TH genome. This was further confirmed by the re-evaluation of *M* haplotype in relation to flesh textural phenotypes in 412 accessions, as described below.

Re-evaluation of *M* Locus in Relation to Flesh Textural Phenotypes

In this study, we revealed that M^0 was not only a unique *M* haplotype as shown in TH, but also a widely spread haplotype in MF accessions, particularly popular peach cultivars grown in Japan, and was responsible for the MF phenotype in these accessions (**Figure 6**, **Supplementary Figure S10B**, and **Supplementary Table S5**). Based on the results obtained from the re-evaluation of *M* locus in 412 accessions in relation to flesh textural traits, we proposed the scenario in which four *M* alleles/haplotypes, M^0 to M^3, were involved in the determination of flesh texture, with M^0 and M^1 dominantly controlling MF texture over M^2 and M^3.

Various alleles/haplotypes have been proposed for *M* locus. The correspondence of *M* alleles/haplotypes in previous studies to those in this study is summarized in **Supplementary Tables S7, S8**. Peace et al. (2005) classified *endoPGs* at *M* locus into four alleles, F, f1, f, and null, on the basis of the results obtained from germplasm derived from peach cultivars GB and DD with f allele being hypothesized to be segregated via outcross from an unknown origin. Morgutti et al. (2017) assumed the same four haplotypes F, f1, f, and f_{null} by referring to Peace's classification and further found two variations, PG^{SH} and PG^{BT}, in f haplotype. The haplotype structures of H_1, H_2, and H_3 reported by Gu et al. (2016) corresponded to those of F, f1, and f_{null} alleles, respectively, although the haplotype corresponding to f was not reported by Gu et al. (2016). In this study, we structurally identified four main haplotypes M^0 to M^3. Judging from S49F substitution and indel at the third intron detected between *PGM*-M^0 and *PGM*-M^1, M^0 appeared to be identical to f haplotype. However, the derivation of

f(M^0) haplotype assumed in this study was different from that in Morgutti et al. (2017), in which f (M^0) was expected to be derived from F(M^1) via fl(M^2). We detected sequence diversifications and large structural differences between M^0 and M^1/M^2 and assumed that M^0 was not derived from M^1/M^2 directly. This assumption was supported by a structural comparison of *M* loci of other *Prunus* species (**Figure 9**). A similar specific structure to peach M^1, such as M1 insertion and/or tandem duplication of *endoPG*, was found in *M* haplotypes of almond and apricot. On the other hand, there was no insertion to disrupt *NADH* in peach M^0 or *M* haplotypes of the Japanese apricot, sweet cherry, and *P.* x *yedoensis*. These findings suggested that the ancestral haplotypes of M^0 and M^1 diverged relatively early, before subgenus divergence, and evolved independently of each other. On the other hand, we could not find any SNP-level variation among M^1, M^2, and M^3 (**Supplementary Table S4**), suggesting that the divergence of M^1 into M^2 and M^3 occurred relatively recently after *P. persica* speciation. It was also suggested that M^2 did not lead to M^1 but rather M^2 was derived from M^1. This might be supported by the fact that the frequencies of M^2 and M^3 were much lower than that of M^1 at least in the accessions investigated in this study (**Figure 6**). In this study, we showed 11 haplotypes in total (**Figure 7**), but more haplotypes are expected to exist. We only examined reference genomes in *Prunus* species other than *P. persica*. Considering the divergence of *M* haplotype before speciation, it would not be surprising to find other species harboring haplotypes similar to both M^0 and M^1 haplotypes.

Gu et al. (2016) did not consider the presence of *PGM*-M^0 (f allele) and defined H_2 as the sole haplotype harboring *PGM* but not *PGF* because they attempted to distinguish each haplotype on the basis of copy number of *endoPG* genes quantified by qPCR. Therefore, not only M^2 but also M^0 was genotyped as H_2 in Gu et al. (2016). This misgenotyping of M^0 as H_2 produced results that included incongruity between genotype and phenotype as M^0 (*PGM*-M^0) and M^2 (*PGM*-M^1) were likely to have different effects on flesh texture. For example, the genotyping in Gu et al. (2016) identified that SM and "Hakuho" (HH), both of which are popular MF cultivars in Japan, were H_2H_3 and H_2H_2, respectively. Supposing *PGM*-M^1 on H_2 is not functional, as assumed in this study, SM and HH should be NMF. Conversely, supposing H_2 (M^2) is a dominant haplotype that determines MF texture, as assumed by Gu et al. (2016), the H_2H_2 genotype shown in DD, "OroA" (OA), and MZ cannot explain their NMF phenotypes (Peace et al., 2005; Morgutti et al., 2006, 2017; Yoshioka et al., 2011).

Re-evaluation of *M* locus in association with MF/NMF phenotypes in this study revealed that M^0 and M^1 were likely to function dominantly over M^2 and M^3. To our knowledge, M^0M^3 was linked to MF, as shown in TH, SM, and BT. LL (M^1M^2) was also reported to exhibit MF phenotype (Font i Forcada et al., 2013), whereas NJF16 (M^2M^3) and MZ ($M^{2b}M^3$) had NMF phenotype (Clark and Finn, 2010; Yoshioka et al., 2011; **Table 1**). Although *PGM*-M^1 was present in M^2, its expression level seemed to be suppressed as reported in OA, whose genotype was determined as M^2M^2 in this study (Morgutti et al., 2006). Thus, the low expression of *PGM*-M^1 was consistent with the feature of M^2, namely, recessive against M^1 and M^0, and comparable to M^3. The hypothesis cannot be excluded that M^2 haplotypes in NMF accessions are specific haplotypes possessing additional mutation(s) that result in the disruption of M^2 function. The sequences of *PGM*-M^1 and its surrounding region on M^2 and M^1 haplotypes were identical with each other. As it was predicted that M^2 was generated from M^1 by deletion of the region including *PGF*, it seemed reasonable to consider that *PGM*-M^1 had lost its function before the emergence of M^2 haplotype and, thus M^2 haplotype in general was not functional. This prediction was supported by Morgutti et al. (2017), who reported that all accessions harboring flfl (M^2M^2) or flf_{null} (M^2M^3) exhibited NMF phenotype, as well as previous reports showing the existence of accessions exhibiting NMF phenotype but not completely lacking *endoPG* genes (Lester et al., 1994, 1996; Callahan et al., 2004; Peace et al., 2005; Morgutti et al., 2006).

It was hypothesized that two tandem *endoPG* genes at *M* locus, *PGM,* and *PGF*, were responsible for peach flesh texture regulation (Gu et al., 2016). In this study, we suggested that *PGM*-M^0 and *PGF* in particular would affect flesh textural quality whereas *PGM*-M^1 would have no effect. Considering the lack of sequence diversification and the relatively recent divergence between M^1 and M^2, it would not be possible that *PGM*-M^1 on M^1 retains its function. Although 11 haplotypes were characterized in this study, it might not be necessary to identify correctly all the haplotypes in order to estimate flesh textural quality in a breeding program. Only an analysis to confirm the presence of *PGM*-M^0 and *PGF* should be sufficient. This means we only need to test whether the PGM/F primer set (**Figure 8** and **Supplementary Figures S9, S10B**) amplifies *PGM*-M^0 or *PGF* fragments to estimate MF/NMF phenotypes in individual accessions and progenies.

M locus is strongly linked to freestone/clingstone (*F*) locus. It seems that *PGM*-M^0 is not responsible for the determination of *F* trait because most M^0M^0 and M^0M^3 accessions have clingstones. Gu et al. (2016) hypothesized that not *PGM* but only *PGF* on H_1 (M^1) haplotype is associated with the freestone phenotype. We re-evaluated the relationship between *M* genotypes and reported freestone/clingstone phenotypes. We found some accessions harboring M^1 haplotype but being reported to have not freestone but clingstone phenotype (data not shown). Further studies are required to unravel the role of *PGF* in the regulation of stone adhesion.

The classification of *M* haplotypes based on genomic structure and the re-evaluation of *M* locus in association with flesh melting traits in this study are expected to provide valuable information for studies on controlling fruit softening and textural quality. For example, BT is a well-known cultivar having slow softening behavior, but reaches MF texture at full maturity (Bassi and Monet, 2008; Ghiani et al., 2011). The *M* genotype of BT was found to be M^0M^3 in this study, which was the same as that of SM, a famous Japanese MF cultivar that softens rapidly (Yamamoto et al., 2003b). Therefore, we suggest that the slow softening behavior of BT is controlled by loci other than *M* locus. Even with the re-evaluated genotypes in this study, there are few incongruities between *M* genotypes and MF/NMF phenotypes

(**Supplementary Table S6**). These incongruities may be due to different conditions and definitions for phenotyping flesh texture among experiments and/or specific mutation(s) that occurred in particular accessions, as well as the involvement of other loci. Further studies addressing the reason for these incongruities are expected to uncover mechanism(s) that determine flesh texture and fruit softening and to improve our understanding of factors related to long shelf life.

CONCLUSION

We found that two ultra-late maturing cultivars, DJ and TH, showed different postharvest properties. DJ did not soften at all during ripening in spite of significant ethylene production, whereas TH showed rapid fruit softening leading to MF texture. Resequencing analyses of DJ and TH demonstrated that DJ was a homozygote of *M* haplotype designated as M^3 and lacked two tandem *endoPG* genes, *PGM* and *PGF*, at *M* locus. On the other hand, TH was a heterozygote of M^3 and a structurally unidentified haplotype designated as M^0 that consisted of only *PGM*-M^0 and was responsible for determining MF texture. Further classification of *M* haplotypes in 412 peach accessions revealed four main haplotypes: M^0; M^1 consisting of *PGM*-M^1 and *PGF*; M^2 consisting of *PGM*-M^1 and M^3; and M^0 was widely spread among MF accessions. We proposed the scenario that combinations of M^0 to M^3 determined flesh texture, and M^0 and M^1 dominantly controlled MF texture over M^2 and M^3. These suggested the possibility that *PGM*-M^0 and *PGF* could confer MF phenotype and *PGM*-M^1 of M^1 and M^2 haplotypes may have lost its function. This scenario was supported by the evolution history of each *M* haplotype assumed from the structural features of *M* locus in *Prunus* species, in which the ancestral haplotypes of M^0 and M^1 diverged before subgenus divergence and evolved independently of each other, whereas M^2 and M^3 were assumed to be derived from M^1 in recent age by deletion mutations.

DATA AVAILABILITY STATEMENT

The datasets analyzed for this study can be found in the DDBJ Sequenced Read Archive database (https://www.ddbj.nig.ac.jp/dra/index-e.html), accession numbers DRR248809-DRR248811 and DRR249197-DRR249201. The contigs A and B of M^0 haplotype will appear in the DDBJ/EMBL/GenBank databases under the accession numbers LC592228 and LC592229, respectively.

AUTHOR CONTRIBUTIONS

RN, TK, KU, and FF designed the study and drafted the manuscript. YF, DT, and MS performed sampling and phenotyping. RN, TK, YF, KA, and SW investigated postharvest ethylene production and flesh firmness. KU, RN, TK, and TA analyzed the genomic sequences of peach accessions and determined the genotypes of *M* locus in various peach accessions. All authors have contributed to manuscript revision and have read and approved the submitted version.

FUNDING

This work was supported in part by the Ministry of Education, Culture, Sports, Science and Technology of Japan (Grant-in-Aid for Scientific Research No. 18H02200 to RN).

ACKNOWLEDGMENTS

Computations were partially performed on the NIG supercomputer at ROIS National Institute of Genetics.

SUPPLEMENTARY MATERIAL

The Supplementary Material for this article can be found online at: https://www.frontiersin.org/articles/10.3389/fpls.2020.554158/full#supplementary-material

Supplementary Figure 1 | Soluble solids contents and juice pH in postharvest TH and DJ. Postharvest changes in **(A–C)** soluble solids content and **(D–F)** juice pH in TH and DJ fruit grown in Okayama Prefecture and DJ grown in Fukushima Prefecture Japan. In **(A,D)**, TH were harvested on November 7 from a commercial orchard in Okayama Prefecture, Japan and held at 25°C for 21 days. In **(B,E)**, DJ from Okayama were harvested on October 12 from the Research Farm of Okayama University, Japan and held at 25°C for 21 days. In **(C,F)** DJ from Fukushima were harvested on October 22 from a commercial orchard in Fukushima Prefecture, Japan, followed by 2-day transport at ambient temperature to Okayama University, where fruit were held at 25°C for 21 days. Fruit were harvested at commercial maturity. Each point in **(A,B,D,E)** and in **(C,F)** represents the mean value of three and four fruits, respectively. Vertical bars indicate ± SE (n = 3–4). Statistical analysis was conducted by Tukey's test after one-way ANOVA. Different letters indicate significant differences among measurement days by Tukey's multiple comparison test ($p < 0.05$).

Supplementary Figure 2 | Ethylene production in propylene treated TH and DJ. Effect of propylene treatment on postharvest ethylene production in **(A)** TH and **(B)** DJ fruit. Harvested fruit were treated with 5,000 ppm of propylene continuously for 7 days. Ethylene production was measured on days 0, 3, and 7. For **(B)** DJ, fruit harvested on October 12 from the Research Farm of Okayama University were used. Each point on days 0, 3, and 7 represents the mean value of four and three fruits, respectively. Vertical bars indicate ± SE (n = 3–4). Statistical analysis was conducted by Tukey's multiple comparison test after one-way ANOVA. Different letters indicate significant differences among measurement days by Tukey's test ($p < 0.05$).

Supplementary Figure 3 | Amino acid sequence comparison of PGM-M^0, PGM-M^1, and PGF. Amino acid sequences of PGM-M^0, PGM-M^1, and PGF of peach and PGM/F of almond "Texas" (PdTX), "Lauranne" (PdLN), *P. kansuensis* (Pkan), apricot (Parm), Japanese apricot (Pmum), sweet cherry (Pavi), and *P.* x *yedoensis* (Pyed) were aligned by CLC Genomics Workbench. Red and blue arrowheads denote amino acid substitution in PGM-M^1 and PGF, respectively. The C-terminal region of PdLN_PGF was truncated because of the frameshift at third exon. Only one PGM/F was found in reference genome of almond "Texas," but it could be orthologous to PGF of reference genome of "Lauranne." PGFs of "Texas" and "Lauranne" shared some amino acid substitutions that were not conserved in PGM of "Lauranne."

Supplementary Figure 4 | Schematic representation of *NADH* genes. We compared the gene structures of *NADH0–3*, *NADH0/2* of M^{2r1}, and *NADH3/1* of M^{2b}. Boxes are exons. Gray exons are gene-specific sequences. Other region sequences are homologous to other genes. Sequence comparison with

Arabidopsis *NADH* indicated that the original *NADH* could be composed of five exons as shown in *NADH3/1* of M^{2b} and *NADH* of Japanese apricot (**Supplementary Figures S5, S6**).

Supplementary Figure 5 | Amino acid sequence comparison of NADH. Putative amino acid sequences of peach NADHs and Arabidopsis NADH (AtNADH; AT3G03080) were aligned by CLC Genomics Workbench.

Supplementary Figure 6 | Comparison of *NADH* gene structures among *Prunus* species. Gene structures of 11 *NADH*s from eight *Prunus* species were compared. Considering exon composition, *NADH3* and *NADH2* of peach were regarded as one gene (*NADH3/2*), although they were annotated as different genes in reference genome. *Pkan NADH* gene was divided into different contigs whose linkages were unknown. Disrupted structures were found in five *NADH*s: *Pkan_NADH*, *NADH3/2*, *Parm_NADH*, *PdLN_NADH3/2*, and *PdTX_NADH*. The others were likely intact structures. The M1 insertion was found at third intron of *NADH3/2* and *Parm_NADH*.

Supplementary Figure 7 | Nucleotide sequence comparison of *PGM-*M^0 and *-*M^{0b}. Sequence comparison showed six mutations in *PGM* of TH (designated as *PGM-*M^{0b} in this figure). Furthermore, a large insertion was predicted at the upstream region of *PGM-*M^{0b}. Of the six mutations, only one was located in CDS region and it was a synonymous substitution. AAC and AAT at 346–348 encode Asn. Therefore, we did not discriminate *PGM-*M^0 and *PGM-*M^{0b} in this study. In the study of Morgutti et al. (2017), *PGM-*M^{0b} was detected by CAPS analysis using *Bst*XI. This restriction enzyme site was caused by the nucleotide substitution at 348 bp of M^{0b} haplotype and the fragment from *PGM-*M^0 was expected to be insensitive to *Bst*XI. *PGM-*M^{0b} could confer the MF phenotype because flesh texture was melting in both TH ($M^{0b}M^3$) and BT ($M^{0b}M^3$). Morgutti et al. (2017) proposed four alleles, *PG_M*, PG^m, PG^{SH}, and PG^{BT}, at *M* locus from OA (M^2M^2), "Bolero" (M^1M^1), "Yumyeong" (M^0M^0), "Ghiaccio" (M^0M^0), and BT ($M^{0b}M^{03}$). Based on **Figure 7**, our classification suggested that *PG_M* and PG^m were derived from M^1 or M^2 haplotype and these were designated as *PGM-*M^1 and *PGF*, respectively, in this study (**Supplementary Table S7**). PG^{SH} and PG^{BT} could correspond to *PGM-*M^0 and *PGM-*M^{0b}, respectively. These might be strictly different alleles because of the nucleotide substitution, but flesh texture was melting in both SM (M^0M^3) and TH ($M^{0b}M^3$), suggesting that their effects on flesh texture were the same and they were not different functionally.

Supplementary Figure 8 | Primers for PCR genotyping. Three primer sets were designed for the discrimination of four main haplotypes, M^0, M^1, M^2, and M^3. **(A)** Primer position at M^1 haplotype. **(B)** Position of PGM/F primer set.

Supplementary Figure 9 | MZ and O3 possessed M^{2b} haplotype. MZ and O3 possessed *PGM-*M^1 and no *PGF*. This pattern indicated the M^2 haplotype, but no amplification to detect the M^2 deletion was observed by PCR (**Figure 8**). In addition to M^2 haplotype, we found the same combination in M^{2b} and M^{2r1} haplotypes, which were rare haplotypes compared with M^2. To determine the genotypes of MZ and O3, we designed three primer sets to discriminate M^2, M^{2b}, and M^{2r1} haplotypes on the basis of the sequences of *NADH* genes (**Supplementary Figure S4**). M2D2 amplified one fragment from M^0, M^{2b} or M^{2r1} haplotype. NDP1 was expected to amplify two fragments: upper for M^0, and lower for M^1, M^2, M^{2b} or M^{2r1}. NDP2 was also expected to amplify two fragments: upper for M^1 or M^{2b}, and lower for M^0 or M^{2r1}. The amplification of M2D2 fragment indicated MZ had M^0, M^{2b} or M^{2r1} but not M^1 and M^2. The lower NDP1 fragment in MZ excluded the possibility of M^0. Furthermore, the upper NPD2 fragment was amplified in PCR, indicating that MZ possessed M^{2b} haplotype. O3 also had M^{2b}, but two fragments were amplified in NDP1 and NDP2 because O3 had M^0 haplotype (**Figure 8**).

Supplementary Figure 10 | Peach cultivars bred in Japan shared M^0 haplotype. HT, Hakuto; HH, Hakuho; AK, Akatsuki; BH, Benihakuto; YZ, Yuzora; TS, Tosui; KN, KawanakajimaHakuto; OB, Okubo; SM, ShimizuHakuto; O3, Okayama-3; HK, HikawaHakuho; LL, Lovell; CC, Chinese Cling (Shanhai Suimitsuto); TW, Tachibanawase; UNK, unknown cultivar. **(A)** Genealogy of peach cultivars in Japan. Green cultivars were the five leading cultivars in Japan in 2016 (e-stat Japan, https://www.e-stat.go.jp/). Their cultivation areas accounted for more than 60% of the total peach cultivation area in Japan. Haplotypes in parentheses were presumed from haplotypes of offspring and another parent. **(B)** PCR haplotyping. CC was imported from China to Japan in the late nineteenth century. HT was reported to be found and selected as a chance seedling of CC in 1899 (Yamamoto et al., 2003a). HT was frequently used as seed parent in breeding programs and many Japanese peach cultivars were the progeny of HT, as described **Supplementary Figure S10A**. We selected 11 Japanese MF cultivars and carried out PCR genotyping to determine the genotypes of their *M* loci. All cultivars shared M^0 haplotype and all cultivars except OB and SM were M^0 homozygous. OB was M^0M^1 and SM was M^0M^3. SM was found as a chance seedling at a mixed orchard of HT and O3. SSR analysis supported the hypothesis that SM was a progeny of HT (Yamamoto et al., 2003a). Because of male sterility of HT, O3 had been regarded as the pollen parent of SM. M^0 haplotype of SM was inherited from HT and seed parent should possess M^3 haplotype, because HT was M^0 homozygous. These indicated that O3 was not the parent of SM.

Supplementary Figure 11 | Structural comparison of *M* loci among *Prunus* species. Circos plots show sequence similarities among M^0, M^1, and *M* haplotypes of other *Prunus* species. Ribbons link homologous regions between haplotypes. *Indicates genes that did not have intact CDS sequence. *PG1* of *P. mume* was translocated to the > 2 Mbp downstream region. To determine the *M* locus region, reference genomes of almond ("Lauranne" and "Texas"), *P. kansuensis*, *P. mira*, Japanese apricot, apricot, sweet cherry, and *P.* x *yedoensis* were searched by Blastn analysis using *PG1*, *PG2*, *PGM/F*, *NADH*, and *F-box* genes as query. *M* locus was found at the right arm of chromosome 4 or LG3 in all *Prunus* species except *P. kansuensis*, in which no pseudomolecule was released. Nucleotide sequences of *M* locus were compared by nucmer and the relationships were drawn by Circos.

Supplementary Table 1 | Climate conditions in peach production areas in Okayama and Fukushima Prefectures, Japan in 2018.

Supplementary Table 2 | Relationships between flesh penetration force measured by the system used in this study and other fruit maturity indexes.

Supplementary Table 3 | Primers used in this study.

Supplementary Table 4 | Comparison of SNP number in regions from *PG1* to *PG2*. Intergenic region 1 was from end of *PG1* to 19,026,185 bp (outside M^3 deletion region). Intergenic region 2 was from 19,026,186 bp (inside M^3 deletion region) to start of *PG2*. Values in parentheses are those of heterozygous SNPs.

Supplementary Table 5 | *M* genotypes of 412 peach accessions.

Supplementary Table 6 | Differences in flesh texture predicted by genotype and reported phenotype. *The reported phenotype matched the predicted one in this study. The 11 accessions showed differences between predicted and reported phenotypes. All except "Early Gold" (EG) were reported by Yoon et al. (2006) and Cao et al. (2016). EG was a canning peach and its parent was "Nishiki" (NK). EG should possess at least one M^2 haplotype because NK was an M^2 homozygote, but resequencing analysis showed that EG was M^1M^1.

Supplementary Table 7 | Correlation of *PGM/F* genes in this study with those in previous reports. PG^{BT} in Morgutti et al. (2017) was *Bst*XI-sensitive (**Supplementary Figure S6**).

Supplementary Table 8 | Correlation of haplotypes in this study with those in previous reports. *M^0 was misidentified as H_2 haplotype in Gu et al. (2016). f haplotype structure in Morgutti et al. (2017) was postulated from M^1 haplotype. *PG* gene composition was correct but the genome structure was not the same as M^0 haplotype in this study. *PGM-*M^0 and *PGM-*M^1 were allelic.

REFERENCES

Bailey, J. S., and French, H. P. (1949). The inheritance of certain fruit and foliage characters in peach. *Mass. Agr. Expt. Sta. Bul.* 452, 2–31.

Bassi, D., and Monet, R. (2008). "Botany and taxonomy," in *The Peach: Botany, Production and Uses*, eds D. R. Layne and D. Bassi (Wallingford: CAB International), 1–36. doi: 10.1079/9781845933869.0001

Biale, J. B., and Young, R. E. (1981). "Respiration and ripening in fruits- retrospect and prospect," in *Recent Advances in the Biochemistry of Fruits and Vegetables*, eds J. Friend and M. J. C. Rhodes (London: Academic Press), 1–39. doi: 10.4324/9781315130590-1

Brecht, J. K., and Kader, A. A. (1984). Ethylene production by fruit of some slow-ripening nectarine genotypes. *J. Am. Soc. Hort. Sci.* 109, 763–767.

Brummell, D. A., Dal Cin, V., Crisosto, C. H., and Labavitch, J. M. (2004). Cell wall metabolism during maturation, ripening and senescence of peach fruit. *J. Exp. Bot.* 55, 2029–2039. doi: 10.1093/jxb/erh227

Burg, S. P., and Burg, E. A. (1967). Molecular requirements for the biological activity of ethylene. *Plant Physiol.* 42, 144–152. doi: 10.1104/pp.42.1.144

Callahan, A. M., Scorza, R., Bassett, C., Nickerson, M., and Abeles, F. B. (2004). Deletions in an endopolygalacturonase gene cluster correlate with non-melting flesh texture in peach. *Funct. Plant Biol.* 31, 159–168. doi: 10.1071/FP03131

Cao, K., Zhou, Z., Wang, Q., Guo, J., Zhao, P., Zhu, G., et al. (2016). Genome-wide association study of 12 agronomic traits in peach. *Nat. Commun.* 7:13246. doi: 10.1038/ncomms13246

Carrasco-Valenzuela, T., Muñoz-Espinoza, C., Riveros, A., Pedreschi, R., Arús, P., Campos-Vargas, R., et al. (2019). Expression QTL (eQTLs) analyses reveal candidate genes associated with fruit flesh softening rate in peach [*Prunus persica* (L.) Batsch]. *Front. Plant Sci.* 10:1581. doi: 10.3389/fpls.2019.01581

Chin, S. W., Shaw, J., Haberle, R., Wen, J., and Potter, D. (2014). Diversification of almonds, peaches, plums and cherries–molecular systematics and biogeographic history of *Prunus* (Rosaceae). *Mol Phylogenet. Evol.* 76, 34–48. doi: 10.1016/j.ympev.2014.02.024

Clark, J. R., and Finn, C. E. (2010). Register of new fruit and nut cultivars List 45. *HortScience* 45, 716–756. doi: 10.21273/HORTSCI.45.5.716

Davis, L. (1937). The gumming of Phillips cling peaches. *Hilgardia* 11, 1–34. doi: 10.3733/hilg.v11n01p001

Eduardo, I., Picañol, R., Rojas, E., Batlle, I., Howad, W., Aranzana, M. J., et al. (2015). Mapping of a major gene for the slow ripening character in peach: co-location with the maturity date gene and development of a candidate gene-based diagnostic marker for its selection. *Euphytica* 205, 627–636. doi: 10.1007/s10681-015-1445-9

Elsadr, H., Sherif, S., Banks, T., Somers, D., and Jayasankar, S. (2019). Refining the genomic region containing a major locus controlling fruit maturity in peach. *Sci. Rep.* 9:7522. doi: 10.1038/s41598-019-44042-4

Fernandez, I., Marti, A., Saski, C. A., Manganaris, G. A., Gasic, K., and Crisosto, C. H. (2018). Genomic sequencing of Japanese plum (*Prunus salicina* Lindl.) mutants provides a new model for *Rosaceae* fruit ripening studies. *Front. Plant Sci.* 9:21. doi: 10.3389/fpls.2018.00021

Fishman, M. L., Levaj, B., Gillespie, D., and Scorza, R. (1993). Changes in the physicochemical properties of peach fruit pectin during on-tree ripening and storage. *J. Amer. Soc. Hort. Sci.* 118, 343–349. doi: 10.21273/JASHS.118.3.343

Font i Forcada, C., Oraguzie, N., Igartua, E., Ángeles Moreno, M., and Gogorcena, Y. (2013). Population structure and marker–trait associations for pomological traits in peach and nectarine cultivars. *Tree Genet. Genomes* 9, 331–349. doi: 10.1007/s11295-012-0553-0

Gapper, N. E., McQuinn, R. P., and Giovannoni, J. J. (2013). Molecular and genetic regulation of fruit ripening. *Plant Mol. Biol.* 82, 575–591. doi: 10.1007/s11103-013-0050-3

Ghiani, A., Negrini, N., Morgutti, S., Baldin, F., Nocito, F. F., Spinardi, A., et al. (2011). Melting of "Big Top" nectarine fruit: some physiological, biochemical, and molecular aspects. *J. Am. Soc. Hort. Sci.* 136, 61–68. doi: 10.21273/JASHS.136.1.61

Giné-Bordonaba, J., Eduardo, I., Arús, P., and Cantín, C. M. (2020). Biochemical and genetic implications of the slow ripening phenotype in peach fruit. *Sci. Hortic.* 259:108824. doi: 10.1016/j.scienta.2019.108824

Gu, C., Wang, L., Wang, W., Zhou, H., Ma, B. Q., Zheng, H. Y., et al. (2016). Copy number variation of a gene cluster encoding endopolygalacturonase mediates flesh texture and stone adhesion in peach. *J. Exp. Bot.* 67, 1993–2005. doi: 10.1093/jxb/erw021

Haji, T., Yaegaki, H., and Yamaguchi, M. (2003). Softening of stony hard peach by ethylene and the induction of endogenous ethylene by 1-aminocyclopropene-1-carboxylic acid (ACC). *J. Japan Soc. Hort. Sci.* 72, 212–217. doi: 10.2503/jjshs.72.212

Haji, T., Yaegaki, H., and Yamaguchi, M. (2005). Inheritance and expression of fruit texture melting, non-melting and stony hard in peach. *Sci. Hortic.* 105, 241–248. doi: 10.1016/j.scienta.2005.01.017

Hayama, H., Shimada, T., Fujii, H., Ito, A., and Kashimura, Y. (2006). Ethylene-regulation of fruit softening and softening-related genes in peach. *J. Exp. Bot.* 57, 4071–4077. doi: 10.1093/jxb/erl178

Hayama, H., Tatsuki, M., and Nakamura, Y. (2008). Combined treatment of aminoethoxyvinylglycine (AVG) and 1-methylcyclopropene (1-MCP) reduces melting-flesh peach fruit softening. *Postharvest Biol. Technol.* 50, 228–230. doi: 10.1016/j.postharvbio.2008.05.003

Hiwasa, K., Nakano, R., Hashimoto, A., Matsuzaki, M., Murayama, H., Inaba, A., et al. (2004). European, Chinese and Japanese pear fruits exhibit differential softening characteristics during ripening. *J. Exp. Bot.* 55, 2281–2290. doi: 10.1093/jxb/erh250

Infante, R., Contador, L., Rubio, P., Aros, D., and Penþa-Neira, A. ì (2011). Postharvest sensory and phenolic characterization of 'Elegant Lady' and 'Carson' peaches. *Chilean J. Agric. Res.* 71, 445–451. doi: 10.4067/S0718-58392011000300016

Jackman, S. D., Vandervalk, B. P., Mohamadi, H., Chu, J., Yeo, S., Hammond, S. A., et al. (2017). ABySS 2.0: resource-efficient assembly of large genomes using a Bloom filter. *Genome Res.* 27, 768–777. doi: 10.1101/gr.214346.116

Kawai, T., Matsumori, F., Akimoto, H., Sakurai, N., Hirano, K., Nakano, R., et al. (2018). Nondestructive detection of split-pit peach fruit on trees with an acoustic vibration method. *Hort. J.* 87, 499–507. doi: 10.2503/hortj.UTD-012

Kurtz, S., Phillippy, A., Delcher, A. L., Smoot, M., Shumway, M., Antonescu, C., et al. (2004). Versatile and open software for comparing large genomes. *Genome Biol.* 5:R12. doi: 10.1186/gb-2004-5-2-r12

Lester, D. R., Sherman, W. B., and Atwell, B. J. (1996). Endopolygalacturonase and the melting flesh (*M*) locus in peach. *J. Amer. Soc. Hort. Sci.* 121, 231–235. doi: 10.21273/JASHS.121.2.231

Lester, D. R., Speirs, G., Orr, G., and Brady, C. J. (1994). Peach (*Prunus persica*) endo-PG cDNA isolation and mRNA analysis in melting and non-melting peach cultivars. *Plant Physiol.* 105, 225–231. doi: 10.1104/pp.105.1.225

Li, H. (2018). Minimap2: pairwise alignment for nucleotide sequences. *Bioinformatics* 34, 3094–3100. doi: 10.1093/bioinformatics/bty191

Liguori, G., Weksler, A., Zutahi, Y., Lurie, S., and Kosto, I. (2004). Effect of 1-methylcyclopropene on ripening of melting flesh peaches and nectarines. *Postharvest Biol. Technol.* 31, 263–268. doi: 10.1016/j.postharvbio.2003.09.007

Liu, H., Qian, M., Song, C., Li, J., Zhao, C., Li, G., et al. (2018). Down-regulation of *PpBGAL10* and *PpBGAL16* delays fruit softening in peach by reducing polygalacturonase and pectin methylesterase activity. *Front. Plant Sci.* 9:1015. doi: 10.3389/fpls.2018.01015

Mathooko, F. M., Tsunashima, Y., Owino, W. Z. O., Kubo, Y., and Inaba, A. (2001). Regulation of genes encoding ethylene biosynthetic enzymes in peach (*Prunus persica* L.) fruit by carbon dioxide and 1-methylcyclopropene. *Postharvest Biol. Technol.* 21, 265–281. doi: 10.1016/S0925-5214(00)00158-7

McMurchie, E. J., McGlasson, W. B., and Eaks, I. L. (1972). Treatment of fruit with propylene gives information about bio-genesis of ethylene. *Nature* 237, 235–236. doi: 10.1038/237235a0

Meneses, C., Ulloa-Zepeda, L., Cifuentes-Esquivel, A., Infante, R., Cantin, C. M., Batlle, I., et al. (2016). A codominant diagnostic marker for the slow ripening trait in peach. *Mol. Breed.* 36:77. doi: 10.1007/s11032-016-0506-7

Minas, I. S., Font i Forcada, C., Dangl, G. S., Gradziel, T., Dandekar, A. M., and Crisosto, C. H. (2015). Discovery of non-climacteric and suppressed-climacteric bud sport mutations originating from a climacteric Japanese plum cultivar (*Prunus salicina* lindl.). *Front. Plant Sci.* 6:316. doi: 10.3389/fpls.2015.00316

Moggia, C., Graell, J., Lara, I., González, G., and Lobos, G. A. (2017). Firmness at harvest impacts postharvest fruit softening and internal browning development in mechanically damaged and non-damaged highbush blueberries (*Vaccinium corymbosum* L.). *Front. Plant Sci.* 8:535. doi: 10.3389/fpls.2017.00535

Monet, R. (1989). Peach genetics: past, present and future. *Acta Hortic.* 254, 49–57. doi: 10.17660/ActaHortic.1989.254.8

Morgutti, S., Negrini, N., Ghiani, A., Baldin, F., Bassi, D., and Cocucci, M. (2017). *Endopolygalacturonase* gene polymorphisms: asset of the locus in different peach accessions. *Am. J. Plant Sci.* 8, 941–957. doi: 10.4236/ajps.2017.84063

Morgutti, S., Negrini, N., Nocito, F. F., Ghiani, A., Bassi, D., and Cocucci, M. (2006). Changes in endopolygalacturonase levels and characterization of

a putative *endo-PG* gene during fruit softening in peach genotypes with nonmelting and melting flesh fruit phenotypes. *New Phytol.* 171, 315–328. doi: 10.1111/j.1469-8137.2006.01763.x

Nakano, R., Akimoto, H., Fukuda, F., Kawai, T., Ushijima, K., Fukamatsu, Y., et al. (2018). Nondestructive detection of split pit in peaches using an acoustic vibration method. *Hort. J.* 87, 281–287. doi: 10.2503/hortj.OKD-094

Nimmakayala, P., Tomason, Y. R., Abburi, V. L., Alvarado, A., Saminathan, T., Vajja, V. G., et al. (2016). Genome-wide differentiation of various melon horticultural groups for use in GWAS for fruit firmness and construction of a high resolution genetic map. *Front. Plant Sci.* 7:1437. doi: 10.3389/fpls.2016.01437

Nishiyama, K., Guis, M., Rose, J. K., Kubo, Y., Bennett, K. A., Wangjin, L., et al. (2007). Ethylene regulation of fruit softening and cell wall disassembly in *Charentais* melon. *J. Exp. Bot.* 58, 1281–1290. doi: 10.1093/jxb/erl283

Nuñez-Lillo, G., Cifuentes-Esquivel, A., Troggio, M., Micheletti, D., Infante, R., Campos-Vargas, R., et al. (2015). Identification of candidate genes associated with mealiness and maturity date in peach [*Prunus persica* (L.) Batsch] using QTL analysis and deep sequencing. *Tree Genet. Genomes* 11:86. doi: 10.1007/s11295-015-0911-9

Pan, L., Zeng, W., Niu, L., Lu, Z., Liu, H., Cui, G., et al. (2015). *PpYUC11*, a strong candidate gene for the stony hard phenotype in peach (*Prunus persica* L. Batsch), participates in IAA biosynthesis during fruit ripening. *J. Exp. Bot.* 66, 7031–7044. doi: 10.1093/jxb/erv400

Peace, C. P., Callahan, A., Ogundiwin, E. A., Potter, D., Gradziel, T. M., Bliss, F. A., et al. (2007). Endopolygalacturonase genotypic variation in *Prunus*. *Acta Hortic.* 738, 639–646. doi: 10.17660/actahortic.2007.738.83

Peace, C. P., Crisosto, C. H., and Gradziel, T. M. (2005). Endopolygalacturonase: a candidate gene for freestone and melting flesh in peach. *Mol. Breed.* 16, 21–31. doi: 10.1007/s11032-005-0828-3

Pressey, R., and Avants, J. K. (1978). Differences in polygalacturonase composition of clingstone and freestone peaches. *J. Food Sci.* 43, 1415–1423. doi: 10.1111/j.1365-2621.1978.tb02507.x

Tatsuki, M., Haji, T., and Yamaguchi, M. (2006). The involvement of 1−aminocyclopropane−1−carboxylic acid synthase isogene, *Pp−ACS1*, in peach fruit softening. *J. Exp. Bot.* 57, 1281–1289. doi: 10.1093/jxb/erj097

Tatsuki, M., Soeno, K., Shimada, Y., Sawamura, Y., Suesada, Y., Yaegaki, H., et al. (2018). Insertion of a transposon−like sequence in the 5'−flanking region of the *YUCCA* gene causes the stony hard phenotype. *Plant J.* 96, 815–827. doi: 10.1111/tpj.14070

Tonutti, P., Casson, P., and Ramina, A. (1991). Ethylene biosynthesis during peach fruit development. *J. Amer. Soc. Hort. Sci.* 116, 274–279. doi: 10.21273/JASHS.116.2.274

Tucker, G., Yin, X., Zhang, A., Wang, M., Zhu, Q., Liu, X., et al. (2017). Ethylene and fruit softening. *Food Qual. Safe* 1, 253–267. doi: 10.1093/fqsafe/fyx024

Verde, I., Jenkins, J., Dondini, L., Micali, S., Pagliarani, G., Vendramin, E., et al. (2017). The Peach v2.0 release: high-resolution linkage mapping and deep resequencing improve chromosome-scale assembly and contiguity. *BMC Genomics* 18:225. doi: 10.1186/s12864-017-3606-9

Wang, Z.-H., and Lu, Z.-X. (1992). Advances of peach breeding in China. *HortScience* 27, 729–732. doi: 10.21273/HORTSCI.27.7.729

Yamamoto, T., Mochida, K., and Hayashi, T. (2003a). Shanhai suimitsuto, one of the origins of Japanese peach cultivars. *J. Japan. Soc. Hort. Sci.* 72, 116–121. doi: 10.2503/jjshs.72.116

Yamamoto, T., Mochida, K., Imai, T., Haji, T., Yaegaki, H., Yamaguchi, M., et al. (2003b). Parentage analysis in Japanese peaches using SSR markers. *Breed. Sci.* 53, 35–40. doi: 10.1270/jsbbs.53.35

Yamazaki, T., and Suzuki, K. (1980). Color charts: useful guide to evaluate the fruit maturation. I. Colorimetric specifications of color charts for Japanese pear, apple, peach, grape, kaki and citrus fruits. (In Japanese with English summary). *Bull. Fruit Tree Res. Sta. A* 19–44.

Yoon, J., Liu, D., Song, W., Liu, W., Zhang, A., and Li, S. (2006). Genetic diversity and ecogeographical phylogenetic relationships among peach and nectarine cultivars based on simple sequence repeat (SSR) markers. *J. Am. Soc. Hort. Sci.* 131, 513–521. doi: 10.21273/JASHS.131.4.513

Yoshida, M. (1981). Recent trend of peach breeding in Japan. *JARQ* 15, 106–109.

Yoshioka, H., Hayama, H., Tatsuki, M., and Nakamura, Y. (2010). Cell wall modification during development of mealy texture in the stony-hard peach "Odoroki" treated with propylene. *Postharvest Biol. Technol.* 55, 1–7. doi: 10.1016/j.postharvbio.2009.08.005

Yoshioka, H., Hayama, H., Tatsuki, M., and Nakamura, Y. (2011). Cell wall modifications during softening in melting type peach "Akatsuki" and non-melting type peach "Mochizuki". *Postharvest Biol. Technol.* 60, 100–110. doi: 10.1016/j.postharvbio.2010.12.013

Zhang, X., Su, M., Du, J., Zhou, H., Li, X., Li, X., et al. (2019). Comparison of phytochemical differences of the pulp of different peach [*Prunus persica* (L.) Batsch] cultivars with alpha-glucosidase inhibitory activity variations in China using UPLC-Q-TOF/MS. *Molecules* 24:1968. doi: 10.3390/molecules24101968

Conflict of Interest: The authors declare that the research was conducted in the absence of any commercial or financial relationships that could be construed as a potential conflict of interest.

frontiers in Plant Science

ORIGINAL RESEARCH
published: 23 December 2020
doi: 10.3389/fpls.2020.594156

Proteomic Changes in Antioxidant System in Strawberry During Ripening

Jun Song[1], Leslie CampbellPalmer[1], Mindy Vinqvist-Tymchuk[1], Sherry Fillmore[1], Charles Forney[1], Honghui Luo[2] and Zhaoqi Zhang[2]*

[1] Agriculture and Agri-Food Canada, Kentville Research and Development Centre, Kentville, NS, Canada, [2] College of Horticulture, South China Agriculture University, Guangzhou, China

OPEN ACCESS

Edited by:
Cai-Zhong Jiang, Crops Pathology and Genetics Research Unit, USDA-ARS, United States

Reviewed by:
David Obenland, San Joaquin Valley Agricultural Sciences Center (USDA ARS), United States
Barbara Blanco-Ulate, University of California, Davis, United States
Jingying Shi, Shandong Agricultural University, China

***Correspondence:**
Jun Song
jun.song@canada.ca

Specialty section:
This article was submitted to Crop and Product Physiology, a section of the journal Frontiers in Plant Science

Received: *12 August 2020*
Accepted: *27 November 2020*
Published: *23 December 2020*

Citation:
Song J, CampbellPalmer L, Vinqvist-Tymchuk M, Fillmore S, Forney C, Luo H and Zhang Z (2020) Proteomic Changes in Antioxidant System in Strawberry During Ripening. Front. Plant Sci. 11:594156. doi: 10.3389/fpls.2020.594156

To investigate the strawberry antioxidant defense system during fruit ripening, a targeted quantitative proteomic approach using multiple reaction monitoring (MRM) was developed to investigate targeted proteins in the antioxidant enzyme system in strawberry fruit. We investigated 46 proteins and isoforms with 73 identified peptides which may be involved in this antioxidant enzyme system. Among the proteins that changed during ripening, aldo/keto reductase (AKR), superoxide dismutase (SOD) and glutathione transferase (GT) increased significantly, while dehydroascorbate reductase, 2-Cys peroxiredoxin, catalase (CAT), 1-Cys peroxiredoxin and L-ascorbate peroxidase (APX) decreased significantly. These results suggest that fruit ripening of strawberry activates the enzymes of an SOD/glutathione metabolism system. The methodologies used in this study will be useful for systematically characterizing the role of antioxidant enzymes in fruit ripening of other plants.

Keywords: *Fragaria* × *ananassa*, fruit ripening, quality, multiple reaction monitoring, OFFGEL, proteomics

SIGNIFICANCE

Gaining insights into the fundamental mechanisms at molecular level in association with the antioxidant enzyme system and its regulation during strawberry fruit ripening is challenging caused by limited research tools and lack of established hypotheses. Despite intensive molecular and biochemical research into fruit ripening, quantitative proteomic studies through an MRM approach have been rare. Using LC-MS/MS analysis and developing quantitative MRM, this study provides a systematic and multi-targeted investigation of the antioxidant enzymes in strawberry fruit at different ripening stages. Targeted detection of proteins in association with the antioxidant enzyme system used for quantitative approaches of MRM was developed. It is possible to examine their changes as the strawberry fruit matures. Our results demonstrate the usefulness of this technique for the analysis of regulatory proteins. These results provide evidence of the dynamic changes in SOD/glutathione metabolism that occur during fruit ripening.

Abbreviations: AKR, aldo/keto reductase; APX, L-ascorbate peroxidase; CAT, catalase; GT, glutathione transferase; GST, glutathione synthase; GR, glutathione reductase; H_2O_2, hydrogen peroxide; MRM, multiple reaction monitoring; PRXs, 1-Cys peroxiredoxin and 2-Cys peroxiredoxin; ROS, reactive oxygen species; SOD, superoxide dismutase.

INTRODUCTION

Strawberry (*Fragaria* × *ananassa*) fruit is one of the popular fruit in the world, with significant economic benefits to the fruit and food industry. It is estimated that the world production of strawberry fruit was 9.1 million tons, with an associated value of $2.9 billion in 2016 (FAOSTAT, 2016). The attractiveness of strawberry fruit to consumers is dependent on a number of quality attributes including color, flavor and nutritional value. From a post-harvest perspective, however, strawberries have a relatively short market life. Research focusing on fruit ripening and quality is therefore important in order to develop new storage and marketing strategies to maintain and improve the quality and shelf-life of strawberry fruit.

Significant research has investigated the biology of fruit ripening and senescence in strawberry fruit resulting in the identification of a number of genes involved in ripening such as anthocyanin biosynthesis, cell wall degradation, sucrose and lipid metabolism, protein synthesis and degradation, and respiration (Manning, 1998). In addition, a number of genes were identified that encode proteins believed to participate in the signal and regulation cascades involved in maturation of achene maturation as well as acquisition of stress. As well, genes associated with stress, cell wall metabolism, DNA/RNA/protein interaction and primary metabolism were highly represented in the receptacle tissues (Nam et al., 1999). Various studies have investigated strawberry fruit during ripening and identified regulating genes involved in ethylene reception (Trainotti et al., 2005), firmness (Redondo-Nevado et al., 2001; Villarreal et al., 2008), allergens (Hjernø et al., 2006) and anthocyanin biosynthesis (Griesser et al., 2008; Carbone et al., 2009; Kadomura-Ishikawa et al., 2015). Metabolomic studies empolying gas chromatography-mass spectrometry (GC/MS) and liquid chromatography-mass spectrometry (LC/MS) revealed dynamic changes of primary and secondary metabolies reflecting organ and development stages of strawberry fruit separately, in achene and receptacle during ripening of strawberry fruit (Fait et al., 2008). Strawberry is recognized as a non-climacteric fruit, which ripens without the autocatalytic ethylene response (Symons et al., 2012). It was reported that the fruit was able to continue ripening after being detached at the green stage, however, reduced content of malic acid, glucose, fructose and sucrose content was found to be lower than fruit ripened on the plant. This would indicate that normal fruit ripening requires a continuous supply of photosynthetic assimilates, water and nutrients by the plant (Van de Poel et al., 2014). It has been shown that auxins and abscisic acid (ABA) related metabolism and signaling in strawberry play an important role in fruit ripening and strawberry has been used as a model of non-climacteric fruit ripening (Medina-Puche et al., 2016). Hormone interplay was reported during strawberry fruit ripening and an increase in carbohydrates, phenylpropanoids, flavonoids, glutathione, and methionine is controlled by ABA, while auxins are mainly responsible for the receptacle development. Ethylene and gibberellins seem to play a minor role in strawberry ripening (Medina-Puche et al., 2016). Gene expression studies on strawberry fruit using auxin treatment showed the reduced genes expression in flavonoids metabolism, pigmentation as well as tubulin and profilin (Aharoni et al., 2002). In addition, it was also reported that the strawberry fruit ripening is induced by a transcriptional program in response to oxidative stress. In non-climacteric fruit, it was proposed that gene expression is induced to cope with oxidative stress that occurs during ripening. Therefore one of the strawberry ripening transcriptional programs is an oxidative stress-induced process (Aharoni et al., 2002). From both fruit ripening physiology and nutritional perspectives, research into redox and antioxidant enzymes in association with strawberry fruit ripening is important (Decros et al., 2019).

Although numerous biochemical and physiological studies have been conducted to reveal the mechanism of fruit ripening and senescence of strawberry, limited proteomic data is available to provide in-depth information in our understanding of strawberry fruit ripening and senescence beyond the above identified genes (Bianco et al., 2009; Palma et al., 2011; Li et al., 2013).

Proteomics is the study of "the entire protein complement expressed by a genome in a cell or tissue" (Pandey and Mann, 2004). Proteomics has become an essential tool of "omic" approaches and is contributing to a better understanding of biological systems by measuring gene products, which are the active agents in cells. More importantly, modifications of proteins and post-translational modifications can be determined only by proteomic methodologies (Fridman and Pichersky, 2005). Proteomic studies using LC/MS, have been developed and applied to investigate the fruit ripening, physiological disorder and abundance of allergens at proteomic level. These studies investigated and identified proteins in association with fruit ripening, cell wall metabolism, natural defense and allergens in apple and strawberry fruit (Pedreschi et al., 2007; Bianco et al., 2009; Zheng et al., 2013). Employing labeling techniques, a quantitative proteomic study was conducted and identified a number of significantly changed proteins in association with fruit ripening. Significantly increased proteins associated with various metabolic pathways including flavonoid/anthocyanin biosynthesis, volatile biosynthesis, antioxidant metabolism, stress responses and allergen formation were found. Meanwhile, proteins that are involved in methionine metabolism, antioxidant-redox, energy metabolism and protein synthesis decreased during fruit ripening. Quantitative proteomic research identified certain proteins that increased during fruit ripening, including aldo/keto reductase (AKR), quinone oxidoreductase and ascorbate peroxidase (APX). Another group of proteins found to decrease as ripeness advanced included 1-Cys peroxiredoxin (PRX), 2-Cys PRX, isoflavone reductase related protein, as well as cytoplasmic SOD[Cu/Zn] (Li et al., 2013). Selected reaction monitoring (SRM) and/or multiple reaction monitoring (MRM) technologies have come out as a major development for targeted quantitative proteomic analysis (Lange et al., 2008). In an SRM experiment, it is usually conducted on a triple quadrupole instrument equipped with two mass filters. Therefore, it can detect and monitor predefined precursor ion and one of its fragments. As a result, series of transitions (precursor/fragment ion pairs) can be established and analyzed. With the help of LC

and the retention time of peptides, targeted peptides can be quantitatively measured in a complex biological sample (Song et al., 2015a). MRM studies offer very good sensitivity and a wide dynamic range, which provide new technological advantages in plant biotechnological and biological applications to quantify targeted proteins. Targeted quantitative proteomic studies using MRM reported the key regulating points responsible for the biosynthesis of anthocyanins, flavonoids and volatile biosynthesis pathways in strawberry fruit in correlation with fruit ripening (Song et al., 2015a,b). These results demonstrate that strawberry fruit ripening is regulated by a complex network involving multiple active processes. With development of analytical techniques, specialized pathways including redox and antioxidant enzymes in fruit such as apple have been reported (Qin et al., 2009). All these findings provided some initial understanding of the involvement of redox systems in the physiological responses of fruit, including regulation of fruit ripening and senescence.

In order to analyze the changes of antioxidant enzyme isoforms involved in redox-antioxidant systems during strawberry fruit ripening, we reanalyzed results previously collected from OFFGEL electrophoresis (OGE) fractionation of a complex mixture of strawberry fruit peptides analyzed with LC-MS/MS (Yang et al., 2014). We evaluated and established the MRM transitions for those peptides, and then quantified proteins in two strawberry cultivars at three different ripening stages. The objectives of this study were to quantitatively determine the changes of protein abundance in association with redox and antioxidant system at different stages of fruit ripening, and to demonstrate links between redox protein changes and ripening physiology in order to gain better insight of strawberry fruit ripening at the proteomic level.

MATERIALS AND METHODS

Fruit Materials

Strawberry (*Fragaria* × *ananassa*, Cv. "Honeoye" and "Mira") fruit were planted at the Kentville Research and Development Centre, Agriculture and Agri-Food Canada, Kentville, NS, Canada. Fruit were harvested at three harvest maturities (white, pink, and red). Collection of fruit samples has been previously described (Li et al., 2013). Briefly, fruit maturities were determined by using 14, 18, and 22 days after anthesis, respectively. The experiment was conducted in triplicates with three harvests. For each cultivar and harvest, three blocks of plants were randomly selected, harvested and pooled. Samples were frozen in liquid nitrogen, then ground to a fine powder in using a stainless steel blender followed by a mortar and pestle. Ground tissue were stored at −85°C until used.

Protein Extraction

Protein sample preparation and extraction were previously reported employing a phenol protocol (Zheng et al., 2007). Quantification of protein, tryptic in-solution digestion and desalting were described previously (Zheng et al., 2007).

Protein Digest Fractionation

Protein digest fractionation was performed on a 3100 OFFGEL fractionator equipped with 24-wells (Agilent Technologies, Palo Alto, CA, United States). The detailed procedure and settings were similar to the manufacturer's protocol with minor modifications and were previously reported (Yang et al., 2014).

LC/MS/MS and Data Analysis

Liquid chromatography-mass spectrometry analysis and parameter have been previously described (28 and 29). Briefly, chromatographic separation of peptides was conducted on a nano-flow LC system (Ultimate 3000, Dionex, Sunnyvale, CA, United States). MS analysis was analyzed on a QTRAP 4000 (AB Sciex, Toronto, ON, Canada) on all 24 fractions via OFFGEL. Collected MS/MS data was manually inspected and searched against NCBI *viridiplantae* entries with 903,371 sequences (NIH, Bethesda, MD, United States) and Swiss-Prot database with 515,203 sequences (Sprot version 57.15) on Mascot (Version 2.4, Matrix Science, London, United Kingdom). Peptide ion scores greater than 43 were accepted as identification as with significant hits or extensive homology ($p < 0.05$).

MRM Assays of Selected Proteotypic Peptides of Strawberry Fruit

Similar approaches were taken to select MRM transitions for proteins in relation to redox and antioxidant system as previously reported for volatile and anthocyanin biosynthesis (25 and 26). Briefly, selections of protein sequences for all proteins and isoforms in association with redox and antioxidant systems were performed. Further evaluation of MRM transitions were conducted on the peptides with at least 7 amino acids and without methionine and cysteine. To confirm the identification of proteins, Peptides were blasted against the NCBI database and Uniprot[1]. The selected peptides and proteins for MRM study are provided in **Supplementary Table S1**.

Validation of the MRM assay was conducted on a mass spectrometer (QTRAP 4000, AB Sciex, Toronto, ON, Canada) with MRM mode. When an MRM trace was detected, a full MS2 spectrum was triggered to an acquisition using a threshold of 100 ion counts, which was operated with Q1 and Q3 at unit resolution (0.7 m/z half maximum peak width). Detailed MRM settings and parameters were reported previously (24, 25, and 26). Protein Pilot v1.5.2 and MRMPilot v2.0 (AB Sciex, Toronto, ON, Canada) and Skyline (v2.5)[2] were used to characterize and validate the MRM transitions (25 and 26).

Two synthesized peptide standards, which were isotopically labeled by incorporating $^{13}C/^{15}N$ on Leu were purchased from Thermo Fisher at concentration of 1.0 nmol μL^{-1}. (Fisher Scientific, Toronto, ON, Canada). Chromatographic behavior and fragmentation spectra of standards were also confirmed by LC-MS/MS analysis. The reference standards were spiked into samples at a final concentration of 125 fmole μL^{-1} to quantify the candidate proteins and isomers. Integration of MRM transitions

[1]http://www.ncbi.nlm.nih.gov/

[2]http://proteome.gs.washington.edu/software/skyline

(peak areas) was performed using MultiQuant (Vison.2.1.1. AB Sciex, Toronto, ON, Canada) and exported for further statistical analysis (25 and 26).

Statistical Analysis

The analysis was completed using a mixed model procedure (ANOVA) in GenStat (16th edition, VSN International, Hemel Hempstead, United Kingdom). The random effects used were harvest with cultivars and maturity used as fixed effects within a randomized block design. All data was tested for normality resulting in a log transformation being used and a significance cut off of $\leq$0.05. The cluster software[3] was applied to the proteomic data. Proteins were clustered according to their expression profile across cultivars and ripeness stages (25 and 26).

RESULTS

Identification of Proteins and Characterization of Peptide Transitions Involved in Antioxidant Defense System in Strawberry Fruit

Identification of Protein

Protein identification in strawberry fruit was conducted on a data set collected previously from OGE with 24 fractions (Yang et al., 2014). Based on the identifications and characterization, 62 proteins and their corresponding peptide transitions in association with antioxidant enzymes were selected for the MRM study. Targeted protein and peptide information is provided in **Supplementary Table S1**.

Evaluation of Peptide Transitions

Only the peptides that were identified and associated with antioxidant enzymes/related proteins were further selected and characterized for the MRM study. MRM transitions were detected and optimized (**Supplementary Table S2**).

In total, we identified 105 strawberry proteins from 24 fractions of OFFGEL as our initial targets for the MRM study. Only peptides with at least four transitions and without any modification were selected and optimized. Ultimately, 73 peptides transitions with optimized CE were established and used for proteins and isoforms related to strawberry antioxidant enzymes. Information on the MRM transitions of peptides, Q_1/Q_3 transitions and proteins are provided in **Supplementary Table S2**. Based on the detection of peptide transitions from all 24 OGE fractions, Some fractions were combined into three groups of fractions (1–5, 9–15, and 19–24).

Quantitative Changes in Proteins Involved in Antioxidant Defense System in Strawberry in Association With Fruit Maturity and Cultivar

Significant changes in abundance of some protein and isomers in association with redox and antioxidant enzymes were found. ANOVA analysis revealed that maturities resulted in significant changes ($p < 0.05$) of 12 proteins and isomers from three groups of combined fractions. In fraction group 1–5, protein abundance of AKR and isomers (gi| 53988164 and gi| 255542314), superoxide dismutase (SOD) (gi| 470102209). two APXs (gi| 5257500 and gi| 189163449), as well as glutathione reductase (GR) (gi| 470121124) increased significantly as fruit ripened from white to red stage (**Figure 1A**). In fraction group 9–15, two AKRs (gi| 62526573 and gi| 63988164) and glutathione transferase (GT) (gi| 476490875) significantly increased. In addition, another AKR isomers (gi| 63988164) was found to increase in fraction group 19–24 (**Figure 1B**).

On the other hand, significantly reduced protein abundance was determined from all fractions (**Figure 2**). Cytosolic ascorbate peroxidise (CAP) (gi| 62910196) decreased significantly in fraction 1–5. Meanwhile, 2-Cys peroxiredoxin (gi| 47027073) and 1-Cys peroxiredoxin (gi| 54306593) decreased significantly in fraction 1–5 and 19–24, respectively in red as compared to white stage (**Figure 2**). In addition, catalase (CAT) (gi| 476490841) decreased in ripe fruit (at red stage) in fraction 1–5 and 19–24, although the decrease of CAT (gi| 476490841) was only significantly in "Mira."

Differences in some proteins and isomers were found between "Mira" and "Honeoye." Abundance of GR (gi| 470121124), AKR (gi| 53988164), monodehydroascorbate reductase (gi| 4760483), peroxiredoxin-2B (gi| 470128097) as well as thioredoxin h (gi| 71534922) was higher in "Honeoye" than in "Mira." However, changes in interaction between cultivar and maturity was not significant.

Hierarchical Cluster Analysis of Differentially Changed Proteins and Isomers

Employing cluster analysis, the dynamics and correlations of the protein abundance profiles from this study are shown (**Figure 3**). In total, there are four clusters that can be demonstrated. The first cluster constitutes only one protein, an AKR and its isoforms that increased significantly in abundance from white to red stage and showed high abundance in red fruit. The second cluster contains 17 proteins and isomers with increasing trends slightly during ripening but showed some difference between the "Mira" and "Honeoye" cultivars. Among them, key proteins such as SOD [Cu-Zn] and glutathione synthase (GST) up-regulated in pink and red fruit as compared to white fruit, especially in "Honeoye." The third cluster includes 16 proteins and isoforms with decreased abundance in both cultivars and with notably decreased abundance only in red ripe fruit. The fourth cluster contains 10 proteins and isomers that decreased significantly during ripening. This cluster includes CAT, APX, 1-cys peroxiredoxin (1-Cys PRX), 2-cys peroxiredoxin (2-Cys PRX), nucleoside diphosphate kinase 1, ascorbate oxidase and dehydroascorbate reductase, which decreased in both cultivars. Analysis of these proteins demonstrated dynamic changes and correlation of antioxidant enzymes to different fruit ripening stages.

[3]http://biit.cs.ut.ee/clustvis/

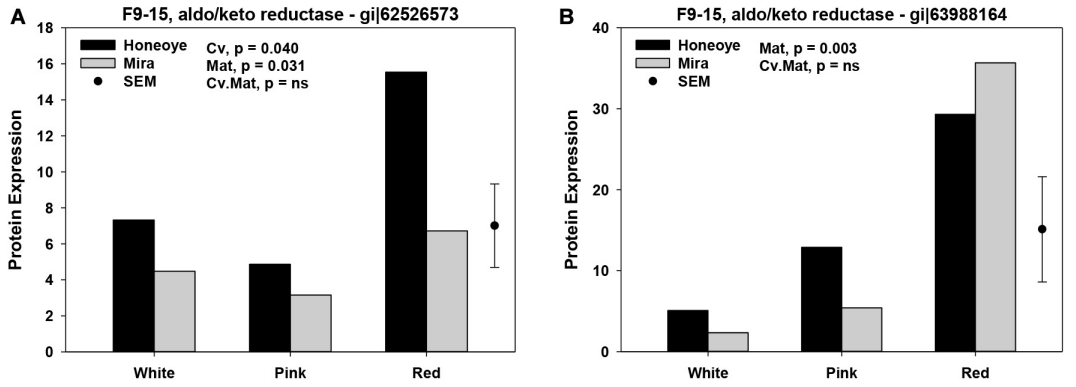

FIGURE 1 | Significantly increased proteins and isomers in association with antioxidant enzymes of strawberry fruit at three ripening stages. Protein expression was calculated based on the intensity of MRM transitions of protein and weighed average from corresponding peptides. **(A)** Significant increased abundance of protein and isomers in fractions 1–5; **(B)** Significant increased abundance of protein and isomers in fractions 9–15 and 19–24. The random effects used were harvest with cultivars (Cv) and maturity (Mat.) as fixed effects. SEM: standard error of mean.

DISCUSSION

Eating quality plays an important role in fruit and vegetable and is comprised of major characteristics including appearance, texture, color, flavor and nutritional components. Despite for the development of technologies to maintain and improve the quality, fundamental research is necessary to reveal regulating mechanism of quality of fruits and vegetables at gene, protein and metabolite levels. Strawberry fruit undergo many significant physiological changes during maturation that drive color formation (through anthocyanin biosynthesis), softening, sugar accumulation, acid loss, and flavor volatile production. Despite the various genes that have been identified related to fruit ripening in strawberries, many of the biosynthetic pathways associated with fruit quality are not fully understood. Although strawberry fruit are considered to be non-climacteric, it showed a different pattern of hormones changes as other non-climacteric fruit such as grape during ripening. Therefore, it is proposed that there may be no consistent hormone changes for non-climacteric fruit due to the variation of fruit structure and phylogenetic relationships (Symons et al., 2012). Strawberry fruit behave differently from climacteric fruit in terms of ACO gene expression and response to auxin treatment (Symons et al., 2012). Therefore, fundamental metabolomic investigations into the role of factors other than ethylene production or reception are needed to increase our understanding of strawberry fruit ripening (Wang et al., 2017).

It has been proposed that fruit ripening is associated with metabolites of antioxidants that respond to or process ROS (Jimenez et al., 2002). Molecular and genomic investigations have also been conducted on redox and antioxidant enzymes including CAT, APX, GST, GR, and peroxidase that respond to ROS and play a role in stress in strawberry fruit (Aharoni et al., 2002). Reduced accumulation of ROS levels was observed in tomato fruit of the ripening mutants *rin*, *nor*, and *Nr* compared to the wild type fruit, as well as down regulation of CATs and CuZnSOD. Gene expression in association with maintaining cellular redox state was found which provided additional evidence for the involvement of ROS in tomato ripening and senescence (Kumar et al., 2016). Most prior research has focused on the measurement of enzyme activity and gene expression. A few proteomic studies employing a gel-based approach and labeling analysis reported some quantitative changes in proteins and isomers in relation to redox and antioxidant system in strawberry fruit (17 and 18). To our knowledge, there has been no targeted quantitative analysis at the protein or isomer level to comprehensively investigate quantitative changes in all enzymes and isomers due to technical limitations.

Multiple reaction monitoring technologies offers significant advantages in good sensitivity and accurate quantification of proteins/peptides in a biological sample (Rödiger and Baginsky, 2018). Based on the results from LC/MS proteomic analysis, MRM assays can be characterized and established for a set of peptides that can be monitored and quantify protein changes in certain metabolic pathways. Protein abundance changed in association with increased volatile production, color formation (biosynthesis of anthocyanins) and other fruit maturity indicators as previously reported (Song et al., 2015a,b). Recently, MRM techniques have been employed to quantify ethylene receptors (CTR and EIN2) during tomato fruit ripening (Mata et al., 2018).

Fruit at harvested at different maturities showed significant differences in quality indices (Li et al., 2013). Significant increase of soluble solids content (SSC) increased to 7.6 and 8.6% in "Honeoye" and "Mira," respectively was found. Meanwhile, decrease of titratable acidity (TA) by 50% in red fruit was reported. Total anthocyanin content, representing cyanidin-3-glucoside or pelargonidin-3-glucoside, increase 200–300% in red as compared to white fruit (Li et al., 2013).

In the present study, we investigated the quantitative changes in redox and antioxidant system proteins during strawberry fruit ripening. We found that AKR and its isomers increased significantly during fruit ripening, with similar trends found in SOD, APXs, GR, and GSTs as fruit ripened from white to red.

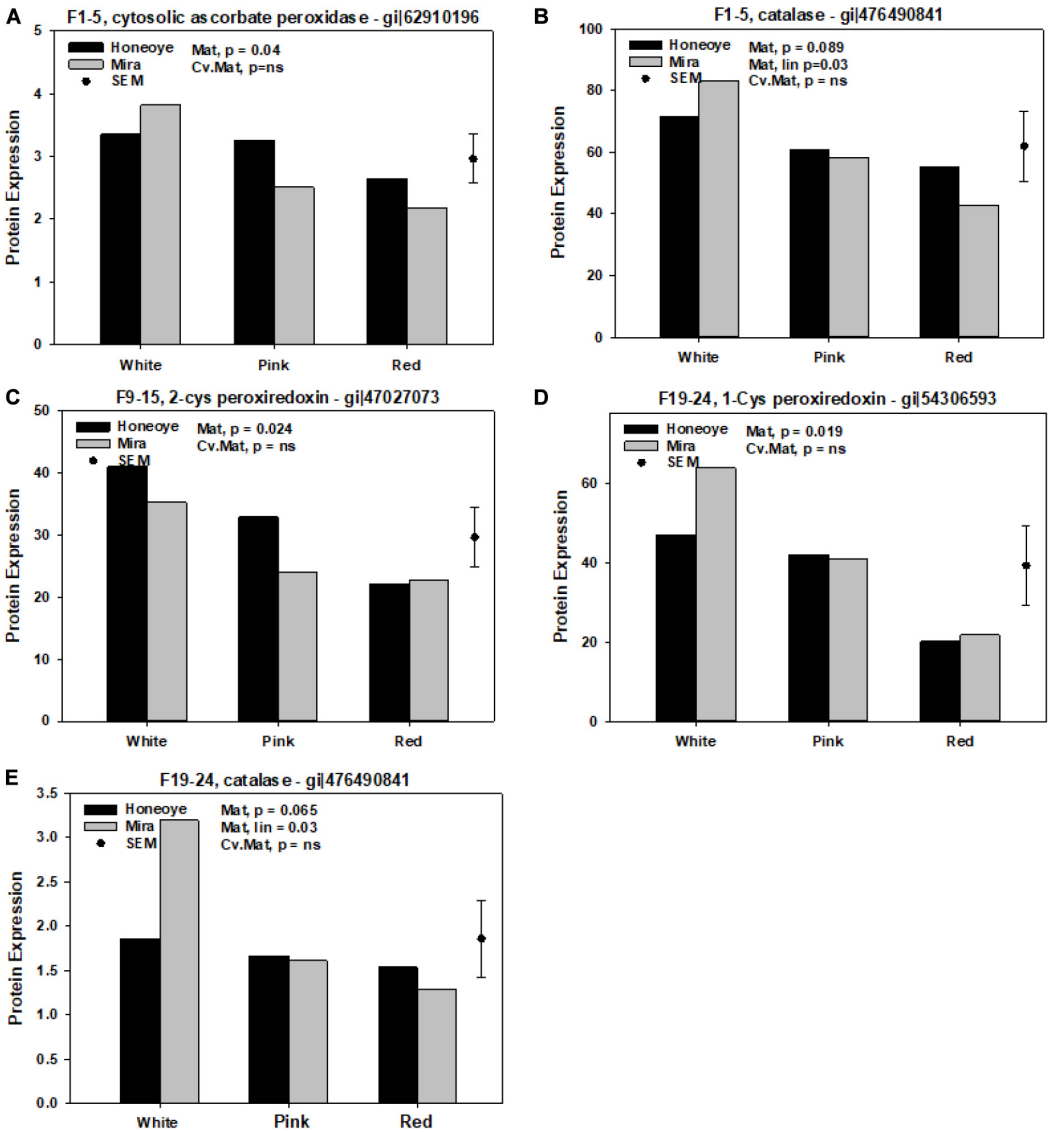

FIGURE 2 | Significantly decreased proteins and isomers in association with antioxidant enzymes of strawberry fruit at different ripening stages. Protein expression was calculated based on the intensity of MRM transitions of protein and weighed average from corresponding peptides. The random effects were harvest with cultivars (Cv.) and maturity (Mat.) used as fixed effects. **(A,B)** Significantly decreased abundance of protein and isomers in fractions 1–5. **(C)** Significantly decreased abundance of protein and isomers in fractions 9–15. **(D,E)** 19–24. SEM: standard error of mean.

In contrast, we observed a significant decrease in abundance of cytosolic APX, 1-Cys and 2-Cys PRX and CAT.

The AKRs belong to the superfamily of NADP (H) dependent oxidoreductases, comprised of a large number of primarily monomeric proteins. Some major and important functional roles of AKRs in plants has been summarized as reactive aldehyde detoxification, biosynthesis of osmolytes, secondary metabolism and membrane transport (Sengupta et al., 2015). In addition, AKRs have functions as biotic and abiotic stress defense and production of commercially important secondary metabolites in plants (Suekawa et al., 2016; Vemanna et al., 2017). In strawberry, an AKR isozyme was classified as AKR4B and was reported to be involved in an increase of ascorbic acid during fruit ripening and linked with remobolizing hydrolytic pectin compounds (Agius et al., 2002). In tomato fruit, gene expression of AKR 4B was detected in senescent leaves and ripening fruit. It did not correlate with L-ascorbate content, but was induced by hydrogen peroxide (H_2O_2), NaCl, and plant hormones such as salicylic acid and jasmonic acid, suggesting AKR is involved in stress response. In addition, it was determined that the promoter region of SlAKR4B contains *cis*-elements for abiotic stress induced response (Sengupta et al., 2015). At this point, it is very difficult to explain the exact role of AKR in strawberry fruit ripening, however, the significant increase of AKRs in association with ripening is clearly evident in this study. This reflects the complex nature of fruit development and the participation of AKRs in this

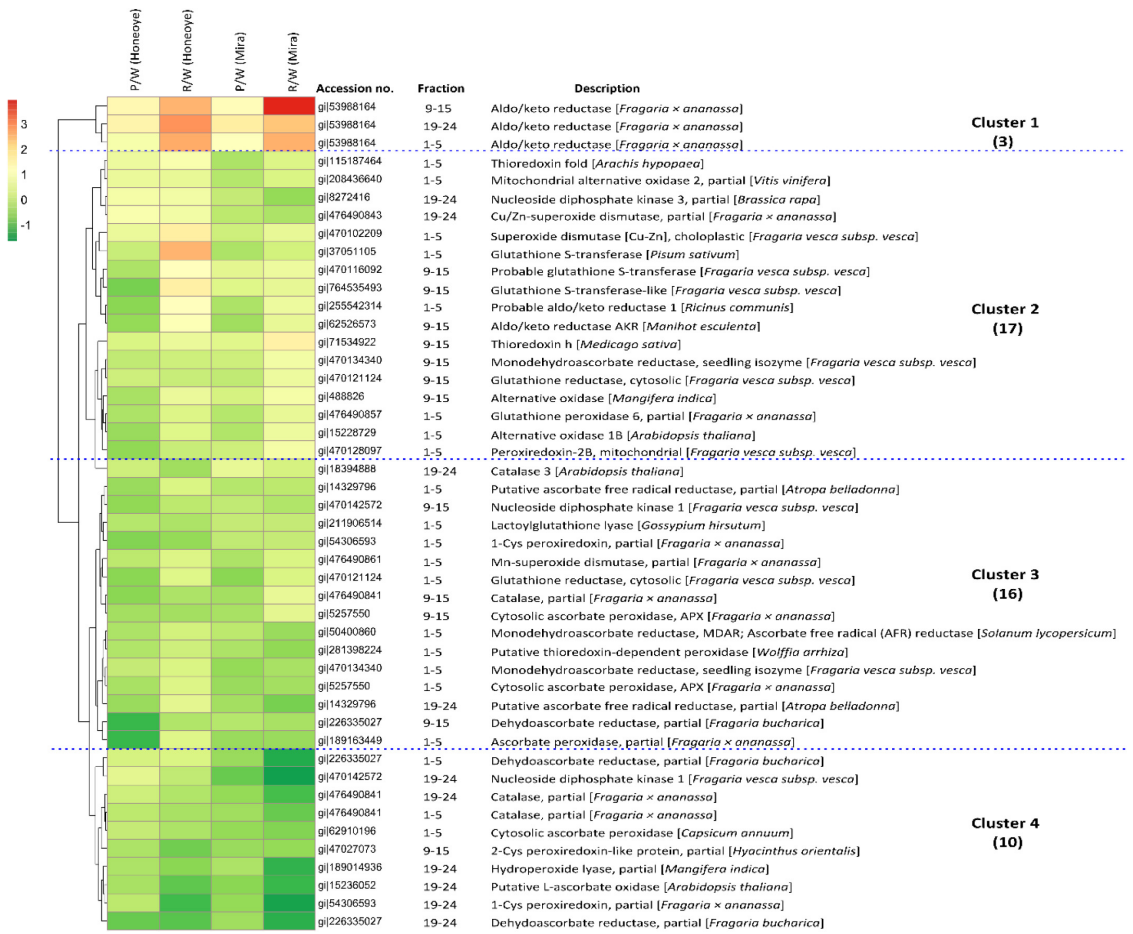

FIGURE 3 | Hierarchical cluster analysis of 46 proteins and isoforms involved in antioxidant and redox enzymes in strawberry fruit ("Honeoye" and "Mira") at three different maturities. The ratio between pink/white and red/white was calculated as log2 fold changes. Four major clusters of protein changes were demonstrated: Cluster 1: increased proteins and isomers in both "Honeoye" and "Mira" in both pink and red fruit; Cluster 2: differently changed proteins and isomers between "Honeoye" and "Mira." Cluster 3: decreased protein and isomers differently in "Honeoye" and "Mira" in pink and red fruit; Cluster 4: decrease protein and isomers in both "Honeoye" and "Mira" in both pink and red fruit. Increasing intensities of red or green color represents differentially increase and decrease abundance of protein and isomers as compared with the control at white stage, respectively.

process, which may involve stress response, hormone interaction and/or substrate metabolism. In addition, key enzymes such as SOD [Cu-Zn] and GST were also found to up-regulate in pink and red fruit compared to white fruit, especially in the cultivar "Honeoye." In general, plant stress is characterized by an increase of reactive oxygen species (ROS) that are harmful to plants, requiring an efficient ROS scavenging system to maintain redox system balance. Antioxidant enzymes such as SOD, APX, and GR are among the dominant H_2O_2 scavengers in chloroplasts and mitochondria (Foyer et al., 2020). Gene expression during grape berry ripening showed an increase of a Cu/ZnSOD and a MnSOD among the 12 investigated SODs (Guo et al., 2020). SOD has been reported to increase in apple fruit during ripening (Zheng et al., 2007). While in another study on apples, SOD activity in both pulp and peel increased and later decreased, which coincided with the change of respiration rate and H_2O_2 content (Lv et al., 2020), indicating that ethylene may play a role in the regulation of gene expression of SOD in apples.

In addition, APX was reported to increase during ripening of strawberry fruit (Pandey and Mann, 2004). The increase of APX was confirmed in this study. Two GSTs were also found to increase during fruit ripening (**Figure 1**). GSTs belong to a super family of proteins encoded by a large gene family (Mhamdi et al., 2010). GSTs have been reported to respond to a wide range of biotic stresses and function to detoxify toxic substances, respond to stress and pathogen attack, and attenuate oxidative stress (Foyer et al., 2020). There is also a tight link between GSTs and plant defense hormones. GSTs response to auxins and played a role in plant secondary metabolism of such as anthocyanins and cinnamic acid (Marrs, 1996). GST was repressed by auxin and identified as one of the ripening regulated genes during strawberry fruit ripening (Aharoni et al., 2002).

Enzymes such as CAT and peroxidase also have a role in removing H_2O_2 and free radicals. A significant decrease of CAT and isomers 1-Cys and 2-Cys PRX was found in this study. CAT is a ubiquitous oxidoreductase in plant peroxisomes

that decomposes H_2O_2 to water and molecular oxygen and removes toxic peroxides during photorespiration (Foyer et al., 2020). Environmental stress can reduce the activity of CATs under conditions such as chilling, drought and hypoxia (Mhamdi et al., 2010). Decrease of *CAT2* gene expression in *Arabidopsis* plants after flowering was shown, suggesting an integral part in H_2O_2 triggered leaf senescence (Zimmermann et al., 2006). Reduction in CAT activity under stress conditions has been attributed to the inactivation of enzymes due to ROS (Lv et al., 2020). Measuring the activities of CAT, SOD and peroxidase in "Chandler" strawberry fruit during development and fruit ripening reported that activity of CAT increased, while SOD and peroxidase decreased from white to red ripe fruit (López et al., 2010). A decline in abundance of CAT under the present study may suggest a reduced capacity in removal of H_2O_2 and toxic peroxides which may resulted in an increase in the free radical initiation of lipid peroxidation with fruit ripening. In the CAT deficient lines of *Arabidopsis* plants, GSTs were induced (Lv et al., 2020). This relationship between CAT and GSTs is confirmed in this study and may reflect a simple association with the loss of chloroplast function as the fruit ripen from white to red. However, more biochemical evidence is required to reveal the dynamic changes in CAT and its interaction with other antioxidant enzymes.

Peroxiredoxins (Cys-PRXs) are important plant specific peroxide detoxifying enzymes whose roles include acting as peroxidases, chaperones, transmitters of redox signal and degradation of H_2O_2. Of the two Cys-PRX identified, 1-Cys-PRX is found in the cytosol, while 2-Cys-PRX is found in the chloroplast (Dietz et al., 2006). The 2-Cys PRX seems to serve an unique function in photosynthesis and many metabolic pathways in chloroplast (Koenig et al., 2002). Research strongly supports that PRX plays an important role to the detoxification of Mehler-derived H_2O_2 in the chloroplast through mediated peroxide reduction and as an alternative to APX. Its role in ROS detoxification network in chloroplast should also be considered (Dietz et al., 2006). Research indicates that Cys PRX related post-translational modifications (PTMs) are also essential regulators of plant stress signaling and ROS (Foyer et al., 2020). In the present study, both Cys-PRXs isomers decreased significantly during strawberry fruit ripening, which agrees with the theory that Cys-PRX content is negatively related to fruit ripening (Li et al., 2013). The decrease in Cys-PRXs may be also linked with the decrease of CAT, simply due to the metabolic activities shifting away from photosynthetic activity as the fruit turns from white to pink to red. Significantly higher amounts of L-ascorbic acid, with higher transcriptional activation of the L-galactose pathway, were identified in green (immature) achenes compared to red fruit (Aragüez et al., 2013). However, considering the possibility of signal transduction of ROS and PRX (Nikkanen et al., 2016), it is also possible that the significant changes in redox and antioxidant activities not only maintain the ROS homeostasis of the fruit cell, but also contribute to signal transduction involving fruit ripening. Further research is required to investigate the complex regulatory network of antioxidant enzymes involved in non-climacteric fruit with low ethylene production during fruit ripening and senescence.

CONCLUSION AND FUTURE PERSPECTIVES

Significant research has been conducted on antioxidant capacity and phenolic compounds in strawberry during ripening, but little is known about the changes in redox and antioxidant enzymes. Despite intensive efforts using molecular biology tools in the past, it has been a challenge to fully understand the molecular mechanisms controlling fruit ripening. To explore the possible biological effects of the antioxidant enzyme system in strawberry fruit, a targeted quantitative proteomics approach employing LC-MS analysis and MRM was conducted. This study reveals significant quantitative changes of antioxidant enzymes (redox) in ripening strawberry fruit. This targeted approach, which used MRM on multi-targeted proteins, allowed us to investigate the multiple proteins and isomers simultaneously and provides direct quantitative evidence of the dynamic changes in these enzymes during fruit ripening. The results support previous reports that had lacked quantitative proteomics, as well as provide novel insight through quantitative proteomic evidence on the control of the antioxidant (redox) pathway that occur during strawberry fruit ripening.

DATA AVAILABILITY STATEMENT

The data presented in the study in the PASSEL (www.peptideatlas.org/passel/) repository accession number PASS01641.

AUTHOR CONTRIBUTIONS

JS conceived, designed, and supervised the study. LC conducted the experiment and collected the data. LC, MV-T, SF, and HL conducted the data analysis and interpretation. JS wrote the manuscript with input from CF and ZZ. All authors read and approved the final manuscript.

FUNDING

This project was funded by the A-Base Research (RBPI 197) of Agriculture and Agri-Food Canada.

ACKNOWLEDGMENTS

We would like to thank the MOE and AAFC for the Ph.D. fellowships provided to HL. Lina Du, at the South China Agriculture University for partially data analysis. We would also like to thank the reviewers and editor for their constructive comments and suggestions.

SUPPLEMENTARY MATERIAL

The Supplementary Material for this article can be found online at: https://www.frontiersin.org/articles/10.3389/fpls.2020.594156/full#supplementary-material

REFERENCES

Agius, F., González-Lamothe, R., Caballero, J. L., Muñoz-Blanco, J., Botella, M. A., and Valpuesta, V. (2002). Engineering increased vitamin C levels in plants by overexpression of a D-galacturonic acid reductase. *Nat. Biotechnol.* 21, 177–181. doi: 10.1038/nbt777

Aharoni, A., Keizer, L. C. P., Van den Broeck, H. C., Blanco-Portales, R., Muñoz-Blanco, J., Bois, G., et al. (2002). Novel insight into vascular, stress, and auxin-dependent and -independent gene expression programs in strawberry, a non-climacteric fruit. *Plant Physiol.* 129, 1019–1031. doi: 10.1104/pp.003558

Aragüez, I., Cruz-Rus, E., Botella, M. Á, Medina-Escobar, N., and Valpuesta, V. (2013). Proteomic analysis of strawberry achenes reveals active synthesis and recycling of l-ascorbic acid. *J. Proteom.* 83, 160–179. doi: 10.1016/j.jprot.2013.03.016

Bianco, L., Lopez, L., Scalone, A. G., Di Carli, M., Desiderio, A., Benvenuto, E., et al. (2009). Strawberry proteome characterization and its regulation during fruit ripening and in different genotypes. *J. Proteom.* 72, 586–607. doi: 10.1016/j.jprot.2008.11.019

Carbone, F., Preuss, A., De Vos, R. C. H., D'Amico, E., Perrotta, G., Bovy, A. G., et al. (2009). Developmental, genetic and environmental factors affect the expression of flavonoid genes, enzymes and metabolites in strawberry fruits. *Plant Cell Environ.* 32, 1117–1131. doi: 10.1111/j.1365-3040.2009.01994.x

Decros, G., Baldet, P., Beauvoit, B., Stevens, R., Flandin, A., Colombié, S., et al. (2019). Get the balance right: ROS homeostasis and redox signalling in fruit. *Front. Plant Sci.* 10:1091. doi: 10.3389/fpls.2019.01091

Dietz, K.-J., Jacob, S., Oelze, M.-L., Laxa, M., Tognetti, V., Nunes de Miranda, S. M., et al. (2006). The function of peroxiredoxins in plant organelle redox metabolism. *J. Exp. Bot.* 57, 1697–1709. doi: 10.1093/jxb/erj160

Fait, A., Hanhineva, K., Beleggia, R., Dai, N., Rogachev, I., Nikiforova, V. J., et al. (2008). Reconfiguration of the achene and receptacle metabolic networks during strawberry fruit development. *Plant Physiol.* 148, 730–750. doi: 10.1104/pp.108.120691

FAOSTAT (2016). *FAOSTAT, Production. Crops. Value of Agriculture Production*. Rome: Food and Agriculture Organization of the United Nations (FAO).

Foyer, C. H., Baker, A., Wright, M., Sparkes, I. A., Mhamdi, A., Schippers, J. H. M., et al. (2020). On the move: redox-dependent protein relocation in plants. *J. Exp. Bot.* 71, 620–631. doi: 10.1093/jxb/erz330

Fridman, E., and Pichersky, E. (2005). Metabolomics, genomics, proteomics, and the identification of enzymes and their substrates and products. *Curr. Opin. Plant Biol.* 8, 242–248. doi: 10.1016/j.pbi.2005.03.004

Griesser, M., Hoffmann, T., Bellido, M. L., Rosati, C., Fink, B., Kurtzer, R., et al. (2008). Redirection of flavonoid biosynthesis through the down-regulation of an anthocyanidin glucosyltransferase in ripening strawberry fruit. *Plant Physiol.* 146, 1528–1539. doi: 10.1104/pp.107.114280

Guo, D., Ji, X., Li, Q., Zhang, G., and Yu, Y. (2020). Genome-wide characterisation of superoxide dismutase genes in grape and their expression analyses during berry development process. *J. Horticult. Sci. Biotechnol.* 95, 53–64. doi: 10.1080/14620316.2019.1647799

Hjernø, K., Alm, R., Canbäck, B., Matthiesen, R., Trajkovski, K., Björk, L., et al. (2006). Down-regulation of the strawberry Bet v 1-homologous allergen in concert with the flavonoid biosynthesis pathway in colorless strawberry mutant. *Proteomics* 6, 1574–1587. doi: 10.1002/pmic.200500469

Jimenez, A., Creissen, G., Kular, B., Firmin, J., Robinson, S., Verhoeyen, M., et al. (2002). Changes in oxidative processes and components of the antioxidant system during tomato fruit ripening. *Planta* 214, 751–758. doi: 10.1007/s004250100667

Kadomura-Ishikawa, Y., Miyawaki, K., Takahashi, A., and Noji, S. (2015). RNAi-mediated silencing and overexpression of the FaMYB1 gene and its effect on anthocyanin accumulation in strawberry fruit. *Biol. Plant.* 59, 677–685. doi: 10.1007/s10535-015-0548-4

Koenig, J., Baier, M., Horling, F., Kahmann, U., Harris, G., Schuermann, P., et al. (2002). The plant-specific function of 2-Cys peroxiredoxinmediated detoxification of peroxides in the redox-hierarchy of photosynthetic electron flux. *Proc. Natl. Acad. Sci. U.S.A.* 99, 5738–5743. doi: 10.1073/pnas.072644999

Kumar, V., Irfan, M., Ghosh, S., Chakraborty, N., Chakraborty, S., and Datta, A. (2016). Fruit ripening mutants reveal cell metabolism and redox state during ripening. *Protoplasma* 253, 581–594. doi: 10.1007/s00709-015-0836-z

Lange, V., Picotti, P., Domon, B., and Aebersold, R. (2008). Selected reaction monitoring for quantitative proteomics: a tutorial. *Mol. Syst. Biol.* 4:422.

Li, L., Song, J., Kalt, W., Forney, C., Tsao, R., Pinto, D., et al. (2013). Quantitative proteomic investigation employing stable isotope labeling by peptide dimethylation on proteins of strawberry fruit at different ripening stages. *J. Proteom.* 94, 219–239. doi: 10.1016/j.jprot.2013.09.004

López, A. P., Gochicoa, M. T. N., and Franco, A. R. (2010). Activities of antioxidant enzymes during strawberry fruit development and ripening. *Biol. Plant.* 54, 349–352. doi: 10.1007/s10535-010-0061-8

Lv, J., Zhang, J., Han, X., Bai, L., Xu, D., Ding, S., et al. (2020). Genome wide identification of superoxide dismutase (SOD) genes and their expression profiles under 1-methylcyclopropene (1-MCP) treatment during ripening of apple fruit. *Sci. Horticult.* 271:109471. doi: 10.1016/j.scienta.2020.109471

Manning, K. (1998). Isolation of a set of ripening-related genes from strawberry: Their identification and possible relationship to fruit quality traits. *Planta* 205, 622–631. doi: 10.1007/s004250050365

Marrs, K. A. (1996). The functions and regulation of glutathione S -transferases in plants. *Annu. Rev. Plant Physiol. Plant Mol. Biol.* 47, 127–158. doi: 10.1146/annurev.arplant.47.1.127

Mata, C. I., Fabre, B., Parsons, H. T., Hertog, M. L. A. T. M., Van Raemdonck, G., Baggerman, G., et al. (2018). Ethylene receptors, CTRS and EIN2 target protein identification and quantification through parallel reaction monitoring during tomato fruit ripening. *Front. Plant Sci.* 871:1626. doi: 10.3389/fpls.2018.01626

Medina-Puche, L., Blanco-Portales, R., Molina-Hidalgo, F. J., Cumplido-Laso, G., García-Caparrós, N., Moyano-Cañete, E., et al. (2016). Extensive transcriptomic studies on the roles played by abscisic acid and auxins in the development and ripening of strawberry fruits. *Funct. Integrat. Genom.* 16, 671–692. doi: 10.1007/s10142-016-0510-3

Mhamdi, A., Queval, G., Chaouch, S., Vanderauwera, S., Van Breusegem, F., and Noctor, G. (2010). Catalase function in plants: a focus on *Arabidopsis* mutants as stress-mimic models. *J. Exp. Bot.* 61, 4197–4220. doi: 10.1093/jxb/erq282

Nam, Y. W., Tichit, L., Leperlier, M., Cuerq, B., Marty, I., and Lelièvre, J. M. (1999). Isolation and characterization of mRNAs differentially expressed during ripening of wild strawberry (*Fragaria vesca* L.) fruits. *Plant Mol. Biol.* 39, 629–636.

Nikkanen, L., Toivola, J., and Rintamäki, E. (2016). Crosstalk between chloroplast thioredoxin systems in regulation of photosynthesis. *Plant Cell Environ.* 39, 1691–1705. doi: 10.1111/pce.12718

Palma, J. M., Corpas, F. J., and del Río, L. A. (2011). Proteomics as an approach to the understanding of the molecular physiology of fruit development and ripening. *J. Proteom.* 74, 1230–1243. doi: 10.1016/j.jprot.2011.04.010

Pandey, A., and Mann, M. (2004). Proteomic to study genes and genomes. *Nature* 405, 837–846.

Pedreschi, R., Vanstreels, E., Carpentier, S., Hertog, M., Lammertyn, J., Robben, J., et al. (2007). Proteomic analysis of core breakdown disorder in Conference pears (*Pyrus communis* L.). *Proteomics* 7, 2083–2099. doi: 10.1002/pmic.200600723

Qin, G., Wang, Q., Liu, J., Li, B., and Tian, S. (2009). Proteomic analysis of changes in mitochondrial protein expression during fruit senescence. *Proteomics* 9, 4241–4253. doi: 10.1002/pmic.200900133

Redondo-Nevado, J., Moyano, E., Medina-Escobar, N., Caballero, J. L., and Muñoz-Blanco, J. (2001). A fruit specific and developmentally regulated endopolygalacturonase gene from strawberry (*Fragaria x ananassa* cv. Chandler). *J. Exp. Bot.* 52, 1941–1945. doi: 10.1093/jexbot/52.362.1941

Rödiger, A., and Baginsky, S. (2018). Tailored use of targeted proteomics in plant-specific applications. *Front. Plant Sci.* 9:1204. doi: 10.3389/fpls.2018.01204

Sengupta, D., Naik, D., and Reddy, A. R. (2015). Plant aldo-keto reductases (AKRs) as multi-tasking soldiers involved in diverse plant metabolic processes and stress defense: a structure-function update. *J. Plant Physiol.* 179, 40–55. doi: 10.1016/j.jplph.2015.03.004

Song, J., Du, L., Li, L., Kalt, W., Palmer, L. C., Fillmore, S., et al. (2015a). Quantitative changes in proteins responsible for flavonoid and anthocyanin biosynthesis in strawberry fruit at different ripening stages: a targeted quantitative proteomic investigation employing multiple reaction monitoring. *J. Proteom.* 122, 1–10. doi: 10.1016/j.jprot.2015.03.017

Song, J., Du, L., Li, L., Palmer, L. C., Forney, C. F., Fillmore, S., et al. (2015b). Targeted quantitative proteomic investigation employing multiple

reaction monitoring on quantitative changes in proteins that regulate volatile biosynthesis of strawberry fruit at different ripening stages. *J. Proteom.* 126, 288–295. doi: 10.1016/j.jprot.2015.06.004

Suekawa, M., Fujikawa, Y., Inada, S., Murano, A., and Esaka, M. (2016). Gene expression and promoter analysis of a novel tomato aldo-keto reductase in response to environmental stresses. *J. Plant Physiol.* 200, 35–44. doi: 10.1016/j.jplph.2016.05.015

Symons, G. M., Chua, Y. J., Ross, J. J., Quittenden, L. J., Davies, N. W., and Reid, J. B. (2012). Hormonal changes during non-climacteric ripening in strawberry. *J. Exp. Bot.* 63, 4741–4750. doi: 10.1093/jxb/ers147

Trainotti, L., Pavanello, A., and Casadoro, G. (2005). Different ethylene receptors show an increased expression during the ripening of strawberries: does such an increment imply a role for ethylene in the ripening of these non-climacteric fruits? *J. Exp. Bot.* 56, 2037–2046. doi: 10.1093/jxb/eri202

Van de Poel, B., Vandendriessche, T., Hertog, M. L. A. T. M., Nicolai, B. M., and Geeraerd, A. (2014). Detached ripening of non-climacteric strawberry impairs aroma profile and fruit quality. *Postharvest Biol. Technol.* 95, 70–80. doi: 10.1016/j.postharvbio.2014.04.012

Vemanna, R. S., Babitha, K. C., Solanki, J. K., Amarnatha Reddy, V., Sarangi, S. K., and Udayakumar, M. (2017). Aldo-keto reductase-1 (AKR1) protect cellular enzymes from salt stress by detoxifying reactive cytotoxic compounds. *Plant Physiol. Biochem.* 113, 177–186. doi: 10.1016/j.plaphy.2017.02.012

Villarreal, N. M., Rosli, H. G., Martínez, G. A., and Civello, P. M. (2008). Polygalacturonase activity and expression of related genes during ripening of strawberry cultivars with contrasting fruit firmness. *Postharvest Biol. Technol.* 47, 141–150. doi: 10.1016/j.postharvbio.2007.06.011

Wang, Q. H., Zhao, C., Zhang, M., Li, Y. Z., Shen, Y. Y., and Guo, J. X. (2017). Transcriptome analysis around the onset of strawberry fruit ripening uncovers an important role of oxidative phosphorylation in ripening. *Sci. Rep.* 7:41477. doi: 10.1038/srep41477

Yang, X., Li, L., Song, J., Palmer, L. C., Li, X., and Zhang, Z. (2014). Peptide prefractionation is essential for proteomic approaches employing multiple-reaction monitoring of fruit proteomic research. *J. Separat. Sci.* 37, 77–84. doi: 10.1002/jssc.201301041

Zheng, Q., Song, J., Campbell-Palmer, L., Thompson, K., Li, L., Walker, B., et al. (2013). A proteomic investigation of apple fruit during ripening and in response to ethylene treatment. *J. Proteom.* 93, 276–294. doi: 10.1016/j.jprot.2013.02.006

Zheng, Q., Song, J., Doncaster, K., Rowland, E., and Byers, D. M. (2007). Qualitative and quantitative evaluation of protein extraction protocols for apple and strawberry fruit suitable for two-dimensional electrophoresis and mass spectrometry analysis. *J. Agricult. Food Chem.* 55, 1663–1673. doi: 10.1021/jf062850p

Zimmermann, P., Heinlein, C., Orendi, G., and Zentgraf, U. (2006). Sencsence-speccific reguulaiton of catalase in *Arabidopsis thaliana* (L.) *Planr. Cell Environ.* 29, 1049–1056.

Conflict of Interest: The authors declare that the research was conducted in the absence of any commercial or financial relationships that could be construed as a potential conflict of interest.

frontiers in Plant Science

ORIGINAL RESEARCH
published: 02 February 2021
doi: 10.3389/fpls.2021.640601

Differential Tissue-Specific Jasmonic Acid, Salicylic Acid, and Abscisic Acid Dynamics in Sweet Cherry Development and Their Implications in Fruit-Microbe Interactions

David H. Fresno[1,2] *and Sergi Munné-Bosch*[1,2]*

[1]*Department of Evolutionary Biology, Ecology and Environmental Sciences, University of Barcelona, Barcelona, Spain,*
[2]*Institute of Nutrition and Food Safety (INSA), University of Barcelona, Barcelona, Spain*

OPEN ACCESS

Edited by:
Carlos R. Figueroa, University of Talca, Chile

Reviewed by:
Sofia Correia, Centre for the Research and Technology of Agro-Environmental and Biological Sciences (CITAB), Portugal
Asunción Amorós, Miguel Hernandez University, Spain

***Correspondence:**
Sergi Munné-Bosch
smunne@ub.edu

Specialty section:
This article was submitted to Crop and Product Physiology, a section of the journal Frontiers in Plant Science

Received: *11 December 2020*
Accepted: *12 January 2021*
Published: *02 February 2021*

Citation:
Fresno DH and Munné-Bosch S (2021) Differential Tissue-Specific Jasmonic Acid, Salicylic Acid, and Abscisic Acid Dynamics in Sweet Cherry Development and Their Implications in Fruit-Microbe Interactions. Front. Plant Sci. 12:640601. doi: 10.3389/fpls.2021.640601

Sweet cherry is an important non-climacteric fruit with a high commercial interest, but exploitation of sweet cherry trees (*Prunus avium* L.) in orchards is usually subject to important economic losses due to fruit decay by pathogenic fungi and other microorganisms. Sweet cherries development and ripening are characterized by profound physiological changes in the fruit, among which the phytohormone abscisic acid (ABA) plays a pivotal role. In addition, sweet cherries are usually affected by fruit decay pathogens, and the role of other stress-related hormones such as jasmonic acid (JA) and salicylic acid (SA) may also be of paramount importance, not only from a developmental point of view, but also from a fruit-microbe interaction perspective. Here, a tissue-specific hormone quantification by LC-MS/MS, including the contents of JA, SA, and ABA, in the fruit exocarp and mesocarp of sweet cherries during fruit development from trees growing in a commercial orchard was carried out. Additionally, this study was complemented with the characterization of the culturable epiphytic and endophytic microbial communities of sweet cherries at various stages of fruit development and during cracking lesion formation. Our results revealed a completely differential behavior of phytohormones between both tissues (the exocarp and mesocarp), with a more dynamic exocarp in front of a more stable mesocarp, and with marked variations during fruit development. Microbial epiphytic community was mainly composed by yeasts, although rot-causing fungi like *Alternaria* spp. were always also present throughout fruit development. Endophytic colonization was poor, but it increased throughout fruit development. Furthermore, when the exocarp was naturally disrupted in sweet cherries suffering from cracking, the colonization by *Alternaria* spp. markedly increased. Altogether, results suggest that the fruit exocarp and mesocarp are very dynamic tissues in which endogenous phytohormones not only modulate fruit development and ripening but also fruit-microbe interactions.

Keywords: exocarp, jasmonic acid, microbiome, plant-microbe interaction, salicylic acid, *Prunus avium* L.

INTRODUCTION

Sweet cherry (*Prunus avium* L.) is an important stone fruit crop which has recently received increased interest due to both its organoleptic and visual characteristics and high nutritional value (Kelley et al., 2018). Most sweet cherries are marketed globally as a fresh product (Chockchaisawasdee et al., 2016) but they are highly perishable due to different factors, among which microbial decay caused by pre- and post-harvest pathogens is one of the most relevant (Alonso and Alique, 2006). Although necrotrophic filamentous fungi like *Botrytis cinerea* and *Alternaria* spp. are known to be the main pathogens affecting cherry fruits (Habib et al., 2015; Chockchaisawasdee et al., 2016), very little is still known on how endogenous phytohormone contents might influence their decay. Sweet cherry is a non-climacteric fruit, which is characterized, in contrast to climacteric fruits, by a progressive abscisic acid (ABA) accumulation, a lower respiration rate and almost no ethylene release during ripening (Pérez-Llorca et al., 2019). However, although cherry fruits are composed by an outer layer, the exocarp, an edible mesocarp, and a stony endocarp, no studies have focused thus far on better understanding the contribution of these tissues on fruit decay.

Plant-microbe interactions and their underlying mechanisms are increasingly receiving attention in the exploitation of commercial orchards of stone fruity trees because of their economic relevance. In this respect, not only plant pathogens, which are able to colonize the plant inner tissues causing disease to the host (Schlechter et al., 2019), but also epiphytic microorganisms, those that live on the plant surfaces, and endophytes, when they colonize inner tissues without affecting the host's fitness (Takken and Rep, 2010), may play a major role. Furthermore, plant physical barriers, like the cuticle or cell walls in leaves or the exocarp in fruits, as well as the immune responses elicited by endogenous phytohormones, keep microbial communities under control (Schlechter et al., 2019). Indeed, physical barriers and immunity are tightly interconnected, so that when physical barriers fail, immune responses such as pathogen associated molecular pattern (PAMP)- and effector-triggered immunity (PTI and ETI, respectively) take place to halt the microbial invasion (Bigeard et al., 2015; Cui et al., 2015).

Plant immune responses have been extensively studied, and the role of specific phytohormones like salicylic acid (SA), jasmonic acid (JA), ABA, or ethylene has been described in detail in previous studies using model plants (reviewed by Pieterse et al., 2012). In addition, the role of these hormones in physiological processes like ripening of non-climacteric fruits is already well-known (Leng et al., 2014; Tijero et al., 2019). However, it remains unclear how the interactions between these hormones and ripening may affect fruit specific immune responses to pathogens and, eventually, fruit susceptibility to fruit decay, most particularly in fruits of non-model plants. Previous research proved that ABA has a negative effect in tomato resistance to the necrotrophic pathogen *B. cinerea*, and ABA signaling has been shown to antagonize with SA and JA-dependent responses to biotic stress in tomato plants (Asselbergh et al., 2007; Pieterse et al., 2012). However, due to technical limitations and the difficulty of performing studies in commercial orchards, most of this information has been obtained in model plants and using whole fruits. However, plant immune responses take place in a localized manner, and the role of different plant tissues in these responses may be relevant in plant-pathogen interactions. Thus, it is highly relevant to monitor how hormones vary during fruit development at the tissular level to unravel specific responses in the exocarp and mesocarp of fruits.

It is generally known that fruits become more susceptible to pathogen attack at later stages of ripening, although the main molecular and biochemical mechanisms underlying this susceptibility have not been unveiled yet (Forlani et al., 2019). Besides, one of the main physical barriers that protects fruits from pathogens is the exocarp. Fruit cracking is a physiological process in which lesions are produced on the fruit skin and flesh, disrupting the fruit's main physical barrier, leading to severe microbial infections of the fruit (Correia et al., 2018). Thus, finding new ways to protect fruits, and especially sweet cherries from microbial decay is of major importance for fruit production. Previous studies have described the role of different phytohormones during sweet cherry fruit development, ripening, and overripening (Teribia et al., 2016; Tijero et al., 2016), and others have described the microbiome of different fruits (Granado et al., 2008; Zhang et al., 2018). In the present study, we combine these approaches by studying sweet cherries from a commercial orchard on the tree with the aim of unveiling the possible underlying physiological and biochemical causes of fruit decay in sweet cherries during ripening. With this aim, we examined the variations in the endogenous contents of the hormones ABA, SA, and JA at a tissue-specific level (exocarp and mesocarp) throughout fruit development, combined with a microbial analysis of the culturable epiphytic and endophytic populations. As profound physiological changes take place during fruit development, we hypothesized that variations in ABA, SA, and JA contents in different fruit tissues occur, which might have implications on the fruit culturable microbiome. We found that both the exocarp as a physical barrier and the hormone dynamics in specific fruit tissues may influence fruit responses to fruit microbiome and pathogens.

MATERIALS AND METHODS

Experimental Design, Treatments, and Samplings

Sweet cherries (*P. avium* L. var. Prime Giant; rootstock SL-64) were obtained from eight trees (hereafter referred as $n = 8$) located in a commercial sweet cherry orchard at Partida Vall del Sector III (Lleida, Spain). Trees were organized in rows (5 m separation between rows) and all the fruit samples were collected from trees at the same row (with a separation of 3 m between trees). Fruits were harvested at stages of development I, II, and III and at commercial harvest on May 10th, 14th, 21st, and 31st, 2019, respectively, between 9 and 10 AM local time. Fruits were visually characterized, and stages defined as described by Teribia et al. (2016) but with some modifications:

stage I, green fruits; stage II, fruits with green coloration turning to yellow and red; stage III, red-pink color with maximum 30% green; and Harvest, commercial harvest. Fruits were always collected from bunches located in the outer branches of each tree.

For fruit hormone analysis, a pooled sample of six fruits per tree was used as one replicate and a total of eight replicates from different trees were used. Every cherry was quickly cut by half to discard the endocarp, immediately frozen in liquid nitrogen, and stored at −80°C until further processing. For microbial analysis, a pooled sample of three fruits per tree was used as one replicate and a total of eight replicates from different trees were used. Cherries were introduced inside sterile bags, and immediately transported under refrigeration to the lab for further processing.

Finally, for cracking analyses, three sweet cherries suffering from natural cracking were collected at harvest from another tree located at the same row, stored in sterile bags, and transported under refrigeration to the lab until further use.

Microbial Extraction and Isolation

Under sterile conditions, three cherries were gently shaken for 5 min inside a sterile bottle containing a saline solution (NaCl, 9 g/L) to extract the fruit epiphytic microorganisms. Afterward, 10 ml of that solution was collected and stored in sterile falcon tubes at 4°C until further processing. After epiphyte extraction, three measures from each cherry (**Supplementary Figure 1**) were taken to estimate the skin surface (cm^2). Cherries were surface sterilized by immersion in 70% ethanol for 5 min, in 1% sodium hypochlorite for 2 min, and rinsing three times with sterile distilled water. For each sample, 10 ml of the last rinsing water was collected and stored as a sterility control.

For endophyte extraction, after surface sterilization, one half from each cherry was cut and weighed under sterile conditions. Then, they were ground on a sterile mortar containing 10 ml of saline solution using a sterile pestle, and the homogenate was collected and stored in sterile falcon tubes at 4°C until further use. Prior to grinding, both mortar and pestle were washed with 10 ml of sterile distilled water, which were stored and further used as a sterility control.

The falcon tubes containing epiphytes and endophytes, as well as the sterility control tubes, were centrifuged for 15 min at 6000 rpm (Hettich Universal 32R) and the microbial pellet was resuspended in 3 ml of fresh sterile saline solution. For the epiphyte suspension, a 1:10 dilution was done, and 500 µl of it were plated on nutrient agar (NA) and potato dextrose agar (PDA) plates. For the homogenate containing endophytes and the sterility controls, 500 µl of the suspension were directly plated on NA and PDA plates. The plates were incubated at room temperature (22 ± 1°C) and dark conditions for 7 days, when colony forming units (CFU) were scored. Eventually, epiphytic CFU per cm^2 of fruit exocarp, per fruit, or endophytic CFU per gram of fresh mesocarp were calculated. Microbial isolates were tagged as yeast, bacteria, or other fungi. The proportion of every microbial group in each sample was calculated. The most abundant yeast and bacterial isolates were morphologically characterized according to their colony type, colony edge, colony color, and texture (Krishnan et al., 2012). The most frequent fungal isolates were morphologically identified by colony structure and microscopic characteristics.

Tissue-Specific Hormone Analysis

Exocarp and mesocarp from each cherry were separated for a differential hormone analysis of both tissues. The exocarp of every frozen cherry (−80°C) was separated from the mesocarp using a scalpel by scraping the fruit surface. Afterward, both tissues were ground separately using a pestle and a TissueLyser (Qiagen). These processes were always performed using liquid nitrogen to avoid sample defrosting. Plant hormones, including ABA, SA, and JA, were extracted and quantified by LC-MS/MS. Ground exocarp (50 mg) and mesocarp (100 mg) samples were extracted with 250 µl pure methanol and deuterium-labeled internal standards (d6-ABA, d5-JA, and d4-SA) before ultrasonication and vortexing (Branson 2510 ultrasonic cleaner, Bransonic, United States) for 30 min. After centrifugation, the supernatant was collected and the pellet was re-extracted using the same procedure. Both supernatants were merged and filtered through a 0.22 µm PTFE filter (Waters, United States). Hormone levels were analyzed by UHPLC-ESI-MS/MS as described by Müller and Munné-Bosch (2011). The ultrahigh-performance liquid chromatography (Aquity UPLCTM System, Waters Milford, MA, United States) was coupled to a triple quadrupole mass spectrometer (API 3000, PE Sciex, Concord, Ont., Canada). A Kinetex C18 (Phenomenex Inc., United States) column (1,7 µm, 100 × 2.1 mm) was used. Solvent A was water with 0.05% glacial acetic acid and solvent B was acetonitrile with 0.05% glacial acetic acid. Flow rate was set at 0.6 ml/min. Quantification was made considering recovery rates for each sample by using the deuterium-labeled internal standards as described by Müller and Munné-Bosch (2011).

Fruit Cracking Analysis

Three cherries suffering from natural cracking were collected at harvest. Every cherry had the same degree of cracking located on the fruit cheek. Each cherry was divided into three different regions, including the cracking lesion itself, the area around the cracking lesion (zone 1), and the region opposite to the cracking lesion (zone 2). For the isolation of endophytic microorganisms from cracked cherries, fruits were surface sterilized by immersion in 70% ethanol for 5 min, in 1% sodium hypochlorite for 2 min, and rinsed three times with sterile distilled water. Five-hundred microliter of the last rinsing water was plated on PDA plates to certify complete surface disinfection. For each cherry, using a sterile scalpel, approximately 25 mesocarp pieces (0.5 × 0.5 cm) from zone 1 and zone 2 were cut and plated on PDA plates. Plates were incubated at room temperature (22°C) and dark conditions for 7 days, and microbial outgrowth from the pieces was scored. Microbial isolates were morphologically characterized (Krishnan et al., 2012) and, if possible, identified. For *Alternaria* spp. colonization percentage calculation, for each zone, the number of pieces showing pathogen outgrowth was divided by the total number of mesocarp pieces plated.

Antagonistic Activity of Endophytic Isolates Against *Botrytis cinerea*

The "killer stroke" method was performed as described before (Pretscher et al., 2018). In brief, microbial isolates showing an endophytic behavior in healthy or cracked cherries were streaked in the centre of PDA plates and incubated for 4 days at 22°C. *Botrytis cinerea* plugs from a well-grown PDA plate were placed 2–3 cm away on both sides of the streak. Plates were incubated at 22°C for 7 days, and fungal growth was monitored daily to observe *B. cinerea* growth inhibition.

Statistical Analysis

A linear regression model was performed to predict the cherry skin surface out from three specific measures (**Supplementary Figure 1**): (a) fruit width, (b) fruit height from the apex to the base of the peduncle, and (c) width at the top of the fruit. After measuring (a), (b), and (c) on 24 cherries at stages III and harvest, the skin from these fruits was scanned and its area (cm^2) was quantified using ImageJ. A linear regression model was performed, showing the following model to predict fruit skin area: area (cm^2) = −33.6695 − 0.3837(b) + 20.064(c). The (a) variable was discarded during the analysis due to multicollinearity.

To estimate the effect of "Stage of Development" in epiphytic populations and epiphytic composition, mean values were tested by one-way ANOVA and *post-hoc* Tukey honestly significant difference (HSD) test to determine statistical differences. To determine the effect of "Stage of development" in endophytic colonization, a non-parametric Kruskal Wallis test was performed, followed by a *post-hoc* Fisher least significant difference test. To analyze differences in *Alternaria* spp. colonization rate between zones in cracked cherries, a non-parametric Kruskal Wallis test was performed. Finally, to determine the effect of "Stage of development" and "Fruit tissue" in endogenous ABA, SA, and JA contents, mean values were tested by two-way ANOVA followed by *post-hoc* Tuckey HSD. In addition, Spearman's rank correlation analyses were performed between hormone levels at different tissues and endophyte CFU/gFW. For ANOVA analyses, data were $\log_{10}$ or square root transformed to accomplish normal distribution and homogeneity of variance, if needed. In all cases, differences were considered significant at a probability level $p < 0.05$. All statistical tests were performed with RStudio.

RESULTS

Tissue-Specific Hormone Contents Vary Depending on the Stage of Development

Endogenous contents of JA, SA, and ABA differed between the exocarp and mesocarp at different stages of development (**Figure 1**). A clear differential behavior in both JA and SA contents was observed in the exocarp in comparison to the mesocarp. A significant effect of the "Stage of development" and "Tissue" was observed in the endogenous contents of both JA and SA, although the interaction of both factors was not significant.

In the case of JA, an increase in JA contents was observed at initial steps of fruit development in the exocarp, specially between stages I and II, contents remaining stable afterward until harvest. On the contrary, in the mesocarp, JA contents did not significantly vary all through fruit development (**Figure 1**).

Regarding SA, there was a significant drop in the SA content in the exocarp at the beginning of fruit development, from stage I to II. Afterward, SA content remained relatively constant until harvest. No differences in SA levels, however, were reported in the mesocarp, where endogenous SA barely decreased throughout development. Furthermore, SA differentially accumulated in the exocarp, showing higher levels than in the mesocarp both at the beginning of fruit development (stage I) and at harvest (**Figure 1**).

In contrast to JA and SA contents, ABA levels gradually increased during fruit development regardless the fruit tissue, showing a similar accumulation both in the exocarp than in the mesocarp during fruit development and ripening (**Figure 1**).

Spearman's rank correlation analyses revealed interactions between different hormone levels. A strong significant positive correlation was observed between ABA levels in the exocarp and in the mesocarp. In addition, ABA levels in the exocarp were also correlated with other hormones, like JA (positively) and SA (negatively), not only in the exocarp but also, although to a lesser extent, in the mesocarp (**Table 1**).

Culturable Epiphytic Community Remained Stable Through Fruit Development

Microbial load per cm^2 of cherry skin remained stable throughout fruit development, from the beginning of development until commercial harvest time. However, the total amount of epiphytic microorganisms per fruit significantly increased during fruit development (**Figure 2A**).

To have a deeper insight into the composition of culturable epiphytic microorganisms on sweet cherry surfaces, epiphytes were categorized into three different microbial groups: yeasts, bacteria, and other fungi. Stage of development did not significantly affect proportion of microbial groups. Despite being some variability between samples, yeast was clearly the most abundant microbial group during fruit development, as 70–80% of total epiphytes belonged to this group. Other fungi and bacteria proportions varied from 7 to 16 and 0 to 20%, respectively (**Figure 2B**).

Presence of Microbial Isolates, Including Fruit Rot-Causing Fungi, on the Fruit Surface

Different yeast, bacterial, and other fungi isolates were observed during cherry development. Those microbial isolates that were found in a recurrent manner, at several stages of development, were selected, morphologically characterized and, if possible, identified according to morphological criteria. Two yeast isolates (Ep-1 and Ep-2) and one bacterial isolate (Ep-4) were repeatedly obtained from fruit surface throughout development (**Supplementary Table 1**). Other yeast and bacterial isolates

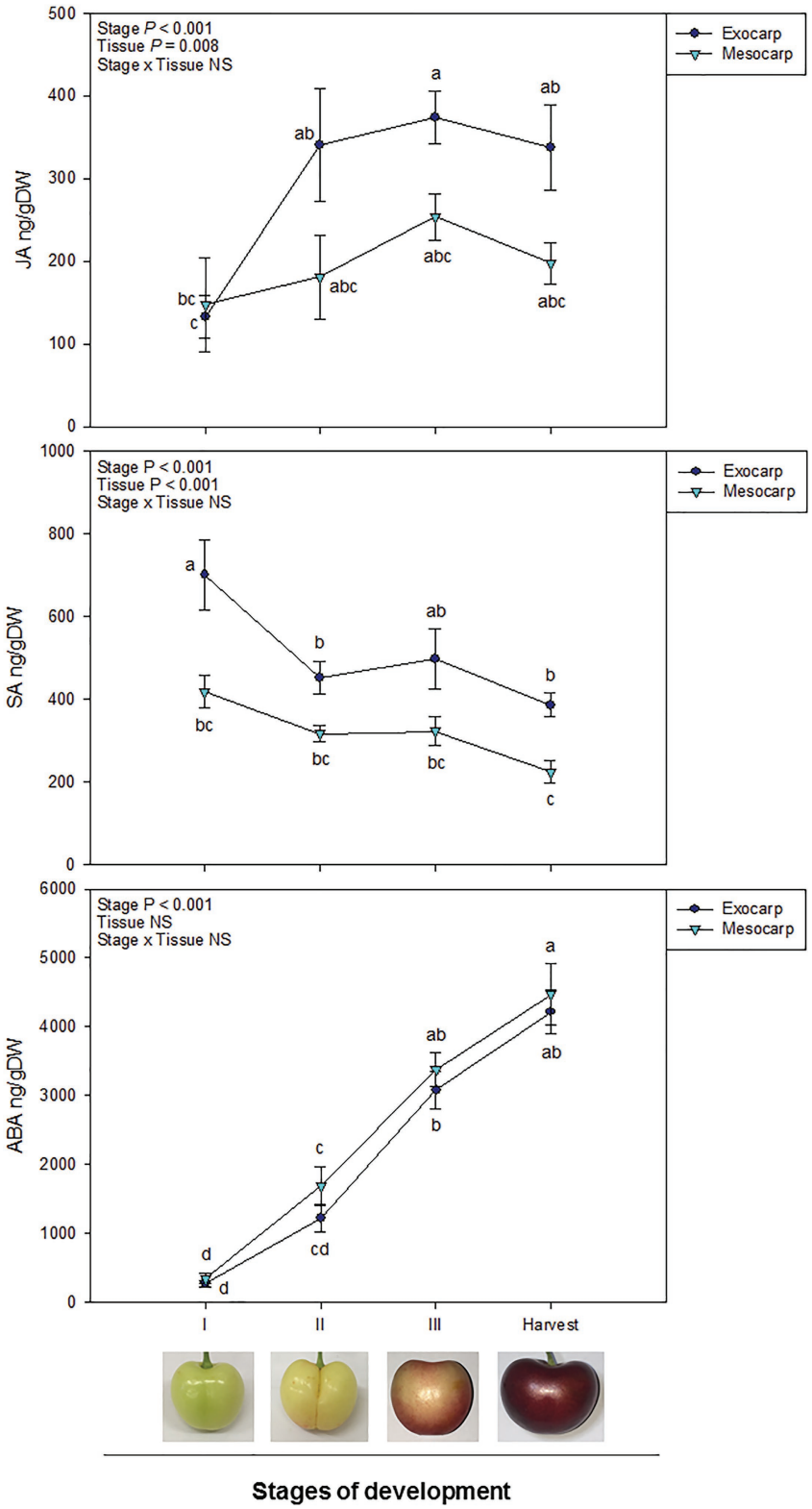

FIGURE 1 | Endogenous contents of jasmonic acid (JA), salicylic acid (SA), and abscisic acid (ABA) in the exocarp and mesocarp of sweet cherries during different stages of natural fruit development in trees from a commercial orchard. Data are means ± SE of $n = 8$. Statistical comparisons were performed by two-way ANOVA, followed by a *post-hoc* Tukey honestly significant difference (HSD) test. Different letters indicate significant differences between stages of development and tissues ($p < 0.05$).

TABLE 1 | Spearman correlation analysis between exocarp and mesocarp hormone levels and endophytic colony forming units (CFU) per gram of fresh weight.

	ABA-meso	SA-exo	SA-meso	JA-exo	JA-meso	CFU/gFW
ABA-exo	0.848***	−0.390*	−0.482**	0.566***	0.386*	0.430*
ABA-meso		−0.393*	−0.534**	0.456**	0.337	0.481**
SA-exo			0.231	−0.266	−0.227	−0.348
SA-meso				−0.198	−0.163	−0.271
JA-exo					0.624***	0.234
JA-meso						0.174

*Rho values are represented, and significant correlations are marked by asterisks (*represents $p < 0.05$; **represents $p < 0.01$; and ***represents $p < 0.001$). ABA, abscisic acid; SA, salicylic acid; JA, jasmonic acid; CFU/gFW, endophytic colony forming units per gram of mesocarp fresh weight.*

were found as well at specific points of the experiment, but, as they were occasional observations, they were not quantified. Identification by morphological characteristics could not be carried out. In the case of other fungi, several isolates were obtained. A thorough analysis of colony morphology and microscopical characteristics revealed that *Aureobasidium*, and the rot-causing fungi *Alternaria* and *Cladosporium* were the main fungal genera present on sweet cherry skin (**Figure 3**). *Aureobasidium* spp. isolates presented hyphae with multiple lateral pegs, lateral accumulation of conidia and intercalary conidiophores (Zalar et al., 2008). *Alternaria* spp. isolates had characteristic catenulate and muriform conidia (Woudenberg et al., 2013) and, finally, *Cladosporium* spp. isolates showed fragile conidiophores with a really typical structure (Pitt and Hocking, 1985). Within each fungal genus, different isolates showed phenotypical variability, both in colony morphologies and in microscopic features. Representative microscopic structures from each genus are shown (**Figure 3**). Quantitatively, *Cladosporium* was the most abundant genus, followed by *Aureobasidium* and, finally, by *Alternaria* (data not shown).

Fruit Colonization by Endophytes Increases During Ripening

No endophytic growth was detected at stages I or II. Mesocarp colonization was only observed after the onset of fruit ripening: at stages III and harvest. A significant increase in endophytic colonization was reported from stages II until harvest. Endophytic colonization, when present, was, however, relatively low, with mean values ranging from 1 up to 4 CFU/gFW (**Figure 4**). Correlation analyses between tissue-specific hormone levels and endophytic colonization revealed a significant positive correlation between both ABA exocarp and mesocarp levels and CFU/gFW (**Table 1**).

Three endophytic isolates were detected in the analyzed cherries, but only one of them, named as En-1, was repeatedly obtained from most of the samples at both stages III and harvest. Consequently, only En-1 was morphologically characterized (**Supplementary Table 1**). In addition, the antagonistic activity *in vitro* of En-1 against *B. cinerea*, a well-known rot-causing fungus, was assessed by the "killer stroke" method (Pretscher et al., 2018), showing no biocontrol ability.

Fruit Cracking Allows Fruit Mesocarp Colonization by Epiphytic and Pathogenic Microorganisms

The effect of natural disruption of sweet cherry exocarp in fruits affected by cracking on fruit-endophyte interactions was assessed. Yeast and other fungi outgrowth were observed at zone 1 (near the cracking lesion; **Figure 5A**). Two endophytic yeast isolates were detected and morphologically characterized (**Supplementary Table 1**). One of them was tagged as En-2, and the other one displayed equal characteristics to the epiphytic yeast isolate Ep-2 isolated during fruit development, and it was considered the same isolate.

Two fungal isolates were identified. On the one hand, an isolate from the genus *Aureobasidium* was obtained from one replicate in both zones of the fruit. On the other hand, *Alternaria* spp. isolates were found in every cracked fruit, colonizing both zones 1 and 2. Quantification of *Alternaria* colonization percentage of cracked cherries per zone was done, and a statistical analysis revealed that zone 2 was significantly less colonized by *Alternaria* than zones nearby the cracking lesion (**Figure 5B**), suggesting that the cracking lesion was the entry point for this rot-causing pathogen.

Endophytic isolates En-2, Ep-2, and *Aureobasidium* showed *in vitro* biocontrol ability of *B. cinerea* by the "killer stroke" method (Pretscher et al., 2018). *Alternaria* spp. isolates were not tested, as they are well known post-harvest pathogens.

DISCUSSION

A fruit tissue-specific behavior of two of the major phytohormones related with plant-microbe interactions, JA and SA, was observed in cherry fruits during fruit development in a commercial tree orchard. Previous studies on sweet cherry development have shown marked variations in different hormone levels during fruit development, showing a substantial increase of ABA, and an important decrease in JA and SA contents in whole fruits (Teribia et al., 2016; Tijero et al., 2016, 2019). However, these previous studies did not focus on the role that specific fruit tissues may have in fruit development, despite, as shown here, the differentiation between tissues may provide important hints toward better understanding the physiology and biochemistry of fruit ripening. We provide here evidence of variations in the endogenous contents of JA, SA, and ABA in the exocarp and mesocarp of sweet cherries and examine its possible relationship with the interaction of the exocarp and mesocarp of these fruits with its own microbiome and potential rot-causing pathogens. These results have important implications for biotic stress management in sweet cherry commercial orchards, as biotic stress can cause severe reductions in sweet cherry yields both during pre- and post-harvest.

Results showed sharp increases in JA levels in the exocarp during early stages of fruit development. More specifically, JA contents increased by 3-fold between stages I and II to remain constant later in development, while JA contents in the mesocarp remained stable throughout fruit development. In other words, JA accumulation was activated in the exocarp, not in the

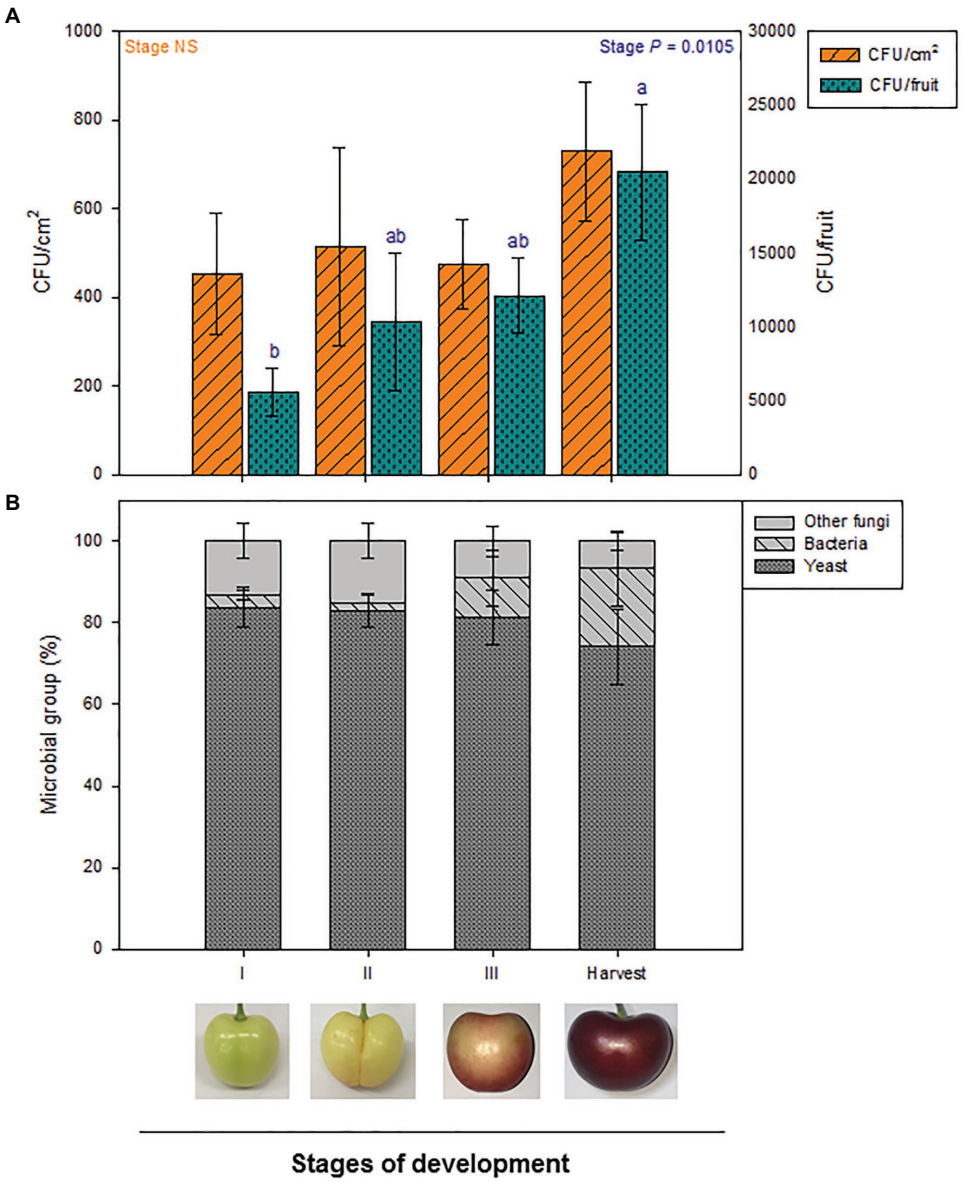

FIGURE 2 | Quantification and composition of total culturable epiphytic microorganisms at different stages of fruit development in the exocarp of sweet cherries during different stages of natural fruit development in trees from a commercial orchard. **(A)** Total epiphytic CFU per cm^2 of sweet cherry skin and per fruit are represented. **(B)** Main microbial groups present on the culturable epiphytic community of sweet cherries during fruit development. Data are means ± SE of $n = 8$. Statistical comparisons were performed by two-way ANOVA, followed by a *post-hoc* Tukey HSD test. Different letters show significant differences between groups ($p < 0.05$).

mesocarp, and most particularly only during early stages of fruit development. Similarly, an exocarp-specific SA decrease was observed during fruit development, while this hormone remained at constant levels in the mesocarp. In contrast, ABA contents increased evenly in both tissues. These results highlight the relevance of the fruit exocarp as a more active and dynamic tissue than the mesocarp, where SA and JA shifts are negligible, which could have strong implications in fruit-microbe interactions. On the other hand, it brings forward the issue that hormone analyses on whole fruits, although necessary and informative, should be complemented with tissue specific analyses in order to have a complete and accurate view of hormonal regulation of fruit development. In addition, correlation analyses showed significant corelations between different hormone levels and tissues, suggesting a certain hormone crosstalk between ABA, SA, and JA during fruit development. Indeed, this crosstalk could have not only strong implications in fruit ripening, as previously shown (Fuentes et al., 2019; Tijero et al., 2019), but also in the fruit ability to mount an effective defense against fruit-decay pathogens.

FIGURE 3 | *Aureobasidium*, *Cladosporium*, and *Alternaria* as the most frequent culturable filamentous fungi found in the exocarp of sweet cherries. Micrographs of reproductive structures (conidia and conidiophores) for each main fungal epiphytic isolate are shown. According to morphological criteria, fungal isolate Ep-3 was identified as *Aureobasidium* sp., Ep-5 as *Alternaria* sp., and Ep-6 as *Cladosporium* sp. Scale bar = 10 μm.

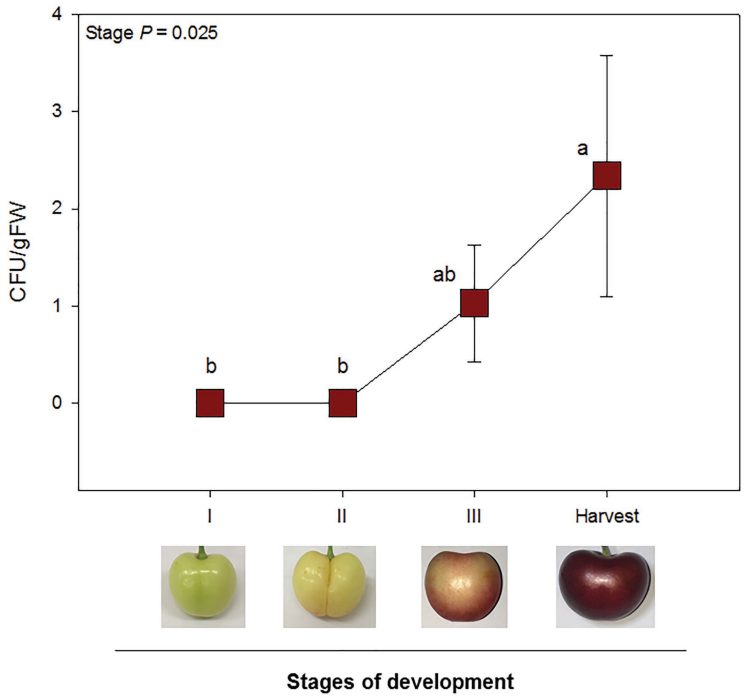

FIGURE 4 | Endophytic colonization was only observed after the onset of ripening (stage III and harvest). CFU per gram of fruit flesh from sweet cherries at different stages of development are represented. Data are means ± SE of $n = 8$. A non-parametric Kruskal Wallis test was performed, followed by a *post-hoc* Fisher least significant difference test ($p < 0.05$). Different letters mean significant differences between groups.

Plant immune responses are characterized by a certain balance between several hormones, including SA, JA, ethylene, and ABA (Robert-Seilaniantz et al., 2011). SA-dependent responses usually confer resistance to biotrophic pathogens, and higher SA levels in the exocarp at early stages of development, as observed in this experiment, could be essential in front of infections by necrotrophic pathogens that remain in the exocarp at their quiescent phase (Prusky et al., 2013). In addition, SA can also confer resistance to necrotrophic pathogens like *Monilinia fructicola* (Yao and Tian, 2005). On the other hand, JA is involved in resistance to nectrotrophic pathogens through the ETHYLENE RESPONSE FACTOR (ERF) branch of JA signaling (Pieterse et al., 2012; Campos et al., 2014), and varying levels of JA during fruit development in the exocarp could affect this response. Finally, ABA has a negative effect on plant resistance. The lack of this hormone increases resistance in tomato plant to *B. cinerea*, and ABA signaling antagonizes with SA-dependent responses and the ERF branch of JA signaling

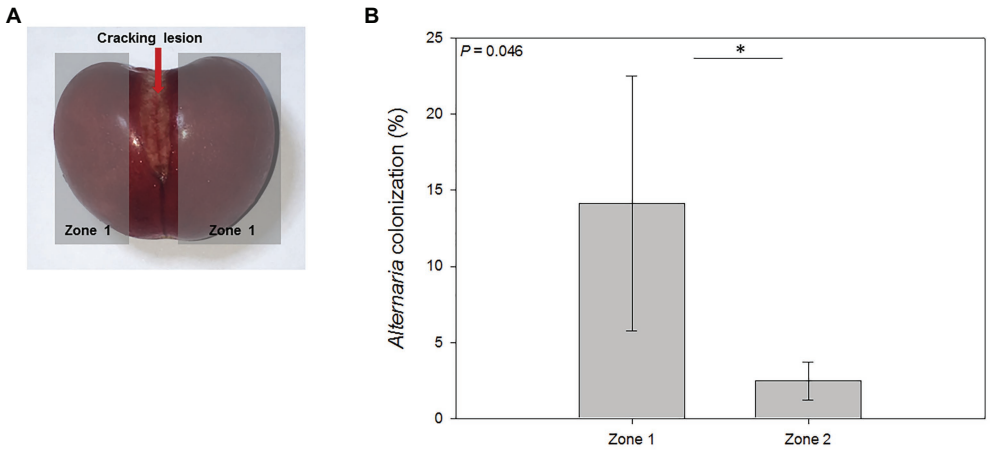

FIGURE 5 | Mesocarp colonization of cracked cherries by *Alternaria* spp. **(A)** Cherries suffering from natural cracking were divided into three areas: cracking lesion, areas around the lesion (zone 1), and the area opposite to the cracking lesion (zone 2, not shown in this plane). **(B)** Percentage of endophytic colonization by *Alternaria* sp. near and opposite (zones 1 and 2, respectively) the cracking lesion. Data are means ± SE of $n = 3$. Statistical comparisons were performed by a non-parametric Kruskal Wallis test and significant differences are shown by an asterisk ($p < 0.05$).

(Asselbergh et al., 2007; Robert-Seilaniantz et al., 2011; Pieterse et al., 2012). Therefore, the tissue-specific variations observed in the exocarp and mesocarp of sweet cherries in our study strongly support the idea that the hormonal changes observed during fruit ripening will influence the susceptibility of fruits to the infection by specific pathogens. Sustained increases in ABA contents both in the exocarp and the mesocarp, together with sustained decreases of SA contents (most particularly in the exocarp) and increases of JA contents in the exocarp (but during early stages of development only), suggest that not only the exocarp, but also the mesocarp, will be most sensitive to pathogen infection during fruit ripening, and contrariwise, it will be better protected from microbial attack during early stages of fruit development. The fact that both JA and SA contents were higher in the exocarp than in the mesocarp also suggests that the exocarp acts not only as a physical barrier but also as an immune barrier against biotrophic and necrotrophic pathogens.

Epiphytic microbial quantification and characterization showed a constant microbial population per area in the sweet cherry skin. However, the epiphytic microbial load per fruit significantly increased during fruit ripening, suggesting an active microbial reproduction on the fruit outer surface. Culturable epiphytic microbial community was mainly composed by yeasts, followed by other fungi and bacteria. Specifically, several fungal decay pathogens were recurrently found from the beginning of fruit development in the epiphytic culturable microbiome, such as *Cladosporium* and *Alternaria* species. These genera have been extensively described as important post-harvest decay pathogens in sweet cherries and other fruits (Granado et al., 2008; Tarbath et al., 2014). Additionally, different *Aureobasidium* isolates were recurrently found. Previous reports have described the biocontrol ability of certain *Aureobasidium* strains against certain post-harvest decay pathogens like *B. cinerea*, but other strains can behave as opportunistic pathogens in apples and sweet cherries (Kim, 2014; Wang et al., 2018). Altogether, our data confirmed that fungal post-harvest decay pathogens were already present at the field not only prior to harvest, but also at very early stages of fruit development.

Some fruit decay fungal genera such as *Botrytis*, *Monilinia*, or *Alternaria* can infect fruits during flowering and at unripe stages of development, behaving as biotrophic pathogens, and remaining in a quiescent state at the fruit outermost layers waiting for the right conditions to become active and cause the disease (Prusky et al., 2013). The early presence of some fruit decay pathogens in sweet cherry development in our study suggests that fungal infections could be taking place as soon as fruits are at stage I of development. Higher SA in the exocarp during early sweet cherry development, as observed in this study, could be an advantage to orchestrate a specific immune response against these infections (Prusky et al., 2013). On the other hand, increased JA levels in the exocarp could be beneficial at later stages of development, when these quiescent infections switch to a necrotrophic lifestyle and as observed in this study, when the microbial epiphytic load substantially increases.

According to our results, endophytic colonization of sweet cherries in the field was not a common event, with few CFU/gFW, suggesting that this colonization could be limited and opportunistic rather than active and widespread. Nevertheless, the onset of fruit ripening could be described as a tipping point in endophytic colonization, as endophytes were only observed in fruits at stages III and at harvest, but not before. Furthermore, endophytic amounts tended to increase throughout development. Several physiological changes take place in sweet cherries during fruit development, and specially at the onset of ripening, including an increase in total soluble sugars, pH decreases and, therefore, an enhanced sugar availability (Prusky et al., 2013; Teribia et al., 2016), which could explain this observation. Our correlation analyses suggest that ABA mesocarp content could be an additional key factor in regulating this

endophytic colonization, although its exact molecular mechanism could not yet be unraveled. It is likely that the increase of ABA during ripening may have an antagonistic effect in front of SA and JA-dependent immune responses, limiting the fruit to mount an effective defense response (Asselbergh et al., 2007; Pieterse et al., 2012; Alkan and Fortes, 2015), but further investigations will be required to support this contention.

Fruit cracking is characterized by a deep disruption of the fruit exocarp (Correia et al., 2018). A microbiological analysis of cracked cherries revealed a heavy colonization by the rot-causing fungi *Alternaria* spp., and other microorganisms like *Aureobasidium* spp. Interestingly, these microorganisms were present as epiphytes on the fruit skin during fruit development, but never as endophytes in healthy cherries. This proves that the exocarp is a physical barrier not only for pathogenic microorganisms, but also for a wide variety of microbes, and when it is broken, it can lead to fruit colonization by different pathogenic and non-pathogenic microorganisms. Several studies have aimed to prevent sweet cherry cracking to reduce fruit loss in the field (Thomidis and Exadaktylou, 2013; Correia et al., 2018). Recently, it was reported that exogenous application of ABA at early stages of development could reduce sweet cherry cracking (Balbontín et al., 2018). Paradoxically, even though ABA could have negative effects on plant immune responses to pathogens, it could indirectly be beneficial by preventing fruit cracking and subsequent fruit infection by pathogens.

In conclusion, tissue-specific hormone variations may be very useful to better understand fruit-microbiome interactions, which may have important implications to reduce yield losses in sweet cherry commercial orchards. Our results suggest a differential SA and JA hormone behavior between tissues, suggesting that fruit exocarp is a key tissue in fruit development and in fruit-microbe relations, not only by acting as a physical barrier in front of epiphytic pathogens, but also providing important hormonal signals that influence fruit-microbiome interactions. Further research is, however, needed to better understand putative causal relationships between specific hormonal variations in the exocarp and mesocarp and the increased occurrence of pathogen infection during fruit ripening. A better exploration of possible microbiome interactions is also required to better understand possible biocontrol strategies to prevent fruit decay in sweet cherries.

DATA AVAILABILITY STATEMENT

The raw data supporting the conclusions of this article will be made available by the authors, without undue reservation.

AUTHOR CONTRIBUTIONS

DF and SM-B conceived and designed the experiments. DF performed the experiments and wrote the manuscript with the help of SM-B. Both authors contributed to the discussion and revised and approved the final manuscript.

FUNDING

This project was funded by Generalitat de Catalunya, project number 2017 SGR 980.

ACKNOWLEDGMENTS

We thank Paula Muñoz for her advice and collaboration during experimental design and samplings, as well as Maren Müller and Serveis Científico-Tècnics (University of Barcelona) for their help with hormone analyses.

SUPPLEMENTARY MATERIAL

The Supplementary Material for this article can be found online at: https://www.frontiersin.org/articles/10.3389/fpls.2021.640601/full#supplementary-material

REFERENCES

Alkan, N., and Fortes, A. M. (2015). Insights into molecular and metabolic events associated with fruit response to post-harvest fungal pathogens. *Front. Plant Sci.* 6:889. doi: 10.3389/fpls.2015.00889

Alonso, J., and Alique, R. (2006). "Sweet cherries" in *Handbook of fruits and fruit processing*. ed. Y. H. Hui (Hoboken, NJ, USA: Blackwell Publishing), 359–367.

Asselbergh, B., Curvers, K., Franc, S. C., Audenaert, K., and Vuylsteke, M. (2007). Resistance to *Botrytis cinerea* in sitiens, an abscisic acid-deficient tomato mutant, involves timely production of hydrogen peroxide and cell wall modifications in the epidermis. *Plant Physiol.* 144, 1863–1877. doi: 10.1104/pp.107.099226

Balbontín, C., Gutiérrez, C., Wolff, M., and Figueroa, C. R. (2018). Effect of abscisic acid and methyl jasmonate preharvest applications on fruit quality and cracking tolerance of sweet cherry. *Chil. J. Agric. Res.* 78, 438–446. doi: 10.4067/S0718-58392018000300438

Bigeard, J., Colcombet, J., and Hirt, H. (2015). Signaling mechanisms in pattern-triggered immunity (PTI). *Mol. Plant* 8, 521–539. doi: 10.1016/j.molp.2014.12.022

Campos, M. L., Kang, J. H., and Howe, G. A. (2014). Jasmonate-triggered plant immunity. *J. Chem. Ecol.* 40, 657–675. doi: 10.1007/s10886-014-0468-3

Chockchaisawasdee, S., Golding, J. B., Vuong, Q. V., Papoutsis, K., and Stathopoulos, C. E. (2016). Trends in food science & technology sweet cherry: composition, postharvest preservation, processing and trends for its future use. *Trends Food Sci. Technol.* 55, 72–83. doi: 10.1016/j.tifs.2016.07.002

Correia, S., Schouten, R., Silva, A. P., and Gonçalves, B. (2018). Sweet cherry fruit cracking mechanisms and prevention strategies: a review. *Sci. Hortic.* 240, 369–377. doi: 10.1016/j.scienta.2018.06.042

Cui, H., Tsuda, K., and Parker, J. E. (2015). Effector-triggered immunity: from pathogen perception to robust defense. *Annu. Rev. Plant Biol.* 66, 487–511. doi: 10.1146/annurev-arplant-050213-040012

Forlani, S., Masiero, S., and Mizzotti, C. (2019). Fruit ripening: the role of hormones, cell wall modifications, and their relationship with pathogens. *J. Exp. Bot.* 70, 2993–3006. doi: 10.1093/jxb/erz112

Fuentes, L., Figueroa, C. R., and Valdenegro, M. (2019). Recent advances in hormonal regulation and cross-talk during non-climacteric fruit development and ripening. *Horticulturae* 5:45. doi: 10.3390/horticulturae5020045

Granado, J., Thürig, B., Kieffer, E., Petrini, L., Flie, A., Tamm, L., et al. (2008). Culturable fungi of stored 'Golden Delicious' apple fruits: a one-season comparison study of organic and integrated production systems in Switzerland. *Microb. Ecol.* 56, 720–732. doi: 10.1007/s00248-008-9391-x

Habib, M., Bhat, M., Dar, B. N., and Wani, A. A. (2015). Sweet cherries from farm to table: a review. *Crit. Rev. Food Sci. Nutr.* 57, 1638–1649. doi: 10.1080/10408398.2015.1005831

Kelley, D. S., Adkins, Y., and Laugero, K. D. (2018). A review of the health benefits of cherries. *Nutrients* 10:368. doi: 10.3390/nu10030368

Kim, Y. K. (2014). First report of a new postharvest rot in sweet cherries caused by *Aureobasidium pullulans*. *Plant Dis.* 98:424. doi: 10.1094/PDIS-07-13-0740-PDN

Krishnan, P., Bhat, R., Kush, A., and Ravikumar, P. (2012). Isolation and functional characterization of bacterial endophytes from *Carica papaya* fruits. *Appl. Microbiol.* 113, 308–317. doi: 10.1111/j.1365-2672.2012.05340.x

Leng, P., Yuan, B., Guo, Y., and Chen, P. (2014). The role of abscisic acid in fruit ripening and responses to abiotic stress. *J. Exp. Bot.* 65, 4577–4588. doi: 10.1093/jxb/eru204

Müller, M., and Munné-Bosch, S. (2011). Rapid and sensitive hormonal profiling of complex plant sample by liquid chromatography coupled to electrospray ionization tandem mass spectrometry. *Plant Methods* 7:37. doi: 10.1186/1746-4811-7-37

Pérez-Llorca, M., Muñoz, P., Müller, M., and Munné-Bosch, S. (2019). Biosynthesis, metabolism and function of auxin, salicylic acid and melatonin in climacteric and non-climacteric fruits. *Front. Plant Sci.* 10:136. doi: 10.3389/fpls.2019.00136

Pieterse, C. M. J., Van der Does, D., Zamioudis, C., Leon-Reyes, A., and Van Wees, S. C. M. (2012). Hormonal modulation of plant immunity. *Annu. Rev. Cell Dev. Biol.* 28, 489–521. doi: 10.1146/annurev-cellbio-092910-154055

Pitt, J. I., and Hocking, A. D. (1985). *Fungi and food spoilage*. Sydney, Australia: Academic Press.

Pretscher, J., Fischkal, T., Branscheidt, S., Jäger, L., Schlander, M., Thines, E., et al. (2018). Yeasts from different habitats and their potential as biocontrol agents. *Fermentation* 4:31. doi: 10.3390/fermentation4020031

Prusky, D., Alkan, N., Mengiste, T., and Fluhr, R. (2013). Quiescent and necrotrophic lifestyle choice during postharvest disease development. *Annu. Rev. Phytopathol.* 51, 155–176. doi: 10.1146/annurev-phyto-082712-102349

Robert-Seilaniantz, A., Grant, M., and Jones, J. D. G. (2011). Hormone crosstalk in plant disease and defense: more than just JASMONATE-SALICYLATE antagonism. *Annu. Rev. Phytopathol.* 49, 317–343. doi: 10.1146/annurev-phyto-073009-114447

Schlechter, R. O., Miebach, M., and Remus-Emsermann, M. N. P. (2019). Driving factors of epiphytic bacterial communities: a review. *J. Adv. Res.* 19, 57–65. doi: 10.1016/j.jare.2019.03.003

Takken, F., and Rep, M. (2010). The arms race between tomato and *Fusarium oxysporum*. *Mol. Plant Pathol.* 11, 309–314. doi: 10.1111/j.1364-3703.2009.00605.x

Tarbath, M. P., Measham, P. F., Glen, M., and Barry, K. M. (2014). Host factors related to fruit rot of sweet cherry (*Prunus avium* L.) caused by *Botrytis cinerea*. *Australas. Plant Pathol.* 43, 513–522. doi: 10.1007/s13313-014-0286-7

Teribia, N., Tijero, V., and Munné-Bosch, S. (2016). Linking hormonal profiles with variations in sugar and anthocyanin contents during the natural development and ripening of sweet cherries. *New Biotechnol.* 33, 824–833. doi: 10.1016/j.nbt.2016.07.015

Thomidis, T., and Exadaktylou, E. (2013). Effect of a plastic rain shield on fruit cracking and cherry diseases in Greek orchards. *Crop Prot.* 52, 125–129. doi: 10.1016/j.cropro.2013.05.022

Tijero, V., Muñoz, P., and Munné-Bosch, S. (2019). Melatonina as an inhibitor of sweet cherries ripening in orchard trees. *Plant Physiol. Biochem.* 140, 88–95. doi: 10.1016/j.plaphy.2019.05.007

Tijero, V., Teribia, N., Muñoz, P., Munné-bosch, S., and Kiel, C. (2016). Implication of abscisic acid on ripening and quality in sweet cherries: differential effects during pre- and post-harvest. *Front. Plant Sci.* 7:602. doi: 10.3389/fpls.2016.00602

Wang, X., Glawe, D. A., Kramer, E., Weller, D., and Okubara, P. A. (2018). Biological control of *Botrytis cinerea*: interactions with native vineyard yeasts from Washington state. *Phytopathology* 108, 691–701. doi: 10.1094/PHYTO-09-17-0306-R

Woudenberg, J. H. C., Groenewald, J. Z., Binder, M., and Crous, P. W. (2013). Alternaria redefined. *Stud. Mycol.* 75, 171–212. doi: 10.3114/sim0015

Yao, H., and Tian, S. (2005). Effects of pre- and post-harvest application of salicylic acid or methyl jasmonate on inducing disease resistance of sweet cherry fruit in storage. *Postharvest Biol. Technol.* 35, 253–262. doi: 10.1016/j.postharvbio.2004.09.001

Zalar, P., Gostinčar, C., de Hoog, G. S., Uršič, V., and Sudhadham, M. (2008). Redefinition of Aureobasidium pullulans and its varieties. *Stud. Mycol.* 61, 21–38. doi: 10.3114/sim.2008.61.02

Zhang, J., Wang, E. T., Singh, R. P., Guo, C., Shang, Y., Chen, J., et al. (2018). Grape berry surface bacterial microbiome: impact from the varieties and clones in the same vineyard from Central China. *J. Appl. Microbiol.* 126, 204–214. doi: 10.1111/jam.14124

Conflict of Interest: The authors declare that the research was conducted in the absence of any commercial or financial relationships that could be construed as a potential conflict of interest.

frontiers in Plant Science

ORIGINAL RESEARCH
published: 27 April 2021
doi: 10.3389/fpls.2021.647035

Single and Double Mutations in Tomato Ripening Transcription Factors Have Distinct Effects on Fruit Development and Quality Traits

*Jaclyn A. Adaskaveg, Christian J. Silva, Peng Huang and Barbara Blanco-Ulate**

Department of Plant Sciences, University of California, Davis, Davis, CA, United States

Spontaneous mutations associated with the tomato transcription factors COLORLESS NON-RIPENING (SPL-CNR), NON-RIPENING (NAC-NOR), and RIPENING-INHIBITOR (MADS-RIN) result in fruit that do not undergo the normal hallmarks of ripening but are phenotypically distinguishable. Here, we expanded knowledge of the physiological, molecular, and genetic impacts of the ripening mutations on fruit development beyond ripening. We demonstrated through phenotypic and transcriptome analyses that *Cnr* fruit exhibit a broad range of developmental defects before the onset of fruit ripening, but fruit still undergo some ripening changes similar to wild type. Thus, *Cnr* should be considered as a fruit developmental mutant and not just a ripening mutant. Additionally, we showed that some ripening processes occur during senescence in the *nor* and *rin* mutant fruit, indicating that while some ripening processes are inhibited in these mutants, others are merely delayed. Through gene expression analysis and direct measurement of hormones, we found that *Cnr*, *nor*, and *rin* have alterations in the metabolism and signaling of plant hormones. *Cnr* mutants produce more than basal levels of ethylene, while *nor* and *rin* accumulate high concentrations of abscisic acid. To determine genetic interactions between the mutations, we created for the first time homozygous double mutants. Phenotypic analyses of the double ripening mutants revealed that *Cnr* has a strong influence on fruit traits and that combining *nor* and *rin* leads to an intermediate ripening mutant phenotype. However, we found that the genetic interactions between the mutations are more complex than anticipated, as the *Cnr/nor* double mutant fruit has a *Cnr* phenotype but displayed inhibition of ripening-related gene expression just like *nor* fruit. Our reevaluation of the *Cnr*, *nor*, and *rin* mutants provides new insights into the utilization of the mutants for studying fruit development and their implications in breeding for tomato fruit quality.

Keywords: fruit ripening, fruit senescence, fruit quality, CNR, NOR, RIN, ethylene, abscisic acid

OPEN ACCESS

Edited by:
Carlos R. Figueroa, University of Talca, Chile

Reviewed by:
Ruud A. De Maagd, Wageningen University & Research, Netherlands
James Giovannoni, Cornell University, United States

****Correspondence:***
Barbara Blanco-Ulate
bblanco@ucdavis.edu

Specialty section:
This article was submitted to Crop and Product Physiology, a section of the journal Frontiers in Plant Science

Received: *28 December 2020*
Accepted: *25 March 2021*
Published: *27 April 2021*

Citation:
Adaskaveg JA, Silva CJ, Huang P and Blanco-Ulate B (2021) Single and Double Mutations in Tomato Ripening Transcription Factors Have Distinct Effects on Fruit Development and Quality Traits. Front. Plant Sci. 12:647035. doi: 10.3389/fpls.2021.647035

INTRODUCTION

Fleshy fruit gain most of their quality traits, such as color, texture, flavor, and nutritional value, as a result of physiological and biochemical changes associated with ripening. Fruit ripening has been studied for decades, yet there are still many unanswered questions about the timing and coordination of the biological processes related to this developmental program. Much of this research has been done in the model for fleshy fruit ripening, tomato (*Solanum lycopersicum*), and has utilized the spontaneous single ripening mutants *Cnr* (*Colorless non-ripening*), *nor (non-ripening)*, and *rin (ripening inhibitor)* (Robinson and Tomes, 1968; Tigchelaar et al., 1973; Thompson et al., 1999; Giovannoni et al., 2004; Manning et al., 2006). Each of these mutations produces pleiotropic defects to ripening and occur in or near genes encoding the transcription factors (TFs) SPL-CNR, NAC-NOR, and MADS-RIN, belonging to the SQUAMOSA promoter binding protein-like (SPL), NAM, ATAF1/2, CUC2 (NAC) and, MCM1, AG, DEF, SRF (MADS) TF families, respectively. Each TF family functions in diverse developmental processes and have distinct spatiotemporal expression patterns (Karlova et al., 2014; Shinozaki et al., 2018).

These mutants were used to study ripening under the assumption that the mutations cause a complete loss of function to the corresponding protein. Recently, it has been discovered that the *nor* and *rin* mutations produce proteins that are still functional and gain the ability to negatively regulate their targets (Ito et al., 2017; Li et al., 2018, 2019b; Gao et al., 2019, 2020; Wang et al., 2019). In *nor*, the two base pair deletion truncates the protein but still produces a functional DNA-binding and dimerizing NAC domain (Gao et al., 2020). In *rin*, a large deletion creates a chimeric protein with the neighboring gene *MACROCALYX* (*MC*), producing a functional protein with suppression activity (Ito et al., 2017). The *Cnr* mutation is also thought to be a gain of function mutation, although the mechanism has yet to be understood (Gao et al., 2019). The *Cnr* mutation results from hypermethylation upstream of the gene near the promoter and has been shown to inhibit the genome-wide demethylation cascade associated with normal tomato ripening (Zhong et al., 2013). Previously, these TFs were regarded as master regulators of ripening; however, given the new information about the nature of the mutations in *Cnr*, *nor*, and *rin*, it is less clear the precise roles the TFs are playing in ripening (Giovannoni et al., 2017; Wang et al., 2020a).

The *nor* and *rin* mutants have been utilized in breeding for developing tomato hybrids with extended shelf life or extended field harvest depending on their purpose for the fresh market and processing tomato industries (Kopeliovitch et al., 1979; Kitagawa et al., 2005; Garg et al., 2008; Osei et al., 2017). Hybrids between elite varieties and the ripening mutants have a delayed ripening progression, but with the tradeoff of decreased fruit quality attributes, such as color, taste, and aroma (Kitagawa et al., 2005; Tieman et al., 2017). Although there are some publications dedicated to evaluating the physiological characteristics of mutant or hybrid fruit (Tigchelaar et al., 1978; Agar et al., 1994; Garg et al., 2008), up to this point, much of what we know about the ripening mutations is based on controlled greenhouse experiments with limited fruit and few ripening stages examined. A complete dataset of phenotypic data produced from large-scale field trials evaluating fruit ripening and senescence is lacking to provide information relevant to breeding, particularly in the new context of the molecular mechanisms behind the *nor* and *rin* mutations.

The *Cnr* mutant provides a unique opportunity to study the role of epigenetics in fruit ripening but is not used in breeding because the mutant phenotype is dominant. *Cnr* has been regarded as a ripening mutant due to its unique colorless phenotype and additional ripening defects (Thompson et al., 1999). It has been suggested that *Cnr* fruit undergo normal growth and development (Lai et al., 2020); however, fruit appear different from wild type (WT) even before ripening, with a smaller size, alterations in cell wall enzyme expression, and earlier chlorophyll degradation (Eriksson et al., 2004; Wang et al., 2020b). To better utilize *Cnr* as a tool for studying fruit development and ripening, a broader understanding of the physiological and transcriptomic alterations in this mutant is necessary.

These spontaneous single mutants need to be reevaluated as tools to understand the wide-ranging biological processes regulated by each TF. Previous literature has generally assumed that the mutations block ripening, resulting in similar processes affected (Giovannoni, 2007; Karlova et al., 2014; Giovannoni et al., 2017; Osorio et al., 2020). This study demonstrates that each mutant has a unique ripening phenotype, resulting from a combination of inhibited and delayed developmental processes. We integrated phenotypic data with gene expression data and hormone measurements in the *Cnr, nor*, and *rin* mutants across ripening and senescence to characterize the extent and timing of the ripening defects. Tomatoes grown under field conditions were assessed for fruit traits over multiple seasons. We then performed a transcriptomic analysis to gain more definition of the timing in which mutant fruit deviated from WT in their development and to determine specific molecular functions altered in each mutant. Due to their pivotal role in regulating ripening, we focused on defects in hormone networks, including biosynthesis and accumulation. We analyzed the influence of each mutation on the expression of the other TF throughout ripening and senescence. Finally, to better understand the combined genetic effects of the mutants on fruit ripening, we generated homozygous double mutants of *Cnr*, *nor*, and *rin* and used phenotyping and transcriptional data to evaluate the relationships between the mutants.

MATERIALS AND METHODS

Plant Material

Tomato plants (*Solanum lycopersicum)* of *c.v.* 'Alisa Craig' and the isogenic ripening mutants *Cnr, nor*, and *rin* were grown in randomized plots under standard field conditions in Davis, CA, United States, during the 2016, 2017, 2018, and 2020 seasons. Fruit tagged at 10 days post-anthesis (dpa), which corresponds to 7 mm in fruit diameter, were harvested at stages equivalent to the WT fruit. Fruit were sampled at the mature green (MG), turning

(T), red ripe (RR), and overripe (OR) stages, corresponding to 37, 45, 50, and 57 dpa, respectively. The term "RR" is used throughout the manuscript to refer to the 50 dpa stage of all genotypes, even when the mutant fruit do not turn red. Fruit stages for each of the mutants were further validated by external color analysis (see details on fruit trait phenotyping).

Double mutant fruit were generated through reciprocal crosses: *Cnr* × *nor*, *nor* × *Cnr, Cnr* × *rin*, *rin* × *Cnr, nor* × *rin*, and *rin* × *nor*. Fruit were selfed after the initial cross to generate an F2 segregating generation. The double mutants were initially selected in the F2 generation through genotyping and phenotyping. At least two additional generations after F2 were obtained through selfing to ensure the stability of the double mutations and to perform the experiments in this study. Three seasons of data were collected for the *Cnr/nor* fruit (2016, 2017, and 2020) while only one season of data was collected for the *rin/nor* and *Cnr/rin* crosses.

Mutant Genotyping

The mutant lines were genotyped for their respective mutations. For *nor*, the Phire Plant Direct PCR Kit (Thermo Fisher Scientific, United States) was used to extract DNA and amplify the region of the gene containing the 2 bp mutation using the primers listed in **Supplementary Table 1**. The PCRs were run on a SimpliAmp Thermal Cycler (Applied Biosystems, United States) with the following conditions denaturation: 99°C for 5 min; 35 cycles of 98°C for 5 s, 56°C for 25 s, and 72°C for 25 s; with a final extension of 72°C for 1 min. The PCR products were purified using Wizard SV Gel and PCR Clean-Up System (Promega, United States) and then sequenced with Sanger technology to confirm the absence of the two (AA) nucleotides. For *rin*, the Phire Plant Direct PCR Kit (Thermo Fisher Scientific, United States) was used to extract DNA and perform end-point PCRs using primers specific for the mutant and WT alleles (**Supplementary Table 1**). The following PCR conditions were used for the WT allele primers: denaturation 99°C for 5 min; 35 cycles of 98°C for 5 s, 55°C for 25 s, and 72°C for 25 s; with a final extension of 72°C for 1 min. The PCR conditions for the mutant allele primers were: denaturation 98°C for 5 min; 40 cycles of 98°C for 5 s, 58°C for 25 s, and 72°C for 25 s; with a final extension of 72°C for 1 min. The PCR products were visualized as bands using a 1% agarose gel.

The *Cnr* epimutation was genotyped by bisulfite sequencing. Extracted DNA was treated with the Zymo Gold bisulfite kit (Zymo Research, United States). Bisulfite treated-DNA was PCR amplified for the *CNR* promoter region containing the methylation changes (Manning et al., 2006) using the primers listed in **Supplementary Table 1**. The following PCR conditions were used: 94°C for 2 min; 40 cycles of 94°C for 30 s, 54°C for 30 s, and 60°C for 45 s, and a final extension of 60°C for 10 min. The PCR products were then Sanger sequenced and compared to the same region amplified in untreated controls with primers (**Supplementary Table 1**). The following conditions were used to amplify the untreated DNA: 95°C for 2 min; 35 cycles of 95°C for 30 s, 56°C for 30 s and 72°C for 1 min, and a final extension of 72°C for 10 min. To ensure mutants were homozygous for the locus, we confirmed the double mutants by allowing the plants to self for at least two additional generations and checking that the progeny were not segregating for any fruit phenotypes.

Fruit Trait Phenotyping

Fruit trait data were collected across four field seasons (2016, 2017, 2018, and 2020). The genotypes, developmental stages, number of biological replicates, and number of field seasons used for fruit trait phenotyping can be found in **Supplementary Table 2**. One season of phenotyping was performed for *Cnr/rin* and *rin/nor* double mutant fruits for color, firmness, and ethylene. Three seasons of data were collected for the *Cnr/nor* double mutant fruit for ethylene and two seasons of data for color and firmness. Fruit were collected from multiple plots or harvests to capture environmental variability. Fruit trait measurements were taken on the same day of harvest for all samples unless noted. Intact and halved fruit were imaged using the VideometerLab 3 (Videometer, Denmark) facilitated by Aginnovation LLC[1]. External color measurements were obtained from individual fruit with the CR-410 Chroma Meter (Konica Minolta Inc, Japan) and recorded in the L*a*b* color space, where L* quantifies lightness, a* quantifies green/red color, and b* quantifies blue/yellow color. Principal component analysis (PCA) of the color parameters was performed with the *FactoMineR* package and graphed with the *FactoExtra* package in R (Lê et al., 2008; Kassambara et al., 2017). Non-destructive firmness measurements were taken on the TA.XT2i Texture Analyzer (Texture Technologies, United States) using a TA-11 acrylic compression probe, a trigger force of 0.035 kg, and a test speed of 2.00 mm/sec with Exponent software (Texture Technologies Corporation, United States). Firmness values are reported as kilograms (kg) force. The size was measured by taking the largest diameter (mm) of the fruit with a handheld caliper.

Tomato juice was produced by pressing the fruit tissues with a juicer and filtering with cheesecloth to measure total soluble solids (TSS) and titratable acidity (TA). At least five biological replications of tomato juice were obtained from independent pools of 10–12 fruit from distinct plots in the field or at different harvest dates within the field season. TSS were measured as percent Brix with a Reichert AR6 Series automatic bench refractometer (Reichert Inc., United States) from the prepared juice with three technical replicates. TA was measured using the tomato juice with the TitraLab TIM850 Titration Manager (Radiometer Analytics, Germany). Four grams of juice were diluted with water in 20 mL of deionized water to measure TA based on citric acid equivalents. Significant differences in fruit traits across genotypes and ripening stages were determined in R (R foundation for Statistical Computing) using Type I analysis of variance (ANOVA) tests, followed by a *post hoc* test (Tukey Honest Significant Differences, HSD) using the R package *agricolae* (De et al., 2017).

RNA Extraction

On the day of harvest, the fruit pericarp tissues were dissected and flash-frozen in liquid nitrogen. Frozen tissues were then ground to a fine powder with the Retsch Mixer Mill MM 400

[1]https://www.aginnovationusa.com

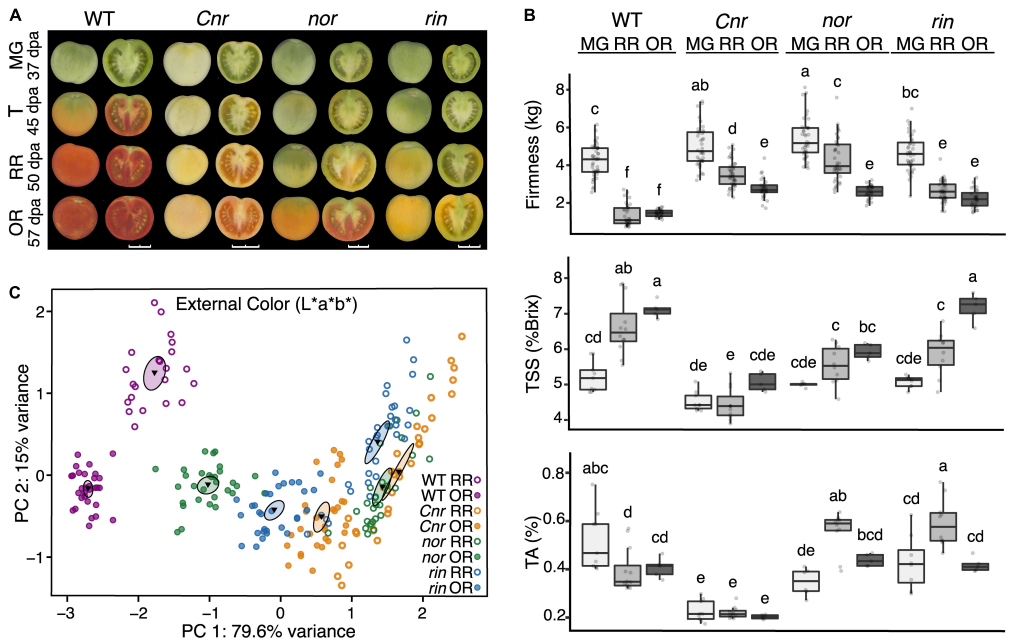

FIGURE 1 | Fruit traits of the tomato single ripening mutants. **(A)** Ripening progression of wild type (WT), *c.v.* 'Ailsa Craig,' compared to the isogenic mutants *Cnr*, *nor*, and *rin* across four developmental stages: mature green [MG, 37 days post anthesis (dpa)], turning (T, 45 dpa), red ripe (RR, 50 dpa), and overripe (OR, 57 dpa) shown at left whole and at right in longitudinal sections. Images were captured and processed with the VideometerLab instrument. Bars correspond to 2 cm. **(B)** Measurements of fruit firmness (n = 28–44), total soluble solids (TSS) (n = 5–12), and titratable acidity (TA) (n = 5–12) for each MG, RR, and OR stages are presented. Error bars represent standard error between biological replicates of each sample. Letters indicate significant differences among genotypes and stages calculated by ANOVA and Tukey HSD ($P \leq 0.05$). **(C)** Principal component analysis of external color measured on the L*a*b* color scale of each genotype at the RR (n = 22–34) and OR stage (n = 28–40). The center of gravity is represented by a triangle with surrounding ellipses indicating 95% confidence interval.

(Verder Scientific, Netherlands). One gram of ground tissue was used for RNA extractions as described in Blanco-Ulate et al. (2013). RNA concentrations were quantified with Nanodrop One Spectrophotometer (Thermo Scientific, United States) and Qubit 3 (Invitrogen, United States). RNA integrity was then assessed on an agarose gel. Six biological replicates composed of 8–10 independent fruit were extracted per genotype and ripening stage from the 2016 and 2018 seasons.

cDNA Preparation and RT-qPCR

cDNA was prepared from 1 μg of RNA of all samples using M-MLV Reverse Transcriptase (Promega, United States) in the SimpliAmp Thermal Cycler (Applied Biosystems, United States). RT-qPCRs were performed using PowerSYBR Green PCR Master Mix (Applied Biosystems, United States) in the QuantStudio3 (Applied Biosystems, United States) following the preset qPCR conditions for the 'Comparative CT method.' The tomato *SlUBQ* (*Solyc12g04474*) was used as the reference gene for all relative expression analyses. Primers for the genes of interest were designed using Primer-BLAST (Ye et al., 2012) or obtained from previous studies (**Supplementary Table 1**). For all new qPCR primer sets, efficiency was confirmed to be higher than 90% using fourfold DNA or cDNA dilutions (0, 1:1, 1:4, 1:16, 1:64, and 1:256) in triplicate. Then, specificity was checked by analyzing the melting curves at temperatures ranging from 60 to 95°C. Relative gene expression was calculated using the formula $2^{(referencegeneCt - geneof\ interest\ Ct)}$.

cDNA Library Preparation, RNA Sequencing, and Sequencing Data Processing

Four biological replicates each of *Cnr/nor* MG and RR fruit RNA were used to prepare cDNA libraries. cDNA libraries were prepared with Illumina TruSeq RNA Sample Preparation Kit v.2 (Illumina, United States) from the extracted RNA. The quality of the barcoded cDNA libraries was assessed with the High Sensitivity DNA Analysis Kit in the Agilent 2100 Bioanalyzer (Agilent Technologies, United States) and then sequenced (50 bp single-end reads) on the Illumina HiSeq 4000 platform by the DNA Technologies Core at UC Davis Genome Center.

Raw RNAseq data from WT, *Cnr*, *nor*, and *rin* at MG and RR were obtained from a published dataset by our group (Silva et al., 2021), GEO accession GSE148217), while raw RNAseq data from the immature stages of the ripening mutants were extracted from Lü et al. (2018) (GEO accession GSE116581). The RNAseq datasets for the *Cnr/nor* double mutant were generated in this study. The raw sequencing reads from the different datasets were analyzed *de novo* following the bioinformatics pipeline described below. Raw reads were trimmed for quality and adapter sequences using Trimmomatic v0.39 (Bolger et al., 2014) with the following parameters: maximum seed mismatches = 2,

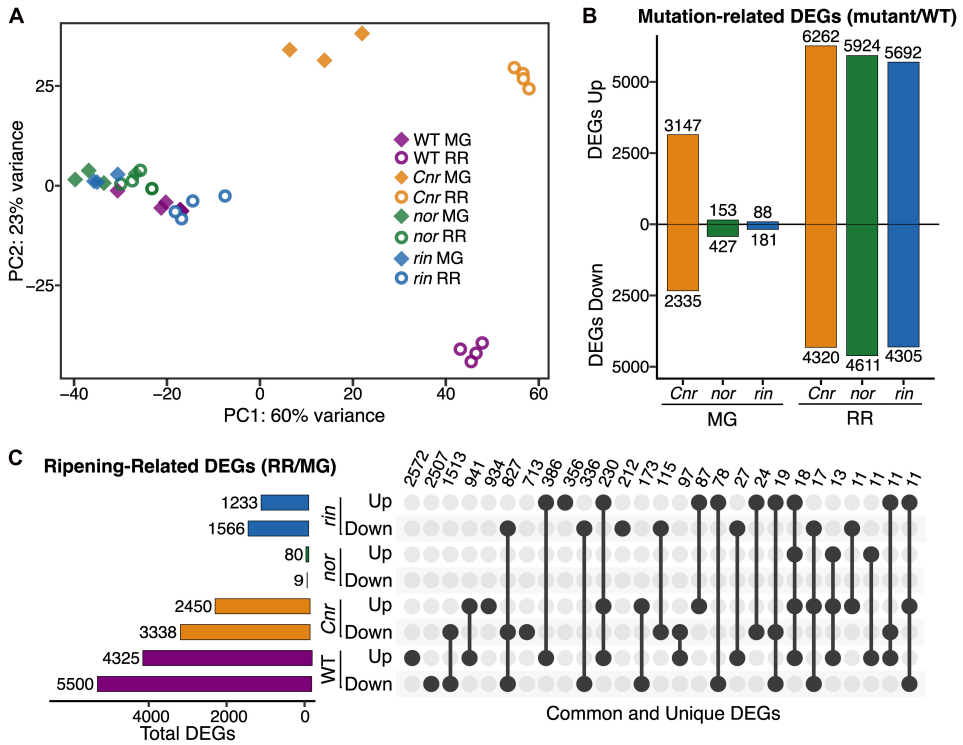

FIGURE 2 | Transcriptional misregulation in fruit from the single ripening mutants *Cnr, nor*, and *rin*. **(A)** Principal component analysis of total mapped RNAseq reads for *Cnr*, *nor*, *rin* and wild type (WT) fruit at the mature green (MG) and red ripe (RR) stages. **(B)** Number of differentially expressed genes (DEGs; $P_{adj} \leq 0.05$) up- or down-regulated for each mutant compared to WT. **(C)** Total, unique, and intersecting up- and down-regulated DEGs across ripening (RR/MG) for each genotype visualized using *UpSetR*. Dots connected by lines indicate common DEGs between categories and single dots indicate unique DEGs, with the number of genes in each category listed above.

palindrome clip threshold = 30, simple clip threshold = 10, minimum leading quality = 3, minimum trailing quality = 3, window size = 4, required quality = 15, and minimum length = 36. Trimmed reads were then mapped using Bowtie2 (Langmead and Salzberg, 2012) to the tomato transcriptome (SL4.0 release[2]). Count matrices were made from the Bowtie2 results using sam2counts.py v0.91[3]. A summary of all read mapping results can be found in **Supplementary Table 3**.

Differential Expression Analysis, Functional Annotations, and Enrichment Analysis

The Bioconductor package *DESeq2* (Love et al., 2014) in R was used to normalize read counts and perform PCAs and differential expression analyses for various comparisons (**Supplementary Tables 4, 5**). Differentially expressed genes (DEGs) for each comparison had an adjusted *P*-value of less than or equal to 0.05. Gene functional annotations were retrieved from the Kyoto Encyclopedia of Genes and Genomes (KEGG) using the KEGG Automatic Annotation Server (Moriya et al., 2007). Enrichment analysis for all functional annotations was performed using a Fisher test. The *P*-values obtained from the Fisher test were adjusted with the Benjamini and Hochberg method (Benjamini and Hochberg, 1995). Shared and unique DEGs among the comparisons were determined using the R package *UpSetR* (Conway et al., 2017).

Hormone Extraction and Analysis

Ethylene production measurements were taken from MG, RR, and OR fruit on the day of harvest. At least five biological replicates of 5–7 fruit were used for the measurements. The genotypes, developmental stages, and number of biological replicates used for ethylene analysis in each field season can be found in **Supplementary Table 2**. Fruit were weighed and placed in 1 L airtight glass jars. Headspace gas (3 ml) was extracted from the sealed containers after 60 min and was injected into a Shimadzu CG-8A gas chromatograph (Shimadzu Scientific Instruments, Japan). Sample peaks were measured against an ethylene standard. The rate of ethylene production (nL kg^{-1} fresh weight h^{-1}) was calculated from the peak, fruit mass, and incubation time.

Frozen ground tissue prepared from the tomato fruit pericarp was lyophilized, weighed, and extracted in isopropanol:H2O:HCL1MOL(2:1:0.005) with 100 l of internal standard solution (1000 pg) as described in Casteel et al. (2015). Abscisic acid (ABA) and 1-aminocyclopropane-1-carboxylate (ACC) were measured using liquid chromatography coupled to

[2]http://solgenomics.net

[3]https://github.com/vsbuffalo/sam2counts/

TABLE 1 | Differential expression of key genes associated with tomato fruit traits in the single ripening mutants *Cnr*, *nor*, and *rin*.

			Mutation comparison (Log_2FC mutant/WT)						Ripening comparison (Log_2FC RR/MG)			
Fruit trait	**Gene accession**	**Gene name**	***Cnr* MG**	***nor* MG**	***rin* MG**	***Cnr* RR**	***nor* RR**	***rin* RR**	**WT**	***Cnr***	***nor***	***rin***
Color	*Solyc03g031860*	Phytoene synthase 1 (*SlPSY1*)	–2.41	–1.93	–1.81	–4.08	–3.97	–5.33	3.32	1.65	1.29	
	Solyc03g123760	Phytoene desaturase (*SlPDS1*)	–0.63			–0.70						
	Solyc01g097810	ζ-carotene desaturase (*SlZDS*)	–0.81			–1.45	–1.19	–1.02	0.96			
	Solyc04g040190	Lycopene β-cyclase (*SlLCY1*)	–0.76				2.15	1.94	–2.02	–1.19		
	Solyc10g079480	Lycopene β-cyclase (*SlLCY2*)				4.07	4.15	4.48	–3.73			
Firmness	*Solyc10g080210*	Polygalacturonase (*SlPG2A*)	–3.39	–4.40	–3.58	–5.03	–11.38	–8.33	7.54	5.90		2.80
	Solyc03g111690	Pectate lyase (*SlPL*)				–2.23	–4.14	–4.64	3.05	1.42		
	Solyc12g008840	β-galactosidase 4 (*TBG4*)				–1.97	–2.89	–1.87	1.71			
	Solyc07g064170	Pectin methylesterase 1 (*SlPME1*)	–8.27			–8.66		–1.02	–1.21	–1.60		–2.41
	Solyc07g064180	Pectin methylesterase 2 (*SlPME2*)	–5.53			–7.65				–2.60		–1.38
	Solyc01g008710	Mannan endo-1,4-β-mannosidase (*SlMAN*)	–9.69	–9.11	–4.11	–7.63	–5.66					3.85
Total soluble solids	*Solyc03g083910*	Sucrose accumulator (*SlSUCR*)	–2.50	–2.33	–2.27	–3.88	–5.57	–5.85	2.52			
	Solyc11g017010	Sucrose transporter (*SlSUT1*)	1.59			3.67				1.76		
	Solyc05g007190	Sucrose transporter (*SlSUT2*)				1.48				1.08		
	Solyc04g076960	Sucrose transporter (*SlSUT4*)	0.93			2.27	0.86	2.01	–1.29			0.62
Acidity	*Solyc12g005860*	Aconitate hydratase (*SlACO*)				–0.58	–1.71	–1.55	1.38	1.14		

Two comparisons were performed: one to capture differences between mutant vs. wild type (WT) fruit at the mature green (MG) and red ripe (RR) stages, and the other to detect differences across ripening (RR vs. MG) in the WT and mutant fruit. Only significant fold changes (Log_2FC, $P_{adj} \leq 0.05$) are presented.

tandem mass spectrometry and internal standards as described in Casteel et al. (2015). The hormone concentrations were expressed as ng/g of dry weight. Four to six biological replicates composed of 8–10 fruit were used for these measurements for the 2017 season. Significant differences in hormone accumulation across genotypes and ripening stages were determined using Type I ANOVA in R, followed by an HSD test using the R package *agricolae* (De et al., 2017). In some cases, pairwise comparisons in hormone accumulation were also conducted by Student's *t-test* in R.

RESULTS

Ripening Mutants Display Distinct Phenotypes and Transcriptional Profiles Throughout Fruit Development

Fruit from the *Cnr*, *nor*, and *rin* mutants fail to acquire most ripening-associated traits that make them appealing for consumption. Yet, each mutant can be distinguished by their unique phenotypes (**Figure 1**). To determine the impact of *Cnr*, *nor,* and *rin* mutations on the key fruit traits, we measured external color, firmness, total soluble solids (TSS), and titratable acidity (TA) at multiple ripening stages. Fruit from the isogenic mutants *Cnr*, *nor*, and *rin*, were harvested alongside WT from an experimental field at selected ripening stages, mature green (MG; 37 dpa), turning (T; 45 dpa), red ripe (RR; 50 dpa), and overripe (OR; 57 dpa) (**Figure 1A**). We captured field variability through large sample sizes and validated across two to four independent field seasons. A summary of all seasons is displayed in **Figure 1** while a breakdown of the data by field season can be found in **Supplementary Table 2**.

As expected, between the MG and RR stages WT fruit turned red internally and externally, reduced firmness, accumulated TSS, and became less acidic during ripening. *Cnr* fruit showed visual differences compared to all of the genotypes at the MG stage and continuing through subsequent stages, including significantly smaller size and its characteristic colorless flesh, marked by an opaque yellow coloration of the pericarp (**Figure 1** and **Supplementary Figure 1**). Statistical analyses performed for color and size confirmed *Cnr* exhibited significant differences ($P \leq 0.05$) consistently across each field season, as reported in **Supplementary Table 2**. Fruit of *nor* and *rin* displayed a distinct absence of any red coloration compared to WT at the RR stage; instead, these fruit began to turn yellow externally. Fruit of all ripening mutants were significantly firmer across all stages than the WT, though this difference was especially pronounced in *Cnr* (**Figure 1B**). Overall, *Cnr* was consistently different from the other genotypes before and during ripening, while *nor* and *rin* remained similar to WT MG fruit.

The OR stage was selected to investigate if the ripening mutants displayed phenotypic changes at later time points that could be associated with a delay in fruit development. At this stage, *nor* fruit started to turn orange-red externally and red internally, similar to WT fruit. The *nor* OR fruit resembled WT fruit between the T and RR stages. We performed a PCA of the color data (L*a*b measurements) to compare the genotypes at the RR and OR stage, and found *nor* OR measured closely with WT RR in external coloration (**Figure 1C**). A summary of

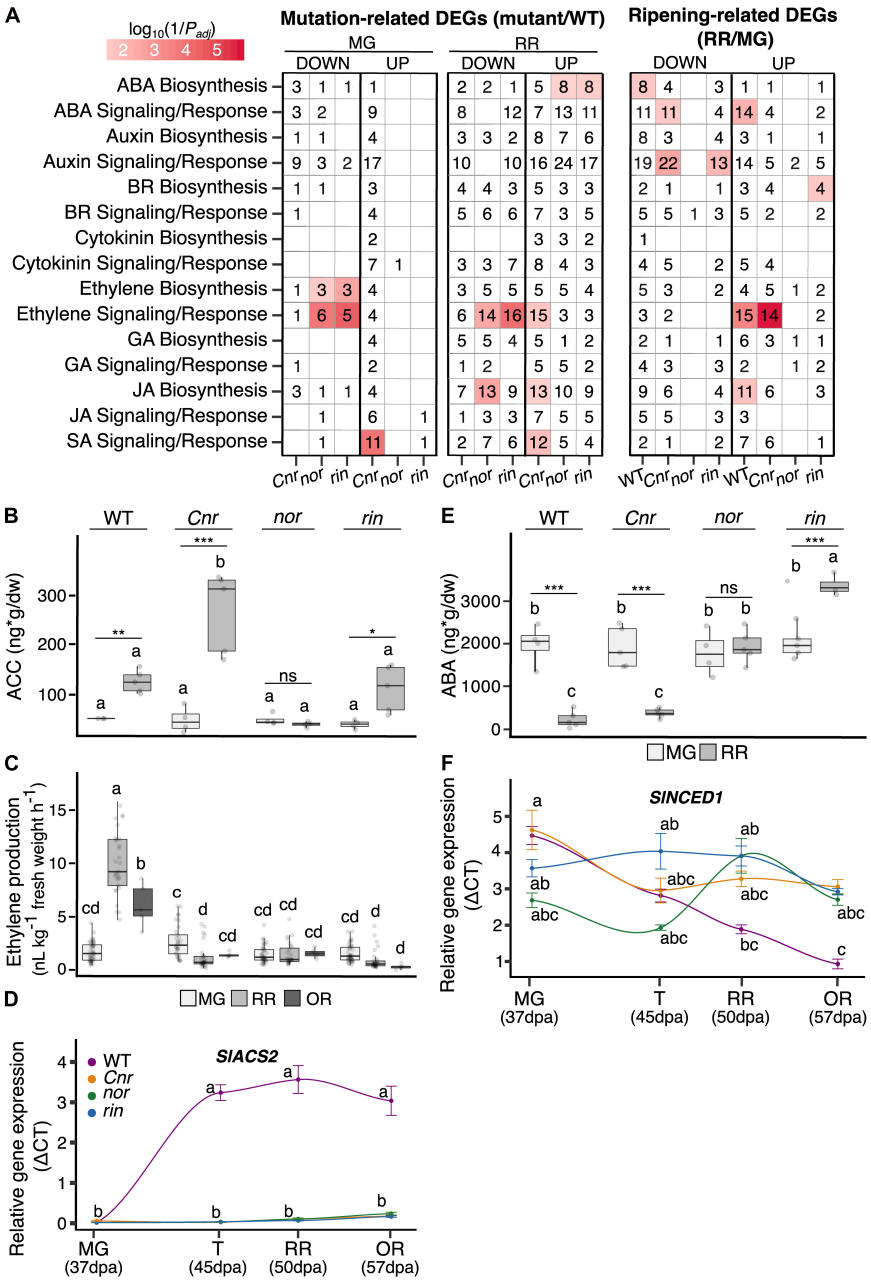

FIGURE 3 | Plant hormone networks altered in the single ripening mutants *Cnr*, *nor*, and *rin*. **(A)** Functional enrichments in hormone functions among differentially expressed genes (DEGs; $P_{adj} \leq 0.05$) in two comparisons: mutation-related DEGs obtained when comparing each mutant to the wild type (WT) at the mature green (MG) and red ripe (RR) stages, and ripening-related DEGs when the RR stage was compared against MG for each genotype. Each comparison is separated into significant down- and up-regulated DEGs. The heat map colors indicate the significance of the functional enrichment using a $\log_{10}(1/P_{adj})$ scale. Numbers in each tile indicate the number of DEGs within each category. Only significant ($P_{adj} \leq 0.05$) functional enrichments are shown. Hormone measurements of the **(B)** ethylene precursor 1-aminocyclopropane-1-carboxylate (ACC) (n = 4–6), **(C)** ethylene (n = 5–45), and **(E)** abscisic acid (ABA) (n = 4–6) for WT, *Cnr*, *nor*, and *rin* fruit at the MG, RR, and/or overripe (OR) stages. Relative gene expression by RT-qPCR of key hormone biosynthesis genes of **(D)** ethylene and **(F)** ABA across (n = 6) across four ripening stages MG, turning (T), RR, and OR for each genotype. Error bars represent standard error between biological replicates of each sample. Letters in **(B–F)** indicate significant differences among genotypes and ripening stages calculated by ANOVA and Tukey HSD ($P \leq 0.05$). Asterisks in **(B,C,E)** denote significant differences (*$P \leq 0.05$, **$P \leq 0.01$, ***$P \leq 0.001$) between two ripening stages within a single genotype calculated by Student's t-test.

the color data and statistical analyses performed can be found in **Supplementary Table 2**. While *nor* OR fruit visually looked most similar to WT RR fruit, *rin* OR fruit consistently measured similarly to WT fruit at the RR and OR stages in the taste-related traits of TSS and TA. These phenotypes were especially noticeable in the OR stage, suggesting that *rin* exhibits a delay

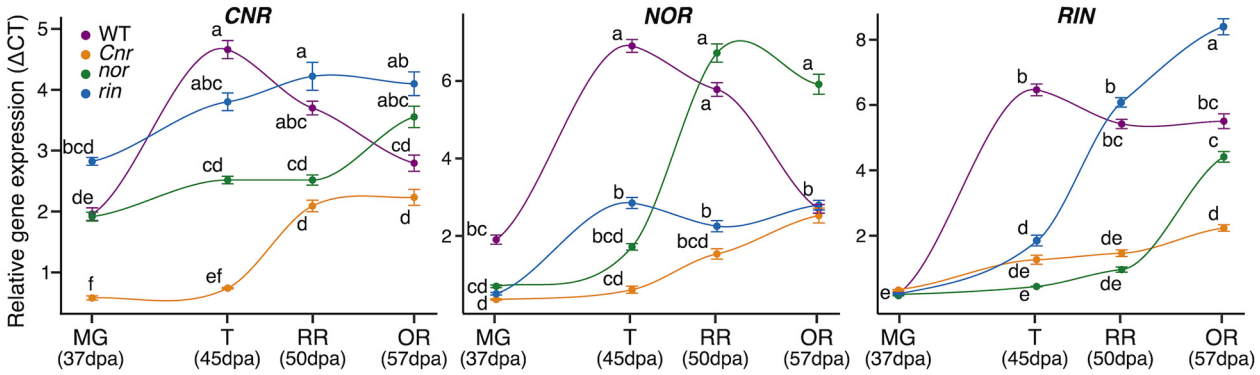

FIGURE 4 | Impact of ripening mutations on the *CNR*, *NOR*, and *RIN* transcription factors. Relative gene expression of the three transcription factors across ripening in the wild type (WT), *Cnr*, *nor*, and *rin* genotypes measured by quantitative reverse transcription (qRT)-PCR. The measurements were done with fruit ($n = 6$) collected at 37 days post anthesis (dpa), equivalent to the mature green stage (MG), 45 dpa, equivalent to the turning stage (T), 50 dpa, equivalent to the red ripe stage (RR), and 57 dpa, equivalent to the overripe (OR) stage. Error bars represent standard error between biological replicates of each sample. Letters indicate significant differences among genotypes and ripening stages calculated by ANOVA and Tukey HSD ($P \leq 0.05$).

in these traits. In contrast, *Cnr* remained distinct from WT and the other mutants at the OR stage in all measurements (**Figure 1B**). Thus, in the OR stage, *nor* and *rin* behaved more similar to WT, suggesting they display more ripening phenotypes after the RR stage.

The distinct phenotypic differences observed between the ripening mutants indicate that each mutation has a unique impact on fruit molecular processes at specific developmental stages. We performed an RNAseq study of WT, *Cnr*, *nor*, and *rin* fruit at the MG and RR stages to gain insights into the observed phenotypes. A principal component analysis (PCA) was performed using mapped normalized reads to the tomato predicted transcriptome (34,075 genes; SL4.0 release) from WT and mutant samples at MG and RR stages (**Figure 2A**). The PCA revealed that the genotypes were mainly separated by ripening stage (PC1, 60% variance) and that *Cnr* was distinct from WT and the other mutants (PC2, 23% variance). Remarkably, *Cnr* displayed the most similar pattern to WT across PC1 than any other mutant. Like their phenotypes suggested, *nor* and *rin* transcriptomic profiles showed little change between the MG and RR stage and clustered with the WT MG fruit. The separation driven by PC2 supported our observations that *Cnr* fruit was phenotypically different from other genotypes.

Cnr Fruit Display Transcriptional Differences From Wild Type Before Ripening

Because *Cnr* showed deviation from WT at the MG stage in both phenotype and transcriptional profiles, we hypothesized that gene expression across the genome was affected prior to the MG stage. To determine when the transcriptional profile of *Cnr* began to diverge from WT and other mutants, we obtained and reanalyzed raw RNAseq data from all genotypes at four early stages of fruit growth and development (7, 17, 27, and 37 dpa) (Lü et al., 2018). We performed a PCA for each developmental stage and found that *Cnr* was separated from other genotypes as early as 7 dpa in fruit development, while *nor* and *rin* were similar to WT throughout early development (**Supplementary Figure 2**). When evaluating differentially expressed genes (DEGs, $P_{adj} \leq 0.05$) between *Cnr* and WT fruit at 7 dpa, we detected 1,320 mutation-related DEGs while *nor* and *rin* had only 173 and 392, respectively (**Supplementary Table 5**). These results suggest that *Cnr* fruit have different gene expression profiles from WT throughout fruit growth and maturation, even before ripening begins.

Transcriptional Misregulation in the Ripening Mutants Leads to Inhibition or Delay of Molecular Processes

We determined DEGs ($P_{adj} \leq 0.05$) from the MG and RR stages to identify specific molecular functions altered in *Cnr*, *nor*, and *rin* fruit. First, we compared the ripening mutants to the WT at each stage and obtained a total of 16,085 mutation-related DEGs across all comparisons (**Figure 2B**). Like the PCA suggested (**Figure 2A**), *Cnr* MG fruit presented the largest amount of mutation-related DEGs (5,482), while *nor* and *rin* MG had considerably fewer DEGs when compared to the WT counterpart (580 and 269 DEGs, respectively). At the RR stage, large differences between each mutant and WT were observed, with *Cnr* RR fruit displaying once again the largest differences in the amount of mutation-related DEGs (10,582, **Figure 2B**). The large number of mutation-related DEGs shown by *Cnr* fruit further supports our hypothesis that the *Cnr* mutation more broadly affects fruit development and that *nor* and *rin* appear to be more ripening-specific mutations.

We examined molecular functions based on KEGG annotations that were significantly ($P_{adj} \leq 0.05$) enriched among the mutation-related DEGs for each *Cnr, nor*, and *rin* fruit at MG and RR (**Supplementary Figure 3**). Large differences in enriched functions were detected in the *Cnr* MG fruit, which mainly corresponded to alterations in carbohydrate and amino acid metabolism, chlorophyll, and carotenoid biosynthesis,

and interestingly many processes related to DNA replication and repair. The lack of green color in *Cnr* MG fruit could be explained by lower expression of photosynthesis and carbon fixation genes. The *nor* MG and *rin* MG fruit showed few alterations compared to WT and were mainly noted in amino acid metabolism and plant hormone signal transduction. In contrast, at the RR stage, the three ripening mutants showed significant alterations across multiple molecular pathways that range from primary and secondary metabolism to transcription, translation, and signaling processes.

We proceeded to mine the mutation-related DEGs for key genes known to affect the fruit traits evaluated in the ripening mutants: color, firmness, TSS, and acidity. We selected five carotenoid biosynthesis genes involved in fruit pigmentation, six genes encoding cell wall degrading enzymes (CWDEs) that promote fruit softening, four genes related to sugar accumulation and transport that impact the fruit's TSS, and one gene that regulates the levels of citric acid then affecting the fruit's acidity (**Table 1**). At the MG stage, we observed that *Cnr* fruit showed significantly lower expression than WT for several of these key genes, consistent with our phenotypic data (**Figure 1**), including firmness related enzymes and carotenoid biosynthesis genes. MG fruit from the three ripening mutants showed significantly lower gene expression in an important invertase in fruit (*SlSUCR*), which may contribute to the lower levels of TSS observed in all the mutants (**Table 1**; Klann et al., 1993). At the RR stage, most of the fruit trait-associated genes surveyed in the ripening mutants had a significantly lower expression than WT, in support of the phenotypic data and reinforced by the numerous functional enrichments among the mutation-related DEGs (**Supplementary Figure 3**). The critical carotenoid biosynthesis gene that encodes *PHYTOENE SYNTHASE 1* (*PSY1)* was significantly lower expressed than WT in the mutant fruit across all stages, accounting for the lack of red pigmentation at the RR stage. Also, downstream genes in the pathway encoding Lycopene β-cyclases (*SlLCY1 and SlLCY2*) were highly expressed in the mutants at the RR stage, suggesting that not only was less lycopene being produced but more was being metabolized. CWDEs were negatively affected across all genotypes, with *Cnr* having the most mutation-related DEGs in this category.

We were interested in examining if the *Cnr*, *nor*, and *rin* mutant fruit displayed altered ripening progression or if they were completely inhibited or delayed in ripening events. We performed another set of differential expression analyses comparing RR against MG fruit for WT and each of the mutants to reveal ripening-related DEGs. As anticipated, WT had the largest number of ripening-related DEGs (9,825), while *nor* showed almost no change between the two ripening stages with only 89 DEGs detected (**Figure 2C**). *Cnr* and *rin* had fewer ripening-related DEGs compared to WT but still exhibited significant changes during the transition between stages with 5,788 and 2,799 DEGs, respectively. Although *Cnr* showed the most differences from WT in mutation-related DEGs (**Figure 2B**), it had the largest number of ripening-related DEGs (2,454) in common with WT fruit (**Figure 2C**). *Cnr* also displayed similar functional enrichments ($P_{adj} \leq 0.05$) to WT among their respective ripening-related DEGs, including photosynthesis-related pathways, carbohydrate, and amino acid metabolism, and plant hormone signal transduction (**Supplementary Figure 4**). Compared to *Cnr*, *rin* shared a smaller number of ripening-related DEGs (722) and functional enrichments with WT fruit (**Figure 2C** and **Supplementary Figure 4**). The number of ripening-related DEGs shared between *nor* and WT fruit was negligent, and no functional enrichments were detected in this set of DEGs.

Similar to our previous analysis, we mined the ripening-related DEGs to determine the patterns of expression of key genes involved in fruit quality traits (**Table 1**). We observed that *Cnr* and WT showed similar gene expression of *SlPSY1*, *SlLCY1, POLYGALACTURONASE 2A* (*SlPG2A*), pectate lyase (*SlPL*), *PECTIN METHYLESTERASE 1* (*SlPME1*), and *ACTINATE HYDRATASE* (*SlACO*). Fruit from *nor* and *rin* did not have similar ripening expression patterns to WT fruit for those genes, except for the *SlPG2A* and *SlPME1* in *rin*. Altogether, these data indicate that *Cnr* fruit undergo the most similar ripening progression to WT fruit, while *nor* and *rin* fruit have moderate to minimal changes between the MG and RR stages.

Ripening Mutants Present Alterations in Hormone Networks

Alterations in transcriptional and hormone control likely cause the extensive gene expression differences that lead to the pleiotropic ripening defects in the mutants. Our transcriptional data pointed out that both mutation-related and ripening-related DEGs were significantly enriched ($P_{adj} \leq 0.05$) in functions related to hormone regulation (**Supplementary Figures 3, 4**). Thus, we decided to look closer at defects in hormone biosynthesis and signaling in the mutant fruit, with a particular focus on ethylene and ABA as they are known to promote tomato ripening (Zhang et al., 2009; Kumar et al., 2014; Mou et al., 2016).

It has been reported multiple times that ethylene production is negatively affected in the *Cnr*, *nor*, and *rin* mutants (Giovannoni, 2007; Liu et al., 2015; Li et al., 2019a). We confirmed that the three ripening mutants do not present the ethylene burst associated with climacteric fruit ripening at any of the stages evaluated, MG, RR, and OR (**Figure 3**). However, in a one-way ANOVA and Tukey HSD test comparing all genotypes at the MG stage we noted that *Cnr* fruit produced significantly ($P = 0.0004$) more ethylene at the MG stage than WT MG fruit and the other mutants at the equivalent stages. We validated these results with field-grown tomatoes across four field seasons. The results from each season can be found in **Supplementary Table 2**. To give a sense if ethylene was inhibited at an early step in biosynthesis in the mutants, we measured the accumulation of the immediate ethylene precursor ACC at the MG and RR stages. ACC accumulates typically at the RR stage in WT fruit, reflecting the increase in ethylene biosynthesis and ethylene production. Surprisingly, ACC concentrations also increased in *Cnr* and *rin* fruit during ripening, reaching values similar to WT fruit (**Figure 3B**); yet the fruit did not produce normal ethylene levels. Moreover, the ACC accumulation in *Cnr* RR fruit was the highest across all genotypes and ripening stages, significantly more than WT RR fruit. These results suggest that the low levels of ethylene

in *Cnr* and *rin* RR fruit may be partially explained by inhibition of the final enzymatic step in ethylene biosynthesis.

We found ethylene biosynthesis significantly enriched ($P_{adj} \leq 0.05$) among mutation-related and ripening-related DEGs in several of the mutants (**Figure 3A**). At the MG stage, *nor* and *rin* fruit had significantly lower expression of the primary ripening ACC synthases (*SlACS2* and *SlACS4*) and ACC oxidases (*SlACO1* and *SlACO4*). At RR, this pattern was maintained except for *SlACO4*, which was higher than WT for both mutants. *SlACS2* was significantly down-regulated across all mutants and stages compared to WT. We validated the expression patterns of *SlACS2* by RT-qPCR experiment using independent samples from WT and the mutant fruit obtained from another field season (**Figure 3C**). We included fruit at the T and OR stages in the validation experiment to capture the gene expression dynamics across fruit ripening and senescence.

In *Cnr* MG fruit, *SlACS4* was significantly lower expressed than WT, like the other mutants, but *SlACS2* showed no significant difference. Interestingly, *Cnr* MG fruit had higher gene expression of four ACC oxidases than WT MG fruit, including *SlACO3*, which is involved in System 1 of ethylene biosynthesis. The increased ACC oxidase expression in *Cnr* MG fruit could explain the high ethylene levels detected in these fruit (**Figure 3B**). At RR, four *ACO* genes had significantly higher expression than WT, except for *SlACO1* that showed no significant differences in RT-qPCR relative expression shown in **Supplementary Table 6**.

Ethylene signaling and response genes, including *ETHYLENE INSENSITIVE 3* (*EIN3*) and *EIN3-BINDING F-BOX* (*EBF*) homologs, were generally higher expressed in *Cnr* than WT at MG and RR stages. *Nor* and *rin* displayed the opposite trend, with generally lower expression than WT at both stages in these genes (**Supplementary Table 4**). These patterns were also reflected in significant enrichments ($P_{adj} \leq 0.05$) of ethylene signaling and response genes at the RR stage (**Figure 3**). Interestingly, ethylene receptor encoding genes (ETRs) were lower expressed across all genotypes and stages compared to WT. In contrast, ethylene response TFs (ERFs) were generally higher expressed in all genotypes at the RR stage.

We measured ABA levels present in the WT and mutant fruit at the MG and RR stages. A decrease of ABA during ripening was found in WT, consistent with previous reports (Mou et al., 2016). This pattern was also present in *Cnr* fruit. However, in *nor* fruit, ABA remained at the same level across both stages, and *rin* showed a significant increase at the RR stage. ABA biosynthesis was significantly enriched among mutation-related DEGs in *nor* and *rin* RR fruit, consistent with the high ABA levels observed (**Figure 3A**). We looked at specific ABA biosynthesis genes enriched in *nor* and *rin* that were also down-regulated in WT at the RR stage and found *SlNCED1*, encoding the 9-*cis*-epoxycarotenoid dioxygenase that catalyzes the rate-limiting step in ABA biosynthesis (Ji et al., 2014). We validated the expression of *SlNCED1* with independent samples and additional stages (T and OR) using RT-qPCR (**Figure 3C**). We also confirmed the expression of an upstream biosynthesis gene, *SlZEP*, encoding a zeaxanthin epoxidase, which was also significantly up-regulated in *nor* at the RR stage and in *rin* at the T stage (**Supplementary Table 6**). While *Cnr* accumulated ABA, signaling and response genes were altered in at MG and RR fruit, including higher expression in ABRE-binding protein (AREB)/ABRE binding factors (ABFs) at both stages compared to WT. *Nor* and *rin* showed alterations in signaling and response at the RR stage, such as lower expression of receptor protein (PYR/PYL) genes and higher expression of the PP2C phosphatase (**Supplementary Table 4**).

We observed changes in biosynthesis and signaling of other plant hormones implicated in fruit development, such as auxins, cytokinins, jasmonic acid, and brassinosteroids (**Figure 3A**). *Cnr* MG fruit had alterations in all hormone pathways examined, further supporting the differences present in *Cnr* phenotype before ripening begins. At the RR stage, all mutants presented multiple defects in hormone metabolism compared to WT. Ripening-related DEGs with hormone functions displayed a similar expression pattern in WT and *Cnr* fruit, whereas *nor* and *rin* displayed low numbers of ripening-related DEGs from these categories.

Ripening Mutations Influence the Expression Dynamics of *CNR, NOR*, and *RIN* in Fruit

Another way in which the mutations in the *CNR*, *RIN*, and *NOR* may affect gene expression of ripening processes is through direct or indirect interactions with each other. We performed RT-qPCR on fruit from the MG, T, RR, and OR stages in each genotype for each of the genes encoding the ripening TFs (**Figure 4**). In WT, each TF follows a ripening pattern, peaking in expression at the T stage. Mutations in any of the three TFs led to a decrease or delay in the expression of the other TFs compared to WT. For example, *RIN* expression does not begin to show an increase until the OR stage for *nor* and *Cnr*. A similar pattern was exhibited in *CNR* expression for *nor* and *rin* and *NOR* expression in *rin* and *Cnr*. The *Cnr* fruit displayed the most dramatic decreases in expression across the TFs, while the *nor* fruit showed the most delays.

Phenotypic Differences in Double Mutants Reveal Genetic Relationships

The changes in gene expression of *CNR*, *NOR*, and *RIN* in the ripening mutants indicate that the genes are interconnected during fruit development. In addition, *Cnr* consistently showed earlier defects in fruit traits, gene expression, and hormone pathways. To characterize the combined genetic effects of the mutations on tomato fruit, we generated homozygous double mutants through reciprocal crosses of the single mutants. We then phenotyped the double mutants for fruit traits and ethylene production (**Figure 5**). Because the reciprocal crosses produced fruit indistinguishable from each other, we report them as only one double mutant (**Supplementary Table 7** and **Supplementary Figure 5**). Fruit of *nor*/*rin* double mutants were almost indistinguishable from both *nor* and *rin* fruit in appearance and external color. Fruit resulting from any cross with *Cnr* as a parent presented similar visual characteristics (**Figure 5A**). We

also performed a PCA of the color measurements to compare the double mutants to their parental lines at the RR stage and confirmed this observation (**Figure 5B** and **Supplementary Table 7**). Based on these observations and our earlier phenotypic and transcriptional data, we confirmed that the *Cnr* mutation affects early fruit development. In contrast, the *nor* and *rin* mutations act during fruit ripening.

If defects in *Cnr* occur earlier in fruit development than those caused by *nor* or *rin*, we expected the *Cnr/rin* and *Cnr/nor* double mutants to behave similarly to *Cnr* and display similar phenotypes (**Figures 5C,D**). *Cnr/rin* fruit were significantly ($P \leq 0.05$) less firm than either parent at the MG stage but performed most similarly to *Cnr* at the RR stage. *Cnr/nor* fruit was not distinguishable from either parent in firmness at MG but was firmer ($P \leq 0.05$) than *Cnr* RR fruit. Interestingly, *Cnr/nor* fruit exhibited high ethylene production at the MG stage like the *Cnr* fruit. At the RR stage, *Cnr/nor* showed a less pronounced decrease in ethylene production, resulting in higher hormone levels than either parent. Although some phenotypic differences were detected, we verified that *Cnr/rin* and *Cnr/nor* resembled the *Cnr* parent for most of the fruit traits measured.

If *nor* and *rin* act synergistically during ripening, the *rin/nor* double mutants would have a more extreme phenotype than either on their own. At the MG stage, *rin/nor* fruit firmness was statistically similar to *rin* ($P \leq 0.05$; **Figure 5C**) but became an intermediate phenotype at the RR stage. For ethylene, *rin/nor* fruit produced less than either parent at both stages, although not significant, suggesting a combined effect of both mutations.

Double Mutant *Cnr/nor* Shows Gene Expression Unique From Both Parents

The strong effect of *Cnr* in the double mutant phenotypes led us to investigate if gene expression in the fruit was altered in a similar way. We selected the *Cnr/nor* double mutant to perform an RNAseq experiment of fruit at MG and RR stages and assessed the overall transcriptional changes resulting from the two mutations combined. We conducted a PCA of total mapped reads for MG and RR fruit of *Cnr/nor* and the single mutant parents (**Figure 6A**). In this analysis, *Cnr/nor* expression appeared more similar to *Cnr* than *nor* in PC1 (66% of variance), but PC2 (20% of variance) accounted for differences between *Cnr* and *Cnr/nor*.

We analyzed mutation-related DEGs ($P_{adj} \leq 0.05$) in the *Cnr/nor* fruit by comparing the gene expression patterns of the double mutant against WT at both MG and RR stages. We then determine which of these mutation-related DEGs were also differentially expressed between the single mutant parents and WT (**Figure 6B**). Similar to *Cnr*, *Cnr/nor* fruit started with a high number of mutation-related DEGs (10,643) at the MG stage, showing defects in development before the initiation of ripening. However, *Cnr/nor* MG and RR fruit showed more mutation-related DEGs than either *nor* or *Cnr* fruit, including 634 unique DEGs at the MG stage and 948 at the RR stage. These data indicate that the *Cnr/nor* fruit present additional defects than *Cnr* fruit prior to ripening.

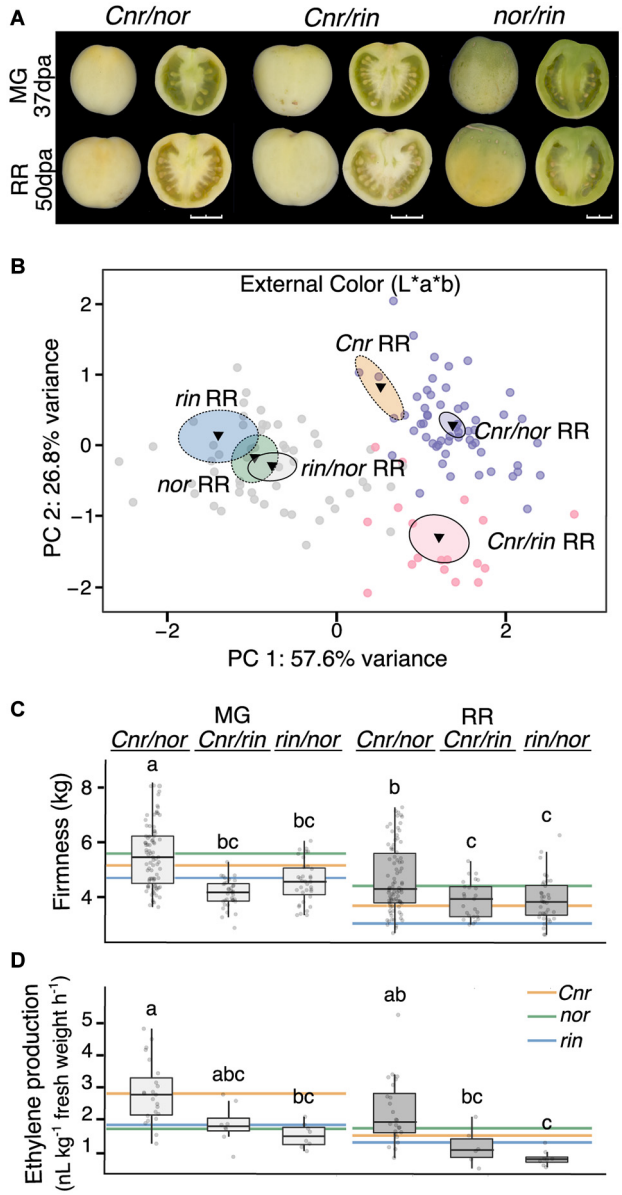

FIGURE 5 | Fruit traits of the homozygous double ripening mutants. **(A)** Homozygous double mutants pictured at the mature green (MG) and red ripe (RR) stages. Fruit shown whole at left and in longitudinal sections at right. Images were extracted and processed with the VideometerLab instrument. Bar represents 2 cm. **(B)** Principal component analysis of fruit external color (n = 18–54). The center of gravity is represented by a triangle with surrounding ellipses indicating 95% confidence interval. Dashed ellipses indicate the values of the single mutant parents. **(C)** Texture analysis of fruit firmness at MG and RR stages (n = 25–86). **(D)** Ethylene production of MG and RR fruit (n = 6-24). Letters indicate significant differences among genotypes and stages ($P \leq 0.05$). Colored lines indicate averages of the parents at each stage for comparison.

Interestingly, *Cnr/nor* and both its parents at the RR stage shared many mutation-related DEGs (1,980) (**Figure 6B**). These shared mutation-related DEGs were significantly ($P_{adj} \leq 0.05$) enriched in glycolysis, starch and

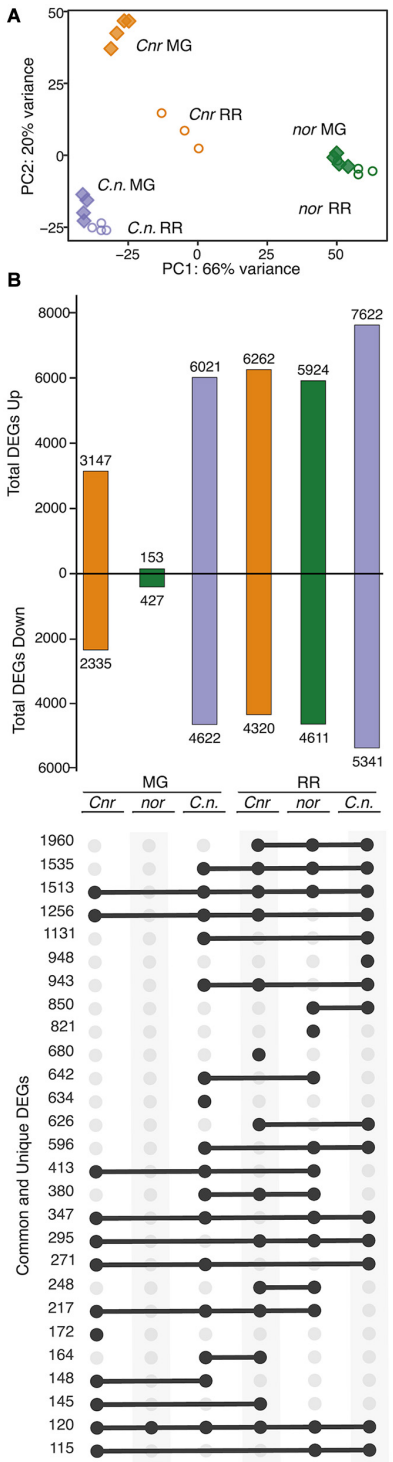

FIGURE 6 | Comparison of *Cnr/nor* double mutant gene expression to parents. **(A)** Principal component analysis of total mapped RNAseq reads for the double mutant *Cnr/nor* (*C.n.*), and the parents *Cnr* and *nor* at the mature green (MG) and red ripe (RR) stages. **(B)** Total, unique, and intersecting differentially expressed genes (DEGs) compared to wild type (WT) for each genotype (mutant/WT) visualized using *UpSetR*. Dots connected by lines indicate common DEGs between categories and single dots indicate unique DEGs, with the numbers of shared or unique genes at the left.

sucrose metabolism, fructose and mannose metabolism, among others, suggesting that carbohydrate metabolism is altered in all three genotypes (**Supplementary Table 4**). When we looked again at the key genes associated with fruit traits, we observed greater defects in the double mutant compared to the single mutant parents (**Supplementary Table 8**).

We only identified 272 ripening-related DEGs ($P_{adj} \leq 0.05$) in *Cnr/nor* fruit, indicating that the double mutant fruit changed very little between the MG and RR stages (**Supplementary Table 4**). This inhibition of ripening progression is similar to the ripening-related DEG patterns exhibited by *nor* (**Figure 2**), highlighting a critical difference between *Cnr/nor* and *Cnr*. Overall, the transcriptional data indicate that *Cnr/nor* have stronger alterations in fruit development and more significant inhibition of fruit ripening than the *Cnr* and *nor* fruit.

DISCUSSION

The spontaneous ripening mutants, *Cnr*, *nor*, and *rin*, are essential genetic tools to untangle the complexity of climacteric fruit ripening (Chen et al., 2020) and to breed for extended shelf-life or field harvest traits in tomato (Kitagawa et al., 2005; Garg et al., 2008). However, thorough phenotyping of the fruit traits affected by these mutants using plants grown under field conditions has been neglected. Here, we produced an extensive quantitative study of fruit quality in the tomato ripening mutants and corroborated it across multiple field seasons. We were able to carefully describe physiological and molecular differences between the mutants by sampling large numbers of fruit and surveying distinct stages through ripening in ways not feasible with greenhouse experiments.

Delay or Inhibition of Ripening Events Vary in *nor* and *rin*

We determined that some ripening events in the mutants *nor* and *rin* were not completely blocked but severely delayed. By examining the OR stage, we found that the mutation in *nor* may strongly affect firmness and taste while pigment accumulation was only delayed and slightly perturbed (**Figure 1**). These phenotypes were supported by higher expression of carotenoid biosynthesis genes in *nor* RR than WT and an increase in *SlPSY1* between the MG and RR stages (**Table 1** and **Supplementary Figure 3**). The accumulation of pigments in *nor* fruit, particularly at late stages in development, has gone unnoticed in previous studies, but it partially resembles the CRISPR-NOR mutants (Gao et al., 2019; Wang et al., 2019). In contrast, *rin* fruit showed strong inhibition of pigment accumulation but less dramatic alterations to fruit taste-related traits, only delaying the accumulation of sugars and decrease in acidity (**Figure 1**). The lack of upregulation of *SlPSY1* in *rin* (**Table 1**) appears to contribute to the color defects, consistent with evidence that RIN directly regulates this gene (Fujisawa et al., 2013). Both *nor* and *rin* exhibited severe delays or inhibition of ripening-related gene expression changes. While highly similar to WT at the MG stage, *nor* and *rin* fruit showed large deviations from WT at the RR stage

(**Figure 2B**). In fact, the gene expression profiles of *nor* and *rin* RR fruit remained similar to those from WT MG fruit.

The physiological data generated in this study show *nor* and *rin* mutations have different impacts on fruit quality traits. Soluble solids and acid accumulation are negatively impacted in both mutants, but more dramatically in *nor* fruit. In addition, previous reports have demonstrated a similar pattern among volatile profiles of the mutants at the red ripe stage, with *rin* again showing more similarity to WT in flavor related traits (Kovács et al., 2009). This suggests *rin* fruit are less likely to hinder flavor profiles than *nor* fruit when breeding for fresh-market hybrid varieties with extended shelf-life. Although *nor* showed lower quality flavor attributes, its coloration at overripe stages was most similar to WT compared to *rin;* and thus, it can be useful in breeding hybrid varieties when coloration is a critical fruit trait, such as in the case of processing tomato varieties. Overall, this knowledge will provide valuable information on these tradeoffs of using either loci for breeding programs.

Because the *Cnr*, *nor*, and *rin* mutants never acquire equivalent colorations to WT, their ripening stages have been determined based on the fruit's age expressed as days after anthesis (dpa) or days after the breaker (BR) stage. Sometimes described as BR + 7 days, the RR stage has been the primary developmental time employed for studying the ripening mutants. As we showed here, the OR stage could provide better comparisons against WT RR fruit for mutants with delayed ripening phenotypes. We demonstrated that in the *nor* fruit, the *RIN* and *CNR* genes only begin to increase in expression in a way comparable to WT at the OR stage (**Figure 4**). This observation corresponds to over a 10-day delay for some of the ripening processes to begin. The delayed ripening events observed in the OR fruit have not been described before in the spontaneous *nor* mutant.

Cnr Is More Than a Ripening Mutant

Although the *Cnr* mutant has been assumed to have normal fruit development before ripening (Lai et al., 2020), there have been indications that the *Cnr* mutant displays defects that are not ripening-specific, such as earlier chlorophyll degradation and altered expression of CWDE (Eriksson et al., 2004; Wang et al., 2020b). We showed that the *Cnr* mutation causes substantial defects in fruit prior to ripening as seen through statistically significant deviations in fruit size, color, firmness, and TA, ethylene production, and gene expression at the MG stage (**Supplementary Table 2** and **Figures 1–3**). Therefore we propose *Cnr* may be more accurately described as a developmental mutant and not exclusively a ripening mutant. Further complementing these results, the *Cnr* fruit displayed large transcriptional deviations from WT that can be traced back as far as 7 dpa (**Figure 2** and **Supplementary Figure 2**). These early development defects are likely a result of reduced *CNR* expression in the mutant, which is typically expressed in locular tissue before fruit maturity (Giovannoni et al., 2017).

Our analysis of ripening-related gene expression in *Cnr* showed striking similarities to WT in the number and functions of genes changing between stages. Moreover, 69.5% of ripening-related DEGs in *Cnr* were shared with WT (**Figure 2**). These results further support the hypothesis that *Cnr* is not exclusively a ripening mutant. Instead, *Cnr* fruit undergoes gene expression changes consistent with WT "ripening." However, the ripening-related changes in gene expression that occur in *Cnr* are not enough to compensate for the large defects accumulated in the fruit during growth and maturation. In a recent report, a knockout mutation to the gene body of *CNR* yielded little visible effects on fruit development and ripening (Gao et al., 2019), which suggests that the *Cnr* mutant phenotype may result from more than just a reduced expression of the *CNR* gene as previously reported (Manning et al., 2006). It has also been demonstrated that *Cnr* fruit have genome-wide methylation changes that inhibit ripening-related gene expression (Zhong et al., 2013). The developmental defects observed in *Cnr* are likely caused by these methylation changes, directly or indirectly caused by the *Cnr* mutation (Chen et al., 2018). Thus, to better understand the *Cnr* mutation, more physiological data at earlier stages of development needs to be analyzed and complemented with more in-depth functional analysis of gene expression alterations at the corresponding stages. In addition, further molecular and genetic studies need to be performed and compared against complete *CNR* knockout mutants.

The *Cnr* Mutant Produces Ethylene Beyond Basal Levels

Previous reports have shown ethylene levels to be very low or even undetectable in the ripening mutants (Giovannoni et al., 2017). Our data support that the mutants never produce a burst in ethylene production, even at the OR stage where more ripening phenotypes are observed (**Figure 3B**). The orange-red pigmentation in *nor* OR fruit and the similarities of *rin* OR fruit in texture and taste-related attributes to WT RR fruit occur independently of an ethylene burst. These observations evidence that other regulatory mechanisms exist to initiate ripening events outside of ethylene (Li et al., 2019b).

Unlike previous reports, our data consistently showed that *Cnr* presented increased ethylene levels at the MG stage compared to WT (Wang et al., 2020b). Interestingly, *Cnr* fruit produced more of the ethylene precursor ACC than WT at the RR stage. Also, *rin* made equivalent levels to WT fruit. Ethylene biosynthesis is divided into two programs: System 1 produces basal levels of the hormone during development, and System 2 generates the climacteric rise in ethylene during ripening (Mcmurchie et al., 1972). Each of these systems is catalyzed by a different set of ethylene biosynthetic enzymes (Liu et al., 2015). It is clear that all mutants show defects to System 2 of ethylene biosynthesis, but they also appear to have alterations specific to System 1. For example, we observed that *SlACO3*, a System 1-specific ACC oxidase, was higher expressed in *Cnr* fruit than WT (**Supplementary Table 6**).

ABA Biosynthesis and Accumulation Is Affected in *nor* and *rin*

The role of ABA in climacteric ripening is not as well explored but has been reported to be complementary to ethylene (Ji et al., 2014). Previous reports in WT fruit have shown that ABA increases until the breaker stage, just before the ethylene burst (Zhang et al., 2009; Mou et al., 2016). ABA has also been

shown to induce ethylene production and linked to the NOR transcription factor (Mou et al., 2018). We found that *nor* and *rin* fruit did not show decreases in ABA concentration during ripening like WT did (**Figure 3**). For *nor*, the constant levels of ABA between MG and RR stages are another example of how fruit ripening events are delayed or inhibited. *RIN* and ABA have been demonstrated to have an inverse relationship where *RIN* expression is repressed with the induction of ABA (Diretto et al., 2020). The significant increase of ABA accumulation in *rin* during ripening suggests that ABA biosynthesis and metabolism are misregulated in this mutant. *rin* fruit appear to present a delayed peak in ABA levels compared to WT fruit. Our results support the indirect interaction between the TFs and ABA during ripening. More developmental stages, genetic manipulations, and exogenous hormone treatments are needed to investigate further the trends of ABA accumulation seen in the ripening mutants.

CNR, NOR, and RIN Act Interdependently

The interactions between the CNR, NOR, and RIN in ripening have been debated in the literature (Chen et al., 2020). The TF RIN directly interacts with *NOR* and *CNR*, binding to their respective promoters, and therefore has been proposed to be the most upstream TF among the three regulators (Fujisawa et al., 2013). Here we provided evidence that the three TFs display at least indirect effects on each other. We have argued that the *Cnr* mutant shows a wide breadth of defects across fruit development before ripening begins, and thus, we propose the *Cnr* mutation is acting before NOR or RIN. This further supports the hypothesis made in Wang et al. (2020b) that *Cnr* acts epistatically to *nor* and *rin*. The gene expression patterns of *CNR*, *NOR*, and *RIN* across ripening stages were decreased or delayed in each of the single ripening mutants. The most substantial variation in gene expression was the downregulation of *NOR* and *RIN* expression across all stages in the *Cnr* mutant (**Figure 4**).

We present for the first time double ripening mutants, homozygous for both loci, that can be used to see the combined effects of each mutation on fruit development and quality traits. We successfully generated the double mutants by establishing reliable and high throughput genotyping protocols for each mutation and evaluating segregation of the mutant phenotypes in field trials across multiple growing seasons. We obtained double mutants from both reciprocal crosses but saw no fruit phenotypic differences between them, suggesting that the ripening mutations are not influenced by maternal or paternal effects (**Supplementary Table 7**). Because the *nor* and *rin* mutants look so similar, it was hard to visually determine the individual effects of each mutation on the appearance of *rin/nor* fruit. However, when specific fruit traits were measured, we could detect additive or intermediate fruit phenotypes in this double mutant, supporting the proposed relationship in Wang et al. (2020b; **Figure 5**). Thus, *nor* and *rin* appear to influence similar fruit traits and act in coordination.

The *Cnr* mutation had a significant effect on the *Cnr/nor* and *Cnr/rin* mutants resulting in fruit with similar appearance and ethylene production to the *Cnr* fruit (**Figure 5**). When analyzing the gene expression profiles of the *Cnr/nor* fruit, we also observed multiple similarities to the *Cnr* parent, but also several deviations (**Figure 6**). Surprisingly, *Cnr/nor* was also reminiscent of *nor*, as it displayed few ripening-related gene expression changes, suggesting the inhibition or delay of specific ripening events in *nor* carried over to the double mutant. Here, we proposed that the *Cnr* mutation causes defects throughout fruit development while the *nor* mutation causes defects predominantly in ripening. However, the *Cnr/nor* double mutant showed additional phenotypic and transcriptional defects before ripening than both mutant parents (**Figure 6**). These observations indicate that in combination with *Cnr*, *nor* may contribute to alterations in early fruit development and the inhibition of ripening progression.

CONCLUSION

Our study contributes new information about the spontaneous tomato ripening mutants, which have been employed to study fruit ripening for at least the past two decades. Also, given the importance of both *nor* and *rin* for tomato breeding, the fruit trait data generated in this study could be applied to improve quality in tomato hybrids or at least identify tradeoffs between fruit traits. Ultimately, our results extend knowledge of underlying genetic and molecular factors affecting fruit ripening and quality while providing insights into fruit physiological changes through ripening and senescence.

DATA AVAILABILITY STATEMENT

The datasets presented in this study can be found in online repositories. The names of the repository/repositories and accession number(s) can be found below: https://www.ncbi.nlm.nih.gov/geo/, GSE163745.

AUTHOR CONTRIBUTIONS

BB-U conceived the original research plan. JA and BB-U designed the experiments and generated the double ripening mutant lines. JA established the genotyping strategies for the single and double mutants, performed the fruit trait phenotyping, measured ethylene emissions, extracted RNA, did the qRT-PCRs, and completed other molecular experiments. JA, CS, and PH performed the bioinformatic analyses. JA and CS analyzed and interpreted the data. JA wrote the manuscript with contributions of CS and BB-U. All authors contributed to the article and approved the submitted version.

FUNDING

This work was supported by start-up funds from the College of Agricultural and Environmental Sciences and the Department of Plant Sciences (UC Davis) to BB-U. Funding to JA was partially provided by the Plant Sciences GSR Award (UC Davis) and the Henry A. Jastro Research Scholarship Award.

ACKNOWLEDGMENTS

We would like to acknowledge and thank Casper van den Abeele for preparing the cDNA libraries for RNAseq; Dr. Baljeet Gill for helping establish a genotyping protocol for *Cnr* by bisulfite sequencing; Dr. Ann L. T. Powell for the initial tomato plant materials; Dr. Clare L. Casteel for performing part of the hormone measurements; Dr. Yasihiro Ito for sharing the primer sequences to genotype *rin*; and Sarah Ream, Emily Lam, and Aaron Lee, for their assistance in genotyping the double mutants.

SUPPLEMENTARY MATERIAL

The Supplementary Material for this article can be found online at: https://www.frontiersin.org/articles/10.3389/fpls.2021.647035/full#supplementary-material

Supplementary Figure 1 | External color of single ripening mutant fruit at the mature green (MG) stage. Principal component analysis of the external color of wild type (WT), *Cnr*, *rin*, and *nor* fruit measured on the L*a*b* color scale. The center of gravity is represented by a triangle with surrounding ellipses indicating 95% confidence interval.

Supplementary Figure 2 | Principal component analysis (PCA) of normalized RNAseq reads for *Cnr*, *nor*, and *rin* wild type fruit at immature and mature green (MG) stages. The RNAseq data of the single mutants at 7 days post anthesis (dpa), 17, 27, and 37 dpa (MG) were obtained from Lü et al. (2018) and reanalyzed using our bioinformatics pipeline.

Supplementary Figure 3 | Functional enrichments in Kyoto Encyclopedia of Genes and Genomes (KEGG) functions among differentially expressed genes (DEGs; $P_{adj} \leq 0.05$). Mutation-related DEGs were obtained by comparing each mutant to the wild type (WT) at the mature green (MG) and red ripe (RR) stages. Each comparison is separated into significant down- and up-regulated DEGs. The heat map colors indicate the significance of the functional enrichment using a $\log_{10}$ ($1/P_{adj}$) scale. Numbers in each tile indicate the number of DEGs within each category. Only significant ($P_{adj} \leq 0.05$) functional enrichments are shown.

Supplementary Figure 4 | Functional enrichments in Kyoto Encyclopedia of Genes and Genomes (KEGG) functions among differentially expressed genes (DEGs; $P_{adj} \leq 0.05$). Ripening-related DEGs were obtained by comparing the RR stage against MG for each genotype. Each comparison is separated into significant down- and up-regulated DEGs. The heat map colors indicate the significance of the functional enrichment using a $\log_{10}$ ($1/P_{adj}$) scale. Numbers in each tile indicate the number of DEGs within each category. Only significant ($P_{adj} \leq 0.05$) functional enrichments are shown.

Supplementary Figure 5 | Representative fruit from the reciprocal crosses of the double mutants. The maternal genotype is listed first for each double mutant. Fruit are pictured at the mature green (MG) and red ripe (RR) stages. Fruit shown whole at left and in longitudinal sections at right. Images were extracted and processed with the VideometerLab instrument. Bar represents 1.5 cm.

Supplementary Table 1 | Primers sequences used for genotyping and RT-qPCRs. Forward (F) and reverse (R) samples are listed for each primer pair.

Supplementary Table 2 | Phenotypic data of ripening mutants at the mature green (MG) and red ripe (RR) by field season. Averages, standard deviations (SD), number of biological replicates (N), and statistical differences are listed for each fruit trait measured. Color was measured in the L*a*b* color space. Letters indicate significant differences among both genotypes and stages calculated by an ANOVA and Tukey HSD ($P \leq 0.05$).

Supplementary Table 3 | Summaries of RNAseq read mapping of tomato wild type, single mutant, and double mutant genotypes across immature, mature green (MG), and red ripe (RR) stages. The study each sample originates from is listed under dataset. Immature stages correspond to 7 days post anthesis (dpa), 17, and 27 dpa. Parsed reads are those that passed through quality and adapter trimming.

Supplementary Table 4 | Differential expression output from DESeq2 (Love et al., 2014) with functional annotations for the two main comparisons: one to capture differences between mutant vs. wild type (WT) fruit at the mature green (MG) and red ripe (RR) stages, and the other to detect differences across ripening (RR vs. MG) in the WT and double mutant fruit. The RNAseq data of the single mutants at 7 days post anthesis (dpa), 17, 27, and 37 dpa (MG) were obtained from Lü et al. (2018) and reanalyzed using our bioinformatics pipeline. Comparisons are listed in the header of each section. Sub-headers are values returned by the results function in DESeq2. baseMean, the mean of normalized counts of all samples for that gene; log2FoldChange, the logarithm (base 2) of the fold change between each comparison; lfcSE, the standard error of the log2FoldChange; stat, the Wald test statistic for each comparison; *P* = *P*-value generated from the Wald test statistic; *P*adj, adjusted *P*-value as calculated via the Benjamini and Holchberg method. AHRD, Automated Assignment of Human Readable Descriptions; KEGG, Kyoto Encyclopedia of Genes and Genomes.

Supplementary Table 5 | Differential expression output from DESeq2 (Love et al., 2014) with functional annotations for the comparisons between mutant vs. wild type (WT) fruit at 7 days post anthesis (dpa), 17, 27, and 37 dpa (MG) were obtained from Lü et al. (2018) and reanalyzed using our bioinformatics pipeline. Comparisons are listed in the header of each section. Sub-headers are values returned by the results function in DESeq2. baseMean, the mean of normalized counts of all samples for that gene; log2FoldChange, the logarithm (base 2) of the fold change between each comparison; lfcSE, the standard error of the log2FoldChange; stat, the Wald test statistic for each comparison; *P*, *P*-value generated from the Wald test statistic; *P*adj, adjusted *P*-value as calculated via the Benjamini and Holchberg method. AHRD, Automated Assignment of Human Readable Descriptions; KEGG, Kyoto Encyclopedia of Genes and Genomes.

Supplementary Table 6 | Relative gene expression by RT-qPCR of hormone biosynthesis genes in wild type and ripening mutant (*Cnr*, *nor*, and *rin*) fruit at the mature green (MG; 37 dpa), turning (T; 45 dpa), red ripe (RR; 50 dpa), and overripe (OR; 57 dpa) stages. The tomato *SlUBQ* gene was used as reference gene.

Supplementary Table 7 | Fruit phenotypic data of the double mutants obtained by reciprocal crosses. The maternal genotype is listed first in each double mutant genotype. Fruit traits were measured at the mature green (MG) and red ripe (RR) stages. Averages, standard deviations (SD), and number of biological replicates (n) are presented for ethylene emissions and color (measured in the L*a*b* color space).

Supplementary Table 8 | Differential expression of key genes associated with tomato fruit traits in the double ripening mutant *Cnr/nor*. Two comparisons were performed: one to capture differences between mutant vs. wild type (WT) fruit at the mature green (MG) and red ripe (RR) stages, and the other to detect differences across ripening (RR vs. MG) in the *Cnr/nor* mutant fruit. Only significant fold changes (Log_2FC, $P_{adj} \leq 0.05$) are presented.

REFERENCES

Agar, I. T., Abak, K., and Yarsi, G. (1994). Effect of Different Maturity Stages on the Keeping Quality of nor (non-ripening), rin (ripening-inhibitor) and Normal Type Tomatoes. *Acta Hortic* 742–753. doi: 10.17660/actahortic.1994.368.88

Benjamini, Y., and Hochberg, Y. (1995). Controlling the False Discovery Rate: A Practical and Powerful Approach to Multiple Testing. *J. R. Stat. Soc. Ser. B* 57, 289–300. doi: 10.1111/j.2517-6161.1995.tb02031.x

Blanco-Ulate, B., Vincenti, E., Powell, A. L. T., and Cantu, D. (2013). Tomato transcriptome and mutant analyses suggest a role for plant stress hormones in the interaction between fruit and Botrytis cinerea. *Front. Plant Sci.* 4:142. doi: 10.3389/fpls.2013.00142

Bolger, A. M., Lohse, M., and Usadel, B. (2014). Trimmomatic: A flexible trimmer for Illumina sequence data. *Bioinformatics* 2014:170. doi: 10.1093/bioinformatics/btu170

Casteel, C. L., De Alwis, M., Bak, A., Dong, H., Whitham, S. A., and Jander, G. (2015). Disruption of ethylene responses by Turnip mosaic virus mediates suppression of plant defense against the green peach aphid vector. *Plant Physiol.* 169, 209–218. doi: 10.1104/pp.15.00332

Chen, T., Qin, G., and Tian, S. (2020). Regulatory network of fruit ripening: current understanding and future challenges. *New Phytol.* 228, 1219–1226. doi: 10.1111/nph.16822

Chen, W., Yu, Z., Kong, J., Wang, H., Li, Y., Zhao, M., et al. (2018). Comparative WGBS identifies genes that influence non-ripe phenotype in tomato epimutant Colourless non-ripening. *Sci. China Life Sci.* 61, 244–252. doi: 10.1007/s11427-017-9206-5

Conway, J. R., Lex, A., and Gehlenborg, N. (2017). UpSetR: An R package for the visualization of intersecting sets and their properties. *Bioinformatics* 2017:364. doi: 10.1093/bioinformatics/btx364

De, F., Maintainer, M., and De Mendiburu, F. (2017). *Package "agricolae" Title Statistical Procedures for Agricultural Research. Stat. Proced. Agric. Res. Version 1.3-3*.

Diretto, G., Frusciante, S., Fabbri, C., Schauer, N., Busta, L., Wang, Z., et al. (2020). Manipulation of β-carotene levels in tomato fruits results in increased ABA content and extended shelf life. *Plant Biotechnol. J.* 18, 1185–1199. doi: 10.1111/pbi.13283

Eriksson, E. M., Bovy, A., Manning, K., Harrison, L., Andrews, J., De Silva, J., et al. (2004). Effect of the Colorless non-ripening Mutation on Cell Wall Biochemistry and Gene Expression during Tomato Fruit Development and Ripening 1[w]. *Am. Soc. Plant Biol.* 136, 4184–4197. doi: 10.1104/pp.104.045765

Fujisawa, M., Nakano, T., Shima, Y., and Ito, Y. (2013). A large-scale identification of direct targets of the tomato MADS box transcription factor RIPENING INHIBITOR reveals the regulation of fruit ripening. *Plant Cell* 25, 371–386. doi: 10.1105/tpc.112.108118

Gao, Y., Wei, W., Fan, Z., Zhao, X., Zhang, Y., Jing, Y., et al. (2020). Re-evaluation of the nor mutation and the role of the NAC-NOR transcription factor in tomato fruit ripening. *J. Exp. Bot* 2020:131. doi: 10.1093/jxb/eraa131

Gao, Y., Zhu, N., Zhu, X., Wu, M., Jiang, C.-Z., Grierson, D., et al. (2019). Diversity and redundancy of the ripening regulatory networks revealed by the fruitENCODE and the new CRISPR/Cas9 CNR and NOR mutants. *Hortic. Res.* 6:39. doi: 10.1038/s41438-019-0122-x

Garg, N., Cheema, D. S., and Dhatt, A. S. (2008). Utilization of rin, nor, and alc alleles to extend tomato fruit availability. *Int. J. Veg. Sci.* 14, 41–54. doi: 10.1080/19315260801890526

Giovannoni, J. J. (2007). Fruit ripening mutants yield insights into ripening control. *Curr. Opin. Plant Biol.* 10, 283–289. doi: 10.1016/j.pbi.2007.04.008

Giovannoni, J., Nguyen, C., Ampofo, B., Zhong, S., and Fei, Z. (2017). The Epigenome and Transcriptional Dynamics of Fruit Ripening. *Annu. Rev. Plant Biol.* 68, 61-84. doi: 10.1146/annurev-arplant-042916

Giovannoni, J., Tanksley, S., Vrebalov, J., and Noensie, F. (2004). *NOR gene composition and methods for use thereof*. U.S. Patent No US 6,762,347,B1. Washington, DC: U.S. Patent and Trademark

Ito, Y., Nishizawa-Yokoi, A., Endo, M., Mikami, M., Shima, Y., Nakamura, N., et al. (2017). Re-evaluation of the rin mutation and the role of RIN in the induction of tomato ripening. *Nat. Plants* 1:5. doi: 10.1038/s41477-017-0041-5

Ji, K., Kai, W., Zhao, B., Sun, Y., Yuan, B., Dai, S., et al. (2014). SlNCED1 and SlCYP707A2: Key genes involved in ABA metabolism during tomato fruit ripening. *J. Exp. Bot.* 65, 5243–5255. doi: 10.1093/jxb/eru288

Karlova, R., Chapman, N., David, K., Angenent, G. C., Seymour, G. B., and De Maagd, R. A. (2014). Transcriptional control of fleshy fruit development and ripening. *J. Exp. Bot.* 65, 4527–4541. doi: 10.1093/jxb/eru316

Kassambara, A., Mundt, F., Kassambara, A., and Mundt, F. (2017). Factoextra: extract and visualize the results of multivariate data analyses. *R. Packag. Version* 1, 337–354.

Kitagawa, M., Ito, H., Shiina, T., Nakamura, N., Inakuma, T., Kasumi, T., et al. (2005). Characterization of tomato fruit ripening and analysis of gene expression in F1 hybrids of the ripening inhibitor (rin) mutant. *Physiol. Plant.* 123, 331–338. doi: 10.1111/j.1399-3054.2005.00460.x

Klann, E. M., Chetelat, R. T., and Bennett, A. B. (1993). Expression of Acid Invertase Gene Controls Sugar Composition in Tomato (Lycopersicon) Fruit. *Plant Physiol.* 103, 863–870. doi: 10.1104/pp.103.3.863

Kopeliovitch, E., Rabinowitch, H. D., Mizrahi, Y., and Kedar, N. (1979). The potential of ripening mutants for extending the storage life of the tomato fruit. *Euphytica* 1979:BF00029179. doi: 10.1007/BF00029179

Kovács, K., Fray, R. G., Tikunov, Y., Graham, N., Bradley, G., Seymour, G. B., et al. (2009). Effect of tomato pleiotropic ripening mutations on flavour volatile biosynthesis. *Phytochemistry* 70, 1003–1008. doi: 10.1016/j.phytochem.2009.05.014

Kumar, R., Khurana, A., and Sharma, A. K. (2014). Role of plant hormones and their interplay in development and ripening of fleshy fruits. *J. Exp. Bot.* 65, 4561–4575. doi: 10.1093/jxb/eru277

Lai, T., Wang, X., Ye, B., Jin, M., Chen, W., Wang, Y., et al. (2020). Molecular and functional characterization of the SBP-box transcription factor SPL-CNR in tomato fruit ripening and cell death. *J. Exp. Bot.* 71, 2995–3011. doi: 10.1093/jxb/eraa067

Langmead, B., and Salzberg, S. L. (2012). Fast gapped-read alignment with Bowtie 2. *Nat. Methods* 9, 357–359.

Lê, S., Josse, J., and Husson, F. (2008). FactoMineR: An R package for multivariate analysis. *J. Stat. Softw* 2008:01. doi: 10.18637/jss.v025.i01

Li, S., Chen, K., and Grierson, D. (2019a). A critical evaluation of the role of ethylene and MADS transcription factors in the network controlling fleshy fruit ripening. *New Phytol.* 221, 1724–1741. doi: 10.1111/nph.15545

Li, S., Xu, H., Ju, Z., Cao, D., Zhu, H., Fu, D., et al. (2018). The RIN-MC Fusion of MADS-Box Transcription Factors Has Transcriptional Activity and Modulates Expression of Many Ripening Genes. *Plant Physiol.* 176, 891–909. doi: 10.1104/pp.17.01449

Li, S., Zhu, B., Pirrello, J., Xu, C., Zhang, B., Bouzayen, M., et al. (2019b). Roles of RIN and ethylene in tomato fruit ripening and ripening-associated traits. *New Phytol.* 2019:16362. doi: 10.1111/nph.16362

Liu, M., Pirrello, J., Chervin, C., Roustan, J.-P., and Bouzayen, M. (2015). Ethylene Control of Fruit Ripening: Revisiting the Complex Network of Transcriptional Regulation. *Plant Physiol.* 169, 2380–2390. doi: 10.1104/pp.15.01361

Love, M. I., Huber, W., and Anders, S. (2014). Moderated estimation of fold change and dispersion for RNA-seq data with DESeq2. *Genome Biol.* 15:550. doi: 10.1186/s13059-014-0550-8

Lü, P., Yu, S., Zhu, N., Chen, Y.-R., Zhou, B., Pan, Y., et al. (2018). Genome Encode Analyses Reveal the Basis of Convergent Evolution of Fleshy Fruit. *Ssrn* 2018:3155803. doi: 10.2139/ssrn.3155803

Manning, K., Tor, M., Poole, M., Hong, Y., Thompson, A. J., King, G. J., et al. (2006). A naturally occurring epigenetic mutation in a gene encoding an SBP-box transcription factor inhibits tomato fruit ripening. *Nat. Genet.* 38, 948–952. doi: 10.1038/ng1841

Mcmurchie, E. J., Mcglasson, W. B., and Eaks, I. L. (1972). Treatment of fruit with propylene gives information about the biogenesis of ethylene. *Nature* 1972:237235a0. doi: 10.1038/237235a0

Moriya, Y., Itoh, M., Okuda, S., Yoshizawa, A. C., and Kanehisa, M. (2007). KAAS: An automatic genome annotation and pathway reconstruction server. *Nucleic Acids Res.* 35, W182–W185. doi: 10.1093/nar/gkm321

Mou, W., Li, D., Bu, J., Jiang, Y., Khan, Z. U., Luo, Z., et al. (2016). Comprehensive Analysis of ABA Effects on Ethylene Biosynthesis and Signaling during Tomato Fruit Ripening. *PLoS One* 11:e0154072. doi: 10.1371/journal.pone.0154072

Mou, W., Li, D., Luo, Z., Li, L., Mao, L., and Ying, T. (2018). SlAREB1 transcriptional activation of NOR is involved in abscisic acid-modulated ethylene biosynthesis during tomato fruit ripening. *Plant Sci.* 276, 239–249. doi: 10.1016/J.PLANTSCI.2018.07.015

Osei, M. K., Danquah, A., Danquah, E., and Adu-Dapaah. (2017). An overview of tomato fruit-ripening mutants and their use in increasing shelf life of tomato fruits. *Afr. J. Agric. Res.* 12, 3520–3528. doi: 10.5897/ajar2017.12756

Osorio, S., Carneiro, R. T., Lytovchenko, A., McQuinn, R., Sørensen, I., Vallarino, J. G., et al. (2020). Genetic and metabolic effects of ripening mutations and vine detachment on tomato fruit quality. *Plant Biotechnol. J.* 18, 106–118. doi: 10.1111/pbi.13176

Robinson, R. W., and Tomes, M. L. (1968). Ripening inhibitor: a gene with múltiple effects on ripening. *Tomato Genet. Coop.* 18, 36–37.

Shinozaki, Y., Nicolas, P., Fernandez-Pozo, N., Ma, Q., Evanich, D. J., Shi, Y., et al. (2018). High-resolution spatiotemporal transcriptome mapping of tomato fruit development and ripening. *Nat. Commun.* 9:364. doi: 10.1038/s41467-017-02782-9

Silva, C. J., van den Abeele, C., Ortega-Salazar, I., Papin, V., Adaskaveg, J. A., Wang, D., et al. (2021). Host susceptibility factors render ripe tomato fruit vulnerable to fungal disease despite active immune responses. *J. Exp. Bot.* 2021:601. doi: 10.1093/jxb/eraa601

Thompson, A. J., Tor, M., Barry, C. S., Vrebalov, J., Orfila, C., Jarvis, M. C., et al. (1999). Molecular and genetic characterization of a novel pleiotropic tomato-ripening mutant. *Plant Physiol.* 120, 383–390. doi: 10.1104/pp.120.2.383

Tieman, D., Zhu, G., Resende, M. F. R., Lin, T., Nguyen, C., Bies, D., et al. (2017). A chemical genetic roadmap to improved tomato flavor. *Science* 355, 391–394. doi: 10.1126/science.aal1556

Tigchelaar, E. C., Tomes, M. L., Kerr, E. A., and Barman, R. J. (1973). A new fruit ripening mutant, non-ripning (nor). *Rep. Tomato Genet. Coop.* 23, 33–34.

Tigchelaar, E., McGlasson, W., and Franklin, M. (1978). Natural and ethephon-stimulated ripening of F_1 hybrids of the ripening inhibitor (*rin*) and non-ripening (*nor*) mutants of tomato (*Lycopevsicon esculentum* Mill.). *Aust. J. Plant Physiol.* 1978:PP9780449

Wang, R., Angenent, G. C., Seymour, G., and de Maagd, R. A. (2020a). Revisiting the Role of Master Regulators in Tomato Ripening. *Trends Plant Sci.* 25, 291–301. doi: 10.1016/j.tplants.2019.11.005

Wang, R., da Rocha, Tavano, E., Lammers, M., Martinelli, A., Angenent, G., et al. (2019). Re-evaluation of transcription factor function in tomato fruit development and ripening with CRISPR/Cas9-mutagenesis. *Sci. Rep.* 2019, 1–10. doi: 10.1038/s41598-018-38170-6

Wang, R., Lammers, M., Tikunov, Y., Bovy, A. G., Angenent, G. C., and de Maagd, R. A. (2020b). The rin, nor and Cnr spontaneous mutations inhibit tomato fruit ripening in additive and epistatic manners. *Plant Sci.* 294:110436. doi: 10.1016/j.plantsci.2020.110436

Ye, J., Coulouris, G., Zaretskaya, I., Cutcutache, I., Rozen, S., and Madden, T. L. (2012). Primer-BLAST: a tool to design target-specific primers for polymerase chain reaction. *BMC Bioinformatics* 2012:134. doi: 10.1186/1471-2105-13-134

Zhang, M., Yuan, B., and Leng, P. (2009). The role of ABA in triggering ethylene biosynthesis and ripening of tomato fruit. *J. Exp. Bot.* 60, 1579–1588. doi: 10.1093/jxb/erp026

Zhong, S., Fei, Z., Chen, Y.-R., Zheng, Y., Huang, M., Vrebalov, J., et al. (2013). Single-base resolution methylomes of tomato fruit development reveal epigenome modifications associated with ripening. *Nat. Biotechnol.* 31, 154–159. doi: 10.1038/nbt.2462

Conflict of Interest: The authors declare that the research was conducted in the absence of any commercial or financial relationships that could be construed as a potential conflict of interest.

Advantages of publishing in Frontiers

OPEN ACCESS
Articles are free to read for greatest visibility and readership

FAST PUBLICATION
Around 90 days from submission to decision

HIGH QUALITY PEER-REVIEW
Rigorous, collaborative, and constructive peer-review

TRANSPARENT PEER-REVIEW
Editors and reviewers acknowledged by name on published articles

Frontiers
Avenue du Tribunal-Fédéral 34
1005 Lausanne | Switzerland

Visit us: www.frontiersin.org
Contact us: frontiersin.org/about/contact

REPRODUCIBILITY OF RESEARCH
Support open data and methods to enhance research reproducibility

DIGITAL PUBLISHING
Articles designed for optimal readership across devices

FOLLOW US
@frontiersin

IMPACT METRICS
Advanced article metrics track visibility across digital media

EXTENSIVE PROMOTION
Marketing and promotion of impactful research

LOOP RESEARCH NETWORK
Our network increases your article's readership